Centre Armand-Frappier Santé Biotechnologie

La régulation des fimbriae de type 1 chez les *Escherichia coli* uropathogènes

Par

Hicham Bessaiah

Thèse présentée pour l'obtention du grade de Philosophiae Doctor (Ph.D.)
en Biologie

Jury d'évaluation

Président du jury et Examinateur interne	Dr. Éric Déziel INRS Centre Armand-Frappier Santé Biotechnologie
Examinateur externe	Dr. George Szatmari Département de microbiologie, infectiologie et immunologie Université de Montréal (UdeM)
Examinateur externe	Dr. Marylise Duperthuy Département de microbiologie, infectiologie et immunologie Université de Montréal (UdeM)
Directeur de recherche	Dr. Charles M. Dozois INRS Centre Armand-Frappier Santé Biotechnologie

REMERCIEMENTS

Une thèse, c'est un engagement et un accomplissement personnel certes, mais impossible à réaliser sans la présence de nombreuses personnes que je tiens maintenant à remercier. Tout d'abord, je tiens à remercier mon directeur Dr. Charles M. Dozois qui m'a formé, soutenu et accompagné durant ces quatre années. Son encadrement m'a permis de gagner en confiance et en maturité scientifique. Charles, je te remercie tout particulièrement pour ton enthousiasme et ta rigueur scientifique. Travailler dans ton laboratoire a été incroyablement agréable et, grâce à tes conseils, j'ai appris à aborder chaque nouveau défi avec confiance et une vision positive.

Je remercie Dr. George Szatmari et Dre. Marylise Duperthuy d'avoir accepté d'évaluer ces travaux de thèses, malgré des emplois du temps chargés. Je tiens à remercier également Dr. Éric Déziel, pour sa présence en tant que président du jury et également pour ses conseils et sa bienveillance au cours de nos quelques discussions ces quatre dernières années.

Je me rends compte que je suis extrêmement chanceux d'avoir côtoyer Dr. Pravil Pokharel. Tu es plus qu'un ami. Merci pour ton enthousiasme pour la découverte scientifique et pour ton soutien et encouragement continu. Je t'en suis éternellement reconnaissant pour ton rôle durant mon doctorat.

Merci à Sébastien Houle pour ses conseils et ses remarques scientifiques tellement utiles, sa disponibilité et son aide pour l'avancement de mes projets

Durant ces travaux, j'ai été amené à travailler avec plusieurs équipes de l'INRS et de l'Université de Sherbrooke dont l'aide et les conseils ont toujours été d'une grande utilité. C'est pourquoi j'adresse toute ma gratitude à l'équipe Dr. Julien Van Grevenynghe de l'INRS en particulier à mon ami et frère Hamza Loucif, merci pour ton enthousiasme et ta disponibilité et ton implication. Un grand merci à Merve Kulbay de l'équipe du Dr. Jaques Bernier pour ton implication et tous les moments formidables et les rires que nous avons partagé ensemble. Nous serons toujours de bons amis. Un immense merci au Dr. Charles Calmettes et son équipe. Merci également à l'équipe du Dr. Éric Massé d'avoir participé à l'avancement de mon projet.

Je tiens à remercier les organismes subventionnaires (CRSNG & CRIPA-FRQNT) d'avoir financé notre recherche.

Je tiens également à remercier tous les membres du laboratoire de Dozois qui ont fait de chaque jour en laboratoire un lieu de travail formidable, et je suis très honoré d'avoir pu entrer en contact avec tant de personnes formidables au cours de ces dernières années. Merci Hajer, Katerina,

DÉDICACE

Je dédie ce travail à ma mère, Laila, et à la mémoire de mon père, Ahmed (1959-2010), pour tous leurs sacrifices et tous leurs efforts qui m'ont permis d'arriver là où j'en suis.

RÉSUMÉ

Les *E. coli* pathogènes extra-intestinaux (ExPEC) sont responsables d'un large éventail d'infections invasives chez l'homme et les animaux. Les *E. coli* uropathogènes (UPEC) sont le principal agent étiologique des infections du tractus urinaire (ITU). Ces infections constituent une des formes d'infection bactérienne les plus fréquentes chez l'homme et affectent annuellement des millions de personnes. Les fimbriae de type 1, codés par les gènes *fim*, sont l'un des facteurs de virulence les plus importants impliqués dans la pathogenèse des souches ExPEC. Par exemple, les fimbriae de type 1 sont essentiels pour la colonisation de la vessie par les UPEC, afin de stimuler directement l'invasion des UPEC dans les cellules épithéliales et aider à la formation de communautés bactériennes intracellulaires qui peuvent persister en tant que réservoirs et seront responsables des infections récurrentes. Comprendre la régulation des fimbriae de type 1 pourrait aider à identifier des nouvelles cibles thérapeutiques et à ouvrir de nouvelles avenues dans les approches thérapeutiques et préventives des ITU et d'autres infections causées par des ExPEC.

Dans un premier temps, nous nous sommes intéressés à comprendre davantage la régulation des fimbriae type 1 chez les UPEC. Pour déterminer les facteurs impliqués dans l'expression des fimbriae type 1, nous avons développé un système rapporteur luciférase (système *lux*) à simple copie fusionnée à la région promotrice de l'opéron *fim*, qui est situé sur un élément inversible, *fimS*. L'utilisation du système *lux* permet de mesurer l'activité des promoteurs et d'autres éléments régulateurs de la transcription, ainsi que les effets des activateurs et des inhibiteurs. Dans ce contexte, nous avons généré une banque de mutants par transposition chez la souche sauvage CFT073 portant une fusion transcriptionnelle du promoteur *fimS*. Les mutants générés par le transposon Tn*10* ont été criblés pour le niveau de production des fimbriae type 1 suivi de séquençage à haut débit afin d'identifier des gènes qui, lorsqu'ils sont altérés, affectaient l'expression des fimbriae de type 1.

Deuxièmement, nous avons montré que *yqhG*, codant pour une protéine de fonction inconnue, est l'un des médiateurs importants contribuant à une diminution de l'expression des fimbriae de type 1 chez la souche CFT073. Nos résultats démontrent que la délétion de *yqhG* altère l'expression des fimbriae de type 1 et réduit la capacité du mutant à coloniser le tractus urinaire murin. De plus, l'atténuation de la virulence du mutant *yqhG* est concomitante avec la répression de l'expression des fimbriae de type 1. Nous avons démontré aussi que le mutant *yqhG* est plus sensible au stress oxydatif.

En dernier lieu, nous avons démontré que le petit ARN non-codant RyfA est important pour la résistance au stress oxydatif et osmotique chez les souches UPEC CFT073 et 536 et la souche d'*E. coli* pathogène aviaire (APEC) CH138. Nous constatons que l'inactivation de RyfA atténue la virulence à la fois de la souche CFT073 dans le modèle d'ITU murin et la souche CH138 dans le modèle septicémique aviaire. L'atténuation de la virulence de ces souches est concomitante avec la répression de l'expression des fimbriae de type 1. Par analyse transcriptomique du mutant *ryfA* de la souche CFT073, nous avons observé une modulation de l'expression des gènes associés aux réponses générales au stress, le métabolisme, la formation de biofilm et les gènes codant pour les structures de surface. Finalement, nous avons démontré que la perte du *ryfA* réduit la survie des UPEC dans les macrophages humain et murin.

Mots clés : *Escherichia coli* uropathogène, Infection du tractus urinaire, Volaille, Fimbriae de type 1, Adhésion, Réponse au stress,

ABSTRACT

Extra-intestinal pathogenic *E. coli* (ExPEC) strains are responsible for a wide range of invasive infections in humans and animals, often leading to sepsis. Uropathogenic *E. coli* (UPEC) is the main etiologic agent of urinary tract infections (UTIs). These infections are one of the most common forms of bacterial infection in humans and affect millions of people annually. Type 1 fimbriae, encoded by the *fim* genes, are one of the most important virulence factors involved in the pathogenesis of ExPEC strains. For example, type 1 fimbriae are essential for UPEC colonization of the bladder, to directly stimulate the invasion of UPEC into epithelial cells, and to aid in the formation of intracellular bacterial communities that can persist as reservoirs and will be responsible for recurrent infections. Understanding the regulation of type 1 fimbriae could help to identify new therapeutic targets and open up new avenues in therapeutic and preventive approaches to UTI.

First, we were interested in further understanding the regulation of type 1 fimbriae in UPEC. To determine the factors involved in the expression of type 1 fimbriae, we developed a single copy luciferase reporter system (*lux* system) fused to the promoter region of the *fim* operon, which is located on an invertible element, *fimS*. The use of the *lux* system allows the activity of promoters and other transcriptional regulatory elements to be measured, as well as the effects of activators and inhibitors. In this context, the CFT073 carrying *fimS* phase variable reporter was subjected to transposon mutagenesis using a Tn*10*. The mutants were screened for the level of type 1 fimbriae production followed by high-throughput sequencing to identify genes that affect the expression of type 1 fimbriae once they were disrupted.

Second, we showed that *yqhG*, encoding a protein of unknown function, is one of the important mediators contributing to a decrease in the expression of type 1 fimbriae in strain CFT073. Our results demonstrate that the deletion of *yqhG* alters the expression of type 1 fimbriae and significantly decreases the ability of the mutant to colonize the murine urinary tract. In addition, the attenuation of the virulence of the *yqhG* mutant is concomitant with the repression of the expression of type 1 fimbriae. We demonstrated that the *yqhG* mutant is more sensitive to oxidative stress.

Finally, we demonstrated that the small non-coding RNA RyfA is important for resistance to oxidative and osmotic stress in the UPEC strains CFT073 and 536 and the avian pathogenic *E. coli* (APEC) strain CH138. We demonstrated that RyfA inactivation attenuates the virulence of both strains CFT073 in the murine ITU model and strain CH138 in the avian sepsis model. The

attenuation of the virulence of these strains is concomitant with the repression of the expression of type 1 fimbriae. Transcriptomic analysis of the *ryfA* mutant of the strain CFT073 showed a modulation of the expression of the genes associated with the general stress responses, metabolism, biofilm formation and genes encoding surface structures. Finally, we demonstrated that the loss of *ryfA* reduces the survival of UPEC strains in human and murine macrophages.

TABLE DES MATIÈRES

LISTE DES FIGURES

LISTE DES TABLEAUX

LISTE DES ABRÉVIATIONS

ADN : Acide désoxyribonucléique

AMPc : AMP cyclique

ANOVA : Analysis of variance

APEC : Avian pathogenic *E. coli* (*E. coli* pathogène aviaire)

ARN : Acide ribonucléique

ARNm : ARN messager

BEC : Bladder epithelial cells

CNF1 : Cytotoxic necrotizing factor 1 (facteur nécrosant cytotoxique 1)

CU : Chaperone-Usher

EI : Élément interconvertible

ExPEC : Extraintestinal Pathogenic *E. coli (E. coli* pathogène extraintestinal)

Fe : Fer

IBC : Intracellular Bacterial Communities (communautés bactériennes intracellulaires)

InPEC : Intestinal Pathogenic *E. coli* (*E. coli* pathogène intestinal)

ITU : Infection du tractus urinaire

LPS : Lipopolysaccharide

LT : Toxine thermolabile

M : Molaire

ME : Membrane Externe

MI : Membrane interne

NMEC : Neonatal meningitis *E. coli* (*E. coli* de la méningite néonatale)

PCR : Polymerase Chain Reaction

ppGpp : Guanosine tétraphosphate

Pst : Système de transport spécifique du phosphate inorganique

qRT-PCR : Réaction de polymérase en chaîne quantitative en temps réel

RID : Région inversé droite

RIG : Région inversé gauche

RNS : Reactive nitrogen species (espèces réactives d'azote)

ROS : Reactive oxygen species (espèces réactives d'oxygène)

SPATE : Sérine Protéase Autotransporteur des *Enterobacteriaceae*

sRNA : Small RNA (petit ARN non-codant)

TLR : Toll-like receptor

UPEC : Uropathogenic *E. coli* (*E. coli* uropathogène)

WT : Wild-type (sauvage)

µ : Micro

Unités de mesure

X *g* : nombre de *g* (gravitationnel)

rpm : Rotation par minute

pb : Paires de bases

D.O. : Densité optique

nm : Nanomètre

mM : Millimolaire

Mb : Mégabase

M : Molaire

kDa : KiloDalton

Kb : Kilobase

CFU : Unité formatrice de colonie

µM : micromolaire

µm : micromètre

µl : microlitre

µg : microgramme

Symboles

Ω : Ohm

χ : Chi

σ : Sigma

β : Beta

α : Alpha

< : Plus petit que

> : Plus grand que

1   INTRODUCTION

Escherichia coli est un habitant commun du microbiote intestinal des humains et des animaux. Habituellement, *E. coli* forme une relation symbiotique bénéfique avec son hôte et joue un rôle important dans la promotion de la stabilité de la flore microbienne luminaire et dans le maintien d'une homéostasie intestinale normale. Il existe plusieurs sous-types d'*E. coli* hautement adaptés qui ont acquis des attributs de virulence spécifiques, ce qui leur confère une grande capacité à s'adapter à de nouvelles niches et leur permet de provoquer un large spectre de maladie (Kaper *et al.*, 2004). Les souches d'*E. coli* extra-intestinales sont des souches commensales et maintiennent la capacité d'exister dans l'intestin sans conséquence, mais ont la capacité de se disséminer et de coloniser d'autres organes de l'hôte, y compris le sang, le système nerveux central et les voies urinaires, ce qui entraîne une maladie (Wiles *et al.*, 2008b).

Les infections du tractus urinaire (ITU) constituent une des formes d'infections bactériennes les plus fréquentes chez les humains, et sont une cause importante de morbidité et de mortalités aux dans le monde. Les infections urinaires sont plus fréquentes chez les femmes que chez les hommes, en grande partie à cause des différences anatomiques, et on estime que la moitié des femmes subissent au moins une infection urinaire au cours de leur vie (Bien *et al.*, 2012). Bien que ces infections puissent souvent être traitées par un traitement antibiotique de courte durée, l'infection récurrente est un problème grave.

E. coli uropathogène (UPEC) est l'agent étiologique prédominant des ITU, cependant, beaucoup d'autres uropathogènes sont également capables de causer ce type d'infection. Les souches UPEC agissent comme des pathogènes intracellulaires opportunistes, en tirant profit du comportement et de la susceptibilité de l'hôte en utilisant un répertoire diversifié de facteurs de virulence pour coloniser les voies urinaires. Les adhésines étant sans doute les déterminants les plus importants de la pathogénicité (Subashchandrabose *et al.*, 2013). L'aptitude des UPEC à se lier aux tissus de l'hôte est l'un des facteurs primordiaux qui facilitent la colonisation des voies urinaires, permettant aux bactéries de résister au flux massique d'urine et favorisant l'invasion des cellules urothéliales par les UPEC. Les fimbriae de type 1 sont hautement conservés et extrêmement fréquents chez les isolats d'UPEC et commensaux et sont l'un des facteurs de virulence les plus importants impliqués dans la mise en place des ITU. Le traitement de ces infections se fait par antibiotique, mais leur utilisation massive et abusive a favorisé le développement et l'émergence de souches antibiorésistantes, rendant ainsi les antibiotiques inefficaces. Ainsi, en cette ère d'augmentation rapide de la résistance aux antibiotiques, une

avenue prometteuse est de développer des agents antimicrobiens capables de lutter contre les bactéries en ciblant des facteurs importants pour la virulence.

Ce projet de thèse visait à comprendre davantage la régulation des fimbriae de type 1 chez la souche UPEC CFT073. Plus précisément, l'objectif était d'identifier de nouveaux facteurs qui pourraient être impliqués dans la régulation de ces fimbriae dans une souche sauvage. Ainsi, nous désirions caractériser ces facteurs et leurs importances pour la virulence des souches UPEC. Enfin, ceci permettra de mieux comprendre les mécanismes moléculaires reliant l'expression de fimbriae type 1, les nouveaux régulateurs et la virulence. L'objectif global de ce projet permettra d'approfondir les connaissances par rapport à la régulation des fimbriae de type 1 et la virulence des souches UPEC.

2   REVUE DE LITTERATURE

2.1   *Escherichia coli,* une bactérie diversifiée et versatile

Le bacille *Bacterium coli commune* a été décrit pour la première fois en 1885 après avoir été isolé dans des selles de nourrissons par l'allemand Theodor Escherich comme une bactérie qui croît rapidement (Escherich, 1988).

Le genre *Escherichia,* ainsi que *Salmonella* ou encore *Shigella,* appartiennent à la famille des *Enterobacteriaceae*, qui regroupe des bacilles à coloration Gram négatif, non sporulés, aérobies-anaérobies facultatifs. Le genre *Escherichia* compte cinq espèces, les autres étant : *E. blattae*, *E. fergusonii*, *E. hermanii*, et *E. vulneris* (Freter *et al.*, 1983). Les souches d'*E. coli* sont actuellement subdivisées en huit groupes phylogénétiques principaux A, B1, B2, C, D, E F et Clade I (Clermont *et al.*, 2013).

E. coli est considéré comme un hôte normal de la microflore bactérienne du tractus digestif des humains ainsi que de celle de nombreux animaux à sang chaud. Il a la particularité de coloniser le tractus gastro-intestinal dans les premières heures de la vie où il vit en symbiose avec son hôte (Kaper *et al.*, 2004). Dans le tube digestif, les souches commensales *d'E. coli* sont localisées dans le gros intestin, en particulier dans le caecum et le côlon.

Ces souches commensales d'*E. coli,* manquant généralement des traits de virulence spécialisés, restent inoffensives dans la lumière intestinale et provoquent rarement des maladies, sauf chez les hôtes immunodéprimés ou lorsque les barrières gastro-intestinales normales sont brisées - comme dans le cas de la péritonite (Kaper *et al.*, 2004) .

La combinaison des antigènes de surface, à savoir lipopolysaccharidiques (antigène O), flagellaires (antigène H) et capsulaires (antigènes K), détermine plusieurs milliers de sérotypes en théorie (Ørskov & Ørskov, 1992). Un total de 181 antigènes O différents, chacun définissant un sérogroupe, sont actuellement reconnus (Liu *et al.*, 2020).

E. coli est une espèce bactérienne avec un génome présentant une forte plasticité. Il est important de noter que toutes les souches d'*E. coli* partagent un noyau de gènes (environ 1976 gènes) conservés entre elles, appelé le « core » génome (Hendrickson, 2009). Ce dernier encode les fonctions vitales de la cellule (Kaper *et al.*, 2004). L'ensemble des gènes de l'espèce *E. coli* constitue le pan-génome de cette espèce bactérienne où actuellement plus de 17838 gènes ont été répertoriés (Hendrickson, 2009; Van Elsas *et al.*, 2011). Il est à noter que 39,2 % des protéines produites par la souche commensale *E. coli* K-12 MG1655 sont conservées chez les souches

intestinales EDL933 et urinaires CFT073 (Welch *et al.*, 2002). De plus, les souches pathogènes possèdent plusieurs gènes, absents chez les souches commensales, codant pour des facteurs de virulence permettant à la bactérie de coloniser un plus grand nombre de sites. Ces gènes sont localisés soit sur des plasmides ou sur des îlots de pathogénicité (Dobrindt, 2005; Hacker & Kaper, 2000; Kaper *et al.*, 2004).

D'un point de vue génétique et clinique, les souches d'*E. coli* peuvent être classées comme : souches commensales ou souches pathogènes capables de tuer plus de 2 millions de personnes par an. Ces pathogènes sont associés à des infections intra-intestinales (InPEC : Intestinal Pathogenic *E. coli*) ou extra-intestinales (ExPEC : Extraintestinal Pathogenic *E. coli*) (Tenaillon *et al.*, 2010).

Sur la base des modes d'interactions hôte / bactérie et des signes cliniques de l'infection, les souches sont classées en « pathovars » ou « pathotypes » (Croxen *et al.*, 2013; Pohl, 1993). Ces souches sont hautement adaptées et elles ont acquis des attributs de virulence spécifique, qui leur confèrent une grande capacité d'adaptation à des nouvelles niches et leur permet de causer un large spectre de maladies. Un pathotype est un groupe de souches provenant d'une seule espèce causant une même maladie en utilisant un ensemble commun de facteurs de virulence (Kaper *et al.*, 2004).

2.1.1 Les *E. coli* pathogènes intestinaux

Les pathotypes faisant partie de cette famille causent différents types de maladies entériques (diarrhées) (Fig. 2.1). Les souches responsables de ce type d'infection ont en commun de se multiplier dans l'intestin de leur hôte.

Les maladies diarrhéiques entraînent une forte mortalité dans le monde, en particulier chez les enfants de moins de 5 ans et notamment dans les pays d'Afrique subsaharienne et d'Asie du Sud, où les enfants souffrent de nombreux décès liés à la diarrhée (Kotloff *et al.*, 2013).

Les *E. coli* entériques font partie de la flore naturelle de nombreux animaux. Les infections chez les humains se produisent par la consommation de produits alimentaires, d'eau contaminée par des déchets de sources animales ou humaines, ou par la propagation directe de personne à personne en raison d'une mauvaise hygiène (Clements *et al.*, 2012).

Ce premier groupe de pathogène est subdivisé en sept pathovars majeurs : les EPEC (*E. coli* entéropathogènes), les ETEC (*E. coli* entérotoxinogènes), les EAEC (*E. coli* entéroagrégatifs),

les DAEC (*E. coli* à adhérence diffuse), les EHEC (*E. coli* entérohémorragiques), les EIEC (*E. coli* entéroinvasifs) et les *E. coli* entéroagregatifs-hémorragiques (EAHEC).
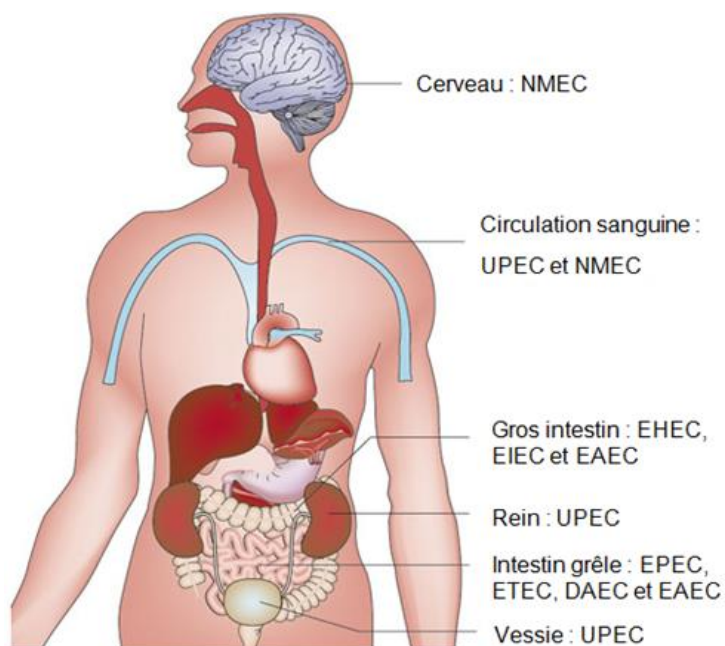
Figure 2.1. Les différents pathotypes d'*E. coli* et leurs sites de colonisations

Les EPEC, les ETEC et les DAEC colonisent l'intestin et sont à l'origine de diarrhées, les EHEC et les EIEC colonisent plutôt le côlon, tandis que les EAEC peuvent coloniser les deux sites. Les UPEC colonisent le tractus urinaire jusqu'à la vessie et peuvent remonter jusqu'aux reins et entraîner une pyélonéphrite. Les NMEC sont à l'origine de méningites néonatales (NMEC). Adapté de Croxen and Finlay (2010).

Les *E. coli* entéropathogènes (EPEC)

Les infections gastro-intestinales restent une cause majeure de morbidité et de mortalité dans la population pédiatrique dans le monde entier. Parmi eux, les infections à EPEC présentent une cause majeure de diarrhée infantile chez les nourrissons âgés de 0 - 11 mois, et sévissent surtout dans les pays en voie de développement (Kaper *et al.*, 2004; Kotloff *et al.*, 2013).

Les EPEC sont non invasifs et provoquent des lésions intestinales appelées lésions d'attachement et d'effacement (A/E) (Croxen *et al.*, 2013), caractérisées par l'adhérence spécifique de la bactérie à la cellule épithéliale intestinale (Fig. 2.2), l'effacement des microvillosités intestinales, le réarrangement du cytosquelette de la cellule infectée, et la

formation d'une structure en piédestal formée de diverses fibres du cytosquelette, dont l'actine (Neves et *al.*, 1998). La plupart des éléments responsables du phénotype A/E sont contenus sur un îlot de pathogénicité de 35 kb appelé locus d'effacement des entérocytes (Locus of Enterocytes Effacement, LEE) (McDaniel *et al.*, 1995).

Les *E. coli* entérotoxinogènes (ETEC)

Les *E. coli* entérotoxinogènes provoquent des diarrhées aqueuses aiguës chez les enfants de moins de 3 ans dans les pays en développement et sont également une cause majeure de diarrhée du voyageur à destination de pays en développement (Nataro & Kaper, 1998). Les diarrhées aqueuses varient de modérées à sévères, sont peu fébriles et associées à des nausées et à des crampes abdominales (Croxen *et al.*, 2013). Ces bactéries sont aussi responsables de diarrhées chez d'autres espèces animales, en particulier le veau et le mouton (diarrhée néonatale), le porc (diarrhée néonatale et après sevrage, maladie de l'œdème en combinaison avec des STEC) et le chien (diarrhée) (Gyles et Fairbrother, 2004). Après adhésion à la muqueuse intestinale, les ETEC sont capables de produire une ou plusieurs entérotoxines (Fig. 2.2), soit la toxine thermolabile LT (heat-labile enterotoxin), soit les toxines thermostables STa et / ou STb (heat-stable enterotoxin) (Levine, 1987; Nataro & Kaper, 1998). Ces toxines stimulent la sécrétion de fluide intestinal et amènent ainsi l'apparition de diarrhée (Dubreuil, 1999).

Les *E. coli* entérohémorragiques (EHEC)

L'ensemble des souches d'*E. coli* possédant au moins un gène *stx* (*Shiga-like toxin*) (Fig. 2.2) représente le groupe des STEC (Shiga-toxin-producing *E. coli*) précédemment appelé VTEC (verotoxin-producing *E. coli*) selon l'ancienne dénomination internationale. Il est important de souligner que tandis que tous les EHEC sont des STEC, tous les STEC ne sont pas nécessairement responsables d'infection ni isolés de cas cliniques (Levine, 1987).

Les infections causées par les EHEC constituent un problème majeur de santé publique en raison de l'extrême sévérité des manifestations cliniques telles que le Syndrome Hémolytique et Urémique (SHU) ou le Purpura Thrombotique et Thrombocytopénique (PTT) qui peuvent mener à la mort du patient ou occasionner des graves séquelles (Zhou *et al.*, 2010), principalement chez les jeunes enfants et chez les personnes âgées. Le principal réservoir d'EHEC est le tractus intestinal bovin et les premiers foyers ont été associés à la consommation de hamburgers insuffisamment cuits (Kaper *et al.*, 2004).

Le sérotype d'EHEC le plus fréquemment mis en cause lors d'infections sporadiques ou d'épidémies est *E. coli* O157: H7 (Gerber *et al.*, 2002). Ce sérotype a la capacité d'induire des

lésions A/E (Fig. 2.2) en adhérant intimement à la paroi intestinale (Ebel *et al.*, 1998), comme le font les EPEC. Les gènes nécessaires à l'induction des lésions A/E sont aussi contenus sur le LEE et sont, pour la plupart, homologues à ceux retrouvés chez les EPEC. Outre chez l'humain, les STEC sont aussi responsables de désordres intestinaux chez le veau (Dean-Nystrom *et al.*, 2003).

Les *E. coli* entéroinvasifs (EIEC)

Les *E. coli* entéroinvasifs présentent de nombreuses similarités avec les shigelles et partagent plusieurs facteurs de virulence. Les EIEC ne sont différenciables de *Shigella* que par des caractéristiques biochimiques (Kaper *et al.*, 2004). Ces souches ont la capacité d'envahir la muqueuse colique et de produire des toxines de type Shigelle (Fig. 2.2), provoquant ainsi des syndromes dysentériques (forte fièvre, crampes abdominales, nausées et diarrhées aqueuses) qui évoluent rapidement en une dysenterie (selles contenant du sang et du mucus) (Croxen & Finlay, 2010). Les EIEC possèdent divers facteurs de virulence, dont des invasines et des entérotoxines (Nataro & Kaper, 1998). La phase précoce de la pathogenèse comprend l'internalisation par des cellules épithéliales, suivie de la lyse de la vacuole endocytaire et la multiplication intracellulaire. Puis les bactéries induisent la polymérisation de l'actine cellulaire à un de leur pôle, permettant ainsi leur dissémination aux cellules épithéliales adjacentes (Kaper *et al.*, 2004).

Les *E. coli* à adhérence diffuse (DAEC)

Les *E. coli* à adhérence diffuse sont responsables de diarrhées, en particulier chez les enfants de plus de 12 mois. *In vitro*, les DAEC adhèrent aux cellules épithéliales HEp-2 et HeLa de façon uniforme (adhésion diffuse) (Fig. 2.2). Cette capacité est due à l'expression d'adhésines codées par les opérons *afa/dra/daa*. Ces adhésines peuvent être fimbriaires (Dr et F1845) ou non-fimbriaires (Afa) et sont toutes de la famille Afa/Dr (Servin, 2005). Environ 75% des souches DAEC produisent une adhésine appelée F1845 ou adhésine connexe (Nataro & Kaper, 1998). Les souches DAEC produisent un effet cytopathique caractérisé par la formation de grandes extensions cellulaires qui s'enroulent autour de la bactérie (Bernet-Camard *et al.*, 1996). D'autres facteurs de virulence pourraient être impliqués dans le pouvoir pathogène, en particulier en induisant une inflammation intestinale (Kaper *et al.*, 2004).
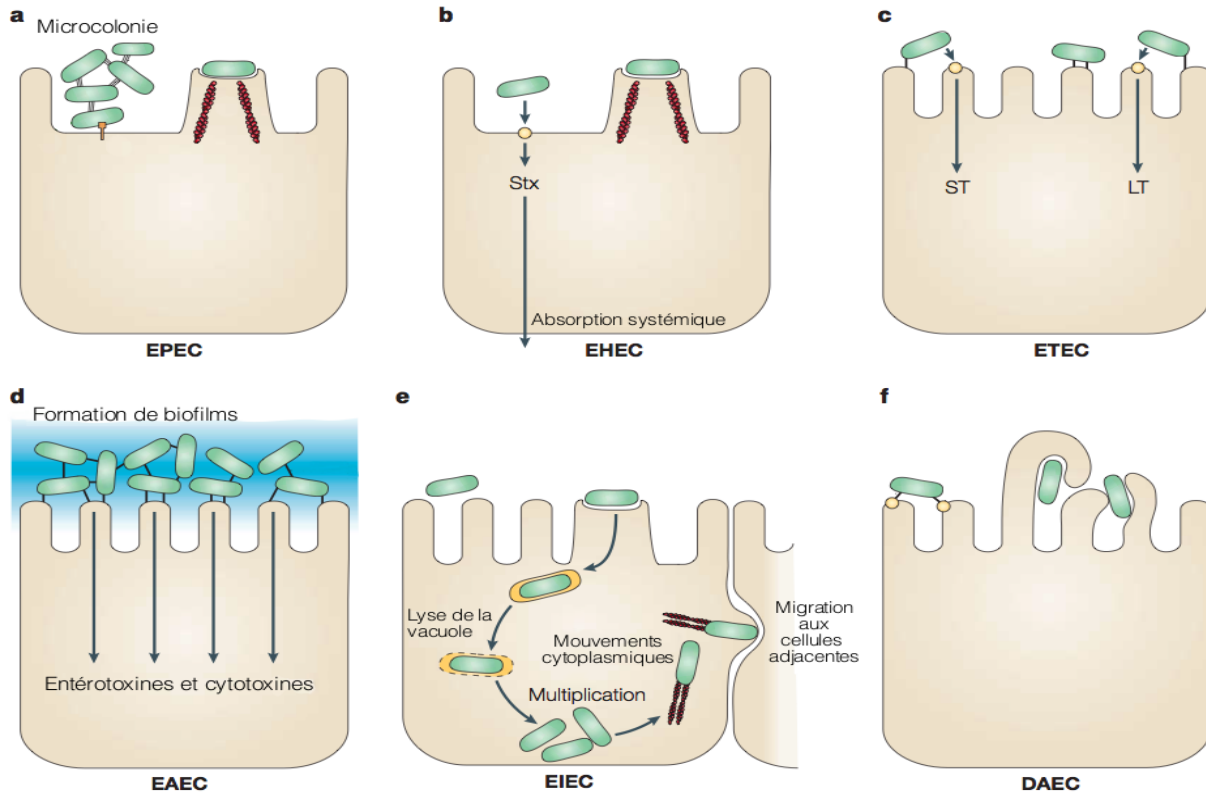
Figure 2.2. Schéma pathogénique des _E. coli_ de la famille des InPEC

Les six pathotypes de la famille des InPEC interagissent différemment avec les cellules de l'hôte. Ces interactions sont schématisées ici. a) Les EPEC adhèrent aux entérocytes de l'intestin grêle, en formant des microcolonies et en détruisant les microvillosités, induisant des lésions d'attachements et d'effacement. Les dérangements cytosquelettiques s'accompagnent d'une réponse inflammatoire et de diarrhée. b) Les EHEC forment aussi un piédestal et détruisent les microvillosités en induisant également des lésions d'attachements et d'effacement. De plus, ils produisent la Shiga toxine, dont l'absorption systémique entraîne des complications potentiellement mortelles. c) Les ETEC adhèrent aux entérocytes de l'intestin grêle et produisent deux entérotoxines (ST et LT) qui induisent une diarrhée aqueuse. d) Les EAEC adhèrent aux épithéliums de l'intestin, forment des biofilms et sécrètent des entérotoxines et cytotoxines. e) Les EIEC envahissent la cellule hôte et induisent une réponse inflammatoire destructrice. Les bactéries peuvent se déplacer latéralement à travers l'épithélium par propagation directe de cellule à cellule ou peuvent sortir et rentrer dans la membrane plasmique baso-latérale. f) Les DAEC induisent la croissance des projections cellulaires en forme de doigts qui enveloppent les bactéries. Adaptée de Kaper _et al._ (2004).

Les _E. coli_ entéroagrégatifs (EAEC)

Les EAEC sont de plus en plus reconnus comme une cause de diarrhées persistantes chez les enfants et les adultes dans les pays en développement et développés, et ont été identifiés comme étant la cause de plusieurs foyers à travers le monde (Nataro & Kaper, 1998). À l'heure actuelle,

les EAEC sont définis comme des *E. coli* qui ne sécrètent pas d'entérotoxines et qui sont caractérisés par une adhérence agrégative aux cellules HEp-2 (Fig. 2.2) (Nataro & Kaper, 1998; Nataro *et al.*, 1987). Les bactéries adhèrent les unes aux autres en formant des " briques empilées ", qui sont à l'origine de nécroses du pôle apical des villosités avec œdème inflammatoire et hémorragique de la sous muqueuse (Nataro & Kaper, 1998).

Les *E. coli* entéroagrégatifs-hémorragiques (EAHEC)

L'épidémie due à une souche d'*E. coli* O104:H4 en Allemagne ainsi qu'en France en 2011 se distingue particulièrement du fait de la souche impliquée. En effet, cette souche épidémique appartenait au sérotype O104:H4 et possédait le gène *stx2* qui code la Shiga-toxine de type 2, caractéristique typique des EHEC (Brzuszkiewicz *et al.*, 2011). Cette souche présentait un profil de multi-résistance aux antibiotiques grâce à un plasmide codant pour des β-lactamases à spectre étendu (ESBL). Elle ne possédait pas le gène *eae* mais portait le gène *aggR* présent sur le plasmide pAA caractéristique des EAEC et n'aurait donc pas la même origine clonale que les autres EHEC. La souche épidémique de l'Allemagne combine des caractéristiques génomiques uniques des EHEC et des EAEC. Cela suggère que cette souche représente un nouveau pathotype émergeant appelé Entero-Aggregative-Haemorrhagic *Escherichia coli* (EAHEC) (Brzuszkiewicz *et al.*, 2011).

2.1.2   Les *E. coli* pathogènes extra-intestinaux

Les souches ExPEC, comme les souches commensales, colonisent le tractus digestif sans causer d'infection, mais elles ont la capacité de causer des maladies chez les humains et les animaux si elles se retrouvent dans un autre site, comme le sang, le système nerveux central ou encore le tractus urinaire (Wiles *et al.*, 2008b). Les ExPEC sont des pathogènes opportunistes, c'est-à-dire qu'ils peuvent être retrouvés dans les selles des sujets sains avec une fréquence variable selon les individus et les populations humaines étudiées (Nataro & Kaper, 1998).

Les animaux sont reconnus comme réservoirs d'*E. coli* pathogène intestinal humain, cependant l'hypothèse selon laquelle les animaux sont à l'origine des ExPEC humains reste encore un sujet de débat. Bien qu'il soit difficile de retracer la source des ExPEC causant des infections humaines, il est possible que les ExPEC provenant d'animaux puissent contaminer les humains. En effet, les ExPEC sont répandus dans les réservoirs animaux, où ils provoquent également des maladies (Bélanger *et al.*, 2011). Plusieurs rapports ont démontré des similitudes entre les diverses souches d'ExPEC ; les origines phylogénétiques communes des souches isolées chez l'homme et l'animal, ainsi que leur flexibilité génomique soulèvent des inquiétudes quant au potentiel des

ExPEC de causer des zoonoses (Brzuszkiewicz *et al.*, 2009). Les réservoirs animaux des ExPEC pourraient être à l'origine d'infections, mais aussi propager la résistance aux antimicrobiens, augmentant ainsi le risque d'incidence des infections humaines et compliquant leur traitement.

Les ExPEC comprennent des souches à l'origine d'infection du tractus urinaire (UPEC : uropathogenic *E. coli*), de méningites (NMEC : neonatal meningitis associated *E. coli*) et de septicémies (SePEC) (Fig. 2.1), ou de nécroses (NTEC : necrotoxigenic *E. coli*). Par ailleurs, il existe également des souches ExPEC associées à des infections chez les animaux en particulier chez les volailles appelées APEC (avian pathogenic *E. coli*) (Kaper *et al.*, 2004). Les ExPEC appartiennent principalement aux groupes phylogénétiques B2 et D (Picard *et al.*, 1999)

Les *E. coli* de la méningite néonatale (NMEC)

Enfin, le pronostic des méningites néonatales, bien que rares, est très défavorables. *E. coli* est l'une des deux principales causes de méningite néonatale (avec streptocoque du groupe B), provoquant 20-40% de mortalité, dont 400 cas par an aux États-Unis, et 33% à 50% des survivants développent des séquelles neurologiques (de Louvois, 1994). Environ 80% des isolats de méningite néonatale possèdent une capsule polysaccharidique K1 (Kaper *et al.*, 2004) et la plupart de ces isolats K1 sont présents dans les sérogroupes comme O18, O7, O16, O1 et O45 (Bonacorsi *et al.*, 2003).

Actuellement, les streptocoques du groupe B et les *E. coli* représentent entre 70% et 80% des cas de méningite bactérienne néonatale dans les pays industrialisés (May *et al.*, 2005). Dans les pays en développement, les méningites à streptocoque du groupe B sont beaucoup moins fréquentes que les formes dues à des entérobactéries. Chaque année, dans les pays en développement, environ 50 000 nouveau-nés meurent de méningite (taux de mortalité de 40%).

L'infection du nouveau-né débute par la colonisation du tractus intestinal de l'enfant suite à l'acquisition du pathogène du liquide amniotique ou de la flore vaginale de la mère (Watt *et al.*, 2003). Par la suite, il y a translocation bactérienne du lumen intestinal à la circulation sanguine, passage à travers la barrière hémato-encéphalique et invasion de l'espace arachnoïde (Bonacorsi & Bingen, 2005). Afin d'infecter les nouveau-nés, les *E. coli* doivent pouvoir s'adapter dans diverses niches écologiques. En premier, les conditions physico-chimiques particulières de la cavité vaginale, qui diffèrent considérablement de celles du tractus intestinal. En second lieu, les bactéries doivent traverser le col cervical et survivre dans le liquide amniotique. Enfin, les bactéries peuvent être soumises à une forte pression de sélection par ces conditions avant de générer la septicémie et la méningite néonatale (Watt *et al.*, 2003).

L'antigène capsulaire K1, l'alpha-hémolysine, les systèmes d'acquisition de fer (comme le sidérophore aérobactine), les adhésines (fimbriae F1C, P, et S), la protéine de la membrane externe OmpA, la protéine IbeA et la toxine CNF1 (le facteur nécrosant cytotoxique 1) sont considérés comme les principaux facteurs de virulence liés à la pathogénicité des NMEC (Bingen *et al.*, 1997; Bingen *et al.*, 1998).

Les *E. coli* pathogènes aviaires (APEC)

Les *E. coli* aviaires représentent à l'heure actuelle l'une des plus importantes causes de pertes économiques dans l'industrie de la volaille dans le monde et constituent aussi l'un des motifs de saisie les plus fréquents à l'abattoir (Bélanger *et al.*, 2011).

Ils sont présents dans la flore intestinale des oiseaux sains et la plupart des pathologies qui leur sont associées sont secondaires à l'action de facteurs prédisposants (Dho-Moulin & Fairbrother, 1999). La maladie commence comme une infection des voies respiratoires, conduisant à une infection systémique des organes internes avec une septicémie qui s'installe. Les animaux s'infectent en respirant des particules fécales contaminées par les APEC (présentent naturellement dans la flore intestinale de la volaille), qui sont contenues dans la poussière (La Ragione *et al.*, 2002; Antao *et al.*, 2008).

Les APEC sont associées à plusieurs infections et syndromes chez la volaille, tels que les infections de la membrane vitelline des œufs, le syndrome de la tête enflée, la salpingite, la péritonite, la cellulite aviaire et la colibacillose aviaire dont les lésions et les manifestations peuvent être variables suivant l'âge de l'animal (Dho-Moulin & Fairbrother, 1999; La Ragione & Woodward, 2002). Les souches APEC appartiennent généralement à trois sérogroupes, O1, O2 et O78, bien que de nombreux sérogroupes différents aient été identifiés chez les APEC et les trois sérogroupes ne sont pas toujours prédominants dans certaines études (Ewers *et al.*, 2007).

Les principaux facteurs de virulences associés aux APEC sont : les fimbriae de type P et de type 1 (Kariyawasam & Nolan, 2009; La Ragione *et al.*, 2000), la capsule K1(Mellata *et al.*, 2003), l'autotransporteur hémagglutinine sensible à la température (*tsh*) (Dozois *et al.*, 2000), l'aérobactine (*iucD*) (Gao *et al.*, 2015), les salmochelines (*iroN*) (Caza *et al.*, 2008), la protéine de résistance au sérum (*iss*) (Nolan *et al.*, 2003), la protéine de transfert (*traT*), et l'opéron ColV retrouvés sur les plasmides R et ColV (Stordeur & Mainil, 2002).

Les APEC partagent des similarités avec les ExPEC d'origine humaine (Ewers *et al.*, 2007). Bien qu'il soit difficile de retracer l'origine des ExPEC provoquant des infections humaines, il est possible que les ExPEC affectant les humains auraient une origine aviaire (Bélanger *et al.*, 2011).

Les *E. coli* uropathogènes

L'appareil urinaire est parmi les sites les plus courants de l'infection bactérienne et *E. coli* est l'agent infectieux le plus commun à ce site. Les *E. coli* qui provoquent une cystite, une pyélonéphrite aiguë et une urosepticémie font partie des souches commensales d'*E. coli* qui constituent la majeure partie du genre *Escherichia* peuplant la partie inférieure du côlon de l'être humain (Kaper *et al.*, 2004).

Parmi les ExPEC, les souches UPEC sont le plus souvent associées aux infections humaines. L'agent causal le plus fréquemment isolé lors des ITU simples (75%) et complexes (65%) est l'UPEC (Flores-Mireles *et al.*, 2015a), et ce sont seulement six sous-groupes « O » qui provoquent 75% des ITU (Manges *et al.*, 2001). Les UPEC ont la capacité de coloniser le tractus urinaire humain et sont responsables de cystites (non compliquées, compliquées et récurrentes), de pyélonéphrites et d'urosepticémies (Kaper *et al.*, 2004; Russo & Johnson, 2003).

La flore fécale des humains et des animaux est considérée comme un réservoir des UPEC. Les souches UPEC isolées chez les chiens, les chats et les humains sont dans certains cas phylogénétiquement étroitement liées (Johnson *et al.*, 2008). De plus, ces souches peuvent franchir la barrière des espèces et coloniser les humains ainsi que les animaux de compagnie tels que les chiens et les chats.

2.2 Les infections du tractus urinaire

2.2.1 Site d'infection

Les voies urinaires peuvent être divisées en voies urinaires supérieures et inférieures. Les voies urinaires supérieures se composent des reins et des uretères, et les voies urinaires inférieures se composent de la vessie et de l'urètre (Fig. 2.3). Ce dernier est une porte de sortie de l'urine, mais permet également l'entrée de microbes, y compris des agents pathogènes, dans les voies urinaires. En effet, les bactéries vivent autour de l'ouverture urétrale chez les humains et colonisent fréquemment l'urine dans l'urètre, mais sont éjectées avec l'urine pendant la miction (Foxman, 2010).

Les ITU se produisent dans l'une ou l'autre partie des voies urinaires, mais le plus souvent, les ITU surviennent lorsque des bactéries colonisant le tractus gastro-intestinal accèdent à l'urètre et remontent jusqu'à la vessie (Foxman & Brown, 2003).

L'urètre est plus court chez les femmes permettant aux bactéries d'atteindre plus aisément la vessie avant d'être éliminées par miction. En outre, l'ouverture urétrale chez la femme est proche

de la cavité vaginale et du rectum, qui abritent de grandes communautés bactériennes (Kaper *et al.*, 2004; Foxman & Brown, 2003). Les manipulations urogénitales associées aux activités de la vie quotidienne et aux interventions médicales facilitent le déplacement des bactéries de la cavité vaginale, de l'ouverture rectale et de la zone péri-urétrale dans l'urètre. Cependant, même si les bactéries atteignent la vessie et se multiplient en nombre significatif, la colonisation bactérienne ne provoque que rarement des symptômes. Par conséquent, les ITU sont parmi les infections bactériennes les plus courantes (Foxman, 2010).

2.2.2   Les infections du tractus urinaire (ITU)

Les ITU sont classées cliniquement comme simples (non compliquées) ou compliquées. Les ITU non compliquées affectent généralement les individus en bonne santé et qui ne présentent aucune anomalie structurale ou fonctionnelle des voies urinaires. Ces infections se manifestent chez une personne qui n'est pas enceinte ou qui n'a pas été cathétérisée (Foxman, 2014; Hannan *et al.*, 2012). Ces infections se différencient en ITU inférieures (cystite) et en ITU supérieures (pyélonéphrite) (Hooton, 2012). Plusieurs facteurs de risque sont associés à la cystite, notamment le sexe féminin, une infection urinaire antérieure, l'activité sexuelle, l'infection vaginale, le diabète, l'obésité et la susceptibilité génétique (Foxman, 2014; Hannan *et al.*, 2012).

Les ITU compliquées sont des infections urinaires associées à des facteurs qui compromettent les voies urinaires ou la défense de l'hôte et augmentent le risque d'échec du traitement. Ces facteurs comprennent la présence de corps étrangers (calculs et des cathéters), l'obstruction urinaire, la rétention urinaire causée par une maladie neurologique, l'insuffisance rénale, la transplantation rénale, l'immunosuppression et la grossesse (Lichtenberger & Hooton, 2008).

Les ITU sont diagnostiquées à l'aide d'une combinaison de symptômes urinaires et d'une culture d'urine démontrant le nombre d'un uropathogène connu au-dessus d'un seuil donné avec la présence de neutrophiles (généralement défini comme > 10^5 CFU/ml d'urine, mais des seuils aussi bas que 100 CFU/ml et jusqu'à 100 000 CFU/ml sont également utilisés) (Rubin *et al.*, 1992).

La présence de bactéries dans l'urine, sans signes cliniques d'ITU, est appelée *stricto sensu* « bactériurie asymptomatique » et est la forme la plus bénigne de colonisation par *E. coli* dans les voies urinaires. Par conséquent, les symptômes urinaires et la bactériurie surviennent le plus souvent indépendamment les uns des autres. Par ailleurs, les cultures d'urine sont négatives chez près de 20% des femmes présentant des symptômes d'ITU classiques. Ainsi, un nombre

important de bactéries se trouvent souvent dans l'urine d'individus en santé (Ferry *et al.*, 2007; Foxman, 2010).

La prévalence globale de la bactériurie asymptomatique chez les femmes est de 3,5%, mais elle est beaucoup plus élevée après les rapports sexuels (Evans *et al.*, 1978). Chez les hommes comme chez les femmes, la prévalence de la bactériurie asymptomatique augmente avec l'âge. Bien que la bactériurie asymptomatique augmente le risque d'ITU symptomatique, elle ne doit pas être traitée sauf chez les femmes enceintes ou chez les personnes subissant des procédures génito-urinaires (Foxman, 2010).

Les ITU sont causées à la fois par des bactéries à Gram négatif et à Gram positif, ainsi que par certains champignons. Cependant, la maladie est principalement causée par les UPEC. Plusieurs espèces bactériennes ont été isolées des ITU, y compris *Klebsiella pneumoniae* (environ 7%)*, Proteus mirabilis* (environ 5%), *Staphylococcus saprophyticus, Enterococcus faecalis, Streptococcus* du groupe B, *Pseudomonas aeruginosa, Staphylococcus aureus* et des levures *Candida* spp (pour le pourcentage restant) (Foxman, 2014; Nielubowicz & Mobley, 2010). Plusieurs de ces espèces ont montré des niveaux croissants de résistance aux antibiotiques couramment utilisés pour traiter ces infections (Tabibian *et al.*, 2008).

Les ITU affectent 150 millions de personnes chaque année dans le monde. En 2007, aux États-Unis seulement, on estimait le nombre à 10,5 millions de visites pour les symptômes à ITU (2 - 3 millions de visites aux services d'urgence). Aux États-Unis, les coûts annuels estimés de ces infections sont d'environ 5 milliards de $ (Flores-Mireles *et al.*, 2015a; Foxman, 2010; Foxman, 2014; Schappert & Rechtsteiner, 2011). Les taux d'incidence sont quatre fois plus élevés chez les femmes que chez les hommes, et environ un quart de ces femmes affectées souffriront d'une ITU récurrente (défini comme trois ITU ou plus sur une période de 12 mois) dans les 6 à 12 mois (Epp *et al.*, 2010).

 Pour traiter les ITU récurrentes, ces femmes sont soumises à une antibiothérapie fréquente au moment où les symptômes apparaissent ou immédiatement après un rapport sexuel (Hooton, 2012). Les personnes particulièrement sensibles aux ITU comprennent les femmes enceintes et ménopausées, les patients subissant un cathétérisme urétral, et les personnes atteintes de diabète (Griebling, 2007). Également, les enfants prépubères sont sensibles à la cystite récurrente et chronique (Foxman & Brown, 2003). La pyélonéphrite aiguë chez l'adulte entraîne une hospitalisation de 10% à 30% des patients avec des coûts estimés à 2,9 milliards de dollars en 2013 (Foxman, 2014). Ces infections sont responsables d'une morbidité significative entraînant une grave détérioration de la qualité de vie, notamment: douleur, inconfort,

perturbation des activités quotidiennes et peu d'options de traitement autres que la prophylaxie antibiotique à long terme (Foxman, 2014; Foxman & Brown, 2003). Cependant, les ITU deviennent de plus en plus difficiles à traiter en raison de l'émergence rapide de la résistance aux antibiotiques chez les bactéries, y compris les UPEC.

2.2.3   Physiopathologie des infections à UPEC

Le tractus gastro-intestinal est considéré comme le principal réservoir des UPEC chez l'homme (Wiles *et al.*, 2008a). L'infection commence lorsque les UPEC qui résident dans le tractus gastro-intestinal contaminent la région périurétrale, puis d'une façon ascendante la colonisation de l'urètre et la migration ultérieure de l'agent pathogène à la vessie (Fig. 2.3) (Flores-Mireles *et al.*, 2015a). Les UPEC peuvent aussi arriver au système urinaire de l'environnement ou par une transmission entre individus. Par la suite, l'UPEC migre dans la lumière de la vessie où elle envahit l'épithélium de la vessie. Plusieurs adhésines bactériennes reconnaissent les récepteurs sur l'épithélium de la vessie (uroépithélium) et médient la colonisation.

Le cycle infectieux est complexe impliquant : a) colonisation des zones périurétrale et vaginale par les UPEC puis colonisation de l'urètre; (b) ascension dans la lumière de la vessie et croissance sous forme de cellules planctoniques dans l'urine; (c) adhérence à la surface et interaction avec le système de défense de l'épithélium de la vessie; (d) formation de biofilm; (e) invasion et réplication en formant des communautés bactériennes intracellulaires (IBC) où des réservoirs intracellulaires au repos (réservoir quiescent) se forment et résident dans l'urothélium sous-jacent; (f) colonisation des reins et lésions tissulaires de l'hôte avec risque accru de bactériémie/septicémie (Andersen *et al.*, 2012; Terlizzi *et al.*, 2017).

Les UPEC ont la capacité de se lier directement à l'épithélium de la vessie, qui est composé des cellules superficielles en forme de parapluie, des cellules intermédiaires et des cellules basales. En effet, le nouvel environnement de la vessie favorise l'expression des fimbriae de type 1, qui ont un rôle important dans le développement précoce d'une infection urinaire (Gunther *et al.*, 2002). Ces fimbriae reconnaissent des résidus mannosylés, appelés uroplakines, qui sont les principaux composants protéiques de la membrane apicale des cellules parapluie (Khandelwal *et al.*, 2009). En plus des uroplakines, les intégrines α3β1 des cellules moins différenciées des couches sous-jacentes, qui sont exprimées à la surface des cellules uroépithéliales, peuvent également servir de récepteurs pour les UPEC (Eto *et al.*, 2007). Les intégrines sont des molécules d'adhésion de surface qui relient les protéines de la matrice extracellulaire au cytosquelette d'actine. Suite à la colonisation de la vessie, les UPEC provoquent une cystite (Fig.

2.3), qui est généralement associée à des symptômes classiques d'ITU, qui sont, la sensation de douleurs au moment d'uriner, ce qui rend la miction douloureuse et difficile, l'impression d'avoir un besoin urgent et fréquent d'uriner sans en être capable, ainsi qu'une pyurie (leucocytes dans l'urine) (Flores-Mireles *et al.*, 2015a; Scholes *et al.*, 2005). Si les infections ne sont pas traitées, les UPEC peuvent passer de la vessie, à travers les uretères vers le rein, pour provoquer la pyélonéphrite, avec la possibilité de provoquer des lésions rénales irréversibles et parfois la mort (Scholes *et al.*, 2005). La pyélonéphrite se distingue cliniquement de la cystite par la présence de douleurs aux flancs, de fièvre et de nausées (Grabe *et al.*, 2015). Les ITU symptomatiques sont traitées par antibiotiques, mais jusqu'à 25% subiront une récidive de l'infection dans les 6 mois suivant le traitement des infections urinaires initiales (Foxman, 2014).

Les cellules épithéliales de la vessie alertent non seulement le système immunitaire pendant l'infection, mais interviennent également directement dans la clairance bactérienne en sécrétant des composés antimicrobiens dans l'urine et en expulsant les bactéries envahissantes dans la lumière de la vessie pour réduire la charge intracellulaire (Abraham & Miao, 2015).

Pour atteindre le système urinaire haut, les UPEC doivent se détacher de l'épithélium. À ce stade, le système de production de fimbriae de type 1 est régulé négativement, les bactéries peuvent être libérées et donc migrer de façon ascendante (Gunther *et al.*, 2002). Une fois au niveau des reins (Fig. 2.3), la bactérie se fixe, grâce à la production des fimbriae qui reconnaissent des récepteurs digalactoside exprimés à la surface de l'épithélium rénal (Korhonen *et al.*, 1986). Une fois le rein atteint, la production de toxines telles l'hémolysine et Sat, des composants bactériens comme le lipopolysaccharide (LPS), déclenchent une pyélonéphrite. Tout comme la cystite, si la pyélonéphrite n'est pas traitée, l'infection évoluera puisque les bactéries détruiront les reins, et sont capables de traverser la paroi des tubules proximaux ainsi que les cellules endothéliales. Ensuite, les bactéries pénètrent dans la circulation sanguine et déclenchent une bactériémie pouvant évoluer en septicémie (Kaper *et al.*, 2004).
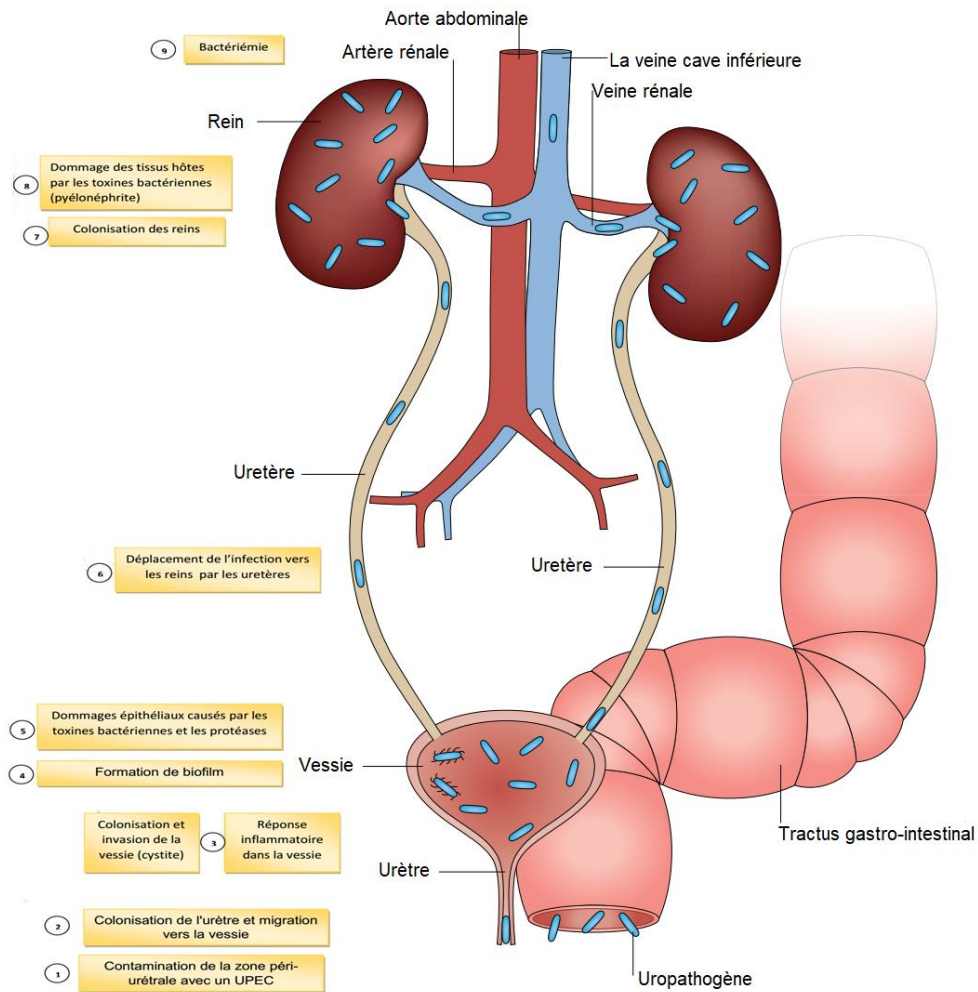
Figure 2.3. Représentation des étapes d'une infection du tractus urinaire

Les ITU non compliquées commencent lorsque les uropathogènes qui résident dans l'intestin contaminent la région périurétrale (Étape 1) et sont capables de coloniser l'urètre. La migration subséquente vers la vessie (étape 2) et l'expression de fimbriae et d'adhésines conduit à la colonisation et à l'invasion des cellules de la vessie (étape 3). Les réponses inflammatoires de l'hôte, y compris l'infiltration de neutrophiles, commencent à éliminer les bactéries extracellulaires. Certaines bactéries échappent au système immunitaire, soit par invasion des cellules de l'hôte, soit par des modifications morphologiques qui entraînent une résistance aux neutrophiles, et ces bactéries subissent une multiplication et forment un biofilm (étape 4). Ces bactéries produisent des toxines et des protéases qui induisent des lésions des cellules de l'hôte (étape 5), libérant des nutriments essentiels qui favorisent la survie bactérienne et l'ascension vers les reins (étape 6). La colonisation du rein (étape 7) entraîne une production de toxine bactérienne et des lésions tissulaires de l'hôte (étape 8). Si elles ne sont pas traitées, les ITU peuvent progresser vers la bactériémie si le pathogène traverse la barrière épithéliale tubulaire dans les reins (étape 9). Figure adaptée de Klein and Hultgren (2020).

2.2.4 Cycle d'infection de la vessie

Au cours du cycle infectieux intracellulaire, les UPEC subissent divers changements morphologiques entraînant un phénotype filamenteux, ce qui contribue à leur survie et à la pathogenèse des ITU.

Attachement des bactéries et invasion des cellules de l'hôte

En raison de la présence d'urine, qui représente un milieu de croissance, les bactéries prolifèrent dans un laps de temps relativement court. Cependant, la miction constitue une ligne de défense de l'hôte qui élimine la majorité des bactéries qui accèdent à la lumière de la vessie. Pour persister dans la vessie malgré le flux urinaire, les bactéries sont capables de se lier étroitement aux cellules épithéliales qui tapissent la vessie en utilisant des fimbriae (Fig. 2.3) (Mulvey, 2002).

Les fimbriae de type 1 reconnaissent les récepteurs glycoprotéiques de l'hôte contenant du mannose comme les uroplakines mannosylées sur la surface luminale de l'épithélium de la vessie via l'adhésine FimH (Welch *et al.*, 2002). L'interaction FimH-récepteur déclenche alors une cascade de signalisation qui active les GTPases de la famille Rho (Martinez & Hultgren, 2002), entraînant des réarrangements dynamiques du cytosquelette qui permettront l'enveloppement et l'invasion des bactéries attachées (Mulvey *et al.*, 1998). Ce réarrangement d'actine formera des protrusions qui envelopperont les bactéries. Celles-ci se retrouveront dans des vacuoles ressemblant aux endosomes tardifs (Eto *et al.*, 2007). À l'intérieur de la cellule hôte, les UPEC peuvent résister aux défenses de l'hôte et aux antibiotiques. Cependant, l'environnement des vacuoles limite la croissance des bactéries en raison de la diminution de l'absorption des nutriments (Eto *et al.*, 2006). Le LPS libéré par les UPEC est détecté par le récepteur Toll-like 4 (TLR4) des cellules uroépithéliales, ce qui induit la production d'AMP cyclique (AMPc) via l'activation de l'adénylyl cyclase 3 (AC3), entraînant une exocytose des UPEC vésiculaires à travers la membrane plasmique apicale des cellules parapluie où une croissance rapide peut se produire (Berry *et al.*, 2009; Song *et al.*, 2009).

Communauté bactérienne intracellulaire (IBC)

Après que les UPEC aient eu accès au cytoplasme, une phase de croissance exponentielle commence qui se traduit par la formation de communautés bactériennes intracellulaires (IBC) (Fig. 2.4). Les IBC sont de larges inclusions intracellulaires composées de plusieurs milliers de bactéries (10^5 à 10^6) qui ont des propriétés de biofilm (Anderson *et al.*, 2003). Environ 24 h après l'invasion, les IBC se développent et submergent la cellule épithéliale de l'hôte. Ensuite, les bactéries se détachent des IBC et quittent la cellule-hôte en passant d'une forme coccoïde à une

forme de bâtonnet motile. Un processus d'exfoliation est déclenché et il y a initiation de l'apoptose caspase-dépendante. Ce processus permet l'expulsion des cellules infectées, mais qui, en contrepartie met à nu les cellules des couches sous-jacentes qui vont être envahies (Justice *et al.*, 2004). Lors de leur sortie, les bactéries se filamenteront et adhèreront aux cellules voisines et démarreront un autre cycle infectieux. Les bactéries filamenteuses sont formées par une croissance continue et un allongement cellulaire avec un arrêt de la division cellulaire normale. La forme filamenteuse des UPEC peut aider à fournir une plus grande fixation aux surfaces des voies urinaires et éviter l'élimination par le système immunitaire de l'hôte (Anderson *et al.*, 2003). Pour contrer l'infection, une réponse inflammatoire et immunitaire est déclenchée suite à l'exfoliation (Fig. 2.3). Cependant, le processus d'exfoliation expose les cellules profondes aux bactéries, les rendant ainsi susceptibles à l'invasion.
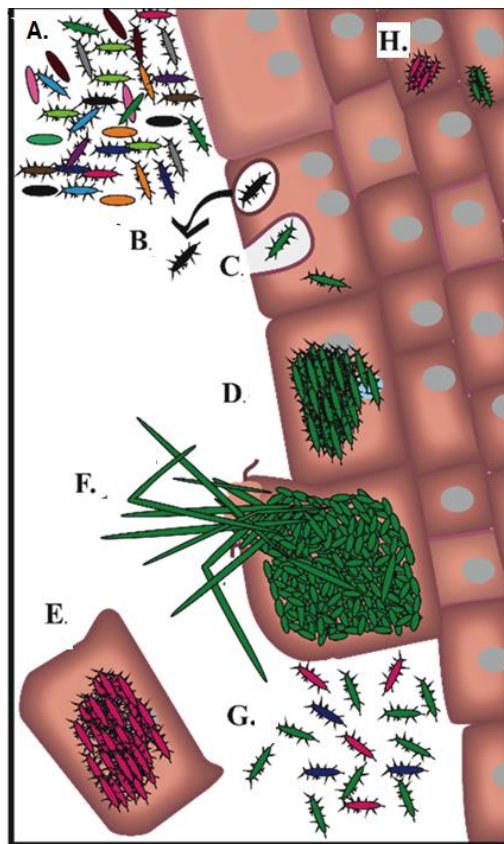
Figure 2.4. Cycle de vie des UPEC pendant la cystite

(A) Lors de l'accès à la vessie, l'UPEC adhère à la surface des cellules superficielles qui tapissent la lumière de la vessie d'une manière dépendant du fimbriae de type 1. (B) Les bactéries adhérentes envahissent les cellules et sont soit expulsées dans la lumière par la cellule d'une manière dépendante de TLR4. (C) ou s'échappe de la vésicule endocytaire dans le cytoplasme. (D) Lors de l'invasion, les bactéries se répliquent dans le cytoplasme en formant des IBC. (E) Un mécanisme de défense de l'hôte contre les UPEC intracellulaire

est l'excrétion de cellules urothéliales dans l'urine, ce qui réduit le nombre total d'UPEC dans la vessie. (F) Au cours des derniers stades de la formation du IBC, les bactéries filamenteuses se dissocient des IBC, éclatent hors de la cellule et retournent dans la lumière de la vessie où elles restent ou peuvent envahir une cellule à adjacente. Chez la souris, deux issues potentielles de l'infection existent : la cystite chronique ou la résolution de l'infection. (G) La réplication bactérienne incontrôlée dans l'urine se produit chez les souris qui développent une cystite chronique. (H) Chez les souris qui résolvent l'infection, de petites poches de bactéries, appelées réservoirs intracellulaires quiescents, se forment et résident dans l'urothélium sous-jacent et peuvent recommencer un nouveau cycle infectieux. Adapté de Spaulding et Hultgren (2016).

Formation de réservoir quiescent

Dans les IBC, les UPEC peuvent entrer en quiescence (quiescent intracellular reservoirs) et perdurer pendant des mois dans le cytoplasme des cellules urothéliales (Fig. 2.4). De plus, les UPEC survivent dans l'environnement hostile de la vessie en sécrétant plusieurs facteurs importants pour l'acquisition des nutriments (Hannan *et al.*, 2012). Les bactéries en quiescence sont protégées contre les traitements antibiotiques et le flux de cisaillement de l'urine et des mécanismes d'immunosurveillance de l'hôte, et peuvent persister dans l'urothélium pendant plusieurs semaines (Blango & Mulvey, 2010). Les bactéries en quiescence peuvent être réactivées pour déclencher une ITU récurrente (Fig. 2.4) (Hannan *et al.*, 2012). Lors du renouvellement des cellules uroépithéliales, dans lequel les cellules immatures sous-jacentes se différencient de manière terminale en cellules parapluie, la redistribution de l'actine pourrait déclencher la réactivation des UPEC à partir des bactéries en quiescence, relâchant ces dernières dans la lumière de la vessie (Blango *et al.*, 2014).

2.2.5   Réponses métaboliques des UPEC durant la pathogenèse

Les UPEC doivent s'adapter rapidement à de nouveaux environnements lors de leur transition entre la lumière intestinale et les voies urinaires. Dans les voies urinaires, l'urine est l'une des principales sources de nutriments rencontrées par les UPEC pendant la phase extracellulaire du cycle d'infection (Alteri *et al.*, 2015). L'urine est un environnement à haute osmolarité et modérément oxygéné. Il est pauvre en nutriments en raison des faibles quantités de l'arginine, la méthionine, la valine, l'uracile, l'adénine, l'isoleucine et le fer (Vejborg *et al.*, 2012).

Bien qu'il soit considéré comme un milieu pauvre, l'urine est un milieu de croissance complexe et contient des concentrations élevées de nombreux métabolites pouvant être utilisés par les UPEC. Il contient des concentrations élevées d'urée, de créatinine, d'acides aminés, de sels inorganiques (chlorure, sodium et potassium), d'acides organiques, d'ammoniac, les purines, les pyrimidines et de nombreuses toxines hydrosolubles, qui doivent être utilisées ou tolérées par les

UPEC (Bouatra *et al.*, 2013). Les métabolites les moins abondants dont disposent les UPEC dans l'urine sont les sucres, en particulier le glucose, des peptides spécifiques et des hormones telles que l'ocytocine, l'angiotensine et la mélatonine. Ainsi, alors que l'urine est peut-être plus difficile sur le plan nutritionnel pour permettre la croissance bactérienne que l'environnement intestinal, les souches UPEC ont une capacité métabolique bien développée pour survivre dans cet environnement (Mann *et al.*, 2017). En effet, la gluconéogenèse et le cycle de l'acide tricarboxylique sont requis durant les ITU, en particulier pendant l'infection intracellulaire de la vessie, tandis que la glycolyse est importante dans la colonisation des reins (Alteri *et al.*, 2009a).

L'utilisation des acides aminés et de petits peptides par les UPEC est soutenue par la surexpression des gènes impliqués dans le catabolisme des acides aminés pendant la croissance dans l'urine humaine, tels que le DsdA (D-sérine désaminase), permettant ainsi le catabolisme du D-sérine (Snyder *et al.*, 2004b). Ce dernier se trouve en quantité importante dans l'urine humaine.

2.2.6   Réponse immunitaire de l'hôte à l'infection à UPEC

Les tissus muqueux tels que le tractus gastro-intestinal et le vagin abritent une communauté microbienne importante qui contribuent à la santé globale de l'organisme. Par conséquent, la colonisation par des bactéries provoque une réponse inflammatoire robuste qui serait à l'origine des symptômes associés à la maladie. Une réponse immunitaire innée est initiée lorsque des motifs moléculaires associés aux pathogènes (PAMP, Pathogen-associated molecular patterns) sont reconnus par des Récepteurs de reconnaissance de motifs moléculaires (PRR, Pattern recognition receptor) sur les cellules épithéliales et les cellules immunitaires résidentes (Abraham & Miao, 2015) (Fig. 2.5).

Les cellules épithéliales qui tapissent les voies urinaires sont la première ligne de défense contre les agents pathogènes. Ces cellules regorgent de récepteurs PRR pour diverses bactéries. Par exemple, la reconnaissance des LPS par TLR4 est une étape essentielle de la réponse pro-inflammatoire dans la vessie (Schilling *et al.*, 2003). En plus du LPS, le TLR4 semble également reconnaître les fimbriae de type 1 et P (Ashkar *et al.*, 2008; Hedlund *et al.*, 2001). La stimulation de TLR2 et TLR5 par les lipoprotéines bactériennes et la flagelline, respectivement, contribue également à une réponse pro-inflammatoire (Andersen-Nissen *et al.*, 2007; Jeannin *et al.*, 2002). Lors de la liaison du ligand, les récepteurs Toll-like activent les cascades de signalisation, y compris la voie NF-κB, qui entraînent des changements dans l'expression de cytokines et de chimiokines (Agace *et al.*, 1993).

Les cellules épithéliales sécrètent une pléthore de composés solubles allant des cytokines pro-inflammatoires aux agents antibactériens. Les cytokines telles que l'interleukine-1 (IL-1), IL-6, IL-8 et IL-1β sont détectables dans l'urine après l'infection (Fig. 2.5), et elles sont importantes pour le recrutement des leucocytes, principalement les leucocytes polymorphonucléaires (neutrophiles) et les phagocytes dans la vessie ou le tissu rénal pour contrer l'infection bactérienne (Agace *et al.*, 1993; Song *et al.*, 2007). Suite à la stimulation des PRR lors de l'entrée de bactéries, les cellules épithéliales produisent de l'IL-8. Cette dernière conduit au recrutement de neutrophiles dans l'épithélium superficiel et la lumière de la vessie, où se trouvent des bactéries (Godaly *et al.*, 2001). Ces cellules immunitaires innées sont les cellules primaires responsables de l'élimination bactérienne une fois la réponse inflammatoire déclenchée. Dans les modèles murins d'ITU, les neutrophiles peuvent être détectés dans l'urine dès 2 heures post-infection, et leur nombre atteint un pic à 6 heures. Le nombre de neutrophiles est étroitement parallèle à la charge bactérienne dans les voies urinaires, et à mesure que le nombre de bactéries diminue, le nombre de neutrophiles diminue également (Agace *et al.*, 1995; Shahin *et al.*, 1987). De plus, les neutrophiles contrôlent l'infection via de multiples mécanismes facilités par divers facteurs solubles dans l'urine, tels que les pentraxines (PTX3, pentraxin-related protein 3). La PTX3 est produite par de nombreux types cellulaires, y compris les cellules urothéliales. La PTX3 se lie aux surfaces bactériennes, ce qui conduit à une destruction médiée par le complément et à une absorption accrue par les phagocytes (Fig. 2.5) (Jaillon *et al.*, 2014). En raison de la libération des espèces réactives d'oxygène (ROS) et d'autres produits cytotoxiques, les neutrophiles activés causent des dommages inflammatoires aux tissus de la vessie et prédisposent la vessie à des infections persistantes (Hannan *et al.*, 2014).

L'adhésion des bactéries aux épithéliums tapissant les voies urinaires peut être empêchée par la libération de protéines incluant les peptides antimicrobiens tels que les β-défensines, la cathélicidine, et la ribonucléase 7 (Fig. 2.5) (Chromek *et al.*, 2006; Valore *et al.*, 1998). Les peptides antibactériens peuvent également avoir des effets immunomodulateurs, comme l'augmentation de la production de cytokines et la promotion de l'infiltration des neutrophiles.

L'uromoduline, une glycoprotéine majeure à haute teneur en mannose, est spécifiquement produite dans les voies urinaires par les cellules rénales (Bates Jr *et al.*, 2004). Elle exerce un effet protecteur contre les infections urinaires en concurrençant la liaison de l'UPEC via FimH à l'uroplakine (Fig. 2.5). En effet, lors de sa liaison à l'UPEC, l'uromoduline empêche les bactéries d'interagir avec la surface des cellules épithéliales tout en les induisant simultanément à s'agréger, ce qui facilite l'élimination précoce de l'UPEC dans l'urine (Mo *et al.*, 2004).

L'uromoduline peut déclencher directement le TLR4 et induire la maturation de certaines cellules telles que les cellules dendritiques myéloïdes (CD). Ainsi, l'uromoduline peut également avoir une fonction immunomodulatrice.
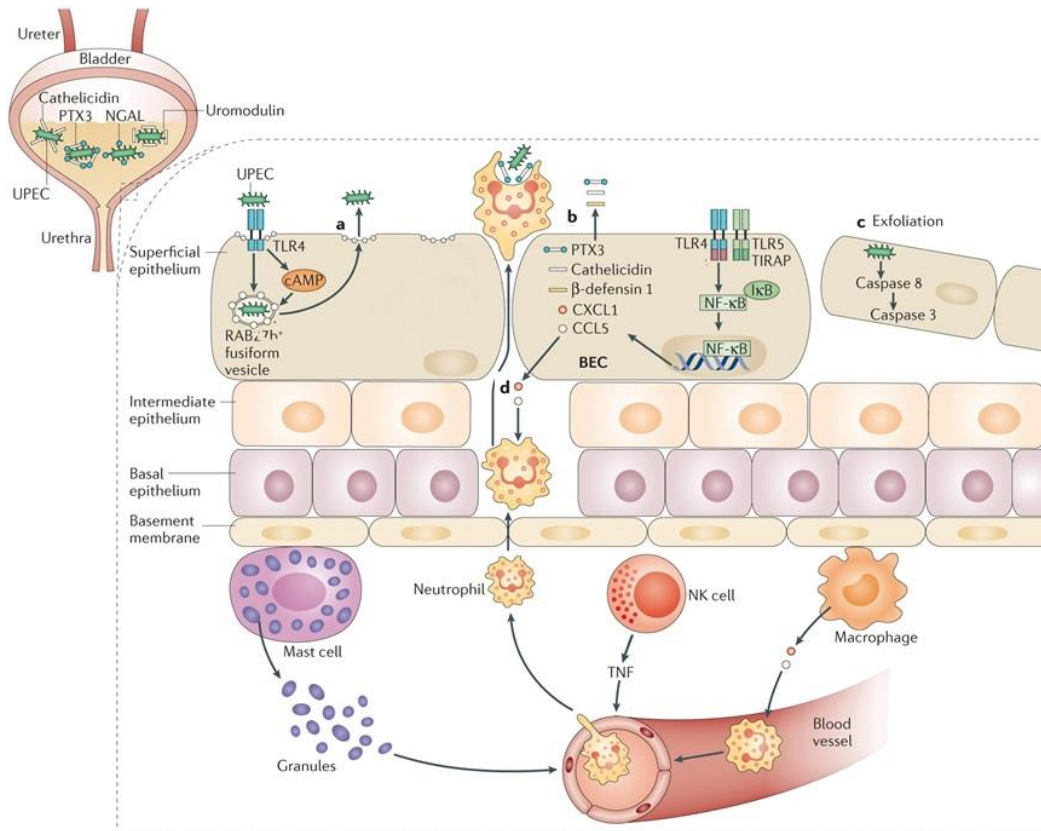
Figure 2.5. Représentation de la réponse immunitaire innée dans la vessie

Un réseau complexe de réponses immunitaires innées peut être initié dans la vessie en réponse à une ITU. A) Après l'invasion par les UPEC et l'encapsulation dans les vésicules RAB27b+ des cellules épithéliales de la vessie (BEC, bladder epithelial cells), le TLR4 reconnaît les UPEC intracellulaires et augmente les niveaux d'AMPc intracellulaire. Cela conduit à une exocytose des vésicules RAB27b+ hébergeant les UPEC et à l'expulsion des UPEC intracellulaires dans la lumière de la vessie. B) Suite à la détection de bactéries pathogènes par le TLR4, un large éventail de facteurs solubles est sécrété par les BEC, y compris des peptides antimicrobiens (tels que la cathélicidine et la β-défensine 1), des protéines antimicrobiennes (telles que la pentraxine 3 (PTX3)) et chimiokines (telles que CXC-chimiokine ligand 1 (CXCL1) et CC-chimiokine ligand 5 (CCR5)). C) L'infection bactérienne déclenche l'apoptose dépendante de la caspase 3 et de la caspase 8 des BEC infectés, qui se répandent dans la lumière de la vessie. Cela représente un autre mécanisme efficace pour réduire la charge bactérienne. D) Les cellules immunitaires résidentes, comme les mastocytes, les lymphocytes cytotoxiques naturels (NK, Natural Killer) et les macrophages, peuvent détecter la présence des

infections et sécréter diverses cytokines pour recruter d'autres cellules immunitaires innées de la circulation sanguine, en particulier les neutrophiles, pour éliminer les infections. Abraham & Miao (2015).

Les CD, les monocytes et les macrophages jouent un rôle important dans la réponse immunitaire innée à l'UPEC en favorisant l'élimination des UPEC (Abraham & Miao, 2015). Les macrophages qui résident dans la lamina propria de la vessie sont des macrophages Ly6C−, qui lors de l'infection, recrutent à la fois des neutrophiles et des macrophages Ly6C+ hors de la circulation dans la lamina propria de la vessie par la sécrétion de chimiokines telles que CXCL1 et CXCL2 (Schiwon *et al.*, 2014). Ainsi, alors que les macrophages LY6C− résidants fonctionnent comme les principales cellules pro-inflammatoires, les macrophages LY6C+ recrutés jouent un rôle clé pour garder les neutrophiles à proximité avant de cibler l'agent pathogène (Abraham & Miao, 2015).

Bien que les macrophages soient le principal type de cellules immunitaires innées à phagocyter les UPEC dans les 48 premières heures de l'infection, l'épuisement des macrophages provoque une phagocytose accrue des UPEC par les CD. Cela suggère que les CD peuvent jouer un rôle important dans l'élimination de l'UPEC (Mora-Bau *et al.*, 2015).

2.3   Facteurs de virulence

La différence entre une souche pathogène et une souche non pathogène est l'acquisition de facteurs de virulence (Tableau 2.1), permettant à la bactérie pathogène de mieux coloniser l'hôte et surtout d'envahir des organes normalement non propices au développement bactérien. Ces facteurs peuvent provenir de différentes sources comme des plasmides, des bactériophages ou des éléments génétiques mobiles (Braun, 1981; Clancy & Savage, 1981; Waters & Crosa, 1991).

Pour surmonter les restrictions environnementales et les défenses de l'hôte lors d'ITU, les souches UPEC utilisent de nombreux facteurs de virulence qui leur permettent de s'adhérer, de faciliter l'acquisition des nutriments, se multiplier dans un environnement hostile, d'endommager les tissus, et se disséminer dans l'appareil urinaire (Subashchandrabose *et al.*, 2013). Ces facteurs de virulences sont codés par des gènes situés dans des îlots de pathogénicité (PAI), qui ont souvent une teneur en nucléotides GC distinct du reste du génome (Hacker & Kaper, 2000).

Les facteurs de virulence qui sont impliqués pour établir des ITU peuvent être répertoriés en deux groupes : (i) facteurs de virulence associés à la surface des cellules bactériennes et (ii) facteurs de virulence qui sont sécrétés et exportés (Tableau 2.1).

2.3.1　Les structures de surface

Pour s'adhérer aux cellules de l'hôte, les bactéries expriment des molécules qui leur permettent de s'accrocher et d'éviter d'être expulsées par les fluides corporels. Suite à ce contact intime, les bactéries peuvent aussi relâcher des toxines ou d'autres effecteurs dans les cellules de l'hôte afin de favoriser le passage aux étapes subséquentes de l'infection. En effet, les adhésines contribuent à la virulence en favorisant l'adhérence et la colonisation des surfaces des cellules de l'hôte. Les fimbriae ou pili sont des organelles en forme de filaments utilisées par les bactéries pour s'adhérer à diverses surfaces (Spurbeck *et al.*, 2011a); et qui sont impliquées dans l'invasion et la formation de biofilm. Les adhésines se comportent comme des lectines, reconnaissant les résidus d'oligosaccharides des glycoprotéines ou des glycolipides qui se trouvent à la surface des cellules hôtes.

Ces appendices non-flagellaires peuvent être répertoriés en cinq classes principales sur la base de la voie de biosynthèse impliquée: les fimbriae de la voie « Chaperone-Usher » (CU), curli, pili de type IV, système de sécrétion (seringue) de type III et le système de sécrétion de type IV (Waksman & Hultgren, 2009). Parmi ces cinq classes, les fimbriae de la voie CU sont les plus étudiés.

La voie CU est un système omniprésent parmi les entérobactéries, utilisé pour l'assemblage des fimbriae exposés en surface. Les CU sont organisés en opérons codant pour un fimbriae, une chaperon périplasmique et un placier de la membrane externe (Clegg & Gerlach, 1987a); (Waksman & Hultgren, 2009). Les souches UPEC possèdent plusieurs opérons fimbriaires. Ces opérons sont *fim* (type 1), *pap* (P), F17-like, *sfa* (S), *yad*, *auf*, *yfc*, *ygi*, *yeh*, *fml* et *foc* (F1C), *yde* (F9), *dra*/*afa* (Dr family), *fso* (F7), *fst* et *pix* (Korea *et al.*, 2011). En général, les souches UPEC portent un nombre significativement plus élevé de systèmes fimbriaires comparativement aux souches fécales/commensales (Spurbeck *et al.*, 2011a). Il existe également des adhésines dites afimbriaires, c'est-à-dire que la sous-unité adhérente ne semble pas se trouver à l'extrémité d'un filament. En effet, les différentes adhésines qu'une seule souche peut exprimer permettraient de coloniser différentes niches. C'est aussi ce qui peut permettre à une même souche d'infecter différents organes d'un même hôte. La voie CU de biogenèse des fimbriae utilise une chaperon périplasmique qui se lie et assiste au repliement des différentes composantes sous-unitaire. La chaperon facilite plusieurs étapes essentielles de la voie; elle intervient dans le repliement des sous-unités fimbriaires, empêche leur polymérisation dans le périplasme et dirige leur passage vers l'usher (Sauer *et al.*, 1999; Sauer *et al.*, 2004).

Les différentes sous-unités forment un complexe avec la protéine chaperon. Ce complexe est dirigé vers la membrane externe, où le placier forme un pore à travers lequel les sous-unités de fimbriae sont exportées et assemblées. Les fimbriae CU sont assemblés en polymères linéaires non ramifiés constitués de plusieurs centaines à milliers de sous-unités de fimbriae (également appelées pilines) dont la taille varie de ~12 kDa à ~20 kDa. Les sous unités CU diffèrent largement en complexité et en morphologie, allant des fibres minces aux tiges épaisses composées d'un cylindre enroulé en hélice et d'une pointe fibrillaire distincte (Waksman & Hultgren, 2009). Puisque la biogenèse du fimbriae ne peut pas être initiée en leur absence, les adhésines sont toujours assemblées dans les fimbriae en premier et se situent donc à l'extrémité distale du fimbriae. L'assemblage de l'adhésine en premier, est nécessaire pour amorcer/activer le placier pour la biogenèse du fimbriae (Geibel & Waksman, 2014).

Les fimbriae de type 1 et P, assemblés par la voie CU, sont parmi les fimbriae bactériens les mieux caractérisés. Tandis que les gènes de fimbriae type 1 se retrouvent dans le génome des souches d'*E. coli* fécales/commensales, les gènes de fimbriae P sont localisés sur des îlots de pathogénicité des souches UPEC (Subashchandrabose *et al.*, 2013).

Le génome d'une souche UPEC, soit le CFT073, contient 12 régions de gènes fimbriaires dont 10 appartiennent à la famille CU, y compris les fimbriae de type 1, deux copies de fimbriae P (F1C, F9 et Auf) et 2 pili putatifs de type IV (c2394-c2395 et ppdD-hofBC) (Welch *et al.*, 2002).

2.3.1.1   Les fimbriae type 1

Bien que les UPEC puissent exprimer plusieurs variétés de fimbriae, les fimbriae de type 1 sont les plus importants pour la colonisation de l'appareil urinaire humain. Outre *E. coli*, le fimbriae de type 1 est produit par d'autres espèces de la famille *Enterobacteriaceae* (Clegg & Gerlach, 1987b). Ces fimbriae sont impliqués dans l'attachement des bactéries à différents types de surfaces, biotiques ou abiotiques et constituent un élément essentiel dans l'étape initiale de formation de biofilms (Pratt & Kolter, 1998; Schembri *et al.*, 2003b). Ainsi, ils jouent un rôle important dans la virulence des souches UPEC. Ils se présentent sous la forme d'une tige filamenteuse, d'un diamètre d'environ 7 nanomètres (nm) et une longueur de 0,1 à 2 micromètres (µM) (Hahn *et al.*, 2002).

La synthèse des fimbriae de type 1 est sous le contrôle de l'expression de l'opéron *fimAICDFGH,* qui code pour les protéines impliquées dans la biosynthèse et la structure des fimbriae (Fig. 2.6). *fimA*, *fimF*, *fimG* et *fimH* encodent les protéines structurales, *fimC*, est le gène de la chaperon ; *fimD*, exprime le placier (Fig. 2.7) ; alors que le rôle du produit de *fimI* n'est toujours pas clair, il est requis pour la biosynthèse des fimbriae de type 1 (Klemm & Schembri, 2004; Valenski *et al.*, 2003).
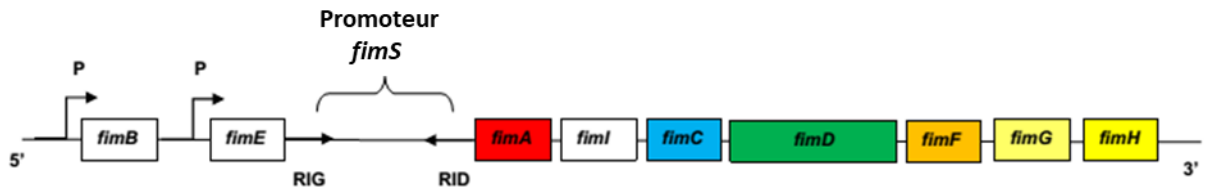
Figure 2.6. Schéma de la région génétique *fim*

Chaque rectangle de couleur représente un gène. Les couleurs correspondent aux protéines illustrées. *fimBE* sont des gènes de régulation, ils possèdent chacun un promoteur (représenté par une fine flèche noire) ; *fimA* code pour la piline; *fimI* code pour une protéine qui aurait le rôle d'ancrage ; *fimC* code pour la chaperon ; *fimD* pour le placier ; *fimFG* codent pour les protéines de liaison et enfin *fimH* pour l'adhésine. Adaptée de Schwan (2011).

Étant des organelles complexes, leur production demande une coordination très précise entre le repliement, la sécrétion et l'ordre d'assemblage des protéines qui les composent (Hahn *et al.*, 2002). Le corps du fimbriae est sous forme d'hélice et est composé seulement d'une répétition de la sous-unité majeure FimA. La piline est aussi responsable du caractère antigénique. Les protéines FimFGH provoquent l'initialisation de l'extension du fimbriae et se retrouvent vers le bout externe du fimbriae (Fig. 2.7). En effet, la production commence par l'adhésine FimH, puis vient le tour des protéines FimFG et de la protéine FimA (Klemm & Christiansen, 1987; Lowe *et al.*, 1987; Russell & Orndorff, 1992). Aucune énergie, telle que l'ATP, n'est nécessaire pour l'assemblage et l'extension du fimbriae.
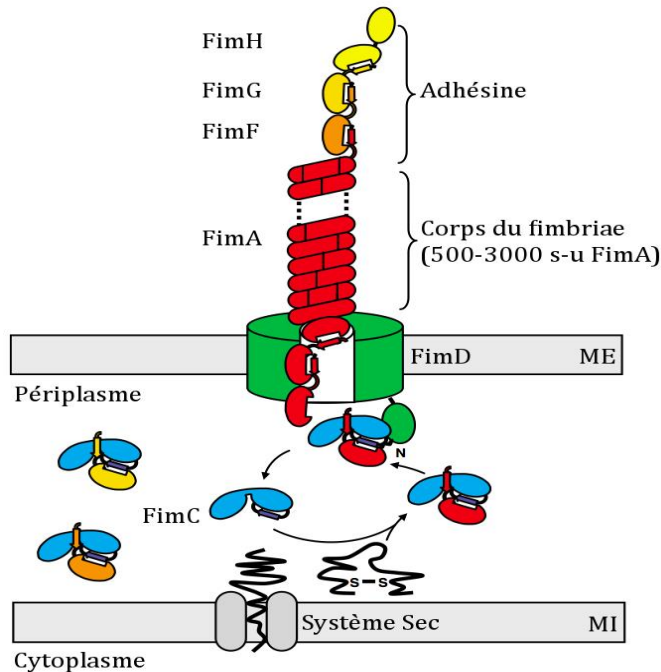
Figure 2.7. Modèle de l'assemblage des fimbriae type 1 par la voie « chaperon-placier »

La protéine FimH est l'adhésine, elle reconnaît les récepteurs à la surface des cellules de l'hôte. Les protéines FimG et FimF servent de connecteur entre FimH et le corps du fimbriae composé d'une répétition de la sous-unité majeure FimA. FimD est la protéine placier et enfin FimC est la chaperon. Ces protéines sont excrétées au niveau du périplasme grâce au système Sec. Abréviation : s-u pour sous-unité ; ME pour membrane externe ; MI pour membrane interne. Adaptée de Nishiyama et al. (2005)

Toutes les protéines structurales des fimbriae sont sécrétées dans le périplasme à travers la membrane interne par le système de translocation SecYEG, ce qui demande la présence d'un peptide signal sur chacune des séquences natives. La protéine chaperon FimC est composée de deux domaines de types immunoglobulines et a un rôle important (avec FimD) dans la biogenèse du fimbriae (Pratt & Kolter, 1998; Schembri *et al.*, 2003a). En effet, lors de la sécrétion des protéines par le système Sec et par reconnaissance de séquence en C-terminale et N-terminale, la protéine chaperon va directement prendre en charge ces protéines. Ceci étant afin de pouvoir effectuer le relargage effectif dans le périplasme par le système Sec. La formation des complexes avec la chaperon empêche la formation d'agrégats des sous-unités dans le périplasme, ainsi que leur dégradation par des protéases (Hung *et al.*, 2002). La première fonction de la protéine FimC est, bien entendu, le repliement des protéines, pour qu'elles adoptent leur configuration tertiaire. En effet, elles sont sécrétées de façon linéaire dans le périplasme. Passé toutes les étapes de sécrétions et de repliements, les protéines structurelles sont prêtes à être prises en charge par la

protéine placier FimD (Mulvey, 2002; Zhou *et al.*, 2001b). Une forte interaction se produit entre le placier et le complexe chaperon-protéine. La partie N-terminale du placier va reconnaître la chaperon chargée, s'ensuit une modification de sa conformation spatiale pour permettre le transfert de la protéine chargée par la chaperon au placier et ainsi faire l'assemblage du fimbriae. Les protéines structurelles passent à travers le placier, qui forme un pore de 2 à 3 nm, de façon linéaire : la taille du pore est trop petite pour faire traverser la membrane externe à une hélice de sous-unité majeure d'un diamètre de 6 nm. En somme, l'hélice se forme à l'extérieure de la cellule bactérienne. Enfin, la taille du fimbriae dépend essentiellement de la concentration en sous-unités présente dans le périplasme. De même, le nombre de fimbriae exprimés dépend du nombre de protéines FimFGH disponible pour l'initialisation de la production (Mulvey, 2002; Zhou *et al.*, 2001b). En effet, les sous-unités sont ajoutées à la base du fimbriae en croissance, l'adhésine FimH étant d'abord incorporée. En conséquence, le placier FimD a l'affinité la plus élevée pour les complexes FimC-FimH (Saulino *et al.*, 1998). Après l'incorporation de FimH, une seule sous-unité de FimG et FimF est ajoutée pour compléter la pointe fimbriaire. Les complexes FimC-FimA sont ensuite ajoutés séquentiellement pour produire une tige de fimbriae entièrement formée contenant ~ 1000 sous-unités FimA disposées dans un cylindre hélicoïdal avec environ 3,2 sous-unités par tour (Bullitt *et al.*, 1996). La sous-unité majeure FimA permet l'ancrage du fimbriae à la surface bactérienne et l'adhésine FimH, située à l'extrémité distale des fimbriae (Hung *et al.*, 2002), reconnaît les résidus D-mannose retrouvés à la surface des cellules uroépithéliales (Mulvey *et al.*, 1998). Les résidus D-mannose sont également présents au niveau des récepteur glycoprotéiques retrouvés au niveau de l'intestin, des poumons ainsi que sur les cellules inflammatoires (La Ragione *et al.*, 2002; Mulvey *et al.*, 1998(Antao *et al.*, 2008). Également, les fimbriae de type 1 permettent la fixation bactérienne au collagène de type I et IV, la laminine et la fibronectine (Mulvey, 2002; Zhou *et al.*, 2001b).

Dans l'urine de patients souffrant d'ITU et/ou chez la souris, l'expression des fimbriae de type 1 est variable (Gunther *et al.*, 2001; Spaulding & Hultgren, 2016). Plusieurs études, chez la souris et l'homme, ont démontré que les UPEC attachés à l'excrétion des cellules épithéliales dans l'urine expriment les fimbriae de type 1, tandis que les UPEC planctoniques trouvés dans l'urine n'expriment pas les fimbriae (Gunther *et al.*, 2001; Hultgren *et al.*, 1985). Cela suggère que l'expression des fimbriae de type 1 est spécifique à la niche, ceux-ci étant exprimés par les UPEC qui sont attachés à la surface épithéliale.

2.3.1.2   Les fimbriae P

Les fimbriae Pap (fimbriae P) sont associés aux souches causant des pyélonéphrites (pyelonephritis-associated pili). Ils jouent un rôle important dans la colonisation des tissus de l'hôte lors de l'infection du tractus urinaire supérieur (Lane & Mobley, 2007). Les génomes des souches 536 et UTI89 contiennent chacun une copie de l'opéron *pap* codant pour les fimbriae P, tandis que le génome de CFT073 a deux copies fonctionnelles dans des îlots de pathogénicités séparés (Wiles *et al.*, 2008b). Les fimbriae P sont codés par le groupe de gènes *pap*, constitué de 11 gènes *papIBAHCDJKEFG* localisés sur le chromosome. La morphologie de ces fimbriae est très semblable à celui de type 1, avec un diamètre de 5 à 7 nm et une longueur variant de 0,5 à 2 μm (Brauner *et al.*, 1985). La sous-unité majeure PapA forme le corps basal ancrant le fimbriae à la surface bactérienne et les trois protéines PapE, PapF et PapK s'associent à la protéine PapG pour former l'extrémité distale de fimbriae. L'adhésine PapG varie en spécificité et peut reconnaître des motifs Galα(1->4)Gal présents à la surface des érythrocytes ainsi qu'au niveau des cellules uroépithéliales du rein et du tractus urinaire (Stapleton *et al.*, 1998; Stromberg *et al.*, 1991).

Les fimbriae P ne sont pas exprimés au niveau de la vessie, mais ils sont nécessaires pour l'attachement des UPEC au niveau des reins chez un animal vivant (Melican *et al.*, 2011a). En outre, l'expression ectopique de l'opéron *pap* dans la souche de bactériurie asymptomatique *E. coli* 83972 est suffisante pour améliorer la colonisation des voies urinaires humaines (Wullt *et al.*, 2000). Par conséquent, la production de fimbriae P favorise l'établissement plus rapide de la bactériurie. Les fimbriae P sont impliqués également dans la régulation de la motilité flagellaire via PapX, un gène non structurel trouvé dans le groupe de gènes fimbriaire P. PapX est un acteur essentiel dans la régulation croisée entre l'adhésion et la motilité (Simms & Mobley, 2008b).

2.3.1.3   Les autres fimbriae

D'autres régions codant pour des fimbriae confirmés ou putatifs trouvés chez certaines souches UPEC comprennent Auf, Dr, F1C, F9, Pix, S, Yad, Yeh, Yfc et Ygi. Les fimbriae F1C sont codés par les gènes *foc* et ressemblent, génétiquement et structuralement, aux fimbriae de type 1 et se lient aux glycosphingolipides, y compris les galactosylcéramides qui sont répandus sur les cellules épithéliales présentes dans les reins, les uretères et la vessie, et les globotriaosylcéramides retrouvés sur les cellules rénales (Bäckhed *et al.*, 2002; Bäckhed *et al.*, 2001; Khan *et al.*, 2000). De plus, l'attachement des fimbriae F1C aux cellules épithéliales rénales

humaines induit la sécrétion de la cytokine IL-8, où des niveaux élevés d'IL-8 dans l'urine sont une indication d'une infection urinaire en cours (Bäckhed *et al.*, 2002). Les fimbriae F1C sont fortement exprimés dans une souche dépourvue à la fois de fimbriae type 1 et P, suggérant la régulation croisée entre les protéines régulatrices qui affectent l'expression de divers fimbriae (Snyder *et al.*, 2005). La production des fimbriae F1C peut contribuer à la formation de biofilms sur une surface abiotique par la souche *E. coli* Nissle 1917 (Lasaro *et al.*, 2009).

Les fimbriae Dr et les adhésines afimbriaires Afa (afimbrial adhesin) d'*E. coli* sont associées aux infections urinaires, en particulier à la pyélonéphrite gestationnelle et à la cystite récurrente (Garcia *et al.*, 1996; Servin, 2005). Les données cliniques suggèrent que les souches d'*E. coli* avec des adhésines Afa ont des propriétés favorisant potentiellement l'établissement d'une infection chronique et/ou récurrente. Les adhésines Afa sont responsables de l'agglutination mannose-résistante des érythrocytes humains exprimant l'antigène du système Cromer sur le facteur DAF (Decay-Accelerating Factor) (Le Bouguénec, 2005; Nowicki *et al.*, 1990). Également, les fimbriae Dr agglutinent les érythrocytes humains et favorisent l'insuffisance rénale en se liant à la membrane basale de l'épithélium tubulaire rénal et à la capsule de Bowman (Nowicki *et al.*, 1988b).

Les fimbriae S permettent l'adhérence des UPEC aux cellules tubulaires proximales rénales en se liant au α-sialyl-2-3-β-galactoside. Les gènes codant pour les fimbriae S, *sfa*, sont plus fréquemment présent chez les isolats cliniques d'UPEC isolés de patients atteints de méningite néonatale et ces fimbriae jouent un rôle potentiel dans les ITU ascendantes (Castelain *et al.*, 2010; Kreft *et al.*, 1995). Il a été mis en évidence que les fimbriae Yad sont impliqués dans l'adhérence à la lignée cellulaire épithéliale de la vessie humaine et dans la formation de biofilm. La délétion de ces gènes fimbriaires a augmenté la motilité (Spurbeck *et al.*, 2011a). Les fimbriae Ygi sont impliqués dans l'adhérence à une lignée cellulaire de rein embryonnaire. Un double mutant Δ*ygi*Δ*yad* est atténué dans le modèle murin d'ITU, démontrant que ces fimbriae contribuent à l'uropathogenèse (Spurbeck *et al.*, 2011a).

2.3.1.4   Les curli

Les curli, aussi appelés les fimbriae agrégatifs minces « thin aggregative fimbriae », appartiennent à une classe de fibres connues sous le nom d'amyloïdes (Barnhart & Chapman, 2006) et sont présents chez plusieurs membres de la famille des *Enterobacteriaceae* et chez environ 50% des isolats urinaires. Ils sont exprimés de manière optimale à température ambiante (Pátri *et al.*, 2002). Chez *E. coli*, les curli favorisent à la fois l'adhérence, l'invasion, la colonisation

et le développement du biofilm (Prigent-Combaret *et al.*, 2000). Ils sont trouvés à des niveaux détectables dans les échantillons d'urine lors d'une infection urinaire. Les gènes impliqués dans la production des curli sont regroupés en deux opérons divergents génétiquement opposés : l'opéron *csgBAC* encodant les composants structurels des curli et l'opéron *csgDEFG* codant pour les gènes nécessaires à l'exportation des sous-unités des curli et à la stabilisation des fibres (les gènes *csgE-G*). *csgD* encode un régulateur transcriptionnel appartenant à la famille *luxR* qui induit l'expression de *csgAB* codant pour CsgA, la principale sous-unité de fibre curli, et CsgB, qui assure la nucléation de CsgA (Chapman *et al.*, 2002; Hammar *et al.*, 1995). L'expression du promoteur *csgD* est affectée, positivement ou négativement, par plusieurs régulateurs transcriptionnels, y compris RpoS, Crl, H-NS et OmpR (Romling *et al.*, 1998).

2.3.1.5   Régulation croisée entre les différentes adhésines

Comme mentionné précédemment, la souche CFT073 possède les gènes pour au moins 12 fimbriae distincts et plusieurs adhésines afimbriaires (Welch *et al.*, 2002)*. E. coli* exprime principalement qu'un type de fimbriae à la fois (Nowicki *et al.*, 1984). Les adhésines bactériennes sont soumises à une régulation transcriptionnelle appelée « variation de phase » ; un mécanisme du tout ou rien. Cette propriété permet à des bactéries individuelles d'activer ou de réprimer l'expression de facteurs de virulence spécifiques à un moment donné (pour plus de détails, voir section 2.4.2). Certaines adhésines fimbriaires exprimées par *E. coli* sont contrôlées par une variation de phase et, par conséquent, seul un sous-ensemble d'une population bactérienne exprimera une adhésine particulière à un temps précis. L'expression des fimbriae peut être stochastique et influencée par de nombreuses conditions environnementales. De plus, une co-régulation existe entre les différents fimbriae dans le but d'exprimer, au moment opportun, le type de fimbriae approprié. Cela permettrait aux bactéries d'adhérer aux tissus de l'hôte et de s'adapter aux microenvironnements qu'elles rencontrent au cours de l'infection.

En effet, chez la souche CFT073, l'accroissement de l'expression des gènes *fim* est corrélée à une diminution de l'expression de *pap*. Ainsi, la délétion des deux opérons *fim* et *pap* a induit la production de F1C fimbriae (Snyder *et al.*, 2005). En revanche, le mécanisme responsable de la sous-expression des gènes *pap* en réponse à l'expression de *fim* n'est pas bien compris. Par exemple, chez la souche *E. coli* F11, lorsque le promoteur *fimS* était verrouillé en phase ON, il n'y avait aucun effet sur l'expression *pap* (Buckles *et al.*, 2015).

Les voies urinaires sont un exemple d'environnement diversifié. Une bactérie pathogène doit posséder des adhésines spécifiques pour les différentes niches, comme la vessie, les uretères

et les reins. Au niveau de la vessie, les fimbriae de type 1 sont exprimés et les fimbriae P sont réprimés chez les UPEC (Snyder *et al.*, 2004a), indiquant ainsi qu'il y a co-régulation entre les différents fimbriae. De plus, des mutations au niveau de *fimS* inhibent l'expression des fimbriae de type 1 et activent l'expression des fimbriae P (Snyder *et al.*, 2005). Il est possible que l'expression des fimbriae de type 1 réprime celle des autres fimbriae. Ainsi, les fimbriae de type 1 sont importants pour la colonisation des voies urinaires, et les fimbriae P sont utilisés plus tard lorsque les bactéries peuvent remonter pour établir une infection rénale. Il semble donc évident que l'expression des fimbriae de type 1 active un ou des facteurs réprimant l'induction des fimbriae P et F1C. Également, les régulateurs transcriptionnels PapB et FocB, codés respectivement par les opérons *pap* et *foc*, assurent la régulation croisée entre les opérons *pap*, *foc* et *fim*, et fonctionnent comme deux régulateurs des opérons *pap* et *foc* en fonction de la concentration en protéines (Holden *et al.*, 2006; Lindberg *et al.*, 2008; Xia *et al.*, 2000b). Plus précisément, PapB peut réprimer la transcription de *fim* en inhibant la transcription de *fimB*, codant pour une recombinase responsable de l'inversement du promoteur *fimS* dans les deux sens. En même temps, PapB favorise l'expression de *fimE*, codant la recombinase médiant l'inversion du promoteur *fimS* de la phase ON à OFF (Gally *et al.*, 1996a; Holden *et al.*, 2001; Xia *et al.*, 2000a) (pour plus de détails, voir section 2.4.1). Ainsi, le régulateur SfaB (régulateur de fimbriae S) inhibe l'expression de fimbriae de type 1 via l'inhibition de FimB (Holden *et al.*, 2001). Les mécanismes moléculaires reliant l'expression des fimbriae de type 1 et la répression des autres fimbriae ne sont pas connus.

2.3.1.6 Conclusion facteurs d'adhésion

Pour les bactéries pathogènes, les adhésines sont essentielles lors des premiers stades de l'infection, afin d'initier le contact avec les cellules hôtes, de coloniser les différents tissus et d'établir l'infection. La capacité à s'adhérer aux tissus de l'hôte est particulièrement importante pour les bactéries qui colonisent des sites tels que le tractus urinaire, où le flux d'urine maintient la stérilité du site en éliminant les agents pathogènes non adhérents. La diversité des adhésines exprimées par les bactéries uropathogènes reflète l'importance de l'adhésion dans la colonisation. En outre, les adhésines exprimées doivent pouvoir résister aux forces mécaniques exercées par l'écoulement de l'urine, pour éviter d'être cisaillées une fois qu'elles se sont attachées à leurs récepteurs sur la surface urothéliale. Ceci démontre l'importance des adhésines telles que le fimbriae de type 1 et P, qui sont adaptées pour fonctionner dans les voies urinaires (Chahales & Thanassi, 2015).

Il est évident que les bactéries coordonnent l'expression des gènes afin de s'adapter aux microenvironnements qu'elles rencontrent au cours de l'infection. Ainsi, les signaux environnementaux rencontrés au niveau de chaque organe du système urinaire auront pour effet d'activer ou de réprimer la transcription des gènes afin de permettre aux bactéries de survivre (Chahales & Thanassi, 2015).

Tableau 2.1. Facteurs impliqués dans la virulence des UPEC

Facteur de virulence	Localisation	Fonction	Référence
Fimbriae de type 1	Surface bactérienne	Colonisation initiale sur le site de l'infection Adhésion à l'épithélium muqueux et à la matrice tissulaire, invasion, formation de biofilm	(Martinez *et al.*, 2000; Schembri & Klemm, 2001)
Fimbriae P	Surface bactérienne	Adhésion à l'épithélium muqueux et à la matrice tissulaire, induction de cytokines	(Lane & Mobley, 2007; Stapleton *et al.*, 1998)
Fimbriae S	Surface bactérienne	Adhésion à l'épithélium des reins et de la vessie	(Korhonen *et al.*, 1984; Korhonen *et al.*, 1986)
Fimbriae Dr	Surface bactérienne	Médie la reconnaissance des récepteurs DAF (decayaccelerating factor) dans les reins	(Nowicki *et al.*, 1990; Nowicki *et al.*, 1988a)
Fimbriae F1C	Surface bactérienne	Adhésion aux cellules épithéliales rénales	(Bäckhed *et al.*, 2002; Khan *et al.*, 2000; Lasaro *et al.*, 2009)
Curli	Surface bactérienne	Adhésion et formation de biofilm	(Pátri *et al.*, 2002; Prigent-Combaret *et al.*, 2000)
Flagelle	Surface bactérienne	Motilité, adaptation, fitness	(Schwan, 2008b)
Capsule	Surface bactérienne	Protection contre la phagocytose, résistance au sérum, développement des IBC	(Anderson *et al.*, 2010; Snyder *et al.*, 2004a)
Lipopolysaccharide	Surface bactérienne	Effets endotoxiques, induction de cytokines, résistance au sérum,	(Bäckhed *et al.*, 2001; Tomás *et al.*, 1988)
Protéines de la membrane externe	Surface bactérienne	Récepteur et fonction de transport	(Chaffer *et al.*, 1999)

α-Hémolysine	Sécrété	Cytotoxicité, hémolyse	(Jonas *et al.*, 1993; Stanley *et al.*, 1998)
Facteur nécrosant cytotoxique (CNF1)	Exporté	Interférence avec la phagocytose et l'apoptose	(Mills *et al.*, 2000; Rippere-Lampe *et al.*, 2001)
Les autotransporteurs	Exporté	Cytotoxicité	(Guyer *et al.*, 2002; Maroncle *et al.*, 2006; Wiles *et al.*, 2008b)
Entérobactine	Exporté	Croissance en milieu pauvre en fer	(Gao *et al.*, 2012; Hantke *et al.*, 2003; Massip *et al.*, 2020)
Aérobactine	Exporté		
Yersiniabactine	Exporté		
Salmochélines	Exporté		

2.3.2   Les flagelles

Les flagelles sont des organelles complexes qui assurent la motilité et le chimiotactisme, et sont composés d'un stator et rotor, d'un crochet et d'un filament (Berg & Anderson, 1973). Certaines espèces bactériennes sont capables de se déplacer en faisant tourner la portion filamenteuse du flagellum, qui est un ensemble de sous-unités de flagelline codées par le gène *fliC* (Chilcott & Hughes, 2000). La nature ascendante de la plupart des cas d'ITU a conduit à la spéculation selon laquelle les flagelles pourraient être des facteurs de virulence critiques pour les UPEC. L'expression des gènes flagellaires chez les UPEC coïncide avec l'ascension de l'uretère et la colonisation des reins, suggérant le rôle des flagelles dans le développement de la pyélonéphrite (Schwan, 2008b).

2.3.3   LPS et capsule

Les facteurs de virulence situés sur la surface bactérienne comprennent également la capsule et le LPS. La capsule est principalement une structure polysaccharidique couvrant et protégeant la bactérie du système immunitaire de l'hôte. Les UPEC produisent des capsules de type II (Whitfield, 2006). Cette dernière fournit une protection contre la phagocytose et l'effet bactéricide assuré par le complément dans l'hôte. Les gènes impliqués dans la biosynthèse de la capsule sont surexprimés lors d'une infection urinaire dans un modèle murin (Snyder *et al.*, 2004a). La

souche UPEC UTI89 produit une capsule de type K1 et cette capsule est importante pour le développement des IBC dans la vessie dans un modèle d'ITU murin (Anderson *et al.*, 2010).

Le LPS est une composante intégrante de la paroi cellulaire des bactéries à Gram-négatif. Le LPS joue un rôle principal dans la résistance des UPEC à l'activité bactéricide du sérum humain (Tomás *et al.*, 1988). Il est connu pour activer la réponse de l'hôte et induire l'oxyde nitrique et la production de cytokines (Backhed *et al.*, 2001). Également, le LPS offre une résistance aux antibiotiques hydrophobes (Zhang *et al.*, 2013).

Plus de 180 sérotypes différents ont été répertoriés chez *E. coli*, certains types d'antigènes O tels que O1, O2, O4, O6, O7, O8, O16, O18, O25 et O75 sont courants parmi les souches UPEC (Raetz & Whitfield, 2002). Bien que le LPS des souches UPEC soit important dans l'activation de la réponse pro-inflammatoire durant les ITU non compliquées, il n'est pas clair si le LPS joue un rôle dans la médiation d'une insuffisance rénale chez les patients atteints d'infections urinaires ascendantes (Bien *et al.*, 2012).

2.3.4   Les toxines

Plusieurs toxines exprimées par *E. coli* ont été répertoriées. L'utilisation de toxines sécrétées par des bactéries pathogènes est bien connue. Les UPEC ne possèdent pas le système de sécrétion de type III que certains autres agents pathogènes utilisent pour injecter des molécules effectrices dans des cellules hôtes et utilisent plutôt les systèmes de sécrétion de type I et de type V (Wiles *et al.*, 2008a).

Les souches UPEC sont connues pour produire l'hémolysine, le facteur nécrosant cytotoxique 1 (CNF1) et les autotransporteurs Vat (vacuolating autotransporter toxin) et Sat (secreted autotransporter toxin). Les toxines les plus étudiées chez les UPEC seront discutées ci-dessous.

2.3.4.1   L'hémolysine

L'hémolysine A (HlyA) est l'une des toxines de formation de pores les mieux caractérisées, de type RTX (repeats in toxin). Les gènes nécessaires à l'activité hémolytique et à la sécrétion de HlyA sont codés par l'opéron *hlyCABD*. Les souches UPEC CFT073 et UTI89 contiennent chacune une copie de l'opéron *hlyCABD*, tandis que la souche 536 possède deux copies (Wiles *et al.*, 2008a). HlyA est une protéine de 110 kDa dépendante du calcium sécrétée par un système de sécrétion de type 1. La toxine est codée par le gène *hlyA* et le gène *hlyC* code pour une acyltransférase qui est requise pour l'activation de la toxine (Bhakdi *et al.*, 1988; Boehm *et al.*,

1990). L'hémolysine traverse donc les deux membranes bactériennes, sans subir de modification, à l'aide de HlyB, HlyD et TolC, respectivement un transporteur de type ABC, une protéine de fusion de la membrane et une protéine formatrice de la membrane externe (Stanley *et al.*, 1998). HlyA s'insère et forme des pores de 2 nm dans la membrane plasmique des cellules de l'hôte. Cette insertion mène ainsi à la lyse cellulaire, ce qui a pour effet de libérer des nutriments et d'autres facteurs permettant la croissance bactérienne (Subashchandrabose & Mobley, 2015; Wiles *et al.*, 2008a). Par exemple, la lyse des érythrocytes permet la libération de fer, qui est peu disponible chez l'hôte. HlyA n'est pas seulement une hémolysine, mais présente également une toxicité vis-à-vis d'autres types cellulaires, y compris les leucocytes (Jonas *et al.*, 1993). HlyA stimule la protéolyse des protéines de l'hôte impliquées dans l'adhésion cellulaire, provoquant ainsi l'exfoliation des cellules urothéliales (Nagy *et al.*, 2006; Dhakal & Mulvey, 2012), expliquant aussi les phénotypes associés à HlyA, soit l'induction d'hématuries, des dommages rénaux et l'augmentation des risques de septicémie (Smith *et al.*, 2008). HlyA est trouvé dans environ 50% des isolats cliniques d'ITU récurrentes de femmes âgées de 18 à 39 ans contre 37% des isolats des premières infections urinaires et 31% des isolats des secondes infections urinaires (Klein & Hultgren, 2020).

2.3.4.2   Facteur nécrosant cytotoxique

CNF1 est un facteur de virulence non négligeable pour la colonisation et l'invasion des cellules du tractus urinaire. Il est produit par un tiers des souches provenant de pyélonéphrite. Cette protéine sécrétée par *E. coli* pénètre dans la cellule et stimule la formation des fibres de stress, et aussi induit des froissements (ruffling) membranaires et la modulation des réseaux de signalisation inflammatoire (Rippere-Lampe *et al.*, 2001). Des études *in vitro* ont démontré que le CNF1 aide à la survie des bactéries en diminuant la faculté de phagocytose des leucocytes polymorphonucléaire et ainsi entraine l'apoptose des cellules épithéliales de la vessie (Fiorentini *et al.*, 1997; Mills *et al.*, 2000). *In vivo,* le CNF1 peut conduire à une exfoliation des cellules de la vessie et à l'accès des bactéries au tissu sous-jacent (Mills *et al.*, 2000). Le CNF1 active les GTPases Rho chez des cellules de son hôte. Par cette activation, les protéines Rho sont activées en permanence, causant des perturbations cellulaires. Les principaux effets sont une forte production d'une pléiade d'immunomodulateurs, ainsi qu'une importante réorganisation du cytosquelette d'actine menant à la formation de cellules géantes multinuclées (Lemonnier *et al.*, 2007; Mobley *et al.*, 2009).

2.3.4.3   Les toxines Sat et Vat

Les ExPEC codent pour plusieurs toxines autotransporteurs sécrétées par le système de sécrétion de type V (Henderson *et al.*, 2004). Les toxines Vat et Sat sont souvent exprimées par des isolats d'UPEC (Maroncle *et al.*, 2006). Ces protéases sont membres de la sous-famille des SPATE, pour sérine protéase autotransporteurs des *Enterobacteriaceae*. C'est-à-dire que ces protéases présentent un motif de sérine (Maroncle *et al.*, 2006). CFT073 code à la fois Vat et Sat, tandis que 536 et UTI89 expriment uniquement Vat (Wiles *et al.*, 2008b).

Vat et Sat ont été initialement caractérisés pour leur capacité à induire une variété d'effets cytopathiques dans les cellules hôtes cibles, y compris la vacuolisation et l'enflure (le gonflement). Bien que le rôle de Vat dans la pathogenèse des ITU n'ait pas été bien étudié, cette toxine contribue à la virulence des APEC dans les modèles d'infection respiratoire chez les poulets (Parreira & Gyles, 2003). L'expression de Sat par CFT073 induit des dommages aux reins dans un modèle d'ITU murin, provoquant la dissolution de la membrane glomérulaire, la perte de cellules épithéliales tubulaires et la vacuolisation du tissu rénal (Guyer *et al.*, 2002; Maroncle *et al.*, 2006). Ainsi, Sat semble être impliqué dans la sévérité de l'infection et prépare les bactéries à se disséminer dans la circulation sanguine.

2.3.5   Les systèmes d'acquisition du fer par les sidérophores

Pour tous les microorganismes, l'acquisition des ions métalliques est essentielle pour la survie dans leur environnement ou chez l'hôte infecté. Ces métaux sont trouvés presque exclusivement en tant que constituants des protéines, incluant les enzymes, les protéines de stockage et les facteurs de transcription (Hood & Skaar, 2012). Par exemple, les bactéries pathogènes rencontrent une carence en fer chez l'hôte. En effet, un aspect important du système immunitaire inné est de limiter la disponibilité du fer aux bactéries pathogènes dans un processus appelé immunité nutritionnelle (Cassat & Skaar, 2013). Étant donné que le fer dans sa forme utilisable est plutôt rare dans les organes généralement touchés par les ExPEC, ainsi que dans le sang, les bactéries ont développé plusieurs stratégies afin de se procurer ce métal. Il existe deux systèmes de capture du fer, le premier reconnaissant directement les protéines liant le fer, le deuxième consistant en la sécrétion de sidérophores (Wandersman & Stojiljkovic, 2000). Les sidérophores sont des molécules sécrétées de faibles poids moléculaires qui sont des chélateurs de fer. Ces molécules ont une très forte affinité pour le fer ferrique (Fe^{3+}) et elles sont capables de rivaliser avec la transferrine et la lactoferrine pour lier le fer (Porcheron *et al.*, 2013). Les bactéries récupèreront les complexes sidérophore-fer à l'aide de récepteurs membranaires où

le fer sera libéré au niveau du cytoplasme bactérien (Wiles *et al.*, 2008a). Chez les souches UPEC, les sidérophores qui sont impliqués dans la pathogenèse incluent l'aérobactine, l'entérobactine, la salmochéline et la yersiniabactine. Ils ne présentent pas tous la même affinité pour le fer (Subashchandrabose & Mobley, 2015).

2.4 Caractérisation, régulation et facteurs affectant l'expression des fimbriae de type 1 chez les ExPEC

2.4.1 Organisation génétique de l'opéron *fim*

La plupart des souches d'*E. coli*, autant commensales que pathogènes, expriment les fimbriae de type 1 (Klemm, 1994). Les gènes *fim* d'*E. coli* comprennent 9 gènes (*fimA, fimI, fimC, fimD, fimF, fimG, fimH, fimB* et *fimE*) (Fig. 2.6). Cet opéron est formé de deux unités transcriptionnelles distinctes ; l'une codant pour FimB et FimE, les recombinases spécifiques, et l'autre pour l'opéron polycistronique codant pour les gènes de structure (*fimA, fimF, fimG, fimH*) et du système d'assemblage du fimbriae. Le gène structurel *fimA* code pour un polypeptide de 158 à 159 acides aminés (Orndorff & Falkow, 1985). L'expression de l'opéron dépend de l'orientation du promoteur *fimS* qui se trouve en amont de *fimA* (Abraham *et al.*, 1985a). Ce promoteur est une séquence nucléotidique de 314 pb situé sur un élément interconvertible (EI) et bordé de chaque côté par des séquences inversées répétées de 9 pb flanquant ce segment d'ADN (5 'TTGGGGCCA 3') , marqué RID « région inversée droite » et RIG « région inversée gauche » (Fig. 2.8) (Abraham *et al.*, 1985a; Spears *et al.*, 1986).

La séquence du promoteur *fimA* est soumise à une recombinaison spécifique du site, positionnant l'élément interconvertible en Phase ON ou en Phase OFF (Schwan, 2011). Lorsque l'EI est en phase ouverte (ON), les fimbriae sont produits, tandis qu'ils sont réprimés lorsque *fimS* est en phase fermée (OFF) puisque le promoteur se trouve en direction inverse de l'opéron *fim*, bloquant ainsi sa transcription (Fig. 2.8). Ce phénomène de changement d'orientation est connu sous le nom de variation de phase. Deux gènes en amont de l'EI *fimS*, *fimB* et *fimE*, codent pour des protéines qui sont impliquées dans le positionnement de l'ADN de *fimS* (Gally *et al.*, 1996b; Klemm, 1986b).
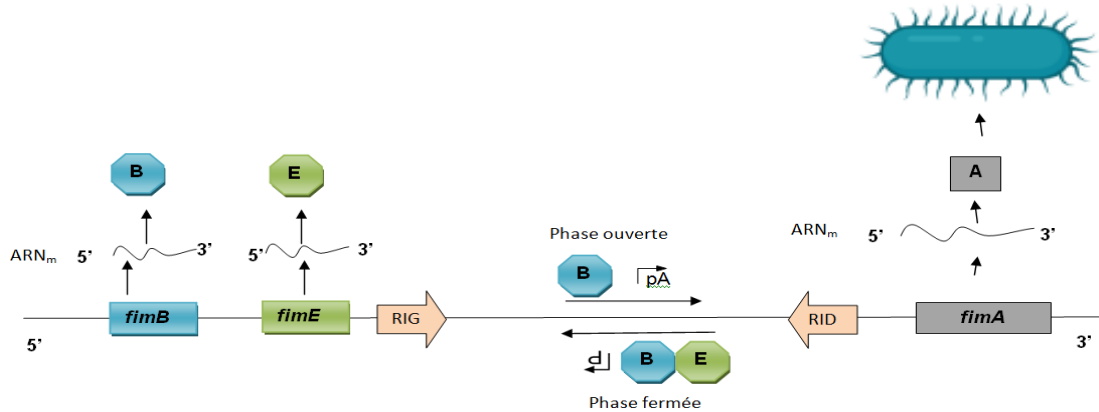
Figure 2.8. Organisation de l'élément interconvertible (en position ouverte et fermée)

Le promoteur des fimbriae de type 1 se trouve sur un élément interconvertible (EI) alternant entre les phases ouvertes et fermées. Ce dernier est bordé de régions inversées de 9 pb (RIG et RID) et contient les sites de fixation des régulateurs des fimbriae de type 1, i.e. FimB, FimE. Les deux recombinases FimB et FimE catalysent l'inversion de la phase ouverte à la phase fermée, bien que l'inversion de la phase fermée à la phase ouverte soit catalysée principalement par FimB. Abréviations : EI, élément interconvertible; RID, région inversée droite; RIG, région inversée gauche; p, promoteur de *fimA*. L'orientation de la flèche associée à pA indique l'orientation de la transcription. Adaptée de Schwan (2011).

2.4.2 Rôle de la variation de phase dans l'expression des fimbriae type 1

La variation de phase en général se réfère à un phénomène réversible entre une phase d'expression « tout ou rien » (ON / OFF), entraînant une variation du niveau d'expression d'une ou plusieurs protéines entre des cellules individuelles d'une population clonale (van der Woude & Baumler, 2004). Cette propriété permet à une bactérie de transiter entre deux états distincts, soit l'expression (phase ON) et la répression (phase OFF) d'un gène ou d'un complexe génétique. Ce phénomène est le résultat de différents mécanismes moléculaires sous-jacents, qui peuvent être identifié comme génétiques lorsqu'ils impliquent un changement de séquence d'ADN (recombinaison spécifique du site et phénomène d'insertion / excision) ou épigénétique lorsqu'ils impliquent un état de méthylation de l'ADN (Davidson & Surette, 2008). Dans une population clonale, après la division cellulaire, la majorité des cellules filles conserveront la phase d'expression de la cellule parentale, mais une minorité aura changé sa phase d'expression.

Chez les UPEC, la variation de phase conduit à une alternance entre les cellules exprimant les fimbriae (Phase-ON) et les cellules qui n'expriment pas ces derniers (Phase-OFF). Le site spécifique de recombinaison qui permet la variation de phase nécessite deux facteurs situés en

amont de *fimS*, codé par *fimB* et *fimE*. Les recombinases FimB et FimE ont 48% d'homologie d'acides aminés entre elles. Klemm (1986) a d'abord suggéré que FimB et FimE puissent agir indépendamment pour inverser l'élément *fimS*, soit de la phase ouverte à la phase fermée ou inversement, via les deux régions répétées inversées, RIG et RID. FimB peut se lier à l'élément *fimS* pour effectuer le changement de la phase ON à la phase OFF ou inversement (Fig. 2.8) (Gally *et al.*, 1996a; Kulasekara & Blomfield, 1999). En revanche, FimE se lie pour inverser *fimS* de la phase ON à la phase OFF (Fig. 2.8). FimE peut inverser l'EI *fimS* de la phase ON à OFF à une fréquence beaucoup plus élevée que FimB. De plus, FimE s'est avérée avoir une affinité de liaison plus élevée lorsque la région inversible est orientée en position ON, l'inversant ainsi préférentiellement en position OFF (Kulasekara & Blomfield, 1999). L'orientation de l'élément *fimS* dans la position fermée mène à la production de transcrits antisens à partir du promoteur de *fimA* (Schwan *et al.*, 1992). Dans de rares cas, FimE peut inverser *fimS* dans le sens contraire chez la souche *E. coli* MG1655 dans des conditions de croissance statique (Stentebjerg-Olesen *et al.*, 2000a).

La recombinaison assurée par FimB se produit à raison de 10^{-3} à 10^{-4} par cellule. Cependant, l'alternance assurée par FimE se produit plus souvent à une fréquence de 0,3 par cellule par génération (Blomfield *et al.*, 1991; Gally *et al.*, 1993).

Outre FimB et FimE, il existe trois autres recombinases qui pourraient affecter la variation de phase de l'élément *fimS* : IpuA (48% d'identité avec FimB), IpuB (49% d'identité avec FimB) et IpbA (55% d'identité avec FimB) (Bryan *et al.*, 2006a; Hannan *et al.*, 2008). Ces recombinases ont été découvertes par analyse de séquence du génome de la souche CFT073 en raison de leur haute homologie avec les gènes *fimB* et *fimE*.

Les recombinases IpuA et IbpA se lient à l'élément *fimS* et interviennent dans la variation de phase (Fig. 2.9). IpuA fonctionne comme FimB, ce qui permet une inversion dans l'une ou l'autre orientation, tandis qu'IpbA peut inverser *fimS* uniquement de la phase OFF à la phase ON. Par contre, ces trois recombinases ne sont pas présentes chez toutes les souches d'*E. coli* (Bryan *et al.*, 2006a; McClain *et al.*, 1993). HbiF est une autre recombinase qui peut inverser l'EI principalement de la phase OFF à la phase ON en l'absence de FimB et FimE. Ainsi, l'expression constitutive de HbiF a permis de verrouiller *fimS* en phase ouverte chez la souche *E. coli* YX101, une dérivée de la souche RS218 d'*E. coli* K1 causant la méningite (Stentebjerg-Olesen *et al.*, 1999). Il n'est pas clair dans quelles conditions environnementales de croissance ces recombinases affectent l'orientation de l'élément *fimS* (Schwan, 2011). L'expression de *fimB* et

fimE ainsi que leur activité dépendent de divers régulateurs et de diverses conditions environnementales.
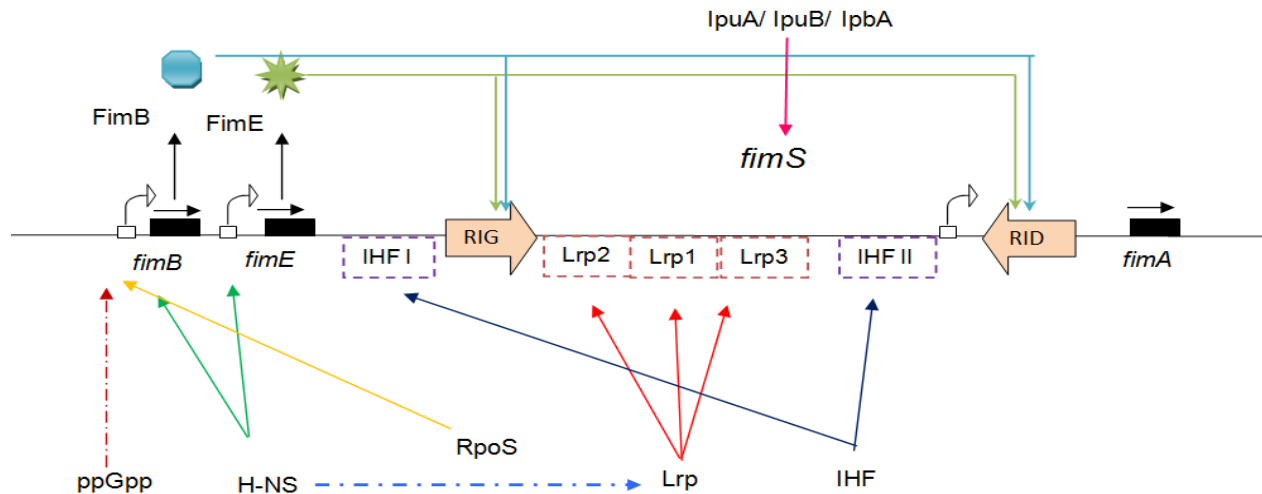
Figure 2.9. Modèle schématique d'action de quelques protéines et cofacteurs sur la régulation des fimbriae de type 1

Les sous-unités structurales des fimbriae sont codées par *fimA* et d'autres gènes en aval, qui sont transcrits lorsque l'EI *fimS* est en position ON. Les recombinases FimB et FimE se lient à RID / RIG et inversent l'EI. La protéine, H-NS, réprime l'expression des deux recombinases. Lrp stimule et inhibe l'inversion de *fimS* en fonction du site occupé (1, 2 ou 3), tandis que son expression est également réprimée par H-NS. IHF est requis pour toute variation de phase, il joue un rôle structurel au cours de l'inversion de phase par sa capacité à produire des courbures de l'ADN. L'accumulation de ppGpp active la transcription de *fimB*. Pour plus de détails, se référer à la section régulation de l'expression des fimbriae de type 1, adaptée de Schwan (2011).

2.4.3   Autres cofacteurs affectant la variation de phase

Bien que FimB et FimE soient des acteurs majeurs dans le contrôle de la variation de phase, plusieurs autres protéines affectent l'expression du fimbriae de type 1 à la fois en stimulant l'inversion de *fimS* directement ou indirectement en affectant l'expression de *fimB* ou *fimE.* En effet, l'expression de *fimS* est dépendante des cofacteurs IHF (Integration host factor), Lrp (Leucine-responsive protein) et H-NS (Histone-like protein). L'expression des recombinases est finement régulée pour permettre la recombinaison de la phase ouverte à la phase fermée. H-NS est un régulateur global impliqué dans la condensation de la chromatine bactérienne. Il contrôle la variation de phase de la région *fimS* directement et indirectement (Donato *et al.*, 1997; Schembri *et al.*, 1998; Schwan *et al.*, 2002a). Pour un effet potentiel direct, H-NS se lie aux

séquences adjacentes de l'élément inversible *fimS*, bloquant ainsi l'activité recombinase de FimB (Donato & Kawula, 1999).

La mutation de *hns* augmente sensiblement la transcription de *fimB* et par conséquent la fréquence de recombinaison de FimB (Donato *et al.*, 1997; Kawula & Orndorff, 1991). Cette inhibition prend place puisque H-NS se fixe en amont du site de fixation de FimB (RIG) au niveau de l'EI (Fig. 2.9), causant ainsi un encombrement stérique à ce site. Indirectement, H-NS réprime la transcription de *fimB* et *fimE*, influençant ainsi la position de l'élément *fimS*, ce qui affecterait la variation de phase (Bjarke Olsen & Klemm, 1994a; Olsen *et al.*, 1998). H-NS se lie, avec une grande spécificité, à la région promotrice de *fimB* (Fig. 2.9) (Donato & Kawula, 1999). De plus, la protéine SlyA active l'expression de *fimB* en déplaçant H-NS, annulant ainsi les effets inhibiteurs de H-NS (McVicker *et al.*, 2011). H-NS réprime également la transcription de *lrp* (Oshima *et al.*, 1995), ce qui affecterait à son tour l'inversion de l'élément *fimS*.

Plusieurs études ont démontré que IHF est nécessaire pour la variation de phase de *fimS* (Dorman & Higgins, 1987; Eisenstein *et al.*, 1987). IHF est une protéine à deux composants codés par *ihfA* et *ihfB* (Flamm & Weisberg, 1985; Miller & Friedman, 1980). Des sites de liaisons d'IHF ont été identifiés, appelé IHF I, entre RIG et l'extrémité 3' de *fimE*, et IHF II, près de la RID (Fig. 2.9) (Blomfield *et al.*, 1993). Des mutations dans *ihfA* ou *ihfB* verrouille la région *fimS* dans l'orientation ouverte ou fermée en diminuant la variation de phase promue par FimB (100 fois) et FimE (15000 fois) chez la souche MG1655 (Blomfield *et al.*, 1997a).

La protéine Lrp est une autre protéine qui affecte l'EI. Lrp est un régulateur global des gènes impliqués dans les fonctions métaboliques et dans la synthèse de fimbriae chez *E. coli* (Brinkman *et al.*, 2003a). La fixation de Lrp au niveau de l'IE est requise dans la variation de phase. La mutation du gène *lrp* entraîne une diminution de 100 fois de la fréquence de recombinaison de l'élément *fimS*, mais l'expression de *fimB* et *fimE* n'est que légèrement affectée (Blomfield *et al.*, 1993). De plus, des niveaux plus élevés de Lrp devraient inhiber directement la recombinaison de FimB. Les acides aminés leucine, isoleucine, valine et alanine interagissent avec Lrp et modifient sa liaison à *fimS* pour stimuler la variation de phase (Lahooti *et al.*, 2005; Roesch & Blomfield, 1998). En effet, l'activité recombinase de FimB est inhibée par les acides aminés à chaîne latérale (isoleucine, leucine, valine) et l'alanine via l'empêchement de l'appariement de Lrp au niveau de l'ADN (Fig. 2.9), ce qui a pour effet d'inhiber la variation de phase et de favoriser la positionnement de *fimS* en phase OFF (Lahooti *et al.*, 2005). Ainsi, Lrp se lie à trois sites distincts dans l'élément *fimS* qui sont plus proches du site RIG (Fig. 2.9). Lorsque les sites à forte affinité 1 et 2 sont mutés, la fréquence de recombinaison de l'EI diminue (Blomfield *et al.*, 1997a).

La liaison de Lrp au site à faible affinité 3 inhibe la recombinaison (Corcoran & Dorman, 2009). Bien que Lrp se lie à de multiples sites dans l'élément *fimS*, Lrp ne régule pas directement *fimB* et *fimE*.

L'appariement d'IHF et de Lrp au niveau de l'EI introduit des courbures de l'ADN pouvant atteindre 180°. La fixation d'IHF et de Lrp au niveau de l'EI devrait entraîner la formation d'une boucle en forme d'épingle à cheveux au niveau de l'ADN et la formation de cette boucle a pour effet de juxtaposer les RID et RIG et de ce fait, favoriser la recombinaison par FimB et FimE (Blomfield *et al.*, 1993; Blomfield *et al.*, 1997a). Lorsque Lrp et IHF sont présents à des niveaux insuffisants, H-NS se lie et maintient l'orientation en phase fermée.

L'alarmone guanosine tétraphosphate ppGpp est un second messager produit en cas de stress nutritionnel et initie l'adaptation physiologique globale (Potrykus & Cashel, 2008). Cette alarmone est liée à la régulation de plusieurs gènes chez *E. coli*, y compris l'opéron *fim*. Les mutants incapables de synthétiser ppGpp présentent une diminution de l'expression des fimbriae de type 1 par rapport à la souche sauvage, et ceci s'explique par un déficit dans la transcription de *fimB* (Aberg *et al.*, 2008). Étant donné que les fimbriae de type 1 sont essentiels à la colonisation de la vessie, et que celle-ci est carencée en nutriments, cet environnement est favorable à la production du ppGpp. Le ppGpp active le promoteur de *fimB* (Åberg *et al.*, 2008). Puisque *lrp* est également stimulé par le ppGpp (Landgraf *et al.*, 1996), la carence en acides aminés à chaîne ramifiée induit vraisemblablement des effets antagonistes sur l'expression de *fimB* (Lahooti *et al.*, 2005).

Une étude a mis en évidence le rôle de RpoS dans la régulation de l'expression des fimbriae de type 1. La transcription de *fimA* diminuerait lorsque les bactéries entrent en phase stationnaire de croissance. Le facteur sigma (σ) RpoS, qui est activé pendant la phase stationnaire, inhibe l'expression de fimbriae de type 1 en réprimant la transcription de *fimB* (*Dove et al., 1997*). Ceci contredit l'étude menée par Old and Duguid (1970a), qui suggérait que l'expression des fimbriae type 1 soit favorisée en phase stationnaire de croissance lorsque les bactéries étaient cultivées en statique sur une période de 24 à 48h (Old & Duguid, 1970a). D'autre part, l'expression de l'opéron *fim* est maximale lorsque les bactéries entrent en phase stationnaire de croissance (Aberg *et al.*, 2006).

Le glucose agit comme un répresseur catabolique en augmentant les concentrations internes d'AMPc, ce qui permet de plus grandes interactions avec sa protéine réceptrice, CRP. Le complexe CRP-AMPc contrôle un réseau important de gènes chez les bactéries à Gram négatifs et est associé à l'état énergétique de la cellule (Göransson *et al.*, 1989). Pour l'expression du

fimbriae de type 1, le rôle de l'AMPc et du glucose reste opaque. Les premières études ont démontré que l'AMPc affectait l'expression du fimbriae dans certaines souches d'*E. coli* (Eisenstein *et al.*, 1981). Cependant, Eisenstein and Dodd (1982) dans une étude ultérieure ont démontré que le glucose n'a aucun effet sur l'expression du fimbriae, même lorsqu'il a été ajouté avec de l'AMPc exogène ou lorsqu'il a été testé chez des mutants de l'adénylate cyclase (*cya*). Il est à noter que certaines études ont été effectuées avec la souche *E. coli* CSH50, qui a une mutation *fimE :: IS1* (Blomfield *et al.*, 1991), de sorte que le rôle de la répression des catabolites soit resté flou jusqu'à récemment. Une étude plus récente de Müller *et al.* (2009a) a démontré que le complexe CRP-AMPc réprime directement le promoteur *fimA* et affecte indirectement la variation de phase en limitant l'inversement de la phase fermée à la phase ouverte, médié par la recombinase FimB, en phase logarithmique de croissance. Cependant, la répression des fimbriae de type 1 par CRP-cAMP est atténuée pendant la phase stationnaire de croissance, ce qui concorde avec une implication des fimbriae de type 1 dans l'adaptation au stress en favorisant la croissance du biofilm ou l'entrée dans les cellules hôtes. Une baisse de la concentration intracellulaire d'AMPc, due à une croissance en présence de glucose, augmente le pourcentage de cellules exprimant les fimbriae dans la population bactérienne (Müller *et al.*, 2009a).

Les protéines SlyA et RcsB activent la transcription de *fimB*. Le régulateur SlyA est impliqué dans l'activation du gène fimB (McVicker *et al.*, 2011), mais les conditions de croissance qui favoriseraient l'expression de *slyA* n'ont pas été déterminées. RcsB fait partie du système de régulation à deux composants RcsC/RcsB (Majdalani & Gottesman, 2005). RcsB influence l'expression du fimbriae de type 1 en contrôlant la transcription *fimB* et *fimE* (Schwan *et al.*, 2007). En effet, dans des conditions de croissance à pH neutre et faible osmolalité, RcsB semble activer *fimB.* Ainsi, à pH neutre, RcsB favorise la transcription de *fimA* soit en augmentant la transcription *fimB* (milieu faible en sel), soit en diminuant la transcription *fimE* (milieu riche en sel). Également, RcsC peut influencer le positionnement de l'EI dans des conditions de croissance à forte teneur en sel (Schwan *et al.*, 2007).

2.4.4 Effet de l'environnement sur la variation de phase

L'expression des fimbriae de type 1 est sensible aux variations environnementales rencontrées par les bactéries, telles que la température, l'osmolarité, les conditions de culture, la présence de certains acides aminés et le stress.

Les voies urinaires humaines ou murines sont un environnement dynamique. Dans le tractus urinaire inférieur, il existe de nombreux récepteurs de mannose pour l'attachement des UPEC

exprimant les fimbriae de type 1 (Virkola *et al.*, 1988). La température dans les voies urinaires est d'environ 37°C, pourtant les fimbriae de type 1 sont préférentiellement exprimés lorsque les bactéries se retrouvent au niveau de la vessie (Snyder *et al.*, 2004a). Plusieurs études contradictoires démontrent le rôle de la température sur l'expression des fimbriae de type 1. Par exemple, le groupe de Dorman (1992) ont démontré que l'expression des fimbriae de type 1 est favorisée lorsque les bactéries croissent à 30°C, comparé à 37°C. Paradoxalement, l'expression des fimbriae est induite au niveau de la vessie où la température de l'urine se situe aux environs de 37°C (Snyder *et al.*, 2004a; Snyder *et al.*, 2005). D'autres études ont démontré que l'inversion du promoteur *fim*S de la phase ouverte à la phase fermée est biaisée chez les bactéries poussées en bouillon à 20°C (Olsen *et al.*, 1998). Cependant, un autre groupe a démontré que l'expression de *fimB* est favorisée lorsque les bactéries se trouvent à des températures se situant entre 37 et 41°C et qu'en contrepartie, *fimE* est réprimé à ces températures (Gally *et al.*, 1993).

Les voies urinaires représentent différentes niches de croissance, et il est connu que les conditions environnementales spécifiques telles que la température, le pH et l'osmolarité peuvent affecter l'orientation du promoteur *fimS*. Par exemple, la combinaison bas pH et forte osmolarité a un effet synergique sur l'expression des gènes *fim*. FimB est favorisée dans un environnement à pH neutre et faible osmolarité (Schwan *et al.*, 2002a). Ainsi, dans les conditions de pH légèrement acide avec une faible salinité trouvée sur la surface vaginale, des protéines telles que SlyA ou RcsB peuvent activer FimB et empêcher H-NS de se lier (Tableau 2.2), permettant ainsi l'expression des fimbriae de type 1 (McVicker *et al.*, 2011; Schwan *et al.*, 2007). Cependant, l'expression de *fimE*, donc l'inhibition de l'expression des fimbriae de type 1, est favorisée lorsque les bactéries sont cultivées en conditions de haute osmolarité avec un pH acide (conditions retrouvées dans les reins) (Schwan *et al.*, 2002a). Une expression plus faible du fimbriae de type 1 a été observée dans les cellules UPEC trouvées dans un environnement à pH 5,5 par rapport à un environnement à pH 7,0 (Schwan *et al.*, 2018). Les voies urinaires humaines sont baignées dans l'urine avec un pH compris entre 5,0 et 8,0. L'urine humaine peut également affecter l'expression du fimbriae de type 1 (Hagan *et al.*, 2010; Schwan *et al.*, 2002a). Il semblerait que la régulation de *fim* sous stress osmotique s'effectue via le système de régulation à deux composants EnvZ/OmpR. En effet, à une osmolarité élevée, il y a une augmentation du niveau d'OmpR phosphorylée, qui à son tour se lie aux séquences d'ADN et active ou réprime la transcription des gènes (Tableau 2.2). Le mutant *ompR* semble induire une dérépression de *fimB* dans un milieu à forte osmolarité et pH faible. L'OmpR non phosphorylé se lie au promoteur de *fimB* pour réprimer sa transcription (Rentschler, 2010).

Tableau 2.2. Régulateurs influençant l'expression des recombinases *fimB* et *fimE*

	fimB	*fimE*	Références
SylA	+		(McVicker *et al.*, 2011)
RcsB	+		(Schwan *et al.*, 2007)
H-NS	-	-	(Donato *et al.*, 1997)
OmpR	-		(Rentschler, 2010)
RpoS	-		(Dove *et al.*, 1997)
CpxRA			(Matter *et al.*, 2018)
Pst	-	+	(Crepin *et al.*, 2012)
NagC	-		(El-Labany *et al.*, 2003; Sohanpal *et al.*, 2007)
NanR	-		(El-Labany *et al.*, 2003; Sohanpal *et al.*, 2007)

Le sigle « + » signifie induction tandis que le sigle « – » signifie répression

Les infections à UPEC sont des infections ascendantes, par conséquent, la présence de flagelles sur les UPEC permettrait aux bactéries d'atteindre les reins. L'expression des flagelles peut désactiver de façon coordonnée l'expression des fimbriae de type 1 (Lane *et al.*, 2007a). À mesure que les bactéries remontent vers les reins, le pH diminue et l'osmolalité augmente. À ce moment, H-NS peut se lier et réprimer à la fois *fimB* et *fimE* verrouillant ainsi l'élément *fimS* en position fermée (Tableau 2.2), par conséquent les UPEC deviennent afimbriaire. Ensuite, les UPEC passent en phase stationnaire, où la transcription du gène *rpoS* est activée (Dove *et al.*, 1997). L'environnement acide à osmolalité élevée entraînerait une plus grande traduction des transcrits *rpoS* et par conséquent mène à la production de la protéine RpoS, ce qui provoque la répression de la transcription de *fimB*. Ces observations peuvent donc expliquer, en partie, la cascade de régulation des fimbriae de type 1 observées lors d'une infection, *i.e.* expression des fimbriae de type 1 dans la vessie et leur inhibition dans les reins. Les différences dans l'expression

du fimbriae de type 1 chez les bactéries trouvées dans chaque organe peuvent être partiellement attribuées à moins de récepteurs du mannose dans le rein par rapport à la vessie. Il est évident que la régulation négative du fimbriae de type 1 dans les reins pourrait être avantageuse pour les bactéries en raison que les fimbriae sont immunogènes.

Nos travaux antérieurs ont démontré que la délétion du gène *treA* codant pour une tréhalase périplasmique chez la souche APEC MT78 conduit à une augmentation de la résistance au stress osmotique causé par l'urée et à une diminution de l'expression des fimbriae de type 1, et par conséquent une réduction de la colonisation de l'uroépithélium murin (Pavanelo *et al.*, 2018). *treA* code la tréhalase périplasmique qui est une protéine impliquée dans le catabolisme du tréhalose. Le tréhalose peut être métabolisé et utilisé directement en tant que source de carbone ou, sous des conditions de stress osmotiques, il peut servir d'agent osmoprotecteur. L'effet de la suppression de *treA* sur la production des fimbriae de type 1 est probablement dû à un effet post-transcriptionnel ou post-traductionnel (Pavanelo *et al.*, 2018).

Le système de réponse Cpx affecte l'expression du fimbriae de type 1 chez la souche APEC MT78 (Matter *et al.*, 2018). Le système de régulation à deux composants CpxRA répond au stress de la membrane externe et détecte les protéines mal repliées dans le périplasme bactérien (Vogt & Raivio, 2012). Chez le mutant Δ*cpxA*, la transcription de *fimA* est significativement réprimée. La phosphorylation de CpxR par la voie acétate kinase (AckA) et la phosphotranscétylase (Pta) affecte négativement l'expression du fimbriae de type 1 chez la souche Δ*cpxA*. En effet, CpxR phosphorylé se lie directement au promoteur *de fimA*, verrouillant ainsi la région *fimS* du fimbriae de type 1 dans l'orientation phase fermée (Matter *et al.*, 2018).

D'autres études ont démontré que la mutation du groupe de gènes *pst* codant pour le système de transport spécifique au phosphate (Pst) affecte plusieurs traits de virulence, entre autres les fimbriae de type 1. En effet, l'inactivation du système Pst active de manière constitutive le système de régulation à deux composants PhoBR et atténue la virulence des bactéries pathogènes (Bertrand *et al.*, 2010a; Crepin *et al.*, 2012; Crépin *et al.*, 2008). Chez la souche UPEC CFT073, l'atténuation par inactivation de *pst* est principalement due à la répression des fimbriae de type 1. Cette répression est concomitante avec l'expression différentielle des régulateurs de ces fimbriae, soit les recombinases *fimB*, *fimE*, *ipuA* et *ipbA* (Tableau 2.2) (Crepin *et al.*, 2012). Ainsi, la diminution de l'expression des fimbriae de type 1 dans un mutant *pst* est concomitante avec l'augmentation de l'expression du gène *yaiC*. La délétion du gène *yaiC* dans un mutant *pst* restaure partiellement l'expression des fimbriae de type 1. De plus, le regain de l'expression des fimbriae de type 1 dans le double mutant Δ*pst*Δ*yaiC* augmente l'adhérence aux cellules de la

vessie médiée par les fimbriae de type 1, de même que la souche sauvage. Comme *yaiC* est induit dans le mutant *pst* et sa délétion restaure l'expression des fimbriae de type 1, *yaiC* pourrait être considéré comme un répresseur de ces fimbriae (Crépin *et al.*, 2017).

Trois autres protéines ont des effets inexpliqués sur l'expression du fimbriae de type 1: OmpX, IbeA et IbeT. Par exemple, l'inactivation de *ompX*, codant pour une protéine de la membrane externe, a provoqué une surexpression de *fimA* (Otto & Hermansson, 2004). Une surproduction de OmpX est connue en tant que réponse à des stress environnementaux. Par conséquent, la perte d'OmpX modifierait la surface cellulaire, ce qui affecterait les interactions cellule-surface. Il est probable qu'OmpX puisse agir indirectement pour réguler l'expression du fimbriae de type 1. Une autre protéine, IbeA, influence l'expression du fimbriae de type 1. En effet, la délétion du gène *ibeA*, chez la souche APEC BEN2908, a provoqué une diminution de l'expression de *fimA*, ainsi qu'une sous-expression de *fimB* et *fimE*. Également, l'inactivation d'*ibeT* provoque une diminution du fimbriae de type 1 en raison de l'orientation OFF de l'EI *fimS* (Cortes *et al.*, 2008). Le fonctionnement de chacune de ces protéines pour réguler les gènes *fim* n'a pas été déterminé. Il est à noter que IbeA est impliquée dans la résistance au stress oxydatif induit par le H_2O_2 (Fléchard *et al.*, 2012). Il n'est pas surprenant que la modulation du stress puisse affecter la production des fimbriae de type 1 et d'autres facteurs de virulence. Par exemple, le gène *yeaR* est surexprimé en IBC et il contribue à la résistance au stress oxydatif. Ainsi, l'inactivation de *yeaR* chez la souche UTI89 semble causer une diminution de l'expression de *fimA* (Conover *et al.*, 2016).

Durant les ITU, la production des fimbriae de type 1 par les UPEC induit une réponse inflammatoire (Malaviya *et al.*, 1996), conduisant à des niveaux élevés d'acide sialique et de N-acétylglucosamine dans l'urine qui, à leur tour, activeront deux protéines régulatrices qui inhibent la transcription de *fimB*. Les deux protéines, NagC (a N-acetylglucosamine-6P-responsive protein) et NanR (a sialic acid-responsive protein), liées à l'acide sialique et au catabolisme de la N-acétylglucosamine (Plumbridge & Kolb, 1991; Plumbridge & Vimr, 1999), se lient au promoteur de *fimB* (Tableau 2.2) (El-Labany *et al.*, 2003; Sohanpal *et al.*, 2007). La libération d'acide sialique serait une étape importante dans l'activation de la réponse inflammatoire. Par conséquent, il est suggéré qu'*E. coli* peut reconnaître l'acide sialique libre comme un indicateur d'inflammation et que l'acide sialique libre peut inactiver l'expression de *fimB*, empêchant ainsi l'adhérence bactérienne et par conséquent permettant une évasion du système immunitaire.

Le manque d'oxygène diminue la production de fimbriae connues pour être critiques pour l'adhérence aux cellules de la vessie. Ainsi, l'expression des fimbriae de type 1 est réduite en

absence totale d'O$_2$ chez la souche UTI89 (Floyd *et al.*, 2015a). L'étude de Hung et al. a révélé que les bactéries sur la couche exposée à l'air d'un biofilm pelliculaire flottant sont morphologiquement distinctes de celles à l'interface liquide (Hung *et al.*, 2013). L'O$_2$ est l'accepteur terminal d'électron permettant la formation d'un biofilm plus robuste. Chez les UPEC, la formation de biofilm est diminuée en condition anoxique. Ainsi, il semble que l'O$_2$ améliore la production de biofilm et que donc les UPEC se retrouvent dans des conditions idéales à la formation de ces biofilms dans les vessies (Floyd *et al.*, 2015; Eberly *et al.*, 2017). Des études antérieures ont rapporté que les souches UPEC dépendent du cycle TCA pendant l'infection (Alteri *et al.*, 2009a) et que les perturbations du cycle TCA conduisent à une répression de l'expression des gènes *fim* et à l'abrogation de la formation des IBC (Hadjifrangiskou *et al.*, 2011).

3   CONTEXTE DE RECHERCHE

Les pathotypes d'*Escherichia coli* uropathogènes (UPEC) provoquent différents types d'infections urinaires. Les UPEC possèdent un répertoire diversifié de facteurs de virulence qui favorisent l'apparition des ITU. Non seulement la présence et la contribution des gènes de virulence, mais aussi le niveau d'expression des gènes détermine la forme de l'infection. L'adhérence aux cellules épithéliales de l'hôte est une étape cruciale dans la pathogenèse des UPEC. L'un des facteurs de virulence les plus importants impliqués dans l'attachement est les fimbriae de type 1. Au cours de l'infection, les bactéries doivent réguler de façon coordonnée l'expression de leurs gènes en réponse aux stimuli environnementaux.

4   PROBLEMATIQUE

Les fimbriae de type 1 sont produits à la fois par des souches commensales et pathogènes d'*E. coli*. Les fimbriae de type 1 aident à la virulence des souches ExPEC à différents stades de leur pathogenèse. Ces fimbriae sont importants pour l'urovirulence et déclenchent l'association des UPEC avec des cellules de la vessie en se liant aux récepteurs mannosylés permettant aux bactéries de s'établir au sein des tissus de l'hôte.

Les fimbriae de type 1 sont également impliqués dans la modulation des voies de signalisation des cellules hôtes, l'invasion bactérienne dans les cellules hôtes et la formation de biofilm. La compréhension du mécanisme de régulation des fimbriae de type 1 permettrait le développement d'approches visant à contrôler les infections causées par les ExPEC.

Hypothèse

Première hypothèse : des facteurs régulent l'expression de fimbriae de type 1, en affectant le taux de variation de phase « ON/OFF », l'expression ou la stabilité de l'ARNm (transcrit).

Deuxième hypothèse : ces régulateurs sont reliés directement ou indirectement à l'expression différentielle des recombinases FimB, FimE, IpuA et IpbA.

Par conséquent, l'altération de l'expression des fimbriae de type 1 influence la pathogénicité de CFT073.

4.1 Les objectifs

L'objectif principal de ce projet de thèse est d'identifier des nouveaux régulateurs qui pourraient être impliqués dans l'expression de fimbriae de type 1 et qui affectent le taux de variation de phase « ON/OFF ».

I. **Identifier des nouveaux régulateurs impliqués dans l'expression des fimbriae de type 1 (Article 1)**

Nous avons développé un système rapporteur transcriptionnel luciférase (système *lux*) à simple copie fusionnée à la région promotrice de l'opéron *fim*, qui est situé sur un élément inversible, *fimS*. L'utilisation du système *lux* permet de mesurer l'activité des promoteurs et d'autres éléments régulateurs de la transcription, ainsi que les effets des activateurs et des inhibiteurs. Dans ce contexte, nous avons généré une banque de mutants aléatoire par transposition chez la souche CFT073. Nous avons par la suite, criblé les mutants générés par le transposon Tn*10* pour le niveau de transcription de l'opéron *fim* suivi de séquençage à haut débit afin d'identifier des gènes qui, lorsqu'ils sont altérés, affecter l'expression des fimbriae de type 1.

II. **Déterminer le rôle des facteurs identifiés dans la virulence en utilisant un test phénotypique et des modèles d'infection de souris (Articles 1 & 2)**

Sur la base des données de séquençage, montrant l'effet de l'interruption de plusieurs régulateurs sur l'expression du fimbriae de type 1, nous avons étudié :

II.1. Le rôle de *yqhG*, codant pour une protéine de fonction inconnue, dans l'expression des fimbriae de type 1, le stress et la pathogenèse de la souche CFT073

II.2. L'importance du petit ARN non-codant RyfA dans la virulence des souches ExPEC

5   ARTICLE 1: Identifying genes that alter expression of type 1 fimbriae in uropathogenic *Escherichia coli*

yqhG Contributes to Oxidative Stress Resistance and Virulence of Uropathogenic *Escherichia coli* and Identification of Other Genes Altering Expression of Type 1 Fimbriae

yqhG contribue à la résistance au stress oxydatif et à la virulence d'*Escherichia coli* uropathogène et à l'identification d'autres gènes altérant l'expression des fimbriae de type 1

Auteurs : **Hicham Bessaiah**[1,2], Pravil Pokharel[1,2], Hajer Habouria[1,2], Sébastien Houle[1,2], Charles M. Dozois[1,2*]

[1]INRS-Institut Armand-Frappier, Laval, Québec, Canada

[2]CRIPA-Centre de recherche en infectiologie porcine et avicole, Saint-Hyacinthe, Québec, Canada

Recherche publiée dans le cadre de la 1ère partie de mon doctorat

Contribution des auteurs :

J'ai effectué presque la totalité des expérimentations. J'ai écrit la totalité de l'article, qui a été corrigé par mon directeur et mes collaborateurs. **Pravil Pokharel** et **Hajer Habouria :** Contribué aux infections de souris et l'interprétation des résultats. **Sébastien Houle :** Assistance technique avec les infections dans le modèle murin d'UTI. **Charles M Dozois :** Planification et conception de l'étude, analyse et discussion des résultats, commentaires et révision du manuscrit.

*Corresponding author: Charles M. Dozois

INRS-Institut Armand-Frappier 531 boul des Prairies Laval, Quebec CANADA, H7V 1B7
E-mail : Charles.dozois@iaf.inrs.ca

5.1   Résumé en français

Les infections du tractus urinaire (ITU) sont des infections bactériennes courantes et la grande majorité des ITU sont causées par des souches d'*Escherichia coli* pathogènes extra-intestinales (ExPEC) appelées *E. coli* uropathogènes (UPEC). La colonisation des voies urinaires humaines par l'UPEC est médiée par des facteurs de virulence sécrétés ou exposés en surface comme : les toxines, les systèmes de transport du fer et les adhésines telles que les fimbriae de type 1 (pili). Afin d'identifier les facteurs impliqués dans l'expression des fimbriae de type 1, nous avons développé un système rapporteur transcriptionnel à luciférase (système *lux*) à simple copie fusionné à la région promotrice de l'opéron *fim, fimS*. Cette fusion a été insérée dans le génome de la souche UPEC de référence CFT073 au site *att*Tn*7*. La souche possédant la fusion *fimS-lux* a été utilisée pour générer une banque de mutants par transposition aléatoire du transposon Tn*10*, couplée à un séquençage à haut débit pour identifier les gènes qui affectent l'expression des fimbriae de type 1. Les sites d'insertion d'un transposon étaient liés à des gènes impliqués dans la synthèse des protéines, le métabolisme énergétique, l'adhérence, la régulation transcriptionnelle et le transport. Nous avons montré que YqhG, une protéine prédite pour être périplasmique, est l'un des médiateurs importants qui contribuent à l'activation de l'expression des fimbriae de type 1 chez la souche UPEC CFT073. La délétion de *yqhG* altère l'expression des fimbriae de type 1 et diminue significativement la capacité du mutant *yqhG* à coloniser le tractus urinaire murin. La répression des fimbriae de type 1 est concomitante avec la position OFF du promoteur *fimS*. De plus, le mutant Δ*yqhG* est plus mobile que la souche WT et est également plus sensible au peroxyde d'hydrogène. En somme, la délétion de *yqhG* atténue la virulence dans le modèle murin d'infection urinaire, en raison d'une diminution de la production de fimbriae de type 1 et d'une plus grande sensibilité au stress oxydatif.

5.2   Abstract

Urinary tract infections (UTIs) are common bacterial infections and the vast majority of UTIs are caused by extraintestinal pathogenic *Escherichia coli* (ExPEC) strains referred to as uropathogenic *E. coli* (UPEC). Successful colonization of the human urinary tract by UPEC is mediated by secreted or surface exposed virulence factors - toxins, iron transport systems, and adhesins such as type 1 fimbriae (pili). To identify factors involved in the expression of type 1 fimbriae, we constructed a chromosomal transcriptional reporter consisting of *lux* under the control of the fimbrial promoter region, *fimS* and this construct was inserted into the reference UPEC strain CFT073 genome at the *att*Tn*7* site. This *fimS* reporter strain was used to generate

a Tn*10* transposon mutant library, coupled with high-throughput sequencing to identify genes that affect the expression of type 1 fimbriae. Transposon insertion sites were linked to genes involved in protein fate and synthesis, energy metabolism, adherence, transcriptional regulation, and transport. We showed that YqhG, a predicted periplasmic protein, is one of the important mediators that contribute to the decreased expression of type 1 fimbriae in UPEC strain CFT073. The Δ*yqhG* mutant had reduced expression of type 1 fimbriae and a decreased capacity to colonize the murine urinary tract. Reduced expression of type 1 fimbriae correlated with an increased bias for orientation of the *fim* switch in the OFF position. Interestingly, the Δ*yqhG* mutant was more motile than the WT strain and was also significantly more sensitive to hydrogen peroxide. Taken together, loss of *yqhG* may decrease virulence in the urinary tract due to a decrease in production of type 1 fimbriae and a greater sensitivity to oxidative stress.

5.3   Introduction

Urinary tract infections (UTIs) can occur throughout the urinary tract within the urethra, bladder, ureters, or kidneys. UTIs are a common infectious disease with over 150 million cases documented worldwide each year (Foxman, 2014; Stamm & Norrby, 2001). Furthermore, the overwhelming majority of uncomplicated UTI cases (≥80%) are caused by extraintestinal pathogenic *Escherichia coli* (ExPEC), referred to as uropathogenic *E. coli* (UPEC) (Ronald, 2002), which can belong to a diversity of phylogenetic groups or sequence types (Chen *et al.*, 2013; Russo & Johnson, 2000). An estimated 50% of women experience at least one UTI during their life, and up to a quarter of those women are prone to recurrent UTIs (Foxman, 2002). Adherence of UPEC to host cells is a key event in initiating UTI pathogenesis and is important for overcoming strong urine flow, and to promote urinary tract colonization (Flores-Mireles *et al.*, 2015a; Ulett *et al.*, 2013).

Fimbriae (pili) are filamentous structures that can mediate adherence of bacteria to host cell receptors (Mulvey *et al.*, 1998; Nielubowicz & Mobley, 2010). For instance, type 1 fimbriae are critical for colonization of the bladder by UPEC (Gunther IV *et al.*, 2002), to directly stimulate UPEC invasion into epithelial cells and aid in formation of intracellular reservoirs that may contribute to recurrent infection (Mysorekar & Hultgren, 2006). Type 1 fimbriae encoded by the *fimAICDFGH* (*fim*) genes, are one of the best-characterized UPEC chaperone-usher fimbriae. These fimbriae are produced by most *E. coli* strains including UPEC (Buchanan *et al.*, 1985; Sivick & Mobley, 2010). The *fimA* gene encodes the type 1 major fimbrial subunit and the tip-located adhesin, encoded by *fimH*, mediates binding to α-d-mannosylated receptors, such as

uroplakins, which are abundant in the bladder and other host surfaces containing mannosides (Connell *et al.*, 1996; Wu *et al.*, 1996). The *fim* promoter is located on a 314-bp invertible DNA promoter element (*fimS*), the orientation of which determines the transcriptional status (ON or OFF) (Abraham *et al.*, 1985b; Bjarke Olsen & Klemm, 1994b). The switching orientation of *fimS* is controlled by two recombinases. FimB, which promotes inversion in both orientations, and FimE, which mediates the switching from phase-on to phase-off (Gally *et al.*, 1996b; Klemm, 1986b). Two additional recombinases, IpuA and IpbA, present in UPEC strain CFT073 can also mediate switching of the invertible element independent of FimB and FimE (Bryan *et al.*, 2006b). Regulation of *fim* genes is affected by multiple environmental factors (including pH, osmolarity, temperature and oxygen levels) and at least three regulatory proteins are directly implicated (Lrp, IHF, and H-NS) (Unden & Kleefeld, 2004).

To establish a UTI, UPEC strains must resist environmental stresses in the bladder and kidneys including pH stress and wide fluctuations in osmolarity (Cahill *et al.*, 2003; Culham *et al.*, 2001). The high osmolality, high urea concentration, acidic pH and organic acids in urine can limit the growth and survival of *E. coli* within the urinary tract (Mulvey *et al.*, 2000). Thus, an important aspect of UPEC virulence is the capacity to resist high osmolality and the denaturing effects of urea, and rapidly adapt to changes and stress encountered in these niches during establishment of the infection.

Previously, we showed that interference with phosphate homeostasis decreased the expression of type 1 fimbriae in strain CFT073 and attenuated UPEC virulence (Crépin *et al.*, 2012b). The phosphate-specific transport (Pst) system negatively regulates the activity of the two-component signal transduction system PhoBR and also transports inorganic phosphate. Inactivation of the Pst system results in constitutive activation of PhoBR regardless of environmental phosphate availability (Wanner, 1996). As such, a *pst* mutant responds as if it is always under phosphate-limiting conditions. In UPEC, we showed that decreased virulence of a *pst* mutant is largely due to reduced expression of type 1 fimbriae. In avian pathogenic *E. coli* (APEC), an altered membrane homeostasis was also observed in a *pst* mutant (Lamarche & Harel, 2010) and caused increased sensitivity to acid, cationic antimicrobial peptides, and serum (Bertrand *et al.*, 2010b; Crépin *et al.*, 2008; Lamarche *et al.*, 2005).

In order to identify genes affecting the expression of type 1 fimbriae, we constructed a transcriptional luciferase (*lux*) reporter consisting of *lux* under the control of the *fimS* invertible promoter and this construct was inserted into the CFT073 genome at the *att*Tn*7* site. This *fimS* reporter containing strain was used to generate a Tn*10* transposon mutant library, coupled with

high-throughput sequencing to identify the location of transposon insertions that altered the expression of type 1 fimbriae. In this report, we show that YqhG is one of the important mediators that contribute to decreased expression of type 1 fimbriae in UPEC strain CFT073. Our results demonstrated that the deletion of *yqhG* in CFT073 reduced the expression of type 1 fimbriae and reduced urinary tract colonization of the *yqhG* mutant in the murine model. We also examined whether deletion of *yqhG* as well as the *pst* system also reduced resistance to environmental stresses, suggesting that altered expression of type 1 fimbriae can be linked to changes in bacterial adaptation to environmental stresses such as oxidative or osmotic stress.

5.4   Materials and Methods

Bacterial strains, growth conditions and plasmids

E. coli strains and plasmids used in this study are listed in Table 5.1. *E. coli* CFT073 was isolated from the blood and urine of a patient with acute pyelonephritis (Mobley *et al.*, 1990). Bacteria were routinely grown in lysogeny broth (LB) (Alpha Bioscience, Baltimore, MD) at 37°C and in human urine. Urine was obtained from healthy female volunteers, 20 to 40 years old, with no occurrence of a UTI or antibiotic use within the last 2 months prior to collection. A protocol for obtaining biological samples from human donors was reviewed and approved by the ethics committee – Comité d'éthique en recherche (CER 19-507) of INRS. Urine was immediately filter sterilized (0.2-μm pore size), pooled, and frozen at −80°C and used within 2 weeks of sampling. Antibiotics and reagents when required were added at the following concentrations: kanamycin, 50 μg/ml; ampicillin, 100 μg/ml; chloramphenicol 30 μg/ml and diaminopimelic acid (DAP), 50 μg/ml.

Table 5.1. Bacterial strains and plasmids used in this study

Strain or plasmid	Relevant characteristics	Reference or source
Strains		
CFT073	UPEC wild-type pyelonephritis strain (O6:K2:H1)	(Mobley *et al.*, 1990) (Welch *et al.*, 2002)

QT1324	CFT073 Δ*oxyR*::Km; Km^r	(Crépin *et al.*, 2012b)
QT1911	CFT073 Δ*pstSCA*::FRT	(Crépin *et al.*, 2012b)
QT2087	MGN-617 + pLOF/Km; Apr, Km^r	(Crépin *et al.*, 2017)
QT2117	QT1911:: Tn*7*T-Gm::*pstSCA*; Gm^r	(Crépin *et al.*, 2012b)
QT2138	CFT073 Δ*fimAICDFGH*::km; Km^r	(Crépin *et al.*, 2012b)
QT2496	CFT073 + pSTNSK, Km^r	(Crépin *et al.*, 2012a)
QT4791	χ7213 + pGP-Tn*7*-Cm-*PfimA L-ON luxCDABE*, Ap^r, Cm^r, Km^r	This study
QT4792	χ7213 + pGP-Tn*7*-Cm-*PfimA L-ON luxCDABE*, Ap^r, Cm^r, Km^r	This study
QT4793	χ7213 + pGP-Tn*7*-Cm-*PfimA* phase variable *luxCDABE*, Apr, Cm^r, Km^r	This study
QT4794	QT2496::Tn*7*T-Cm::*PfimA L-ON luxCDABE*, Cm^r	This study
QT4795	QT2496::Tn7T-Cm::*PfimA-L-OFF luxCDABE*, Cm^r	This study
QT4796	QT2496::Tn*7*T-Cm::*PfimA* phase variable *luxCDABE*, Cm^r	This study
QT4976	CFT073 Δ*pstSCA*::FRT +pSTNSK, Km^r	This study
QT5018	QT4976::Tn*7*T-Cm- *PfimA* phase variable *luxCDABE*, Cm^r	This study
QT5134 (BW25123)	*E. coli* BW25123, *yqhG*::Km	(Baba *et al.*, 2006)

QT5178	CFT073 Δ*yqhG*::FRT	This study
QT5235	QT5178::Tn*7*T-Cm::*yqhGH*, Cm^r	This study
χ7213 (MGN-617)	thi thr leu tonA lacY glnV supE Δ*asdA4* *recA*::RP4 2-Tc::Mu [λpir], Km^r	(Kaniga *et al.*, 1998)
Plasmids		
pCP20	FLP helper plasmid Ts replicon; Ap^r Cm^r	(Datsenko & Wanner, 2000)
pGP-Tn7-Cm	pGP-Tn7-FRT:: Cm, Ap^r, Cm^r	(Crépin *et al.*, 2012a)
pSTNSK-	pST76-K::*tnsABCD*, Km^r	(Crépin *et al.*, 2012a)
pIJ461	pGP-Tn7-Cm::*luxCDABE* ; Ap^r,Cm^r	This study
pIJ514	pGP-Tn7-Cm::*luxCDABE* ;rbs Ap^r,Cm^r	This study
pIJ516	pGP-Tn7-Cm ::*PfimA L-ON luxCDABE*, Ap^r, Cm^r	This study
pIJ517	pGP-Tn7-Cm::*PfimA-L-OFF luxCDABE*, Ap^r, Cm^r	This study
pIJ518	pGP-Tn7-Cm ::*PfimA* phase variable *luxCDABE*, Ap^r,Cm^r	This study
pIJ543	pGP-Tn7-Cm::*yqhGH*, Ap^r, Cm^r	This study
pKD3	Template plasmid for the amplification of the *cat* gene bordered by FRT sites	(Datsenko & Wanner, 2000)
pKD4	Template plasmid for the amplification of the *km* cassette bordered by FRT sites	(Datsenko & Wanner, 2000)

pKD46	λ-Red recombinase plasmids replicon; Ap^r	(Datsenko & Wanner, 2000)
pLOF/km	Tn*10*-based transposon vector delivery plasmid; Ap^r Km^r	Herrero et al., 1990

Construction of the *fim-lux* Reporter Fusions

E. coli CFT073 harboring the *fimS* reporter was obtained by site-specific transposition of the *fimS-lux* genes at the chromosomal *att*Tn*7* site as described by Crépin *et al.*, (2012a). Briefly, the promoterless *lux* operon of *Photorhabdus luminescens* (*luxCDABE*) (Kevin James Allen, 2000) was amplified with the primers CMD1733 and CMD1734 (Table 5.4). This DNA fragment was digested with KpnI and ApaI (New England Biolabs), purified with the Biobasic kit and ligated into the multiple-cloning sites (MCS) of the mini-Tn7-containing vector pGP-Tn7-Cm, generating the vector pGP-Tn7-*lux* (pIJ461). An optimized ribosome-binding site, RBS, was then added to plasmid pIJ461 to generate the pIJ514 vector. Then, the plasmid pIJ514 was used to generate the vectors, pIJ516 *pfimA* phase L-ON, pIJ517 *pfimA* phase L-OFF and pIJ518 *pfimA* variable phase. The *fim* promoter from strain CFT073 was amplified by PCR with primers CMD1645 and CMD1646 (see Table 5.4 in the supplemental material). Genomic DNA, digested with the restriction enzymes EcoRI and SalI, and ligated to pIJ514 previously digested with EcoRI and XhoI. Transformation into *E. coli* DH5α cells was followed by selection on LB plates containing chloramphenicol. Using the approach described by Gunther et al. (2002), point mutations in primer CMD1133 were introduced to block the promoter switch in the ON position, digested with the restriction enzymes SmaI and SalI, and ligated to pIJ514 plasmid digested with SmaI and XhoI. The resulting vectors pIJ516, pIJ517, pIJ518 were transformed in *E. coli* SM10 λ*pir*-derivative strain MGN-617.

Strain MGN-617 (pGP-Tn7-*fimS-lux*) was conjugated overnight with strain CFT073, containing plasmid pSTNSK, which encodes the Tn7 *tnsABCD* transposase genes, at 30°C on LB agar plates supplemented with DAP. Following overnight culture, the bacteria from agar plates were suspended in 1 ml of phosphate-buffered saline (PBS), washed twice in PBS, serially diluted, and cultured on LB agar supplemented with gentamicin, and incubated at 37°C. Colonies that grew were then tested for sensitivity to kanamycin and ampicillin, indicating the likelihood of integration

at *att*Tn*7* and loss of the transposase-encoding plasmid pSTNSK. Insertion of Tn7 into the *att*Tn7 site was verified by PCR (primers CMD26 and CMD1416 (see Table 5.4).

Testing the *fim-lux* fusions under different pH conditions

To measure the changes following growth in media at different pH, LB was buffered using 0.1 M Na_2HPO_4-NaH_2PO_4 buffer. The media were prepared with a pH ranging between 4.4 and 7.0. *E. coli* containing *pfimA* phase-variable, *pfimA* L-ON and *pfimA*-L-OFF *lux* fusions were incubated overnight at 37°C, 250 rpm in 5 ml LB medium. The next day 3 µl of each overnight culture was transferred to 180 µL of buffered LB at a specific pH and incubated with agitation until mid-logarithmic phase had been reached in 96-well plates at 37°C. The luminescence and $O.D._{600}$ was measured each 15 minutes for 4 hours using a Cytation™ 3 Cell Imaging Multi-Mode Reader (BioTek Instruments Inc). The luminescence results were reported as relative luminescence units (RLU). The luminescence readings were normalized to the $O.D._{600nm}$ values. The luminescence of *lux* fusion-containing strains streaked on LB agar plates was recorded with a ChemiDoc XRS system equipped with Quantity One 1-D analysis software (Syngene Chemi Genius), with an integration time of 30 seconds.

Transposon mutagenesis

Transposon mutagenesis was performed as described by Simms & Mobley, (2008a). Briefly, the MGN-617/pLOF-Km donor strain and recipient strain CFT073 carrying *fimS* phase variable reporter were cultured overnight (O/N) at 37°C in LB with appropriate antibiotics and supplements. Mixed cultures were prepared as a 1:4 donor-to-recipient ratio, placed onto LB agar plates supplemented with IPTG and DAP, and incubated O/N at 37°C. After incubation, cells were suspended in 1 ml of PBS, washed twice in PBS, serially diluted, and plated onto LB agar supplemented with kanamycin and incubated O/N at 37°C to select for the recovery of kanamycin-resistant transposon mutants of the CFT073 *fimS-lux* recipient strains. Colonies were screened for susceptibility to ampicillin to confirm loss of pLOF-Km.

Measurement of luminescence of insertion mutants in CFT073 carrying *PfimA-lux*

Transposon mutants of CFT073 carrying *fimS-lux* were cultured at 250 rpm in 150 µL of LB in a 96-well plate (Corning White With Clear Flat Bottom), and luminescence was measured at $O.D._{600}$. In total, 5,904 transformants were analyzed. The luminescence readings were normalized to the $O.D._{600}$ values to account for any differences in growth. Mutants with disrupted genes that resulted in higher or lower levels of luminescence than the WT *pfim-lux*-fusion containing strain, were confirmed phenotypically by quantification of type 1 fimbriae by yeast agglutination assays as

described below. Mutants of interest were then streaked on LB agar over three successive rounds of subculture and then stored individually in 25% glycerol at −80°C.

Evaluation of type 1 fimbriae production

The production of type 1 fimbriae was determined by yeast agglutination assay (Crépin *et al.*, 2008). Briefly, the transposon mutants were cultured at 37°C in LB broth or human urine to mid-log phase. In our experiment, log-phase (period of steady-state growth in LB) is estimated to occur at OD_{600} between 0.6 and 0.8. However, for growth in urine, cells reach a stationary phase at an OD_{600} of 0.5 to 0.9. As such, we used a growth of cells to an OD_{600} of 0.6 for cells for mid-log growth in LB and an OD_{600} of 0.4 for mid-log growth in human urine. Following centrifugation, 40 µl of an initial suspension of approximately 2×10^{11} cells ml^{-1} in PBS was transferred and serially diluted 2-fold in microtiter wells containing equal volumes of a 3% commercial yeast suspension in PBS. After 30 min of incubation on ice, yeast aggregation was monitored visually, and the agglutination titer was recorded as the most diluted bacterial sample giving a positive aggregation reaction.

Site-specific integration of Tn*10*

Genomic DNA of 32 clones was extracted from cultures using phenol-chloroform. DNA was sequenced at the Génome Québec Innovation Centre, McGill University. DNA concentrations were determined using the Quant-iT™ PicoGreen® dsDNA Assay Kit (Life Technologies). DNA samples were generated using the NEB Next Ultra II DNA Library Prep Kit for Illumina (New England BioLabs) as per the manufacturer protocol. TruSeq adapters and PCR primers were purchased from IDT. Size selection of libraries containing the desired insert size was obtained using SPRI select beads (Beckman Coulter). Briefly, genomic DNA was fragmented and tagged with adapter sequence via one enzymatic reaction (tagmentation). We initially amplified by PCR the region between the end of the insertion (primer Tn_pLOF-Km-CS1:(5′ACACTGACGACATGGTTCTACAcgttgcgctgcccggattac 3′ [transposon-specific sequence is in lowercase])), and the Illumina adapter with primer 2 (5′ TACGGTAGCAGAGACTTGGTCTCTAGCATAGAGTGCGTAGCTCTGCT 3′) to enrich for transposon insertion sites and allow multiplex sequencing. The thermocycler program was 94°C for 2 min, 94°C for 30 s, 55°C for 30 s 72°C for 30 s for 33 cycles and 72°C for 7 min. Each library was prepared with a unique Illumina barcode. We amplified this region to add the Illumina adapters for MiSeq sequencing: PE1-CS1 (AATGATACGGCGACCACCGAGATCTACACTGACGACATGGTTCTACA) and primer 2. The

libraries were then pooled in equimolar concentration and sequencing was performed on an Illumina MiSeq using the MiSeq Reagent Kit v2 Kit (500-cycles).

After determining the location of the transposon, the clones in the pool carrying the specific mutations were determined using a primer complementary to the transposon end and another primer complementary to the identified transposon-interrupted gene. Following DNA amplification of each clone by PCR, we were able to determine which specific clones contained some of the identified site-specific insertions.

Construction of site-directed mutants

Mutations were introduced by lambda-red recombination as described using plasmids pKD3 and pKD4 as templates for chloramphenicol and kanamycin resistance cassettes, respectively (Datsenko & Wanner, 2000). Primers are listed in Table 5.4. Antibiotic cassettes flanked by FLP recombination target (FRT) sites were excised by introduction of vector pCP20 expressing the FLP recombinase (Cherepanov & Wackernagel, 1995).

Preparation of fimbrial extracts and Western blotting

Preparation of fimbrial extracts and western blotting were performed as described previously (Crépin *et al.*, 2008), with anti-type 1 fimbriae serum from *E. coli* strain B_{AM}. Briefly, after the growth to log phase, the bacteria were harvested and resuspended in 5 ml of 150 mM NaCl-0.5 mM Tris-HCl (pH 7.8). Following incubation at 56°c for 1h and centrifugation (3,000 × g for 10 min), the aliquot was precipitated with 10 % trichloroacetic acid. Followed by centrifugation 20,000 × g for 15 min at 4°C, the pellet was washed twice with 0.5 M Tris-HCl-0.5 M EDTA (pH 12.0) and resuspended in 0.5 M Tris-EDTA.

Further, fimbrial extracts were separated by sodium dodecyl sulphate-polyacrylamide gel electrophoresis, the proteins were stained with Coomassie brilliant blue and transferred to a nitrocellulose membrane (Bio-Rad) for 60 min at 100 V. The membrane was blocked with supplemented with 0.05% Tween 20 (Pierce). Incubations with primary rabbit anti-*fim* (1:5,000) and secondary goat anti-rabbit (1:25,000) antibodies were carried out for 1 h at room temperature. SuperSignal West Pico chemiluminescent substrate (Pierce) was used for detection.

Detection and quantification of the on/off state of the *fimS* region

The orientation of the *fimS* region was determined as described previously (Müller *et al.*, 2009a). Briefly, the *fimS* region was PCR amplified with the primers CMD1258 and CMD1259 (see Table 5.4), to produce a 650 bp fragment. The DNA was then digested with HinfI and analyzed on a 2% agarose gel. Following digestion, the ON orientation produces fragments of 128 bp and 522 bp, whereas the OFF orientation generates fragments of 411 bp and 239 bp. Quantification of the ratio of cells in ON or OFF position was performed as described (Wu & Outten, 2009). The WT strain was cultured statically for 48 h at 37°C for use as a control for increased orientation of the ON position. The WT strain was also cultured for 24 h on LB agar plates at room temperature as a control to favor orientation in the OFF position.

Experimental UTI in CBA/J mice

The animal study was reviewed and approved by the animal ethics evaluation committee – Comité Institutionel de Protection des Animaux (CIPA No 1608-02) of INRS. The murine experimental UTIs were carried out as described previously (Hagberg et al., 1983), using a single-strain infection model. Prior to inoculation, strains were grown for 16 h at 37°C with shaking (250 rpm) in 55 ml of LB medium. Six-week-old CBA/J female mice were inoculated through a catheter inserted in the urethra with 20 µl of the pellet containing 2×10^9 CFU of either UPEC strain CFT073, CFT073 Δ*yqhG* (QT5178) or the complemented strain (QT5235). After 48 h, mice were euthanized; kidneys and bladders were sampled, homogenized, diluted, and plated on MacConkey agar for enumeration of colonies.

Adhesion assays

5637 human bladder cells (ATCC HTB-9) were grown in RPMI 1640 medium (Wisent Bioproducts) supplemented with 10% fetal bovine serum, 2 mM l-glutamine, 10 mM HEPES, 1 mM sodium pyruvate, 4.5 g/liter glucose, and 1.5 g/liter sodium bicarbonate. For the assays 5637 cells were grown to confluency in RPMI 1640 and 2×10^5 cells/well were distributed in 24-well plates. Strain CFT073 and isogenic mutants were grown in LB medium at 37°C to the mid-log phase of growth (O.D. 0.6). Immediately before infection, cultures were washed with PBS, suspended in medium and inoculated at a multiplicity of infection (MOI) of 10 CFU per epithelial cell. Bacteria-epithelial cell contact was enhanced by a centrifugation at 600 × *g* for 5 min. After 2 h, cells were washed three times and lysed with PBS–0.1% sodium deoxycholate (DOC), serially diluted, and plated on LB agar plates. Quantification of cell-associated bacteria was performed as previously described (Martinez et al., 2000). To block adherence mediated by type 1 fimbriae, 2.5% α-d-mannopyranose was added.

Motility assay

Motility assays were as previously described (Lane *et al.*, 2005) with modification. Following overnight growth at 37°C, strains were cultured at 37°C in LB broth to mid-log phase. Strains were stabbed into the surface of soft agar (1% tryptone, 0.5% NaCl, 0.25% agar) using an inoculating needle. Care was taken not to touch the bottom of the plate during inoculation to ensure only swimming motility was assessed. After 16 h of incubation, the diameters of motility zones were measured. Three independent motility experiments for each strain were performed. Results were analyzed using a paired t-test.

Growth under conditions of osmotic stress

Strains were tested for growth under conditions of osmotic stress using NaCl or urea. Cultures were diluted 1:100 from overnight cultures grown in LB, grown until mid-log phase with shaking. They were serially diluted and plated on LB agar alone and LB agar supplemented with 0.3 M NaCl, 0.6 M NaCl, 0.3 M urea, or 0.6 M urea. Colonies were enumerated, and growth under each condition was compared to growth on LB agar.

Hydrogen peroxide sensitivity assay

Sensitivity to H_2O_2 was determined by using an agar overlay diffusion method (Boyer *et al.*, 2002). Briefly, overnight cultures were used to inoculate (1/100) fresh LB medium, and incubated until the O.D. $_{600}$ reached 0.6. Then, 100 µl of each culture were mixed with 3 ml molten top agar and poured onto an LB agar plate. A 6-mm-diameter Whatman filter disk containing 10 µl 30 % H_2O_2 was placed on the agar surface and plates were incubated overnight at 37°C. Inhibition zone diameters were then measured.

Statistical analyses

Statistical tests were obtained using the Prism 7.04 software package (GraphPad Software). Statistically significance between two groups was determined by unpaired t-test and comparison among three or more groups was obtained by one-way analysis of variance (ANOVA). For the independent infections, comparisons of the CFU mL^{-1} or CFU g^{-1} distributions were analyzed using the Mann–Whitney test.

5.5   RESULTS

5.5.1   The single-copy integrated CFT073 *fimS-lux* reporter system

To identify systems that alter the expression of type 1 fimbriae, we used a promoterless *lux* reporter system fused to the *fim* type 1 fimbriae promoter region, *fimS*. A *luxCDABE* reporter system originally from *Photorhabdus luminescens* (Allen, 2000) was used. The system encodes all the enzymes needed to produce a luminescent signal. The *lux* genes were introduced into the pGP-Tn7-*Cm* vector. An optimized ribosome binding site, *RBS*, was added to plasmid pIJ461 to generate pIJ514 vector. Further, we generated phase variable, *pfimA* phase variable-*lux* (pIJ518) to measure the expression of type 1 fimbriae in various conditions (Fig. 5.1A). Using the same approach as described by Gunther IV *et al.*, (2002), point mutations were introduced in order to lock the promoter in the ON- and OFF-position respectively to generate *pfimA L-ON-lux* (pIJ516) and *pfimA L-OFF-lux (*pIJ517) (Fig. 5.1).

A
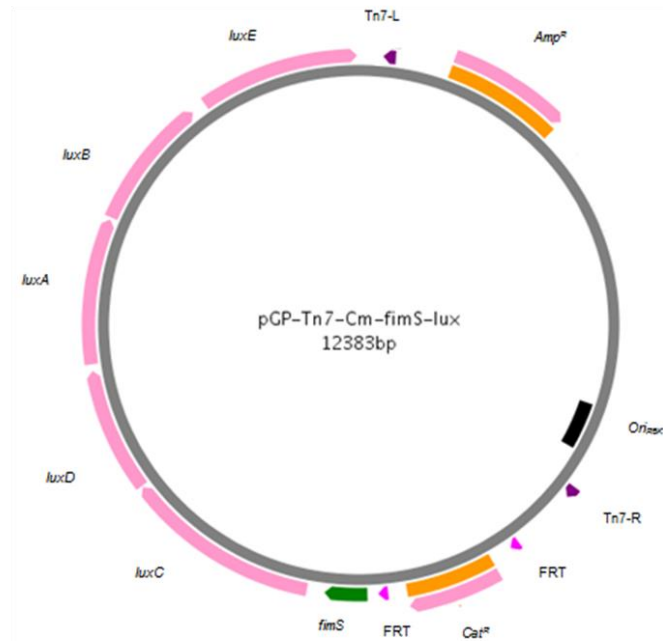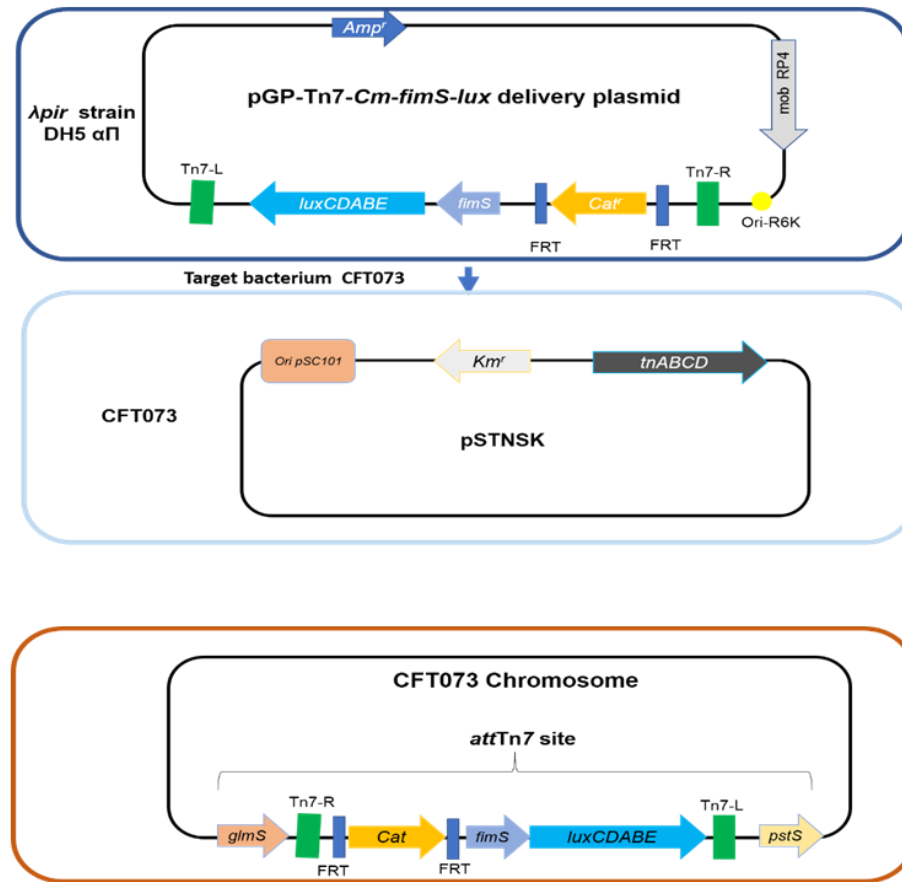
Figure 5.1. Methods for site-specific insertion of *fimS-lux* fusions using mini-Tn*7-lux* vector

(A) The mobilizable suicide vector pGP-Tn7-Cm-*fimS-lux* contains the conjugative transfer Mob RP4 and the ori R6K. A multiple cloning site is integrated between the two Tn*7* ends, where the promoterless *lux* reporter system is fused to the fimbrial promoter region, *fimS*. (B) Tn7-based transposition at the chromosomal *att*Tn7 site was achieved by conjugation, where the donor strain (*E. coli* SM10λpir) harbored the mini-Tn*7* vector and the recipient strain CFT073 contained the thermosensitive suicide vector pSTNSK pSC101-temperature sensitive origin and transposases *tnsABCD*. The Tn7 transposon integrates at the site-specific *attTn7*, located downstream of the highly conserved *glmS* gene.

5.5.2   Analysis of the *fim-lux* fusions in UPEC CFT073 grown under different pH conditions

To better characterize the reporter system upon dynamic transcriptional changes, we set out to assay the response kinetics of the *pfimA* promoter, driving the expression of the type 1 fimbriae using the *lux* reporter system. This promoter has been extensively studied in *E. coli* and used to validate a *lux* reporter system and *lacZYA* fusion implemented on a single copy number plasmid (Schwan & Ding, 2017; Schwan *et al.*, 2002b). Thus, it has been reported that growth conditions

play a substantial role in the ability of *E. coli* cells to undergo phase variation and alter expression of type 1 fimbriae. Of note, transcription of all of the *fim* genes was shown to be repressed in a low pH environment (Schwan *et al.*, 2002b). Following a similar protocol, the *fim-lux* reporter containing variant of CFT073 or its isogenic *pst* mutant was grown in LB adjusted at different pH conditions ranging from 4.4 to 7. To verify any differences in expression, the *E. coli* cells were grown to mid-logarithmic phase (OD_{600} of 0.6). The *fimS*-Locked ON fusion had the highest expression level and did not vary regardless of the pH during growth (Fig. 5.2A). However, the neutral pH influenced the expression of the *fim* switch. A shift from pH 4.4 to a neutral pH of 7 in LB media resulted in a two-fold increase in expression of *fim*. Decrease in pH also diminished the production of type 1 fimbriae (Supplemental Fig. 5.9). In addition, no significant change in growth rates was observed for growth of the CFT073 parent strain and the *PfimA*-Locked ON and *PfimA* variable *lux* derivatives, suggesting that the expression of the *lux* operon and its gene products had no adverse effects on bacterial growth (Supplemental Fig. 5.10).

CFT073 derivatives carrying the *PfimA* promoter in either direct (*PfimA*-Locked ON) or opposite (*PfimA*-Locked OFF) orientation with respect to the *luxCDABE* operon were streaked on LB agar plates, together with the CFT073 strain and a *pst* mutant carrying the *PfimA* phase-variable *lux* fusion. Stronger emission was detected from the *fimS*-Locked ON fusion (Fig. 5.2B), with single colonies producing a strong signal. By contrast, there was no luminescence signal detected in the negative control carrying the *PfimA-Locked-OFF* fusion or the CFT073 strain or its *pst* mutant carrying the *PfimA*-phase-variable-*lux fusion*, although a dim light emission could be detected for CFT073 containing the *PfimA*-phase-variable fusion after longer exposure. In addition, the stability of the *fimS*-Locked-ON-*lux* strain was evaluated after 10 passages without antibiotic selection and the maintenance and luminescence expression of this fusion was found to be stable.

The expression of *lux* derivatives was also compared in LB liquid media overnight. As expected, there was a high signal for the *fimS*-Locked ON strain (QT4794)*,* no signal for the *fimS*-Locked OFF strain (QT4795) and an intermediate signal for the *fimS-lux* variable strain (QT4796) (Fig. 5.2C). In contrast, the signal for Δ*pst, fimS-phase variable-lux* (QT5018) increased significantly (Fig. 5.2C) when compared with the same mutant at OD_{600} 0.6. (Fig. 5.2A). This result was similar to what was previously observed (Supplemental Fig. 5.9) (Crépin *et al.*, 2012b).
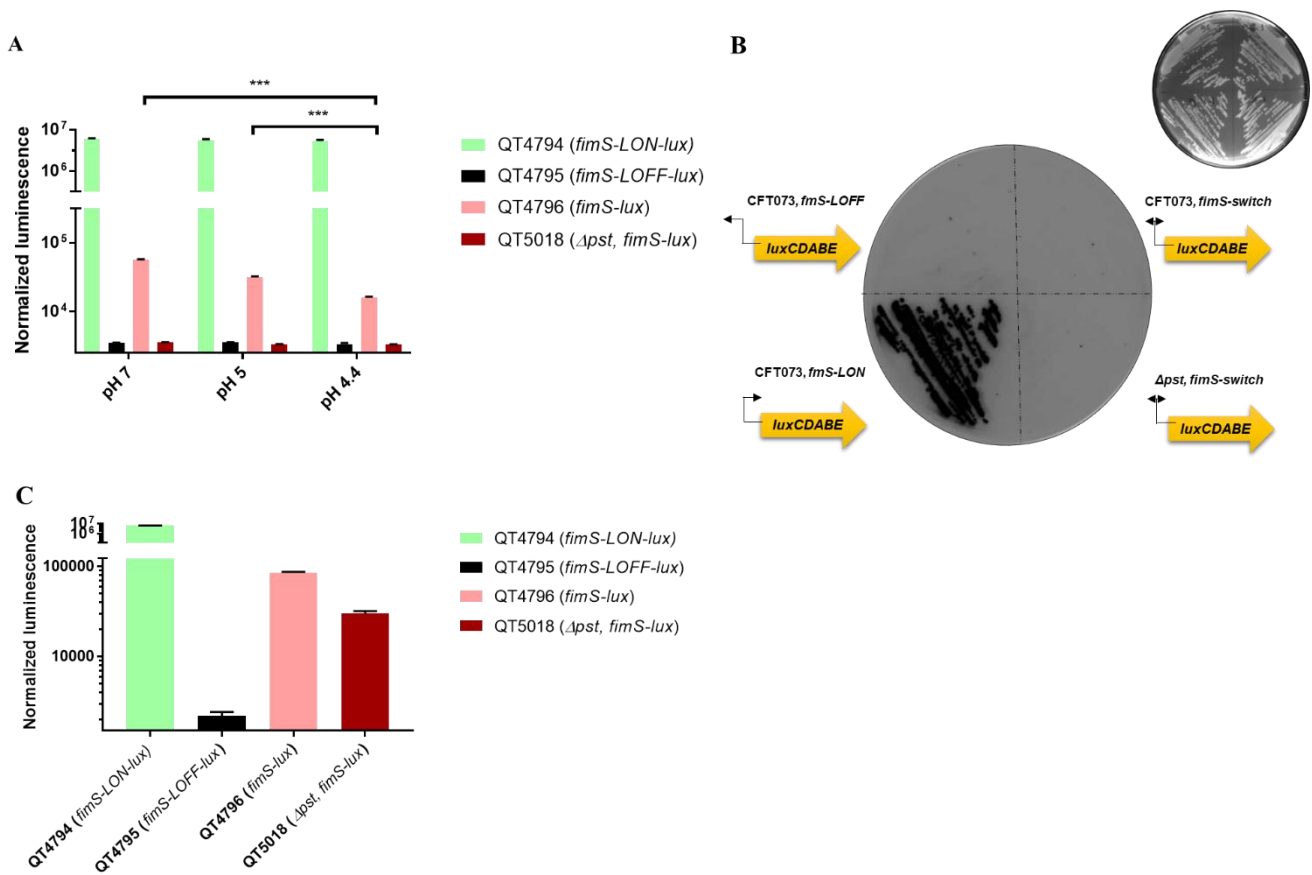
Figure 5.2. Response of the *lux* reporter system in exponential-phase, overnight cultures and on agar

(A) Effects of pH on *fimS*-phase variable, *fimS*-Locked ON and *fimS*-Locked OFF expression was determined with *luxABCDE* transcriptional fusions in strain CFT073. Luminescence was normalized to the O.D.$_{600}$ of the culture compared to CFT073; means ± standard deviations are indicated from at least three separate runs. (B) Inverted darkfield image of luminescence emitted on plates by CFT073 and pst reporter strains carrying *PfimA* from the constitutively expressed promoter (*fimS*-LON) or inverted promoter (*fimS*-LOFF) or switch variable (*fimS*-phase variable) direction with respect to *luxCDABE*. Colonies were grown overnight at 37°C and imaged using white light 400 ms (top right corner) or luminescence imaging for 30 s exposure time. Exposure images were acquired through ChemiDoc XRS system using high sensitivity chemiluminescence settings. (C) Response of the *lux* reporter system in overnight cultures in LB broth. Statistical significance was calculated by the Student t-test: *, $P < 0.05$; **, $P < 0.005$; ***, $P < 0.0001$.

5.5.3 Screening for transposon mutants with increased or decreased *lux* expression and altered production of type 1 fimbriae

To identify genes affecting the expression of type 1 fimbriae, *E. coli* CFT073 carrying the *fimS* phase-variable reporter (Fig. 5.1B) was subjected to transposon mutagenesis. A mini-Tn*10* transposon carrying a kanamycin resistance marker pLOF/Km (Herrero *et al.*, 1990) was

randomly inserted into the bacterial chromosome. A transposon bank was screened for luminescence. Clones demonstrating increased or decreased light emission were identified. Transposon insertions that produced high or low levels of luminescence may identify genes encoding transcriptional repressors or activators of *fim*. Transposon insertions that result in low levels of luminescence suggest that the disrupted genes may promote *fim* transcription and production of type 1 fimbriae. A total of 5904 transposon mutants were generated and stored individually in 96-well plates stored at −80°C. The mutants were assessed for luminescence at O.D.$_{600}$ 0.6 with shaking at 37°C (Fig. 5.3A). A subset of 65 transposon mutants demonstrating the highest and lowest levels of luminescence compared to the control CFT073 (*att*Tn*7 PfimA-lux*) were further evaluated. Mutants that produced more or less luminescence than the control strain were further tested for levels of production of type 1 fimbriae by yeast agglutination assay (Crépin *et al.*, 2012b). From this secondary screen, 48 transposon mutants were confirmed and there was at least a 4-fold increase or decrease in yeast agglutination ($p<0.0001$) (Fig. 5.3B). Some of these mutants are currently being investigated to determine the transposon insertion site locations. In addition, 32 of the individual mutants were pooled and their transposon insertions were determined (Supplemental Fig. 5.11) as described in the methods section.
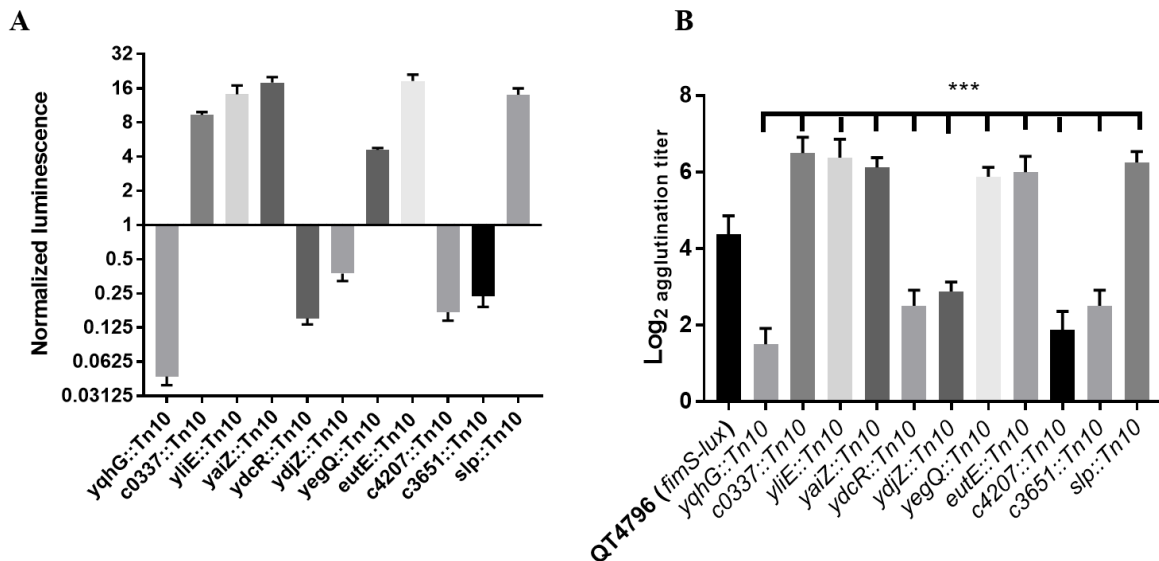
Figure 5.3. Screening of transposon mutants based on *lux* expression and the production of type 1 fimbriae

(A) A decrease or increase of luminescence corresponding to the expression of type 1 fimbriae was observed in the transposon mutants, (B) Production of type 1 fimbriae in transposon mutants cultured to the mid-log phase in LB broth determined by yeast agglutination. The QT4796 (*fimS-lux*) strain was used as a control and showed baseline luminescence. Results are the mean values and standard deviations for three biological

5.5.4 Identification of mutations affecting type 1 fimbriae expression

Analysis of the 32 mutants generated 6733 sequence reads that mapped to the CFT073 genome. The insertions were linked to genes involved in protein fate and synthesis, energy metabolism, adherence, transcriptional regulation, and transport, regulatory functions, etc. (Table 5.2). A number of transposon mutations were also inserted in genes predicted to encode proteins of unknown function (Supplemental Fig. 5.11).

Table 5.2. Transposon mutants with altered *pfimA::lux* expression in CFT073*

Insertion site [a]	CDS	Gene symbol	Gene product description
Energy metabolism			
yecK	*c2287*	*yecK*	Cytochrome c-type protein TorY
eutE	*c2980*	*eutE*	Ethanol amine utilization protein EutE
sseB	*c3047*	*sseB*	Serine sensitivity enhancing B (SseB)
nadB	*c3098*	*nadB*	L-aspartate oxidase
iucC	*c3625*	*iucC*	IucC protein
tdcB	*c3875*	*tdcB*	Threonine dehydratase
Fimbrial adhesins, transporters or outer membrane proteins			
ydeS	*c1933*		YdeS - fimbrial-like protein ydeS precursor (minor subunit proteins F9 fimbriae)
aufG	*c4207*	*aufG*	Putative fimbrial adhesin precursor
fimD	*c5396*	*fimD*	Outer membrane usher protein FimD precursor
dnaJ	*c0020*	*dnaJ*	Chaperone protein DnaJ
yaiO	*c0467*		Outer membrane protein YaiO
ydcS	*c1864*	*ydcS*	ABC transporter periplasmic-binding protein (polyhydroxybutyrate synthase)

nmpC	*c2348*	*nmpC*	Outer membrane porin protein NmpC precursor
emrK	*c2904*	*emrK*	Multidrug resistance protein K
Adjacent to *kpsM*	*c3698*	*kpsM*	Capsule synthesis
slp	*c4304*	*slp*	Outer membrane protein Slp precursor
ytfR	*c5326*	*ytfR*	Putative ATP-binding component of a transport system
Regulators			
yliE	*c0918*	*yliE*	Putative c-di-GMP phosphodiesterase PdeI
lrp	*C1026*	*lrp*	Leucine-responsive transcriptional regulator
rstA	*c2000*	*rstA*	DNA-binding transcriptional regulator RstA
	c3750		Putative regulator
kguS	*c5041*	*kguS*	α-ketoglutarate utilization sensor
fimB	*c5391*	*fimB*	FimB recombinase regulator for *fimA*
Unknown function			
	c0337		Putative conserved protein
yaiZ	*c0486*	*yaiZ*	Hypothetical protein
	c1269		Hypothetical protein
	c1555		Putative DNA N-6-adenine-methyltransferase of bacteriophage
ynjA	*c2154*	*ynjA*	Hypothetical protein
yegQ	*c2611*	*yegQ*	Putative protease yegQ
yqhG	*c3747*	*yqhG*	Hypothetical protein YqhG precursor

Adjacent to **yqhG**	*c3746-c3747*	*yqhG*	Hypothetical protein YqhG precursor

*List includes insertions identified that had at least 4-fold greater or 4-fold less relative light units compared to the CFT073 control level of *lux* expression. Genetic locus with the closest match to the sequence interrupted by the transposon in each mutant. Locations of specific Tn insertions are presented in Supplemental Fig. 5.11.

[a] Genes in bold are present in the genome of *E. coli* K-12 strain MG1655 genome.

Insertions within genes contributing to amino acid biosynthesis and metabolism

Several clones carried an insertion within genes with metabolic functions. For instance, one of these clones was inserted in *tdcB* (Table 5.2) that encodes a catabolic threonine dehydratase involved in the first step in threonine degradation. It is one of several enzymes carrying out the first step in the anaerobic breakdown of L-threonine to propionate (Umbarger & Brown, 1957). However, TdcB is activated by cAMP. Following a transition from aerobic to anaerobic growth, cAMP levels rise dramatically, which leads to increased expression of *tdcB* and consequently high levels of catabolic threonine deaminase (Hobert & Datta, 1983).

Similarly, another insertion was in *nadB* (Tritz *et al.*, 1970) which is involved in NAD biosynthesis under both aerobic and anaerobic conditions (Messner & Imlay, 2002). Another mutant had an insertion in a pathogen-specific iron acquisition gene, *iucC*, which encodes a protein required for synthesis of aerobactin (De Lorenzo & Neilands, 1986). Likewise other insertion sites were *yecK,* encoding a membrane anchored pentaheme *c*-type cytochrome involved in an anaerobic respiratory system (Gon *et al.*, 2000); *eutE* which codes for a protein that increases the level of acetylating acetaldehyde dehydrogenase activity (Rodriguez & Atsumi, 2012) and *sseB* involved in increased rhodanese activity (Hama *et al.*, 1994).

Insertions within genes encoding other fimbrial adhesins, transporters or outer membrane proteins in *E. coli* CFT073

A number of mutants with altered *lux* expression were found to contain insertions in genes encoding fimbriae, outer membrane proteins and transport proteins. Among these mutants, three carried insertions in fimbrial systems. One insertion was identified in *fimD* which is the usher of the chaperone-usher pathway of type 1 fimbriae (Supplemental Fig. 5.11) (Klemm & Christiansen, 1990), the other mutant had an insertion in *aufG* which codes for a putative fimbrial-like adhesin protein, and another insertion was identified in c1933 (*ydeS*) encoding the minor fimbrial subunit of F9 fimbriae (Table 5.2). These loci have been previously characterized (Buckles *et al.*, 2004;

Ulett *et al.*, 2007). We also identified insertions in genes encoding a putative ABC transporter periplasmic binding protein, *ydcS*, a predicted outer membrane protein, *yaiO,* and an outer membrane porin, *nmpC* (Table 5.2). Chaperone genes involved in protein fate, such as *dnaJ* coding a chaperone protein were also identified. DnaJ acts as a sensor for non-native proteins (Siegenthaler & Christen, 2006) and is involved in many cytoplasmic events, such as promotion of protein folding and translocation of nascent polypeptides (Hartl, 1996).

Insertions within regulatory genes

Further, sequencing also identified insertions in well-known regulatory genes such as *lrp* (Calvo & Matthews, 1994). Insertion within *fimB,* which mediates switching in both directions was also identified. An insertion was identified within the *c0918* (*yliE*) gene (Table 5.2). *yliE* encodes a hypothetical conserved inner membrane protein which contains a phosphodiesterase EAL domain. This protein is involved in hydrolysis of the bacterial second messenger cyclic di-GMP (c-di-GMP), a key factor in processes such as flagellar motility, biofilm formation, the cell cycle, and virulence of pathogenic bacteria (Jenal & Malone, 2006; Römling *et al.*, 2013). Similarly, another clone contained an insertion in *c5041* (*kguS*) which was identified as a sensor protein of a two-component signaling system involved in α-ketoglutarate utilization. This system is involved in utilization of α-ketoglutarate, an abundant metabolite during UPEC infection, which regulates target genes that encode α-ketoglutarate dehydrogenase and a succinyl-CoA synthetase. This two-component signaling system has been shown to be important for UPEC fitness during UTI (Cai *et al.*, 2013). Also, *rstA*, a member of the two-component regulatory system RstB/RstA (Calvo & Matthews, 1994) was disrupted in one of the mutants.

Insertions within hypothetical genes

Several of the mutations disrupted genes predicted to encode hypothetical proteins of unknown function, and the roles of such genes for *E. coli* physiology as well as their influence on expression of type 1 fimbriae and UPEC pathogenesis are unknown (Table 5.2). Sequence analysis identified an independent insertion within the *yqhG* gene and an insertion immediately upstream of the *yqhG* coding region (Fig. 5.4A), strongly suggesting the involvement of YqhG in type 1 fimbriae production. Thus, we focused the rest of our investigation on this gene of unknown function and its role for production of type 1 fimbriae and UPEC pathogenesis.

5.5.5   Disruption of *yqhG* reduces expression of type 1 fimbriae

A transposon was inserted in the opposite orientation of *yqhG* in one mutant and in the middle of the gene in another mutant (Fig. 5.4A), suggesting that the *yqhG* gene was involved in regulation of expression of type 1 fimbriae. Since type 1 fimbriae contribute to UPEC pathogenicity (Nielubowicz & Mobley, 2010), the production of type 1 fimbriae was then evaluated by yeast agglutination at the mid-log phase of growth in LB (O.D.$_{600}$ 0.6) and urine (O.D.$_{600}$ 0.4). As expected, loss of *yqhG* had an effect on the production of type 1 fimbriae (Fig. 5.4B). After mid-log growth with shaking in LB, and overnight growth in human urine with shaking, the agglutination titer of CFT073Δ*yqhG* was reduced by 4-fold as compared to strain CFT073. Agglutination titers of the complemented mutant regained titers similar to that of the WT strain (Fig. 5.4B). To confirm that yeast agglutination was mediated by type 1 fimbriae, the assay was also performed in the presence of 2.5% mannopyranose, which blocks type 1 fimbriae-mediated agglutination. As expected, no yeast agglutination was observed when 2.5% mannopyranose was added to the bacteria. These results indicate that the deletion of *yqhG* caused a substantial decrease of type 1 fimbriae expression. Since the *yqhG* mutant demonstrated a defect in type 1 fimbriae production (Fig. 5.4B), we further investigated the ability of the mutant to grow in human urine. Loss of the *yqhG* in strain CFT073 did not affect growth in human urine. To confirm that production of type 1 fimbriae was reduced in the *yqhG* mutant, Western blotting against the type 1 major subunit FimA was determined. Western blotting confirmed an important decrease of the FimA protein in the *yqhG* mutant compared to parent strain CFT073 and the complemented strain (Fig. 5.4D).
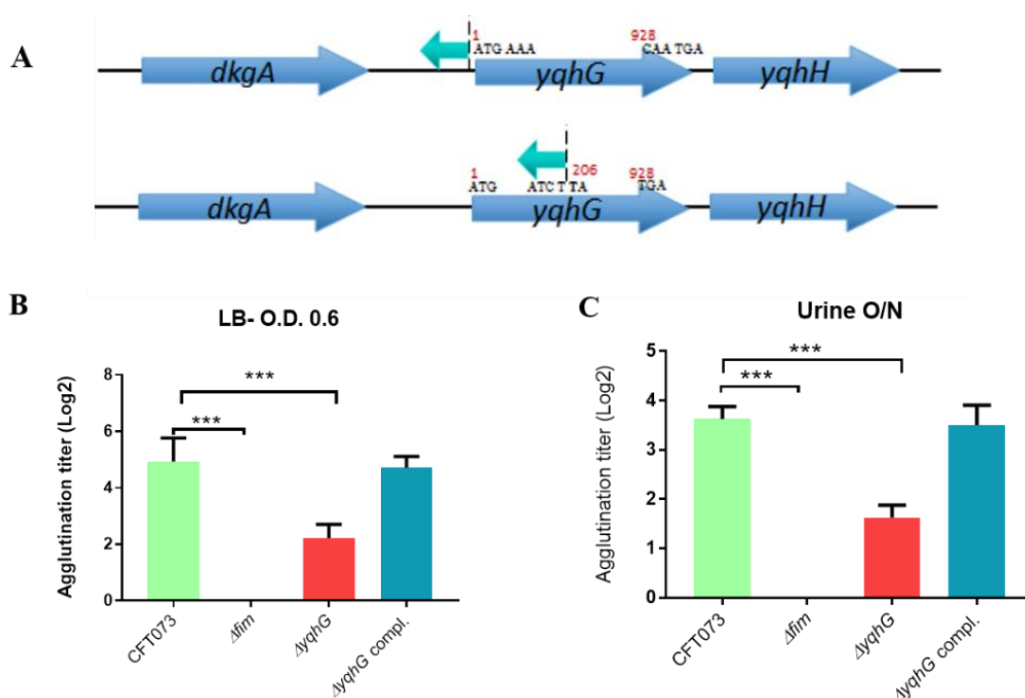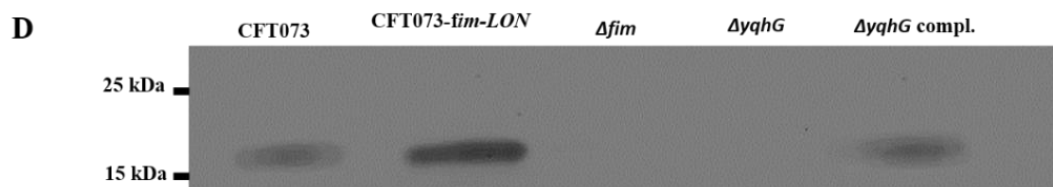
Figure 5.4. Inactivation of the *yqhG* gene reduced expression of type 1 fimbriae

(A) Schematic representation of a transposon insertion which caused a decrease in expression of type 1 fimbriae. (B) Production of type 1 fimbriae in strains cultured to the mid-log phase of growth in LB broth and O/N in urine. The Δ*fim* strain was used as a negative control and showed no agglutination. (C) Production of type 1 fimbriae in strains cultured O/N in human urine. (D) Western blot of fimbrial extracts of strains cultured to the mid-log phase of growth in LB broth. Results are the mean values and standard deviations for six biological experiments. Statistical significance was calculated by the Student t test: *, $P < 0.05$; **, $P < 0.005$; ***, $P < 0.0001$.

5.5.6   The *yqhG* mutant demonstrates reduced adherence to human bladder epithelial cells.

The adherence of the *yqhG* mutant to 5637 human bladder epithelial cells was compared to that of the parental strain CFT073. Figure 5.5 shows that the adherence of the Δ*yqhG* mutant was reduced approximately two-fold compared to that of WT strain. Further, the decrease in epithelial cell adherence was rescued by complementation of the *yqhG* gene. Addition of 2.5% α-d-mannopyranose to block the effect of type 1 fimbriae greatly reduced cell association of all strains tested in the cell association assay (Fig. 5.5A).

To determine if the reduction of type 1 fimbriae was due to orientation bias of the phase-variable promoter, we determined orientation of the *fimS* promoter region. The orientation of *fimS* was evaluated in strains grown under agitation to mid-log phase in LB broth. Using the procedure described by (Stentebjerg-Olesen *et al.*, 2000b), we observed that the *fim* promoter clearly had an increased bias for the OFF position in the *yqhG* mutant (Fig. 5.5B).
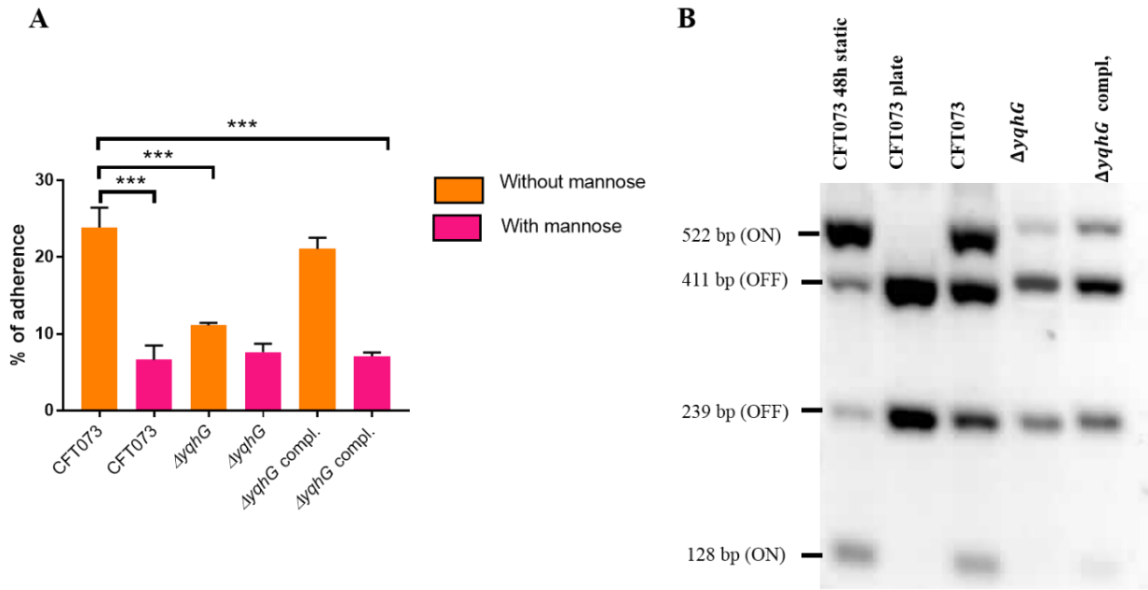
Figure 5.5. Effect of inactivation of *yqhG* and production of type 1 fimbriae on adherence of uropathogenic *E. coli* CFT073 to human bladder epithelial cells *in vitro*

(A) Adherence of strain CFT073 and its derivatives to human 5637 bladder epithelial cells in the presence or absence of 2.5% α-d-mannopyranose was determined. (B) Effect of inactivation of *yqhG* on orientation of the *fim* promoter switch (*fimS*) *in vitro*. The *fimS* region was PCR amplified, and the product was digested with HinfI. Fragments of different sizes indicate the ON or OFF orientation. All results shown are the mean values and standard deviations for four biological experiments. Statistical significance was calculated by the Student *t* test (A) *, $P < 0.05$; **, $P < 0.005$; ***, $P < 0.0001$.

5.5.7   The *yqhG* mutant demonstrates reduced bladder and kidney colonization in mice

Type 1 fimbriae are important for ExPEC colonization of the bladder during UTIs. Since the *yqhG* mutant demonstrated decreased type 1 fimbriae production, we tested its capacity to cause urinary tract infection in the CBA/J mouse model. Forty-eight hours after urethral inoculation, the *yqhG* mutant was attenuated 100-fold in bladder and 10,000-fold in kidneys ($P < 0.0001$) compared to the WT parent strain (Fig. 5.6). Further, the complemented mutant regained the capacity of colonization. This reduction in colonization from inactivation of *yghG* could be due to reduced production of type 1 fimbriae, and potentially other changes in the Δ*yqhG* mutant that could decrease colonization of the murine urinary tract (Fig. 5.6).
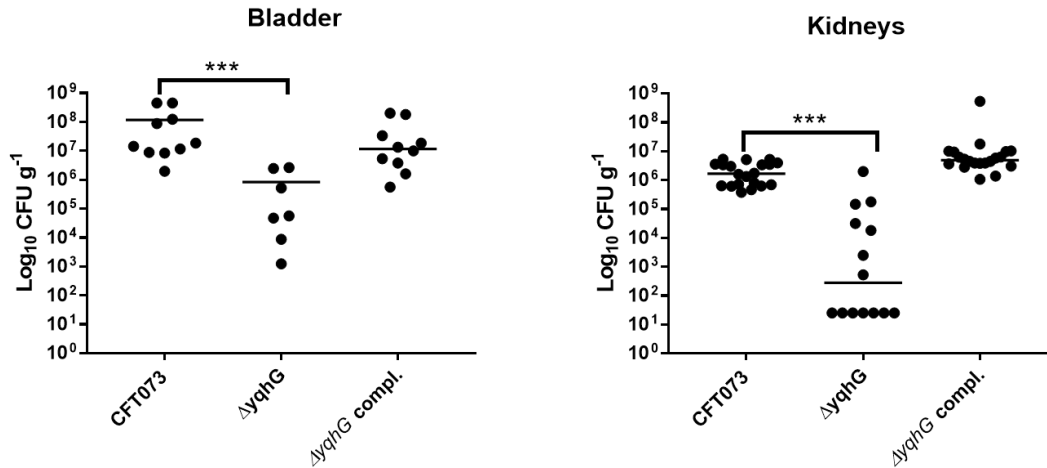
Figure 5.6. Deletion of *yqhG* reduces colonization of the murine urinary tract

CBA/J mice were infected transurethrally and the animals were euthanized, and organs were collected 48 h postinfection. Each data point represents a sample from an individual mouse, and horizontal bars indicate the medians. Two independent infections were performed: with CFT073 WT and CFT073Δ*yqhG* and with CFT073 WT and CFT073Δ*yqhG*-Tn7T-Cm::*yqhGH*. Each kidney was sampled separately (Mann-Whitney test). *, P < 0.05; **, P < 0.005; ***, P < 0.0001.

5.5.8   The *yqhG* mutant demonstrates increased motility

Since flagella and swimming motility play a pivotal role in colonization and persistence in the urinary tract (Lane et al., 2005), we investigated whether the loss of *yqhG* affected swimming motility. The *yqhG* mutant was considerably more motile than the UPEC CFT073 parental strain. Complementation of the *yqhG* mutant (strain QT5235) effectively restored motility to wild-type levels. Further, a *fimS* Locked-ON reference strain was shown to be non-motile in the swimming assays (Fig. 5.7).
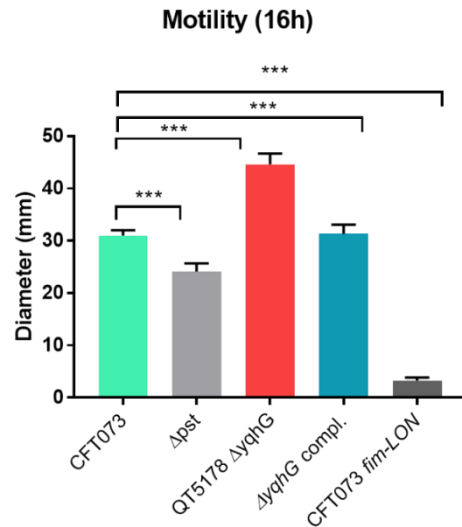
Figure 5.7. Effect of deletion of *yqhG* on motility

Diameters of swimming motility of CFT073, mutants and complemented mutant. Data represent the averages of five separate experiments. Error bars represent the SEM. Significant differences in motility between mutants and complemented mutants were determined using a paired Student t-test. *, P < 0.05; **, P < 0.005; ***, P < 0.0001.

5.5.9   *yqhG* contributes to oxidative stress resistance

During the course of a UTI, UPEC come across a variety of environmental stresses that can potentially limit survival and growth (Mulvey *et al.*, 2000). Envelope stress response pathways are likely to be critical for UPEC, in order to detect and respond to potentially harmful environmental insults during the course of infection. In an effort to determine the mechanism by which *yqhG* influences type 1 fimbriae expression, we first sought to determine if this gene is involved in hydrogen peroxide resistance. Our observations revealed that the Δ*yqhG* strain was more sensitive to oxidative killing compared to wild-type strain CFT073. This result indicates that *yqhG* contributes to resistance to oxidative stress mediated by hydrogen peroxide (Table 5.3). Further, screening of specific transposon mutants that were also shown to have decreased expression of type 1 fimbriae including clones with insertions in the *slp or yegQ* genes also showed increased sensitivity to hydrogen peroxide-mediated oxidative stress (Table 5.3).

Table 5.3. Growth inhibition zones of UPEC CFT073, isogenic mutants, and complemented strains exposed to 10 μl of hydrogen peroxide

Strain	Mean diameter inhibition zone (mm) in LB ± SDa
CFT073	25.56 ± 0.49
Δ*pst*	**31.25 ± 0.70**
Δ*pst* compl.	26.0625 ± 0.41
Δ*yqhG*	**28.62± 0.51**
Δ*yqhG* compl.	25.12 ± 0.58
QT1324 (*oxyR*::Km)	**39.35 ± 1.04**
QT4937 (*slp*::Tn*10*)	**28.93 ± 0.67**
QT4940 (*yegQ*::Tn*10*)	**28.87 ± 0.23**

Data presented are the means ± standard deviations for eight independent experiments. The compound used was 10 μl of H_2O_2 (30%) on LB or agar plates. a Mean of eight determinations per strain. All strains were tested in parallel each day. Values indicated in bold text are significantly different, $P < 0.05$, from the mean for the wild-type strain as calculated by Student's t test.

5.5.10   The *pst* mutant of UPEC CFT073 is sensitive to osmotic and oxidative stress

In a previous study, in avian pathogenic *E. coli* (APEC) strain χ7122, inactivation of the *pst* system mimicked phosphate-limiting conditions and caused pleiotropic effects (Lamarche *et al.*, 2008). In the APEC *pst* mutant, membrane homeostasis was altered and included modification of phospholipids (Lamarche *et al.*, 2008). Accordingly, the same mutant appeared to modulate the expression of some genes regulating antioxidant activities (Crépin *et al.*, 2008). In the UPEC strain CFT073 *pst* mutant, attenuation of urinary tract virulence was shown to mainly be attributed to reduced production of type 1 fimbriae (Crépin *et al.*, 2012b). As stress resistance is crucial for the survival of UPEC strains in the host, we also evaluated the capacity of the UPEC CFT073-derived *pst* mutant to resist oxidative and osmotic stresses. Sensitivity to hydrogen peroxide was

analyzed from exponential growth cultures of CFT073 and the Δ*pst* derivative by using the H_2O_2 agar overlay diffusion method. Under phosphate-sufficient conditions (LB), the *pst* mutant was more sensitive to oxidative stress, as diameters of inhibition zones were significantly larger with the *pst* mutant than with the CFT073 parental strain (P<0.001) (Table 5.3). Complementation of the Δ*pstCAB* mutant restored the wild-type phenotype (Table 5.3). Given the significant decrease in the colonization of the mouse bladder by the *pst* mutant, we also tested whether this strain displayed increased susceptibility to osmotic stress by using an established protocol (Pavanelo *et al.*, 2018). We, therefore, tested the growth of the wild-type, *pst* mutant, and a complemented mutant on modified LB agar containing different concentrations of NaCl or urea. Both strains were able to grow on LB agar with 0.3 M NaCl (Fig. 5.8A) and with 0.3 M urea (Fig. 5.8B), and no strain could grow on LB agar with 1 M NaCl and 1 M urea. In contrast, the *pst* mutant was significantly more sensitive to 0.6 M NaCl (Fig. 5.8C) and 0.6 M urea (Fig. 5.8D) compared to parent strain CFT073. The complemented mutant grew similarly to the WT strain (Fig. 5.8). Taken together, the *pst* mutant was found to show increased sensitivity to both oxidative and osmotic stresses.
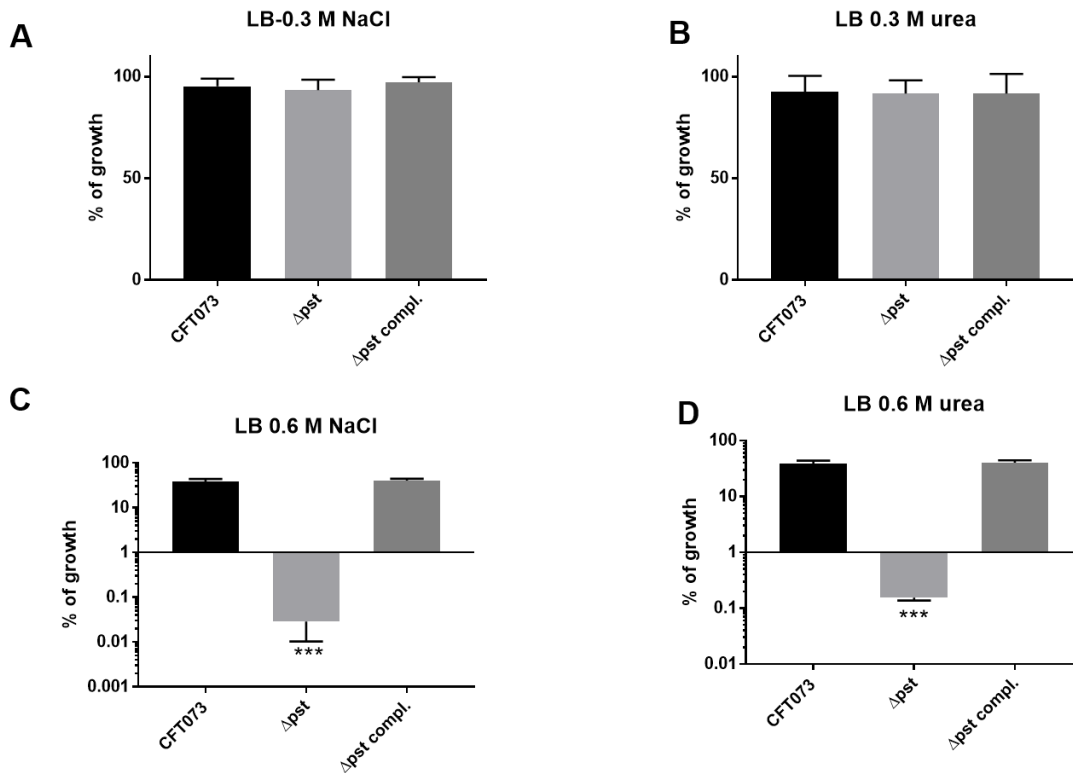
Figure 5.8. Growth in conditions of osmotic stress

Strains were grown under shaking in LB medium until mid-log phase (O.D.$_{600}$ 0.6) and plated on LB agar (taken as 100% growth) and (A) LB agar with 0.3 M of NaCl, (B) 0.3 M of urea (C) 0.6 M NaCl and (D) 0.6 M of urea.

Graphs show the mean of growth relative to regular LB with standard error bars. Assays were performed three times in duplicates (Kruskal-Wallis test). *, *P* < 0.05; **, *P* < 0.005; ***, *P* < 0.0001.

5.6   Discussion

The ability to adhere to host epithelial cells is an important factor for initial colonization and persistence during a UTI. Therefore, type 1 fimbriae are crucial for the establishment of UPEC infections (Schaeffer *et al.*, 1987). Bacterial adherence to the uroepithelium limits the effect of shear forces produced by urine flow and thereby improves colonization (Thomas *et al.*, 2002). Urine is considered to be a nutrient limiting environment with relatively low levels of available sugars and metabolites. Consequently, UPEC metabolism is tightly regulated and highly responsive to nutrient availability, and UPEC adapted to utilization of a wide range of nutrients from this nutrient-limited environment (Mann *et al.*, 2017). Further, most bacteria are unable to thrive within the urinary tract environment due to its high osmolarity, elevated urea concentrations, low pH, and limited iron availability (Mann *et al.*, 2017). Due to this transition, bacteria that enter the urinary tract encounter a harsh environment and are subject to numerous stresses, and stringent competition due to a drastic reduction in the abundance of nutrients. Further, environmental cues, such as pH and osmolality, have been shown to regulate *fim* genes and to affect the orientation of the *fim* switch (Schwan *et al.*, 2002b).

The expression of type 1 fimbriae is controlled by an invertible DNA element that upon inversion changes the promoter orientation through two site-specific recombinases, FimB and FimE. Thus affecting the transcription of the *fimAICDFGH* genes (Abraham *et al.*, 1985b). This inversion phenomenon known as phase variation, reversibly switches between the expression of type 1 fimbriae (Phase-ON) and loss of expression (Phase-OFF) (Klemm, 1986b). Besides the *fim* gene cluster, other genes and their gene products contribute to the expression of type 1 fimbriae. The global regulator histone-like nucleoid-structuring protein (H-NS), integration host factor (IHF), leucine-responsive protein (Lrp), and cyclic adenosine monophosphate (cAMP) receptor protein (CRP)/cAMP, control the expression of type 1 fimbriae directly and indirectly (Blomfield *et al.*, 1997b; Kelly *et al.*, 2006; Schembri *et al.*, 1998). Other proteins affect type 1 fimbriae expression in *E. coli* such us OmpX (Otto & Hermansson, 2004), IbeA, and IbeT (Cortes *et al.*, 2008), although mechanisms of control are unknown. The regulatory alarmone, ppGpp, has been connected to the regulation of the *fim* operon (Åberg *et al.*, 2006). Alteration of phosphate metabolism through inactivation of the phosphate specific transporter (*pst)* was shown to contribute to expression of type 1 fimbriae and attenuated UPEC virulence (Crépin *et al.*, 2012b). Further, inactivation of *pst* was linked to increased production of the signaling molecule c-di-GMP,

which in turn decreased the expression of type 1 fimbriae in UPEC CFT073 (Crépin *et al.*, 2017). It has been shown that under a slightly acidic pH and low salt growth conditions found on the vaginal surface, that proteins such as SlyA or RcsB may activate *fimB* and prevent H-NS from binding, allowing type 1 fimbriae to be expressed on the surface of the UPEC cells (McVicker *et al.*, 2011; Schwan *et al.*, 2007). Recently, the *treA* gene coding for a periplasmic trehalase that contributes to osmotic stress resistance was also shown to affect type 1 fimbriae production in an APEC strain and this mutation significantly reduced adherence to and invasion of epithelial cell and bladder colonization in a murine model of UTI (Pavanelo *et al.*, 2018). Taken together, there is a body of evidence indicating that type 1 fimbriae expression is important for UPEC colonization of the urinary tract and that multiple factors, including adaptation to osmotic and oxidative stress, that influence expression of these fimbriae play a role in *E. coli* UTI pathogenesis.

Given the importance of type 1 fimbriae and control of its expression, in the present report we devised a means to randomly identify different genes involved in the regulation of type 1 fimbriae by using a *luxCDABE* reporter fusion and genetic screening of a transposon bank. We constructed a *fimS-lux* reporter fusion integrated on a single-copy at the chromosomal *att*Tn*7* of pyelonephritis strain CFT073 (Fig. 5.1B). Integrating the *lux* reporter into the chromosome results in a reduced level of promoter expression compared to fusions on multi-copy vectors, but has the added advantage of stability of the signal during long term localization studies and more relevant comparison to regulatory effects on the native *fim* switch, as the single-copy fusion will not be as biased by titration of regulator proteins or recombinases that could occur with multi-copy fusion vectors. Moreover, the luciferase bioluminescence system may overcome some limitations of fluorescent reporters used in *in vivo* imaging, such a background signals associated with cellular autofluorescence, poor penetration of the excitation wavelength, slow turnover of the fluorescent protein, etc. (Riedel *et al.*, 2007).

The *fimS-lux* fusion was shown to undergo a change in signal in accordance to changes in regulation of the *fimA* promoter observed under different pH conditions (Fig. 5.2A), demonstrating its potential value at investigating environmental cues that could affect transcription of the *fim* gene cluster. A shift from pH 4.4 to a neutral pH 7.0 resulted in a significant increase of *fimS* expression. Furthermore, and in accordance with previous reports (Schwan & Ding, 2017; Schwan *et al.*, 2002b)), the expression of *fimS* was increased when bacteria were cultured in LB (neutral pH) and decreased at lower pH (Fig. 5.2A). The *in vitro* results with the *fim-lux* fusions were similar to previous studies (Schwan & Ding, 2017; Schwan *et al.*, 2002b), and helped validate the reporter system that we developed. Our *lux* fusion was highly sensitive with low

background noise, which makes this reporter rapid enough to enable a delicate monitoring of quick response kinetics. Indeed, such vectors have also been developed for transposon-based systems with random integration of *lux* into the chromosomes of both Gram-negative and Gram-positive bacteria (De Lorenzo *et al.*, 1990; Francis *et al.*, 2001). However, these systems are based on random integration of the transposon into the chromosome, followed by selection of clones which retain viability but demonstrate high levels of *lux* expression. Hence, our *lux* system seems more efficient with single-copy integration of recombinant genes at the *att*Tn*7* site that does not require selective pressure and can be used in a variety of *Enterobacteriaceae.* This system provides a useful tool for studying promoter regulation without introducing unforeseen genetic changes that influence the behavior of the strain *in vitro* and *in vivo.* The application of the *lux* reporter in combination with transposon mutagenesis and high-throughput sequencing herein provided a novel and valid approach to identify specific genes and begin to dissect genetic pathways linked to expression of type 1 fimbriae.

Our transposon library screening resulted in the identification of numerous insertions that deregulated expression of type 1 fimbriae. In this study, we initially screened 5904 transposon mutants by measuring the level of luminescence following growth on LB broth and phenotypic screening for production of type 1 fimbriae by using a yeast agglutination assay (Fig. 5.3). Here, we searched for genes with a significant increase or decrease in luminescence levels from specific transposon mutants compared to the control strain (CFT073, *fimS-lux*). The insertion of transposons in specific clones were shown to repress or activate *lux* expression *fimS* and hence deregulate type 1 fimbriae production (Fig. 5.3A). Using high throughput sequencing, we then mapped the Tn*10* insertion sites of these mutants (Supplemental Fig. 5.11), leading to the identification of numerous genes that significantly altered type 1 fimbriae production (Table 5.2). In addition to known structural and regulatory genes, genes identified included those involved in biogenesis of type 1 fimbriae and other fimbriae, amino acid biosynthesis, membrane transport, chaperones involved in protein fate and genes that are currently of unknown function. Confirmation of the role of these genes in type 1 fimbriae expression via the construction and characterization of specific mutants will be required to more clearly determine their mechanisms of action in the regulation of expression type 1 fimbriae and potential roles in UTI pathogenesis. Several clones had insertions within genes with metabolic functions. One of these clones disrupted *tdcB* (catabolic threonine dehydratase). Many nutrient transport systems and genes related to carbohydrate metabolism have been reported to be involved in the virulence of ExPEC strains. For example, the periplasmic trehalase *treA* affects type 1 fimbriae production and

virulence of APEC strain MT78 (Pavanelo *et al.*, 2018). The metabolic *frz* operon has also been shown to link the metabolic capacity of ExPEC with expression of genes required for adherence to the bladder epithelium; the presence of the *frz* operon favors the ON orientation of the invertible type 1 fimbriae promoter (Rouquet *et al.*, 2009). The two-component-system (TCS), KguSR, involved in the control of utilization of α-ketoglutarate, has also been shown to be important for UPEC fitness during UTI (Cai *et al.*, 2013). Interestingly, this system was disrupted in our mutant bank. As such, the roles of this TCS in type 1 fimbriae expression in UPEC merit further investigation. Moreover, proteins involved in the transport and catabolism of sialic acid, xylose, arabinose, and the biosynthesis of arginine and serine are highly expressed in UPEC cultured in human urine (Alteri *et al.*, 2009b). It has also been reported that sialic acid regulates type 1 fimbriae by inhibiting FimB switching in UPEC (Sohanpal *et al.*, 2004). Tn insertions also disrupted well studied regulators, Lrp, a global regulator of genes involved in metabolic functions within *E. coli* including fimbriae production (Brinkman *et al.*, 2003a; Kelly *et al.*, 2006) and *fimB* which regulates phase variable expression of the *fim* operon (Blomfield *et al.*, 1997b). It is intriguing to see a potential connection of iron acquisition mechanisms and type 1 fimbriae production as disruption of the aerobactin precursor *iucC* (De Lorenzo & Neilands, 1986) affected the fimbriae production. However, the specific mechanisms underlying how certain genes involved in metabolism influence the expression of type 1 fimbriae and to what extent this alone may influence UPEC pathogenesis during UTI remain to be elucidated.

Further, some of the genes in our bank have been reported earlier for the correlation with strong virulence and pathogenesis of UPEC. Loss of *nadB* rendered NAD auxotrophy and contributes to the virulence in *Shigella* (Prunier *et al.*, 2007) however the colonization of CFT073 and UTI89 in murine UTI model was not influenced by NAD auxotrophy (Li *et al.*, 2012). We identified an insertion in *rstA* which is a part of low pH sensing RstBA two- component system which is directly involved in the regulation of *csgD*, which encodes a regulator responsible for curli and cellulose production (Ogasawara *et al.*, 2010). Interestingly, mutation in *emrK* in *E. coli* caused a significant drop in biofilm formation (Matsumura *et al.*, 2011). So, these observations show the possible correlation between inhibition of fimbriae and a reduction in biofilm formation.

This relation has been documented before in terms of aerobic respiration in the bladder. Biofilm production in UPEC has been shown to be affected by different terminal electron acceptors (Eberly *et al.*, 2017a). In addition, type 1 fimbriae production was reduced in the absence of oxygen, and UPEC strain UTI89 had increased type 1 fimbriae production on the air exposed region of biofilm due to increased oxygen level (Floyd *et al.*, 2015a). In conjugation with biofilm

forming capacity, cytochrome *bd* provided a fitness advantage for UTI89 under hypoxic growth conditions as well as increased nitric oxide tolerance (Beebout *et al.*, 2019). So, our insertion in cytochrome c-type gene, *yecK/torY*, may also affect the adherence due to type 1 fimbriae as well as respiration in various oxygen gradient in the complex biofilm community.

Interestingly, many of the genes identified in our bank that influenced type 1 fimbriae expression are uncharacterized genes of hypothetical or unknown function. We were particularly interested in further investigating the role of the *yqhG* gene encoding a hypothetical protein containing DUF3828 domains that is conserved in *E. coli*. Although, the function of this gene is still unknown, transcription of *yqhG* was shown to be positively regulated by the BglJ-RcsB complex (Salscheider *et al.*, 2013) in *E. coli* K-12. A putative binding site for BglJ-RcsB with a significant score was also identified upstream of the *yqhG* promoter (Salscheider *et al.*, 2013). Interestingly, RcsB is the response regulator of the Rcs phosphorelay which is conserved in *Enterobacteriaceae*. RcsB plays a pleiotropic role in the control of biofilm formation, motility behavior and responds to membrane stress, specifically outer membrane stress, and is best known for its positive regulatory effect on capsule synthesis (Majdalani & Gottesman, 2005; Majdalani *et al.*, 2005). Further, BglJ is a positive DNA-binding transcriptional regulator of transport and utilization of the aromatic β-glucosides arbutin and salicin (Madhusudan *et al.*, 2005). It has been shown that it is completely dependent on RcsB (Venkatesh *et al.*, 2010). It will therefore be of interest to further investigate potential regulatory links between these regulators and *yqhG* expression in UPEC.

A more pronounced reduction of yeast agglutination occurred when the *yqhG* mutant was grown to mid-log phase in LB or urine compared to O/N growth. Similarly, other mutations in genes such as the *pst* system also resulted in a marked change in expression of type 1 fimbriae during growth to mid-log phase compared to after overnight static growth (Crépin *et al.*, 2012b). Because the CFT073 Δ*yqhG* mutant displayed a decreased capacity to agglutinate yeast in LB and urine (Fig 5.4B and C), we performed Western blotting against type 1 fimbriae to investigate any effect on type 1 fimbriae production. As shown in Figure 5.4D in comparison to the WT strain, the mutant had a reduced production of type 1 fimbriae. This reduction in type 1 fimbriae was also in line an increased bias for the OFF position with *fim* promoter in the *yqhG* mutant in LB broth at O.D.$_{600}$ 0.6 (Fig. 5.5B). Interestingly, we also found that the *yqhG* mutant was more motile than the WT strain (Fig. 5.7). UPEC strains coordinately regulate motility and adherence to mediate colonization and dissemination during the pathogenesis of UTIs. It is widely believed that when adhesin genes are expressed, motility genes are repressed and *vice versa* (Simms & Mobley,

2008a). They represent opposing forces. Thus, by mediating adherence, fimbriae would promote a sessile state and flagellar-based motility would be expected to be decreased. By contrast, increased motility by flagella would reduce the ability of bacteria to adhere at one site. Accordingly, Lane *et al.*, (2007b) and Bryan *et al.*, (2006b) have shown that constitutive expression of type 1 fimbriae (CFT073 *fim* L-ON) leads to repression of swimming motility in strain CFT073. The decreased expression of type 1 fimbriae may therefore also lead to increased production of other adhesins or biofilm associated factors under certain growth conditions. Further experiments, will be required to confirm whether loss of *yqhG* may promote expression of other fimbriae while reducing expression of type 1 fimbriae.

In the murine UTI model, the *yqhG* mutant was attenuated (Fig. 5.6). Loss of *yghG* in CFT073 caused an important decrease in colonization of both the bladder and kidneys, whereas loss of type 1 fimbriae by deletion of the *fim* operon, mainly results in a decrease in colonization of the bladder in the mouse model (Gunther IV *et al.*, 2002). As such, we investigated whether loss of *yqhG* also affected resistance to certain stress conditions including oxidative stress and osmolarity. A $\Delta yqhG$ derivative of CFT073 was significantly more sensitive than its wild-type parent to oxidative stress from H_2O_2 challenge (Table 5.3), and complementation of this mutant with a single-copy of *yqhG* restored wild-type resistance to H_2O_2 killing. Although, it is clear that YqhG plays a role in regulating expression of type 1 fimbriae and promoting adherence of UPEC CFT073 to host cells, YqhG likely plays a greater role in UPEC, including adaptation to environmental stresses, as it is also required for resistance to oxidative stress. A plausible mechanism for this drop could be due to reduced catalase activity in the mutant to counteract the oxidative burst from immune cells during infection. The *yghG* mutant colonies also demonstrated less bubbling upon addition of H_2O_2 compared to wild type. So, mutation in *yqhG* may also lead to increased sensitivity to reactive oxygen radicals as well as reduced production of type 1 fimbriae. Nevertheless, our results shed new light on the importance of *yqhG* for UPEC virulence, and it will be of interest to further elucidate what other factors that are, directly or indirectly, regulated by *yqhG,* including type 1 fimbriae, and determine its importance for resistance of *E. coli* to host innate immune response during infection.

Finally, we investigated whether inactivation of *pst,* in addition to repression of expression of type 1 fimbriae also reduced resistance to stresses including oxidative and osmotic stress. Decreased virulence of the *pst* mutant of UPEC CFT073 was mainly attributed to the decreased expression of type 1 fimbriae (Crépin *et al.*, 2012b). The ability sense, adapt to, and resist different types of stress can also play an important role in regulation of gene expression, including regulation of

type 1 fimbriae. As such, we investigated the capacity of the *pst* mutant to resist oxidative and osmotic stresses. The conditions were chosen to simulate the effects of NaCl and urea that UPEC cells may encounter during colonization of the urinary tract. Urea can permeate through the cell membrane and destabilize the native structure of proteins inside cells (Withman *et al.*, 2013). According to our results, CFT073 showed a higher resistance to 0.6 M urea and 0.6 NaCl than the *pst* mutant grown to mid-log phase (Fig. 5.8C and Fig. 5.8D). Similarly, the *pst* mutant was much more sensitive to hydrogen peroxide than the CFT073 parent strain (Table 5.3). Therefore, inactivation of *pst* in CFT073 resulted in increased sensitivity to both osmotic and oxidative stress, and this may importantly also in part be linked to changes in levels of expression of type 1 fimbriae. In APEC strain χ7122, inactivation of the Pst system induced deregulation of phosphate sensing and important changes in cell surface composition that led to reduced virulence in a chicken infection model, decreased production of type 1 fimbriae and lower resistance to oxidative stress (Crépin *et al.*, 2008; Lamarche *et al.*, 2005)**.** Several studies concerning osmotic stress and expression of type 1 fimbriae were also reported for UPEC. In UPEC strain NU149, type 1 fimbriae expression was downregulated under osmotic stress caused by NaCl (Schwan *et al.*, 2002b). Further, loss of *treA* in ExPEC strain MT78 also resulted in a change in osmotic resistance to urea, concomitant with a decreased expression of type 1 fimbriae and reduced urinary tract colonization in the mouse model (Pavanelo *et al.*, 2018). Transcriptome analyses also showed upregulation of type 1 fimbriae expression and the genes that are regulated by the osmotic stress response in CFT073 during UTI (Snyder *et al.*, 2004b).

Overall, generation of a transposon bank and a single-copy *lux*-based reporter fusion system integrated at the *att*Tn7 site in UPEC strain CFT073, has led to successful identification of insertions in a number of genes including heretofore unknown sites that altered expression of type 1 fimbriae. Interestingly, these insertions include a variety of genes involved in a diversity of functions including protein fate and synthesis, energy metabolism, adherence, transcriptional regulation, and transport, and genes of hypothetical or unknown function including *yqhG*, that we have shown to play an important role in UPEC colonization in the mouse model as well as resistance to oxidative stress. It will be of interest to more fully elucidate how some of these different systems influence expression of type 1 fimbriae as well as their potential roles in metabolism and bacterial regulatory networks as well as sensing, adaptation and resistance to environmental stresses such as osmotic and oxidative stresses that may be encountered during the course of colonization and infection of the host.

5.7   Data Availability

The datasets generated for this study are available on request to the corresponding author.

5.8   Author Contributions

HB was the primary author and performed most of the experiments and writing of the manuscript. PP and HH contributed to some of the experiments and writing of the text. SH contributed the technical assistance including mouse infections with other co-authors. CD conceived the planning of the study, design of experiments, mentored the researchers, and revised the manuscript.

5.9   Funding

5.10   Conflict of Interest Statement

The authors declare that the research was conducted in the absence of any commercial or financial relationships that could be construed as a potential conflict of interest.

5.11 References

1. Åberg, A., Shingler, V., and Balsalobre, C. (2006). (p) ppGpp regulates type 1 fimbriation of *Escherichia coli* by modulating the expression of the site-specific recombinase FimB. *Molecular microbiology* 60**,** 1520-1533.
2. Abraham, J.M., Freitag, C.S., Clements, J.R., and Eisenstein, B.I. (1985). An invertible element of DNA controls phase variation of type 1 fimbriae of *Escherichia coli*. *Proceedings of the National Academy of Sciences* 82**,** 5724-5727.
3. Alteri, C.J., Smith, S.N., and Mobley, H.L. (2009). Fitness of *Escherichia coli* during urinary tract infection requires gluconeogenesis and the TCA cycle. *PLoS Pathogens* 5**,** e1000448.
4. Baba, T., Ara, T., Hasegawa, M., Takai, Y., Okumura, Y., Baba, M., Datsenko, K.A., Tomita, M., Wanner, B.L., and Mori, H. (2006). Construction of *Escherichia coli* K-12 in-frame, single-gene knockout mutants: the Keio collection. *Molecular systems biology* 2.
5. Beebout, C.J., Eberly, A.R., Werby, S.H., Reasoner, S.A., Brannon, J.R., De, S., Fitzgerald, M.J., Huggins, M.M., Clayton, D.B., and Cegelski, L. (2019). Respiratory heterogeneity shapes biofilm formation and host colonization in uropathogenic *Escherichia coli*. *mBio* 10**,** e02400-02418.
6. Bertrand, N., Houle, S., Lebihan, G., Poirier, É., Dozois, C.M., and Harel, J. (2010). Increased Pho regulon activation correlates with decreased virulence of an avian pathogenic *Escherichia coli* O78 strain. *Infection and Immunity* 78**,** 5324-5331.
7. Bjarke Olsen, P., and Klemm, P. (1994). Localization of promoters in the fim gene cluster and the effect of H-NS on the transcription of *fimB* and *fimE*. *FEMS Microbiology Letters* 116**,** 95-100.
8. Blomfield, I.C., Kulasekara, D.H., and Eisenstein, B.I. (1997). Integration host factor stimulates both FimB-and FimE-mediated site-specific DNA inversion that controls phase variation of type 1 fimbriae expression in *Escherichia coli*. *Molecular microbiology* 23**,** 705-707.
9. Boyer, E., Bergevin, I., Malo, D., Gros, P., and Cellier, M. (2002). Acquisition of Mn (II) in addition to Fe (II) is required for full virulence of *Salmonella enterica* serovar Typhimurium. *Infection and Immunity* 70**,** 6032-6042.
10. Brinkman, A.B., Ettema, T.J., De Vos, W.M., and Van Der Oost, J. (2003). The Lrp family of transcriptional regulators. *Molecular microbiology* 48**,** 287-294.
11. Bryan, A., Roesch, P., Davis, L., Moritz, R., Pellett, S., and Welch, R.A. (2006). Regulation of type 1 fimbriae by unlinked FimB-and FimE-like recombinases in uropathogenic *Escherichia coli* strain CFT073. *Infection and Immunity* 74**,** 1072-1083.
12. Buchanan, K., Falkow, S., Hull, R., and Hull, S. (1985). Frequency among Enterobacteriaceae of the DNA sequences encoding type 1 pili. *Journal of Bacteriology* 162**,** 799-803.
13. Buckles, E.L., Bahrani-Mougeot, F.K., Molina, A., Lockatell, C.V., Johnson, D.E., Drachenberg, C.B., Burland, V., Blattner, F.R., and Donnenberg, M.S. (2004). Identification and characterization of a novel uropathogenic *Escherichia coli*-associated fimbrial gene cluster. *Infection and Immunity* 72**,** 3890-3901.
14. Cahill, D.J., Fry, C.H., and Foxall, P.J. (2003). Variation in urine composition in the human urinary tract: evidence of urothelial function in situ? *The Journal of urology* 169**,** 871-874.
15. Cai, W., Wannemuehler, Y., Dell'anna, G., Nicholson, B., Barbieri, N.L., Kariyawasam, S., Feng, Y., Logue, C.M., Nolan, L.K., and Li, G. (2013). A novel two-component signaling system facilitates uropathogenic *Escherichia coli*'s ability to exploit abundant host metabolites. *PLoS pathogens* 9**,** e1003428.
16. Calvo, J.M., and Matthews, R.G. (1994). The leucine-responsive regulatory protein, a global regulator of metabolism in *Escherichia coli*. *Microbiol. Mol. Biol. Rev.* 58**,** 466-490.

17. Chen, S.L., Wu, M., Henderson, J.P., Hooton, T.M., Hibbing, M.E., Hultgren, S.J., and Gordon, J.I. (2013). Genomic diversity and fitness of *E. coli* strains recovered from the intestinal and urinary tracts of women with recurrent urinary tract infection. *Science translational medicine* 5, 184ra160-184ra160.

18. Cherepanov, P.P., and Wackernagel, W. (1995). Gene disruption in *Escherichia coli*: TcR and KmR cassettes with the option of Flp-catalyzed excision of the antibiotic-resistance determinant. *Gene* 158, 9-14.

19. Connell, I., Agace, W., Klemm, P., Schembri, M., Mărild, S., and Svanborg, C. (1996). Type 1 fimbrial expression enhances *Escherichia coli* virulence for the urinary tract. *Proceedings of the National Academy of Sciences* 93, 9827-9832.

20. Cortes, M.A., Gibon, J., Chanteloup, N.K., Moulin-Schouleur, M., Gilot, P., and Germon, P. (2008). Inactivation of ibeA and *ibeT* results in decreased expression of type 1 fimbriae in extraintestinal pathogenic *Escherichia coli* strain BEN2908. *Infection and Immunity* 76, 4129-4136.

21. Crépin, S., Harel, J., and Dozois, C.M. (2012a). Chromosomal complementation using Tn7 transposon vectors in Enterobacteriaceae. *Applied and Environmental Microbiology.* 78, 6001-6008.

22. Crépin, S., Houle, S., Charbonneau, M.-È., Mourez, M., Harel, J., and Dozois, C.M. (2012b). Decreased expression of type 1 fimbriae by a *pst* mutant of uropathogenic *Escherichia coli* reduces urinary tract infection. *Infection and Immunity* 80, 2802-2815.

23. Crépin, S., Lamarche, M.G., Garneau, P., Séguin, J., Proulx, J., Dozois, C.M., and Harel, J. (2008). Genome-wide transcriptional response of an avian pathogenic *Escherichia coli* (APEC) pst mutant. *BMC Genomics* 9, 568.

24. Crépin, S., Porcheron, G., Houle, S., Harel, J., and Dozois, C.M. (2017). Altered regulation of the diguanylate cyclase YaiC reduces production of type 1 fimbriae in a Pst mutant of uropathogenic *Escherichia coli* CFT073. *Journal of Bacteriology* 199, e00168-00117.

25. Culham, D.E., Lu, A., Jishage, M., Krogfelt, K.A., Ishihama, A., and Wood, J.M. (2001). The osmotic stress response and virulence in pyelonephritis isolates of *Escherichia coli*: contributions of RpoS, ProP, ProU and other systems. *Microbiology* 147, 1657-1670.

26. Datsenko, K.A., and Wanner, B.L. (2000). One-step inactivation of chromosomal genes in *Escherichia coli* K-12 using PCR products. *Proceedings of the National Academy of Sciences* 97, 6640-6645.

27. De Lorenzo, V., Herrero, M., Jakubzik, U., and Timmis, K.N. (1990). Mini-Tn5 transposon derivatives for insertion mutagenesis, promoter probing, and chromosomal insertion of cloned DNA in gram-negative eubacteria. *Journal of Bacteriology* 172, 6568-6572.

28. De Lorenzo, V., and Neilands, J. (1986). Characterization of *iucA* and *iucC* genes of the aerobactin system of plasmid ColV-K30 in *Escherichia coli*. *Journal of Bacteriology* 167, 350-355.

29. Eberly, A., Floyd, K., Beebout, C., Colling, S., Fitzgerald, M., Stratton, C., Schmitz, J., and Hadjifrangiskou, M. (2017). Biofilm formation by uropathogenic *Escherichia coli* is favored under oxygen conditions that mimic the bladder environment. *International Journal of Molecular Sciences* 18, 2077.

30. Flores-Mireles, A.L., Walker, J.N., Caparon, M., and Hultgren, S.J. (2015). Urinary tract infections: epidemiology, mechanisms of infection and treatment options. *Nature Reviews Microbiology* 13, 269.

31. Floyd, K.A., Moore, J.L., Eberly, A.R., Good, J.A., Shaffer, C.L., Zaver, H., Almqvist, F., Skaar, E.P., Caprioli, R.M., and Hadjifrangiskou, M. (2015). Adhesive fiber stratification in uropathogenic *Escherichia coli* biofilms unveils oxygen-mediated control of type 1 pili. *PLoS Pathogens* 11, e1004697.

32. Foxman, B. (2002). Epidemiology of urinary tract infections: incidence, morbidity, and economic costs. *The American Journal of Medicine* 113, 5-13.

33. Foxman, B. (2014). Urinary tract infection syndromes: occurrence, recurrence, bacteriology, risk factors, and disease burden. *Infectious Disease Clinics of North America* 28**,** 1-13.

34. Francis, K.P., Yu, J., Bellinger-Kawahara, C., Joh, D., Hawkinson, M.J., Xiao, G., Purchio, T.F., Caparon, M.G., Lipsitch, M., and Contag, P.R. (2001). Visualizing Pneumococcal Infections in the Lungs of Live Mice Using Bioluminescent *Streptococcus pneumoniae*Transformed with a Novel Gram-Positive *lux* Transposon. *Infection and Immunity* 69**,** 3350-3358.

35. Gally, D.L., Leathart, J., and Blomfield, I.C. (1996). Interaction of FimB and FimE with the fim switch that controls the phase variation of type 1 fimbriae in *Escherichia coli* K-12. *Molecular Microbiology* 21**,** 725-738.

36. Gon, S., Patte, J.-C., Méjean, V., and Iobbi-Nivol, C. (2000). The torYZ (*yecK bisZ*) operon encodes a third respiratory trimethylamine N-oxide reductase in *Escherichia coli*. *Journal of Bacteriology* 182**,** 5779-5786.

37. Gunther Iv, N.W., Snyder, J.A., Lockatell, V., Blomfield, I., Johnson, D.E., and Mobley, H.L. (2002). Assessment of virulence of uropathogenic *Escherichia coli* type 1 fimbrial mutants in which the invertible element is phase-locked on or off. *Infection and Immunity* 70**,** 3344-3354.

38. Hama, H., Kayahara, T., Ogawa, W., Tsuda, M., and Tsuchiya, T. (1994). Enhancement of serine-sensitivity by a gene encoding rhodanese-like protein in *Escherichia coli*. *The Journal of Biochemistry* 115**,** 1135-1140.

39. Hartl, F.U. (1996). Molecular chaperones in cellular protein folding. *Nature* 381**,** 571.

40. Herrero, M., De Lorenzo, V., and Timmis, K.N. (1990). Transposon vectors containing non-antibiotic resistance selection markers for cloning and stable chromosomal insertion of foreign genes in gram-negative bacteria. *Journal of Bacteriology* 172**,** 6557-6567.

41. Hobert, E.H., and Datta, P. (1983). Synthesis of biodegradative threonine dehydratase in *Escherichia coli*: role of amino acids, electron acceptors, and certain intermediary metabolites. *Journal of Bacteriology* 155**,** 586-592.

42. Jenal, U., and Malone, J. (2006). Mechanisms of cyclic-di-GMP signaling in bacteria. *Annual Review of Genetics.* 40**,** 385-407.

43. Kaniga, K., Compton, M.S., Curtiss, R., 3rd, and Sundaram, P. (1998). Molecular and functional characterization of *Salmonella enterica* serovar typhimurium *poxA* gene: effect on attenuation of virulence and protection. *Infection and Immunity* 66**,** 5599-5606.

44. Kelly, A., Conway, C., Cróinín, T.Ó., Smith, S.G., and Dorman, C.J. (2006). DNA supercoiling and the Lrp protein determine the directionality of fim switch DNA inversion in *Escherichia coli* K-12. *Journal of Bacteriology* 188**,** 5356-5363.

45. Kevin James Allen, M.W.G. (2000). Construction and application of flaa sigma-28 promoter fusions to the virulence am3 ecology of *Campyloobacter jejuni*. *Thesis*.

46. Klemm, P. (1986). Two regulatory *fim* genes, *fimB* and *fimE*, control the phase variation of type 1 fimbriae in *Escherichia coli*. *The EMBO journal* 5**,** 1389-1393.

47. Klemm, P., and Christiansen, G. (1990). The *fimD* gene required for cell surface localization of *Escherichia coli* type 1 fimbriae. *Molecular and General Genetics MGG* 220**,** 334-338.

48. Lamarche, M.G., Dozois, C.M., Daigle, F., Caza, M., Curtiss, R., Dubreuil, J.D., and Harel, J. (2005). Inactivation of the pst system reduces the virulence of an avian pathogenic *Escherichia coli* O78 strain. *Infection and Immunity* 73**,** 4138-4145.

49. Lamarche, M.G., and Harel, J. (2010). Membrane homeostasis requires intact *pst* in extraintestinal pathogenic *Escherichia coli*. *Current Microbiology* 60**,** 356-359.

50. Lamarche, M.G., Wanner, B.L., Crépin, S., and Harel, J. (2008). The phosphate regulon and bacterial virulence: a regulatory network connecting phosphate homeostasis and pathogenesis. *FEMS Microbiology Reviews* 32**,** 461-473.

51. Lane, M.C., Lockatell, V., Monterosso, G., Lamphier, D., Weinert, J., Hebel, J.R., Johnson, D.E., and Mobley, H.L. (2005). Role of motility in the colonization of uropathogenic *Escherichia coli* in the urinary tract. *Infection and Immunity* 73, 7644-7656.

52. Lane, M.C., Simms, A.N., and Mobley, H.L. (2007). Complex interplay between type 1 fimbrial expression and flagellum-mediated motility of uropathogenic *Escherichia coli*. *Journal of Bacteriology* 189, 5523-5533.

53. Li, Z., Bouckaert, J., Deboeck, F., De Greve, H., and Hernalsteens, J.-P. (2012). Nicotinamide dependence of uropathogenic *Escherichia coli* UTI89 and application of *nadB* as a neutral insertion site. *Microbiology* 158, 736-745.

54. Madhusudan, S., Paukner, A., Klingen, Y., and Schnetz, K. (2005). Independent regulation of H-NS-mediated silencing of the bgl operon at two levels: upstream by BglJ and LeuO and downstream by DnaKJ. *Microbiology* 151, 3349-3359.

55. Majdalani, N., and Gottesman, S. (2005). The Rcs phosphorelay: a complex signal transduction system. *Annual Review of Microbiology.* 59, 379-405.

56. Majdalani, N., Heck, M., Stout, V., and Gottesman, S. (2005). Role of RcsF in signaling to the Rcs phosphorelay pathway in *Escherichia coli*. *Journal of Bacteriology* 187, 6770-6778.

57. Mann, R., Mediati, D.G., Duggin, I.G., Harry, E.J., and Bottomley, A.L. (2017). Metabolic adaptations of uropathogenic *E. coli* in the urinary tract. *Frontiers in Cellular and Infection Microbiology* 7, 241.

58. Matsumura, K., Furukawa, S., Ogihara, H., and Morinaga, Y. (2011). Roles of multidrug efflux pumps on the biofilm formation of *Escherichia coli* K-12. *Biocontrol Science* 16, 69-72.

59. Mcvicker, G., Sun, L., Sohanpal, B.K., Gashi, K., Williamson, R.A., Plumbridge, J., and Blomfield, I.C. (2011). SlyA protein activates *fimB* gene expression and type 1 fimbriation in *Escherichia coli* K-12. *Journal of Biological Chemistry* 286, 32026-32035.

60. Messner, K.R., and Imlay, J.A. (2002). Mechanism of superoxide and hydrogen peroxide formation by fumarate reductase, succinate dehydrogenase, and aspartate oxidase. *Journal of Biological Chemistry* 277, 42563-42571.

61. Mobley, H., Green, D., Trifillis, A., Johnson, D., Chippendale, G., Lockatell, C., Jones, B., and Warren, J. (1990). Pyelonephritogenic *Escherichia coli* and killing of cultured human renal proximal tubular epithelial cells: role of hemolysin in some strains. *Infection and Immunity* 58, 1281-1289.

62. Müller, C.M., Åberg, A., Straseviçiene, J., Emődy, L., Uhlin, B.E., and Balsalobre, C. (2009). Type 1 fimbriae, a colonization factor of uropathogenic *Escherichia coli*, are controlled by the metabolic sensor CRP-cAMP. *PLoS pathogens* 5, e1000303.

63. Mulvey, M.A., Lopez-Boado, Y.S., Wilson, C.L., Roth, R., Parks, W.C., Heuser, J., and Hultgren, S.J. (1998). Induction and evasion of host defenses by type 1-piliated uropathogenic *Escherichia coli*. *Science* 282, 1494-1497.

64. Mulvey, M.A., Schilling, J.D., Martinez, J.J., and Hultgren, S.J. (2000). Bad bugs and beleaguered bladders: interplay between uropathogenic *Escherichia coli* and innate host defenses. *Proceedings of the National Academy of Sciences* 97, 8829-8835.

65. Mysorekar, I.U., and Hultgren, S.J. (2006). Mechanisms of uropathogenic *Escherichia coli* persistence and eradication from the urinary tract. *Proceedings of the National Academy of Sciences* 103, 14170-14175.

66. Nielubowicz, G.R., and Mobley, H.L. (2010). Host–pathogen interactions in urinary tract infection. *Nature Reviews Urology* 7, 430.

67. Ogasawara, H., Yamada, K., Kori, A., Yamamoto, K., and Ishihama, A. (2010). Regulation of the *Escherichia coli csgD* promoter: interplay between five transcription factors. *Microbiology* 156, 2470-2483.

68. Olsen, P.B., Schembri, M.A., Gally, D.L., and Klemm, P. (1998). Differential temperature modulation by H-NS of the *fimB* and *fimE* recombinase genes which control the orientation of the type 1 fimbrial phase switch. *FEMS Microbiology Letters* 162**,** 17-23.

69. Otto, K., and Hermansson, M. (2004). Inactivation of ompX causes increased interactions of type 1 fimbriated *Escherichia coli* with abiotic surfaces. *Journal of Bacteriology* 186**,** 226-234.

70. Pavanelo, D.B., Houle, S., Matter, L.B., Dozois, C.M., and Horn, F. (2018). The periplasmic trehalase affects type 1 fimbria production and virulence of extraintestinal pathogenic *Escherichia coli* strain MT78. *Infection and Immunity* 86**,** e00241-00218.

71. Prunier, A.-L., Schuch, R., Fernandez, R.E., Mumy, K.L., Kohler, H., Mccormick, B.A., and Maurelli, A.T. (2007). nadA and nadB of *Shigella flexneri* 5a are antivirulence loci responsible for the synthesis of quinolinate, a small molecule inhibitor of *Shigella* pathogenicity. *Microbiology* 153**,** 2363-2372.

72. Riedel, C.U., Casey, P.G., Mulcahy, H., O'gara, F., Gahan, C.G., and Hill, C. (2007). Construction of p16Slux, a novel vector for improved bioluminescent labeling of gram-negative bacteria. *Applied and Environmental Microbiology.* 73**,** 7092-7095.

73. Rodriguez, G.M., and Atsumi, S. (2012). Isobutyraldehyde production from *Escherichia coli* by removing aldehyde reductase activity. *Microbial cell factories* 11**,** 90.

74. Römling, U., Galperin, M.Y., and Gomelsky, M. (2013). Cyclic di-GMP: the first 25 years of a universal bacterial second messenger. *Microbiology and Molecular Biology Reviews.* 77**,** 1-52.

75. Ronald, A. (2002). The etiology of urinary tract infection: traditional and emerging pathogens. *The American journal of medicine* 113**,** 14-19.

76. Rouquet, G., Porcheron, G., Barra, C., Répérant, M., Chanteloup, N.K., Schouler, C., and Gilot, P. (2009). A metabolic operon in extraintestinal pathogenic *Escherichia coli* promotes fitness under stressful conditions and invasion of eukaryotic cells. *Journal of Bacteriology* 191**,** 4427-4440.

77. Russo, T.A., and Johnson, J.R. (2000). Proposal for a new inclusive designation for extraintestinal pathogenic isolates of *Escherichia coli*: ExPEC. *The Journal of Infectious Diseases* 181**,** 1753-1754.

78. Salscheider, S.L., Jahn, A., and Schnetz, K. (2013). Transcriptional regulation by BglJ–RcsB, a pleiotropic heteromeric activator in *Escherichia coli*. *Nucleic Acids Research* 42**,** 2999-3008.

79. Schaeffer, A.J., Schwan, W., Hultgren, S., and Duncan, J. (1987). Relationship of type 1 pilus expression in *Escherichia coli* to ascending urinary tract infections in mice. *Infection and Immunity* 55**,** 373-380.

80. Schwan, W.R., and Ding, H. (2017). Temporal regulation of *fim* genes in uropathogenic *Escherichia coli* during infection of the murine urinary tract. *Journal of Pathogens* 2017.

81. Schwan, W.R., Lee, J.L., Lenard, F.A., Matthews, B.T., and Beck, M.T. (2002). Osmolarity and pH growth conditions regulate fim gene transcription and type 1 pilus expression in uropathogenic *Escherichia coli*. *Infection and Immunity* 70**,** 1391-1402.

82. Schwan, W.R., Shibata, S., Aizawa, S.-I., and Wolfe, A.J. (2007). The two-component response regulator RcsB regulates type 1 piliation in *Escherichia coli*. *Journal of Bacteriology* 189**,** 7159-7163.

83. Siegenthaler, R.K., and Christen, P. (2006). Tuning of DnaK chaperone action by nonnative protein sensor DnaJ and thermosensor GrpE. *Journal of Biological Chemistry* 281**,** 34448-34456.

84. Simms, A.N., and Mobley, H.L. (2008). Multiple genes repress motility in uropathogenic *Escherichia coli* constitutively expressing type 1 fimbriae. *Journal of Bacteriology* 190**,** 3747-3756.

85. Sivick, K.E., and Mobley, H.L. (2010). Waging war against uropathogenic *Escherichia coli*: winning back the urinary tract. *Infection and Immunity* 78**,** 568-585.

86. Snyder, J.A., Haugen, B.J., Buckles, E.L., Lockatell, C.V., Johnson, D.E., Donnenberg, M.S., Welch, R.A., and Mobley, H.L. (2004). Transcriptome of uropathogenic *Escherichia coli* during urinary tract infection. *Infection and Immunity* 72**,** 6373-6381.

87. Sohanpal, B.K., El-Labany, S., Lahooti, M., Plumbridge, J.A., and Blomfield, I.C. (2004). Integrated regulatory responses of *fimB* to N-acetylneuraminic (sialic) acid and GlcNAc in *Escherichia coli* K-12. *Proceedings of the National Academy of Sciences* 101**,** 16322-16327.

88. Stamm, W.E., and Norrby, S.R. (2001). Urinary tract infections: disease panorama and challenges. *The Journal of Infectious Diseases* 183**,** S1-S4.

89. Stentebjerg-Olesen, B., Chakraborty, T., and Klemm, P. (2000). FimE-catalyzed off-to-on inversion of the type 1 fimbrial phase switch and insertion sequence recruitment in an *Escherichia coli* K-12 *fimB* strain. *FEMS microbiology letters* 182**,** 319-325.

90. Thomas, W.E., Trintchina, E., Forero, M., Vogel, V., and Sokurenko, E.V. (2002). Bacterial adhesion to target cells enhanced by shear force. *Cell* 109**,** 913-923.

91. Tritz, G.J., Matney, T.S., and Gholson, R.K. (1970). Mapping of the *nadB* locus adjacent to a previously undescribed purine locus in *Escherichia coli* K-12. *Journal of Bacteriology* 102**,** 377-381.

92. Ulett, G.C., Mabbett, A.N., Fung, K.C., Webb, R.I., and Schembri, M.A. (2007). The role of F9 fimbriae of uropathogenic *Escherichia coli* in biofilm formation. *Microbiology* 153**,** 2321-2331.

93. Ulett, G.C., Totsika, M., Schaale, K., Carey, A.J., Sweet, M.J., and Schembri, M.A. (2013). Uropathogenic *Escherichia coli* virulence and innate immune responses during urinary tract infection. *Current Opinion in Microbiology* 16**,** 100-107.

94. Umbarger, H.E., and Brown, B. (1957). Threonine deamination in *Escherichia coli*. II. Evidence for two L-threonine deaminases. *Journal of Bacteriology* 73**,** 105-112.

95. Unden, G., and Kleefeld, A. (2004). "*Escherichia coli* and *Salmonella*: Cellular and Molecular Biology, eds Bock A et al". ASM Press, Washington, DC).

96. Venkatesh, G.R., Koungni, F.C.K., Paukner, A., Stratmann, T., Blissenbach, B., and Schnetz, K. (2010). BglJ-RcsB heterodimers relieve repression of the *Escherichia coli bgl* operon by H-NS. *Journal of Bacteriology* 192**,** 6456-6464.

97. Wanner, B.L. (1996). Phosphorus assimilation and control of the phosphate regulon. *Escherichia coli* and *Salmonella: cellular and molecular biology, 2nd ed. ASM Press, Washington, DC* 41**,** 1357-1381.

98. Welch, R.A., Burland, V., Plunkett, G., 3rd, Redford, P., Roesch, P., Rasko, D., Buckles, E.L., Liou, S.R., Boutin, A., Hackett, J., Stroud, D., Mayhew, G.F., Rose, D.J., Zhou, S., Schwartz, D.C., Perna, N.T., Mobley, H.L., Donnenberg, M.S., and Blattner, F.R. (2002). Extensive mosaic structure revealed by the complete genome sequence of uropathogenic *Escherichia coli*. *Proceedings of the National Academy of Sciences* 99**,** 17020-17024.

99. Withman, B., Gunasekera, T.S., Beesetty, P., Agans, R., and Paliy, O. (2013). Transcriptional responses of uropathogenic *Escherichia coli* to increased environmental osmolality caused by salt or urea. *Infection and Immunity* 81**,** 80-89.

100. Wu, X.-R., Sun, T.-T., and Medina, J.J. (1996). In vitro binding of type 1-fimbriated *Escherichia coli* to uroplakins Ia and Ib: relation to urinary tract infections. *Proceedings of the National Academy of Sciences* 93**,** 9630-9635.

101. Wu, Y., and Outten, F.W. (2009). IscR controls iron-dependent biofilm formation in *Escherichia coli* by regulating type I fimbria expression. *Journal of Bacteriology* 191**,** 1248-1257.

5.12   Supplementary data

A

LB O.D 0.6

■ QT4796 (*fimS-lux*)

B

LB O/N

■ QT4794 (*fimS-LON-lux*)
■ QT4795 (*fimS-LOFF-lux*)
■ QT4796 (*fimS-lux*)
■ QT5018 (*Δpst, fimS-lux*)

C
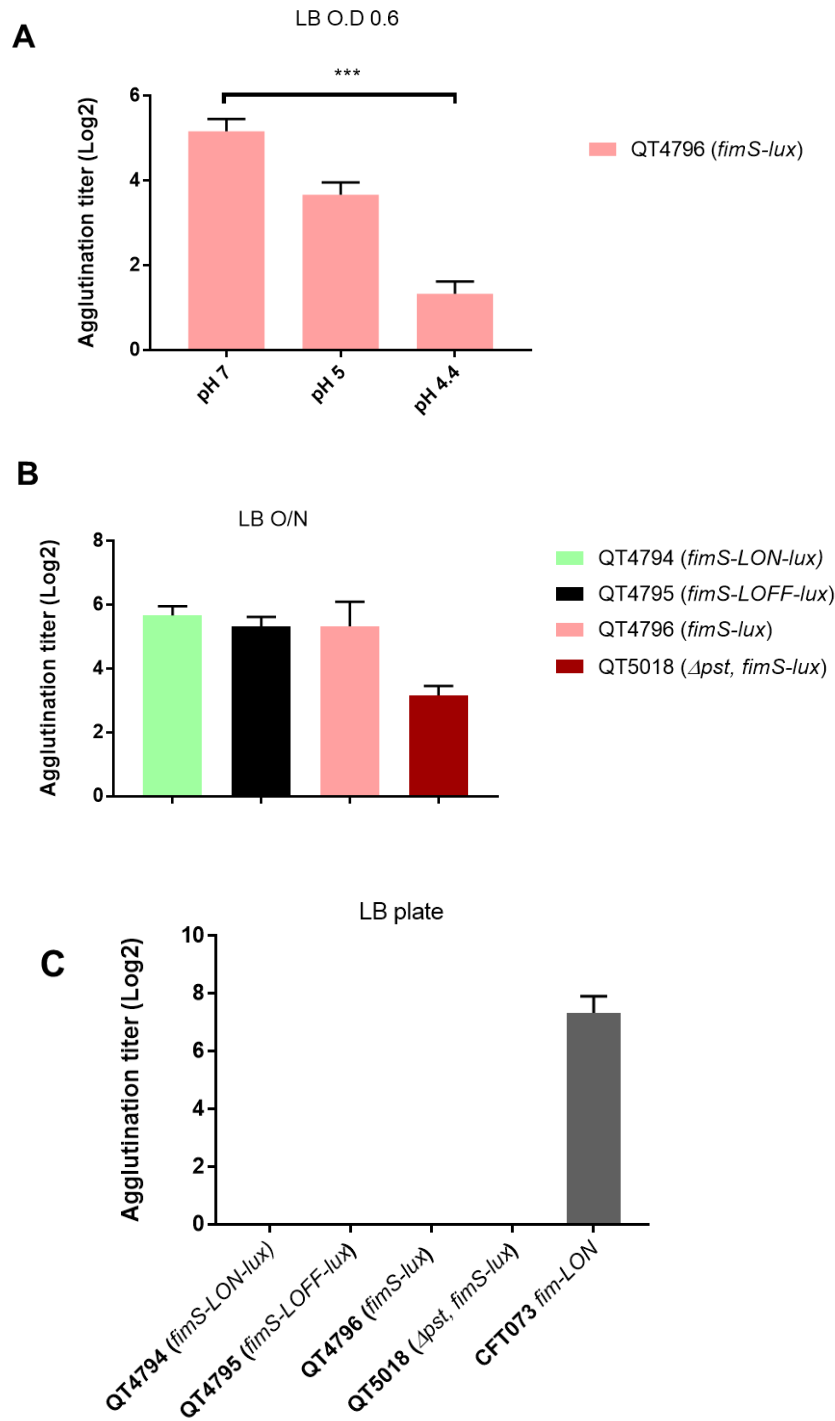
LB plate

Figure 5.9. Production of type 1 fimbriae by uropathogenic *E. coli* CFT073 and its derivative strains

(A) Production of type 1 fimbriae in strains cultured to the mid-log phase of growth in LB broth in different pH
(B) O/N culture (C) in LB plate. The CFT073 *fim*-LON strain was used as a positive control for agglutination.

Results are the mean values and standard deviations for three biological experiments. Statistical significance was calculated by the one-way ANOVA. *, P < 0.05; **, P < 0.005; ***, P < 0.0001.

A

B
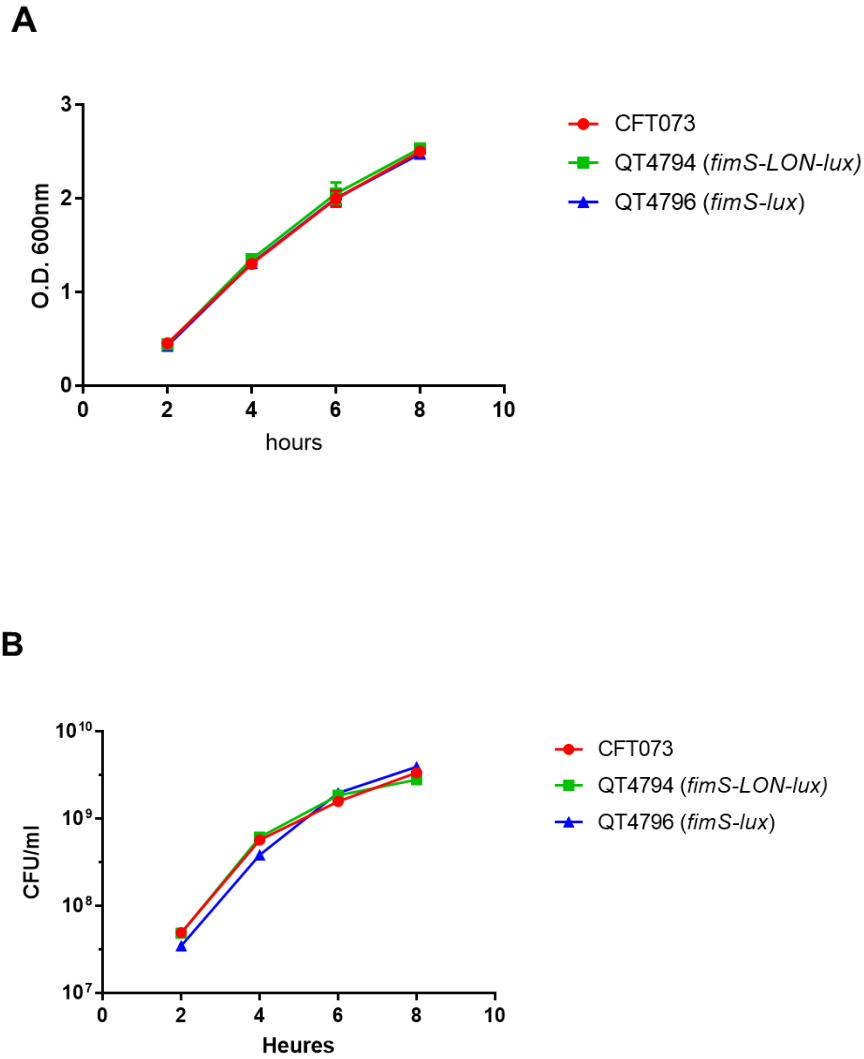
Figure 5.10. Growth curves of wild type CFT073 and its P*fimA*-Locked ON and P*fimA* variable *lux* derivatives

The cells were grown in LB broth. There were no significant differences in the growth phases of all strains.
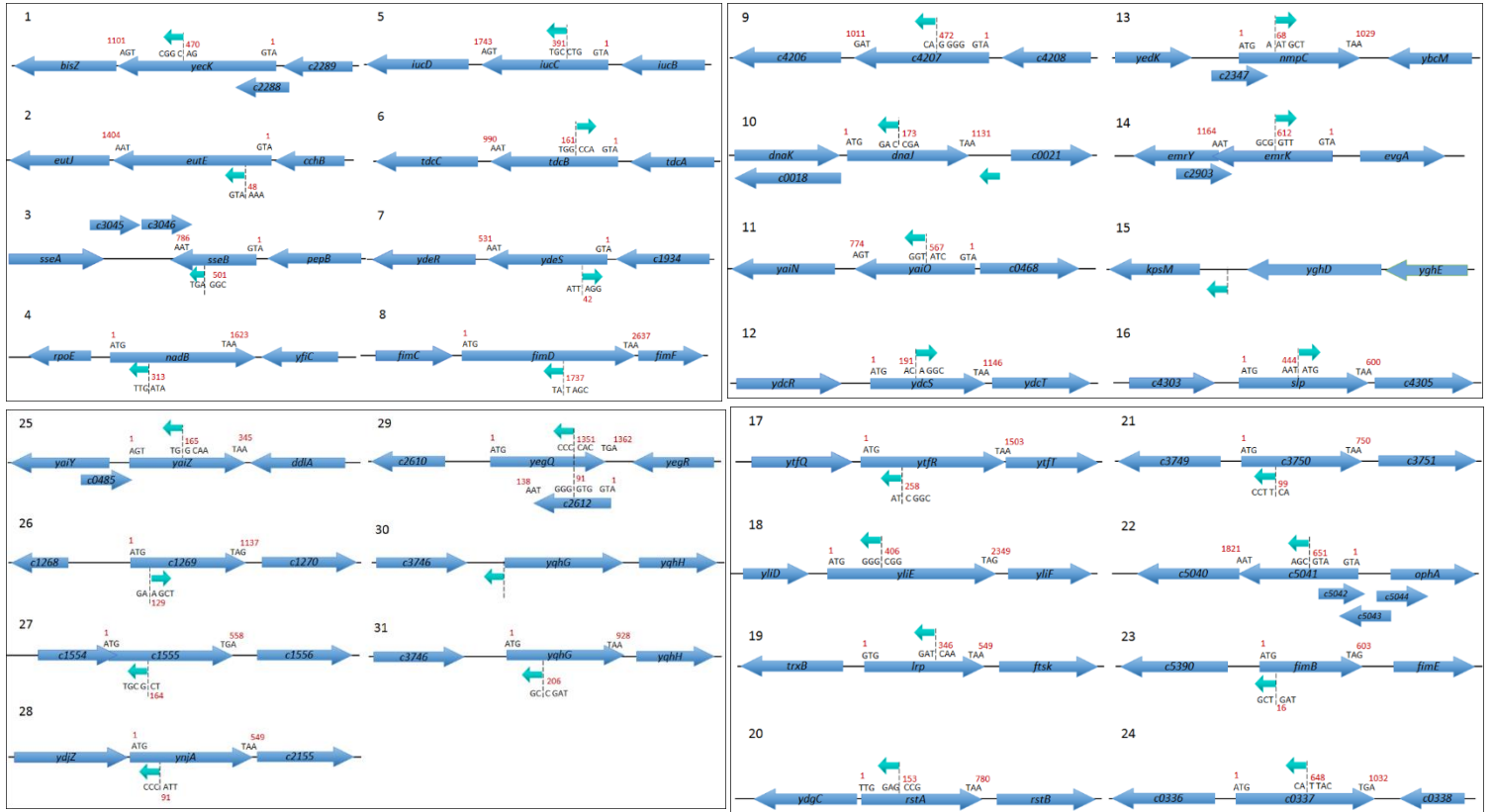
Figure 5.11. Transposon mutants with affected expression of type 1 fimbriae in CFT073

Genetic locus with the closest match to the sequence interrupted by the transposon in each mutant are represented with an arrow (teal) in their respective insertion site.

Table 5.4. Primers used in this study

Primers	Direction	Characteristic (s)	Sequences 5' → 3'
CMD26	Forward	In *glmS* for screening integration in *att*Tn*7* site (used with CMD1416)	GAT CTT CTA CAC CGT TCC GC
CMD1133	Forward	Amplification of *fimS* promoter phase locked ON used with CMD1646)	ACA ATG CCC GGG CTT TTG ACT CAT AGA GGA AAG CAT C
CMD1186	Reverse	Amplification of ON-orientation of *fimS* (used with CMD1185	ΨAAAGTTTGTGCGCGAT GCTTTCCTCTATGAGTC AAAATAGATCTCCTTGA TGGGAATTAGCCATGG TCC
CMD1185	Forward		TGGGAAAGAAATAATCT CATAAACGAAAAATTAA AAAGAGAAGAAGTTTG GTGTAGGCTGGAGCTG CTTC
CMD1246	Forward	Amplification of a *fimE*-IE region (used with CMD1248)	GAT CTT CTA CACCGT TCC GC
CMD1247	Forward	Amplification of a IE-*fimA* region (used with CMD1248)	TGAACGGTCCCACCTTA ACCG
CMD1248	Reverse		TCACATCACCCCGCTAT ATGT
CMD1258	Forward	Amplification of the *fimS* region (used with CMD1259)	TCGTTTTGCCGGATTAT GGG

CMD1259	Reverse		AGTGAACGGTCCCACC ATTAACC
CMD1416	Reverse	In Tn7 (Used with CMD26)	GCT TTT TCA CAGCAT AAC TGG A
CMD1645	Forward	Amplification of *fimS* (used with CMD1646)	TTT AAC GAA TTC ATA ATA AAG TTA AAA AAC AAA TAA ATA CAA GAC
CMD1646	Reverse		CAT GTC GAC TTC CTT TAA AAA AAC TAT TTC TAA ATC GAC ATG GGC
CMD1733	Forward	Amplification of the *luxCDABE* operon without promoter (used with CMD 1734)	CGG TAC CCT AAC TAT CAA ACG CTT CGG TTA AGC TTA AAG CAC
CMD1734	Reverse		CGG TAC CCTAACTAT CAA ACGCTT CGGTTA AGC TTAAAGCAC
CMD2290	Forward	Amplification of the *Km* gene from QT5134 (*yqhG::km*) (used with CMD2291)	TCATCATGCAGAGCC GGAAG
CMD2291	Reverse		CAGGTTGCCAGAACA ACAGC
CMD2318	Forward	Cloning of *yqhGH* into pGP-Tn7-Cm plasmid and amplification of *yqhGH* fragment for complementation (used with CMD2320)	GCAAGGCCTTCGCGAG GTACCACTCTTCCTTGT TCAGGAAT

CMD2320	Reverse		CGGGCTGCAGGAATTC CTCGAG ATATCCCCGG TAACAGAATG

ᵠThe red underlined nucleotides of the CMD 1186 primer were modified from the original sequence to lock the promoter switch (*fimS*) to the ON (L-ON) position.

6 Article 2: The RyfA small RNA serves as a master regulator of stress responses and virulence in uropathogenic *Escherichia coli*

Le petit ARN RyfA sert de régulateur principal de réponse au stress et de la virulence chez *Escherichia coli* uropathogène

Auteurs : **Hicham Bessaiah**[1,2], Pravil Pokharel[1,2], Hamza Loucif[1], Merve Kulbay[1], Charles Sasseville[3], Hajer Habouria[1,2], Sébastien Houle[1,2], Jacques Bernier[1], Éric Massé[3], Julien Van Grevenynghe[1], Charles M. Dozois[1,2*]

[1]INRS-Institut Armand-Frappier, Laval, Québec, Canada

[2]CRIPA-Centre de recherche en infectiologie porcine et avicole, Saint-Hyacinthe, Québec, Canada

[3]Department of Biochemistry, RNA Group, Université de Sherbrooke, Sherbrooke, Quebec, Canada

Recherche effectuée dans le cadre de la 2ème partie de mon doctorat

Journal : Plos Pathogens

Soumis : 3 novembre 2020

Contribution des auteurs :

J'ai réalisé, avec l'aide de mon directeur, toutes les étapes de conceptions de l'étude. J'ai effectué presque la totalité des expérimentation. J'ai écrit la totalité de l'article, qui a été corrigé par mon directeur et mes collaborateurs. **Pravil Pokharel :** Participation dans l'analyse de données transcriptomiques et infections de souris. **Hamza Loucif :** Isolement des HMDM, analyses des donnés de cytométrie en flux et imageStream. **Merve Kulbay :** Infection des RAW264.7 et quantification des ROS. **Charles Sasseville** : Réalisation du Northern blot. **Hajer Habouria :** Contribution aux infections de lignées cellulaires. **Sébastien Houle :** Assistance technique avec les infections dans le modèle murin d'ITU avec d'autres co-auteurs. **Jacques Bernier, Éric Massé et Julien Van Grevenynghe :** Assistance dans la conception de l'étude. **Charles M Dozois :** Planification et conception de l'étude, analyse et discussion des résultats, commentaires et révision du manuscrit.

*Corresponding author : Charles M. Dozois   E-mail : Charles.dozois@iaf.inrs.ca

INRS-Centre Armand-Frappier Santé Biotechnologie 531 boul des Prairies Laval, Quebec CANADA, H7V 1B7

6.1 Résumé en français

Les infections du tractus urinaires (ITU) sont une maladie infectieuse bactérienne courante chez l'homme, et les *Escherichia coli* uropathogènes (UPEC) sont la cause la plus fréquente des infections urinaires. Pendant l'infection, l'UPEC doit faire face à une variété de conditions stressantes dans les voies urinaires. Ici, nous démontrons que le petit ARN (sARN) RyfA des souches UPEC est nécessaire pour la résistance aux stress oxydatifs et osmotiques. L'inactivation de *ryfA* chez la souche UPEC CFT073 a diminué la colonisation des voies urinaires dans le modèle murin d'ITU et le mutant *ryfA* présente une réduction dans la production des fimbriae de type 1 et P, qui sont connus pour être importants pour les infections urinaires. L'analyse transcriptomique du mutant *ryfA* a montré des changements dans l'expression de gènes associés à la réponse générale au stress, au métabolisme, à la formation de biofilm et de gènes codant pour des protéines de surface cellulaire. En outre, la perte de *ryfA* a également réduit la survie des UPEC dans les macrophages humains. Ainsi, *ryfA* joue un rôle régulateur clé dans l'adaptation de l'UPEC au stress, ce qui contribue aux infections urinaires et à la survie dans les macrophages.

Mots clés : *Escherichia coli* uropathogène, infection du tractus urinaire, sARN, RyfA, stress, fimbriae de type 1, macrophage

6.2 Abstract

Urinary tract infections (UTIs) are a common bacterial infectious disease in humans, and uropathogenic *Escherichia coli* (UPEC) are the most frequent cause of UTIs. During infection, UPEC must cope with a variety of stressful conditions in the urinary tract. Here, we demonstrate that the small RNA (sRNA) RyfA of UPEC strains is required for resistance to oxidative and osmotic stresses. Inactivation of *ryfA* in UPEC strain CFT073 decreased urinary tract colonization in mice and the *ryfA* mutant also had reduced production of type 1 and P fimbriae, which are known to be important for UTI. Transcriptomic analysis of the *ryfA* mutant showed changes in expression of genes associated with general stress responses, metabolism, biofilm formation and in genes coding for cell surface proteins. Furthermore, loss of *ryfA* also reduced UPEC survival in human macrophages. Thus, *ryfA* plays a key regulatory role in UPEC adaptation to stress, that contributes to UTI and survival in macrophages.

6.3 Introduction

Urinary tract infections (UTIs) are one of the most prevalent bacterial infections, affecting millions of people each year (Foxman, 2010). UTIs primarily affect women, and up to 50% of adult women will experience at least one UTI episode. Recurrent UTIs are observed in a quarter of women within 6 months of initial diagnosis and in half of the women within one year of a UTI episode even after antimicrobial treatment (Foxman, 1990). Uropathogenic *Escherichia coli* (UPEC) remains, by far, the primary causative agent of uncomplicated UTIs (Foxman, 2010). To establish, maintain, and to circumvent host defenses during an infection, UPEC are equipped with specialized virulence factors. Well-documented examples include adhesins (type 1, P, F1C, and S fimbriae), flagella, iron acquisition systems, a polysaccharide capsule and toxins such as hemolysin (Subashchandrabose *et al.*, 2013; Wiles *et al.*, 2008a).

Bacterial adherence to host cells is critical for initiating pathogenesis and persistence during a UTI. Fimbrial adhesins (type 1, P, F1C, S, and Dr) and nonfimbrial adhesins (TosA) mediate binding to cells lining the urinary tract mucosal surfaces (Nielubowicz & Mobley, 2010; Vigil *et al.*, 2011). Type 1 fimbriae encoded by the *fimAICDFGH* (*fim*) operon are critical for colonization and invasion of bladder epithelial cells. They aid in formation of biofilm-like intracellular bacterial communities (IBCs) that contain large numbers of bacteria which may persist as reservoirs and may lead to recurring infections (Mysorekar & Hultgren, 2006). UPEC type 1 fimbriae bind to mannosylated uroplakin proteins enriched on the apical surface of the bladder (Zhou *et al.*, 2001a). *fimA* encodes the major subunit of type 1 fimbriae and *fimH* encodes the mannose-specific adhesin. The promoter region regulating *fim* expression (*fimS*) is located on a 314-bp invertible element flanked by two 9-bp inverted repeats. The expression of type 1 fimbriae is phase variable, meaning that the *fimS* promoter can switch between two different orientations which allows ("ON" orientation) or prevents ("OFF" orientation) transcription of the structural genes (Abraham *et al.*, 1985a).

 FimB and FimE are site-specific recombinases involved in phase variation (flipping) of *fimS.* FimB mediates the ON-to-OFF or OFF-to-ON inversions of *fimS*, and FimE preferentially mediates the ON-to-OFF inversion of *fimS* (Klemm, 1986a). In addition, in UPEC strain CFT073 there are three additional tyrosine recombinases, IpbA, IpuA, and IpuB, which are also capable of catalyzing inversion of *fimS* (Bryan *et al.*, 2006a). Numerous mechanisms of regulation of the *fimS* switch

and expression of type 1 fimbriae have been described. Regulatory proteins such as host factor (IHF), leucine responsive protein (LRP), and histone-like nucleoid structuring (H-NS) affect *fim* expression (Corcoran & Dorman, 2009). Other factors have also been shown to affect type 1 fimbrial expression, including cross-talk with genes from other fimbriae (Snyder *et al.*, 2005) and environmental conditions such as pH, osmolarity, temperature, metabolite availability and oxygen levels (Müller *et al.*, 2009b; Schwan *et al.*, 2002a).

As with all infectious agents, UPEC must circumvent, suppress, or resist a variety of stressful conditions and host defenses during the course of an infection. In the urinary tract, UPEC may encounter neutrophils and macrophages which produce antimicrobial factors, such as reactive oxygen species (ROS) and reactive nitrogen species (RNS) (Babior, 2000). ROS and RNS cause damage and stresses and have pleiotropic effects on bacterial cells (Nathan & Shiloh, 2000). Indeed, UPEC need to overcome environmental stresses that can be encountered during infection by a variety of mechanisms, and it is thought that resistance to ROS may be important for UPEC pathogenesis.

Bacterial small non-coding RNAs (sRNAs) are regulators of many physiological processes (Waters & Storz, 2009). Several sRNAs play key roles in bacterial adaptation to changing environmental conditions and stress responses, including responses to nutrient availability, envelope and osmotic stresses, oxidative stress, iron deficiency, and pH stress (Altuvia *et al.*, 1997; Guillier & Gottesman, 2006; Massé & Gottesman, 2002). The purpose of this research was to investigate the role of the sRNA RyfA for gene regulation in UPEC and its importance for adaptation to stress and colonization during UTI. Here, we show that RyfA contributes to resistance to oxidative and osmotic stresses in UPEC strain CFT073. In both *in vitro* and *in vivo* experiments, inactivation of *ryfA* resulted in important differences in expression of genes that contribute to protection against environmental stresses, and are known to regulate fimbrial adhesins, cellular processes, and metabolism. These regulatory changes are likely to contribute to attenuation of UPEC and its decreased capacity to survive within macrophages. These data support the hypothesis that RyfA is involved in resistance to oxidative stress in UPEC and that oxidative stress also influences type 1 fimbriae expression, thereby attenuating UPEC virulence. Understanding the link between the RyfA small RNA and its connection between stress responses, and expression of type 1 fimbriae will better elucidate the signals that control UPEC virulence, and may lead to the development of therapeutics that could potentially inhibit the establishment of UTI and thereby reduce the occurrence of this highly prevalent infection.

6.4   Materials and Methods

Ethics Statement

This study was performed in accordance with the ethical standards of the University of Quebec, INRS. A protocol for obtaining biological samples from human donors was reviewed and approved by the ethics committee - *Comité d'éthique en recherche* of INRS (CER 19-507, approved November 19, 2019).

Bacterial strains, growth conditions and plasmids

E. coli strains and plasmids used in this study are listed in Table 6.1. *E. coli* CFT073 was initially isolated from the blood and urine of a patient with acute pyelonephritis (Mobley *et al.*, 1990). Bacteria were grown in lysogeny broth (LB) (Alpha Bioscience, Baltimore, MD) at 37°C and in human urine. Urine was collected from healthy female volunteers that were from 20 to 40 years old and who had no history of UTI or antibiotic use in the prior 2 months. Each urine sample was immediately filter sterilized (0.2-µm pore size), pooled, and frozen at −80°C and was used within 2 weeks. Antibiotics and reagents were added as required at the following concentrations: kanamycin, 50 µg/ml; ampicillin, 100 µg/ml; chloramphenicol 30 µg/ml.

Table 6.1. Bacterial strains and plasmids used in this study

Strain or plasmid	Relevant characteristics	Reference or source
Strains		
CTT073	UPEC wild-type pyelonephritis strain (O6:K2:H1)	(Mobley *et al.*, 1990; Welch *et al.*, 2002)
536	UPEC wild-type pyelonephritis strain (O6:K15:H31)	(Berger *et al.*, 1982)
QT1324	CFT073 Δ*oxyR*::Km; Km^r	(Crepin *et al.*, 2012)
QT2138	CFT073 Δ*fimAICDFGH*::km; Km^r	(Crepin *et al.*, 2012)
QT2081	CFT073 Δ*lacZYA*::FRT	(Sabri *et al.*, 2009)

QT2285	CFT073 *fimS* phase L-ON	(Crepin *et al.*, 2012)
QT2496	CFT073 + pSTNSK, Km^r	(Crepin *et al.*, 2012)
QT2909	CFT073 *araBAD::Gm* - pNM12	This study
QT4437	MGN-617 + pGP-Tn*7*-Cm-Ptrc-mCherryST	This study
QT5255	CFT073 Δ*ryfA::FRT*	This study
QT5261	QT5255 + pSTNSK, Tp^r	This study
QT5305	MGN-617 + pGP-Tn7-*ryfA*	This study
QT5308	QT5255 + pSTNSK, Km^r	This study
QT5309	QT5261 :Tn*7*T-Cm::*ryfA,* Cm^r	This study
QT5325	QT5255 *araBAD::Gm,* Cm^r	This study
QT5399	QT5325-pNM12, Ap^r	This study
QT5404	QT5255 + pKEN2, Ap^r	This study
QT5559	QT2496 :Tn7T-Cm::p*trc-mCherryST ,* Cm^r	This study
QT5560	QT5308 :Tn7T-Cm::p*trc-mCherryST ,* Cm^r	This study
QT5613	536 Δ*ryfA::Km,* Km^r	This study
QT5656	CFT073 + pKEN2, Ap^r	This study
QT5656	QT5309 + pKEN2, Ap^r	This study
QT2799	*Serratia liquefaciens*	ATCC® 27592™
χ7213 (MGN-617)	*thi thr leu tonA lacY glnV supE ΔasdA4 recA*::RP4 2-Tc::Mu [λpir], Km^r	(Kaniga *et al.*, 1998)
Plasmids		
pCP20	FLP helper plasmid Ts replicon; Ap^r Cm^r	(Datsenko & Wanner, 2000)
pGP-Tn7-Cm	pGP-Tn*7*-FRT:: Cm, Ap^r, Cm^r	(Crépin *et al.*, 2012a)

pIJ258 (pSTNSK)	pST76-K::*tnsABCD*, Km^r		(Crépin *et al.*, 2012a)
pIJ360 (pSTNSK)	pST76-K::*tnsABCD*, Tp^r		(Crépin *et al.*, 2012a)
pIJ375-mCherryST	pGP-Tn*7*-Cm-Ptrc-mCherryST		(Knodler *et al.*, 2014)
pIJ546	pGP-Tn*7*-Cm::*ryfA* ; Ap^r,Cm^r		This study
pKD3	Template plasmid for the amplification of the *cat* gene bordered by FRT sites		(Datsenko & Wanner, 2000)
pKD4	Template plasmid for the amplification of the *km* cassette bordered by FRT sites		(Datsenko & Wanner, 2000)
pKD46	λ-Red recombinase plasmid Ts replicon; Ap^r		(Datsenko & Wanner, 2000)
pKEN2	*high copy phagemid constitutively expressing GFP, Ap^r*		(Cormack *et al.*, 1996)
pNM12	pBAD24 derivative, Ap^r		(Majdalani *et al.*, 1998)

Construction of site-directed mutants and complementation of strains

All mutants were generated by the procedure described by Datsenko and Wanner using plasmids pKD3 and pKD4 as the template for chloramphenicol and kanamycin resistance cassettes, respectively (Datsenko & Wanner, 2000). Primers used are listed in Table 6.2. Antibiotic cassettes flanked by FLP recombination target (FRT) sequences were removed by transforming the mutant strains with pCP20 expressing the FLP recombinase (Cherepanov & Wackernagel, 1995).

Table 6.2. Primers used in this study

Primers	Direction	Characteristic (s)	Sequences 5' → 3'

CMD26	Forward	In *glmS* for screening integration in *att*Tn*7* site (used with CMD1416)	GAT CTT CTA CAC CGT TCC GC
CMD1416	Reverse	In Tn*7* (Used with CMD26)	GCT TTT TCA CAGCAT AAC TGG A
CMD2337	Forward	Amplification of the *Km*^r cassette from pKD4 vector (used with CMD2338)	TTTTTGTCAAGCGAAAG AGAGTAATCATTGTTTA TTTAGCGTATTATCGAG TGTAGGCTGGAGCTGC TTC
CMD2338	Reverse		CTTTAAACAGAACCGGA TAATCTAAAATATGCCG CCCCAAAGGGCGGCAT ATGGGAATTAGCCATG GTCC
CMD2356	Forward	Screening for *ryfA* mutation (used with CMD2357)	TATTGGCATTGAAGCCG ATG
CMD2357	Reverse		GATTTACCGGTTGAGC CAGA
CMD2362	Forward	Cloning of *ryfA* into pGP-Tn*7*-Cm plasmid and amplification of *ryfA* fragment for complementation (used with CMD2363)	GCAAGGCCTTCGCGAG GTACCAGCAGATTTACC GGTTGAGC
CMD2363	Reverse		CGGGCTGCAGGAATTC CTCGAGCGTGACTTTAA ACAGAACCG

CMD2364	Forward	Cloning of *ryfA* into pNM12 plasmid and amplification of (used with CMD2365)	CGCAACTCTCTACTGTT TGGCCATCCGGCCCTT TCCGCCGTCT
CMD2365	Reverse		TCCCCGGGTACCATGG TGAATTCCCGAACATAT TGCGCCATTC
EM4969B	Forward	RNA probe antisense to the RyfA sRNA	CCTTTCCGCCGTCTCG CAAA
EM4970	Reverse		TAATACGACTCACTATA GGGAGAAAAATATGCC GCCCCAAAGGG
qRT-PCR			
CMD1267	Forward	*fimA* gene amplification (used with CMD1268)	*ACCGTTCAGTTAGGACA GGTTCGT*
CMD1268	Reverse		*CGAGAGCCAGAACGTT GGTAT*
CMD2370	Forward	*ryfA* gene amplification (used with CMD2371)	GTTTCTGGTGCGCTGTT A
CMD2371	Reverse		GCTTACTTGCTGCTCTG AA
CMD2547	Forward	*ibpA* gene amplification (used with CMD2548)	CTGAGAGCGAACTGGA AATTA
CMD2548	Reverse		ATGCCCTGGTACAGATA GG
CMD2549	Forward	*cadA* gene amplification (used with CMD2550)	ACCAACTTCTCACCGAT TTAC

CMD2550	Reverse		CCAGCAGTTTGTGAGTAGAC
CMD2557	Forward	*treC* gene amplification (used with CMD2558)	ACGTGGAGAGCCTCAATA
CMD2558	Reverse		GACTGTTGTCACGGGATTT
CMD2561	Forward	*cspA* gene amplification (used with CMD2562)	AAAGGCTTCGGCTTCATC
CMD2562	Reverse		GACCTTCGTCCAGAGATTTG
CMD2563	Forward	*soxS* gene amplification (used with CMD2564)	TTATCGCATGGATTGACGAG
CMD2564	Reverse		GGAACATCCGTTGCAAGT
CMD2575	Forward	*marA* gene amplification (used with CMD2576)	CTTCGAGTCCCAACAAACTC
CMD2576	Reverse		GCGATTCACCCTGCATATT
CMD2577	Forward	*bssS* gene amplification (used with CMD2578)	AATAAGTCCGAGCAGGAAGG
CMD2578	Reverse		TGGCGATTCCTGCTTCTAATA
CMD2605	Forward	*rpoH* gene amplification (used with CMD2606)	AACATCGGCCTGATGAAAG

CMD2606	Reverse		ATTCGTGGATCTCTGCT TTG

Growth under conditions of osmotic stress

Strains were tested for the capacity to grow under conditions of osmotic stress caused by NaCl or urea. Strains were inoculated 1:100 from an overnight pre-culture grown in LB and grown until mid-log phase with shaking. They were serially diluted and plated on LB agar alone and LB agar supplemented with 0.3 M NaCl, 0.6 M NaCl, 0.3 M urea, and 0.6 M urea. Colonies were counted, and growth under each condition was compared to growth on LB agar.

Sensitivity of *E. coli* strains to reactive oxygen intermediate (ROI)-generating agents

Sensitivity to oxidative stress generating agents was determined by an agar overlay diffusion method on LB plates (1.5% agar) as described by Sabri *et al.* (2008). Briefly, overnight-grown cultures were used to inoculate (1/100) fresh LB medium without antibiotics, and the resulting cultures were incubated until the O.D. $_{600}$ was 0.6. Then, 100 µl of each culture were mixed with 3 ml molten top agar and poured onto an LB agar plate. Whatman filter disks saturated with 10 µl of hydrogen peroxide (30%), plumbagin (53 mM), phenazine methosulfate (PMS) (15 mM) or phenazine ethosulfate (PES) (15 mM) were spotted onto the disks. The plates were then incubated overnight at 37°C. Following growth, the diameters of inhibition zones were measured.

For sensitivity of bacterial cultures to H_2O_2, bacteria were grown at 37°C in LB broth and approximately 2.5×10^8 CFU/ml of wild-type CFT073 or mutant was inoculated into PBS containing either 5 mM H_2O_2 and or H_2O. The test was carried out under static conditions at room temperature and samples were collected at various time points post-inoculation. Samples were diluted, plated on LB agar to determine bacterial counts.

Experimental UTI in CBA/J mice

Experimental infections were carried out using either competitive coinfection or single-strain infection models as described previously (Sabri *et al.*, 2009). Prior to inoculation, strains were grown for 16 h at 37°C with shaking (250 rpm) in 55 ml of LB medium. For coinfection, cultures were centrifuged and pellets of a *lac*-negative derivative of the wild-type (WT) and mutant or

complemented strains were mixed 1:1. Six-week-old CBA/J female mice were transurethrally inoculated with 20 µl of the 1:1 mixture containing 2×10^9 CFU of the UPEC CFT073 Δ*lacZYA* strain (QT1081) and 5×10^8 CFU of either the CFT073 Δ*ryfA* (QT5255) strain or its complemented derivative (QT5309). At 48 h postinfection (p.i.), mice were euthanized; bladders and kidneys were aseptically removed, homogenized, diluted, and plated on MacConkey agar to determine bacterial counts. In the single-strain experimental UTI model, mice were infected as described above but with only a single strain (10^9 CFU), and 48 h p.i., bacterial counts were determined from the bladders and kidneys. Bladders were dissected; one half was used to determine bacterial counts and the other half was resuspended in TRIzol reagent (Invitrogen) for RNA extraction and subsequent analysis of bacterial gene expression.

RNA extraction and quantification of gene expression.

Bacterial cultures were grown in triplicate in LB broth or human urine. RNAprotect (Qiagen, Toronto, ON, Canada) was added to cultures and RNA extracted using the RNeasy mini kit (Qiagen, Toronto, ON, Canada). Ambion™ Turbo DNase (Thermo Fisher Scientific, St. Laurent, QC, Canada) was used to remove contaminating DNA. RNA integrity was assessed using a Nanodrop (ND-1000). RNA was also extracted from infected bladders at 48 h p.i. with TRIzol reagent (Thermo Fisher Scientific, St. Laurent, QC, Canada), followed by DNase 1 treatment. Total RNAs were then reverse-transcribed to cDNAs using TransScript® All-in-One First-Strand cDNA Synthesis SuperMix Kit (TransGen, Haidian District, Beijing, China). The resulting cDNA was used for qRT PCR with EvaGreen® according to the manufacturer's instructions (TransGen, Haidian District, Beijing, China). The *rpoD* gene was used as housekeeping control. Each qRT-PCR run was done in triplicate, and for each reaction the calculated threshold cycle (C_T) was normalized to the C_T of the *rpoD* gene amplified from the corresponding sample. The fold change was calculated using the $2^{-\Delta\Delta CT}$ method (Livak & Schmittgen, 2001). Genes with a fold-change above or below the defined threshold of 2 were considered as differentially expressed. Primers used for qRT-PCR analysis are listed in Table 6.2.

RNA sequencing, mapping and analyses

Cultures were grown in triplicate as described above, and total RNA was isolated using the Qiagen RNeasy Protect Bacteria Mini kit. RNA-seq was performed at Génome Québec Innovation Centre, McGill University. Total RNA was quantified using a NanoDrop Spectrophotometer ND-1000 (NanoDrop Technologies, Inc.) and its integrity was assessed on a 2100 Bioanalyzer (Agilent

Technologies, St. Laurent, QC, Canada). rRNA were depleted from 250 ng of total RNA using Ribo-Zero rRNA removal kit specific for bacteria RNA (Illumina). Residual RNA was cleaned up using the Agencourt RNA CleanTM XP Kit (Beckman Coulter) and eluted in water. cDNA synthesis was achieved with the NEB Next RNA First Strand Synthesis and NEBNext Ultra Directional RNA Second Strand Synthesis Modules (New England BioLabs, Whitby, ON, Canada). The remaining steps of library preparation were done using and the NEBNext Ultra II DNA Library Prep Kit for Illumina (New England BioLabs, Whitby, ON, Canada). Adapters and PCR primers were purchased from New England BioLabs, Whitby, ON, Canada. Libraries were quantified using the Quant-iT™ PicoGreen® dsDNA Assay Kit (Thermo Fisher Scientific, St. Laurent, QC, Canada) and the Kapa Illumina GA with Revised Primers-SYBR Fast Universal kit (Kapa Biosystems, Wilmington, MA, USA). Average size fragment was determined using a LabChip GX (PerkinElmer, Woodbridge, ON, Canada) instrument (Génome Québec).

Reads were checked for quality using the FASTQC tool, poor quality reads by Trimmomatic were converted to FastQ format, or "groomed", for downstream analysis using the FastQ Groomer tool. Bowtie was used to align RNA-seq reads to the genome of *E. coli* CFT073 (GenBank accession no. AE014075.1) with default parameters. Finally, the number of reads mapping to each annotated feature was obtained with HTSeq. Differential expression between WT CFT073 and the *ryfA* mutant was analyzed using Degust (David R. Powell. Degust: interactive RNA-seq analysis. DOI: 10.5281/zenodo.3258932). Transcripts were considered significant if passing the following cut-offs: adjusted p-value of < 0.05 and $\log_2$ fold change of >1.7 and <-1.7. All processing steps were performed using the Galaxy platform (https://usegalaxy.org/).

RNA-seq data have been deposited in the GEO database, accession number GSE157450 (https://www.ncbi.nlm.nih.gov/geo/query/acc.cgi?acc=GSE157450).

Verification of RNA-seq results (Validation of RNA-seq results by qPCR)

RNA samples were obtained and prepared as described above for RNA-seq. qRT-PCR was performed to verify the transcript levels of 8 genes selected for validation (*soxS*, *ibpA*, *cspA*, *marA*, *bssS*, *rpoH*, *cadA* and *treC*).

Northern Blot Analysis

The hot phenol method was used to extract total RNA (Aiba *et al.*, 1981). A sample of 10 μg of total RNA was loaded on a 5% acrylamide (29:1)/8M urea gel. RNA was electro-transferred to a Hybond-XL membrane (Amersham Biosciences) and UV-crosslinked (1200J). Prehybridization

was done in 50% formamide, 5× SSC, 5× Denhardt reagent, 1% SDS, and 100 µg/ml sheared salmon sperm DNA for 4 h at 60°C. The radiolabeled RNA probe was added and incubated overnight. Three 15 minutes washes of the membranes were made with 1× SSC/0.1% SDS followed by a final wash with 0.1× SSC/0.1% SDS at 65°C.

RNA Probe radio-labeling

The RNA probe antisense to the RyfA sRNA was synthesized *in vitro* using the T7 RNA polymerase. Oligos EM4969B and EM4970 were used to generate the transcription template. Transcription was carried out in the T7 transcription buffer (40 mM Tris-HCL at pH 8.0, 6 mM $MgCl_2$, 10 mM dithiothreitol, 2 mM spermidine), 400 µM NTPs (A, C and G), 10 µM UTP, 3 µl of α-32P-UTP (3000 Ci/mmol), 20 U RNA guard, 20 U T7 RNA polymerase and 0.5 µg DNA template. After 2 h of incubation at 37°C, the mixture was treated with 2 U of Turbo DNAse (Ambion) for 15 minutes. The radio-labeled probe was then purified on a G50-Sephadex column before hybridization.

Evaluation of type 1 and P fimbriae production

The level of production of type 1 fimbriae was determined by a yeast agglutination assay (Crepin *et al.*, 2012). Briefly, the strains were cultured at 37°C / 250 rpm in LB broth or human urine to mid-log phase (conditions which were used for transcriptional analyses), or static in M9-glucose or human urine overnight. Following centrifugation, 40 µl of an initial suspension of approximately 2×10^{11} cells ml^{-1} in PBS was transferred and serially diluted 2-fold in microtiter wells containing equal volumes of a 3% commercial yeast suspension in PBS. After 30 min of incubation on ice, yeast aggregation was monitored visually. The agglutination titer was defined as the most diluted sample showing agglutination.

The mannose-resistant hemagglutination (MRHA) assay was determined using human type O^+ and A^+ erythrocytes to determine HA that could be mediated by P fimbriae. Bacterial strains were grown to mid-log phase or passaged six times on LB agar at 37°C, after which a bacterial sample was transferred to a well containing 50 µl of 3% (vol/vol) human red blood cells. To inhibit type 1 fimbriae-dependent hemagglutination, a final concentration of 2.5% α-d-mannopyranose was added to samples.

Preparation of fimbrial extracts and Western blotting

Preparation of fimbrial extracts and Western blotting were performed as described previously (Crépin *et al.*, 2008), with anti-FimA serum from *E. coli* strain B$_{AM}$ and F1C fimbriae-specific (anti-F165$_2$) antiserum (Harel *et al.*, 1995) .

Adhesion assays

5637 human bladder cells (ATCC HTB-9) were grown in RPMI 1640 medium (Wisent Bioproducts) supplemented with 10% fetal bovine serum, 2 mM l-glutamine, 10 mM HEPES, 1 mM sodium pyruvate, 4.5 g/liter glucose, and 1.5 g/liter sodium bicarbonate. 5637 cells were grown to confluency in RPMI 1640 and 2×10^5 cells/well were distributed in 24-well plates. UPEC CFT073 and its derivative strains were grown in LB medium at 37°C to the mid-log phase of growth (O.D. 0.6). Immediately before infection, cultures were washed once with PBS to remove dead cells, returned to the infection medium, and infected at an estimated multiplicity of infection (MOI) of 20 CFU per cell. The bacterial cells were centrifuged, washed twice with PBS, resuspended in RPMI 1640 medium (Wisent Biocenter, St-Bruno, Canada) supplemented with 10% fetal bovine serum at 10^6 CFU ml^{-1}, and added to each well. Bacterium-host cell contact was enhanced by a 5-min centrifugation at $600 \times g$. After 2 h, cells were washed three times and lysed with PBS–0.1% sodium deoxycholate (DOC), serially diluted, and plated on LB agar plates. Quantification of cell-associated bacteria was performed as previously described (Martinez et al., 2000). To block adherence mediated by type 1 fimbriae, 2.5% α-d-mannopyranose was added to culture medium.

Electron microscopy

Cells for electron microscopy were grown as described above for agglutination assay experiments. A glow-discharged Formvar-coated copper grid was placed under a drop of bacterial culture for 15 min to allow cells to adsorb. Excess liquid was removed using filter paper, just before a drop of 1% phosphotungstic acid (negative stain) was placed onto the grid for 15 sec. Samples were left to air dry and viewed using a Hitachi H-7100 transmission electron microscope.

Swimming Motility assay

Motility assays were done using UPEC strains CFT073 and 536 and its mutant derivatives as previously described (Bessaiah *et al.*, 2019; Lane *et al.*, 2005) with modifications. Following overnight growth at 37°C, strains were cultured at 37°C in LB broth to mid-log phase. Soft agar (1% tryptone, 0.5% NaCl, 0.25% agar) or urine agar, were stabbed in the center of the plate using

an inoculating needle. Care was taken not to touch the bottom of the plate during inoculation to ensure only swimming motility was assessed. After 16 h (soft agar) or 22 h (urine agar) of incubation at 37°C, the motility diameters were measured for each strain. Wild-type *E. coli* CFT073 was always included as a reference, and three independent motility experiments for each mutant were performed. *E. coli* CFT073 *fim* L-ON was used as a negative control. Results were analyzed using a paired t-test.

Infection of human cultured macrophage-like cell line THP-1

The human monocyte cell line THP-1 (ATCC TIB-202) was maintained in RPMI 1640 (Wisent, Saint-Jean-Baptiste, QC, Canada) containing 10% (v/v) heat-inactivated FBS (Wisent, Saint-Jean-Baptiste, QC, Canada), 1 mM sodium pyruvate (Wisent, Saint-Jean-Baptiste, QC, Canada) and 1% modified Eagle's medium with non-essential amino acids (Wisent). A stock culture was maintained as monocyte-like, non-adherent cells at 37 °C in an atmosphere containing 5% (v/v) CO_2. The bacterial strains were cultured at 37°C in LB broth to mid-log phase. Bacterial cells were pelleted, washed with phosphate-buffered saline (PBS) and added to the cell monolayer at a MOI of 20:1, and plates were centrifuged for 5 min at 800 ×g to synchronize bacterial uptake. After 60 min of incubation at 37 °C, extracellular bacteria were removed by washing cells three times with prewarmed PBS, and the infected monolayers were either lysed with PBS-DOC (T0) or incubated for 2 h or 24 h with medium containing 100 µg gentamicin ml^{-1} (Wisent) to kill remaining extracellular bacteria, and then with 12 µg gentamicin ml^{-1} for the remainder of the experiment. Surviving bacteria were determined (c.f.u.) by plating on LB agar. Results are expressed as the mean±SEM of at least three experiments performed in duplicate. One-way ANOVA was used for statistical analysis.

Human Monocyte-derived Macrophage Cultures

Peripheral blood mononuclear cells (PBMC) were obtained from leukaphereses of healthy donors. All participants of the study received approval from the McGill University Health Centre Ethical Review Board (ethic reference number SL-00.069). Human monocytes were purified to at least 96% by using the Human Monocyte Enrichment Kit (Stem Cell Technologies, Vancouver, BC). Afterwards, purified human monocytes were seeded in RPMI 1640 medium supplemented with 2mM glutamine, antibiotics, and 10% FBS in the presence of 50 ng/ml of Human recombinant Macrophage colony-stimulating factor (M-CSF). After 6 days, monocyte-derived macrophages (MDMs) were used for infection assays. Differentiation follow-up during 6 days was assessed by flow cytometry analysis.

Multiparametric and Imaging Flow cytometry analyses

To assess bacterial infection in macrophages, MDMs were harvested after adding non-enzymatic cell dissociation solution (Sigma-Aldrich, Oakville, ON, Canada) for 30 mins at room temperature. Cells were washed with PBS and prepared in FACS tubes. For surface staining, we used the following specific monoclonal antibodies provided from BD Biosciences for phenotypic analysis of human MDMs: anti-CD3 (BV605), anti-CD14 (BV650), anti-CD80 (PE Cy7), anti-CD209 (PE), anti-CD64 (PE) and anti-CD86 (APC). Finally, the viability marker 7-aminoactinomycin D or 7-AAD (ThermoFisher Scientific, St. Laurent, QC, Canada) was used to exclude dead cells from analyses. Afterwards, cells were fixed with 4% paraformaldehyde solution and then washed.

Data analysis

Samples were analyzed by flow cytometry with a BD LSRII Fortessa flow cytometer and DIVA software (BD). Viable gated cell singlets were analyzed for each sample and the percentages of mCherry^{high} CFT073 containing CD14^{+} HMDMs were determined. For Imaging flow cytometry, the same procedures were applied while cells were prepared in Eppendorf tubes. For surface staining, we used CD14-V450 and CD80-APC H7 for phenotypic gating of HMDMs. Samples were acquired using the Image Stream X MKII flow cytometer and analyzed with IDEAS software (Amnis) and representative images of singlets CD14^{+} HMDMs were generated expressing GFP^{high} CFT073 bacterial cells.

Measurement of ROS production

RAW264.7 cells were infected at an MOI 20:1 in complete DMEM medium in 24-well plates. The same conditions as for infection of THP-1 cells were used. After 60 min of incubation at 37 °C, extracellular bacteria were removed by washing cells three times with prewarmed PBS, and the cells were then incubated for 4 h or 6 h with medium containing 100 µg gentamicin ml^{-1} to kill extracellular bacteria. The fluorescent probe 2′, 7′-dichlorodihydrofluorescein diacetate (H$_2$DCF-DA) (ThermoFisher Scientific, St. Laurent, QC, Canada), was solubilized at 5 mM in dimethyl sulfoxide (DMSO) (Sigma). Infected or uninfected cells were incubated with 10 µM H$_2$DCFDA for 45 min at 37°C, and then washed once with PBS 1X. Cells were then trypsin treated, washed once with PBS 1X and cell pellets were suspended in a 1 µg/ml propidium iodide solution (ThermoFisher Scientific, St. Laurent, QC, Canada). The flow cytometer FACSCalibur (Becton Dickinson) was used to measure the fluorescence of the oxidized product dichlorofluorescein at

a λ of 488 nm with excitation at 530 nm. The fluorescence of propidium iodide was measured at a λ of 585 nm with an excitation at 542 nm. A total of 10 000 viable cells were analyzed by sample. For all points, experiments were performed in replicates. Statistical differences between different conditions were determined with a two-tailed Student's t test on the indicated number (n) of experiments.

Statistical analyses

Statistical analyses were performed using the Prism 7.04 software package (GraphPad Software). Statistically significant differences between two groups were established by unpaired t-test and comparison among three or more groups was done by one-way analysis of variance (ANOVA). For the independent infections, comparisons of the CFU mL−1 or CFU g−1 distributions were analyzed using the Mann–Whitney test. A Wilcoxon signed-rank test (two-tailed; $P \leq 0.05$) was used to determine statistical significance for comparison of bacterial numbers in coinfection experiments.

6.5   Results

6.5.1   The *ryfA* gene is involved in resistance to osmotic stress

We previously generated a transposon (Tn) library in UPEC reference strain CFT073 (Bessaiah *et al.*, 2019). The library was subjected to osmotic and oxidative stresses as a selection for potentially decreased fitness in an environment in which the bacteria encounter host-derived stresses including osmolarity in urine and interactions with host immune cells. We screened this Tn library for mutants that exhibited reduced tolerance to osmotic and oxidative stress in order to identify genes that may play a role in UPEC stress tolerance. One mutant that exhibited reduced tolerance to osmotic and oxidative stress carried a transposon insertion adjacent to the *ryfA* gene.

To confirm the direct role of *ryfA* in phenotypes of decreased tolerance to stresses, we generated a site-directed deletion to create a Δ*ryfA* mutant of UPEC strain CFT073. To determine whether *ryfA* contributes to resistance to osmotic stress, the WT parental strain, Δ*ryfA*, and a complemented Δ*ryfA* strain were subjected independently to osmotic stress (0.3 and 0.6 M Urea) and salt stress (0.3 and 0.6 M NaCl), on modified LB agar. The WT and the complemented mutant were able to grow on LB agar containing different concentrations of NaCl or urea (Fig. 6.1A and 6.8A). By contrast, on LB agar with 0.6 M urea or 0.6 M NaCl, the capacity of the *ryfA* mutant to grow was significantly reduced (Fig. 6.1A). This result suggests that RyfA could play a role in resistance to osmotic stress caused by NaCl and urea.
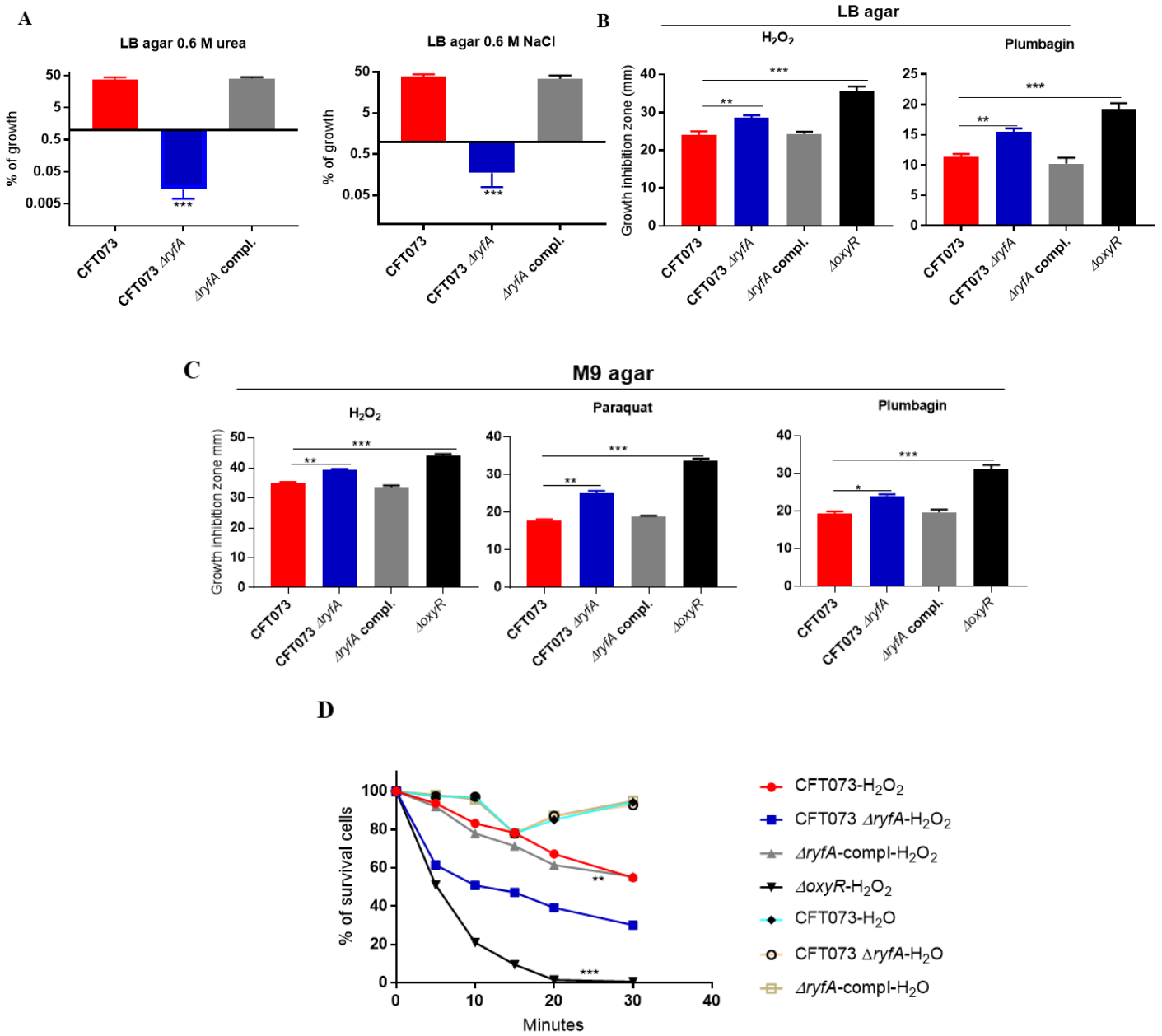
Figure 6.1. Role of RyfA in osmotic and oxidative stress resistance

(A) Growth under conditions of osmotic stress. Strains were grown with shaking in LB medium until mid-log phase (O.D.$_{600}$, 0.6) and plated on LB agar (taken as 100% growth) and LB agar with 0.6 M NaCl and 0.6 M urea. (B) Growth inhibition zones (mm) of UPEC CFT073, *ryfA* mutant and complemented strains to oxidative stress generating compounds. Strains were grown on either LB agar and (C) M9 agar. ROI-generating compounds tested were 30% hydrogen peroxide (H$_2$O$_2$), 53 mM plumbagin, 15 mM PMS or PES, and 40 mM paraquat. Sensitivity to PES was similar to sensitivity to PMS (not shown). (D) Resistance to hydrogen peroxide in LB broth. WT CFT073 and *ryfA* mutant strains were examined in LB medium containing 5mM H$_2$O$_2$ or an equivalent volume of Milli-Q water (H$_2$O). Samples were collected every 5 minutes, diluted, and plated on LB agar to determine CFU. The CFT073 Δ*oxyR* strain was used as a sensitive control strain. The results represent the means of replicate experiments for a minimum of three samples. Vertical bars represent the standard errors of the means. Statistical significance was calculated by one-way ANOVA (A to D) (*, *P* < 0.05; **, *P* < 0.005; ***, *P* < 0.0001).

6.5.2   Loss of *ryfA* increases sensitivity to ROI-generating compounds

To determine if RyfA influences UPEC resistance to oxidative stress, bacterial survival after exposure to oxidative stress was tested using different reactive oxygen intermediate (ROI)-generating agents. We used H$_2$O$_2$ and various superoxide generators such as plumbagin, paraquat, phenazine methosulfate (PMS) and phenazine ethosulfate (PES) during growth on either rich (LB) or minimal (M9-glucose) medium. Sensitivity to these compounds was determined with wild-type UPEC strains CFT073 and 536 and corresponding Δ*ryfA* mutants. On LB medium, the CFT073 Δ*ryfA* strain was more sensitive to the ROI-generating compounds H$_2$O$_2$ (p=0.0022) and plumbagin (p<0.0001) when compared to parent strain CFT073 (Fig. 6.1B). The UPEC 536 Δ*ryfA* mutant, by contrast was only more sensitive to H$_2$O$_2$ when compared to strain 536 (p=0.0065) (Fig. 6.8B). On minimal medium, both UPEC *ryfA* mutants were more sensitive to H$_2$O$_2$, plumbagin, and paraquat (Fig. 6.1C and 6.8B). In addition, in LB broth the CFT073 Δ*ryfA* mutant was killed more readily compared to wild-type CFT073 (p=0.0057) after exposure to 5 mM hydrogen peroxide (Fig. 6.1D). A regain in resistance to the levels of the wild-type was achieved by complementation of the Δ*ryfA* with a single-copy on the chromosome, confirming a role for *ryfA* in resistance to oxidative stress (Fig. 6.1B, C and D). By contrast, Δ*ryfA* mutants of either CFT073 or 536 did not demonstrate any increased sensitivity to the ROI-generating products PES and PMS (data not shown). These results show that loss of the *ryfA* sRNA reduces bacterial resistance to oxidative stress, and that RyfA may contribute to regulation of genes implicated in the oxidative stress response.

6.5.3 RyfA is required for *E. coli* fitness in the murine urinary tract infection model

Based upon increased sensitivity of the Δ*ryfA* mutant to environmental stresses, we hypothesized that the impaired osmotic and oxidative stress response could result in a fitness defect during infection of the urinary tract. To determine if *ryfA* contributed to UTI pathogenesis, a CFT073 Δ*lac* and the CFT073 Δ*ryfA* strain were administered transurethrally as a mixed inoculum to female CBA/J mice in a competition model of ascending UTI. The CFT073 Δ*lac* strain has been shown to colonize the urinary tract as well as the CFT073 wild-type parent and presented no statistical difference in a murine UTI model (Sabri *et al.*, 2009). Forty-eight hours after urethral inoculation, the Δ*ryfA* mutant was significantly outcompeted by the CFT073 Δ*lac* strain with a mean of 124-fold in the bladders (p<0.0001) and 13-fold (p<0.0001) in the kidneys (Fig. 6.2A and 6.9A). In contrast to the fitness decrease identified for the Δ*ryfA* strain during UTI, there was no growth difference between CFT073 and CFT073 Δ*ryfA* when grown *in vitro* in either LB broth or in filtered human urine, which represents an *ex vivo* condition that may reflect nutrient availability and environmental conditions encountered in the bladder (Fig. 6.9B and C). Thus, the competitive defect of the *ryfA* mutant during UTI was not the consequence of a general fitness defect, and that during standard *in vitro* culture conditions, *ryfA* was dispensable.
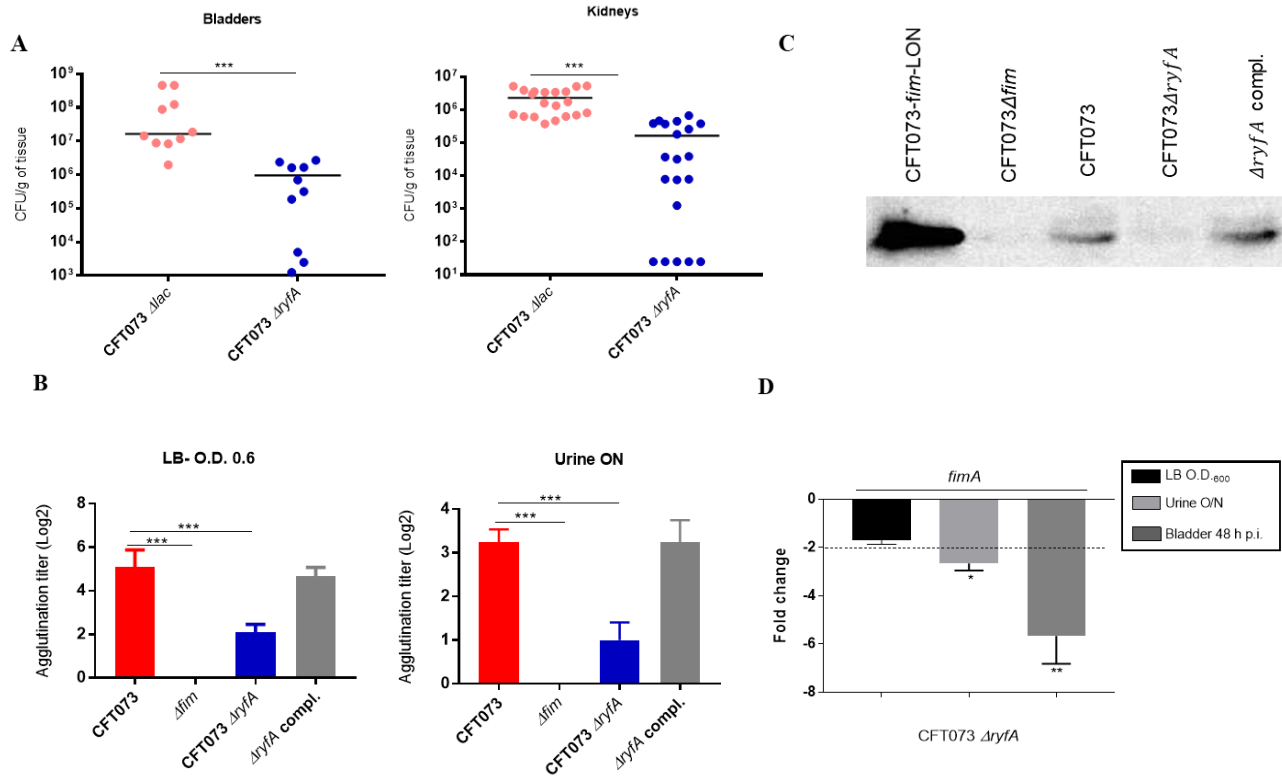
Figure 6.2. Role of *ryfA* for *E. coli* CFT073 Δ*lac* in the murine model of ascending UTI

CBA/J mice were challenged transurethrally with strain CFT073 and an isogenic Δ*ryfA* mutant. Mice were euthanized after 48 h, and bladders and kidneys were harvested for colony counts. (A) Co-infection experiments between the CFT073 Δ*lac* and the Δ*ryfA* mutant. The Δ*ryfA* strain was outcompeted in the bladders and the kidneys by over 10-fold. (B) Yeast agglutination titer demonstrating level of production of type 1 fimbriae in strains cultured to the mid-log phase of growth in LB broth and O/N in urine. The Δ*fim* strain was used as a negative control and showed no agglutination. (C) Western blot of fimbrial extracts of strains cultured to the mid-log phase of growth in LB broth. The CFT073 *fim*-Locked ON strain was used as a positive control. (D) Expression of *fimA* gene in the Δ*ryfA* strain compared to the WT CFT073 strain in LB, human urine and infected bladders. Results are the mean values and standard deviations for four biological experiments. Statistical significance was calculated by the Student t test (B, D) or Mann–Whitney Test. (A) Data are means ± standard errors of the means of 10 mice: *, P < 0.05; **, P < 0.005; ***, P < 0.0001.

6.5.4   Inactivation of RyfA reduces production of type 1 fimbriae *in vitro*

Since the *ryfA* mutant had an important fitness defect during competitive infection and given that type 1 fimbriae play an important role for colonization in the murine UTI model (Nielubowicz & Mobley, 2010), the effect of the *ryfA* mutation on production of type 1 fimbriae was investigated. Production of type 1 fimbriae was determined by yeast agglutination at the mid-log phase of growth in LB (O.D. 0.6) and urine (O.D. 0.4). Following mid-log growth with shaking in LB broth, and overnight growth in human urine with shaking, the agglutination titer of CFT073 Δ*ryfA* was significantly reduced (p<0.0001 and p=0.0062, respectively) as compared to parent strain CFT073 (Fig. 6.2B). Yeast agglutination by the *ryfA* complemented mutant regained titers similar to that of the WT strain. In addition, the production of type 1 fimbriae was reduced by half in the UPEC 536 Δ*ryfA* mutant in mid-log phase of growth in LB (p=0.0005) and in human urine (p=0.0009), respectively (Fig.6.10A). To confirm that yeast agglutination was mediated by type 1 fimbriae, the assay was also performed in the presence of 2.5% mannopyranose, which is a competitive inhibitor of type 1 fimbriae-mediated agglutination. As expected, no yeast agglutination was observed when 2.5% mannopyranose was added (data not shown). Furthermore, agglutination titers were significantly reduced in cultures of the CFT073 Δ*ryfA* mutant compared to the WT strain after static growth in human urine or minimal M9-glucose broth (Fig. 6.10B). Western blotting against the type 1 fimbrial major subunit FimA confirmed a sharp reduction of FimA production by the Δ*ryfA* mutant compared to WT strain CFT073 and the *ryfA* complemented strain (Fig. 6.2C). By comparing expression of *fimA* in the *ryfA* mutant and the complemented strain, in LB and human urine, we observed a significant decrease in *fimA* transcription in human urine (Fig. 6.2D). These results indicate that deletion of the *ryfA* sRNA

caused a substantial decrease in the levels of type 1 fimbriae production and *fimA* gene expression.

6.5.5 Loss of RyfA increases swimming motility

The effect of *ryfA* deletion on motility was determined, since motility contributes to colonization and persistence in the urinary tract (Lane *et al.*, 2005). We compared the motility of the *ryfA* mutant in 0.25% soft and urine agar. We reasoned that since the deletion of *ryfA* decreased expression of type 1 fimbriae (Fig. 6.2B and D), motility of the *ryfA* mutants may potentially be increased. There was a clear and significant increase in motility of both UPEC Δ*ryfA* strains compared to wild-type CFT073 and 536 parent strains in soft agar (Fig. 6.3). On urine agar medium, motility of all UPEC strains tested was significantly lower compared to soft agar. In addition, both *ryfA* mutants showed a higher average motility compared to the wild-type parent strains CFT073 and 536 ((p=0.0007) and (p=0.0016), respectively) (Fig. 6.3B).
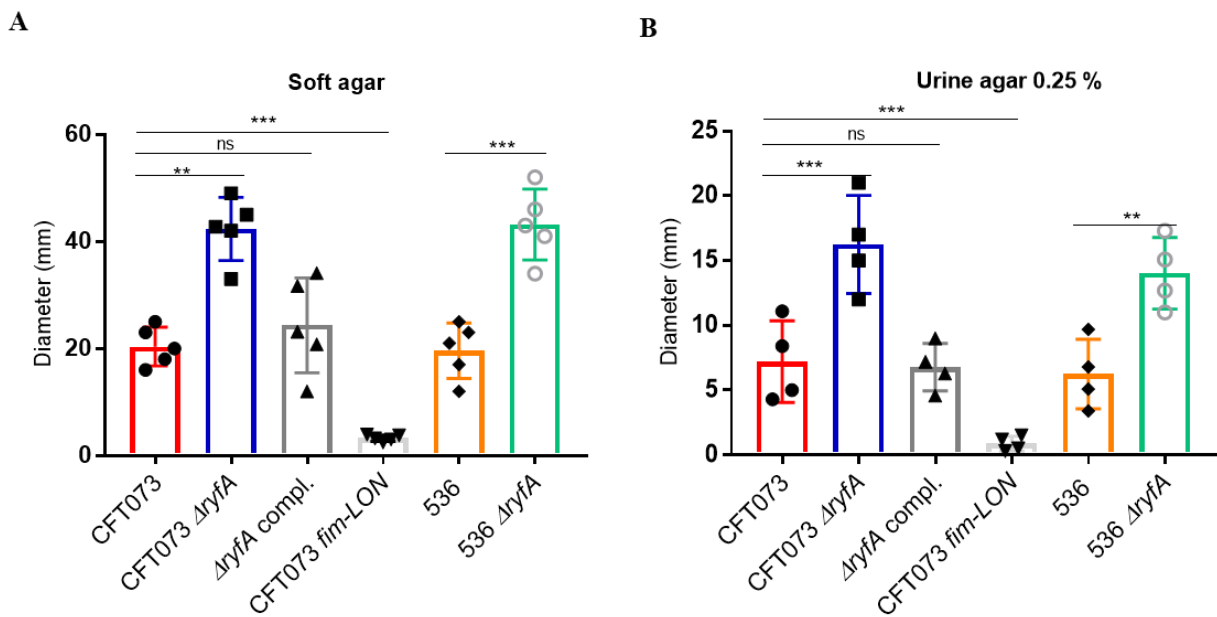
Figure 6.3. Effect of deletion of *ryfA* on motility

Motility of UPEC strains CFT073 and 536 and isogenic *ryfA* mutants on LB medium (A) or urine (B), supplemented with 0.25% agar. Each box and whisker plot (min to max) represents the mean diameter of the motility zone of each culture, based on duplicate measurements. Data represent the averages of four separate experiments. Error bars represent the SEM. Statistical significance was calculated by one-way ANOVA : *, *P* < 0.05; **, *P* < 0.005; ***, *P* < 0.0001.

6.5.6 RyfA is produced in logarithmic phase

RyfA was originally identified by *in silico*-based genomic analyses designed to identify genes encoding previously uncharacterized sRNA molecules (Hershberg *et al.*, 2003). *In silico* analyses revealed that *ryfA* is chromosomally located between *sseA* and *sseB* (Fig. 6.4A). Using BLAST searches, we identified *ryfA* homologues in other species of *Escherichia*, *Salmonella, Shigella, Klebsiella, Enterobacter, Serratia* and *Citrobacter* (Fig. 6.4A). *ryfA* from CFT073 shares 98 % identity at the nucleic acid level with the non-pathogenic K-12 strain MG1655 (Fig. 6.11A), and has greater than 90% sequence identity to *ryfA* sequences from other intestinal and extraintestinal pathogenic *E. coli* and *Shigella* (Fig. 6.4A).

To determine under what conditions CFT073 produces RyfA, we performed northern blotting. Bacteria were grown in LB medium at 37 °C until the culture O.D. of 0.2 to 2.9. Northern blot analysis showed that RyfA was expressed starting at mid-log phase and reached maximal production in late exponential phase (~ 0.9 to 2.3) (Fig. 6.4B and C). We did not detect any signal in the Δ*ryfA* strain, confirming the absence of RyfA in the mutant strain (Fig. 6.4B).
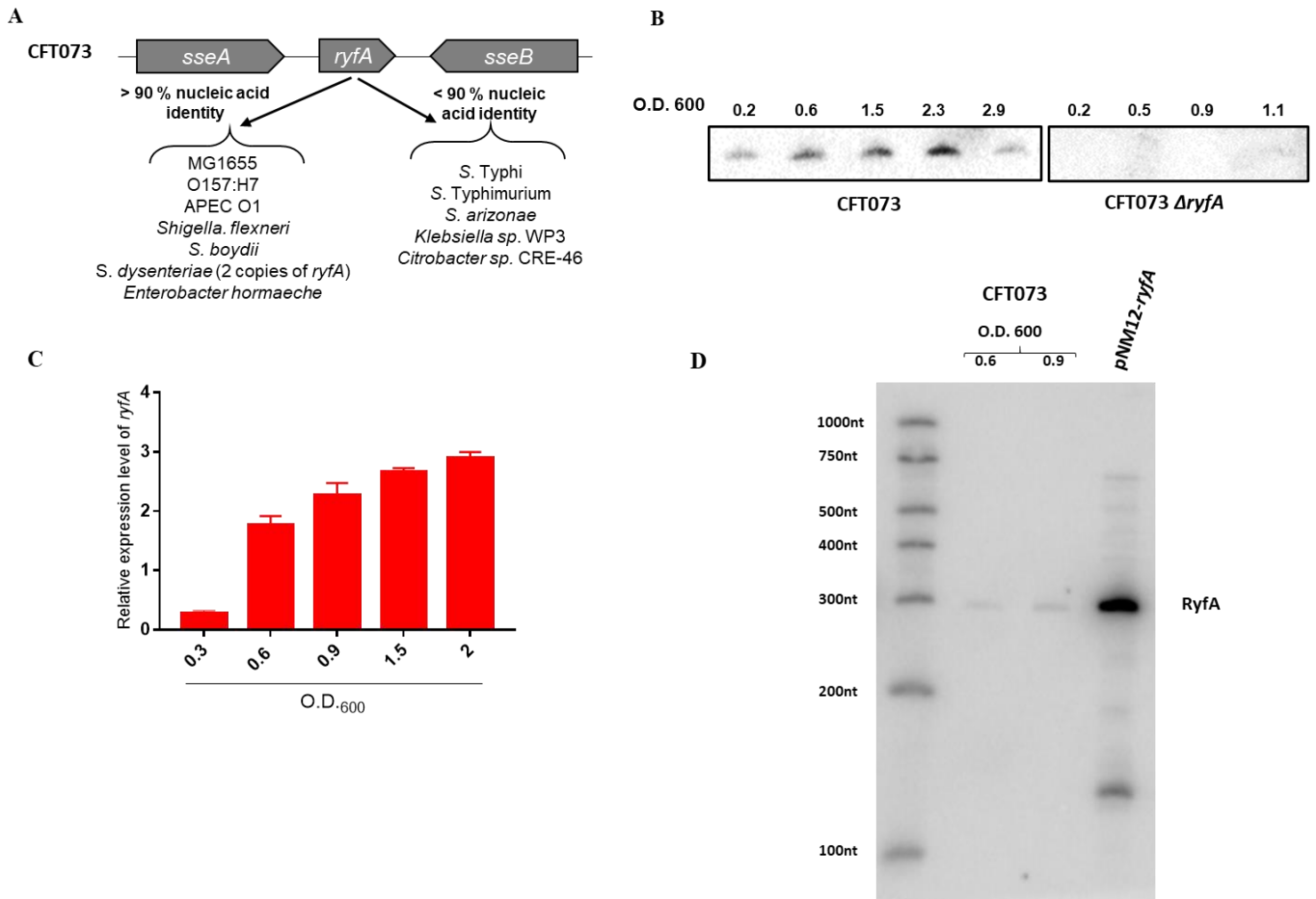
Figure 6.4. CFT073 produces RyfA in mid-logarithmic phase

(A) Schematic depicting the chromosomal location of *ryfA* in *E. coli* CFT073 and other species. (B) Northern blot analysis using 10 ug of total RNA isolated from WT CFT073 following growth to the mid-logarithmic phase at 37 °C. Lack of signal in Δ*ryfA* strain confirms absence of RyfA in the deletion strain. (C) Quantitative real-time PCR (qRT-PCR) analysis demonstrating that RyfA is produced by wild-type CFT073 under the conditions tested. (D) Northern blot showing RyfA expression in a strain overexpressing RyfA. The predicted sizes of RyfA is around 300 nt.

RyfA is predicted to be 305 nt in length (Fig. 6.11A). The production of RyfA was placed under the control of an arabinose inducible promoter and the size of RyfA was confirmed by radiolabeled *ryfA*-specific antisense RNA probe. A single band of approximately 300 nt was detected by northern blot in RNA samples obtained from strain CFT073 and using the inducible promoter construct (Fig. 6.4D). The secondary structure of RyfA was predicted using the Mfold program (Zuker, 2003) (Fig. 6.11B).

6.5.7   Transcriptomic analysis of the effect of loss of *ryfA* on UPEC gene expression

Our *in vitro* and *in vivo* experiments revealed an important role for RyfA in response to stresses and during infection. We reasoned that the decreased fitness and greater sensitivity of the *ryfA* mutant could be due to numerous changes in gene expression that occur in the absence of this regulatory RNA. To examine the role of RyfA, we performed RNA-Seq to compare RNA profiles between wild-type *E. coli* CFT073 and the CFT073 Δ*ryfA* mutant. Bacteria were cultured at 37°C in LB with aeration to mid-logarithmic growth (O.D. 0.6), mRNAs were extracted and RNA-Seq was performed. In total, the deletion of *ryfA* significantly altered the expression of 484 genes (120 were upregulated and 364 were downregulated) with a log2 fold-change (FC) greater than or equal to ± 1.7 (Table 6.4). The genes that were most highly affected in response to *ryfA* mutation are noted in Table 6.3. This functional analysis revealed that the genes belonging to the categories metabolism and stress response were by far the most markedly affected. Indeed, the increased sensitivity to stresses is likely a consequence of altered gene expression and defective regulation of the stress response.

Loss of *ryfA* alters expression of genes regulated by the RpoH (σ³²) (heat shock response) regulon

rpoH encodes σ³², the primary sigma factor controlling the heat shock response during log-phase growth. It is subjected to tight control via a multivalent regulatory system that responds to temperature and the abundance of misfolded proteins within the cell (Zhao *et al.*, 2005). During

exponential growth, in the *ryfA* mutant, *rpoH* gene expression was down-regulated (-1.76-fold) (Table 6.4). The heat shock regulon mediated by σ^{32} controls a major stress response to cope with heat and other stresses in *Escherichia coli* (Morimoto, 2011). The heat-shock response is a protective mechanism that is crucial for bacterial survival and adaptation to hostile environmental conditions. The most down-regulated genes in the *ryfA* mutant were genes encoding both cold shock and heat shock proteins (Table 6.3). These included genes encoding chaperones involved in protein fate, such as those responding to heat shock: *ibpB* (-7.70-fold), *ibpA* (-5.96-fold), *dnaKJ* (-2.20-fold), *htpX* (-2.28-fold) and *cpxP* (-3.37-fold). CpxP functions as both a chaperone and a repressor of the Cpx response. This system is involved in many cytoplasmic events, such as folding of nascent polypeptide chains, rescue of misfolded proteins and assembly and disassembly of protein complexes (Bukau & Horwich, 1998; Mogk *et al.*, 2003).

Table 6.3. Genes significantly affected by deletion of *ryfA*

ibpB	yigI	entS	focA	lamB
ymcE	ydjM	phoE	cheW	malE
ibpA	cpxP	uxuA	lysS	glpD
ynfQ	exuT	yadC	fliN	glpQ
cspG	agaB	proV	c3694	treC
glcD	nanC	cysA	lysA	glpC
cspI	iscR	htpX	flgD	glpT
glcE	c1935	cysT	ompW	glpA
fadB	papC2	cysD	flgG	glpB
soxS	mgtA	gntP	malF	cadB
kbaY	rrfG	kgtP	ghoT	cadA
cspA	yebG	ompG	inaA	
ydfK	agaV	emrY	nikC	
marB	pspA	fruK	malG	
marR	glcF	dnaJ	malM	
pspG	cspH	c1936	nikB	
marA	cyoA	dnaK	nikD	
glcC	kbaZ	cyoB	flgB	
bssS	mntS	c1934	nikA	
pspB	cysJ	papC1	ydfZ	
agaS	uidC	proW	flgC	
pspC	glcA	rpoH	treB	
pspD	fepD	csgB	malK	
mgtS	chaA	fliC	glpK	
lpxP	agaC	rpoF	glpF	

Legend:
- Amino acid metabolism
- Unknown function
- General stress responses
- Metabolism and sugar transport
- Metabolism and iron transport
- Pathospecific
- Flagella and motility
- RNA
- Curli and toxin-antitoxin system
- Fatty acids and respiratory

Downregulated
Upregulated

RNA-seq analysis was performed on RNA samples from strain CFT073 and CFT073 Δ*ryfA* grown in LB at mid-log phase of growth. Genes upregulated (yellow rectangles) and downregulated (blue rectangles) by at least 1.7-fold were considered significant. Dark blue is greater or equal to (≤) a

127

3-fold decrease. Light blue is a decrease from 3-fold to 1.7-fold. Light yellow is an increase from 1.7-fold to 3-fold. Dark yellow is a greater or equal to (≥) 3-fold increase. Genes are classified in different categories with colored squares: General stress responses in red, metabolism and sugar transport in black, metabolism and iron transport in grey, pathospecific in pink, flagella and motility in purple, fatty acids and respiratory chain in green, amino acid metabolism in white, curli and toxin-antitoxin system in orange, RNA in yellow and unknown function in azure. Specific values fold-changes are presented in Table 6.4 (see supplementary data).

Alteration of expression of genes involved in the general stress response

Several genes that are involved in defense against oxidative stress were also down-regulated including *soxS*, which encodes the transcriptional regulator that responds to superoxide-generating species (-5.03-fold) (Table 6.3). The four cold shock genes *cspG*, *cspI*, *cspA* and *cspH* were also down-regulated. Other genes associated with cold-shock were downregulated such as *ymcE* (-6.39-fold) and *ydfK* (-4.07-fold), as well as genes in the *pspABCDG* operon coding for phage shock proteins. The Psp system protects proteins from aggregation and helps maintain the proton motive force (PMF) to counteract stress conditions (such as filamentous phage infection, extreme temperatures, osmolarity changes, and the mislocalization of secretin proteins) (Flores-Kim & Darwin, 2015). The genes *yebG* and *ydjM*, which are induced during stress involving DNA-damage and SOS response were also down-regulated. In addition, *emrY* (-2.22-fold**)**, encoding a multidrug resistance secretion protein and also known to reduce the lethal effects of stress (Table 6.3) was downregulated.

Further, other genes that contribute to resistance to antimicrobials, toxic compounds and oxidative stress were also downregulated in the *ryfA* mutant. These include the *marR* (-4.01-fold) gene encoding the multiple antibiotic resistance regulator and *marAB* (-3.92- to -4.01-fold) encoding multiple antibiotic resistance proteins. Interestingly, *proVW*, encoding systems for the transport of osmoprotectants proline and glycine betaine were also downregulated (-1.94 and -2.29-fold, respectively) (Table 6.3).

Altered expression of genes involved with the cell membrane and transport systems

Other differentially expressed genes in the *ryfA* mutant, included, *ompG* (-2.22-fold) known to increase permeability and *nanC* (-3.28-fold), encoding a protein of the KdgM family of outer membrane-specific channels involved in sialic acid uptake. Some genes coding for transport of molecules were also down-regulated, including fructose, *fruB,* (-3.27-fold), magnesium, *mgtA,* (-

3.02-fold), fructuronate, *gntP,* (-2.24-fold), sodium and potassium ion extrusion, c*haA*, (-2.52-fold) and α-ketoglutarate, *kgtP,* (-2.24-fold) transporters (Table 6.4). In contrast, four genes involved in nickel uptake, *nikABCD* were up-regulated (2.47 to 3.13-fold). Likewise, *malEFG*, *malKM* and *lamB* genes involved in maltose transport and metabolism were upregulated (2.32 to 4.76-fold) (Table 6.3).

Effect on genes involved in metabolism

Some metabolic genes, involved in the catabolism of different carbon sources, were down-regulated. The *kbaZ-agaV* and *kbaY-agaSBC* operons, involved in N-acetyl-D-galactosamine and D-galactosamine transport and metabolism, respectively, were down-regulated in the *ryfA* mutant (-4.54 to -2.46-fold). In addition, repression of genes involved in transport of D-galacturonate and D-glucuronate *exuT* (-3.3-fold), utilization of fructose *fruK* (-2.21-fold) (Table 6.3), and *uxuA* encoding mannonate dehydratase were significantly downregulated. The *uxuA* gene was previously found to be upregulated during UTI (Snyder *et al*., 2004a). On the other hand, we observed increased expression of genes involved in catabolism of glycerol-3-phosphate (G3P), including the G3P transporter encoded by the *glpTQ* genes (6.18-fold), the glycerol-3-dehydrogenase *glpABC* and *glpD* (6.57-fold to 4.96-fold) and the glycerol facilitator *glpF* (4.70-fold). The Glp system mediates utilization of G3P or its precursors, glycerol and glycerophosphodiesters (Boos, 1998). Furthermore, genes involved in transport and metabolism of trehalose *treB* and *treC* were up-regulated (3.89-fold and 5.31-fold, respectively) (Table 6.3). Interestingly, genes encoding the uptake and catabolism of sn-glycerol-3-phosphate and trehalose were previously found to be downregulated *in vivo* during UTI in the mouse (Snyder *et al.*, 2004a). Upregulation of *cadA* (6.48-fold) and *cadB* (5.01-fold) genes which encode the lysine decarboxylase and lysine-cadaverine antiporter, respectively also occurred in the *ryfA* mutant (Table 6.3). This operon is induced in response to acidic pH and plays a role in maintaining pH homeostasis. Disruption of the *cad* genes abrogates cadaverine synthesis and has been shown to severely attenuate bacterial growth of uropathogenic *E. coli* strain UTI89 in the presence of acidified sodium nitrite (Bower & Mulvey, 2006).

Loss of *ryfA* altered expression of genes encoding fimbriae and required for flagella synthesis and motility

RNA-Seq results indicated that deletion of *ryfA* altered expression of genes encoding different types of fimbriae. We observed significant downregulation of the *papC* genes, which

encodes the usher protein required for biogenesis of P fimbriae. The CFT073 genome harbors two copies of the *pap* operon, designated *pap1* and *pap2*, and both *papC1* and *papC2* genes were repressed (-2.02 and -3.16-fold, respectively) (Table 6.3). The *f9* genes, encoding F9 fimbriae (ORFs c1931-c1936), showed decreased expression (-3.18 to -1.61-fold). The *yadC* gene (c0166), encoding a putative fimbrial adhesin protein, was also down-regulated (-2.3-fold). In contrast, *focA* (c1239) encoding the F1C fimbrial major subunit protein was increased (1.81-fold) (Table 6.3 and 6.4). While we identified some differentially regulated fimbria-encoding genes within the *yeh*, *yqi*, and *yfc* operons, most genes within these operons were either not differentially regulated or were excluded due to having mapped reads below the cutoff value. Surprisingly, although production of type 1 fimbriae was reduced in the *ryfA* mutant, we did not observe significant differences in the gene expression of *fim* genes under growth conditions tested.

The gene encoding the sigma factor 28 (σ^{28}), which is responsible for initiation of transcription of a number of genes involved in motility and flagellar synthesis was up-regulated (1.73-fold). In agreement with this, some flagellar biosynthesis and motility genes were also up-regulated (*flgCBGD*) (2.18 to 3.48-fold), the *fliC* gene encoding flagellin (1.60-fold), and *cheW* (1.90-fold), which encodes a positive regulator of chemotaxis (Table 6.3). The upregulation of flagellar and motility genes also corresponds to the increased swimming motility that was observed on motility agar (Fig. 6.3).

Some genes that are involved in biofilm formation were also down-regulated, including, genes important for cellulose synthesis (*bssS*) (-3.79-fold), thin aggregative curli fiber production (*csgB*) (-1,76-fold) and lipid A biosynthesis (*lpxP*) (-3,51-fold) (Table 6.3). We were unable to determine if *csgA, csgD, csgE,* and *csgF* were differentially expressed as their expression levels were too low under the test conditions that were used and were excluded from the final RNA-Seq analysis. Taken together, mutation of *ryfA* affects expression of multiple operons encoding fimbriae, downregulated some genes important for biofilm formation and upregulated genes required for flagellar assembly and motility.

6.5.8   Validation of differentially expressed genes

To validate some of the data obtained from the RNA-Seq results, we performed qPCR using primers specific to a series of genes that were differentially expressed: *soxS, ibpA, cspA, marA, bssS, rpoH, cadA malE* and *treC* to compare log2 fold change in gene expression between the CFT073 Δ*ryfA* and the wild-type parent strain CFT073. Strains were cultured under conditions

identical to our RNA-Seq experiment. We observed highly similar differences in gene expression as compared to our RNA-Seq results. Specifically, we observed downregulation of *soxS*, *ibpA*, *cspA*, *marA, bssS, rpoH* and upregulation of *cadA*, and *treC* (Fig. 6.13A).

6.5.9 Loss of RyfA reduces virulence and expression of type 1 fimbriae in the murine urinary tract

To determine whether type 1 fimbrial expression in the absence of *ryfA* is also downregulated *in vivo*, a single-strain infection in the murine UTI model with strain CFT073 was performed. In the single-strain infection model, the Δ*ryfA* mutant strain showed a marked decrease in bacterial numbers in both bladders (146-fold decrease) (P=0.0021) and the kidneys (10,000-fold decrease) (P<0.0001) compared to the wild-type parent strain (Fig. 6.5A). The *ryfA* complemented mutant colonized the mouse urinary tract as well as parent strain CFT073 (Fig. 6.5A). Likewise, *fimA* transcription was downregulated 6-fold in the bladder (Fig. 6.2D). This reduction in colonization from inactivation of *ryfA* could be due in part to the decrease in expression of *fimA* and reduced production of type 1 fimbriae, which was also observed *in vitro* (Fig. 6.2B and D). However, it is likely that additional factors including decreased resistance to cellular stresses due to loss of *ryfA* contribute to the strong attenuation and decreased bacterial numbers observed during infection with the Δ*ryfA* mutant, particularly in the kidneys. Overall, these results confirm an important role for the RyfA sRNA during colonization and infection of the urinary tract by strain CFT073.

6.5.10 Deletion of *ryfA* decreased the expression of P fimbriae and increased expression of F1C fimbriae

Deletion of the *fim* operon results in increased expression of other types of fimbriae (Crepin *et al.*, 2012; Snyder *et al.*, 2005). Interestingly, our RNA-seq data demonstrated that genes involved in biogenesis of Yad, Pap and F9 fimbriae were down-regulated in the Δ*ryfA* strain (Table 6.3 and 6.4). Further, we also observed that *fimA* (encoding the major type 1 subunit) was also decreased in the *ryfA* mutant during UTI in the mouse model and following growth in human urine (Fig. 6.2D). The *ryfA* mutant also demonstrated a marked decrease in yeast agglutination titer, which indicates a reduced level of production of type 1 fimbriae (Fig. 6.2B and 6.10B).
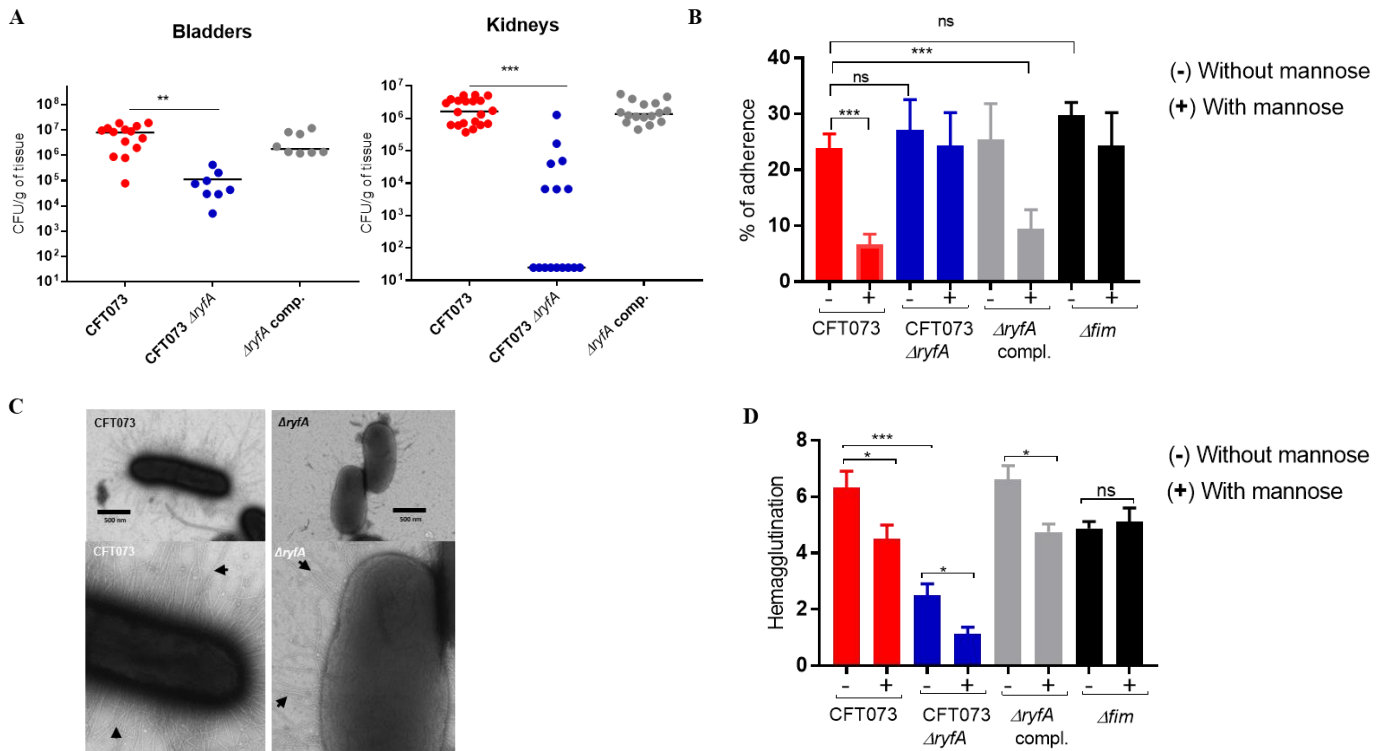
Figure 6.5. Deletion of *ryfA* decreases type 1 and P fimbriae production

A) Single-strain infections to compare wild-type strain CFT073 to Δ*ryfA* mutant. Results are presented as the log$_{10}$ CFU g^{-1}. Each data point represents a sample from an individual mouse, and horizontal bars indicate the medians. Two independent series of infections were performed: with CFT073 WT and CFT073 Δ*ryfA* and with CFT073 WT and the complemented mutant. The Δ*ryfA* mutant was attenuated 146-fold in bladder and 10,000-fold in kidneys compared to the WT parent strain. (B) Adherence of strain CFT073 and its derivatives to human 5637 bladder epithelial cells in the presence or absence of 2.5% α-d-mannopyranose was determined. (C) Electron microscopy of CFT073 and the Δ*ryfA* mutant at magnification ×12,000. Images show a typical field of view of bacteria. Arrows show fimbriae on cell surfaces. (D) Production of Pap fimbriae by hemagglutination assay. Results are the mean values and standard deviations for four biological experiments. Statistical significance was calculated by one-way ANOVA (B and D): *, *P* < 0.05; **, *P* < 0.005; ***, *P* < 0.0001.

Since UPEC strains adhere to bladder epithelial cells and epithelial cell adherence is mediated predominantly by type 1 fimbriae, we therefore hypothesized that the *ryfA* mutant may demonstrate reduced adherence to bladder epithelial cells. To test this possibility, adhesion assays using 5637 human bladder epithelial cells (ATCC HTB-9) were performed. The *ryfA* mutant adhered to human bladder cells as well as the WT strain (Fig. 6.5B). As expected, addition of 1.5% α-d-mannopyranose, which inhibits type 1 fimbriae mediated binding, greatly decreased

adherence of the WT (mean decrease of 17.2%) and complemented strain (mean decrease of 15.9%) (Fig. 6.5B). By contrast, addition of mannopyranose only slightly reduced adherence of the Δ*ryfA* (mean decrease of 2.8%) and Δ*fim* (mean decrease of 5.4%) mutants, to 5637 bladder cells (Fig. 6.5B). In line with these findings, *fimA* expression was also down-regulated by 4.8-fold in the *ryfA* mutant, during adherence to 5637 bladder cells (Fig. 6.10C).

These results suggest that other adhesins such as the *foc*-encoded F1C fimbriae, which were upregulated in the *ryfA* mutant (Table 6.3), could potentially mediate adherence to the bladder epithelial cells. Further, electron microscopy images demonstrate that the type of fimbriae at the surface of cells of the *ryfA* mutant differ from those produced by the CFT073 wild-type strain and that fimbriae are also somewhat reduced in numbers compared to the WT parent strain (Fig. 6.5C). As such, adherence of the *ryfA* mutant to bladder cells is largely independent of type 1 fimbriae and is mediated by other adhesins present at the cell surface. We also investigated production of Pap fimbriae by mannose-resistant hemagglutination (MRHA) of human erythrocytes of strains cultured in LB broth. Interestingly, the MRHA titer of the *ryfA* mutant was significantly reduced compared to parent strain CFT073 (Fig. 6.5D). This supports the hypothesis that P fimbriae production is also reduced in the *ryfA* mutant. In line with these results, expression of both *papA1* and *papA2* was reduced by 3.5-fold and 6.3-fold, respectively (Fig. 6.10C). These results demonstrate that the mannose-resistant adherence of the *ryfA* mutant to bladder epithelial cells is not attributed to increased production of Pap fimbriae, but could be due to increased production of other adhesins such as F1C fimbriae. It was also previously shown that expression of F1C fimbriae increased considerably in a strain lacking the *fim* and *pap* gene clusters (Snyder *et al.*, 2004a). Thereby, we investigated by qRT-PCR and Western blotting whether expression of F1C fimbriae was increased in this background. As shown in Fig. 6.10C and D, F1C fimbriae were upregulated 7.9-fold in the *ryfA* mutant. Therefore, upregulation of F1C fimbriae in the *ryfA* mutant could potentially contribute to the *in vitro* adherence of the *ryfA* mutant to bladder cells.

6.5.11   RyfA contributes to increased uptake and survival of UPEC in professional phagocytes

During infection, inflammatory cells produce a variety of antimicrobial factors. A primary antimicrobial agent in this repertoire is superoxide, which reacts with other molecules to form ROS. The primary source of bactericidal ROS during infection is provided by phagocyte oxidase. We next sought to assess the potential role of *ryfA* for protection from the host-generated oxidative environment during UTI by testing bacterial interaction with human macrophages. To evaluate bacterial uptake, survival and proliferation within macrophages, primary human monocyte-derived

macrophages (HMDMs) and human cultured macrophage-like THP-1 cells were infected with the wild-type strain and the isogenic mutants using a gentamicin protection assay (at a multiplicity of infection (MOI) of 20). The number of bacteria present at different times was determined by viable counts. We also assessed intramacrophage survival of an *oxyR* mutant for comparison as a sensitive control. The uptake of the *ryfA* mutant was significantly reduced in HMDMs when compared with uptake of the wild-type strain (Fig. 6.6A and 6.7). However, for the THP-1 macrophages, similar bacterial loads for the different strains were observed (Fig. 6.6B). In contrast to wild-type strain CFT073, for both the *ryfA* and *oxyR* mutants, viable bacteria decreased at 2 h post-infection in all types of macrophages (Fig. 6.6A, B, C and 6.7). Furthermore, both mutants decreased in the intracellular compartment of macrophages at 24 h post-infection, were unable to reach the number of intracellular bacterial cells observed for the wild-type parent strain. We also obtained similar results by using multi-parameter and imaging flow cytometry (Fig. 6.6D and 6.7). We monitored the uptake of mCherry-tagged CFT073 wild-type and *ryfA* mutant strains in CD14+ HMDMs, which represent a classic phenotype for HMDMs. Results showed a major drop in survival of the *ryfA* mutant in HMDMs compared to the wild-type strain at all-time points (2h, 6h and 10h post-infection) (Fig. 6.6D). Furthermore, we confirmed this assessment of the same GFP-tagged CFT073 strains including the *ryfA*-complemented strain via imaging flow cytometry. Representative images were also generated at 2h post-infection for each GFP[high] labeled strains within intracellular compartments (Fig. 6.7). Of note, we did not observe a significant difference in the uptake of mCherry-labelled CFT073 and *ryfA* mutant by RAW264.7 macrophages (Fig. 6.6C). However, the *ryfA* mutant survived significantly less than the parent wild-type strain at 2 h and 24 h post-infection (Fig. 6.6C). These observations demonstrate that loss of *ryfA* can contribute to decreased virulence and clearance during extra-intestinal infections such as UTI, since cells lacking *ryfA* are more susceptible to host phagocytic cells such as macrophages. Importantly, the complemented mutant had a completely restored uptake and survival capacity in macrophages that was similar to wild-type parental strain CFT073 (Fig. 6.6A, B, C and 6.7). It is of further interest that loss of *ryfA* also resulted in a reduced level of bacterial uptake by phagocytes, suggesting that some of the changes in expression that occur on the bacterial cell surface led to a reduced initial level of phagocytosis by macrophages. This defect of uptake by macrophages by the *ryfA* mutant also is not likely to be linked to increased sensitivity to oxidative stress, since the ROS-sensitive *oxyR* mutant did not demonstrate any differences in uptake by macrophages (Fig. 6.6A, B, C and 6.7). These results support an important role for the *ryfA* regulatory RNA in interactions with the host cellular response by contributing to uptake, survival, and replication of UPEC CFT073 inside human macrophages.
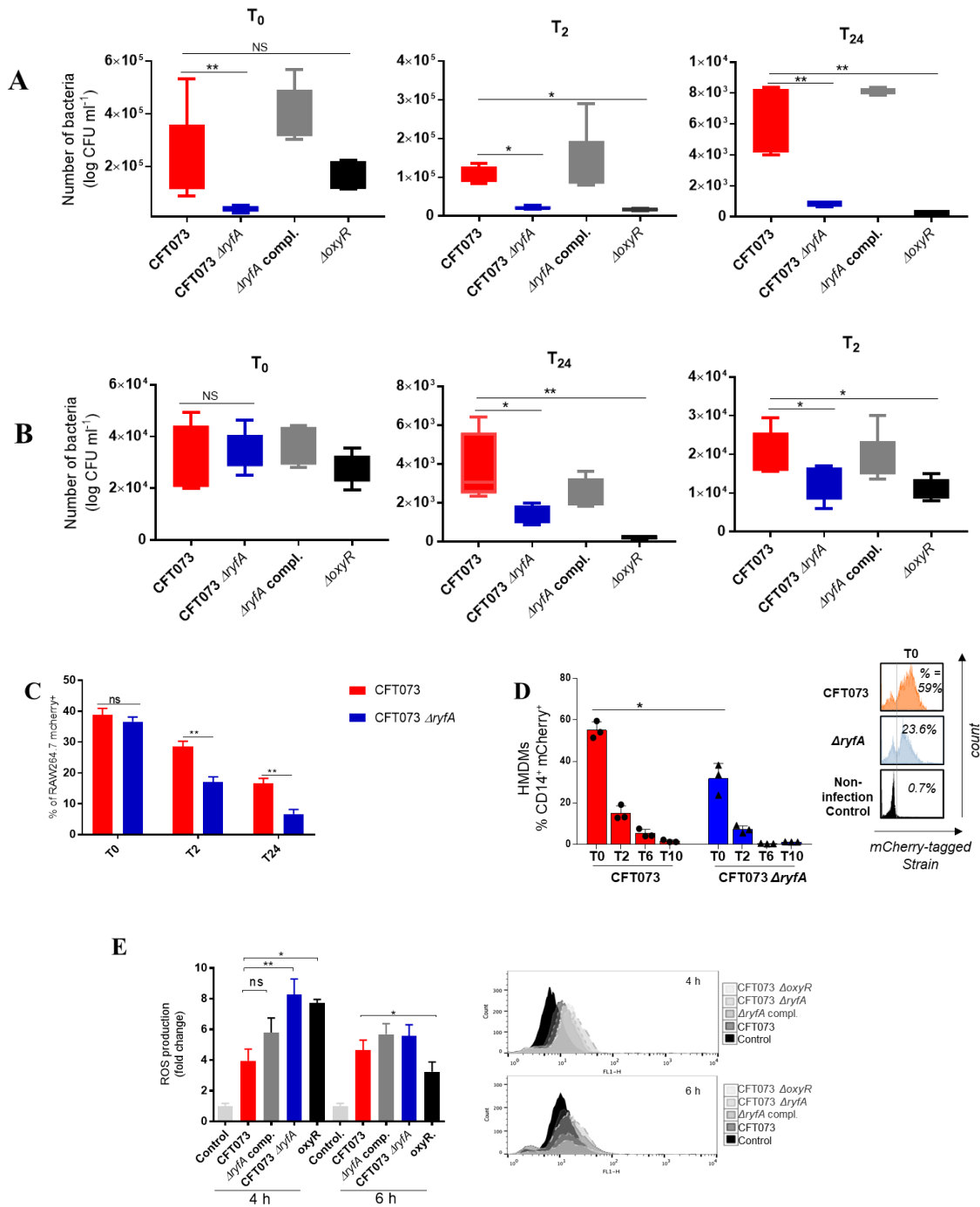
Figure 6.6. Role of RyfA during interaction with professional phagocytes

Human cells were infected with CFT073 wild-type strain, *ryfA* or *oxyR* isogenic mutants or the *ryfA*-complemented strain. (A) *in vitro* differentiated human monocyte-derived macrophages (HMDMs) and (B) THP-1 human macrophages were infected with different strains for 1 h, followed by gentamicin treatment. Cells were lysed and intracellular bacterial counts (c.f.u. ml^{-1}) associated with cells were determined at different

times post-infection (pi). Infection assessment of mCherry tagged CFT073 strains via flow cytometry in (C) RAW264.7 cells and (D) HMDMs. (E) ROS production in RAW264.7 cells. RAW264.7 cells were infected at an MOI of 20 and intracellular generation of ROS was measured at 4 h and 6 h post-infection by using H2DCFDA. Cells were stained with 10 μM H2DCFDA. All assays were conducted in triplicate and repeated independently at least three times. The results are expressed as the mean±sem of the replicate experiments. Significant differences between mutants, WT and complemented mutant strain were determined using a paired Student *t*-test. *, $P < 0.05$; **, $P < 0.005$; ***, $P < 0.0001$.
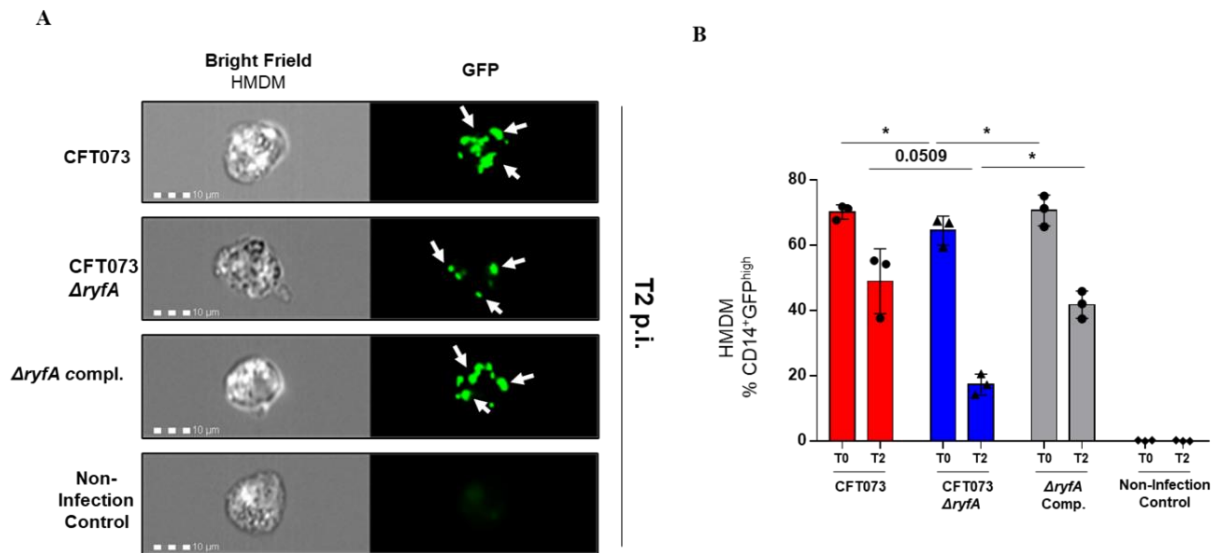
Figure 6.7. Role of RyfA during interaction with human macrophage cells

Imaging flow cytometry analysis of human monocyte-derived macrophages (HMDMs) that were infected with CFT073 wild-type strain, *ryfA* or the *ryfA*-complemented strain at 2 h post-infection. (A) Representative images of HMDMs singlets CD14+GFPhigh at 2h post-infection. (B) Infection assessment for double positive percentages of CD14+GFPhigh HMDMs. Results are expressed as the mean±sem of the replicate experiments. Significant differences between mutant, WT and complemented mutant strain were determined using a paired Student *t*-test. *, $P < 0.05$.

6.5.12 The *ryfA* mutant generates increased ROS production in RAW264.7 murine macrophage-like cells

The phagocyte NADPH oxidase and ROS production play a key role in the elimination of bacteria following phagocytosis. To measure intracellular ROS levels, RAW264.7 macrophages infected with CFT073, the Δ*ryfA*, Δ*oxyR* isogenic mutant, or the Δ*ryfA* complemented strain were incubated for 4 h and 6 h with the membrane-permeant fluorescent probe H2DCFDA. The cells were then stained with a viability marker (propidium iodide) and H2DCFDA fluorescence was quantified in viable cells. Four hours later, the level of intracellular ROS after interaction with WT

strain CFT073 was 3.9-fold higher than that measured in uninfected control cells (p=0.0026) (Fig. 6.6E). The level of intracellular ROS was 25 % (p=0.0093) and 20 % (p=0.0006) higher in cells infected with the Δ*ryfA* and Δ*oxyR* mutants respectively than in cells infected with the WT parent strain. ROS levels remained high (4-fold higher above basal level) up to 6 h p.i. in cells infected with UPEC CFT073 (Fig. 6.6E). The ROS levels were reduced by 3-fold for the *ryfA* mutant and by half for the *oxyR* mutant after 6 h p.i. (Fig. 6.6E), suggesting that both mutants are killed at a faster rate by ROS activity than the wild-type parent. By contrast, no significant difference was observed between the *ryfA* complemented mutant and the WT parent strain in ROS generation. These results also support the likelihood that attenuation of the *ryfA* mutant in the bladder and kidneys during UTI in the mouse model may also be due to a greater sensitivity to killing by host phagocytic cells and an increased generation of ROS within these cells.

6.6   Discussion

During infection of extra-intestinal tissues such as the urinary tract, pathogenic *E. coli* encounters and must adapt to numerous stresses. Bacterial sRNAs of pathogenic *E. coli* and other bacterial pathogens are important regulators of many physiological processes. The role played by sRNAs involves rapid regulation of gene expression which can lead to cellular modifications including stress adaptation in pathogenic bacteria (Ortega *et al.*, 2014). Indeed, sRNAs interact with their specific targets, such as protein, RNA or DNA to exert both positive and negative effects on gene expression, and have received significant attention as central regulators in a variety of cellular processes (Fröhlich & Vogel, 2009).

Given the importance of sRNAs for bacterial physiology and virulence, we investigated the role of the RyfA sRNA for resistance to stresses and its importance during urinary tract infection in a murine model, as well as for adherence to bladder epithelial cells, and survival in human macrophages. RyfA was shown to contribute to resistance to oxidative and osmotic stresses (Fig. 6.1 and 6.8) and virulence in co-infection (Fig. 6.2A) and single-strain (Fig. 6.5A) infection models in the urinary tract. Interestingly, the *ryfA* mutant was less attenuated in the co-infection model. This suggests that a mixed infection with the wild-type strain and *ryfA* mutant somehow alters the host response and/or that the wild-type strain may produce factors that may compensate for the *ryfA* mutant in trans. By contrast, when the *ryfA* mutant alone was tested in the UTI model, it was strongly attenuated. This outcome suggests that the *ryfA* mutant lacks the capacity to adapt to changes and stresses in these tissues and may also induce a more robust immune response during infection leading to more rapid clearance from the bladder and kidneys.

Attenuation of the *ryfA* mutant could be attributed in part to increased sensitivity to osmotic and oxidative stresses, both of which are likely to be encountered during UTI. Further, downregulation of type 1 fimbriae in the *ryfA* mutant may also contribute to reduced colonization during UTI. Deletion of *ryfA* decreased production of type 1 fimbriae or *fim* gene expression *in vitro* and *in vivo* (Fig. 6.2B, C, D and 6.10). It is interesting that there is a link between sensitivity to oxidative stress and altered expression of type 1 fimbriae. Previous studies reported that mutations in other genes, including *yeaR*, *rpoS*, *ibeA* and *yqhG,* increased sensitivity to oxidative stress and concomitantly decreased expression of type 1 fimbriae (Bessaiah *et al.*, 2019; Conover *et al.*, 2016; Dove *et al.*, 1997; Fléchard *et al.*, 2012). Importantly, assembly of type 1 fimbriae is dependent on the oxidative state of subunit proteins in the periplasm and involves the coordinated folding of subunits through action of the oxidoreductase DsbA and the chaperone FimC, underscoring the potential effects of oxidative imbalances on fimbrial biogenesis (Crespo *et al.*, 2012). Collectively, these results suggest that one consequence of loss of *ryfA* may be the reduced expression of type 1 fimbriae due to increased sensitivity of UPEC to oxidative stress.

Based on the transcriptional data during growth *in vitro*, the *ryfA* mutant may be subjected to increased oxidative stress, because it is less able to deploy mechanisms to mediate a global stress response, which may also explain why it is less able to cope with additional stresses from exogenous ROI-generating compounds. The general stress response regulon under control of *rpoH*, the oxidative stress transcriptional factor *soxS*, and genes responding to heat shock and envelope stress were all repressed in the *ryfA* mutant (Table 6.3 and 6.4). Furthermore, *marAB* genes, encoding multiple antibiotic resistance proteins were downregulated. MarA and SoxS are transcription factors belonging to the AraC family and contribute to adaptive responses to many stimuli, such as pH, antibiotics, oxidative stress, and host innate immune responses (Ruiz & Levy, 2010; Ruiz *et al.*, 2008). Furthermore, a triple knockout of a UPEC strain lacking *marA*, *soxS* and *rob* was unable to effectively colonize the kidney in a mouse model (Casaz *et al.*, 2006). Since oxidative stress is increased during infection of the host, a decreased capacity to resist ROS could explain, at least in part, the attenuation observed for *ryfA* mutant.

In the urinary tract, UPEC are subjected to environmental stresses from human urine where both urea and inorganic ions can increase osmotic stress and denature protein structure. As such, UPEC must be able to cope with transient exposure to both high osmolality and the denaturing effects of urea. RyfA contributed to resistance to osmotic stress induced by NaCl or Urea (Fig. 6.1A). Indeed, genes involved in the osmotic stress response, the glycine betaine and proline transporter *proVW*, were downregulated in the *ryfA* mutant (Table 6.3 and 6.4). The *proVW* genes

are induced in response to osmotic stress with NaCl (Withman *et al.*, 2013) and during urinary tract infection (Snyder *et al.*, 2004a) in the mouse model. Loss of *ryfA* may increase sensitivity to osmotic stress due to reduced expression of the *proVW* system. Other genes such as molecular chaperones encoding *ibpA*, *ibpB, cspF,* and *cspH,* which are induced in response to osmotic stress (Withman *et al.*, 2013), were also repressed in the *ryfA* mutant. Interestingly, it was previously reported that *cspC* and *ibpB* genes were highly expressed in UPEC CFT073 isolated from mouse urine (Haugen *et al.*, 2007). Further, *cspA*, *cspG*, *cspH*, *ibpA* and *ibpB* were among the most highly upregulated genes in asymptomatic bacteriuria (ABU) strains during static growth in human urine (Hancock & Klemm, 2007). Moreover, the two cold-shock-associated genes *cspA* and *deaD*, were upregulated in human urine samples (Hagan *et al.*, 2010), by UPEC in murine bladders (Snyder *et al.*, 2004a) and in a ABU strain in the human urinary tract (Roos & Klemm, 2006; Snyder *et al.*, 2004a). Taken together, the decreased capacity of the *ryfA* mutant to express these stress coping chaperones and osmotic stress systems is likely to contribute to its reduced survival during UTI.

Genes belonging to the Cys regulon, *soxS* and *ibpA* were reported to contribute to potassium tellurite (K_2TeO_3) resistance (Pérez *et al.*, 2007). Interestingly, the *ryfA* mutants of UPEC strains were more sensitive to K_2TeO_3 (Fig. 6.8C). The oxidative damage attributed to potassium tellurite is due at least in part to the intracellular generation of superoxide radicals.

The *ryfA* mutant adhered to human bladder cells as well as the WT strain. However, in contrast to the WT strain, which adhered mainly due to mannose-specific type 1 fimbriae, adherence of the *ryfA* mutant was mediated by mannose-resistant adhesins (Fig. 6.5B). Electron microscopy demonstrated a difference in the type of fimbriae present at the cell surface of the *ryfA* mutant compared to the WT strain (Fig. 6.5C), indicating that other adhesins are expressed at the bacterial cell surface and could mediate adherence to bladder epithelial cells. Indeed, RNA-seq data showed increased expression of *focA*, which encodes the major subunit of F1C fimbriae. Interestingly, RNA-seq data revealed that other genes encoding, P fimbriae, F9 and Yad fimbriae were downregulated. Further, the *ryfA* mutant had reduced MRHA compared to the WT strain (Fig. 6.5D), and the expression of both *papA* genes was decreased during adhesion to bladder cells (Fig. 6.10C).

UPEC strain CFT073 contains 12 distinct fimbrial gene clusters and multiple nonfimbrial adhesins (Welch *et al.*, 2002). However, one type of fimbria is predominantly expressed at a time and phase variation of different adhesins involves crosstalk between fimbrial systems that limits production

of fimbriae to a single type for each bacterial cell (Hultgren *et al.*, 1985). Based on gene expression data and immune-based detection, we determined that F1C fimbrial production was increased in the *ryfA* mutant (Fig. 6.10C and D). Since F1C fimbriae mediate adhesion to bladder and kidney epithelial cells (Khan *et al.*, 2000), this likely explains the mannose-resistant adherence demonstrated by the *ryfA* mutant (Fig. 6.5B). Increased expression of F1C fimbrial genes was also observed in a Δ*fim* Δ*pap* mutant of UPEC CFT073 (Snyder *et al.*, 2005). Indeed, in UPEC, the inactivation or constitutive expression of one fimbrial system can alter the expression of other adhesins (Snyder *et al.*, 2005). Thus, it is not surprising that loss of *ryfA* in UPEC CFT073 which caused a decreased expression of type 1 and P fimbriae has resulted in greater expression of another type of fimbrial adhesin. Taken together, these results demonstrate that *ryfA* also plays an important role in regulation and the hierarchy of cross-talk of expression of different fimbrial systems in *E. coli*.

Bacterial virulence factors are often secreted or associated with the cell envelope. In the *ryfA* mutant, many genes encoding cell envelope associated proteins demonstrated significant changes in expression. We observed significant up-regulation of genes encoding flagellar biosynthesis (*flgCBGD* and *fliC*) and chemotaxis (*cheW*) (Table 6.3 and 6.4) and other genes under the control of σ^{28}, encoded by FliA (RpoF) which controls transcription of a number of genes involved in flagellar assembly and swimming motility (Table 6.3 and 6.4). Down-regulation of *fim*, *pap*, *f9* and *yad* fimbrial transcription could also be linked to an increase in flagellar gene expression, since the *ryfA* mutant demonstrated increased swimming motility (Fig. 6.3), and also decreased expression of P and type 1 fimbriae. The production of P fimbriae is coordinated with the repression of swimming motility (Luterbach & Mobley, 2018). Furthermore, Luterbach and Mobley (2018) have demonstrated that PapX, a MarR-like protein encoded by the *pap* operon, repressed *flhD* transcription and the Δ*papX* mutant was hypermotile. Taken together, these observations indicate that type 1, P, and F1C fimbriae, along with motility, can be regulated in some coordinated fashion through a mixture of transcriptional and posttranscriptional mechanisms. Of note, motility in the urinary tract can be important for the translocation of bacteria from bladder to kidneys. In contrast to our results, a previous report on an extraintestinal pathogenic *E. coli* (ExPEC) strain isolated from an ocular infection (L-1216/2010) demonstrated reduced swimming motility compared to the parent strain (Shivaji *et al.*, 2019).

Biofilm formation is an important bacterial adaptation for survival, increased resistance to antibiotics and other stresses. Previous studies investigating contribution of a diversity of sRNAs in *E. coli* demonstrated that loss of *ryfA* decreased biofilm formation in pathogenic and non-

pathogenic *E. coli*. Decreased biofilm formation is likely due to the observed decrease in production of exopolysaccharides, cellulose and curli (Bak *et al.*, 2015; Shivaji *et al.*, 2019). In the current work, the *ryfA* mutants of CFT073 and 536 exhibited a significant decrease in biofilm formation in LB and M63 at different temperatures (Fig. 6.12). Accordingly, we also noted a statistically significant downregulation of some of the genes involved in biofilm formation, including, genes important for cellulose synthesis (*bcsS),* curli fiber production (*csgB)* and lipid A biosynthesis (*lpxP)*. Further, *ibpA* and *ibpB* genes encoding small heat shock chaperone proteins which were downregulated in our mutant, were found to be induced during biofilm formation (Ren *et al.*, 2004), and *ibpB* was also highly expressed by UPEC CFT073 isolated from mouse urine (Haugen *et al.*, 2007). Therefore, these heat shock proteins may also promote resistance to stress by contributing to biofilm formation. Biofilm formation by *E. coli* is a dynamic process that can also involve adhesion to surfaces through type 1 fimbriae and other adhesins (Blumer *et al.*, 2005; Melican *et al.*, 2011b). Taken together, many genes involved in biofilm formation and stress response were downregulated in the *ryfA* mutant, which are normally upregulated when the bacteria are in the biofilm state (Hancock & Klemm, 2007; Ren *et al.*, 2004).

Macrophages employ ROS and RNS, that can contribute to bacterial killing (Flannagan *et al.*, 2009). In this study, the *ryfA* mutant showed significantly reduced uptake by human monocyte derived-macrophages (HMDMs) (Fig. 6.6A and 6.7) as well as decreased survival rates in HMDMs, THP-1 and RAW264.7 cell lines when compared to the WT strain at all time points (Fig. 6.6 and 6.7). These results indicate that RyfA plays an important role for survival in macrophages. The decreased survival inside macrophages could be explained by the numerous defects of the *ryfA* mutant, such as increased sensitivity to oxidative stress. Interestingly, the *ryfA* mutant induced high levels of intracellular ROS in RAW264.7 macrophages at 4 h p.i compared to WT strain CFT073 (Fig. 6.6E), which may explain why the *ryfA* mutant survives less inside macrophages (Fig. 6.6). Thus, a common mechanism used by bacterial pathogens to avoid host innate immune pathways is to employ defense mechanisms against oxidative stress (Imlay, 2013). Interestingly, genes associated with intramacrophage survival including chaperones (*ibpA*, *ibpB*), *trxC*, *phoH* and *soxS* were downregulated in the *ryfA* mutant. Further, genes that were highly expressed and which were shown to be important for persistence of UPEC strain UTI89 within murine macrophages (Mavromatis *et al.*, 2015) including sigma factor H (*rpoH*), the phage shock proteins (*pspACDE*), DNA damage inducible protein (*yebG*), and small heat shock protein (*ibpB*), and biofilm formation regulatory protein (*bssS*) were all repressed in the *ryfA* mutant. The Psp system senses membrane stress and stabilizes the bacterial cell membrane under stress

conditions (Maxson & Darwin, 2004). This system is induced in *Shigella flexneri* infecting macrophage (Lucchini *et al.*, 2005). Interestingly, we found that *pspA*, *rpoH*, *ibpA* and *soxS* where all significantly downregulated in the *ryfA* mutant after 6 h p. i. in HMDM (Fig. 6.13). A previous study, showed that *S. flexneri* harbors two copies of RyfA that contribute to multiplication of *S. flexneri* in host cells. Specifically, the over-expression of RyfA1 negatively impacted the virulence-associated process of cell-to-cell spread by elimination of *ompC* mRNA that encodes the major outer membrane protein C (Fris *et al.*, 2017). We report here that deletion of *ryfA* did not affect the growth of the mutant in LB broth or in human urine (Fig. 6.9B and C). This lends support to our assertion that the observed defect in colonization by the *ryfA* mutant is likely due to an increased sensitivity to certain environmental stresses and changes in metabolic functions that could lead to alterations in production of fimbriae/flagella, and reduced survival in macrophages during infection.

Interestingly, by analyzing the transcriptome profile of a UTI strain isolated directly from patients, *ryfA* was shown to be upregulated in *E. coli* asymptomatic bacteriuria ABU strain 83972 by 1.5 to 8.9-fold in three patients compared with growth in both MOPS and *in vitro* urine (Roos & Klemm, 2006). The ABU strain is an excellent colonizer of the human urinary tract, where it causes long-term bladder colonization.

Taken together, several lines of evidence suggest that inactivation of *ryfA* could attenuate pathogenic *E. coli* by altering regulatory pathways leading to changes in metabolism and decreased adaptation to environmental stresses or may potentially generate an altered response to membrane-associated stress, leading to repression of production of surface structures, including adhesins required for colonization of host tissues. Based on the important number of adaptive and virulence associated genes that are under the control of the RyfA non-coding RNA, it should be considered as a potential target for therapeutic interventions or preventative measures against UPEC and potentially other enterobacterial pathogens. It will also be of future interest to determine regulatory mechanisms through which RyfA regulates multiple bacterial pathways important for adaptive resistance to stresses, production of fimbriae/flagella and virulence of pathogenic *E. coli* and other bacterial pathogens that use this regulatory RNA to mediate an adaptive virulence response during infection.

6.7 Data Availability

The datasets generated for this study are available on request to the corresponding author.

6.8 Author Contributions

H.B. was the primary author and conceived, planned and carried out all the experiments and analysed the results. **H.B and P.P** contributed to the interpretation of the results. **H.B.** took the lead in writing the manuscript. **H.L., M.K., C.S. and H.H.** contributed to some of the experiments. **S.H.** technical assistance. **P.P., H.L., M.K., C.S., S.H., J.B., E.M. J.V and CMD.** Provided critical feedback and helped shape the research, analysis and review and editing of the manuscript. **C.M.D.** supervised the project and acquired grant.

6.9 Funding

6.10 Conflict of Interest Statement

The authors declare that the research was conducted in the absence of any commercial or financial relationships that could be construed as a potential conflict of interest.

6.11   References

Abraham JM, Freitag CS, Clements JR & Eisenstein BI (1985) An invertible element of DNA controls phase variation of type 1 fimbriae of *Escherichia coli*. *Proceedings of the National Academy of Sciences* 82(17):5724-5727.

AIBA, H., ADHYA, S. & DE CROMBRUGGHE, B. 1981. Evidence for two functional gal promoters in intact *Escherichia coli* cells. *Journal of Biological Chemistry,* 256**,** 11905-11910.

ALTUVIA, S., WEINSTEIN-FISCHER, D., ZHANG, A., POSTOW, L. & STORZ, G. 1997. A small, stable RNA induced by oxidative stress: role as a pleiotropic regulator and antimutator. *Cell,* 90**,** 43-53.

BABIOR, B. M. 2000. Phagocytes and oxidative stress. *The American journal of medicine,* 109**,** 33-44.

BAK, G., LEE, J., SUK, S., KIM, D., LEE, J. Y., KIM, K.-S., CHOI, B.-S. & LEE, Y. 2015. Identification of novel sRNAs involved in biofilm formation, motility, and fimbriae formation in *Escherichia coli*. *Scientific reports,* 5**,** 15287.

BERGER, H., HACKER, J., JUAREZ, A., HUGHES, C. & GOEBEL, W. 1982. Cloning of the chromosomal determinants encoding hemolysin production and mannose-resistant hemagglutination in *Escherichia coli*. *Journal of Bacteriology,* 152**,** 1241-1247.

BESSAIAH, H., POKHAREL, P., HABOURIA, H., HOULE, S. & DOZOIS, C. M. 2019. *yqhG* Contributes to Oxidative Stress Resistance and Virulence of Uropathogenic *Escherichia coli* and Identification of Other Genes Altering Expression of Type 1 Fimbriae. *Frontiers in cellular and infection microbiology,* 9**,** 312.

BLUMER, C., KLEEFELD, A., LEHNEN, D., HEINTZ, M., DOBRINDT, U., NAGY, G., MICHAELIS, K., EMÖDY, L., POLEN, T. & RACHEL, R. 2005. Regulation of type 1 fimbriae synthesis and biofilm formation by the transcriptional regulator LrhA of *Escherichia coli*. *Microbiology,* 151**,** 3287-3298.

Boos W. [4] Binding protein-dependent ABC transport system for glycerol 3-phosphate of *Escherichia coli*. Methods in enzymology. 292: Elsevier; 1998. p. 40-51.

Bower, J. M. & Mulvey, M. A. 2006. Polyamine-mediated resistance of uropathogenic *Escherichia coli* to nitrosative stress. *Journal of Bacteriology,* 188**,** 928-933.

Bryan, A., Roesch, P., Davis, L., Moritz, R., Pellett, S. & Welch, R. A. 2006. Regulation of type 1 fimbriae by unlinked FimB- and FimE-like recombinases in uropathogenic *Escherichia coli* strain CFT073. *Infection and Immunity ,* 74**,** 1072-83.

Bukau, B. & Horwich, A. L. 1998. The Hsp70 and Hsp60 chaperone machines. *Cell,* 92**,** 351-366.

Casaz, P., Garrity-Ryan, L. K., Mckenney, D., Jackson, C., Levy, S. B., Tanaka, S. K. & Alekshun, M. N. 2006. MarA, SoxS and Rob function as virulence factors in an *Escherichia coli* murine model of ascending pyelonephritis. *Microbiology,* 152**,** 3643-3650.

Cherepanov, P. P. & Wackernagel, W. 1995. Gene disruption in *Escherichia coli*: TcR and KmR cassettes with the option of Flp-catalyzed excision of the antibiotic-resistance determinant. *Gene,* 158**,** 9-14.

Conover, M. S., Hadjifrangiskou, M., Palermo, J. J., Hibbing, M. E., Dodson, K. W. & Hultgren, S. J. 2016. Metabolic requirements of *Escherichia coli* in intracellular bacterial communities during urinary tract infection pathogenesis. *MBio,* 7**,** e00104-16.

Corcoran, C. P. & Dorman, C. J. 2009. DNA relaxation-dependent phase biasing of the fim genetic switch in *Escherichia coli* depends on the interplay of H-NS, IHF and LRP. *Molecular microbiology,* 74**,** 1071-1082.

Cormack, B. P., Valdivia, R. H. & Falkow, S. 1996. FACS-optimized mutants of the green fluorescent protein (GFP). *Gene,* 173**,** 33-38.

Crépin, S., Harel, J. & Dozois, C. M. 2012. Chromosomal complementation using Tn7 transposon vectors in Enterobacteriaceae. *Applied and Environmental Microbiology.,* 78**,** 6001-6008.

Crepin, S., Houle, S., Charbonneau, M. E., Mourez, M., Harel, J. & Dozois, C. M. 2012. Decreased expression of type 1 fimbriae by a *pst* mutant of uropathogenic *Escherichia coli* reduces urinary tract infection. *Infection and Immunity* , 80**,** 2802-15.

Crépin, S., Lamarche, M. G., Garneau, P., Séguin, J., Proulx, J., Dozois, C. M. & Harel, J. 2008. Genome-wide transcriptional response of an avian pathogenic *Escherichia coli* (APEC) pst mutant. *BMC genomics,* 9**,** 568.

Crespo, M. D., Puorger, C., Schärer, M. A., Eidam, O., Grütter, M. G., Capitani, G. & Glockshuber, R. 2012. Quality control of disulfide bond formation in pilus subunits by the chaperone FimC. *Nature Chemical Biology,* 8**,** 707.

Datsenko, K. A. & Wanner, B. L. 2000. One-step inactivation of chromosomal genes in *Escherichia coli* K-12 using PCR products. *Proceedings of the National Academy of Sciences,* 97**,** 6640-6645.

Dove, S., Smith, S. & Dorman, C. 1997. Control of *Escherichia coli* type 1 fimbrial gene expression in stationary phase: a negative role for RpoS. *Molecular and General Genetics MGG,* 254**,** 13-20.

Flannagan, R. S., Cosío, G. & Grinstein, S. 2009. Antimicrobial mechanisms of phagocytes and bacterial evasion strategies. *Nature Reviews Microbiology,* 7**,** 355-366.

Fléchard, M., Cortes, M. A., Répérant, M. & Germon, P. 2012. New role for the ibeA gene in H2O2 stress resistance of *Escherichia coli. Journal of Bacteriology,* 194**,** 4550-4560.

Flores-Kim, J. & Darwin, A. J. 2015. Activity of a bacterial cell envelope stress response is controlled by the interaction of a protein binding domain with different partners. *Journal of Biological Chemistry,* 290**,** 11417-11430.

Foxman, B. 1990. Recurring urinary tract infection: incidence and risk factors. *American Journal of Public Health,* 80**,** 331-333.

Foxman, B. 2010. The epidemiology of urinary tract infection. *Nature Reviews Urology,* 7**,** 653.

Fris, M. E., Broach, W. H., Klim, S. E., Coschigano, P. W., Carroll, R. K., Caswell, C. C. & Murphy, E. R. 2017. Sibling sRNA RyfA1 influences Shigella dysenteriae pathogenesis. *Genes,* 8**,** 50.

Fröhlich, K. S. & Vogel, J. 2009. Activation of gene expression by small RNA. *Current Opinion in Microbiology,* 12**,** 674-682.

Guillier, M. & Gottesman, S. 2006. Remodelling of the *Escherichia coli* outer membrane by two small regulatory RNAs. *Molecular Microbiology,* 59**,** 231-247.

Hagan EC, Lloyd AL, Rasko DA, Faerber GJ & Mobley HL (2010) *Escherichia coli* global gene expression in urine from women with urinary tract infection. *PLoS Pathogens* 6(11).

Hancock, V. & Klemm, P. 2007. Global gene expression profiling of asymptomatic bacteriuria *Escherichia coli* during biofilm growth in human urine. *Infection and Immunity* , 75**,** 966-976.

Harel, J., Jacques, M., Fairbrother, J. M., Bossé, M. & Forget, C. 1995. Cloning of determinants encoding F1652 fimbriae from porcine septicaemic *Escherichia coli* confirms their identity as F1C fimbriae. *Microbiology,* 141**,** 221-228.

Haugen, B. J., Pellett, S., Redford, P., Hamilton, H. L., Roesch, P. L. & Welch, R. A. 2007. *In vivo* gene expression analysis identifies genes required for enhanced colonization of the mouse urinary tract by uropathogenic *Escherichia coli* strain CFT073 dsdA. *Infection and Immunity* , 75**,** 278-289.

Hershberg, R., Altuvia, S. & Margalit, H. 2003. A survey of small RNA-encoding genes in *Escherichia coli. Nucleic Acids Research,* 31**,** 1813-1820.

Hultgren, S. J., Porter, T. N., Schaeffer, A. J. & Duncan, J. L. 1985. Role of type 1 pili and effects of phase variation on lower urinary tract infections produced by *Escherichia coli. Infection and Immunity* , 50**,** 370-377.

Imlay, J. A. 2013. The molecular mechanisms and physiological consequences of oxidative stress: lessons from a model bacterium. *Nature Reviews Microbiology,* 11**,** 443-454.

Kaniga, K., Compton, M. S., Curtiss, R., 3rd & Sundaram, P. 1998. Molecular and functional characterization of *Salmonella enterica* serovar typhimurium *poxA* gene: effect on attenuation of virulence and protection. *Infection and Immunity* , 66**,** 5599-606.

Khan, A. S., Kniep, B., Oelschlaeger, T. A., Van Die, I., Korhonen, T. & Hacker, J. 2000. Receptor structure for F1C fimbriae of uropathogenic *Escherichia coli*. *Infection and Immunity* , 68**,** 3541-3547.

Klemm, P. 1986. Two regulatory *fim* genes, *fimB* and *fimE*, control the phase variation of type 1 fimbriae in *Escherichia coli*. *EMBO J*, 5**,** 1389-93.

Knodler, L. A., Crowley, S. M., Sham, H. P., Yang, H., Wrande, M., Ma, C., Ernst, R. K., Steele-Mortimer, O., Celli, J. & Vallance, B. A. 2014. Noncanonical inflammasome activation of caspase-4/caspase-11 mediates epithelial defenses against enteric bacterial pathogens. *Cell Host & Microbe,* 16**,** 249-256.

Lane, M. C., Lockatell, V., Monterosso, G., Lamphier, D., Weinert, J., Hebel, J. R., Johnson, D. E. & Mobley, H. L. 2005. Role of motility in the colonization of uropathogenic *Escherichia coli* in the urinary tract. *Infection and Immunity* , 73**,** 7644-7656.

Livak, K. J. & Schmittgen, T. D. 2001. Analysis of relative gene expression data using real-time quantitative PCR and the 2− ΔΔCT method. *Methods,* 25**,** 402-408.

Lucchini, S., Liu, H., Jin, Q., Hinton, J. C. & Yu, J. 2005. Transcriptional adaptation of *Shigella flexneri* during infection of macrophages and epithelial cells: insights into the strategies of a cytosolic bacterial pathogen. *Infection and Immunity* , 73**,** 88-102.

Luterbach, C. L. & Mobley, H. L. 2018. Cross talk between MarR-like transcription factors coordinates the regulation of motility in uropathogenic *Escherichia coli*. *Infection and Immunity* , 86**,** e00338-18.

Majdalani, N., Cunning, C., Sledjeski, D., Elliott, T. & Gottesman, S. 1998. DsrA RNA regulates translation of RpoS message by an anti-antisense mechanism, independent of its action as an antisilencer of transcription. *Proceedings of the National Academy of Sciences,* 95**,** 12462-12467.

Massé, E. & Gottesman, S. 2002. A small RNA regulates the expression of genes involved in iron metabolism in *Escherichia coli*. *Proceedings of the National Academy of Sciences,* 99**,** 4620-4625.

Mavromatis, C., Bokil, N. J., Totsika, M., Kakkanat, A., Schaale, K., Cannistraci, C. V., Ryu, T., Beatson, S. A., Ulett, G. C. & Schembri, M. A. 2015. The co-transcriptome of uropathogenic *E scherichia coli*-infected mouse macrophages reveals new insights into host–pathogen interactions. *Cellular Microbiology,* 17**,** 730-746.

Maxson, M. E. & Darwin, A. J. 2004. Identification of inducers of the *Yersinia enterocolitica* phage shock protein system and comparison to the regulation of the RpoE and Cpx extracytoplasmic stress responses. *Journal of Bacteriology,* 186**,** 4199-4208.

Melican, K., Sandoval, R. M., Kader, A., Josefsson, L., Tanner, G. A., Molitoris, B. A. & Richter-Dahlfors, A. 2011. Uropathogenic *Escherichia coli* P and Type 1 fimbriae act in synergy in a living host to facilitate renal colonization leading to nephron obstruction. *PLoS Pathogens,* 7**,** e1001298.

Mobley, H., Green, D., Trifillis, A., Johnson, D., Chippendale, G., Lockatell, C., Jones, B. & Warren, J. 1990. Pyelonephritogenic *Escherichia coli* and killing of cultured human renal proximal tubular epithelial cells: role of hemolysin in some strains. *Infection and Immunity* , 58**,** 1281-1289.

Mogk, A., Deuerling, E., Vorderwülbecke, S., Vierling, E. & Bukau, B. 2003. Small heat shock proteins, ClpB and the DnaK system form a functional triade in reversing protein aggregation. *Molecular Microbiology,* 50**,** 585-595.

Morimoto, R. I. The heat shock response: systems biology of proteotoxic stress in aging and disease. Cold Spring Harbor symposia on quantitative biology, 2011. Cold Spring Harbor Laboratory Press, 91-99.

Müller, C. M., Åberg, A., Straseviçiene, J., Emődy, L., Uhlin, B. E. & Balsalobre, C. 2009. Type 1 fimbriae, a colonization factor of uropathogenic *Escherichia coli*, are controlled by the metabolic sensor CRP-cAMP. *PLoS Pathogens,* 5 (2): e1000303.

Mysorekar, I. U. & Hultgren, S. J. 2006. Mechanisms of uropathogenic *Escherichia coli* persistence and eradication from the urinary tract. *Proceedings of the National Academy of Sciences,* 103**,** 14170-14175.

Nathan, C. & Shiloh, M. U. 2000. Reactive oxygen and nitrogen intermediates in the relationship between mammalian hosts and microbial pathogens. *Proceedings of the National Academy of Sciences,* 97**,** 8841-8848.

Nielubowicz, G. R. & Mobley, H. L. 2010. Host–pathogen interactions in urinary tract infection. *Nature Reviews Urology,* 7**,** 430.

Ortega, Á. D., Quereda, J. J., Pucciarelli, M. G. & García-Del Portillo, F. 2014. Non-coding RNA regulation in pathogenic bacteria located inside eukaryotic cells. *Frontiers in Cellular and Infection Microbiology,* 4**,** 162.

Pérez, J. M., Calderón, I. L., Arenas, F. A., Fuentes, D. E., Pradenas, G. A., Fuentes, E. L., Sandoval, J. M., Castro, M. E., Elías, A. O. & Vásquez, C. C. 2007. Bacterial toxicity of potassium tellurite: unveiling an ancient enigma. *PloS one,* 2**,** e211.

Ren, D., Bedzyk, L., Thomas, S., Ye, R. & Wood, T. K. 2004. Gene expression in *Escherichia coli* biofilms. *Applied Microbiology and Biotechnology,* 64**,** 515-524.

Roos, V. & Klemm, P. 2006. Global gene expression profiling of the asymptomatic bacteriuria *Escherichia coli* strain 83972 in the human urinary tract. *Infection and Immunity ,* 74**,** 3565-3575.

Ruiz, C. & Levy, S. B. 2010. Many chromosomal genes modulate MarA-mediated multidrug resistance in *Escherichia coli*. *Antimicrobial agents and chemotherapy,* 54**,** 2125-2134.

Ruiz, C., Mcmurry, L. M. & Levy, S. B. 2008. Role of the multidrug resistance regulator MarA in global regulation of the hdeAB acid resistance operon in *Escherichia coli*. *Journal of Bacteriology,* 190**,** 1290-1297.

Sabri, M., Caza, M., Proulx, J., Lymberopoulos, M. H., Brée, A., Moulin-Schouleur, M., Curtiss, R. & Dozois, C. M. 2008. Contribution of the SitABCD, MntH, and FeoB metal transporters to the virulence of avian pathogenic *Escherichia coli* O78 strain χ7122. *Infection and Immunity ,* 76**,** 601-611.

Sabri, M., Houle, S. & Dozois, C. M. 2009. Roles of the extraintestinal pathogenic *Escherichia coli* ZnuACB and ZupT zinc transporters during urinary tract infection. *Infection and Immunity ,* 77**,** 1155-1164.

Schwan, W. R., Lee, J. L., Lenard, F. A., Matthews, B. T. & Beck, M. T. 2002. Osmolarity and pH growth conditions regulate *fim* gene transcription and type 1 pilus expression in uropathogenic *Escherichia coli*. *Infection and Immunity ,* 70**,** 1391-402.

Shivaji, S., Konduri, R., Ramchiary, J., Jogadhenu, P. S., Arunasri, K. & Savitri, S. 2019. Gene targets in ocular pathogenic *Escherichia coli* for mitigation of biofilm formation to overcome antibiotic resistance. *Frontiers in Microbiology,* 10**,** 1308.

Snyder JA, Haugen BJ, Buckles EL, Lockatell CV, Johnson DE, Donnenberg MS, Welch RA & Mobley HL (2004) Transcriptome of uropathogenic *Escherichia coli* during urinary tract infection. *Infection and Immunity* 72(11):6373-6381.

Snyder JA, Haugen BJ, Lockatell CV, Maroncle N, Hagan EC, Johnson DE, Welch RA & Mobley HL (2005) Coordinate expression of fimbriae in uropathogenic *Escherichia coli*. *Infection and Immunity* 73(11):7588-7596.

Subashchandrabose, S., Smith, S. N., Spurbeck, R. R., Kole, M. M. & Mobley, H. L. 2013. Genome-wide detection of fitness genes in uropathogenic *Escherichia coli* during systemic infection. *PLoS Pathogens,* 9 (12)**,** e1003788.

Vigil, P. D., Stapleton, A. E., Johnson, J. R., Hooton, T. M., Hodges, A. P., He, Y. & Mobley, H. L. 2011. Presence of putative repeat-in-toxin gene tosA in *Escherichia coli* predicts successful colonization of the urinary tract. *MBio,* 2**,** e00066-11.

Waters, L. S. & Storz, G. 2009. Regulatory RNAs in bacteria. *Cell,* 136**,** 615-628.

Welch RA, Burland V, Plunkett G, Redford P, Roesch P, Rasko D, Buckles E, Liou S-R, Boutin A & Hackett J (2002b) Extensive mosaic structure revealed by the complete genome sequence of uropathogenic *Escherichia coli. Proceedings of the National Academy of Sciences* 99(26):17020-17024.

Wiles, T. J., Kulesus, R. R. & Mulvey, M. A. 2008. Origins and virulence mechanisms of uropathogenic *Escherichia coli. Experimental and Molecular Pathology,* 85**,** 11-9.

Withman, B., Gunasekera, T. S., Beesetty, P., Agans, R. & Paliy, O. 2013. Transcriptional responses of uropathogenic *Escherichia coli* to increased environmental osmolality caused by salt or urea. *Infection and Immunity ,* 81**,** 80-89.

Zhao, K., Liu, M. & Burgess, R. R. 2005. The global transcriptional response of *Escherichia coli* to induced σ32 protein involves σ32 regulon activation followed by inactivation and degradation of σ32 in vivo. *Journal of Biological Chemistry,* 280**,** 17758-17768.

Zhou, G., Mo, W.-J., Sebbel, P., Min, G., Neubert, T. A., Glockshuber, R., Wu, X.-R., Sun, T.-T. & Kong, X.-P. 2001. Uroplakin Ia is the urothelial receptor for uropathogenic *Escherichia coli*: evidence from in vitro FimH binding. *Journal of Cell Science,* 114**,** 4095-4103.

Zuker, M. 2003. Mfold web server for nucleic acid folding and hybridization prediction. *Nucleic Acids Research,* 31**,** 3406-3415.

6.12   Supplementary data

A

B

C
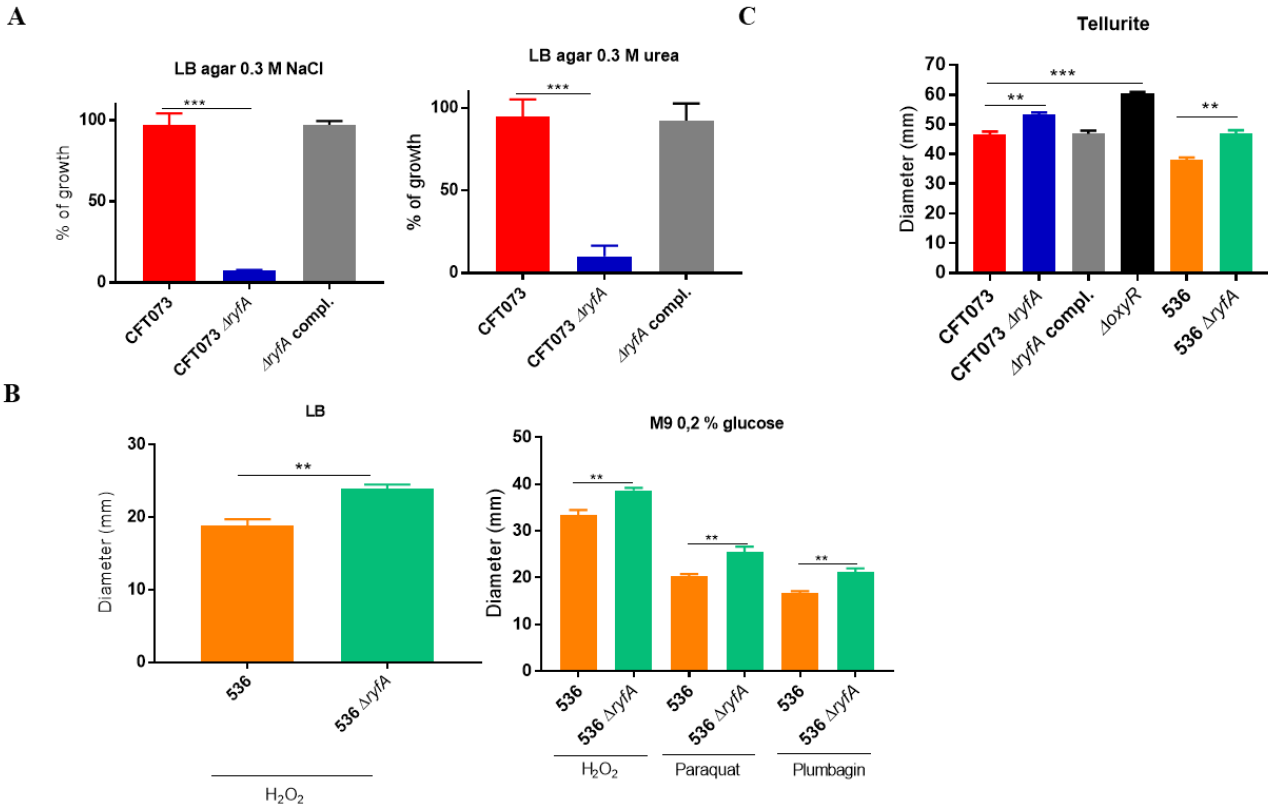
Figure 6.8. Role of RyfA in stress resistance

(A) Growth under conditions of osmotic stress. Strains were grown with shaking in LB medium until mid-log phase (O.D.$_{600}$, 0.6) and plated on LB agar (taken as 100% growth) and LB agar with 0.3 M NaCl and 0.3 M urea. (B) Growth inhibition zones (mm) of UPEC 536 and the *ryfA* mutant to reactive oxygen intermediate compounds on LB and M9 agar. (C) Sensitivities of UPEC strains CFT073 and 536 and their derivatives strains to potassium tellurite on LB agar plates. Tests were performed as described in Materials and Methods. The results represent the means of replicate experiments for a minimum of three samples. Vertical bars represent the standard errors of the means. Statistical significance was calculated by one-way ANOVA (A to C) (*, *P* < 0.05; **, *P* < 0.005; ***, *P* < 0.0001).
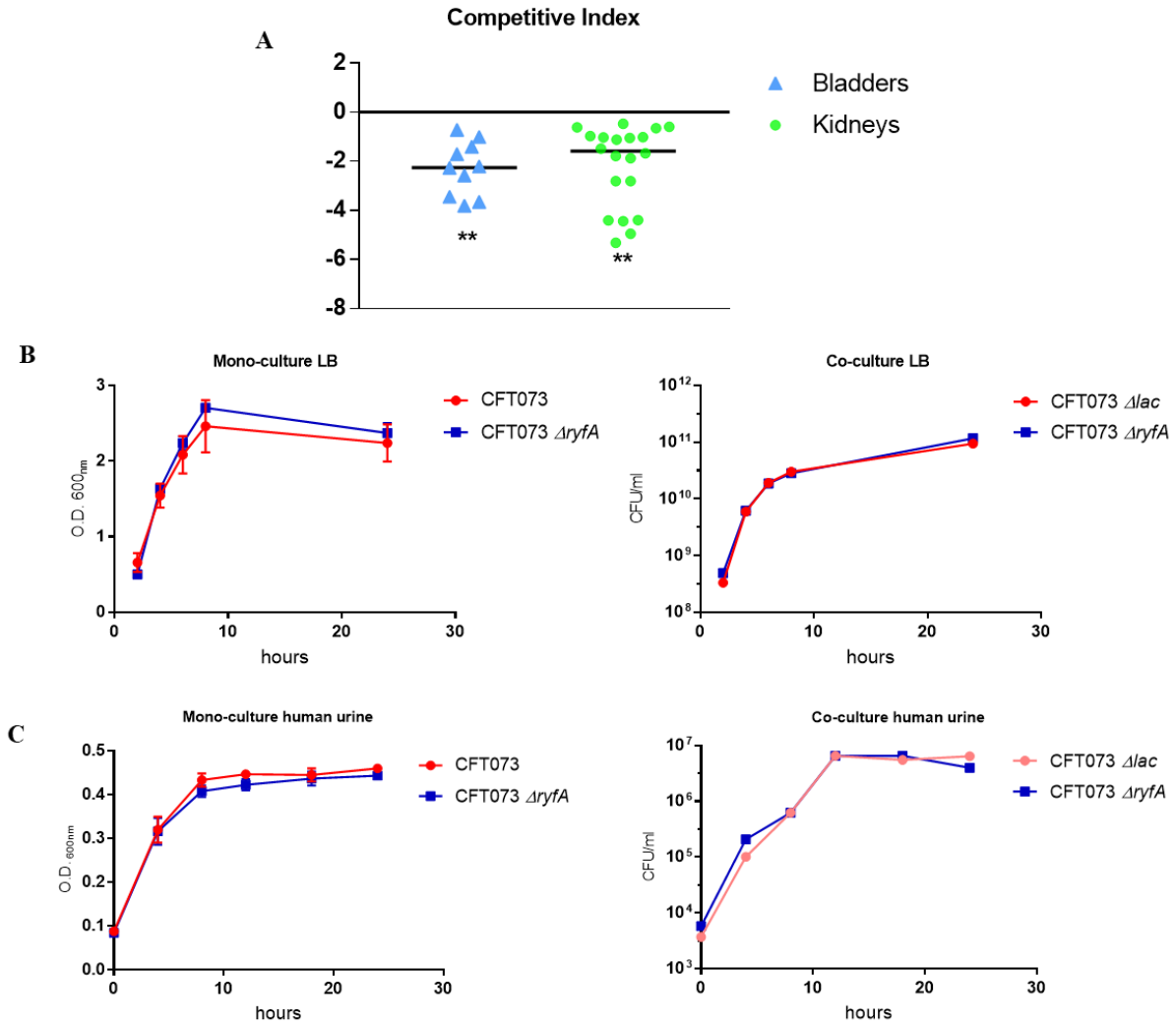
Figure 6.9. Inactivation of *ryfA* in uropathogenic *E. coli* CFT073 reduces competitive colonization of the mouse urinary tract

(A) Co-infection experiments between the CFT073 Δ*lac* and the Δ*ryfA* mutant. Data are means ± standard errors of the means of 10 mice (B) Growth profile of CFT073 and *ryfA* mutant in rich LB broth (C) Comparison of growth characteristics of CFT073 or CFT073 Δ*lac* and *ryfA* mutant in human urine in monoculture and coculture. There were no significant differences in growth between CFT073 and *ryfA* mutant in all conditions tested. Error bars represent the SEM. : *P* < 0.05; **, *P* < 0.005; ***, *P* < 0.000 Mann–Whitney Test.
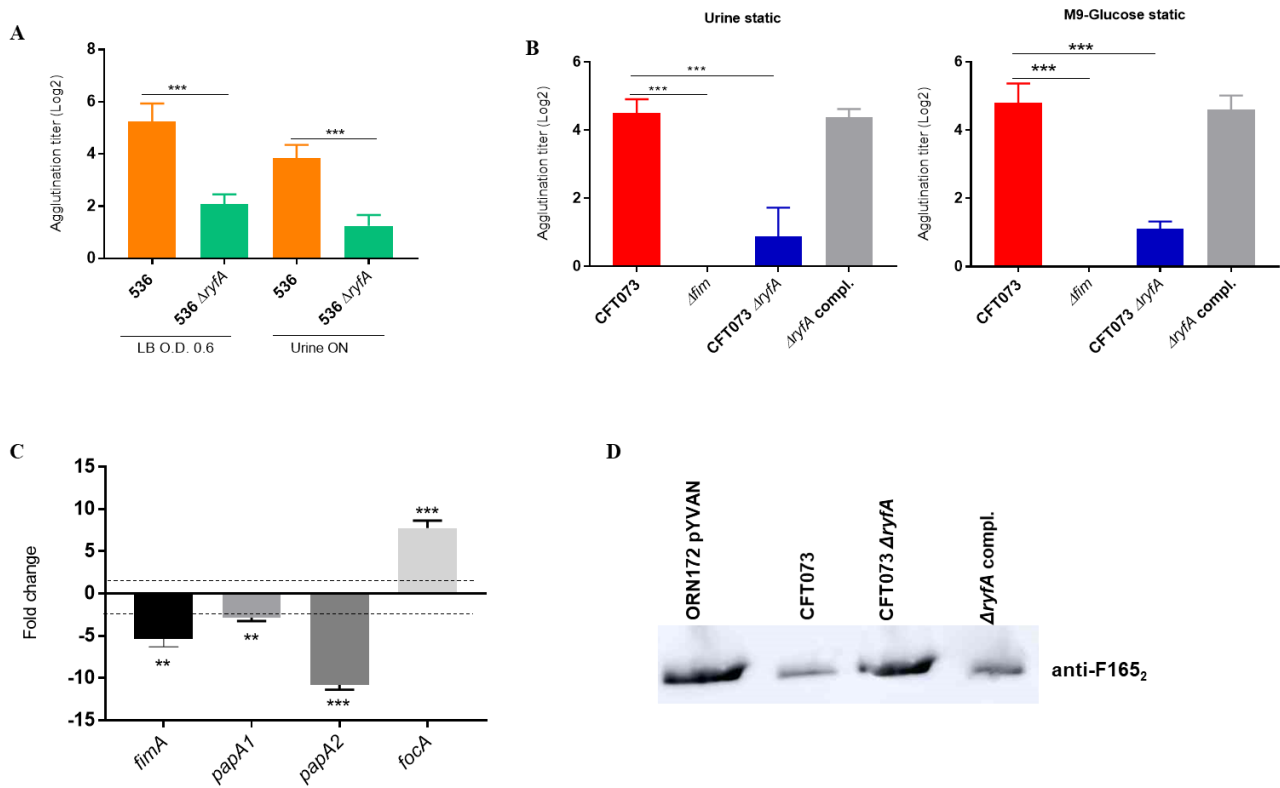
Figure 6.10. Effect of inactivation of *ryfA* on production of type 1 fimbriae and expression of Pap and F1C fimbriae

Type 1 fimbriae production determined by yeast agglutination. The level of type 1 fimbriae production in UPEC strain 536 and *ryfA* mutant (A) and for CFT073 and derivative strains (B) was measured after mid-log growth in LB and human urine and after static growth overnight in human urine and M9 medium containing 0.2% glucose (C) Transcription of *fimA* (Type 1), *papA* (*papA1* and *papA2*-P fimbriae) and *focA* (F1C fimbriae) genes from *ryfA* mutant adhering to 5637 bladder cells compared to results for WT CFT073 strain. The dashed line corresponds to the cutoff for a significant difference in expression. All results shown are the mean values and standard deviations for four biological experiments. Statistical significance was calculated by the one-way ANOVA (A, B and C): *, $P < 0.05$; **, $P < 0.005$; ***, $P < 0.0001$. (D) Western blot of fimbrial extracts using F1C-specific (anti-F165$_2$) antiserum. The *fim*-negative *E. coli* K-12 strain ORN172 carrying the plasmid pYVAN which expresses F1C (F165$_2$) fimbriae was used as positive control.

A

```
CFT073   CCGGCCCTTTCCGCCGTCTCGCAAACGGGCGCTGGCTTAAGGAAAGGATGTTCCATGGCC
MG1655   -CGGCCCTTTCCGCCGTCTCGCAAACGGGCGCTGGCTTTAGGAAAGGATGTTCCGTGGCC
         *********************************** *************** *****

CFT073   GTAAATGCAGGTGTTTCACAGCGCTTGCTATCGCGGCAATATCGCCAGTGGTGCTGTCGT
MG1655   GTAAATGCAGGTGTTTCACAGCGCTTGCTATCGCGGCAATATCGCCAGTGGTGCTGTCGT
         ************************************************************

CFT073   GATGCGGTCTTCGCATGGACCGCACAATGAAGATACGGTGCTTTTGTATCGTACTTATTG
MG1655   GATGCGGTCTTCGCATGGACCGCACAATGAAGATACGGTGCTTTTGTATCGTACTTATTG
         ************************************************************

CFT073   TTTCTGGTGCGCTGTTAACCGAGGTAAATAATAACCGGAGTTTCTCCGGCAACAATTTAC
MG1655   TTTCTGGTGCGCTGTTAACCGAGGTAAATAATAACCGGAGTCTCTCCGGCGACAATTTAC
         ***************************************** ******** *********

CFT073   TGGTGGTTAACAAACTTCAGAGCAGCAAGTAAGCCCGAATGCCGCCCTTTGGGGCGGCAT
MG1655   TGGTGGTTAACAACCTTCAGAGCAGCAAGTAAGCCCGAATGCCGCCCTTTGGG-CGGCAT
         ************* **************************************** ******

CFT073   ATTTT
MG1655   ATTTT
         *****
```

B
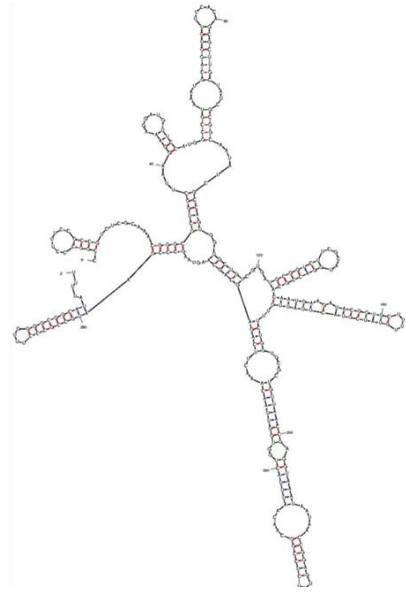
Figure 6.11. RyfA predicted structure and sequence

(A) The predicted genes *ryfA* from the *E. coli* K-12 MG1655 was aligned to *ryfA* from CFT073 using ClustalW (https://www.genome.jp/tools-bin/clustalw). (B) M-fold (http://unafold.rna.albany.edu/?q=mfold) was used to predict the secondary structure of RyfA.
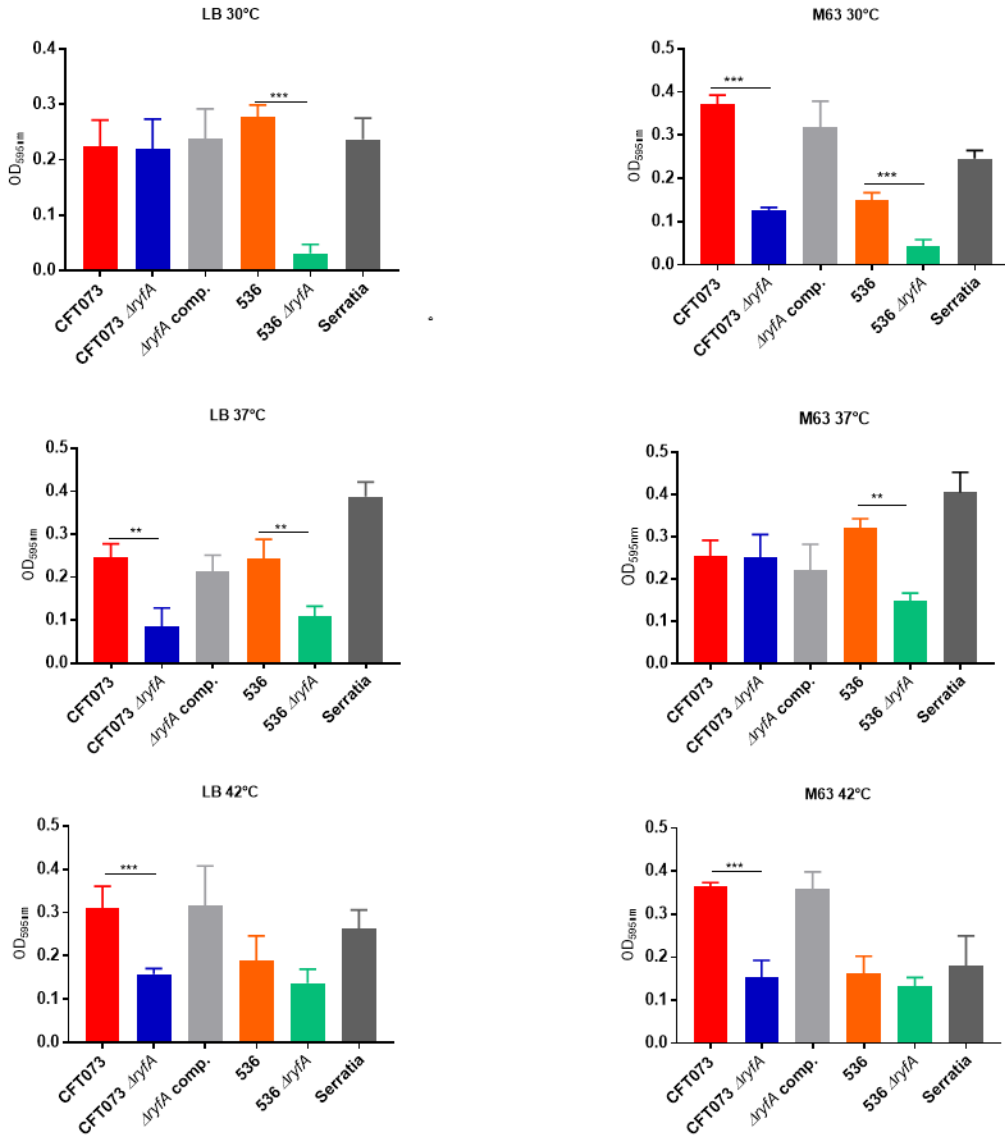
Figure 6.12. Biofilm formation in UPEC strains CFT073 and 536 and respective *ryfA* mutants.

UPEC and a *Serratia liquefaciens* strain were grown at different temperatures (30°C, 37°C, and 42°C) in LB and minimal media M63 in polystyrene plate wells for 48 h and then stained with crystal violet. Remaining crystal violet after washing with acetone was measured as absorbance at 595 nm. Data are the means of three independent experiments, and error bars represent standard errors of the means. The *Serratia liquefaciens* strain was used as positive control for biofilm formation (* $p < 0.05$, **$p < 0.01$, ***$p < 0.001$ compared to CFT073 or 536 using one-way ANOVA).
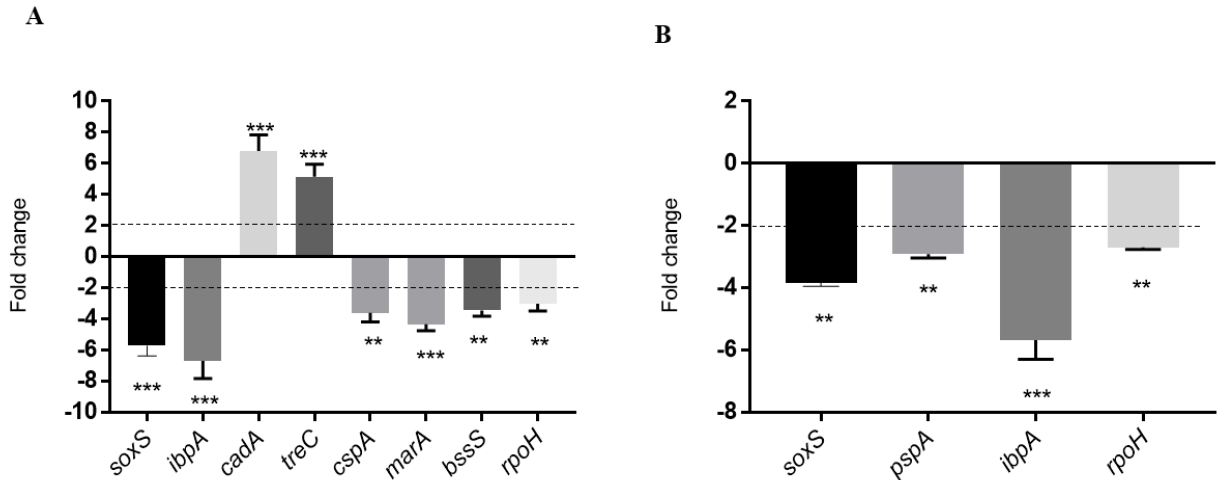
Figure 6.13. Genes whose expression is affected in the absence of *ryfA in vitro* and during infection of human macrophages

(A) Validation of RNA-seq data by qRT-PCR. RNA was isolated from UPEC CFT073 and the Δ*ryfA* mutant in mid-log growth (O.D. 0.6) in LB at 37°C and qRT-PCR analysis was performed. Genes either upregulated or downregulated by at least 2-fold were considered significant. (B) UPEC genes associated with intramacrophage survival. HMDMs were infected at an MOI of 20. Intracellular bacterial survival was assessed at 6 h post-infection and the relative quantity of mRNA of some genes, was determined by RT-qPCR. qPCR data represent means of relative expression ± range (*n* = 3) of three biological replicates (* $p < 0.05$, **$p < 0.01$, ***$p < 0.001$ using one-way ANOVA).

Table 6.4. Examination of transcriptome of CFT073 and Δ*ryfA* mutant in LB at 0.D. 0.6

Gene Locus	Fold change	Upregulated / Gene symbol	Downregulated / CDS	P-value	FDR
ibpB	-7,69	*ibpB*	*c4606*	3,461E-06	8,3E-05
C_RS24315	7,61	*cadA*	*c5140*	6,48E-08	8,6E-06
C_RS24320	7,17	*cadB*	*c5141*	5,02E-07	2,4E-05
C_RS00345	7,05	*araA*	*c0074*	8,71E-07	3,3E-05
glpB	6,58	*glpB*	*c2783*	2,16E-10	1,9E-07
C_RS13205	6,56	*glpA*	*c2782*	1,93E-09	1,0E-06
C_RS26455	-6,40			1,596E-05	2,2E-04
C_RS13200	6,19	*glpT*	*c2781*	1,45E-11	7,0E-08
glpC	6,06	*glpC*	*c2784*	2,09E-10	1,9E-07
ibpA	-5,96	*ibpA*	*c4607*	1,213E-06	4,1E-05
C_RS27365	-5,74			1,51E-07	1,4E-05
cspG	-5,65	*cspG*	*c1123*	1,65E-06	5,2E-05
glcD	-5,63	*glcD*	*c3709*	1,964E-06	5,9E-05
C_RS15120	-5,52	*cspI*	*c3177*	2,53E-09	1,1E-06
glcE	-5,47	*glcE*	*c3708*	8,242E-06	1,4E-04
fadB	-5,40	*fadB*	*c4793*	7,17E-10	4,3E-07
treC	5,31	*treC*	*c5338*	1,66E-07	1,5E-05
C_RS13195	5,23	*glpQ*	*c2780*	2,45E-10	1,9E-07
soxS	-5,03	*soxS*	*c5053*	5,82E-11	1,4E-07
C_RS19895	4,97	*glpD*	*c4203*	3,77E-08	6,3E-06
C_RS27330	-4,92		*c3045*	5,523E-06	1,1E-04
C_RS01705	-4,84	*fadE*	*c0371*	5,17E-08	7,7E-06
malE	4,76	*malE*	*c5004*	4,48E-07	2,2E-05
C_RS23715	4,73	*LamB*	*c5006*	2,92E-06	7,5E-05
C_RS23060	4,71	*glpF*	*c4879*	2,75E-10	1,9E-07
C_RS19900	4,65		*c4204*	3,86E-07	2,2E-05
hokA	-4,56	*hokA*		1,106E-06	3,9E-05
kbaY	-4,55	*kbaY*	*c3894*	3,28E-08	5,9E-06
C_RS02185	-4,46		*c0470*	1,50E-07	1,4E-05

glpK	4,41	*glpK*	*c4878*	2,029E-05	2,5E-04
cspA	-4,35	*cspA*	*c3184*	1,938E-06	5,8E-05
C_RS19040	-4,33		*c4016*	3,11E-08	5,9E-06
C_RS12385	-4,32		*c2610*	1,65E-07	1,5E-05
malK	4,29	*malK*	*c5005*	3,452E-06	8,3E-05
C_RS24310	4,10	*dtpC*	*c5139*	2,01E-07	1,5E-05
C_RS14950	-4,07	*ydfK*	*c3145*	1,02E-07	1,1E-05
C_RS22020	-4,04	*asnA*	*c4672*	6,452E-05	5,5E-04
marB	-4,01	*marB*	*c1954*	3,17E-07	2,0E-05
marR	-4,01	*marR*	*c1952*	3,88E-09	1,6E-06
pspG	-4,00	*pspG*	*c5019*	2,02E-08	5,5E-06
C_RS01750	-3,93		*c0381*	9,74E-07	3,6E-05
marA	-3,93	*marA*	*c1953*	8,47E-08	1,0E-05
treB	3,90	*treB*	*c5339*	2,467E-06	6,7E-05
glcC	-3,85	*glcC*	*c3710*	5,87E-07	2,6E-05
C_RS06495	-3,81	*ycfR*	*c1386*	1,27E-07	1,3E-05
bssS	-3,79	*bssS*	*c1327*	1,506E-06	4,8E-05
C_RS12890	-3,78		*c2718*	1,85E-10	1,9E-07
pspB	-3,67	*pspB*	*c1775*	1,11E-08	3,6E-06
C_RS18475	-3,67	*agaS*	*c3893*	8,23E-09	2,9E-06
C_RS25410	-3,66		*c5385*	2,33E-08	5,6E-06
C_RS29385	-3,65			2,34E-07	1,7E-05
C_RS28080	-3,64		*c5169*	1,828E-06	5,5E-05
C_RS06630	-3,63		*c1416*	1,241E-05	1,8E-04
C_RS06580	-3,62	*dicB*		1,401E-05	2,0E-04
azuC	-3,61	*azuC*		1,15E-07	1,2E-05
C_RS25985	-3,60	*RtT*		3,48E-06	8,3E-05
pspC	-3,60	*pspC*	*c1777*	4,04E-08	6,5E-06
nhaA	-3,59	*nhaA*	*c0024*	6,41E-07	2,7E-05
pspD	-3,56	*pspD*	*c1778*	2,43E-07	1,7E-05
C_RS09235	-3,56	*mgtS*		2,16E-07	1,6E-05
C_RS13825	-3,52	*lpxP*	*c2915*	5,84E-07	2,6E-05
C_RS22405	-3,49		*c4741*	3,57E-07	2,1E-05

flgC	3,48	*flgC*	*c1343*	0,0058544	1,7E-02
ydfZ	3,46	*ydfZ*	*c1967*	0,0001001	7,6E-04
C_RS10055	-3,46	*ydjM*	*c2127*	7,22E-07	2,9E-05
C_RS09055	-3,40	*safA*	*c1929*	0,0003811	2,0E-03
C_RS05530	-3,38		*c1176*	7,94E-07	3,1E-05
cpxP	-3,38	*cpxP*	*c4865*	2,511E-05	2,9E-04
C_RS03695	-3,36		*c0785*	2,545E-05	2,9E-04
C_RS25015	-3,32	*exuT*	*c5298*	3,13E-08	5,9E-06
C_RS01320	-3,30		*c0281*	4,38E-07	2,2E-05
agaB	-3,30	*agaB*	*c3895*	1,02E-06	3,7E-05
C_RS26600	-3,29		*c1249*	0,0012707	5,1E-03
C_RS25430	-3,28	*nanC*	*c5389*	1,187E-06	4,1E-05
C_RS04470	-3,28		*c0943*	2,039E-05	2,5E-04
C_RS12825	-3,27	*fruB*	*c2704*	2,85E-07	1,9E-05
iscR	-3,23	*iscR*	*c3057*	2,49E-09	1,1E-06
C_RS00095	-3,21		*c0021*	4,43E-07	2,2E-05
yrbN	-3,20	*yrbN*		4,227E-06	9,4E-05
C_RS09085	-3,19		*c1935*	9,53E-08	1,1E-05
C_RS17320	-3,18		*c3648*	1,402E-05	2,0E-04
C_RS24510	-3,17	*papC*	*c5186*	0,0038051	4,9E-03
C_RS13805	-3,16	*yfdX*	*c2911*	8,177E-06	1,4E-04
nikA	3,14	*nikA*	*c4269*	5,86E-07	2,6E-05
C_RS01755	-3,14	*prfH*	*c0382*	3,59E-08	6,2E-06
C_RS15140	-3,12	*essQ*	*c3182*	9,749E-05	7,5E-04
C_RS18260	-3,11	*alx*	*c3846*	1,97E-08	5,5E-06
C_RS10360	-3,05	*yeaI*	*c2190*	6,076E-06	1,1E-04
C_RS07455	-3,03		*c1594*	2,29E-05	2,7E-04
nrdH	-3,03	*nrdH*	*c3226*	0,000147	9,8E-04
mgtA	-3,03	*mgtA*	*c5341*	3,336E-05	3,5E-04
C_RS03005	-3,02	*ydfM*	*c0649*	3,81E-07	2,1E-05
rrf	-3,02	*rrf*	*c5615*	0,0051309	1,5E-02
C_RS03010	-3,02	*ybcY*	*c0651*	0,0025381	8,7E-03
C_RS10705	-3,01	*yebG*	*c2260*	3,64E-07	2,1E-05

C_RS17600	-3,01	yghO	c3711	4,55E-07	2,3E-05
flgB	3,00	flgB	c1342	0,0093291	2,5E-02
C_RS06575	-2,98		c1404	2,611E-06	7,0E-05
C_RS20710	-2,98		c4383	0,0076527	2,1E-02
C_RS18450	-2,97	agaV	c3888	7,13E-08	8,9E-06
C_RS04465	-2,97			1,74E-06	5,4E-05
C_RS18455	-2,93		c3889	4,63E-07	2,3E-05
pspA	-2,91	pspA	c1774	5,032E-06	1,0E-04
glcF	-2,91	glcF	c3707	5,341E-05	4,8E-04
cspH	-2,90	cspH	c1122	2,741E-05	3,1E-04
C_RS19660	-2,87	yhfX	c4151	4,475E-06	9,7E-05
C_RS01315	-2,86		c0280	7,18E-08	8,9E-06
C_RS18585	-2,84		c3916	4,40E-09	1,6E-06
C_RS12490	-2,82	rcnA	c2633	2,73E-08	5,9E-06
C_RS21900	-2,82	bglH	c4642	6,20E-07	2,7E-05
C_RS02510	-2,81	cyoA	c0543	4,003E-06	9,0E-05
C_RS05910	-2,80		c5534	6,925E-06	1,3E-04
C_RS06595	-2,80		c1409	1,38E-08	4,2E-06
C_RS08670	-2,79	ycdI	c1847	4,573E-06	9,9E-05
C_RS17375	-2,79		c3658	2,07E-06	6,1E-05
C_RS18445	-2,76	KbaZ	c3887	1,269E-06	4,3E-05
nikD	2,74	nikD	c4272	4,35E-07	2,2E-05
dppB	-2,74	dppB	c4358	3,37E-07	2,1E-05
mntS	-2,73	mntS	c0902	2,103E-06	6,1E-05
C_RS12075	-2,72	YefM	c2545	2,19E-08	5,6E-06
C_RS15790	-2,72	cysJ	c3323	1,02E-07	1,1E-05
nikB	2,71	nikB	c4270	3,42E-07	2,1E-05
C_RS12845	-2,71	yeiQ	c2709	1,32E-07	1,3E-05
C_RS12070	-2,70		c2544	5,26E-08	7,7E-06
C_RS11985	-2,69		c2526	3,875E-06	8,9E-05
uidC	-2,68	uidC	c2007	1,94E-07	1,5E-05
C_RS01970	-2,68	ykgH	c0425	8,259E-05	6,7E-04
C_RS05505	-2,68		c1170	3,12E-07	2,0E-05

tomB	-2,67	*tomB*	*c0579*	9,878E-06	1,6E-04
C_RS27605	-2,67		*c3653*	4,76E-07	2,3E-05
C_RS29025	-2,66		*c0394*	1,461E-05	2,0E-04
C_RS11545	-2,66		*c2437*	0,0002458	1,4E-03
glcA	-2,64	*glcA*	*c3704*	1,49E-05	2,1E-04
fxsA	-2,62	*fxsA*	*c5223*	2,955E-05	3,2E-04
C_RS18695	-2,62	*yhbE*	*c3941*	8,70E-07	3,3E-05
C_RS10155	-2,60	*astC*	*c2148*	0,0004849	2,4E-03
C_RS18050	-2,60		*c3798*	8,094E-06	1,4E-04
C_RS19035	-2,59		*c4015*	4,199E-05	4,1E-04
cysI	-2,59	*cysI*	*c3322*	0,0001279	9,0E-04
nrdI	-2,58	*nrdI*	*c3227*	8,677E-05	6,9E-04
C_RS07160	2,58			0,0071213	2,0E-02
C_RS03155	-2,58	*fepD*	*c0677*	0,0002747	1,6E-03
pepE	2,57	*pepE*	*c4980*	1,993E-05	2,5E-04
C_RS01305	-2,57		*c0278*	1,605E-06	5,1E-05
C_RS18460	-2,56		*c3890*	5,16E-08	7,7E-06
C_RS10280	-2,56	*ydjE*	*c2173*	7,03E-07	2,9E-05
C_RS16725	-2,55		*c3523*	2,00E-07	1,5E-05
C_RS18225	-2,55		*c3839*	6,84E-07	2,9E-05
malM	2,54	*malM*	*c5007*	0,0001484	9,9E-04
C_RS07660	-2,54		*c1638*	0,000155	1,0E-03
C_RS05295	-2,54	*ymcE*	*c1124*	0,001769	6,6E-03
chaA	-2,52	*chaA*	*c1676*	1,31E-07	1,3E-05
C_RS23690	2,51	*malG*	*c5002*	2,561E-06	6,9E-05
C_RS28180	-2,50			0,0276705	5,9E-02
C_RS06010	-2,50		*c1280*	5,347E-05	4,8E-04
C_RS10200	2,48		*c2158*	5,83E-08	8,1E-06
C_RS13960	-2,48		*c2938*	0,003787	1,2E-02
C_RS09375	-2,48			2,781E-05	3,1E-04
nikC	2,47	*nikC*	*c4271*	4,14E-07	2,2E-05
inaA	2,47	*inaA*	*c2779*	0,0057602	1,7E-02
C_RS08255	-2,46		*c1761*	4,98E-07	2,4E-05

agaC	-2,46	*agaC*	*c3896*	2,132E-06	6,1E-05
C_RS01830	2,45		*c0399*	0,0004208	2,2E-03
C_RS12380	-2,45		*c2609*	1,825E-06	5,5E-05
C_RS08845	-2,44		*c1885*	2,44E-07	1,7E-05
C_RS29085	-2,43	*yliM*		7,49E-07	3,0E-05
C_RS23625	-2,43		*c4986*	1,59E-07	1,5E-05
C_RS03205	-2,42	*hcxA*	*c0687*	2,55E-08	5,9E-06
dppC	-2,41	*dppC*	*c4357*	1,71E-07	1,5E-05
C_RS24300	2,41	*ghoT*	*c5136*	1,455E-06	4,7E-05
C_RS29230	-2,40			0,0005263	2,6E-03
entS	-2,40	*entS*	*c0678*	0,0099962	2,6E-02
C_RS01310	-2,40		*c0279*	2,07E-07	1,5E-05
phoE	-2,40	*phoE*	*c0388*	1,03E-07	1,1E-05
C_RS15400	-2,40		*c3243*	3,21E-08	5,9E-06
C_RS03565	-2,40		*c0761*	3,97E-07	2,2E-05
C_RS20455	2,39		*c4329*	2,965E-06	7,6E-05
C_RS03760	-2,39	*sdhC*	*c0798*	6,52E-08	8,6E-06
C_RS24545	-2,39		*c5193*	9,55E-07	3,6E-05
C_RS28500	-2,37	*rzoD*		0,0001781	1,1E-03
C_RS21445	2,36		*c4545*	0,0008421	3,7E-03
C_RS21895	-2,35		*c4641*	5,74E-08	8,1E-06
uxuA	-2,35	*uxuA*	*c5402*	1,153E-05	1,7E-04
C_RS04010	-2,35		*c0846*	0,0001631	1,1E-03
C_RS28535	-2,35		*c1812*	5,141E-06	1,0E-04
C_RS13180	2,34	*nrdB*	*c2777*	1,073E-05	1,7E-04
C_RS17385	-2,34	*tnpB*	*c3660*	1,589E-05	2,2E-04
C_RS00780	-2,33	*yadC*	*c0166*	1,216E-05	1,8E-04
malF	2,32	*malF*	*c5003*	0,0003209	1,8E-03
C_RS06320	2,32	*flgG*	*c1347*	0,0001001	7,6E-04
ompW	2,32	*ompW*	*c1722*	0,0001753	1,1E-03
C_RS29075	-2,31			2,29E-07	1,7E-05
flgD	2,31	*flgD*	*c1344*	0,0082825	2,3E-02
C_RS16305	2,31	*lysA*	*c3435*	5,293E-05	4,8E-04

astD	-2,31	*astD*	*c2146*	0,0023017	8,1E-03
C_RS17515	2,31		*c3694*	2,149E-06	6,1E-05
C_RS04475	-2,31		*c0944*	2,204E-06	6,3E-05
C_RS28530	-2,30		*c1811*	0,000768	3,5E-03
proV	-2,30	*proV*	*c3230*	8,124E-05	6,6E-04
C_RS11445	-2,30		*c2415*	0,0012641	5,1E-03
cysA	-2,29	*cysA*	*c2956*	2,604E-06	7,0E-05
C_RS07625	-2,29		*c1630*	3,353E-06	8,2E-05
htpX	-2,28	*htpX*	*c2238*	1,024E-06	3,7E-05
cysT	-2,28	*cysT*	*c2958*	2,366E-06	6,6E-05
yhcN	-2,28	*yhcN*	*c3993*	8,323E-06	1,4E-04
C_RS28455	-2,28		*c1421*	1,553E-06	5,0E-05
C_RS24230	2,28		*c5121*	1,913E-05	2,4E-04
C_RS11355	-2,28		*c2396*	0,0016343	6,2E-03
C_RS02175	-2,27		*c0468*	0,0001587	1,0E-03
C_RS15430	-2,26		*c5561*	0,0178926	4,2E-02
C_RS27370	2,26			0,0001213	8,7E-04
C_RS25005	-2,26		*c5295*	1,309E-06	4,4E-05
dhaL	2,25	*dhaL*	*c1657*	3,835E-06	8,9E-05
C_RS17410	-2,25		*c3668*	8,206E-06	1,4E-04
C_RS15765	-2,25	*cysD*	*c3319*	4,69E-05	4,4E-04
gntP	-2,24	*gntP*	*c5401*	1,037E-05	1,6E-04
C_RS09685	-2,24		*c2051*	0,0047244	1,4E-02
C_RS14780	-2,24	*kgtP*	*c3112*	2,065E-06	6,1E-05
ilvB	-2,24	*ilvB*	*c4596*	1,356E-05	1,9E-04
fadI	-2,24	*fadI*	*c2887*	5,545E-06	1,1E-04
C_RS02025	-2,23		*c0435*	1,353E-06	4,5E-05
C_RS08390	-2,23	*ompG*	*c1791*	3,921E-05	3,9E-04
C_RS13765	-2,22	*emrY*	*c2902*	6,545E-05	5,6E-04
C_RS11450	-2,22			0,0013515	5,4E-03
C_RS12820	-2,21	*fruK*	*c2703*	4,007E-06	9,0E-05
trxC	-2,21	*trxC*	*c3107*	2,128E-05	2,6E-04
C_RS10530	2,21		*c2226*	0,0015131	5,9E-03

C_RS06215	-2,20		*c1323*	8,06E-06	1,4E-04
higA	-2,20	*higA*	*c3840*	6,044E-06	1,1E-04
dnaJ	-2,20	*dnaJ*	*c0020*	0,0003598	2,0E-03
C_RS04255	-2,20		*c0901*	2,1E-05	2,6E-04
C_RS06220	-2,20		*c1325*	1,122E-05	1,7E-04
C_RS11790	-2,20		*c2489*	0,0008742	3,8E-03
C_RS20705	-2,20		*c4382*	0,0031169	1,0E-02
C_RS10150	-2,20	*astA*	*c2147*	0,0126974	3,2E-02
C_RS07240	-2,19		*c1548*	8,863E-06	1,5E-04
C_RS03045	-2,19	*cusC*	*c0658*	2,951E-05	3,2E-04
C_RS13055	-2,19	*yojI*	*c2752*	0,0114768	2,9E-02
C_RS24260	2,19		*c5127*	6,97E-07	2,9E-05
C_RS19230	-2,19		*c4052*	0,0001539	1,0E-03
C_RS07280	2,19			0,0144299	3,5E-02
nrdD	2,19	*nrdD*	*c5337*	7,97E-08	9,7E-06
yfdV	-2,18	*yfdV*		5,579E-06	1,1E-04
fliN	2,18	*fliN*	*c2363*	0,0195152	4,5E-02
lysS	2,17	*lysS*	*c3469*	3,00E-07	2,0E-05
C_RS17575	-2,17		*c3706*	0,0004278	2,2E-03
C_RS20590	-2,17	*dppD*	*c4356*	6,874E-06	1,2E-04
C_RS21420	-2,17		*c4537*	1,81E-07	1,5E-05
C_RS14640	-2,17	*shoB*		0,0036298	1,2E-02
C_RS23020	2,17	*tpiA*	*c4871*	0,0047317	1,4E-02
C_RS08940	2,17			3,747E-05	3,8E-04
C_RS03820	2,16		*c0812*	0,007351	2,0E-02
hspQ	-2,16	*hspQ*	*c1104*	0,0002693	1,6E-03
cydX	2,16	*cydX*		7,11E-07	2,9E-05
hycA	2,16	*hycA*	*c3285*	0,037791	7,6E-02
lysC	2,16	*lysC*	*c4990*	4,28E-07	2,2E-05
C_RS11435	-2,16		*c2413*	0,0001273	9,0E-04
C_RS24265	2,15		*c5128*	5,855E-06	1,1E-04
C_RS11370	2,15		*c2399*	5,231E-05	4,8E-04
C_RS11125	2,15		*c2348*	0,0001113	8,1E-04

recX	-2,15	*recX*	*c3252*	2,053E-06	6,1E-05
C_RS23905	-2,14		*c5050*	4,20E-07	2,2E-05
C_RS10700	-2,14	*yebF*	*c2259*	0,0081827	2,2E-02
C_RS17815	-2,14		*c3751*	5,106E-05	4,7E-04
C_RS05705	-2,14		*c1214*	1,072E-05	1,7E-04
C_RS14060	-2,13		*c2959*	4,19E-07	2,2E-05
C_RS09045	2,13		*c1927*	7,874E-06	1,3E-04
C_RS11990	-2,13		*c2527*	0,0001667	1,1E-03
gcvH	2,13	*gcvH*	*c3484*	1,229E-05	1,8E-04
C_RS10835	-2,12		*c2287*	0,0001766	1,1E-03
C_RS24390	-2,12		*c5156*	3,508E-05	3,6E-04
C_RS28815	-2,12		*c3674*	3,28E-06	8,2E-05
C_RS05510	-2,11		*c1171*	3,22E-05	3,4E-04
C_RS09090	-2,11		*c1936*	0,0004045	2,1E-03
C_RS25590	2,11		*c5418*	5,393E-05	4,9E-04
metR	-2,11	*metR*	*c4750*	3,62E-07	2,1E-05
C_RS25720	-2,11		*c5444*	4,799E-06	1,0E-04
C_RS23620	-2,11		*c4985*	2,695E-05	3,0E-04
C_RS07330	-2,11	*iss*	*c1564*	0,003833	1,2E-02
glcB	-2,10	*glcB*	*c3705*	0,0001871	1,2E-03
C_RS07550	-2,10		*c1612*	5,223E-05	4,8E-04
C_RS10170	2,10	*ydjY*	*c2152*	1,012E-06	3,7E-05
C_RS02655	-2,09	*hha*	*c0578*	7,575E-05	6,2E-04
C_RS28410	-2,09		*c1258*	5,02E-07	2,4E-05
dhaK	2,09	*dhaK*	*c1658*	0,0002559	1,5E-03
C_RS01650	-2,08		*c0360*	4,326E-05	4,1E-04
umuD	-2,08	*umuD*	*c1631*	9,42E-05	7,4E-04
cydA	2,07	*cydA*	*c0811*	5,667E-05	5,1E-04
C_RS13175	2,07	*nrdA*	*c2776*	1,206E-05	1,8E-04
C_RS13355	-2,07			0,000104	7,8E-04
betI	-2,06	*betI*	*c0433*	0,0004139	2,2E-03
C_RS13955	-2,06	*xapR*	*c2937*	4,875E-06	1,0E-04
C_RS06020	-2,06			0,0016001	6,1E-03

C_RS06585	-2,06			5,363E-06	1,1E-04
nhaR	-2,06	nhaR	c0025	1,74E-07	1,5E-05
C_RS06310	2,06	flgE	c1345	0,0007589	3,4E-03
C_RS02490	-2,05	cyoE	c0539	0,0003581	1,9E-03
C_RS17525	2,05		c3696	0,0001319	9,2E-04
C_RS29405	-2,05			0,0071041	2,0E-02
C_RS09080	-2,05		c1934	7,065E-06	1,3E-04
C_RS01600	-2,05			0,0047572	1,4E-02
C_RS13895	-2,05		c2931	0,0005868	2,8E-03
C_RS15290	-2,04	ygaV	c3216	0,0001118	8,1E-04
C_RS29450	-2,04			1,025E-06	3,7E-05
C_RS14565	-2,04		c3070	0,000144	9,7E-04
C_RS17510	2,04		c3693	2,31E-05	2,7E-04
pyrB	2,04	pyrB	c5345	6,507E-06	1,2E-04
C_RS25190	2,04	nrdG	c5336	1,78E-07	1,5E-05
grcA	2,04	grcA	c3103	0,0038241	1,2E-02
C_RS05525	-2,04		c1175	4,20E-07	2,2E-05
C_RS14050	-2,03	cysW	c2957	2,146E-06	6,1E-05
C_RS01400	-2,03			0,0028376	9,5E-03
C_RS15880	2,03	eno	c3344	0,0048289	1,5E-02
C_RS17030	-2,03	papC	c3590	0,0507879	6,1E-01
C_RS04585	2,02		c0970	0,0002065	1,3E-03
C_RS19855	2,02	malP	c4194	0,0030465	1,0E-02
dnaK	-2,02	dnaK	c0019	0,000463	2,4E-03
recA	-2,01	recA	c3253	0,0066193	1,9E-02
dinD	-2,01	dinD	c4469	1,15E-06	4,0E-05
C_RS11340	2,01		c2393	0,0027358	9,3E-03
C_RS15920	-2,00	gudP	c3353	0,013237	3,3E-02
C_RS19665	-2,00		c4152	0,0004405	2,3E-03
C_RS02505	-2,00	cyoB	c0542	7,534E-05	6,2E-04
C_RS18370	2,00		c3871	0,0145563	3,6E-02
C_RS06625	-2,00		c1414	0,0003864	2,1E-03
C_RS28095	-2,00			0,0271421	5,8E-02

C_RS28025	-1,99			1,6E-05	2,2E-04
C_RS14445	-1,99	ndk	c3041	0,0005129	2,5E-03
C_RS17520	1,99		c3695	3,629E-06	8,5E-05
C_RS09070	-1,99		c1932	3,114E-05	3,3E-04
C_RS15560	-1,99		c3274	0,0002769	1,6E-03
C_RS18420	-1,99	garP	c3882	0,0131747	3,3E-02
C_RS01880	-1,99			0,0016624	6,3E-03
C_RS17705	1,98	hybB	c3732	0,0072012	2,0E-02
C_RS09215	-1,97		c1959	0,0015977	6,1E-03
tkt	1,97	tkt	c2990	0,0005482	2,7E-03
C_RS05790	-1,97			6,188E-05	5,4E-04
cspF	-1,97	cspF	c3185	3,038E-06	7,8E-05
C_RS17690	1,97	hybE	c3729	0,0001552	1,0E-03
C_RS02885	-1,97		c0625	2,424E-05	2,8E-04
sulA	-1,96	sulA	c1095	2,606E-05	3,0E-04
C_RS17700	1,96	hybC	c3731	4,875E-06	1,0E-04
C_RS13785	-1,96	yfdE	c2907	2,336E-06	6,6E-05
C_RS13185	1,96	yfaE	c2778	1,142E-05	1,7E-04
C_RS12810	1,96		c2701	0,0069493	2,0E-02
nikE	1,96	nikE	c4273	9,248E-06	1,5E-04
C_RS24060	-1,96		c5088	0,0013994	5,5E-03
ftnA	1,96	ftnA	c2321	0,002289	8,1E-03
C_RS16650	1,96		c3506	0,0002518	1,5E-03
C_RS18465	-1,96		c3891	0,0021584	7,7E-03
C_RS14945	-1,95		c3144	1,796E-06	5,5E-05
C_RS09210	-1,95		c1958	0,0002001	1,2E-03
pstS	-1,94	pstS	c4653	5,009E-05	4,7E-04
proW	-1,94	proW	c3231	5,9E-05	5,2E-04
C_RS06315	1,94	flgF	c1346	0,0005019	2,5E-03
C_RS04015	-1,94		c0847	4,325E-05	4,1E-04
C_RS10525	1,93	manY	c2224	0,0002219	1,3E-03
C_RS05500	-1,93			5,246E-05	4,8E-04
C_RS16825	1,93	ansB	c3543	0,0632068	1,2E-01

tnaB	-1,92	*tnaB*	*c4632*	0,0118461	3,0E-02
C_RS07215	-1,92			0,0003032	1,7E-03
C_RS11375	1,92		*c2400*	0,0001378	9,5E-04
C_RS07515	-1,92	*bluF*	*c1606*	1,206E-06	4,1E-05
C_RS20265	1,92		*c4285*	0,0001366	9,5E-04
C_RS07870	1,91	*narG*	*c1685*	1,968E-05	2,5E-04
C_RS11855	-1,91		*c2500*	0,0002583	1,5E-03
C_RS25060	-1,91	*cycA*	*c5307*	4,398E-06	9,7E-05
cheW	1,91	*cheW*	*c2302*	0,0266878	5,8E-02
C_RS02635	-1,90		*c0574*	0,0014428	5,7E-03
C_RS24295	1,90	*ghoS*		3,181E-06	8,0E-05
C_RS14955	-1,90		*c3146*	5,421E-06	1,1E-04
C_RS02500	-1,90	*cyoC*	*c0541*	0,0002682	1,5E-03
C_RS14035	-1,89		*c2954*	1,378E-06	4,5E-05
C_RS09245	-1,89	*dgcZ*	*c1963*	9,18E-08	1,1E-05
C_RS10335	1,89		*c2185*	0,0001546	1,0E-03
C_RS02650	-1,89	*maa*	*c0577*	0,0006077	2,9E-03
ypdK	-1,89	*ypdK*		0,0005658	2,7E-03
C_RS15080	-1,88		*c3172*	0,0628645	1,2E-01
C_RS11700	-1,88	*clbC*	*c2468*	0,0005597	2,7E-03
prpB	-1,88	*prpB*	*c0451*	3,906E-06	8,9E-05
C_RS03440	-1,88	*gltI*	*c0739*	0,0001482	9,9E-04
C_RS02495	-1,88		*c0540*	0,0009715	4,1E-03
fliJ	1,88	*fliJ*	*c2359*	0,0087315	2,3E-02
C_RS09035	-1,87		*c1925*	7,148E-05	6,0E-04
C_RS15555	-1,87		*c3273*	0,001263	5,1E-03
C_RS06025	-1,87			0,0030492	1,0E-02
C_RS15425	-1,87		*c5560*	7,098E-05	5,9E-04
C_RS08615	-1,87		*c1835*	3,931E-06	8,9E-05
focA	1,87	*focA*	*c1239*	1,96E-07	1,5E-05
ghrB	1,86	*ghrB*	*c4372*	4,016E-05	4,0E-04
C_RS10420	-1,86		*c2202*	0,0001322	9,2E-04
C_RS17235	-1,85		*c3628*	3,50E-07	2,1E-05

C_RS01295	-1,85		c0275	0,0008908	3,9E-03
nagA	-1,85	nagA	c0752	3,329E-05	3,5E-04
fbaA	1,85	fbaA	c3503	3,269E-05	3,4E-04
C_RS17695	1,84		c3730	1,442E-05	2,0E-04
C_RS01460	-1,84		c0317	0,0021776	7,8E-03
C_RS08830	-1,83		c1882	0,0001121	8,1E-04
nac	-1,83	nac	c2446	7,087E-06	1,3E-04
C_RS03435	-1,83	gltJ	c0738	2,262E-06	6,4E-05
hybA	1,83	hybA	c3733	0,0001115	8,1E-04
C_RS14505	-1,82	iscS	c3056	0,0053559	1,6E-02
C_RS18355	-1,82		c3867	3,216E-05	3,4E-04
C_RS08400	-1,82		c1793	3,217E-05	3,4E-04
C_RS08735	-1,82		c1860	7,028E-06	1,3E-04
C_RS25965	-1,82			0,050099	9,6E-02
C_RS20120	-1,82	livJ	c4253	5,015E-06	1,0E-04
C_RS09075	-1,81		c1933	3,34E-06	8,2E-05
fadA	-1,81	fadA	c4792	8,20E-07	3,2E-05
C_RS17785	1,81	yqhD	c3745	0,0027088	9,2E-03
C_RS17505	1,81		c3692	0,0001025	7,8E-04
C_RS23615	-1,81		c4984	2,808E-05	3,1E-04
aceE	1,81	aceE	c0142	0,0001452	9,7E-04
argO	-1,80	argO	c3501	1,953E-05	2,5E-04
C_RS09250	-1,80			5,93E-07	2,6E-05
C_RS00100	-1,80		c0022	2,127E-05	2,6E-04
dapD	1,80	dapD	c0201	0,000433	2,2E-03
malI	-1,80	malI	c2012	7,026E-05	5,9E-04
C_RS05765	-1,80		c1231	0,0003115	1,7E-03
fruA	-1,80	fruA	c2702	0,0226017	5,1E-02
C_RS17240	-1,80		c3630	3,60E-07	2,1E-05
C_RS05515	-1,80		c1173	6,858E-06	1,2E-04
C_RS01800	-1,79		c0391	8,42E-07	3,2E-05
garL	-1,79	garL	c3881	0,0233892	5,2E-02
xapA	-1,79	xapA	c2940	0,0038022	1,2E-02

C_RS14295	1,79	*bcp*	*c3008*	0,0009348	4,0E-03
C_RS22920	-1,78		*c4849*	6,42E-07	2,7E-05
C_RS19755	-1,78	*hslR*	*c4171*	2,228E-05	2,7E-04
C_RS17405	-1,78		*c3666*	0,0118381	3,0E-02
C_RS00685	-1,78		*c0146*	1,398E-06	4,6E-05
C_RS10285	-1,78		*c2174*	0,0004332	2,2E-03
C_RS16335	-1,77		*c3441*	8,548E-05	6,9E-04
fliR	-1,77	*fliR*	*c2367*	0,0001445	9,7E-04
C_RS01325	-1,77		*c0282*	2,435E-05	2,8E-04
C_RS04485	1,77		*c0946*	0,0001206	8,6E-04
C_RS04580	1,77		*c0969*	0,000778	3,5E-03
C_RS03355	-1,77		*c0721*	0,000752	3,4E-03
cysH	-1,77	*cysH*	*c3321*	4,046E-05	4,0E-04
rpoH	-1,77	*rpoH*	*c4254*	5,152E-05	4,8E-04
C_RS13795	-1,77	*oxc*	*c2909*	2,441E-06	6,7E-05
C_RS25225	1,77	*ridA*	*c5342*	0,0017009	6,4E-03
C_RS29330	-1,77			7,034E-05	5,9E-04
C_RS10365	-1,76		*c2191*	1,41E-05	2,0E-04
C_RS26640	-1,76			3,926E-05	3,9E-04
csgB	-1,76	*csgB*	*c1305*	0,0085802	2,3E-02
C_RS29105	-1,76			7,31E-06	1,3E-04
C_RS25365	1,75		*c5372*	3,434E-05	3,5E-04
gcvT	1,75	*gcvT*	*c3485*	3,558E-05	3,6E-04
C_RS21255	-1,75		*c4502*	1,92E-07	1,5E-05
C_RS18210	-1,74		*c3836*	9,493E-05	7,4E-04
C_RS01605	-1,74		*c0348*	5,05E-05	4,7E-04
C_RS13950	-1,74		*c5558*	0,0191916	4,4E-02
garD	-1,74	*garD*	*c3883*	0,0165608	4,0E-02
C_RS11075	1,74	*rpoF*	*c2337*	0,0420525	1,6E-01
C_RS01440	-1,73		*c0310*	0,0078167	2,1E-02
fadD	-1,73	*fadD*	*c2209*	1,599E-05	2,2E-04
C_RS04480	-1,73		*c0945*	7,385E-05	6,1E-04
C_RS23650	1,73	*pgi*	*c4991*	2,972E-05	3,2E-04

ybgE	1,73	*ybgE*	*c0814*	2,80E-07	1,9E-05
serC	1,73	*serC*	*c1045*	7,54E-07	3,0E-05
C_RS27750	-1,73			0,0027326	9,2E-03
C_RS06050	-1,73		*c1288*	0,0017554	6,6E-03
C_RS01425	-1,72		*c0307*	7,423E-06	1,3E-04
C_RS19460	-1,72	*bfd*	*c4108*	0,00213	7,6E-03
dinI	-1,72	*dinI*	*c1328*	0,0011587	4,8E-03
mdtI	-1,72	*mdtI*	*c1991*	0,0123778	3,1E-02
uspC	1,72	*uspC*	*c2309*	0,0010413	4,4E-03
fliF	1,72	*fliF*	*c2354*	0,0292673	6,2E-02
C_RS02130	-1,72	*lacA*	*c0457*	0,0882183	1,5E-01
C_RS10875	1,72	*cheY*	*c2297*	0,0028406	9,5E-03
C_RS23955	-1,72		*c5063*	3,543E-06	8,3E-05
C_RS26550	-1,71			0,0422969	8,3E-02
mdtJ	-1,71	*mdtJ*	*c1992*	0,011653	3,0E-02
C_RS02180	-1,71		*c0469*	2,069E-05	2,6E-04
fhuF	-1,71	*fhuF*	*c5446*	0,0188576	4,4E-02
C_RS17180	-1,71	*tnpB*	*c3616*	3,662E-05	3,7E-04
C_RS29220	-1,71		*c1892*	0,0155433	3,8E-02
C_RS21545	-1,71		*c4571*	9,447E-06	1,5E-04
garK	-1,71	*garK*	*c3879*	0,0640235	1,2E-01
pepT	1,71	*pepT*	*c1479*	1,187E-05	1,8E-04
C_RS24700	1,71		*c5228*	9,061E-06	1,5E-04
ffs	-1,70	*ffs*		6,239E-05	5,4E-04
C_RS17315	-1,70		*c3647*	0,0006097	2,9E-03
norR	-1,70	*norR*	*c3263*	9,673E-05	7,5E-04

FDR: False Discovery Rate

E. coli CFT073 (GenBank accession no, AE014075,1)

7 Résultats supplémentaires

7.1 Effet de l'inactivation de *yqhG* et *yqhH* sur la production des fimbriae de type 1 et la réponse au stress
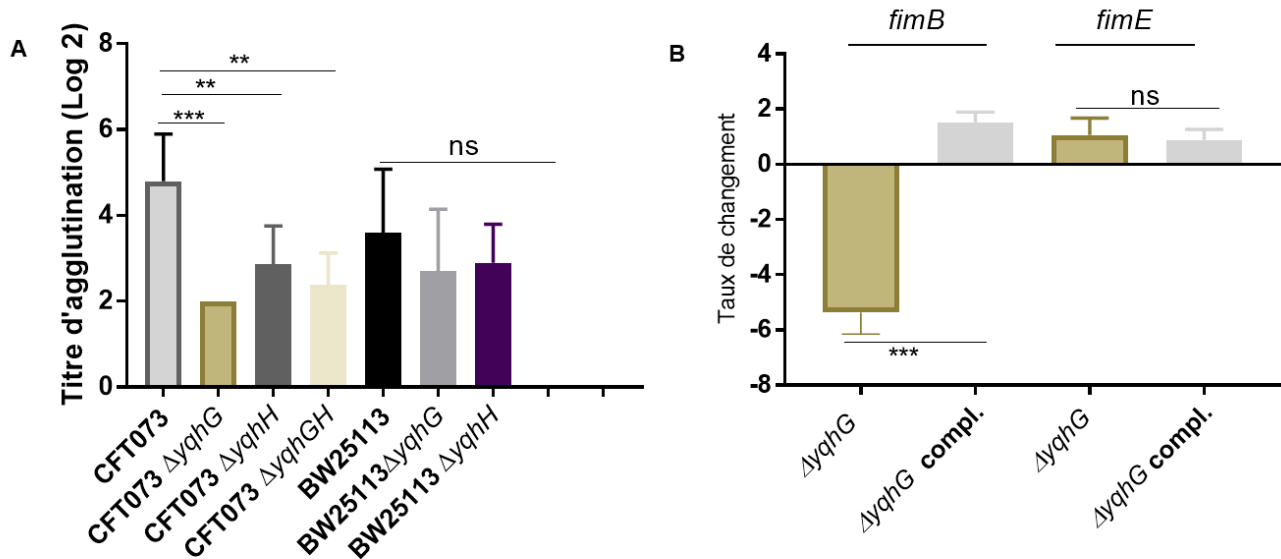
Figure 7.1. Effet de l'inactivation de *yqhG* et *yqhH* sur la production des fimbriae de type 1

(A) Le niveau de production de fimbriae de type 1 a été évalué par le test d'agglutination de levure chez la souche CFT073, la souche non pathogène K-12 BW25113 et les mutants dérivés en milieu LB en phase exponentielle de croissance (O.D. 0,6). (B) Transcription des gènes *fimB* et *fimE* codant des recombinases qui contrôle l'orientation du promoteur *fimS* chez le mutant CFT073Δ*yqhG* et la souche complémentée en milieu LB en phase exponentielle de croissance. Tous les résultats indiqués sont les valeurs moyennes et les écarts types pour trois expériences biologiques ou plus. Le test statistique utilisé est ANOVA : *, P <0,05; **, P <0,005; ***, P <0,0001 (non publié).
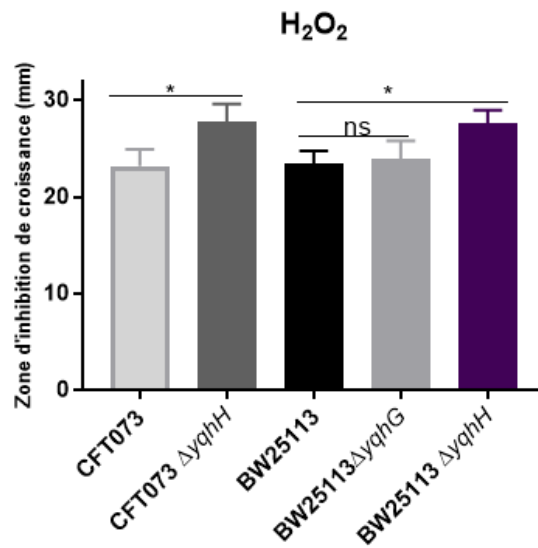
Figure 7.2. Rôle de *yqhG* et *yqhH* dans la résistance au stress oxydatif

Zones d'inhibition de la croissance (mm) de la souche CFT073, la souche non pathogène K-12 BW25113 et les mutants dérivés suite à l'exposition à 10 µl d'H$_2$O$_2$ 30 % sur gélose LB. Tous les résultats indiqués sont les valeurs moyennes et les écarts types pour quatre expériences biologiques. Le test statistique utilisé est ANOVA : *, P <0,05; **, P <0,005; ***, P <0,0001 (non publié).

7.2   Effet de l'inactivation de *ryfA* sur les recombinases

Figure 7.3. Effet de l'inactivation de *ryfA* sur les recombinases

Transcription des gènes de recombinases ***fimE*** et ***ipbA*** chez la souche UPEC CFT073 et son mutant isogénique Δ***ryfA*** dans les vessies de souris 48 h post-infection et après croissance en urine. Le test statistique utilisé est ANOVA : *, P <0,05; **, P <0,005; ***, P <0,0001 (non publié).
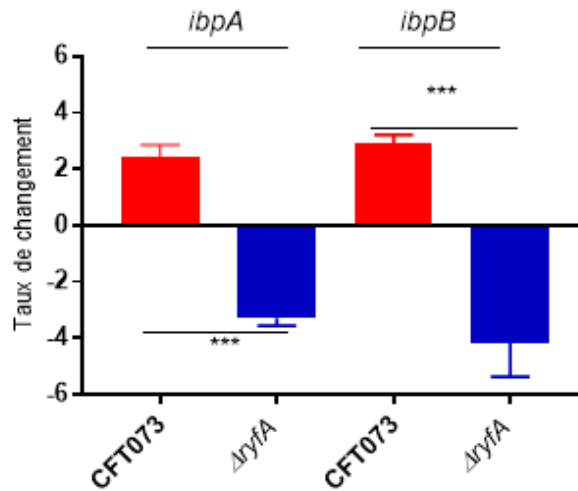
Figure 7.4. Transcription d'*ibpA* et d'*ibpB* chez le mutant *ryfA*

Transcription des gènes de chaperons ***ibpA*** et ***ibpB*** chez la souche UPEC CFT073 et son mutant isogénique *ryfA* dans les vessies de souris 48 h post-infection. Le test statistique utilisé est ANOVA : *, P <0,05; **, P <0,005; ***, P <0,0001 (non publié).

7.3 Production des fimbriae de type 1 et la résistance au stress chez la souche CH138
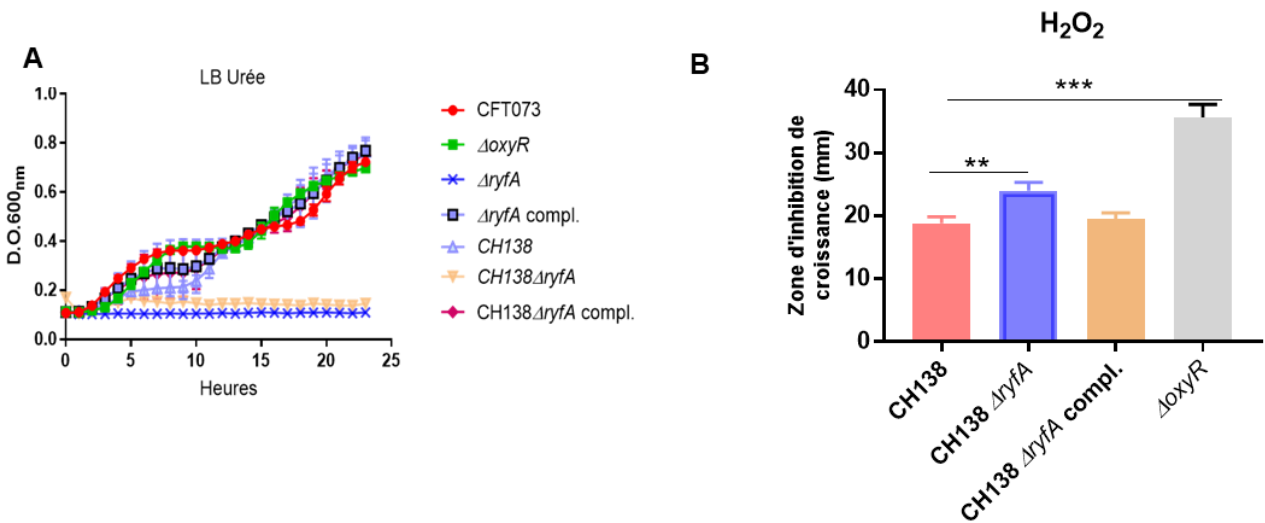
Figure 7.5. Rôle de RyfA dans la résistance au stress chez la souche CH138

(A) Courbe de croissance en conditions de stress osmotique. Les souches ont été cultivées dans du milieu LB 0,6 M urée pendant 24 h à 37°C et les D.O.$_{600}$ sont prises toutes les 15 min par l'appareil _Bioscreen C._ La souche UPEC CFT073 et ses mutants dérivés Δ_ryfA_ et Δ_oxyR_ ont été utilisées comme contrôle. (B) Zones d'inhibition de la croissance (mm) de la souches CH138 et les souches dérivées suite à l'exposition à 10 µl d'H$_2$O$_2$ 30 % sur gélose LB. Le mutant CFT073 Δ_oxyR_ a été utilisé comme contrôle étant plus sensible à l'H$_2$O$_2$. Les barres verticales représentent les erreurs standard des moyennes. Le test statistique utilisé est ANOVA, (*, $P < 0,05$; **, $P < 0,005$; ***, $P < 0,0001$) (non publié).
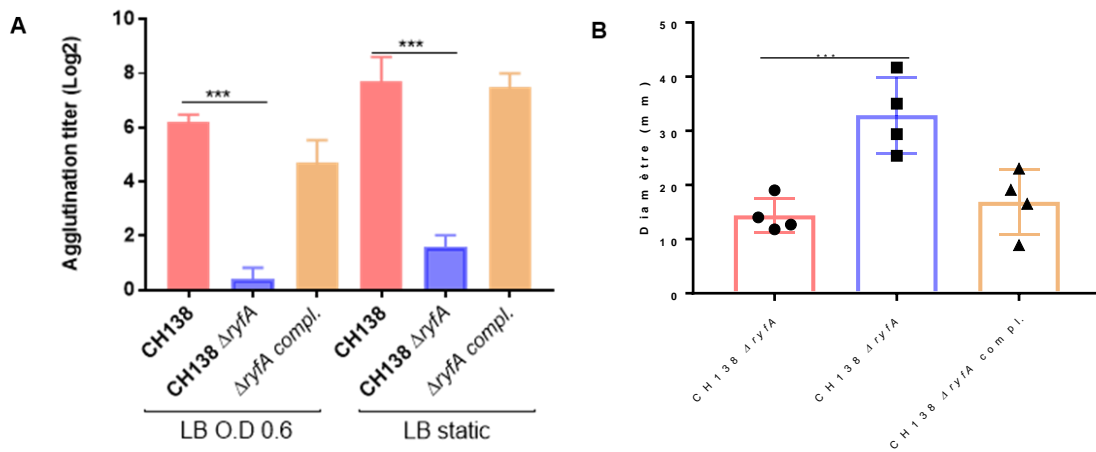
Figure 7.6. Effet de l'inactivation du *ryfA* sur la production de fimbriae de type 1 et la motilité chez CH138

(A) Le niveau de production de fimbriae de type 1 a été évalué par le test d'agglutination de levure chez la souche APEC CH138 et les souches dérivées en milieu LB en phase exponentielle de croissance et après croissance statique pendant 48 h. (B) Diamètre moyen de la zone de motilité en milieu soft agar (0,25 %) après 18 h d'incubation à 37°C. Tous les résultats indiqués sont les valeurs moyennes et les écarts types pour cinq expériences biologiques. Le test statistique utilisé est ANOVA : *, P <0,05; **, P <0,005; ***, P <0,0001 (non publié).

## 7.4   Modèle d'infection systémique aviaire

A

B
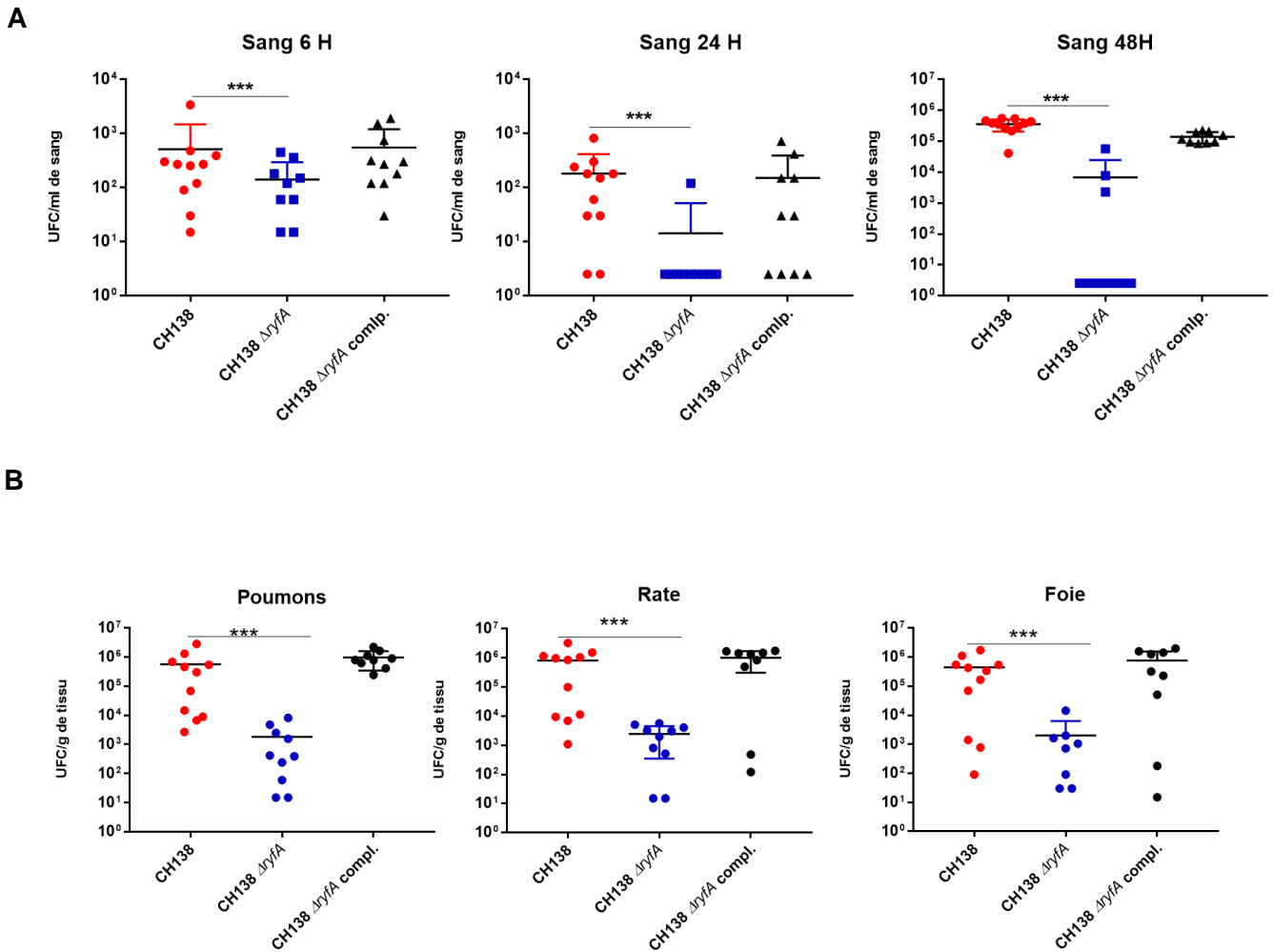
Figure 7.7. Rôle de RyfA chez la souche APEC CH138 dans le modèle aviaire d'infection du sac aérien

(A) le nombre de bactéries présent dans le sang à 6, 24 et 48 heures, (B) dans les poumons, la rate et le foie de poulets infectés. Les résultats sont exprimés en UFC par gramme de tissu ou millilitre de sang. La souche APEC virulente sauvage CH138, le mutant *ryfA* et le mutant complémenté ont été utilisées. Les points de données représentent le nombre de bactéries provenant de tissus isolés de différents poulets (n = 10-11) 48 h après l'infection. Des différences statistiques sont notées : * p <0,05, ** p <0,01, *** p <0,001, **** p <0,0001, test de Mann-Whitney (non publié).
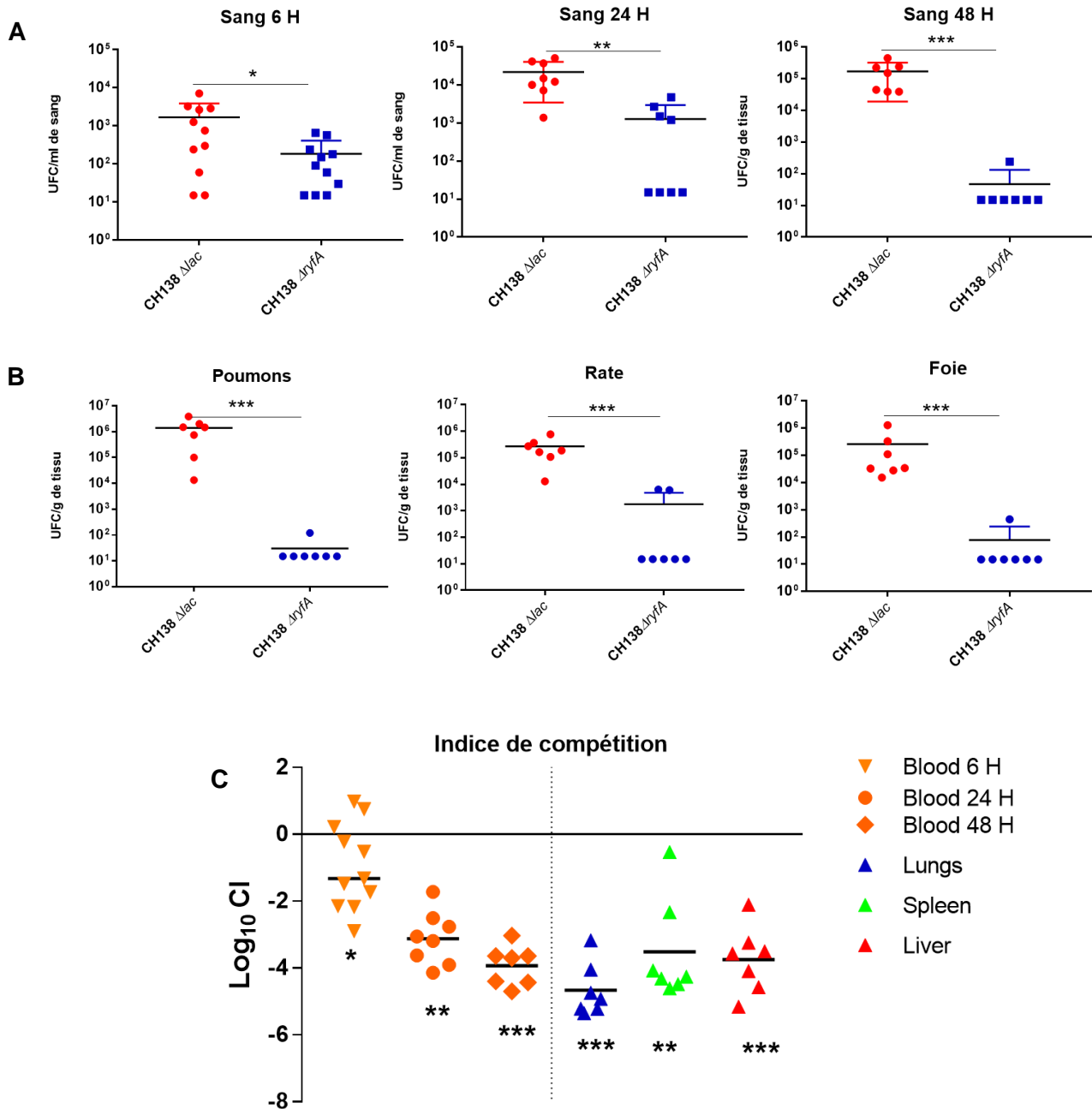
Figure 7.8. RyfA est important pour la compétitivité de la souche CH138 dans le modèle septicémique aviaire

(A) les comptes bactériens dans le sang, (B) et les tissus de poulets infectés par la souche virulente APEC CH138 Δ*lac* et le mutant Δ*ryfA*. (C) Capacité compétitive du mutant *ryfA* dans le modèle de co-infection. Les valeurs de l'indice de compétition (IC) $\log_{10}$ des organes de poulets infectés. Les points de données représentent les comptes bactériens provenant de tissus isolés de différents poulets (n = 11) 48 h après l'infection. Différence statistique : * $p < 0.05$, ** $p < 0.01$, *** $p < 0.001$, Test Two-tailed Wilcoxon signed rank (non publié).

7.5   La résistance au sérum

Test de résistance au sérum

La résistance à 90% de sérum humain a été déterminée comme décrit par (Crepin *et al.*, 2012). Le sang a été prélevé de quatre personnes indépendantes ne travaillant pas avec *E. coli* et n'ayant pas reçu de traitement antibiotique au cours des 3 derniers mois précédents. Les cellules ont été séparées par centrifugation à 1000 x g pendant 10 min, et les fractions de sérum des quatre échantillons ont été collectées, regroupées et stockées en aliquotes à -30°C. Une souche est considérée comme sensible ou résistante s'il y avait une différence dans les comptes bactériens par au moins 2 logs. Nous avons également testé la résistance à 90% de sérum de poulet.
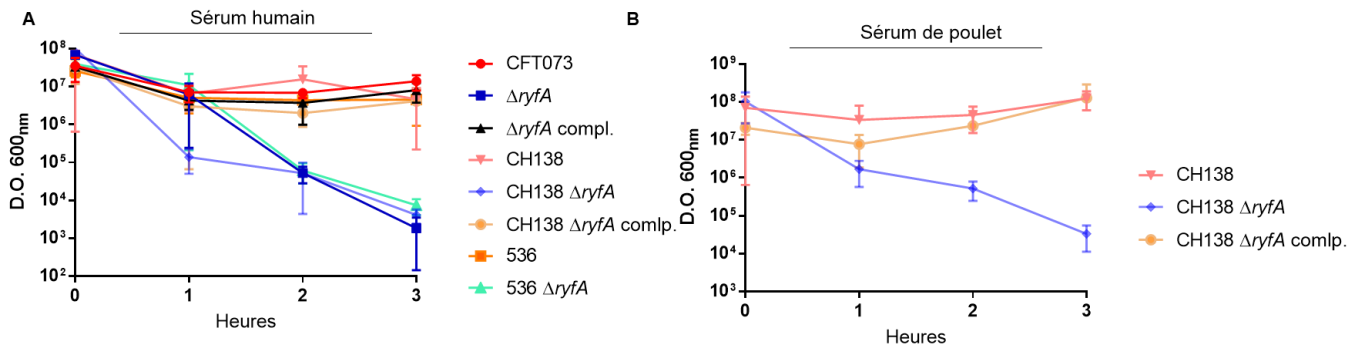
Figure 7.9. Résistance à l'activité bactéricide du complément humain

(A) L'effet de 90% de sérum humain ou de poulet sur la survie des souches ExPEC CFT073, 536, CH138 et les souches dérivées. (B) La sensibilité de la souche APEC CH138, le mutant *ryfA* et la souche complémentée à l'effet de sérum de poulet à 90%. Les suspensions sérum-bactérie ont été incubées à 37 °C pendant 3 h dans avec un inoculum bactérien initial d'environ 10^7 UFC/ml. Le nombre de bactéries viables a été estimé chaque 1 h sur gélose LB. Les résultats sont représentatifs de trois réplicas biologiques indépendants (Non publié).

8 DISCUSSION GENERALE

Les UPEC utilisent les fimbriae de type 1 pour se fixer aux cellules uroépithéliales dans la vessie de l'hôte. Les UPEC peuvent modifier l'expression des fimbriae de type 1 en inversant l'élément *fimS* dans le région promotrice de l'opéron *fim* pour qu'il soit en phase ON ou en phase OFF. L'orientation de *fimS* dépend des signaux environnementaux, tels que la température, le pH et l'osmolarité, à travers une variété de protéines régulatrices (Aberg *et al.*, 2006; Gally *et al.*, 1993; Müller *et al.*, 2009b; Schwan *et al.*, 2002a). Ces protéines affectent la variation de phase directement en interagissant avec *fimS*, ou indirectement en influençant la transcription des gènes codant pour les recombinases spécifiques au site, FimB, FimE, IpuA, IpuB et IpbA qui affectent l'orientation de *fimS* (Bryan *et al.*, 2006a; Hannan *et al.*, 2008).

La régulation des fimbriae de type 1 dans les voies urinaires en réponse à l'hôte n'est toujours pas clair. Par conséquent, la compréhension du réseau de régulation complexe coordonnant l'expression de multiples facteurs d'adhérence chez les UPEC contribuera à terme au développement de stratégies thérapeutiques pour réduire la colonisation des voies urinaires. L'objectif principal de cette thèse était d'identifier des nouveaux régulateurs de fimbriae de type 1 et de caractériser leurs rôles dans la pathogenèse des souches UPEC.

Dans une première partie, nous avons donc voulu identifier les régulateurs de fimbriae de type 1 (article 1). Dans une seconde partie, nous nous sommes intéressés à l'effet de la protéine YqhG et du petit ARN non-codant RyfA sur la production des fimbriae de type 1 et la pathogenèse des souches UPEC (articles 1 et 2).

8.1 Plusieurs nouveaux régulateurs de type 1

Le chapitre V a décrit la méthode d'identification des facteurs affectant l'expression de fimbriae de type 1 chez la souche UPEC CFT073. Pour atteindre cet objectif, la souche CFT073 portant une fusion transcriptionnelle consistant de l'opéron *lux* sous le contrôle du promoteur du fimbriae de type 1, *fimS*, a été utilisée pour générer une banque de mutants par transposon Tn*10*. Les mutants ont été criblés pour la production de la luminescence. Les mutants affectés dans la production de fimbriae de type 1 ont été confirmés *in vitro* par le test d'agglutination de levure.

Au total, nous avons isolé 48 mutants, mais uniquement 32 clones ont été choisis pour avoir un séquençage plus en profondeur. En effet, les clones produisant au moins 4 fois plus ou moins de fimbriae de type 1 comparé à la souche sauvage CFT073 ont été sélectionnés.

En utilisant un séquençage à haut débit, nous avons ensuite identifié les sites d'insertion du transposon dans ces mutants, conduisant à l'identification d'un gène qui est absolument nécessaire pour la production de fimbriae de type 1 et 31 autres gènes qui ont eu un impact sur la production de fimbriae de type 1. Ceci inclus, les gènes codant : le placier *fimD*, la recombinase *fimB* et le régulateur global *lrp*. Nous avons identifié des insertions dans les gènes codant pour les fimbriae Auf et F9, des gènes impliqués dans la biosynthèse des acides aminés, le transport membranaire et les gènes codant des protéines de fonctions inconnues. La confirmation du rôle de ces gènes dans l'expression des fimbriae de type 1 via la construction et la caractérisation de mutants spécifiques est désormais requise.

8.2 YqhG est important pour la réponse au stress oxydatif et la production des fimbriae de type 1

Les résultats présentés dans le chapitre V représentent une caractérisation approfondie des effets de la protéine YqhG, sur l'expression de fimbriae de type 1, la motilité et la réponse au stress oxydatif chez la souche UPEC CFT073. Une approche expérimentale multidimensionnelle a été utilisée à l'aide de tests d'agglutination de levure, de motilité, d'infection de souris et de qPCR pour démontrer que la perte de *yqhG* entraîne une réduction de la production de fimbriae de type 1, de l'adhérence aux cellules uroépithéliales, ce qui explique en partie l'atténuation de la virulence du mutant *yqhG* de la souche UPEC CFT073.

Le gène *yqhG* code pour une protéine hypothétique de fonction inconnue. Dans ce projet de thèse, nous avons montré que l'atténuation de la virulence du mutant *yqhG* de la souche UPEC CFT073 dans la vessie est majoritairement causée par la répression des fimbriae de type 1. Ces derniers étant importants pour la colonisation de la vessie, leur répression diminue la capacité du mutant à coloniser le tractus urinaire de souris et à envahir les cellules urothéliales. La répression du fimbriae de type 1 chez le mutant *yqhG* semble être directement reliée à la répression de la recombinase *fimB* (Fig.7.1B). Aussi, nous avons observé que le mutant *yqhG* est plus motile en milieu soft agar*.* L'augmentation de la motilité n'est pas un phénomène surprenant, car lorsque les fimbriae de type 1 sont réprimés, il a été démontré que les flagelles sont surexprimés (Lane *et al.*, 2007b). L'expression des adhésines et des flagelles est coordonnée. Ainsi, la population de la souche Δ*yghG* peut être hyperflagellée, mais n'exprime pas les fimbriae résultant en une forte réduction de la colonisation rénale, il est possible que l'expression des fimbriae P soit affectée chez le mutant *yqhG*.

Les analyses *in silico* suggèrent que YqhG, est une protéine périplasmique avec deux domaines DUF3828 qui sont conservés chez *E. coli*. Il était donc intéressant de l'étudier plus finement et de déterminer son rôle dans la pathogenèse bactérienne. En aval de *yqhG*, se trouve *yqhH*, codant pour une lipoprotéine. Nous avons émis l'hypothèse qu'il soit possible que *yqhH* puisse influencer la régulation des fimbriae. En phase exponentielle de croissance, l'inactivation de YqhH a entraîné une diminution de l'expression des fimbriae de type 1 chez la souche CFT073 (Fig. 7.1A). Également, le double mutant *yqhGH* a démontré un défaut dans la production de fimbriae de type 1 (Fig. 7.1A). Considérant ce résultat, il semblerait que *yqhH* tout comme *yqhG* puisse jouer un rôle dans la production de fimbriae de type 1 chez la souche UPEC CFT073. Chez la souche non pathogène K-12, la mutation de *yqhG* ou *yqhH* n'a aucun effet sur la production de fimbriae de type 1 dans les mêmes conditions (Fig. 7.1A). Ces résultats indiquent que *yqhG* et *yqhH* pourraient influencer l'expression des fimbriae de type 1 différemment dépendamment des souches.

La capacité des bactéries à détecter et à répondre aux stress est une étape clé pour la survie. Si les bactéries répondent avec succès à un stress rencontré, elles survivent et se multiplient. Si elles échouent ou sont inefficaces dans leur réponse, cela peut entraîner la mort. Ceci est particulièrement crucial pour les bactéries pathogènes qui doivent être capables de tolérer des conditions changeantes principalement pendant la colonisation de l'hôte. Par exemple, les bactéries sont continuellement exposées au stress oxydatif puisque la source primaire des ROS est la chaîne respiratoire (González-Flecha & Demple, 1995). En effet, la respiration aérobie est basée sur le métabolisme de l'oxygène moléculaire et génère des produits toxiques ou les ROS, qui causent un stress oxydatif. Ainsi, au sein de l'hôte, les bactéries doivent faire face à des variations de stress dues à l'environnement de l'hôte telles que les températures, l'osmolarité et les changements de pH, le stress oxydatif, le stress nutritionnel ou le système immunitaire de l'hôte. Pour résister à ces environnements, les bactéries ont une multitude de facteurs de virulence qui doivent être régulés pour répondre correctement à chaque signal stressant.

Le mutant *yqhG* de la souche CFT073 est plus sensible au stress oxydatif induit par le peroxyde d'hydrogène. Ainsi le mutant *yqhH* de la même souche est significativement plus sensible au stress oxydatif indiquant que chez CFT073, *yqhH* semble contribuer à la résistance au stress oxydatif induit par le peroxyde d'hydrogène tout comme *yqhG* (Fig. 7.2). De plus, la délétion de *yqhH* chez la souche K-12 BW25113, mène à une sensibilité accrue au stress oxydatif (Fig. 7.2). Ceci suggère que YqhG et YqhH soient impliqués dans la résistance au stress chez les souches pathogènes et non pathogènes et que possiblement ces deux protéines interagissent ensemble.

Il est clair que l'inactivation des gènes *yqhH* ou *yqhG* provoque des effets pléiotropes selon les souches.

8.3   RyfA un petit ARN régulateur de stress

Dans la deuxième partie de ce travail, nous avons examiné le rôle du petit ARN non-codant, RyfA, dans la régulation de la réponse au stress et la pathogenèse des souches ExPEC. Les résultats présentés au chapitre VI représentent une caractérisation approfondie des effets de l'inactivation de *ryfA* chez les souches UPEC CFT073 et 536 et la souche APEC CH138.

Nous avons montré que la mutation de *ryfA* atténue la virulence des souches CFT073 et CH138. Cette atténuation est causée par des effets pléiotropes. En effet, l'inactivation de RyfA entraîne une sensibilité accrue au stress, la perturbation du métabolisme et la modulation de plusieurs adhésines fimbriaires et des flagelles.

RyfA a été identifié à l'origine par des analyses *in silico* conçues pour identifier des gènes codant pour des sRNAs auparavant non caractérisés (Hershberg *et al.*, 2003). Par analyse *in silico*, nous avons trouvé que RyfA est codé par les souches d'*E. coli* (pathogènes et non pathogènes), *Shigella*, *Salmonella* et d'autres espèces. Chez la souche CFT073, *ryfA* se situe entre les gènes *sseB* et *sseA* et a une taille de 305 pb. Il est à noter que la séquence de *ryfA* de CFT073 est quasiment identique à celle de la souche non pathogène *E. coli* K-12 MG1655 (98 % d'identité en acide nucléique) et la souche UPEC 536 (93 % d'identité). Ainsi, il convient de noter que toutes les souches de *Shigella* possèdent une seule copie de *ryfA* sauf la souche *S. dysenteriae* qui possèdent deux copies de *ryfA* quasiment identique entre elles (Fris *et al.*, 2017). Afin d'étudier le rôle de *ryfA*, nous avons tout d'abord montré que la souche CFT073 produit le sRNA en phase exponentielle de croissance par Northern blot et par qRT-PCR. Une seule bande d'environ 300 nucléotides a été détectée dans l'analyse Northern blot, confirmant que CFTO73 produit RyfA à des D.O. allant de 0.6 à 2. Une bande d'une taille approximative de 120 pb a été également détectée suite à la surexpression de RyfA. Cependant, nous ne savons pas si RyfA subit de l'épissage suite à sa production.

Nous avons montré que l'inactivation de RyfA mène à une sensibilité accrue au stress oxydatif et osmotique. En effet, la perte de *ryfA* chez les souches UPEC CFT073 et 536 ainsi que la souche APEC CH138 provoque une baisse de résistance à la toxicité du H_2O_2. Cependant, uniquement les mutants *ryfA* dérivés des souches CFT073 et CH138 étaient sensibles au stress osmotique (Fig. 7.5).

L'enveloppe des bactéries à Gram-négatifs est en contact avec l'environnement extracellulaire, fonctionnant à la fois comme un senseur de conditions externes et comme une barrière physique sélectivement perméable. Ainsi, les voies de réponse au stress de l'enveloppe sont importantes pour les UPEC afin de détecter et de répondre à des agressions environnementales potentiellement mortelles au cours de l'infection. Nos résultats de transcriptomique indiquent qu'une importante quantité de gènes codant pour des protéines impliquées dans la réponse aux différents stress sont sous-exprimés chez le mutant CFT073 Δ*ryfA*. L'inactivation de RyfA mène à la sous-expression des gènes impliqués dans la réponse aux stress de l'enveloppe tels que *psp*, le gène de la chaperon *cpxP,* le facteur transcriptionnel du stress oxydatif *soxS*, les gènes de réponse au choc froid *csp*, *ymcE* et le locus de résistance multiple aux antibiotiques (*mar*). Afin de s'adapter aux changements des conditions environnementales, les bactéries ont développé des mécanismes de résistance comme la production des protéines de choc froid Csp. Ces protéines sont principalement produites pour contrer la baisse soudaine de la température. Cependant, les Csps contribuent à la tolérance au stress osmotique, oxydatif, nutritionnel, au pH et à l'éthanol ainsi qu'à l'invasion des cellules hôtes (Derman *et al.*, 2015; Loepfe *et al.*, 2010; Schmid *et al.*, 2009). Un autre mécanisme de défense contre divers stress environnementaux est la production de protéines de choc thermique. Par exemple, plusieurs gènes régulés par le facteur sigma RpoH tel que, les gènes *ibpAB*, *dnaKJ* et *htpX* sont significativement sous-exprimés chez le mutant *ryfA*. Ces gènes sont connus pour être induits chez la souche CFT073 face à un stress osmotique (urée) ou un stress de sel (NaCl) (Withman *et al.*, 2013). Également, certains gènes codant pour des protéines de l'enveloppe précédemment associés à la résistance aux stress osmotique et de sel (*proW* et *proV*) sont négativement régulés chez le mutant *ryfA*. Ainsi, la sous-expression des gènes codant pour des chaperons, suggère une diminution des processus cellulaires et du repliement protéique, ce qui peut altérer l'aptitude des bactéries à répondre à divers stress. Bien que les régulateurs impliqués dans l'établissement de la réponse générale au stress (*rpoS*), et la réponse au stress oxydatif (*oxyR* et *oxyS*) et les gènes de la catalase *katE* et de la superoxyde dismutase *sodC* ne soient pas différentiellement exprimés. Cependant, cela n'exclut pas la possibilité qu'ils soient affectés au niveau post-transcriptionnel.

Il est évident que l'inactivation de *ryfA* réprime une multitude de gènes impliqués dans la réponse au stress menant à une sensibilité du mutant face aux stress osmotique et oxydatif. Ceci n'exclut pas la possibilité qu'en absence de *ryfA* les bactéries s'adaptent moins rapidement aux changements environnementaux. Cette adaptation implique deux étapes : une phase transitoire (réponse au choc) qui consiste en des réponses rapides nécessaires pour initier l'adaptation aux nouvelles conditions, et une phase continue (réponse au stress) qui se compose de réponses

nécessaires pour soutenir une croissance exponentielle, dans un environnement modifié. Il est possible que les deux phases soient fortement affectées chez un mutant *ryfA*.

8.3.1 RyfA est important pour la production des fimbriae de type 1 et la virulence des souches ExPEC

Selon les résultats présentés ci-haut, l'inactivation de *ryfA* mène à une atténuation de la virulence de la souche UPEC CFT073 dans la vessie et dans les reins dans le modèle murin d'ITU. L'atténuation de la virulence du mutant *ryfA* dans la vessie pourrait être d'une part due à une répression des fimbriae de type 1 et d'autre part à une sensibilité au stress. Les souches UPEC sont soumises à un stress environnemental périodique due à l'urine. La sous-expression des fimbriae de type 1 diminue la capacité du mutant à envahir les cellules urothéliales. De manière intéressante nous avons constaté que la sous-expression des fimbriae de type 1 pourrait être liée à une augmentation de l'expression des régulateurs *fimE* et une sous-expression de *ipbA in vivo*, ainsi qu'à une sous-expression de *fimB* et *ipbA in vitro* dans l'urine humaine (Fig. 7.3). Également, nous avons constaté une sous-expression des gènes *pstSC.* L'inactivation du système Pst de la souche UPEC CFT073 atténue la virulence et réprime les fimbriae de type 1 (Crepin *et al.*, 2012).

Il est possible que la présence de l'urée dans la vessie soit un signal pour la bactérie afin d'initier l'infection et exprimer les facteurs de colonisation. Parmi ceux-ci, les fimbriae de type 1 qui sont utilisées par les UPEC pour se fixer à l'épithélium de la vessie. Ainsi, l'expression des fimbriae de type 1 est induite en présence d'urée. Cette induction est concomitante avec une induction des gènes de réponse aux stress osmotique (Frick-Cheng *et al.*, 2020; Withman *et al.*, 2013). Cependant, l'inactivation de *ryfA* réprime les fimbriae de type 1 et les gènes de réponse au stress. Il est possible que le mutant *ryfA*, subissant un stress dans les voies urinaires de souris due à la présence d'urée, ne parvienne pas à détecter ou à répondre au stress ce qui pourrait entraîner une modulation de la membrane menant à la répression des fimbriae de type 1 et par conséquent à une diminution de la survie du mutant.

Parmi les gènes fortement sous-exprimés chez le mutant *ryfA*, nous retrouvons les gènes codant les petites protéines *ibpA* et *ibpB*. Ces chaperons de choc thermique se lient aux protéines agrégées et aux corps d'inclusion dans les cellules. La transcription de ces gènes est induite lors de la formation de biofilm (Ren *et al.*, 2004), ce qui pourrait indiquer leur rôle plus général dans la gestion de différentes conditions environnementales. De plus, plusieurs études ont démontré que *ibpB* est fortement exprimé durant les ITU à la fois chez l'humain et chez la souris (Frick-Cheng *et al.*, 2020; Haugen *et al.*, 2007). Ainsi, le gène *ibpB* s'est également révélé fortement

exprimé chez CFT073 isolée à partir d'urine de souris et chez les souches responsables de la bactériurie asymptomatique durant la croissance en urine humaine (Hancock & Klemm, 2007; Haugen *et al.*, 2007; Vejborg *et al.*, 2012).

Par analyse des résultats des autres groupes de recherches, il semble que les gènes *fim* sont exprimés conjointement avec le gène *ibpB* (Frick-Cheng *et al.*, 2020; Haugen *et al.*, 2007; Ren *et al.*, 2004; Vejborg *et al.*, 2012). Cela signifie possiblement que *ibpB* soit impliqué dans la régulation de l'expression des fimbriae de type 1 chez le mutant *ryfA*. Selon ces observations, nous avons donc émis l'hypothèse d'un possible lien entre l'expression des fimbriae de type 1 et *ryfA* via *ibpB*. Ainsi, nous avons constaté que *ibpA* et *ibpB* sont fortement sous-exprimés dans la vessie 48 h p.i chez le mutant *ryfA* (Fig. 7.4). À cet effet, nous suggérons que la sous-expression *in vitro et in vivo* des fimbriae de type 1 pourrait être causée par la sous-expression de *ibpB*.

L'accumulation des protéines mal repliées et endommagées dans l'enveloppe entraîne la formation d'agrégat qui peut mener à la mort de la bactérie, dans le cas où elles ne sont pas dégradées par des protéases ou réparées par des chaperons. Il est donc important que la bactérie puisse détecter les dommages au niveau du protéome de l'enveloppe et induire une réponse adaptée afin de rétablir le défaut de repliement. De nombreuses protéines sont impliquées dans le repliement des polypeptides dans le cytoplasme, par exemple DnaK, DnaJ, GrpE, GroEL et GroES (Gething & Sambrook, 1992; Wülfing & Plückthun, 1994), mais aucune de ces chaperons n'est connue pour être importante pour la voie générale de repliement dans le périplasme et qui intervienne dans la biogenèse et l'assemblage des fimbriae. Il a été suggéré que DnaK contrôle l'homéostasie de la biogenèse de curli (Sugimoto *et al.*, 2018). En effet, DnaK régule la quantité et la qualité de RpoS pour assurer l'expression des gènes *csg* responsables de la production de curli. DnaK s'est avérée également nécessaire pour le repliement du régulateur transcriptionnel CsgD, ce qui conduit à l'expression des composants structurels du curli, CsgA et CsgB (Sugimoto *et al.,* 2018). L'inactivation de *ryfA* réprime les gènes codants DnaK, DnaJ, GrpE, GroEL et GroES. Ces derniers peuvent possiblement affecter la production des fimbriae de type 1. Par exemple, dans notre banque de transposons, nous avons trouvé une insertion au niveau de *dnaJ* qui a mené à la diminution de la production des fimbriae de type 1 suggérant que l'inactivation de DnaJ affecte la production des fimbriae de type 1. Cependant, il n'est pas encore clair comment ces chaperons pourrait affecter l'assemblage des fimbriae. Il serait intéressant de générer des mutants dans les différents gènes codant les chaperons afin de vérifier si leur inactivation affecte la production des fimbriae de type 1.

8.3.2 La régulation croisée entre les fimbriae et la transition entre motilité et adhérence chez les UPEC

L'adhérence médiée par les fimbriae est une étape cruciale pour la colonisation des tissus de l'hôte. Ces fimbriae sont régulés par les variations environnementales, mais ils sont également soumis à une régulation croisée. En effet, les UPEC possèdent plusieurs opérons fimbriaires qui sont produits dans différentes conditions. Par exemple, la souche pyélonéphrite CFT073 code pour 12 adhésines fimbriaires et afimbriaires (Welch *et al.*, 2002). Plusieurs études ont démontré qu'il existe une régulation croisée entre les différents fimbriae chez les souches UPEC afin de n'exprimer qu'un type de fimbriae à la fois (Nowicki *et al.*, 1984; Xia *et al.*, 2000a). Les gènes codés dans les opérons fimbriaires P (*papB*) (Holden *et al.*, 2001), S (*sfaB*) (Lindberg *et al.*, 2008) et F1C (*focB*) (Xia *et al.*, 2000a) codent pour des produits qui répriment la transcription et l'expression ultérieure des fimbriae de type 1.

 Dans le présent travail, nous avons observé que l'inactivation de *ryfA* réprime les fimbriae de type 1, P et F9. Cependant nous constatons une induction de l'expression des fimbriae F1C *in vitro*. L'analyse du transcriptome du mutant *ryfA* en phase exponentielle de croissance démontre une sous-expression des deux copies de *papC,* codant pour la protéine placier, des fimbriae P et plusieurs gènes de l'opéron fimbriaire F9 ainsi qu'une surexpression de *focA* codant la sous unité majeure des fimbriae F1C. Même si les fimbriae de type 1 sont réprimés, nous avons démontré que le mutant *ryfA* est capable d'adhérer aux cellules épithéliales de la vessie via les fimbriae F1C *in vitro*. Ces résultats démontrent qu'il existe une régulation croisée entre les différents fimbriae. Ainsi, ces résultats sont en concordance avec les travaux de Snyder *et al.* (2005) qui démontrent que la suppression des opérons *fim* et *pap* a induit la production de fimbriae F1C et que l'expression des gènes *fim* est corrélée à une diminution de l'expression de *pap* chez la souche CFT073. La délétion du système Pst chez la souche CFT073 s'accompagne d'une sous-expression des fimbriae de type 1 et d'une surexpression des fimbriae F1C (Crepin *et al.*, 2012).

PapX et FocX faisant partie des opérons *pap* et *foc* respectivement, sont deux régulateurs des fimbriae 1, P et F1C. Le gène *papX* est transcrit avec l'opéron *pap*, indiquant que PapX serait synthétisé dans des conditions favorables à l'expression de fimbriae P et que leur expression est positivement corrélée (Simms & Mobley, 2008b). Par exemple, la surexpression de *papX* réprimerait l'expression des fimbriae de type 1 et F1C (Simms & Mobley, 2008b). Cependant, FocX fonctionne comme un répresseur de *papX* (Luterbach & Mobley, 2018). Étant donné que les fimbriae de type 1 et P sont réprimés chez le mutant *ryfA*, ceci suggère que possiblement PapX soit réprimé chez le mutant *ryfA* et que FocX soit induit et agisse comme répresseur des

fimbriae de type 1 et P et comme régulateur positif des fimbriae F1C. Étant donné que les fimbriae F1C permettent, notamment, l'adhésion au niveau des cellules endothéliales de la vessie (Khan *et al.*, 2000; Mulvey, 2002), la sous-expression de ces derniers, causée par l'inhibition de ses répresseurs, peut être un effet compensatoire de la perte des fimbriae de type 1. L'expression des fimbriae peut être influencée par de nombreuses conditions environnementales. De plus, les mécanismes responsables de la sous-expression des gènes *fim* et *pap* en réponse à l'expression de F1C ne sont pas encore connus.

Par analyse des résultats transcriptomique, nous n'avons pas observé de différence significative dans l'expression de *papX* et *focX* en milieu LB en phase exponentielle de croissance (D.O. 0.6). Ceci n'exclut pas la possibilité qu'ils soient affectés au niveau post-transcriptionnel ou chez le mutant *ryfA* en interaction avec les cellules de la vessie *in vivo* et *in vitro.*

L'adhérence et la motilité sont essentielles pour la colonisation des voies urinaires. Les souches UPEC dépendent des flagelles et des fimbriae pour réussir à remonter et à coloniser les diverses niches dans les voies urinaires (Lane & Mobley, 2007; Schwan, 2008a; Wright *et al.*, 2005). Cependant, les mécanismes impliqués dans la coordination de la transition entre adhérence et motilité ne sont pas bien caractérisés. Pour les bactéries, il n'est pas pratique d'être à la fois mobile et adhérente simultanément. Par exemple, il ne serait pas avantageux pour un organisme exprimant les fimbriae et attaché à une surface de tenter de nager soudainement. Ainsi, les isolats UPEC possèdent probablement des mécanismes qui assurent une transition rapide entre les états adhérent et mobile en réponse aux signaux environnementaux lors d'une ITU. Des études ont mis en évidence la régulation réciproque de la motilité et de l'adhérence médiée par les fimbriae chez les bactéries pathogènes. Par exemple, une surexpression de *fimZ*, codée par l'opéron *fim* chez *S.* Typhimurium, conduit à une surexpression des fimbriae de type 1 et par conséquent une répression de la motilité (Clegg & Hughes, 2002). Ainsi, l'induction du système de régulation à deux composants BvgAS chez *Bordetella* induit l'expression de facteurs d'adhérence nécessaires à la colonisation, tout en réprimant la synthèse du flagelle (Akerley *et al.*, 1995). Il est évident qu'une forte expression de fimbriae par un organisme nageur pourrait altérer la motilité.

Lors de cette thèse, un phénotype d'hypermotilité chez les mutants *ryfA* des isolats UPEC CFT073, 536 et l'APEC CH138 a été constaté. Ainsi, les données transcriptomiques démontrent une induction des gènes sous le contrôle du facteur σ^{28}, responsable de l'initiation de la transcription des gènes impliqués dans la motilité et la synthèse des flagelles, tels que *flgCBGD*, *fliC* et *cheW* chez la souche CFT073. On peut émettre l'hypothèse que l'inactivation de RyfA

mène à la sous-expression des fimbriae de type 1, P et F9 et par conséquent l'augmentation de l'expression des gènes flagellaires qui se traduit par un phénotype d'hypermotilité. Plusieurs travaux témoignent de la régulation croisée entre les fimbriae et les flagelles chez les souches UPEC. Ainsi, l'expression des fimbriae de type 1 est probablement coordonnée *in vivo* avec la sous-expression des gènes flagellaires. Par exemple, la production des fimbriae P est coordonnée avec la répression de la motilité (Luterbach & Mobley, 2018). Dans notre étude, la sous-expression des fimbriae P est en concordance avec le phénotype d'hypermotilité observé chez le mutant *ryfA*. De plus, l'expression constitutive des fimbriae de type 1 (*fim* L-ON) mène à la répression de la motilité chez la souche CFT073 via PapX (Simms & Mobley, 2008b). La surexpression de PapX et FocX réprime la motilité (Luterbach & Mobley, 2018). En effet, PapX inhibe la motilité en réprimant l'expression de *flhDC*, ce qui entraîne une répression des gènes flagellaires (Simms & Mobley, 2008b). Cependant, il semble que l'inactivation de PapX ou de FocX ait des effets différents sur la motilité. Contrairement à FocX, la perte de PapX entraîne un phénotype de hypermotilité (Luterbach & Mobley, 2018). Ces observations suggèrent qu'il soit possible que *papX* soit sous-exprimé chez le mutant *ryfA*, menant à la fois à une sous-expression des fimbriae P et une surexpression de *flhDC* conduisant à une induction de l'expression des flagelles.

Contrairement à nos résultats, Shivaji *et al.* (2019) ont démontré que l'inactivation de RyfA chez la souche *E. coli* L-1216/2010 isolée d'une infection oculaire réprime la motilité. Cette différence observée de l'effet de la perte de RyfA sur la motilité pourrait avoir plusieurs explications. En effet, la nature de la souche étudiée étant différente peut impacter la régulation des fimbriae, qui est en partie influencée par la diversité des types de fimbriae codés et des régulateurs présents chez les souches étudiées. Les flagelles sont un facteur de virulence important chez les souches UPEC afin de se déplacer de la vessie aux reins et donc, ils sont finement régulés. Ainsi, notre test de motilité a été réalisé à partir de culture en phase exponentielle de croissance à 37°C sur un milieu contenant 0.25% agar. Cependant, chez la souche *E. coli* L-1216/2010, le test de motilité a été effectué à partir de culture poussée sur la nuit inoculée sur un milieu contenant 0.3 % agar à 30°C. La température et la phase de croissance peuvent grandement affecter les résultats. Ces observations indiquent que les fimbriae de type 1, P et F1C, ainsi que la motilité, peuvent être réguler d'une manière coordonnée par des mécanismes transcriptionnels et post-transcriptionnels encore inconnus.

8.3.3 Rôle de RyfA dans la survie intra-macrophage

Après avoir franchi les barrières cellulaires épithéliales, les UPEC envahissantes atteignent la muqueuse de la vessie et rencontrent des macrophages et des neutrophiles, des cellules phagocytaires qui absorbent et détruisent activement les pathogènes. Les UPEC peuvent induire une forte réponse inflammatoire. Alors que les neutrophiles jouent un rôle essentiel dans l'élimination des UPEC (Abraham & Miao, 2015), le rôle des macrophages dans l'infection par les UPEC est encore flou. De plus, les macrophages représentent près de 40% de toutes les cellules CD45^{+} dans le compartiment des cellules immunitaires de la vessie des souris (Mora-Bau *et al.,* 2015). Par conséquent, ils contribuent à la réponse immunitaire de l'hôte aux infections urinaires de plusieurs manières. La présence de phagocytes et de cellules présentatrices d'antigène dans la vessie suggère que ces cellules jouent un rôle important dans la surveillance immunitaire au niveau local.

Nos données démontrent que le mutant *ryfA* est plus atténué en mono-infection qu'en co-infection dans le modèle murin d'ITU. L'atténuation du mutant *ryfA* pourrait être expliquée en partie par le fait que les bactéries soient rapidement éliminées par le système immunitaire. Il est possible que durant les mono-infections, la réponse immunitaire innée ait été accentuée en raison de la présence de flagelline. Cette dernière est reconnue par le récepteur de l'hôte TLR5 qui peut déclencher une réponse immunitaire innée robuste ciblant les bactéries envahissantes (Yoon *et al.,* 2012). De plus, les bactéries flagellées sont plus susceptibles d'être phagocytées par les cellules immunitaires de l'hôte et ainsi rapidement éliminées au cours de l'infection (Kakkanat et al., 2015). Cette induction accrue de la réponse immunitaire innée pourrait diminuer la survie et la virulence du mutant *ryfA* durant les mono-infections et pourrait expliquer son atténuation sévère après 48 h p.i. dans la vessie et les reins. Cependant, nos résultats avec les macrophages démontrent qu'il n'y avait pas de différence dans l'internalisation du mutant *ryfA* et de la souche sauvage. En revanche, le mutant *ryfA* est rapidement éliminé par les macrophages puisque le mutant induit une production accrue des ROS. Par ailleurs, ces résultats démontrent que les valeurs *in vitro* caractérisent l'internalisation et la survie des bactéries dans les macrophages ce qui peut servir d'indicateur de sensibilité du mutant, mais ne sont certainement pas un reflet parfait de l'atténuation du mutant *ryfA* pendant l'infection du tractus urinaire. De plus, durant les co-infections, il est possible que le mutant tire profit de la présence de la souche sauvage. Il est connu que la population de macrophages Ly6C^{−} résidants dans la vessie joue un rôle essentiel dans la médiation du recrutement des neutrophiles et des macrophages Ly6C^{+} circulants vers la vessie infectée (Schiwon *et al.*, 2014). Une fois recrutés au site d'infection, les macrophages

Ly6C[+] produisent la cytokine TNFα, qui à son tour provoque la sécrétion de CXCL2 par les macrophages Ly6C^{-}. Cette chimiokine active les neutrophiles, permettant leur entrée dans l'uroépithélium pour lutter contre les bactéries. Cependant, certaines souches UPEC peuvent atténuer la fonction et la migration des neutrophiles (Loughman & Hunstad, 2011). Les souches UPEC, telles que CFT073, peuvent déclencher la mort rapide des macrophages (Murthy *et al.*, 2018), qui peut être un mécanisme qui désactive le recrutement des neutrophiles. Par conséquent, il est possible que la présence de CFT073 aide le mutant *ryfA* à résister plus aux cellules immunitaires en causant la mort cellulaire des macrophages et des neutrophiles. Il est possible également que le mutant *ryfA* induise plus fortement les macrophages et par conséquent le recrutement des neutrophiles, menant ainsi à l'élimination subséquente du mutant.

La résistance aux ROS est sans doute un facteur déterminant pour la pathogenèse des UPEC. Les travaux de Haraoka *et al.* (1999) ont démontré que les neutrophiles jouent un rôle critique dans l'élimination des UPEC pendant l'infection. En effet, les neutrophiles produisent de nombreux facteurs antimicrobiens comme les ROS. Ces derniers proviennent du superoxyde (O_2^-), qui est produit par la phagocyte oxydase, un complexe enzymatique exprimé par les cellules phagocytaires (Babior, 2000). Les *E. coli* sont capables de faire face au stress oxydatif par divers mécanismes (Rama *et al.*, 2005), afin de contrecarrer les ROS qui ont des effets pléiotropes sur les cellules bactériennes, où ils réagissent avec les thiols, les lipides et les acides nucléiques (Fang, 2004). L'atténuation du mutant *ryfA* dans le modèle murin d'ITU pourrait être expliquée par le fait que le mutant est plus sensible à l'effet sévère des ROS. En effet, les travaux de Hryckowian and Welch (2013) ont démontré que les niveaux de peroxyde sont élevés dans l'urine de souris infectées par CFT073 après 48 h p.i. Ces résultats suggèrent que le stress oxydatif est généré par l'hôte en réponse à l'infection par les UPEC et que le mutant *ryfA* n'est pas capable de résister face à ce stress *in vivo*.

Il est à noter que le mutant *ryfA* de la souche UPEC CFT073 était capable de croître aussi bien que la souche sauvage en milieu riche (LB) et en urine humaine. Ainsi, aucune différence n'a été observée entre le mutant et la souche parentale en coculture dans les mêmes milieux. Ceci indique que l'atténuation de la virulence du mutant *ryfA* en mono et en co-infection n'est pas due à un défaut de croissance du mutant.

L'atténuation sévère du mutant *ryfA* en mono-infection pourrait être due à un défaut d'adhérence. En effet, nous avons observé une sous-expression des fimbriae de type 1 et une induction des flagelles. Ces derniers sont exprimés lors de l'ascension de l'urètre à la vessie dans le modèle murin d'ITU, en atteignant la vessie, l'expression des gènes flagellaires est rapidement réprimée

(Lane *et al.*, 2007a). À ce stade, l'expression des fimbriae de type 1 est probablement coordonnée *in vivo* avec la régulation négative des gènes flagellaires. Étant donné que le mutant *ryfA* est hypermotile, il est possible qu'il soit rapidement éliminé par le flux d'urine. La miction accrue est un mécanisme de défense efficace de l'hôte pour évacuer les bactéries des voies urinaires. Les fimbriae permettent l'adhérence des UPEC aux cellules urothéliales et améliorent la résistance aux forces de cisaillement produites par la miction (Thomas *et al.*, 2002). Ainsi, le moment précis de la régulation entre l'adhérence et la motilité contribue probablement à la pathogenèse de l'UPEC. L'ensemble de ces résultats suggère qu'une dérégulation dans la coordination de l'expression des fimbriae et des flagelles pourrait être fatale pour la bactérie.

8.3.4   RyfA est important pour la virulence des souches APEC

Nous avons démontré que l'inactivation de RyfA chez la souche APEC virulente CH138 atténue sévèrement la virulence chez le poulet (Fig. 7.7). Ceci confirme l'importance de RyfA pour la virulence des souches ExPEC. Ainsi, lors d'une co-infection, le mutant *ryfA* de la souche CH138 survit nettement moins que la souche sauvage dans le modèle septicémique aviaire (Fig. 7.8), suggérant que le mutant *ryfA* ait des difficultés à survivre *in vivo*. La réintroduction de l'allèle codant pour RyfA en simple copie a démontré un rétablissement complet de la virulence du mutant. L'atténuation du mutant *ryfA* de la souche CH138 pourrait être due en partie à la réduction sévère de la production des fimbriae de type 1 dans cette souche (Fig. 7.6A). Des isolats pathogènes d'*E. coli* exprimant des fimbriae de type 1 adhèrent aux cellules épithéliales respiratoires de poulet *in vitro* (Dho & Lafont, 1984; Gyimah & Panigrahy, 1988). Ainsi, les fimbriae de type 1 sont préférentiellement exprimés *in vivo* par la souche virulente aviaire χ7122, dans les sacs aériens et les poumons, site d'infection primaire de cette souche, chez les poulets infectés par la voie intratrachéale (Dozois *et al.*, 1994; Pourbakhsh *et al.*, 1997). D'autre part, les fimbriae de type 1 sont peut-être moins importants dans le modèle septicémique aviaire comparé au modèle murin d'ITU.

La présence d'*E. coli* dans la circulation sanguine peut entraîner une réponse inflammatoire puissante de l'hôte entraînant une septicémie. Les bactéries présentes dans la circulation sanguine doivent résister aux mécanismes de défense de l'hôte, y compris la phagocytose, le système du complément et les peptides antimicrobiens. Nous avons constaté que l'inactivation de RyfA diminue la survie du mutant dans le sang de poulet à 6, 24 et 48 h et par conséquent l'atténuation subséquente du mutant (Fig.7.7 et 7.8). L'atténuation pourrait être due à une sensibilité accrue du mutant *ryfA* au complément présent dans le sérum. Ce dernier contient plus de trente protéines du système du complément, un élément crucial de la réponse immunitaire

innée qui peut également initier la réponse adaptative (Sarma & Ward, 2011). La position du complément sur la surface bactérienne active la cascade du complément et conduit à la formation du complexe d'attaque membranaire (MAC). Ce complexe se fixe à la surface cellulaire et forme un pore dans les membranes des bactéries sensibles, conduisant ainsi à la mort cellulaire par lyse osmotique (Miajlovic & Smith, 2014; Sarma & Ward, 2011). En effet, nous avons constaté que le mutant *ryfA* de la souche APEC CH138 est plus sensible à la fois au sérum humain et de poulet (Fig. 7.9). Les mécanismes de résistance au sérum utilisés par *E. coli* comprennent la production de capsule polysaccharidique protectrice et l'expression de facteurs qui inhibent ou interfèrent avec la cascade du complément (Burns & Hull, 1998). Le LPS altère ainsi l'efficacité de la formation du CAM en influençant l'accessibilité du complément à la membrane bactérienne (Burns & Hull, 1998).

En réponse à l'activité bactéricide du sérum, les bactéries répriment l'expression des porines de la membrane externe telle que : OmpC, OmpF, OmpN, et NmpC (Miajlovic *et al.*, 2014). La répression de l'expression des porines peut servir de moyen d'échappement au complément. Ainsi, le gène *cadB*, qui code pour un antiporteur cadavérine-lysine, est l'un des gènes les plus réprimés chez la souche CFT073 en présence de sérum (Miajlovic *et al.*, 2014). Nous avons constaté que l'inactivation de *ryfA* chez la souche CFT073 mène à une surexpression des gènes codant les porines NmpC et OmpC ainsi que le gène *cadB*. De plus, la délétion de *ryfA* chez CFT073 mène à une sensibilité au sérum (Fig. 7.9A). Ceci suggère possiblement que le mutant *ryfA* de la souche APEC CH138 soit affecté comme la souche CFT073. Pour croître et survivre dans le sérum, les ExPEC doivent modifier l'expression des facteurs de protection qui favorisent la survie dans un environnement hostile. Il est possible que la sensibilité du mutant *ryfA* de la souche CH138 au stress oxydatif soit en partie responsable de l'atténuation du mutant *in vivo*.

9   CONCLUSION

L'objectif principal de ce projet de thèse était d'identifier des nouveaux régulateurs des fimbriae de type 1 et de caractériser les mécanismes moléculaires reliant ces facteurs, les fimbriae de type 1 et la virulence. Nous avons identifié plusieurs régulateurs qui, lorsqu'ils sont inactivés, pourraient affecter la production des fimbriae de type 1.

J'ai montré que *yqhG*, codant pour une protéine de fonction inconnue, est l'un des médiateurs importants contribuant à une diminution de l'expression des fimbriae de type 1 chez la souche CFT073. Les résultats démontrent que la délétion de *yqhG* altère l'expression des fimbriae de type 1 et diminue significativement la capacité du mutant *yqhG* à coloniser le tractus urinaire murin. J'ai également démontré que le mutant *yqhG* est plus sensible au stress oxydatif. La sous-expression des fimbriae de type 1 chez le mutant *yqhG* pourrait être liée à une augmentation de la sensibilité aux stress environnementaux qui pourrait être rencontrée au cours de l'infection de l'hôte et conduire à des modifications de la surface cellulaire.

Nous avons également caractérisé le rôle du sRNA RyfA dans la virulence des souches ExPEC et son influence sur l'expression des gènes. Nous avons utilisé une combinaison d'approches multidisciplinaires, notamment la biologie moléculaire, les tests phénotypiques et les modèles animaux, pour examiner le rôle potentiel de RyfA dans la virulence et la physiologie des souches ExPEC ainsi que son importance pour l'adhérence et la motilité. Les travaux de cette thèse représentent une première caractérisation approfondie du rôle du RyfA chez les souches ExPEC. Nous avons démontré que RyfA est exprimé en phase logarithmique de croissance et atteint la production maximale à la fin de la phase exponentielle de croissance. L'inactivation de RyfA mène à l'atténuation de la virulence de la souche UPEC CFT073 et de la souche APEC CH138 dans le modèle d'ITU murin et septicémique aviaire, respectivement. Nous avons entrepris une étude transcriptomique comparative globale entre la souche UPEC CFT073 et son mutant isogénique *ryfA* en phase exponentielle de croissance. Globalement, chez le mutant *ryfA*, les gènes

impliqués dans la réponse aux différents stress (réponse générale, choc thermique, choc froid, oxydatif et acide), le métabolisme énergétique, l'adhésion bactérienne (fimbriae type 1, P, F9 et F1C), la motilité et la formation de biofilm sont modulés. Ces résultats montrent que l'inactivation de RyfA a un effet pléiotrope menant à des conséquences néfastes pour les bactéries. À cet effet, l'atténuation sévère de virulence des souches UPEC est principalement due à une sensibilité accrue aux stress osmotique et oxydatif et à la sous-expression des fimbriae de type 1 et P. Ainsi, l'atténuation du mutant *ryfA* de la souche APEC CH138 dans le modèle septicémique aviaire est principalement due à une sensibilité accrue au stress et au sérum. De plus, nos résultats démontrent que RyfA joue un rôle clé dans la survie intra-macrophage.

Les souches UPEC peuvent coder pour 15 systèmes distincts codants des fimbriaires différents. Cependant, les conditions dans lesquelles s'expriment de nombreux autres fimbriae restent méconnues. Ainsi, pourquoi les UPEC codent pour autant de fimbriae est une question intéressante à laquelle il n'y a actuellement pas de réponse. Notre travail a confirmé encore une fois qu'il existe une régulation croisée entre les différents fimbriae. Nous avons élucidé que la sous-expression des fimbriae de type 1 et P soit concomitante avec la surexpression des fimbriae F1C. Nos travaux, comme ceux d'autres groupes suggèrent que l'adhérence et la motilité sont corégulées chez les ExPEC. Par exemple la mutation de *ryfA* diminue la production des fimbriae de type 1 et P et par conséquent les souches deviennent hypermotile.

Selon les résultats présentés ci-haut, il convient de conclure que l'inactivation de *ryfA* pourrait atténuer les souches d'*E. coli* pathogènes en modifiant les voies de régulation menant à des changements du métabolisme et à une diminution de l'adaptation aux stress environnementaux ou peut potentiellement générer une réponse modifiée au stress associé à la membrane, conduisant à la répression de production de structures de surface, y compris les adhésines nécessaires à la colonisation des tissus de l'hôte. Par conséquent, RyfA agit à titre de régulateur global de la réponse au stress et la virulence chez les ExPEC.

En conclusion, ce projet de thèse a contribué à l'avancement de nos connaissances concernant la régulation des fimbriae de type 1 et d'élucider le rôle de YqhG et RyfA dans la pathogenèse des souches ExPEC. Nos données suggèrent que ces deux facteurs sont impliqués dans la résistance au stress chez les UPEC et que le stress influence l'expression des fimbriae de type 1, atténuant ainsi la virulence des souches UPEC. Comprendre le lien entre ces régulateurs et le lien entre les réponses au stress et l'expression des fimbriae de type 1 permettra de mieux élucider les signaux qui contrôlent la production de fimbriae de type 1 et la virulence des UPEC. Ces gènes pourraient être considérés comme des cibles potentielles pour les futures thérapies

contre les infections urinaires, car leur perturbation pourrait inhiber la virulence et la survie des souches UPEC dans le tractus urinaire et ainsi réduire la survenue de cette infection très répandue.

10   PERSPECTIVES

Dans ce projet, j'ai démontré que *ryfA* fait partie d'un réseau complexe de régulation de gènes et que ce sRNA affecte plusieurs traits de virulences. Mes travaux ne lèvent le voile que sur quelques fonctions de RyfA. Continuer dans cette voie d'étude nous permettrait d'en apprendre beaucoup sur la physiologie des UPEC et la façon par laquelle les bactéries peuvent détecter et répondre aux stimuli environnementaux. Les résultats de ce travail offrent un apport considérable sur les connaissances concernant le rôle de RyfA dans la virulence des souches ExPEC et représentent une caractérisation plus approfondie des fonctions de RyfA. Plusieurs expériences seraient intéressantes afin de continuer l'étude de ce régulateur et de mettre en pratique les informations découlant des travaux de cette thèse. Nous avons démontré que l'inactivation de RyfA réprime plusieurs gènes de réponses aux divers stress et des gènes codant pour plusieurs fimbriae chez CFT073, 536 et CH138. Il serait intéressant de déterminer l'implication de RyfA dans la régulation des gènes de réponse aux stress chez les différentes souches ExPEC. Il serait également judicieux d'étudier l'implication de RyfA dans la réponse au stress chez *Salmonella* Typhi et *Salmonella* Typhimurium afin d'élucider si RyfA est un régulateur global de réponse aux stress chez les *Enterobacteriaceae*.

Ainsi, dans les études futures, l'utilisation d'un rapporteur transcriptionnel sous le contrôle du promoteur de *ryfA* pourrait être utile pour déterminer le niveau d'expression pendant l'infection à l'intérieur de l'hôte. Cela pourrait être fait initialement chez un modèle d'infection murin avec les souches UPEC et plus tard étendu chez le poisson zèbre avec les souches APEC en utilisant l'imagerie biophotonique. Cela permettra de construire une image plus complète sur la régulation de RyfA *in vivo*. Nos résultats préliminaires démontrent que le mutant *ryfA* de la souche *S.* Typhimurium LT2 survit moins dans les macrophages murin RAW264.7. Il serait important d'investiguer davantage l'implication de ce sRNA dans la virulence de *S.* Typhimurium à différents niveaux de l'infection chez les souris afin de corroborer les résultats obtenus chez les

macrophages. Ainsi, il serait primordial d'investiguer la capacité du mutant *ryfA* de la souche CH138 à survivre dans les macrophages primaires et la lignée de macrophage de poulet. Ensuite, il sera intéressant d'élucider si l'inactivation de RyfA chez les souches ExPEC et de *Salmonella* impacte la réponse immunitaire de l'hôte comme l'expression des cytokines et chimiokines.

Il serait également important d'identifier les cibles de RyfA par des outils en ligne comme TargetRNA ou CopraRNA et également via la surexpression de ce sRNA suivi d'un séquençage d'ARN. Une autre approche pour caractériser les cibles de RyfA est la technique de capture de transcrits ou la technologie MAPS (MS2-affinity purification coupled with RNA sequencing). Cette technique consiste à utiliser la purification par chromatographie d'affinité MS2 couplée à un séquençage à haut débit (séquençage d'ARN). Nous pouvons appliquer la technique pour trouver les cibles de RyfA chez CFT073 et chez *S.* Typhimurium. Cette technique pourrait être également utilisé lors d'interaction des bactéries avec les macrophages, permettant ainsi d'identifier les cibles de RyfA durant la survie intra-macrophages. Cette méthode nous permettra d'identifier les ARN cibles interagissant avec RyfA, quel que soit le type de régulation (positive ou négative), le type de cibles (ARNm, ARNt, sARN) ou leur abondance. Il serait également important de valider les ARNm cibles putatifs identifiés par MAPS à l'aide de différentes méthodes. Par exemple, utiliser une fusion LacZ avec des cellules exprimant ou non RyfA. L'élucidation des cibles régulées par RyfA peut aider à comprendre comment ce sARN affecte la pathogenèse des souches ExPEC.

Le mutant *ryfA* est sévèrement atténué dans le modèle murin d'ITU et cette atténuation est possiblement due à une sensibilité accrue aux ROS. La principale source de ROS durant l'infection est fournie par la phagocyte oxydase. Afin d'évaluer la contribution du phagocyte oxydase au défaut de colonisation du mutant *ryfA*, il serait important d'infecter des souris dépourvues de la sous-unité p47 du complexe enzymatique la phagocyte oxydase (p47$^{phox\ (-/-)}$). Nous nous attendons à ce que le mutant *ryfA* soit aussi virulent que la souche sauvage.

Parmi les facteurs affectés par RyfA et pouvant affecter l'expression des fimbriae de type 1, nous avons identifié que le gène *agaS*, codant pour une isomérase (deaminase), est sous-exprimé chez le mutant *ryfA*. Le produit du gène *agaS* est important pour l'utilisation des aminosucres le N-acetyl-D-galactosamine et le D- galactosamine. Nos travaux en cours, démontrent que l'inactivation de *agaS* chez la souche CFT073 et UTI89 réprime l'expression des fimbriae de type 1.

Étant donné que la sous-expression d'*ibpB* pourrait diminuer l'expression des fimbriae de type 1, il serait intéressant d'induire l'expression de *ibpB*, chez le mutant *ryfA* et de quantifier l'expression

des fimbriae de type 1. Il serait aussi intéressant de déterminer l'effet de IbpB sur l'expression / activité des différentes recombinases FimB, FimE, IpuA, IpuB et IpbA et conséquemment, l'effet sur l'expression des fimbriae de type 1. Étant donné que *ryfA* soit exprimé en phase exponentielle de croissance, il serait judicieux de mesurer l'activité du promoteur d'*ibpB* en utilisant une fusion transcriptionnelle du promoteur fusionné à *lux* en présence et en absence de *ryfA*. Ainsi pour caractériser au mieux l'effet de *ipbB*, il serait également possible de mesurer l'activité du promoteur dans différentes conditions (LB et en urine) et en condition de stress osmotique et de sel et de quantifier en parallèle la production des fimbriae de type 1.

Il serait primordial de quantifier l'expression différentielle des gènes *papX* et *focX* dans différentes conditions chez la souche CFT073 et le mutant *ryfA in vitro* et dans la vessie 48 h p.i afin d'expliquer la sous-expression des fimbriae de type 1 et P ainsi que la surexpression des fimbriae F1C. Ainsi, il serait important de comparer l'expression de *papX* et *flhDC* chez le mutant *ryfA* en condition de motilité flagellaire.

Nous avons démontré que l'inactivation de RyfA mène à la sous-expression des fimbriae de type 1. Cette sous-expression pourrait être la conséquence de modulation de plusieurs gènes. À cet effet, l'exploration de la banque de transposons nous permettra de décortiquer en détail les mécanismes moléculaires reliant RyfA et l'expression des fimbriae de type 1. Il serait judicieux de générer une banque de mutants par transposition chez le mutant *ryfA* portant une fusion transcriptionnelle *lux* sous le contrôle du promoteur de fimbriae de type 1, *fimS*. Les clones seront criblés pour la production de luminescence et ensuite pour leur capacité à regagner la production des fimbriae de type 1. Étant donné que les fimbriae de type 1 sont réprimés chez cette souche, on suppose que l'inactivation de RyfA induit l'expression d'un (des) facteur (s), qui lui (eux), réprime (nt) l'expression de fimbriae de type 1. Ceci nous permettra d'établir une relation entre RyfA, les gènes qui sembleront affecter l'expression de *fim* et possiblement les gènes impliqués dans la réponse au stress. Ainsi, la délétion de ces gènes aura pour effet d'induire l'expression de fimbriae de type 1. Il serait également intéressant de déterminer à quel niveau RyfA agit sur la régulation des fimbriae de type 1. Est-ce que RyfA agit directement sur la transcription ou la post-transcription de *fimB, fimE* et *ipbA* ou agit-il sur leur activité de recombinase ? S'il s'agit d'une action indirecte, quel est le(s) facteur(s) impliqué dans cette régulation ?

Dans le présent travail, nous avons montré que YqhG, une protéine de fonction inconnue affecte l'expression des fimbriae de type 1. En premier lieu, il serait important de caractériser la structure de YqhG et YqhH et de déterminer leur rôle chez les *E. coli* par des études structurales (cristallographie aux rayons-X) et d'identifier leur localisation cellulaire en

utilisant des fusions GFP. Étant donné que la fonction de ces protéines n'est toujours pas connue, il pourrait être envisageable d'utiliser des MicroArrays (biopuce) de phénotype. Ces MicroArrays sont des plaques de 96 puits préconfigurées contenant différentes classes de composés chimiques conçues pour tester la présence ou l'absence de phénotypes cellulaires spécifiques. Il existe des panels conçus pour vérifier les voies métaboliques ainsi que les effets ioniques, osmotiques et pH, et des panels pour évaluer la sensibilité à divers agents antimicrobiens avec différents mécanismes d'action. De cette manière nous pouvons cribler et mesurer quantitativement des milliers de phénotypes cellulaires à la fois. Le but est de cribler les mutants CFT073 Δ*yqhG* et CFT073 Δ*yqhH* et de les comparer à la souche sauvage pour déterminer les propriétés de sensibilité métabolique et chimique.

11   REFERENCES BIBLIOGRAPHIQUES

Aberg A, Shingler V & Balsalobre C (2006) (p)ppGpp regulates type 1 fimbriation of *Escherichia coli* by modulating the expression of the site-specific recombinase FimB. *Molecular Microbiology* 60(6):1520-1533.

Aberg A, Shingler V & Balsalobre C (2008) Regulation of the *fimB* promoter: a case of differential regulation by ppGpp and DksA *in vivo*. *Molecular microbiology* 67(6):1223-1241.

Abraham JM, Freitag CS, Clements JR & Eisenstein BI (1985a) An invertible element of DNA controls phase variation of type 1 fimbriae of *Escherichia coli*. *Proceedings of the National Academy of Sciences* 82(17):5724-5727.

Abraham SN & Miao Y (2015) The nature of immune responses to urinary tract infections. *Nature Reviews Immunology* 15(10):655.

Agace WW, Hedges SR, Ceska M & Svanborg C (1993) Interleukin-8 and the neutrophil response to mucosal gram-negative infection. *The Journal of Clinical Investigation* 92(2):780-785.

Agace WW, Patarroyo M, Svensson M, Carlemalm E & Svanborg C (1995) *Escherichia coli* induces transuroepithelial neutrophil migration by an intercellular adhesion molecule-1-dependent mechanism. *Infection and Immunity* 63(10):4054-4062.

Aiba H, Adhya S & de Crombrugghe B (1981) Evidence for two functional gal promoters in intact *Escherichia coli* cells. *Journal of Biological Chemistry* 256(22):11905-11910.

Akerley BJ, Cotter PA & Miller JF (1995) Ectopic expression of the flagellar regulon alters development of the Bordetella-host interaction. *Cell* 80(4):611-620.

Alteri CJ, Himpsl SD & Mobley HL (2015) Preferential use of central metabolism in vivo reveals a nutritional basis for polymicrobial infection. *PLoS Pathogens* 11(1):e1004601.

Alteri CJ, Smith SN & Mobley HL (2009a) Fitness of *Escherichia coli* during urinary tract infection requires gluconeogenesis and the TCA cycle. *PLoS Pathogens* 5(5): e1000448.

Altuvia S, Weinstein-Fischer D, Zhang A, Postow L & Storz G (1997) A small, stable RNA induced by oxidative stress: role as a pleiotropic regulator and antimutator. *Cell* 90(1):43-53.

Andersen-Nissen E, Hawn TR, Smith KD, Nachman A, Lampano AE, Uematsu S, Akira S & Aderem A (2007) Cutting edge: Tlr5−/− mice are more susceptible to *Escherichia coli* urinary tract infection. *The Journal of Immunology* 178(8):4717-4720.

Andersen TE, Khandige S, Madelung M, Brewer J, Kolmos HJ & Møller-Jensen J (2012) *Escherichia coli* uropathogenesis in vitro: invasion, cellular escape, and secondary infection analyzed in a human bladder cell infection model. *Infection and Immunity* 80(5):1858-1867.

Anderson GG, Goller CC, Justice S, Hultgren SJ & Seed PC (2010) Polysaccharide capsule and sialic acid-mediated regulation promote biofilm-like intracellular bacterial communities during cystitis. *Infection and Immunity* 78(3):963-975.

Anderson GG, Palermo JJ, Schilling JD, Roth R, Heuser J & Hultgren SJ (2003) Intracellular bacterial biofilm-like pods in urinary tract infections. *Science* 301(5629):105-107.

Antao E-M, Glodde S, Li G, Sharifi R, Homeier T, Laturnus C, Diehl I, Bethe A, Philipp H-C & Preisinger R (2008) The chicken as a natural model for extraintestinal infections caused by avian pathogenic *Escherichia coli* (APEC). *Microbial Pathogenesis* 45(5-6):361-369.

Ashkar AA, Mossman KL, Coombes BK, Gyles CL & Mackenzie R (2008) FimH adhesin of type 1 fimbriae is a potent inducer of innate antimicrobial responses which requires TLR4 and type 1 interferon signalling. *PLoS Pathogens* 4(12).

Baba T, Ara T, Hasegawa M, Takai Y, Okumura Y, Baba M, Datsenko KA, Tomita M, Wanner BL & Mori H (2006) Construction of *Escherichia coli* K-12 in-frame, single-gene knockout mutants: the Keio collection. *Molecular Systems Biology* 2(1): 2006.0008.

Babior BM (2000) Phagocytes and oxidative stress. *The American Journal of Medicine* 109(1):33-44.

Bäckhed F, Alsén B, Roche N, Ångström J, von Euler A, Breimer ME, Westerlund-Wikström B, Teneberg S & Richter-Dahlfors A (2002) Identification of target tissue glycosphingolipid receptors for uropathogenic, F1C-fimbriated *Escherichia coli* and its role in mucosal inflammation. *Journal of Biological Chemistry* 277(20):18198-18205.

Backhed F, Soderhall M, Ekman P, Normark S & Richter-Dahlfors A (2001) Induction of innate immune responses by *Escherichia coli* and purified lipopolysaccharide correlate with organ- and cell-specific expression of Toll-like receptors within the human urinary tract. *Cellular Microbiology* 3(3):153-158.

Bäckhed F, Söderhäll M, Ekman P, Normark S & Richter-Dahlfors A (2001) Induction of innate immune responses by *Escherichia coli* and purified lipopolysaccharide correlate with organ-and cell-specific expression of Toll-like receptors within the human urinary tract. *Cellular Microbiology* 3(3):153-158.

Bak G, Lee J, Suk S, Kim D, Lee JY, Kim K-s, Choi B-S & Lee Y (2015) Identification of novel sRNAs involved in biofilm formation, motility, and fimbriae formation in *Escherichia coli*. *Scientific Reports* 5:15287.

Barnhart MM & Chapman MR (2006) Curli biogenesis and function. *Annual Review of Microbiology* 60:131-147.

Bates Jr JM, Raffi HM, Prasadan K, Mascarenhas R, Laszik Z, Maeda N, Hultgren SJ & Kumar S (2004) Tamm-Horsfall protein knockout mice are more prone to urinary tract infection Rapid Communication. *Kidney International* 65(3):791-797.

Beebout CJ, Eberly AR, Werby SH, Reasoner SA, Brannon JR, De S, Fitzgerald MJ, Huggins MM, Clayton DB & Cegelski L (2019) Respiratory heterogeneity shapes biofilm formation and host colonization in uropathogenic *Escherichia coli*. *mBio* 10(2):e02400-02418.

Bélanger L, Garenaux A, Harel J, Boulianne M, Nadeau E & Dozois CM (2011) *Escherichia coli* from animal reservoirs as a potential source of human extraintestinal pathogenic *E. coli*. *FEMS Immunology & Medical Microbiology* 62(1):1-10.

Berg HC & Anderson RA (1973) Bacteria swim by rotating their flagellar filaments. *Nature* 245(5425):380-382.

Berger H, Hacker J, Juarez A, Hughes C & Goebel W (1982) Cloning of the chromosomal determinants encoding hemolysin production and mannose-resistant hemagglutination in *Escherichia coli*. *Journal of Bacteriology* 152(3):1241-1247.

Bernet-Camard MF, Coconnier MH, Hudault S & Servin AL (1996) Pathogenicity of the diffusely adhering strain *Escherichia coli* C1845: F1845 adhesin-decay accelerating factor interaction, brush border microvillus injury, and actin disassembly in cultured human intestinal epithelial cells. *Infection and Immunity* 64(6):1918-1928.

Berry RE, Klumpp DJ & Schaeffer AJ (2009) Urothelial cultures support intracellular bacterial community formation by uropathogenic *Escherichia coli*. *Infection and Immunity* 77(7):2762-2772.

Bertrand N, Houle S, LeBihan G, Poirier E, Dozois CM & Harel J (2010a) Increased Pho regulon activation correlates with decreased virulence of an avian pathogenic *Escherichia coli* O78 strain. *Infection and Immunity* 78(12):5324-5331.

Bessaiah H, Pokharel P, Habouria H, Houle S & Dozois CM (2019) *yqhG* Contributes to Oxidative Stress Resistance and Virulence of Uropathogenic *Escherichia coli* and Identification of Other Genes Altering Expression of Type 1 Fimbriae. *Frontiers in Cellular and Cnfection Microbiology* 9:312.

Bhakdi S, Mackman N, Menestrina G, Gray L, Hugo F, Seeger W & Holland I (1988) The hemolysin of *Escherichia coli*. *European Journal of Epidemiology* 4(2):135-143.

Bien J, Sokolova O & Bozko P (2012) Role of Uropathogenic *Escherichia coli* Virulence Factors in Development of Urinary Tract Infection and Kidney Damage. *International Journal of Nephrology* 2012:681473: 1-15.

Bingen E, Bonacorsi S, Brahimi N, Denamur E & Elion J (1997) Virulence patterns of *Escherichia coli* K1 strains associated with neonatal meningitis. *Journal of Clinical Microbiology* 35(11):2981-2982.

Bingen E, Picard B, Brahimi N, Mathy S, Desjardins P, Elion J & Denamur E (1998) Phylogenetic analysis of *Escherichia coli* strains causing neonatal meningitis suggests horizontal gene transfer from a predominant pool of highly virulent B2 group strains. *Journal of Infectious Diseases* 177(3):642-650.

Bjarke Olsen P & Klemm P (1994a) Localization of promoters in the fim gene cluster and the effect of H-NS on the transcription of *fimB* and *fimE*. *FEMS Microbiology Letters* 116(1):95-100.

Blango MG & Mulvey MA (2010) Persistence of uropathogenic *Escherichia coli* in the face of multiple antibiotics. *Antimicrobial Agents and Chemotherapy* 54(5):1855-1863.

Blango MG, Ott EM, Erman A, Veranic P & Mulvey MA (2014) Forced resurgence and targeting of intracellular uropathogenic *Escherichia coli* reservoirs. *PLoS One* 9(3).

Blomfield IC, Calie PJ, Eberhardt KJ, McClain MS & Eisenstein BI (1993) Lrp stimulates phase variation of type 1 fimbriation in *Escherichia coli* K-12. *Journal of Bacteriology* 175(1):27-36.

Blomfield IC, Kulasekara DH & Eisenstein BI (1997a) Integration host factor stimulates both FimB- and FimE-mediated site-specific DNA inversion that controls phase variation of type 1 fimbriae expression in *Escherichia coli*. *Molecular Microbiology* 23(4):705-717.

Blomfield IC, McClain MS, Princ JA, Calie PJ & Eisenstein BI (1991) Type 1 fimbriation and fimE mutants of *Escherichia coli* K-12. *Journal of Bacteriology* 173(17):5298-5307.

Blumer C, Kleefeld A, Lehnen D, Heintz M, Dobrindt U, Nagy G, Michaelis K, Emödy L, Polen T & Rachel R (2005) Regulation of type 1 fimbriae synthesis and biofilm formation by the transcriptional regulator LrhA of *Escherichia coli*. *Microbiology* 151(10):3287-3298.

Boehm D, Welch R & Snyder I (1990) Calcium is required for binding of *Escherichia coli* hemolysin (HlyA) to erythrocyte membranes. *Infection and Immunity* 58(6):1951-1958.

Bonacorsi S & Bingen E (2005) Molecular epidemiology of *Escherichia coli* causing neonatal meningitis. *International Journal of Medical Microbiology* 295(6-7):373-381.

Bonacorsi S, Clermont O, Houdouin V, Cordevant C, Brahimi N, Marecat A, Tinsley C, Nassif X, Lange M & Bingen E (2003) Molecular analysis and experimental virulence of French and North American *Escherichia coli* neonatal meningitis isolates: identification of a new virulent clone. *The Journal of Infectious Diseases* 187(12):1895-1906.

Boos W (1998) [4] Binding protein-dependent ABC transport system for glycerol 3-phosphate of *Escherichia coli*. *Methods in Enzymology*, Elsevier, Vol 292. p 40-51.

Bouatra S, Aziat F, Mandal R, Guo AC, Wilson MR, Knox C, Bjorndahl TC, Krishnamurthy R, Saleem F & Liu P (2013) The human urine metabolome. *PloS one* 8(9).

Bower JM & Mulvey MA (2006) Polyamine-mediated resistance of uropathogenic *Escherichia coli* to nitrosative stress. *Journal of Bacteriology* 188(3):928-933.

Boyer E, Bergevin I, Malo D, Gros P & Cellier M (2002) Acquisition of Mn (II) in addition to Fe (II) is required for full virulence of *Salmonella* enterica serovar Typhimurium. *Infection and Immunity* 70(11):6032-6042.

Braun V (1981) *Escherichia coli* cells containing the plasmid ColV produce the iron ionophore aerobactin. *FEMS Microbiology Letters* 11(4):225-228.

Brauner A, Leissner M, Wretlind B, Julander I, Svenson SB & Källenius G (1985) Occurrence of P-fimbriated *Escherichia coli* in patients with bacteremia. *European Journal of Clinical Microbiology* 4(6):566-569.

Brinkman AB, Ettema TJ, De Vos WM & Van Der Oost J (2003a) The Lrp family of transcriptional regulators. *Molecular Microbiology* 48(2):287-294.

Bryan A, Roesch P, Davis L, Moritz R, Pellett S & Welch RA (2006a) Regulation of type 1 fimbriae by unlinked FimB- and FimE-like recombinases in uropathogenic *Escherichia coli* strain CFT073. *Infection and Immunity* 74(2):1072-1083.

Brzuszkiewicz E, Gottschalk G, Ron E, Hacker J & Dobrindt U (2009) Adaptation of pathogenic *E. coli* to various niches: genome flexibility is the key. *Microbial Pathogenomics,* Karger Publishers, Vol 6. p 110-125.

Brzuszkiewicz E, Thurmer A, Schuldes J, Leimbach A, Liesegang H, Meyer FD, Boelter J, Petersen H, Gottschalk G & Daniel R (2011) Genome sequence analyses of two isolates from the recent *Escherichia coli* outbreak in Germany reveal the emergence of a new pathotype: Entero-Aggregative-Haemorrhagic *Escherichia coli* (EAHEC). *Archives of Microbiology* 193(12):883-891.

Buchanan K, Falkow S, Hull R & Hull S (1985) Frequency among Enterobacteriaceae of the DNA sequences encoding type 1 pili. *Journal of Bacteriology* 162(2):799-803.

Buckles EL, Bahrani-Mougeot FK, Molina A, Lockatell CV, Johnson DE, Drachenberg CB, Burland V, Blattner FR & Donnenberg MS (2004) Identification and characterization of a novel uropathogenic *Escherichia coli*-associated fimbrial gene cluster. *Infection and Immunity* 72(7):3890-3901.

Buckles EL, Luterbach CL, Wang X, Lockatell C, Johnson DE, Mobley HL & Donnenberg MS (2015) Signature-tagged mutagenesis and co-infection studies demonstrate the importance of P fimbriae in a murine model of urinary tract infection. *Pathogens and Disease* 73(4).

Bukau B & Horwich AL (1998) The Hsp70 and Hsp60 chaperone machines. *Cell* 92(3):351-366.

Bullitt E, Jones CH, Striker R, Soto G, Jacob-Dubuisson F, Pinkner J, Wick MJ, Makowski L & Hultgren SJ (1996) Development of pilus organelle subassemblies in vitro depends on chaperone uncapping of a beta zipper. *Proceedings of the National Academy of Sciences* 93(23):12890-12895.

Burns SM & Hull SI (1998) Comparison of Loss of Serum Resistance by Defined Lipopolysaccharide Mutants and an Acapsular Mutant of Uropathogenic*Escherichia coli* O75: K5. *Infection and Immunity* 66(9):4244-4253.

Cahill DJ, Fry CH & Foxall PJ (2003) Variation in urine composition in the human urinary tract: evidence of urothelial function in situ? *The Journal of Urology* 169(3):871-874.

Cai W, Wannemuehler Y, Dell'Anna G, Nicholson B, Barbieri NL, Kariyawasam S, Feng Y, Logue CM, Nolan LK & Li G (2013) A novel two-component signaling system facilitates uropathogenic *Escherichia coli*'s ability to exploit abundant host metabolites. *PLoS Pathogens* 9(6):e1003428.

Calvo JM & Matthews RG (1994) The leucine-responsive regulatory protein, a global regulator of metabolism in *Escherichia coli*. *Microbiological reviews.* 58(3):466-490.

Casaz P, Garrity-Ryan LK, McKenney D, Jackson C, Levy SB, Tanaka SK & Alekshun MN (2006) MarA, SoxS and Rob function as virulence factors in an *Escherichia coli* murine model of ascending pyelonephritis. *Microbiology* 152(12):3643-3650.

Cassat JE & Skaar EP (2013) Iron in Infection and Immunity . *Cell host & microbe* 13(5):509-519.

Castelain M, Sjöström AE, Fällman E, Uhlin BE & Andersson M (2010) Unfolding and refolding properties of S pili on extraintestinal pathogenic *Escherichia coli*. *European Biophysics Journal* 39(8):1105-1115.

Caza M, Lépine F, Milot S & Dozois CM (2008) Specific roles of the iroBCDEN genes in virulence of an avian pathogenic *Escherichia coli* O78 strain and in production of salmochelins. *Infection and Immunity* 76(8):3539-3549.

Chaffer M, Heller E & Schwartsburd B (1999) Relationship between resistance to complement, virulence and outer membrane protein patterns in pathogenic *Escherichia coli* O2 isolates. *Veterinary Microbiology* 64(4):323-332.

Chahales P & Thanassi DG (2015) Structure, Function, and Assembly of Adhesive Organelles by Uropathogenic Bacteria. *Molecular Pathogenesis and Clinical Management* 3(5).

Chapman MR, Robinson LS, Pinkner JS, Roth R, Heuser J, Hammar M, Normark S & Hultgren SJ (2002) Role of *Escherichia coli* curli operons in directing amyloid fiber formation. *Science* 295(5556):851-855.

Chen SL, Wu M, Henderson JP, Hooton TM, Hibbing ME, Hultgren SJ & Gordon JI (2013) Genomic diversity and fitness of *E. coli* strains recovered from the intestinal and urinary tracts of women with recurrent urinary tract infection. *Science Translational Medicine* 5(184):184ra160-184ra160.

Cherepanov PP & Wackernagel W (1995) Gene disruption in *Escherichia coli*: TcR and KmR cassettes with the option of Flp-catalyzed excision of the antibiotic-resistance determinant. *Gene* 158(1):9-14.

Chilcott GS & Hughes KT (2000) Coupling of flagellar gene expression to flagellar assembly in *Salmonella enterica* serovar typhimurium and *Escherichia coli*. *Microbiology and Molecular Biology Reviews* 64(4):694-708.

Chromek M, Slamová Z, Bergman P, Kovács L, Podracká Lu, Ehrén I, Hökfelt T, Gudmundsson GH, Gallo RL & Agerberth B (2006) The antimicrobial peptide cathelicidin protects the urinary tract against invasive bacterial infection. *Nature Medicine* 12(6):636-641.

Clancy J & Savage DC (1981) Another Colicin V phenotype: in vitro adhesion of *Escherichia coli* to mouse intestinal epithelium. *Infection and Immunity* 32(1):343-352.

Clegg S & Gerlach G (1987a) Enterobacterial fimbriae. *Journal of Bacteriology* 169(3):934.

Clegg S & Hughes KT (2002) FimZ is a molecular link between sticking and swimming in *Salmonella enterica* serovar Typhimurium. *Journal of Bacteriology* 184(4):1209-1213.

Clements A, Young JC, Constantinou N & Frankel G (2012) Infection strategies of enteric pathogenic *Escherichia coli*. *Gut Microbes* 3(2):71-87.

Clermont O, Christenson JK, Denamur E & Gordon DM (2013) The Clermont *Escherichia coli* phylo-typing method revisited: improvement of specificity and detection of new phylo-groups. *Environmental Microbiology Reports* 5(1):58-65.

Connell I, Agace W, Klemm P, Schembri M, Mårild S & Svanborg C (1996) Type 1 fimbrial expression enhances *Escherichia coli* virulence for the urinary tract. *Proceedings of the National Academy of Sciences* 93(18):9827-9832.

Conover MS, Hadjifrangiskou M, Palermo JJ, Hibbing ME, Dodson KW & Hultgren SJ (2016) Metabolic requirements of *Escherichia coli* in intracellular bacterial communities during urinary tract infection pathogenesis. *MBio* 7(2):e00104-00116.

Corcoran CP & Dorman CJ (2009) DNA relaxation-dependent phase biasing of the fim genetic switch in *Escherichia coli* depends on the interplay of H-NS, IHF and LRP. *Molecular Microbiology* 74(5):1071-1082.

Cormack BP, Valdivia RH & Falkow S (1996) FACS-optimized mutants of the green fluorescent protein (GFP). *Gene* 173(1):33-38.

Cortes MA, Gibon J, Chanteloup NK, Moulin-Schouleur M, Gilot P & Germon P (2008) Inactivation of ibeA and ibeT results in decreased expression of type 1 fimbriae in extraintestinal pathogenic *Escherichia coli* strain BEN2908. *Infection and Immunity* 76(9):4129-4136.

Crépin S, Harel J & Dozois CM (2012a) Chromosomal complementation using Tn7 transposon vectors in Enterobacteriaceae. *Appl. Environ. Microbiol.* 78(17):6001-6008.

Crepin S, Houle S, Charbonneau ME, Mourez M, Harel J & Dozois CM (2012) Decreased expression of type 1 fimbriae by a pst mutant of uropathogenic *Escherichia coli* reduces urinary tract infection. *Infection and Immunity* 80(8):2802-2815.

Crépin S, Lamarche MG, Garneau P, Séguin J, Proulx J, Dozois CM & Harel J (2008) Genome-wide transcriptional response of an avian pathogenic *Escherichia coli* (APEC) *pst* mutant. *BMC Genomics* 9(1):568.

Crépin S, Porcheron G, Houle S, Harel J & Dozois CM (2017) Altered regulation of the diguanylate cyclase YaiC reduces production of type 1 fimbriae in a Pst mutant of uropathogenic *Escherichia coli* CFT073. *Journal of Bacteriology* 199(24):e00168-00117.

Crespo MD, Puorger C, Schärer MA, Eidam O, Grütter MG, Capitani G & Glockshuber R (2012) Quality control of disulfide bond formation in pilus subunits by the chaperone FimC. *Nature Chemical Biology* 8(8):707.

Croxen MA & Finlay BB (2010) Molecular mechanisms of *Escherichia coli* pathogenicity. *Nature Reviews Microbiology* 8(1):26-38.

Croxen MA, Law RJ, Scholz R, Keeney KM, Wlodarska M & Finlay BB (2013) Recent advances in understanding enteric pathogenic *Escherichia coli*. *Clinical Microbiology Reviews* 26(4):822-880.

Culham DE, Lu A, Jishage M, Krogfelt KA, Ishihama A & Wood JM (2001) The osmotic stress response and virulence in pyelonephritis isolates of *Escherichia coli*: contributions of RpoS, ProP, ProU and other systems. *Microbiology* 147(6):1657-1670.

Datsenko KA & Wanner BL (2000) One-step inactivation of chromosomal genes in *Escherichia coli* K-12 using PCR products. *Proceedings of the National Academy of Sciences* 97(12):6640-6645.

Davidson CJ & Surette MG (2008) Individuality in bacteria. *Annual Review of Genetics* 42:253-268.

De Lorenzo V, Herrero M, Jakubzik U & Timmis KN (1990) Mini-Tn5 transposon derivatives for insertion mutagenesis, promoter probing, and chromosomal insertion of cloned DNA in gram-negative eubacteria. *Journal of Bacteriology* 172(11):6568-6572.

De Lorenzo V & Neilands J (1986) Characterization of iucA and iucC genes of the aerobactin system of plasmid ColV-K30 in *Escherichia coli*. *Journal of Bacteriology* 167(1):350-355.

de Louvois J (1994) Acute bacterial meningitis in the newborn. *Journal of Antimicrobial Chemotherapy* 34 Suppl A:61-73.

Dean-Nystrom EA, Melton-Celsa AR, Pohlenz JF, Moon HW & O'Brien AD (2003) Comparative pathogenicity of *Escherichia coli* O157 and intimin-negative non-O157 Shiga toxin-producing *E coli* strains in neonatal pigs. *Infection and Immunity* 71(11):6526-6533.

Derman Y, Söderholm H, Lindström M & Korkeala H (2015) Role of csp genes in NaCl, pH, and ethanol stress response and motility in Clostridium botulinum ATCC 3502. *Food Microbiology* 46:463-470.

Dhakal BK & Mulvey MA (2012) The UPEC pore-forming toxin α-hemolysin triggers proteolysis of host proteins to disrupt cell adhesion, inflammatory, and survival pathways. *Cell Host & Microbe* 11(1):58-69.

Dho-Moulin M & Fairbrother JM (1999) Avian pathogenic *Escherichia coli* (APEC). *Veterinary Research*, 30(2-3):299-316.

Dho M & Lafont J (1984) Adhesive properties and iron uptake ability in *Escherichia coli* lethal and nonlethal for chicks. *Avian Diseases* :1016-1025.

Dobrindt U (2005) (Patho-)Genomics of *Escherichia coli*. *International Journal Of Medical Microbiology* 295(6-7):357-371.

Donato GM & Kawula TH (1999) Phenotypic analysis of random hns mutations differentiate DNA-binding activity from properties of *fimA* promoter inversion modulation and bacterial motility. *Journal of Bacteriology* 181(3):941-948.

Donato GM, Lelivelt MJ & Kawula TH (1997) Promoter-specific repression of fimB expression by the *Escherichia coli* nucleoid-associated protein H-NS. *Journal of Bacteriology* 179(21):6618-6625.

Dorman CJ & Higgins CF (1987) Fimbrial phase variation in *Escherichia coli*: dependence on integration host factor and homologies with other site-specific recombinases. *Journal of Bacteriology* 169(8):3840-3843.

Dove S, Smith S & Dorman C (1997) Control of *Escherichia coli* type 1 fimbrial gene expression in stationary phase: a negative role for RpoS. *Molecular and General Genetics MGG* 254(1):13-20.

Dozois CM, Chanteloup N, Dho-Moulin M, Brée A, Desautels C & Fairbrother JM (1994) Bacterial colonization and *in vivo* expression of F1 (type 1) fimbrial antigens in chickens experimentally infected with pathogenic *Escherichia coli*. *Avian Diseases* :231-239.

Dozois CM, Dho-Moulin M, Brée A, Fairbrother JM, Desautels C & Curtiss R (2000) Relationship between the Tsh autotransporter and pathogenicity of avian *Escherichia coli* and localization and analysis of the Tsh genetic region. *Infection and Immunity* 68(7):4145-4154.

Ebel F, Podzadel T, Rohde M, Kresse AU, Kramer S, Deibel C, Guzman CA & Chakraborty T (1998) Initial binding of Shiga toxin-producing *Escherichia coli* to host cells and subsequent induction of actin rearrangements depend on filamentous EspA-containing surface appendages. *Molecular Microbiology* 30(1):147-161.

Eberly A, Floyd K, Beebout C, Colling S, Fitzgerald M, Stratton C, Schmitz J & Hadjifrangiskou M (2017a) Biofilm formation by uropathogenic *Escherichia coli* is favored under oxygen conditions that mimic the bladder environment. *International Journal of Molecular Sciences* 18(10):2077.

Eisenstein B, Beachey E & Solomon S (1981) Divergent effects of cyclic adenosine 3', 5'-monophosphate on formation of type 1 fimbriae in different K-12 strains of *Escherichia coli*. *Journal of Bacteriology* 145(1):620-623.

Eisenstein B & Dodd D (1982) Pseudocatabolite repression of type 1 fimbriae of *Escherichia coli*. *Journal of Bacteriology* 151(3):1560-1567.

Eisenstein BI, Sweet DS, Vaughn V & Friedman DI (1987) Integration host factor is required for the DNA inversion that controls phase variation in *Escherichia coli*. *Proceedings of the National Academy of Sciences* 84(18):6506-6510.

El-Labany S, Sohanpal BK, Lahooti M, Akerman R & Blomfield IC (2003) Distant cis-active sequences and sialic acid control the expression of *fimB* in *Escherichia coli* K-12. *Molecular Microbiology* 49(4):1109-1118.

Epp A, Larochelle A, Lovatsis D, Walter J-E, Easton W, Farrell SA, Girouard L, Gupta C, Harvey M-A & Robert M (2010) Recurrent urinary tract infection. *Journal of Obstetrics and Gynaecology Canada* 32(11):1082-1090.

Escherich T (1988) The intestinal bacteria of the neonate and breast-fed infant. *Clinical Infectious Diseases* 10(6):1220-1225.

Eto DS, Jones TA, Sundsbak JL & Mulvey MA (2007) Integrin-mediated host cell invasion by type 1–piliated uropathogenic *Escherichia coli*. *PLoS Pathogens* 3(7).

Eto DS, Sundsbak JL & Mulvey MA (2006) Actin-gated intracellular growth and resurgence of uropathogenic *Escherichia coli*. *Cellular Microbiology* 8(4):704-717.

Evans DA, Williams DN, Laughlin LW, Miao L, Warren JW, Hennekens CH, Shimada J, Chapman WG, Rosner B & Taylor JO (1978) Bacteriuria in a population-based cohort of women. *Journal of Infectious Diseases* 138(6):768-773.

Ewers C, Li G, Wilking H, Kießling S, Alt K, Antáo E-M, Laturnus C, Diehl I, Glodde S & Homeier T (2007) Avian pathogenic, uropathogenic, and newborn meningitis-causing *Escherichia coli*: how closely related are they? *International Journal of Medical Microbiology* 297(3):163-176.

Fang FC (2004) Antimicrobial reactive oxygen and nitrogen species: concepts and controversies. *Nature Reviews Microbiology* 2(10):820-832.

Ferry SA, Holm SE, Stenlund H, Lundholm R & Monsen TJ (2007) Clinical and bacteriological outcome of different doses and duration of pivmecillinam compared with placebo therapy of uncomplicated lower urinary tract infection in women: the LUTIW project. *Scandinavian Journal of Primary Health Care* 25(1):49-57.

Fiorentini C, Fabbri A, Matarrese P, Falzano L, Boquet P & Malorni W (1997) Hinderance of apoptosis and phagocytic behaviour induced by *Escherichia coli* cytotoxic necrotizing factor 1: two related activities in epithelial cells. *Biochemical and Biophysical Research Communications* 241(2):341-346.

Flamm EL & Weisberg RA (1985) Primary structure of the hip gene of *Escherichia coli* and of its product, the β subunit of integration host factor. *Journal of Molecular Biology* 183(2):117-128.

Flannagan RS, Cosío G & Grinstein S (2009) Antimicrobial mechanisms of phagocytes and bacterial evasion strategies. *Nature Reviews Microbiology* 7(5):355-366.

Fléchard M, Cortes MA, Répérant M & Germon P (2012) New role for the ibeA gene in H2O2 stress resistance of *Escherichia coli*. *Journal of Bacteriology* 194(17):4550-4560.

Flores-Kim J & Darwin AJ (2015) Activity of a bacterial cell envelope stress response is controlled by the interaction of a protein binding domain with different partners. *Journal of Biological Chemistry* 290(18):11417-11430.

Flores-Mireles AL, Walker JN, Caparon M & Hultgren SJ (2015a) Urinary tract infections: epidemiology, mechanisms of infection and treatment options. *Nature Reviews Microbiology* 13(5):269.

Floyd KA, Moore JL, Eberly AR, Good JA, Shaffer CL, Zaver H, Almqvist F, Skaar EP, Caprioli RM & Hadjifrangiskou M (2015a) Adhesive fiber stratification in uropathogenic *Escherichia coli* biofilms unveils oxygen-mediated control of type 1 pili. *PLoS Pathogens* 11(3):e1004697.

Foxman B (1990) Recurring urinary tract infection: incidence and risk factors. *American Journal of Public Health* 80(3):331-333.

Foxman B (2002) Epidemiology of urinary tract infections: incidence, morbidity, and economic costs. *The American Journal of Medicine* 113(1):5-13.

Foxman B (2010) The epidemiology of urinary tract infection. *Nature Reviews Urology* 7(12):653.

Foxman B (2014) Urinary tract infection syndromes: occurrence, recurrence, bacteriology, risk factors, and disease burden. *Infectious Disease Clinics of North America* 28(1):1-13.

Foxman B & Brown P (2003) Epidemiology of urinary tract infections: transmission and risk factors, incidence, and costs. *Infectious Disease Clinics of North America* 17(2):227-241.

Francis KP, Yu J, Bellinger-Kawahara C, Joh D, Hawkinson MJ, Xiao G, Purchio TF, Caparon MG, Lipsitch M & Contag PR (2001) Visualizing Pneumococcal Infections in the Lungs of Live Mice Using Bioluminescent *Streptococcus pneumoniae*Transformed with a Novel Gram-Positive luxTransposon. *Infection and Immunity* 69(5):3350-3358.

Freter R, Brickner H, Fekete J, Vickerman MM & Carey KE (1983) Survival and implantation of *Escherichia coli* in the intestinal tract. *Infection and Immunity* 39(2):686-703.

Frick-Cheng AE, Sintsova A, Smith SN, Krauthammer M, Eaton KA & Mobley HL (2020) The Gene Expression Profile of Uropathogenic *Escherichia coli* in Women with Uncomplicated Urinary Tract Infections Is Recapitulated in the Mouse Model. *bioRxiv*. doi.org/10.1101/2020.02.18.954842

Fris ME, Broach WH, Klim SE, Coschigano PW, Carroll RK, Caswell CC & Murphy ER (2017) Sibling sRNA RyfA1 influences Shigella dysenteriae pathogenesis. *Genes* 8(2):50.

Fröhlich KS & Vogel J (2009) Activation of gene expression by small RNA. *Current Opinion in Microbiology* 12(6):674-682.

Gally DL, Bogan JA, Eisenstein BI & Blomfield IC (1993) Environmental regulation of the fim switch controlling type 1 fimbrial phase variation in *Escherichia coli* K-12: effects of temperature and media. *Journal of Bacteriology* 175(19):6186-6193.

Gally DL, Leathart J & Blomfield IC (1996a) Interaction of FimB and FimE with the fim switch that controls the phase variation of type 1 fimbriae in *Escherichia coli* K-12. *Molecular Microbiology* 21(4):725-738.

Gao Q, Jia X, Wang X, Xiong L, Gao S & Liu X (2015) The avian pathogenic *Escherichia coli* O2 strain E058 carrying the defined aerobactin-defective iucD or iucDiutA mutation is less virulent in the chicken. *Infection, Genetics and Evolution* 30:267-277.

Gao Q, Wang X, Xu H, Xu Y, Ling J, Zhang D, Gao S & Liu X (2012) Roles of iron acquisition systems in virulence of extraintestinal pathogenic *Escherichia coli*: salmochelin and aerobactin contribute more to virulence than heme in a chicken infection model. *BMC Microbiology* 12(1):1-12.

Garcia MI, Gounon P, Courcoux P, Labigne A & Le Bouguénec C (1996) The afimbrial adhesive sheath encoded by the afa-3 gene cluster of pathogenic *Escherichia coli* is composed of two adhesins. *Molecular Microbiology* 19(4):683-693.

Geibel S & Waksman G (2014) The molecular dissection of the chaperone–usher pathway. *Biochimica et Biophysica Acta (BBA)-Molecular Cell Research* 1843(8):1559-1567.

Gerber A, Karch H, Allerberger F, Verweyen HM & Zimmerhackl LB (2002) Clinical course and the role of shiga toxin-producing *Escherichia coli* infection in the hemolytic-uremic syndrome in pediatric patients, 1997-2000, in Germany and Austria: a prospective study. *Journal of Infectious Diseases* 186(4):493-500.

Gething M-J & Sambrook J (1992) Protein folding in the cell. *Nature* 355(6355):33-45.

Godaly G, Bergsten G, Hang L, Fischer H, Frendeus B, Lundstedt AC, Samuelsson M, Samuelsson P & Svanborg C (2001) Neutrophil recruitment, chemokine receptors, and resistance to mucosal infection. *Journal of Leukocyte Biology* 69(6):899-906.

Gon S, Patte J-C, Méjean V & Iobbi-Nivol C (2000) The torYZ (yecK bisZ) operon encodes a third respiratory trimethylamine N-oxide reductase in *Escherichia coli*. *Journal of Bacteriology* 182(20):5779-5786.

González-Flecha B & Demple B (1995) Metabolic sources of hydrogen peroxide in aerobically growing *Escherichia coli*. *Journal of Biological Chemistry* 270(23):13681-13687.

Göransson M, Forsman K & Uhlin B (1989) Regulatory genes in the thermoregulation of *Escherichia coli* pili gene transcription. *Genes & Development* 3(1):123-130.

Grabe M, Bjerklund-Johansen T, Botto H, Çek M, Naber K, Tenke P & Wagenlehner F (2015) Guidelines on urological infections. *European Association of Urology* 182.

Griebling TL (2007) Urinary tract infection in women. *Urologic diseases in America* 7:587-619.

Guillier M & Gottesman S (2006) Remodelling of the *Escherichia coli* outer membrane by two small regulatory RNAs. *Molecular Microbiology* 59(1):231-247.

Gunther IV NW, Snyder JA, Lockatell V, Blomfield I, Johnson DE & Mobley HL (2002) Assessment of virulence of uropathogenic *Escherichia coli* type 1 fimbrial mutants in which the invertible element is phase-locked on or off. *Infection and Immunity* 70(7):3344-3354.

Gunther NW, Lockatell V, Johnson DE & Mobley HL (2001) In vivo dynamics of type 1 fimbria regulation in uropathogenic *Escherichia coli* during experimental urinary tract infection. *Infection and Immunity* 69(5):2838-2846.

Gunther NW, Snyder JA, Lockatell V, Blomfield I, Johnson DE & Mobley HL (2002) Assessment of virulence of uropathogenic *Escherichia coli* type 1 fimbrial mutants in which the invertible element is phase-locked on or off. *Infection and Immunity* 70(7):3344-3354.

Guyer DM, Radulovic S, Jones F-E & Mobley HL (2002) Sat, the secreted autotransporter toxin of uropathogenic *Escherichia coli*, is a vacuolating cytotoxin for bladder and kidney epithelial cells. *Infection and Immunity* 70(8):4539-4546.

Gyimah J & Panigrahy B (1988) Adhesin-receptor interactions mediating the attachment of pathogenic *Escherichia coli* to chicken tracheal epithelium. *Avian diseases* 32:74-78.

Hacker J & Kaper JB (2000) Pathogenicity islands and the evolution of microbes. *Annual Review of Microbiology* 54:641-679.

Hadjifrangiskou M, Kostakioti M, Chen SL, Henderson JP, Greene SE & Hultgren SJ (2011) A central metabolic circuit controlled by QseC in pathogenic *Escherichia coli*. *Molecular Microbiology* 80(6):1516-1529.

Hagan EC, Lloyd AL, Rasko DA, Faerber GJ & Mobley HL (2010) *Escherichia coli* global gene expression in urine from women with urinary tract infection. *PLoS Pathogens* 6(11).

Hahn E, Wild P, Hermanns U, Sebbel P, Glockshuber R, Häner M, Taschner N, Burkhard P, Aebi U & Müller SA (2002) Exploring the 3D molecular architecture of *Escherichia coli* type 1 pili. *Journal of Moleular Biology* 323(5):845-857.

Hama H, Kayahara T, Ogawa W, Tsuda M & Tsuchiya T (1994) Enhancement of serine-sensitivity by a gene encoding rhodanese-like protein in *Escherichia coli*. *The Journal of Biochemistry* 115(6):1135-1140.

Hammar M, Arnqvist A, Bian Z, Olsen A & Normark S (1995) Expression of two csg operons is required for production of fibronectin- and congo red-binding curli polymers in *Escherichia coli* K-12. *Molecular Microbiology* 18(4):661-670.

Hancock V & Klemm P (2007) Global gene expression profiling of asymptomatic bacteriuria *Escherichia coli* during biofilm growth in human urine. *Infection and Immunity* 75(2):966-976.

Hannan TJ, Mysorekar IU, Chen SL, Walker JN, Jones JM, Pinkner JS, Hultgren SJ & Seed PC (2008) LeuX tRNA-dependent and-independent mechanisms of *Escherichia coli* pathogenesis in acute cystitis. *Molecular Microbiology* 67(1):116-128.

Hannan TJ, Roberts PL, Riehl TE, van der Post S, Binkley JM, Schwartz DJ, Miyoshi H, Mack M, Schwendener RA & Hooton TM (2014) Inhibition of cyclooxygenase-2 prevents chronic and recurrent cystitis. *EBioMedicine* 1(1):46-57.

Hannan TJ, Totsika M, Mansfield KJ, Moore KH, Schembri MA & Hultgren SJ (2012) Host–pathogen checkpoints and population bottlenecks in persistent and intracellular uropathogenic *Escherichia coli* bladder infection. *FEMS Microbiology Reviews* 36(3):616-648.

Hantke K, Nicholson G, Rabsch W & Winkelmann G (2003) Salmochelins, siderophores of *Salmonella enterica* and uropathogenic *Escherichia coli* strains, are recognized by the outer membrane receptor IroN. *Proceedings of the National Academy of Sciences* 100(7):3677-3682.

Haraoka M, Hang L, Frendéus B, Godaly G, Burdick M, Strieter R & Svanborg C (1999) Neutrophil recruitment and resistance to urinary tract infection. *The Journal of Infectious Diseases* 180(4):1220-1229.

Harel J, Jacques M, Fairbrother JM, Bossé M & Forget C (1995) Cloning of determinants encoding F1652 fimbriae from porcine septicaemic *Escherichia coli* confirms their identity as F1C fimbriae. *Microbiology* 141(1):221-228.

Hartl FU (1996) Molecular chaperones in cellular protein folding. *Nature* 381(6583):571.

Haugen BJ, Pellett S, Redford P, Hamilton HL, Roesch PL & Welch RA (2007) In vivo gene expression analysis identifies genes required for enhanced colonization of the mouse urinary tract by uropathogenic *Escherichia coli* strain CFT073 *dsdA*. *Infection and Immunity* 75(1):278-289.

Hedlund M, Frendéus B, Wachtler C, Hang L, Fischer H & Svanborg C (2001) Type 1 fimbriae deliver an LPS-and TLR4-dependent activation signal to CD14-negative cells. *Molecular Microbiology* 39(3):542-552.

Henderson IR, Navarro-Garcia F, Desvaux M, Fernandez RC & Ala'Aldeen D (2004) Type V protein secretion pathway: the autotransporter story. *Microbiology and Molecular Biology Reviews* 68(4):692-744.

Hendrickson H (2009) Order and disorder during *Escherichia coli* divergence. *PLoS Genetics* 5(1):e1000335.

Herrero M, de Lorenzo V & Timmis KN (1990) Transposon vectors containing non-antibiotic resistance selection markers for cloning and stable chromosomal insertion of foreign genes in gram-negative bacteria. *Journal of Bacteriology* 172(11):6557-6567.

Hershberg R, Altuvia S & Margalit H (2003) A survey of small RNA-encoding genes in *Escherichia coli*. *Nucleic Acids Research* 31(7):1813-1820.

Hobert EH & Datta P (1983) Synthesis of biodegradative threonine dehydratase in *Escherichia coli*: role of amino acids, electron acceptors, and certain intermediary metabolites. *Journal of Bacteriology* 155(2):586-592.

Holden NJ, Totsika M, Mahler E, Roe AJ, Catherwood K, Lindner K, Dobrindt U & Gally DL (2006) Demonstration of regulatory cross-talk between P fimbriae and type 1 fimbriae in uropathogenic *Escherichia coli*. *Microbiology* 152(4):1143-1153.

Holden NJ, Uhlin BE & Gally DL (2001) PapB paralogues and their effect on the phase variation of type 1 fimbriae in *Escherichia coli*. *Molecular Microbiology* 42(2):319-330.

Hood MI & Skaar EP (2012) Nutritional immunity: transition metals at the pathogen–host interface. *Nature Reviews Microbiology* 10(8):525-537.

Hooton TM (2012) Uncomplicated urinary tract infection. *New England Journal of Medicine* 366(11):1028-1037.

Hryckowian AJ & Welch RA (2013) RpoS contributes to phagocyte oxidase-mediated stress resistance during urinary tract infection by *Escherichia coli* CFT073. *MBio* 4(1) : 1-6.

Hultgren S, Schwan W, Schaeffer AJ & Duncan J (1986) Regulation of production of type 1 pili among urinary tract isolates of *Escherichia coli*. *Infection and Immunity* 54(3):613-620.

Hultgren SJ, Porter TN, Schaeffer AJ & Duncan JL (1985) Role of type 1 pili and effects of phase variation on lower urinary tract infections produced by *Escherichia coli*. *Infection and Immunity* 50(2):370-377.

Hung C, Zhou Y, Pinkner JS, Dodson KW, Crowley JR, Heuser J, Chapman MR, Hadjifrangiskou M, Henderson JP & Hultgren SJ (2013) *Escherichia coli* biofilms have an organized and complex extracellular matrix structure. *MBio* 4(5):e00645-00613.

Hung CS, Bouckaert J, Hung D, Pinkner J, Widberg C, DeFusco A, Auguste CG, Strouse R, Langermann S, Waksman G & Hultgren SJ (2002) Structural basis of tropism of *Escherichia coli* to the bladder during urinary tract infection. *Molecular Microbiology* 44(4):903-915.

Imlay JA (2013) The molecular mechanisms and physiological consequences of oxidative stress: lessons from a model bacterium. *Nature Reviews Microbiology* 11(7):443-454.

Jaillon S, Moalli F, Ragnarsdottir B, Bonavita E, Puthia M, Riva F, Barbati E, Nebuloni M, Krajinovic LC & Markotic A (2014) The humoral pattern recognition molecule PTX3 is a key component of innate immunity against urinary tract infection. *Immunity* 40(4):621-632.

Jeannin P, Magistrelli G, Goetsch L, Haeuw J-F, Thieblemont N, Bonnefoy J-Y & Delneste Y (2002) Outer membrane protein A (OmpA): a new pathogen-associated molecular pattern that interacts with antigen presenting cells—impact on vaccine strategies. *Vaccine* 20:A23-A27.

Jenal U & Malone J (2006) Mechanisms of cyclic-di-GMP signaling in bacteria. *Annual Review of Genetics* . 40:385-407.

Johnson TJ, Wannemuehler Y, Johnson SJ, Stell AL, Doetkott C, Johnson JR, Kim KS, Spanjaard L & Nolan LK (2008) Comparison of extraintestinal pathogenic *Escherichia coli* strains from human and avian sources reveals a mixed subset representing potential zoonotic pathogens. *Applied and Environmental Microbiology* 74(22):7043-7050.

Jonas D, Schultheis B, Klas C, Krammer PH & Bhakdi S (1993) Cytocidal effects of *Escherichia coli* hemolysin on human T lymphocytes. *Infection and Immunity* 61(5):1715-1721.

Justice SS, Hung C, Theriot JA, Fletcher DA, Anderson GG, Footer MJ & Hultgren SJ (2004) Differentiation and developmental pathways of uropathogenic *Escherichia coli* in urinary tract pathogenesis. *Proceedings of the National Academy of Sciences* 101(5):1333-1338.

Kaniga K, Compton MS, Curtiss R, 3rd & Sundaram P (1998) Molecular and functional characterization of *Salmonella enterica* serovar typhimurium poxA gene: effect on attenuation of virulence and protection. *Infection and Immunity* 66(12):5599-5606.

Kaper JB, Nataro JP & Mobley HL (2004) Pathogenic *Escherichia coli*. *Nature Reviews Microbiology* 2(2):123-140.

Kariyawasam S & Nolan LK (2009) Pap mutant of avian pathogenic *Escherichia coli* O1, an O1: K1: H7 strain, is attenuated in vivo. *Avian Diseases* 53(2):255-260.

Kawula TH & Orndorff PE (1991) Rapid site-specific DNA inversion in *Escherichia coli* mutants lacking the histonelike protein H-NS. *Journal of Bacteriology* 173(13):4116-4123.

Kelly A, Conway C, Cróinín TÓ, Smith SG & Dorman CJ (2006) DNA supercoiling and the Lrp protein determine the directionality of fim switch DNA inversion in *Escherichia coli* K-12. *Journal of Bacteriology* 188(15):5356-5363.

Kevin James Allen MWG (2000) Construction and application of flaa sigma-28 promoter fusions to the virulence am3 ecology of *Campyloobacter jejuni*. *Thesis*. The University of Guelph.

Khan AS, Kniep B, Oelschlaeger TA, Van Die I, Korhonen T & Hacker J (2000) Receptor structure for F1C fimbriae of uropathogenic *Escherichia coli*. *Infection and Immunity* 68(6):3541-3547.

Khandelwal P, Abraham SN & Apodaca G (2009) Cell biology and physiology of the uroepithelium. *American Journal of Physiology-Renal Physiology* 297(6):F1477-F1501.

Klein RD & Hultgren SJ (2020) Urinary tract infections: microbial pathogenesis, host–pathogen interactions and new treatment strategies. *Nature Reviews Microbiology* :1-16.

Klemm P (1986a) Two regulatory fim genes, *fimB* and *fimE*, control the phase variation of type 1 fimbriae in *Escherichia coli*. *EMBO J* 5(6):1389-1393.

Klemm P (1994) *Fimbriae Adhesion, Genetics, Biogenesis, and Vaccines.* CRC Press,

Klemm P & Christiansen G (1987) Three *fim* genes required for the regulation of length and mediation of adhesion of *Escherichia coli* type 1 fimbriae. *Mol Gen Genet* 208(3):439-445.

Klemm P & Christiansen G (1990) The fimD gene required for cell surface localization of *Escherichia coli* type 1 fimbriae. *Molecular and General Genetics MGG* 220(2):334-338.

Klemm P & Schembri M (2004) Type 1 Fimbriae, Curli, and Antigen 43: Adhesion, Colonization, and Biofilm Formation. *EcoSal Plus* 1(1) : 1-18.

Knodler LA, Crowley SM, Sham HP, Yang H, Wrande M, Ma C, Ernst RK, Steele-Mortimer O, Celli J & Vallance BA (2014) Noncanonical inflammasome activation of caspase-4/caspase-11 mediates epithelial defenses against enteric bacterial pathogens. *Cell Host & Microbe* 16(2):249-256.

Korea CG, Ghigo JM & Beloin C (2011) The sweet connection: solving the riddle of multiple sugar-binding fimbrial adhesins in *Escherichia coli*: multiple *E. coli* fimbriae form a versatile arsenal of sugar-binding lectins potentially involved in surface-colonisation and tissue tropism. *Bioessays* 33(4):300-311.

Korhonen T, Väisänen-Rhen V, Rhen M, Pere A, Parkkinen J & Finne J (1984) *Escherichia coli* fimbriae recognizing sialyl galactosides. *Journal of Bacteriology* 159(2):762-766.

Korhonen TK, Parkkinen J, Hacker J, Finne J, Pere A, Rhen M & Holthöfer H (1986) Binding of *Escherichia coli* S fimbriae to human kidney epithelium. *Infection and Immunity* 54(2):322-327.

Kotloff KL, Nataro JP, Blackwelder WC, Nasrin D, Farag TH, Panchalingam S, Wu Y, Sow SO, Sur D, Breiman RF, Faruque AS, Zaidi AK, Saha D, Alonso PL, Tamboura B, Sanogo D, Onwuchekwa U, Manna B, Ramamurthy T, Kanungo S, Ochieng JB, Omore R, Oundo JO, Hossain A, Das SK, Ahmed S, Qureshi S, Quadri F, Adegbola RA, Antonio M, Hossain MJ, Akinsola A, Mandomando I, Nhampossa T, Acacio S, Biswas K, O'Reilly CE, Mintz ED, Berkeley LY, Muhsen K, Sommerfelt H, Robins-Browne RM & Levine MM (2013) Burden and aetiology of diarrhoeal disease in infants and young children in developing countries (the Global Enteric Multicenter Study, GEMS): a prospective, case-control study. *Lancet* 382(9888):209-222.

Kreft B, Placzek M, Doehn C, Hacker J, Schmidt G, Wasenauer G, Daha MR, Van der Woude F & Sack K (1995) S fimbriae of uropathogenic *Escherichia coli* bind to primary human renal proximal tubular epithelial cells but do not induce expression of intercellular adhesion molecule 1. *Infection and Immunity* 63(8):3235-3238.

Kulasekara HD & Blomfield IC (1999) The molecular basis for the specificity of *fimE* in the phase variation of type 1 fimbriae of *Escherichia coli* K-12. *Molecular Microbiology* 31(4):1171-1181.

La Ragione R, Cooley W & Woodward MJ (2000) The role of fimbriae and flagella in the adherence of avian strains of *Escherichia coli* O78: K80 to tissue culture cells and tracheal and gut explants. *Journal of Medical Microbiology* 49(4):327-338.

La Ragione RM & Woodward MJ (2002) Virulence factors of *Escherichia coli* serotypes associated with avian colisepticaemia. *Research in Veterinary Science* 73(1):27-35.

Lahooti M, Roesch PL & Blomfield IC (2005) Modulation of the sensitivity of FimB recombination to branched-chain amino acids and alanine in *Escherichia coli* K-12. *Journal of Bacteriology* 187(18):6273-6280.

Lamarche MG, Dozois CM, Daigle F, Caza M, Curtiss R, Dubreuil JD & Harel J (2005) Inactivation of the pst system reduces the virulence of an avian pathogenic *Escherichia coli* O78 strain. *Infection and Immunity* 73(7):4138-4145.

Lamarche MG & Harel J (2010) Membrane homeostasis requires intact *pst* in extraintestinal pathogenic *Escherichia coli*. *Current Microbiology* 60(5):356-359.

Lamarche MG, Wanner BL, Crépin S & Harel J (2008) The phosphate regulon and bacterial virulence: a regulatory network connecting phosphate homeostasis and pathogenesis. *FEMS Microbiology Reviews* 32(3):461-473.

Landgraf JR, Wu J & Calvo JM (1996) Effects of nutrition and growth rate on Lrp levels in *Escherichia coli*. *Journal of Bacteriology* 178(23):6930-6936.

Lane MC, Alteri CJ, Smith SN & Mobley HL (2007a) Expression of flagella is coincident with uropathogenic *Escherichia coli* ascension to the upper urinary tract. *Proceedings of the National Academy of Sciences* 104(42):16669-16674.

Lane MC, Lockatell V, Monterosso G, Lamphier D, Weinert J, Hebel JR, Johnson DE & Mobley HL (2005) Role of motility in the colonization of uropathogenic *Escherichia coli* in the urinary tract. *Infection and Immunity* 73(11):7644-7656.

Lane MC & Mobley HL (2007) Role of P-fimbrial-mediated adherence in pyelonephritis and persistence of uropathogenic *Escherichia coli* (UPEC) in the mammalian kidney. *Kidney International* 72(1):19-25.

Lasaro MA, Salinger N, Zhang J, Wang Y, Zhong Z, Goulian M & Zhu J (2009) F1C fimbriae play an important role in biofilm formation and intestinal colonization by the *Escherichia coli* commensal strain Nissle 1917. *Applied And Environmental Microbiology* 75(1):246-251.

Le Bouguénec C (2005) Adhesins and invasins of pathogenic *Escherichia coli*. *International Journal Of Medical Microbiology* 295(6-7):471-478.

Lemonnier M, Landraud L & Lemichez E (2007) Rho GTPase-activating bacterial toxins: from bacterial virulence regulation to eukaryotic cell biology. *FEMS Microbiology Reviews* 31(5):515-534.

Levine MM (1987) *Escherichia coli* that cause diarrhea: enterotoxigenic, enteropathogenic, enteroinvasive, enterohemorrhagic, and enteroadherent. *Journal of Infectious Diseases* 155(3):377-389.

Li Z, Bouckaert J, Deboeck F, De Greve H & Hernalsteens J-P (2012) Nicotinamide dependence of uropathogenic *Escherichia coli* UTI89 and application of *nadB* as a neutral insertion site. *Microbiology* 158(3):736-745.

Lichtenberger P & Hooton TM (2008) Complicated urinary tract infections. *Current Infectious Disease Reports* 10(6):499-504.

Lindberg S, Xia Y, Sondén B, Göransson M, Hacker J & Uhlin BE (2008) Regulatory interactions among adhesin gene systems of uropathogenic *Escherichia coli*. *Infection and Immunity* 76(2):771-780.

Liu B, Furevi A, Perepelov AV, Guo X, Cao H, Wang Q, Reeves PR, Knirel YA, Wang L & Widmalm G (2020) Structure and genetics of *Escherichia coli* O antigens. *FEMS Microbiology Reviews.* 44(6):655-683.

Livak KJ & Schmittgen TD (2001) Analysis of relative gene expression data using real-time quantitative PCR and the 2− ΔΔCT method. *Methods* 25(4):402-408.

Loepfe C, Raimann E, Stephan R & Tasara T (2010) Reduced host cell invasiveness and oxidative stress tolerance in double and triple *csp* gene family deletion mutants of *Listeria monocytogenes*. *Foodborne Pathogens And Disease* 7(7):775-783.

Loughman JA & Hunstad DA (2011) Attenuation of human neutrophil migration and function by uropathogenic bacteria. *Microbes and infection* 13(6):555-565.

Lowe MA, Holt SC & Eisenstein BI (1987) Immunoelectron microscopic analysis of elongation of type 1 fimbriae in *Escherichia coli*. *Journal of Bacteriology* 169(1):157-163.

Lucchini S, Liu H, Jin Q, Hinton JC & Yu J (2005) Transcriptional adaptation of *Shigella flexneri* during infection of macrophages and epithelial cells: insights into the strategies of a cytosolic bacterial pathogen. *Infection and Immunity* 73(1):88-102.

Luterbach CL & Mobley HL (2018) Cross talk between MarR-like transcription factors coordinates the regulation of motility in uropathogenic *Escherichia coli*. *Infection and Immunity* 86(12):e00338-00318.

Madhusudan S, Paukner A, Klingen Y & Schnetz K (2005) Independent regulation of H-NS-mediated silencing of the bgl operon at two levels: upstream by BglJ and LeuO and downstream by DnaKJ. *Microbiology* 151(10):3349-3359.

Majdalani N, Cunning C, Sledjeski D, Elliott T & Gottesman S (1998) DsrA RNA regulates translation of RpoS message by an anti-antisense mechanism, independent of its action as an antisilencer of transcription. *Proceedings of the National Academy of Sciences* 95(21):12462-12467.

Majdalani N & Gottesman S (2005) The Rcs phosphorelay: a complex signal transduction system. *Annual Review of Microbiology.* 59:379-405.

Majdalani N, Heck M, Stout V & Gottesman S (2005) Role of RcsF in signaling to the Rcs phosphorelay pathway in *Escherichia coli*. *Journal of Bacteriology* 187(19):6770-6778.

Malaviya R, Ikeda T, Ross E & Abraham SN (1996) Mast cell modulation of neutrophil influx and bacterial clearance at sites of infection through TNF-α. *Nature* 381(6577):77-80.

Manges AR, Johnson JR, Foxman B, O'Bryan TT, Fullerton KE & Riley LW (2001) Widespread distribution of urinary tract infections caused by a multidrug-resistant *Escherichia coli* clonal group. *New England Journal of Medicine* 345(14):1007-1013.

Mann R, Mediati DG, Duggin IG, Harry EJ & Bottomley AL (2017) Metabolic adaptations of uropathogenic *E. coli* in the urinary tract. *Frontiers in Cellular and Infection Microbiology* 7:241.

Maroncle NM, Sivick KE, Brady R, Stokes FE & Mobley HL (2006) Protease activity, secretion, cell entry, cytotoxicity, and cellular targets of secreted autotransporter toxin of uropathogenic *Escherichia coli*. *Infection and Immunity* 74(11):6124-6134.

Martinez JJ & Hultgren SJ (2002) Requirement of Rho-family GTPases in the invasion of Type 1-piliated uropathogenic *Escherichia coli*. *Cellular Microbiology* 4(1):19-28.

Martinez JJ, Mulvey MA, Schilling JD, Pinkner JS & Hultgren SJ (2000) Type 1 pilus-mediated bacterial invasion of bladder epithelial cells. *The EMBO Journal* 19(12):2803-2812.

Massé E & Gottesman S (2002) A small RNA regulates the expression of genes involved in iron metabolism in *Escherichia coli*. *Proceedings of the National Academy of Sciences* 99(7):4620-4625.

Massip C, Chagneau CV, Boury M & Oswald E (2020) The synergistic triad between microcin, colibactin, and salmochelin gene clusters in uropathogenic *Escherichia coli*. *Microbes and Infection*.

Matsumura K, Furukawa S, Ogihara H & Morinaga Y (2011) Roles of multidrug efflux pumps on the biofilm formation of *Escherichia coli* K-12. *Biocontrol Science* 16(2):69-72.

Matter LB, Ares MA, Abundes-Gallegos J, Cedillo ML, Yáñez JA, Martínez-Laguna Y, De la Cruz MA & Girón JA (2018) The CpxRA stress response system regulates virulence features of avian pathogenic *Escherichia coli*. *Environmental Microbiology* 20(9):3363-3377.

Mavromatis C, Bokil NJ, Totsika M, Kakkanat A, Schaale K, Cannistraci CV, Ryu T, Beatson SA, Ulett GC & Schembri MA (2015) The co-transcriptome of uropathogenic *Escherichia coli*-infected mouse macrophages reveals new insights into host–pathogen interactions. *Cellular Microbiology* 17(5):730-746.

Maxson ME & Darwin AJ (2004) Identification of inducers of the *Yersinia enterocolitica* phage shock protein system and comparison to the regulation of the RpoE and Cpx extracytoplasmic stress responses. *Journal of Bacteriology* 186(13):4199-4208.

May M, Daley AJ, Donath S & Isaacs D (2005) Early onset neonatal meningitis in Australia and New Zealand, 1992-2002. *Archives of Disease in Childhood Fetal and Neonatal Edition* 90(4):F324-327.

McClain MS, Blomfield IC, Eberhardt KJ & Eisenstein BI (1993) Inversion-independent phase variation of type 1 fimbriae in *Escherichia coli*. *Journal of Bacteriology* 175(14):4335-4344.

McDaniel TK, Jarvis KG, Donnenberg MS & Kaper JB (1995) A genetic locus of enterocyte effacement conserved among diverse enterobacterial pathogens. *Proceedings of the National Academy of Sciences* 92(5):1664-1668.

McVicker G, Sun L, Sohanpal BK, Gashi K, Williamson RA, Plumbridge J & Blomfield IC (2011) SlyA protein activates *fimB* gene expression and type 1 fimbriation in *Escherichia coli* K-12. *Journal of Biological Chemistry* 286(37):32026-32035.

Melican K, Sandoval RM, Kader A, Josefsson L, Tanner GA, Molitoris BA & Richter-Dahlfors A (2011a) Uropathogenic *Escherichia coli* P and Type 1 fimbriae act in synergy in a living host to facilitate renal colonization leading to nephron obstruction. *PLoS Pathogens* 7(2).

Mellata M, Dho-Moulin M, Dozois CM, Curtiss III R, Brown PK, Arné P, Brée A, Desautels C & Fairbrother JM (2003) Role of virulence factors in resistance of avian pathogenic *Escherichia coli* to serum and in pathogenicity. *Infection and Immunity* 71(1):536-540.

Messner KR & Imlay JA (2002) Mechanism of superoxide and hydrogen peroxide formation by fumarate reductase, succinate dehydrogenase, and aspartate oxidase. *Journal of Biological Chemistry* 277(45):42563-42571.

Miajlovic H, Cooke NM, Moran GP, Rogers TR & Smith SG (2014) Response of extraintestinal pathogenic *Escherichia coli* to human serum reveals a protective role for Rcs-regulated exopolysaccharide colanic acid. *Infection and Immunity* 82(1):298-305.

Miajlovic H & Smith SG (2014) Bacterial self-defence: how *Escherichia coli* evades serum killing. *FEMS Microbiology Letters* 354(1):1-9.

Miller HI & Friedman DI (1980) Am *E. coli* gene product required for [lambda] site-specific recombination. Cell 20(3): 711-719.

Mills M, Meysick KC & O'Brien AD (2000) Cytotoxic necrotizing factor type 1 of uropathogenic *Escherichia coli* kills cultured human uroepithelial 5637 cells by an apoptotic mechanism. *Infection and Immunity* 68(10):5869-5880.

Mo L, Zhu X-H, Huang H-Y, Shapiro E, Hasty DL & Wu X-R (2004) Ablation of the Tamm-Horsfall protein gene increases susceptibility of mice to bladder colonization by type 1-fimbriated *Escherichia coli. American Journal of Physiology-Renal Physiology* 286(4):F795-F802.

Mobley H, Green D, Trifillis A, Johnson D, Chippendale G, Lockatell C, Jones B & Warren J (1990) Pyelonephritogenic *Escherichia coli* and killing of cultured human renal proximal tubular epithelial cells: role of hemolysin in some strains. *Infection and Immunity* 58(5):1281-1289.

Mobley HL, Donnenberg MS & Hagan EC (2009) Uropathogenic *Escherichia coli. EcoSal Plus* 3(2).

Mogk A, Deuerling E, Vorderwülbecke S, Vierling E & Bukau B (2003) Small heat shock proteins, ClpB and the DnaK system form a functional triade in reversing protein aggregation. *Molecular Microbiology* 50(2):585-595.

Mora-Bau G, Platt AM, van Rooijen N, Randolph GJ, Albert ML & Ingersoll MA (2015) Macrophages subvert adaptive immunity to urinary tract infection. *PLoS Pathogens* 11(7).

Morimoto RI (2011) The heat shock response: systems biology of proteotoxic stress in aging and disease. *Cold Spring Harbor symposia on quantitative biology.* Cold Spring Harbor Laboratory Press, p 91-99.

Müller CM, Åberg A, Straseviçiene J, Emődy L, Uhlin BE & Balsalobre C (2009a) Type 1 fimbriae, a colonization factor of uropathogenic *Escherichia coli*, are controlled by the metabolic sensor CRP-cAMP. *PLoS Pathogens* 5(2):e1000303.

Mulvey MA (2002) Adhesion and entry of uropathogenic *Escherichia coli. Cellular Microbiology* 4(5):257-271.

Mulvey MA, Lopez-Boado YS, Wilson CL, Roth R, Parks WC, Heuser J & Hultgren SJ (1998) Induction and evasion of host defenses by type 1-piliated uropathogenic *Escherichia coli. Science* 282(5393):1494-1497.

Mulvey MA, Schilling JD, Martinez JJ & Hultgren SJ (2000) Bad bugs and beleaguered bladders: interplay between uropathogenic *Escherichia coli* and innate host defenses. *Proceedings of the National Academy of Sciences* 97(16):8829-8835.

MV Murthy A, Phan M-D, Peters KM, Nhu NTK, Welch RA, Ulett GC, Schembri MA & Sweet MJ (2018) Regulation of hemolysin in uropathogenic *Escherichia coli* fine-tunes killing of human macrophages. *Virulence* 9(1):967-980.

Mysorekar IU & Hultgren SJ (2006) Mechanisms of uropathogenic *Escherichia coli* persistence and eradication from the urinary tract. *Proceedings of the National Academy of Sciences* 103(38):14170-14175.

Nagy G, Altenhoefer A, Knapp O, Maier E, Dobrindt U, Blum-Oehler G, Benz R, Emody L & Hacker J (2006) Both alpha-haemolysin determinants contribute to full virulence of uropathogenic *Escherichia coli* strain 536. *Microbes and Infection* 8(8):2006-2012.

Nataro JP & Kaper JB (1998) Diarrheagenic *Escherichia coli. Clin Microbiol Rev* 11(1):142-201.

Nataro JP, Kaper JB, Robins-Browne R, Prado V, Vial P & Levine MM (1987) Patterns of adherence of diarrheagenic *Escherichia coli* to HEp-2 cells. *The Pediatric Infectious Disease Journal* 6(9):829-831.

Nathan C & Shiloh MU (2000) Reactive oxygen and nitrogen intermediates in the relationship between mammalian hosts and microbial pathogens. *Proceedings of the National Academy of Sciences* 97(16):8841-8848.

Nielubowicz GR & Mobley HL (2010) Host–pathogen interactions in urinary tract infection. *Nature Reviews Urology* 7(8):430.

Nishiyama M, Horst R, Eidam O, Herrmann T, Ignatov O, Vetsch M, Bettendorff P, Jelesarov I, Grütter MG, Wüthrich K, Glockshuber R & Capitani G (2005) Structural basis of chaperone-subunit complex recognition by the type 1 pilus assembly platform FimD. *EMBO J* 24(12):2075-2086.

Nolan LK, Horne S, Giddings C, Foley S, Johnson T, Lynne A & Skyberg J (2003) Resistance to serum complement, iss, and virulence of avian *Escherichia coli*. *Veterinary Research Communications* 27(2):101-110.

Nowicki B, Labigne A, Moseley S, Hull R, Hull S & Moulds J (1990) The Dr hemagglutinin, afimbrial adhesins AFA-I and AFA-III, and F1845 fimbriae of uropathogenic and diarrhea-associated *Escherichia coli* belong to a family of hemagglutinins with Dr receptor recognition. *Infection and Immunity* 58(1):279-281.

Nowicki B, Moulds J, Hull R & Hull S (1988a) A hemagglutinin of uropathogenic *Escherichia coli* recognizes the Dr blood group antigen. *Infection and Immunity* 56(5):1057-1060.

Nowicki B, Rhen M, Vaisanen-Rhen V, Pere A & Korhonen TK (1984) Immunofluorescence study of fimbrial phase variation in *Escherichia coli* KS71. *Journal of Bacteriology* 160(2):691-695.

Ogasawara H, Yamada K, Kori A, Yamamoto K & Ishihama A (2010) Regulation of the *Escherichia coli* csgD promoter: interplay between five transcription factors. *Microbiology* 156(8):2470-2483.

Old D & Duguid J (1970a) Selective outgrowth of fimbriate bacteria in static liquid medium. *Journal of Bacteriology* 103(2):447-456.

Olsen PB, Schembri MA, Gally DL & Klemm P (1998) Differential temperature modulation by H-NS of the *fimB* and *fimE* recombinase genes which control the orientation of the type 1 fimbrial phase switch. *FEMS Microbiology Letters* 162(1):17-23.

Orndorff PE & Falkow S (1985) Nucleotide sequence of pilA, the gene encoding the structural component of type 1 pili in *Escherichia coli*. *Journal of Bacteriology* 162(1):454-457.

Ørskov F & Ørskov I (1992) *Escherichia coli* serotyping and disease in man and animals. *Canadian Journal of Microbiology* 38(7):699-704.

Ortega ÁD, Quereda JJ, Pucciarelli MG & García-del Portillo F (2014) Non-coding RNA regulation in pathogenic bacteria located inside eukaryotic cells. *Frontiers in Cellular and Infection Microbiology* 4:162.

Oshima T, Ito K, Kabayama H & Nakamura Y (1995) Regulation of lrp gene expression by H-NS and Lrp proteins in *Escherichia coli*: dominant negative mutations in lrp. *Molecular and General Genetics MGG* 247(5):521-528.

Otto K & Hermansson M (2004) Inactivation of ompX causes increased interactions of type 1 fimbriated *Escherichia coli* with abiotic surfaces. *Journal of Bacteriology* 186(1):226-234.

Parreira VR & Gyles CL (2003) A novel pathogenicity island integrated adjacent to the thrW tRNA gene of avian pathogenic *Escherichia coli* encodes a vacuolating autotransporter toxin. *Infection and Immunity* 71(9):5087-5096.

Pátri E, Szabó E, Pál T & Emoődy L (2002) Thin aggregative fimbriae on urinary *Escherichia coli* isolates. *Genes and Proteins Underlying Microbial Urinary Tract Virulence,* Springer. p 219-224.

Pavanelo DB, Houle S, Matter LB, Dozois CM & Horn F (2018) The periplasmic trehalase affects type 1 fimbria production and virulence of extraintestinal pathogenic *Escherichia coli* strain MT78. *Infection and Immunity* 86(8):e00241-00218.

Pérez JM, Calderón IL, Arenas FA, Fuentes DE, Pradenas GA, Fuentes EL, Sandoval JM, Castro ME, Elías AO & Vásquez CC (2007) Bacterial toxicity of potassium tellurite: unveiling an ancient enigma. *PloS one* 2(2):e211.

Pesavento C, Becker G, Sommerfeldt N, Possling A, Tschowri N, Mehlis A & Hengge R (2008) Inverse regulatory coordination of motility and curli-mediated adhesion in *Escherichia coli*. *Genes & Development* 22(17):2434-2446.

Picard B, Garcia JS, Gouriou S, Duriez P, Brahimi N, Bingen E, Elion J & Denamur E (1999) The link between phylogeny and virulence in *Escherichia coli* extraintestinal infection. *Infection and Immunity* 67(2):546-553.

Pichon C, Héchard C, Du Merle L, Chaudray C, Bonne I, Guadagnini S, Vandewalle A & Le Bouguénec C (2009) Uropathogenic *Escherichia coli* AL511 requires flagellum to enter renal collecting duct cells. *Cellular Microbiology* 11(4):616-628.

Plumbridge J & Kolb A (1991) CAP and Nag repressor binding to the regulatory regions of the nagE-B and manX genes of *Escherichia coli*. *Journal of Molecular Biology* 217(4):661-679.

Plumbridge J & Vimr E (1999) Convergent pathways for utilization of the amino sugars N-acetylglucosamine, N-acetylmannosamine, and N-acetylneuraminic acid by *Escherichia coli*. *Journal of Bacteriology* 181(1):47-54.

Pohl P (1993) Les souches pathogènes d'*Escherichia coli*, histoire et classification. *Annales de Médecine Vétérinaire.* p 325-333.

Porcheron G, Garénaux A, Proulx J, Sabri M & Dozois CM (2013) Iron, copper, zinc, and manganese transport and regulation in pathogenic Enterobacteria: correlations between strains, site of infection and the relative importance of the different metal transport systems for virulence. *Frontiers in Cellular and Infection Microbiology* 3:90.

Potrykus K & Cashel M (2008) (p) ppGpp: still Magical? *Annu. Rev. Microbiol.* 62:35-51.

Pourbakhsh SA, Boulianne M, Martineau-Doizé B, Dozois CM, Desautels C & Fairbrother JM (1997) Dynamics of *Escherichia coli* infection in experimentally inoculated chickens. *Avian Diseases* :221-233.

Pratt LA & Kolter R (1998) Pratt *Molecular Microbiology* 30(2):285-293.

Price CT, Lee IR & Gustafson JE (2000) The effects of salicylate on bacteria. *The International Journal Of Biochemistry & Cell Biology* 32(10):1029-1043.

Prigent-Combaret C, Prensier G, Le Thi TT, Vidal O, Lejeune P & Dorel C (2000) Developmental pathway for biofilm formation in curli-producing *Escherichia coli* strains: role of flagella, curli and colanic acid. *Environmental Microbiology* 2(4):450-464.

Prunier A-L, Schuch R, Fernandez RE, Mumy KL, Kohler H, McCormick BA & Maurelli AT (2007) nadA and nadB of Shigella flexneri 5a are antivirulence loci responsible for the synthesis of quinolinate, a small molecule inhibitor of Shigella pathogenicity. *Microbiology* 153(7):2363-2372.

Raetz CR & Whitfield C (2002) Lipopolysaccharide endotoxins. *Annual Review of Biochemistry* 71(1):635-700.

Rama G, Chhina D, Chhina R & Sharma S (2005) Urinary tract infections—microbial virulence determinants and reactive oxygen species. *Comparative Immunology, Microbiology and Infectious Diseases* 28(5-6):339-349.

Ren D, Bedzyk L, Thomas S, Ye R & Wood TK (2004) Gene expression in *Escherichia coli* biofilms. *Applied Microbiology and Biotechnology* 64(4):515-524.

Rentschler A (2010) *In vitro analysis of OmpR regulation of the fimB and fimE genes of uropathogenic Escherichia coli*.).

Riedel CU, Casey PG, Mulcahy H, O'Gara F, Gahan CG & Hill C (2007) Construction of p16Slux, a novel vector for improved bioluminescent labeling of gram-negative bacteria. *Applied Environmental Microbiology.* 73(21):7092-7095.

Rippere-Lampe KE, O'Brien AD, Conran R & Lockman HA (2001) Mutation of the gene encoding cytotoxic necrotizing factor type 1 (cnf(1)) attenuates the virulence of uropathogenic *Escherichia coli*. *Infection and Immunity* 69(6):3954-3964.

Rodriguez GM & Atsumi S (2012) Isobutyraldehyde production from *Escherichia coli* by removing aldehyde reductase activity. *Microbial Cell Factories* 11(1):90.

Roesch PL & Blomfield IC (1998) Leucine alters the interaction of the leucine-responsive regulatory protein (Lrp) with the fim switch to stimulate site-specific recombination in *Escherichia coli*. *Molecular Microbiology* 27(4):751-761.

Römling U, Galperin MY & Gomelsky M (2013) Cyclic di-GMP: the first 25 years of a universal bacterial second messenger. *Microbiology and Molecular Biology Reviews* 77(1):1-52.

Romling U, Sierralta WD, Eriksson K & Normark S (1998) Multicellular and aggregative behaviour of *Salmonella typhimurium* strains is controlled by mutations in the agfD promoter. *Molecular Microbiology* 28(2):249-264.

Ronald A (2002) The etiology of urinary tract infection: traditional and emerging pathogens. *The American Journal of Medicine* 113(1):14-19.

Roos V & Klemm P (2006) Global gene expression profiling of the asymptomatic bacteriuria *Escherichia coli* strain 83972 in the human urinary tract. *Infection and Immunity* 74(6):3565-3575.

Rouquet G, Porcheron G, Barra C, Répérant M, Chanteloup NK, Schouler C & Gilot P (2009) A metabolic operon in extraintestinal pathogenic *Escherichia coli* promotes fitness under stressful conditions and invasion of eukaryotic cells. *Journal of Bacteriology* 191(13):4427-4440.

Rubin RH, Shapiro ED, Andriole VT, Davis RJ & Stamm WE (1992) Evaluation of new anti-infective drugs for the treatment of urinary tract infection. *Clinical Infectious Diseases* 15(Supplement_1):S216-S227.

Ruiz C & Levy SB (2010) Many chromosomal genes modulate MarA-mediated multidrug resistance in *Escherichia coli*. *Antimicrobial Agents and Chemotherapy* 54(5):2125-2134.

Ruiz C, McMurry LM & Levy SB (2008) Role of the multidrug resistance regulator MarA in global regulation of the hdeAB acid resistance operon in *Escherichia coli*. *Journal of Bacteriology* 190(4):1290-1297.

Russell PW & Orndorff PE (1992) Lesions in two *Escherichia coli* type 1 pilus genes alter pilus number and length without affecting receptor binding. *Journal of Bacteriology* 174(18):5923-5935.

Russo TA & Johnson JR (2000) Proposal for a new inclusive designation for extraintestinal pathogenic isolates of *Escherichia coli*: ExPEC. *The Journal of Infectious Diseases* 181(5):1753-1754.

Russo TA & Johnson JR (2003) Medical and economic impact of extraintestinal infections due to *Escherichia coli*: focus on an increasingly important endemic problem. *Microbes and Infection* 5(5):449-456.

Sabri M, Caza M, Proulx J, Lymberopoulos MH, Brée A, Moulin-Schouleur M, Curtiss R & Dozois CM (2008) Contribution of the SitABCD, MntH, and FeoB metal transporters to the virulence of avian pathogenic *Escherichia coli* O78 strain χ7122. *Infection and Immunity* 76(2):601-611.

Sabri M, Houle S & Dozois CM (2009) Roles of the extraintestinal pathogenic *Escherichia coli* ZnuACB and ZupT zinc transporters during urinary tract infection. *Infection and Immunity* 77(3):1155-1164.

Salscheider SL, Jahn A & Schnetz K (2013) Transcriptional regulation by BglJ–RcsB, a pleiotropic heteromeric activator in *Escherichia coli*. *Nucleic Acids Research* 42(5):2999-3008.

Sarma JV & Ward PA (2011) The complement system. *Cell and Tissue Research* 343(1):227-235.

Sauer FG, Fütterer K, Pinkner JS, Dodson KW, Hultgren SJ & Waksman G (1999) Structural basis of chaperone function and pilus biogenesis. *Science* 285(5430):1058-1061.

Sauer FG, Remaut H, Hultgren SJ & Waksman G (2004) Fiber assembly by the chaperone–usher pathway. *Biochimica et Biophysica Acta (BBA)-Molecular Cell Research* 1694(1-3):259-267.

Saulino E, Thanassi D, Pinkner J & Hultgren S (1998) Ramifications of kinetic partitioning on usher-mediated pilus biogenesis. *The EMBO Journal* 17(8):2177-2185.

Schaeffer AJ, Schwan W, Hultgren S & Duncan J (1987) Relationship of type 1 pilus expression in *Escherichia coli* to ascending urinary tract infections in mice. *Infection and Immunity* 55(2):373-380.

Schappert S & Rechtsteiner E (2011) Ambulatory medical care utilization estimates for 2007. *Vital and Health Statistics. Series 13, Data from the National Health Survey* (169):1-38.

Schembri MA, Hjerrild L, Gjermansen M & Klemm P (2003a) Differential expression of the *Escherichia coli* autoaggregation factor antigen 43. *Journal of Bacteriology* 185(7):2236-2242.

Schembri MA & Klemm P (2001) Biofilm formation in a hydrodynamic environment by novel FimH variants and ramifications for virulence. *Infection and Immunity* 69(3):1322-1328.

Schembri MA, Olsen PB & Klemm P (1998) Orientation-dependent enhancement by H-NS of the activity of the type 1 fimbrial phase switch promoter in *Escherichia coli. Molecular and General Genetics MGG* 259(3):336-344.

Schilling JD, Martin SM, Hunstad DA, Patel KP, Mulvey MA, Justice SS, Lorenz RG & Hultgren SJ (2003) CD14-and Toll-like receptor-dependent activation of bladder epithelial cells by lipopolysaccharide and type 1 piliated *Escherichia coli. Infection and Immunity* 71(3):1470-1480.

Schiwon M, Weisheit C, Franken L, Gutweiler S, Dixit A, Meyer-Schwesinger C, Pohl J-M, Maurice NJ, Thiebes S & Lorenz K (2014) Crosstalk between sentinel and helper macrophages permits neutrophil migration into infected uroepithelium. *Cell* 156(3):456-468.

Schmid B, Klumpp J, Raimann E, Loessner MJ, Stephan R & Tasara T (2009) Role of cold shock proteins in growth of Listeria monocytogenes under cold and osmotic stress conditions. *Applied and Environmental Microbiology* 75(6):1621-1627.

Scholes D, Hooton TM, Roberts PL, Gupta K, Stapleton AE & Stamm WE (2005) Risk factors associated with acute pyelonephritis in healthy women. *Ann Intern Med* 142(1):20-27.

Schwan WR (2008a) Flagella allow uropathogenic *Escherichia coli* ascension into murine kidneys. *International Journal of Medical Microbiology* 298(5-6):441-447.

Schwan WR (2011) Regulation of fim genes in uropathogenic *Escherichia coli. World Journal of Clinical Infectious Diseases* 1(1):17-25.

Schwan WR, Beck MT, Hultgren SJ, Pinkner J, Woolever NL & Larson T (2005) Down-regulation of the kps region 1 capsular assembly operon following attachment of *Escherichia coli* type 1 fimbriae to D-mannose receptors. *Infection and Immunity* 73(2):1226-1231.

Schwan WR, Beck MT, Hung CS & Hultgren SJ (2018) Differential regulation of *Escherichia coli* fim genes following binding to mannose receptors. *Journal of Pathogens* 2018.

Schwan WR & Ding H (2017) Temporal regulation of fim genes in uropathogenic *Escherichia coli* during infection of the murine urinary tract. *Journal of Pathogens* 2017.

Schwan WR, Lee JL, Lenard FA, Matthews BT & Beck MT (2002a) Osmolarity and pH growth conditions regulate *fim* gene transcription and type 1 pilus expression in uropathogenic *Escherichia coli. Infection and Immunity* 70(3):1391-1402.

Schwan WR, Seifert HS & Duncan JL (1992) Growth conditions mediate differential transcription of fim genes involved in phase variation of type 1 pili. *Journal of Bacteriology* 174(7):2367-2375.

Schwan WR, Shibata S, Aizawa S-I & Wolfe AJ (2007) The two-component response regulator RcsB regulates type 1 piliation in *Escherichia coli. Journal of Bacteriology* 189(19):7159-7163.

Servin AL (2005) Pathogenesis of Afa/Dr diffusely adhering *Escherichia coli. Clinical Microbiology Reviews* 18(2):264-292.

Shahin R, Engberg I, Hagberg L & Eden CS (1987) Neutrophil recruitment and bacterial clearance correlated with LPS responsiveness in local gram-negative infection. *The Journal of Immunology* 138(10):3475-3480.

Shivaji S, Konduri R, Ramchiary J, Jogadhenu PS, Arunasri K & Savitri S (2019) Gene targets in ocular pathogenic *Escherichia coli* for mitigation of biofilm formation to overcome antibiotic resistance. *Frontiers in Microbiology* 10:1308.

Siegenthaler RK & Christen P (2006) Tuning of DnaK chaperone action by nonnative protein sensor DnaJ and thermosensor GrpE. *Journal of Biological Chemistry* 281(45):34448-34456.

Simms AN & Mobley HL (2008a) Multiple genes repress motility in uropathogenic *Escherichia coli* constitutively expressing type 1 fimbriae. *Journal of Bacteriology* 190(10):3747-3756.

Sivick KE & Mobley HL (2010) Waging war against uropathogenic *Escherichia coli*: winning back the urinary tract. *Infection and Immunity* 78(2):568-585.

Smith YC, Rasmussen SB, Grande KK, Conran RM & O'Brien AD (2008) Hemolysin of uropathogenic *Escherichia coli* evokes extensive shedding of the uroepithelium and hemorrhage in bladder tissue within the first 24 hours after intraurethral inoculation of mice. *Infection and Immunity* 76(7):2978-2990.

Snyder JA, Haugen BJ, Buckles EL, Lockatell CV, Johnson DE, Donnenberg MS, Welch RA & Mobley HL (2004a) Transcriptome of uropathogenic *Escherichia coli* during urinary tract infection. *Infection and Immunity* 72(11):6373-6381.

Snyder JA, Haugen BJ, Lockatell CV, Maroncle N, Hagan EC, Johnson DE, Welch RA & Mobley HL (2005) Coordinate expression of fimbriae in uropathogenic *Escherichia coli*. *Infection and Immunity* 73(11):7588-7596.

Sohanpal BK, El-Labany S, Lahooti M, Plumbridge JA & Blomfield IC (2004) Integrated regulatory responses of *fimB* to N-acetylneuraminic (sialic) acid and GlcNAc in *Escherichia coli* K-12. *Proceedings of the National Academy of Sciences* 101(46):16322-16327.

Sohanpal BK, Friar S, Roobol J, Plumbridge JA & Blomfield IC (2007) Multiple co-regulatory elements and IHF are necessary for the control of *fimB* expression in response to sialic acid and N-acetylglucosamine in *Escherichia coli* K-12. *Molecular Microbiology* 63(4):1223-1236.

Song J, Bishop BL, Li G, Grady R, Stapleton A & Abraham SN (2009) TLR4-mediated expulsion of bacteria from infected bladder epithelial cells. *Proceedings of the National Academy of Sciences* 106(35):14966-14971.

Song J, Duncan MJ, Li G, Chan C, Grady R, Stapleton A & Abraham SN (2007) A novel TLR4-mediated signaling pathway leading to IL-6 responses in human bladder epithelial cells. *PLoS Pathogens* 3(4).

Spaulding CN & Hultgren SJ (2016) Adhesive pili in UTI pathogenesis and drug development. *Pathogens* 5(1):30.

Spears PA, Schauer D & Orndorff PE (1986) Metastable regulation of type 1 piliation in *Escherichia coli* and isolation and characterization of a phenotypically stable mutant. *Journal of Bacteriology* 168(1):179-185.

Spurbeck RR, Stapleton AE, Johnson JR, Walk ST, Hooton TM & Mobley HL (2011a) Fimbrial profiles predict virulence of uropathogenic *Escherichia coli* strains: contribution of ygi and yad fimbriae. *Infection and Immunity* 79(12):4753-4763.

Stamm WE & Norrby SR (2001) Urinary tract infections: disease panorama and challenges. *The Journal of infectious diseases* 183(Supplement_1):S1-S4.

Stanley P, Koronakis V & Hughes C (1998) Acylation of *Escherichia coli* hemolysin: a unique protein lipidation mechanism underlying toxin function. *Microbiology and Molecular Biology Reviews* 62(2):309-333.

Stapleton AE, Stroud MR, Hakomori SI & Stamm WE (1998) The globoseries glycosphingolipid sialosyl galactosyl globoside is found in urinary tract tissues and is a preferred binding

receptor In vitro for uropathogenic *Escherichia coli* expressing pap-encoded adhesins. *Infection and Immunity* 66(8):3856-3861.

Stentebjerg-Olesen B, Chakraborty T & Klemm P (1999) Type 1 Fimbriation and Phase Switching in a Natural*Escherichia coli fimB* Null Strain, Nissle 1917. *Journal of Bacteriology* 181(24):7470-7478.

Stentebjerg-Olesen B, Chakraborty T & Klemm P (2000a) FimE-catalyzed off-to-on inversion of the type 1 fimbrial phase switch and insertion sequence recruitment in an *Escherichia coli* K-12 *fimB* strain. *FEMS Microbiology Letters* 182(2):319-325.

Stordeur P & Mainil J (2002) La colibacillose aviaire. *Annales Medecine Veterinaire* p 11-18.

Stromberg N, Nyholm PG, Pascher I & Normark S (1991) Saccharide orientation at the cell surface affects glycolipid receptor function. *Proceedings of the National Academy of Sciences* 88(20):9340-9344.

Subashchandrabose S & Mobley HL (2015) Virulence and Fitness Determinants of Uropathogenic *Escherichia coli. Microbiology Spectrum* 3(4): UTI-0015-2012.

Subashchandrabose S, Smith SN, Spurbeck RR, Kole MM & Mobley HL (2013) Genome-wide detection of fitness genes in uropathogenic *Escherichia coli* during systemic infection. *PLoS Pathogens* 9(12):e1003788.

Sugimoto S, Arita-Morioka K-i, Terao A, Yamanaka K, Ogura T & Mizunoe Y (2018) Multitasking of Hsp70 chaperone in the biogenesis of bacterial functional amyloids. *Communications Biology* 1(1):1-14.

Tabibian JH, Gornbein J, Heidari A, Dien SL, Lau VH, Chahal P, Churchill BM & Haake DA (2008) Uropathogens and host characteristics. *Journal of Clinical Microbiology* 46(12):3980-3986.

Tenaillon O, Skurnik D, Picard B & Denamur E (2010) The population genetics of commensal *Escherichia coli. Nature Reviews Microbiology* 8(3):207.

Terlizzi ME, Gribaudo G & Maffei ME (2017) UroPathogenic *Escherichia coli* (UPEC) infections: virulence factors, bladder responses, antibiotic, and non-antibiotic antimicrobial strategies. *Frontiers in Microbiology* 8:1566.

Thomas WE, Trintchina E, Forero M, Vogel V & Sokurenko EV (2002) Bacterial adhesion to target cells enhanced by shear force. *Cell* 109(7):913-923.

Tomás JM, Ciurana B, Benedí VJ & Juarez A (1988) Role of lipopolysaccharide and complement in susceptibility of *Escherichia coli* and *Salmonella typhimurium* to non-immune serum. *Microbiology* 134(4):1009-1016.

Tritz GJ, Matney TS & Gholson RK (1970) Mapping of the nadB locus adjacent to a previously undescribed purine locus in *Escherichia coli* K-12. *Journal of Bacteriology* 102(2):377-381.

Ulett GC, Mabbett AN, Fung KC, Webb RI & Schembri MA (2007) The role of F9 fimbriae of uropathogenic *Escherichia coli* in biofilm formation. *Microbiology* 153(7):2321-2331.

Ulett GC, Totsika M, Schaale K, Carey AJ, Sweet MJ & Schembri MA (2013) Uropathogenic *Escherichia coli* virulence and innate immune responses during urinary tract infection. *Current Opinion in Microbiology* 16(1):100-107.

Umbarger HE & Brown B (1957) Threonine deamination in *Escherichia coli*. II. Evidence for two L-threonine deaminases. *Journal of Bacteriology* 73(1):105-112.

Unden G & Kleefeld A (2004) *Escherichia coli* and *Salmonella*: Cellular and Molecular Biology, eds Bock A et al. (ASM Press, Washington, DC).

Valenski ML, Harris SL, Spears PA, Horton JR & Orndorff PE (2003) The Product of the fimI gene is necessary for *Escherichia coli* type 1 pilus biosynthesis. *Journal of Bacteriology* 185(16):5007-5011.

Valore EV, Park CH, Quayle AJ, Wiles KR, McCray PB & Ganz T (1998) Human beta-defensin-1: an antimicrobial peptide of urogenital tissues. *The Journal of Clinical Investigation* 101(8):1633-1642.

Van Elsas JD, Semenov AV, Costa R & Trevors JT (2011) Survival of *Escherichia coli* in the environment: fundamental and public health aspects. *The ISME Journal* 5(2):173-183.

Vejborg RM, de Evgrafov MR, Phan MD, Totsika M, Schembri MA & Hancock V (2012) Identification of genes important for growth of asymptomatic bacteriuria *Escherichia coli* in urine. *Infection and Immunity* 80(9):3179-3188.

Venkatesh GR, Koungni FCK, Paukner A, Stratmann T, Blissenbach B & Schnetz K (2010) BglJ-RcsB heterodimers relieve repression of the *Escherichia coli* bgl operon by H-NS. *Journal of Bacteriology* 192(24):6456-6464.

Vigil PD, Stapleton AE, Johnson JR, Hooton TM, Hodges AP, He Y & Mobley HL (2011) Presence of putative repeat-in-toxin gene tosA in *Escherichia coli* predicts successful colonization of the urinary tract. *MBio* 2(3):e00066-00011.

Vila J & Soto SM (2012) Salicylate increases the expression of marA and reduces in vitro biofilm formation in uropathogenic *Escherichia coli* by decreasing type 1 fimbriae expression. *Virulence* 3(3):280-285.

Virkola R, Westerlund B, Holthofer H, Parkkinen J, Kekomaki M & Korhonen TK (1988) Binding characteristics of *Escherichia coli* adhesins in human urinary bladder. *Infection and Immunity* 56(10):2615-2622.

Vogt SL & Raivio TL (2012) Just scratching the surface: an expanding view of the Cpx envelope stress response. *FEMS Microbiology Letters* 326(1):2-11.

Waksman G & Hultgren SJ (2009) Structural biology of the chaperone-usher pathway of pilus biogenesis. *Nature Reviews Microbiology* 7(11):765-774.

Wandersman C & Stojiljkovic I (2000) Bacterial heme sources: the role of heme, hemoprotein receptors and hemophores. *Current Opinion in Microbiology* 3(2):215-220.

Wanner BL (1996) Phosphorus assimilation and control of the phosphate regulon. *Escherichia coli and Salmonella: cellular and molecular biology, 2nd ed. ASM Press, Washington, DC* 41:1357-1381.

Waters LS & Storz G (2009) Regulatory RNAs in bacteria. *Cell* 136(4):615-628.

Waters VL & Crosa JH (1991) Colicin V virulence plasmids. *Microbiology and Molecular Biology Reviews* 55(3):437-450.

Watt S, Lanotte P, Mereghetti L, Moulin-Schouleur M, Picard B & Quentin R (2003) *Escherichia coli* strains from pregnant women and neonates: intraspecies genetic distribution and prevalence of virulence factors. *Journal of Clinical Microbiology* 41(5):1929-1935.

Welch RA, Burland V, Plunkett G, 3rd, Redford P, Roesch P, Rasko D, Buckles EL, Liou SR, Boutin A, Hackett J, Stroud D, Mayhew GF, Rose DJ, Zhou S, Schwartz DC, Perna NT, Mobley HL, Donnenberg MS & Blattner FR (2002) Extensive mosaic structure revealed by the complete genome sequence of uropathogenic *Escherichia coli*. *Proceedings of the National Academy of Sciences* 99(26):17020-17024.

Whitfield C (2006) Biosynthesis and assembly of capsular polysaccharides in *Escherichia coli*.

Annual Review of Biochemistry 75:39-68.

Wiles TJ, Kulesus RR & Mulvey MA (2008a) Origins and virulence mechanisms of uropathogenic *Escherichia coli*. *Experimental and Molecular Pathology* 85(1):11-19.

Withman B, Gunasekera TS, Beesetty P, Agans R & Paliy O (2013) Transcriptional responses of uropathogenic *Escherichia coli* to increased environmental osmolality caused by salt or urea. *Infection and Immunity* 81(1):80-89.

Wright KJ, Seed PC & Hultgren SJ (2005) Uropathogenic *Escherichia coli* flagella aid in efficient urinary tract colonization. *Infection and Immunity* 73(11):7657-7668.

Wu X-R, Sun T-T & Medina JJ (1996) In vitro binding of type 1-fimbriated *Escherichia coli* to uroplakins Ia and Ib: relation to urinary tract infections. *Proceedings of the National Academy of Sciences* 93(18):9630-9635.

Wu Y & Outten FW (2009) IscR controls iron-dependent biofilm formation in *Escherichia coli* by regulating type I fimbria expression. *Journal of Bacteriology* 191(4):1248-1257.

Wülfing C & Plückthun A (1994) Protein folding in the periplasm of *Escherichia coli*. *Molecular Microbiology* 12(5):685-692.

Wullt B, Bergsten G, Connell H, Röllano P, Gebretsadik N, Hull R & Svanborg C (2000) P fimbriae enhance the early establishment of *Escherichia coli* in the human urinary tract. *Molecular Microbiology* 38(3):456-464.

Xia Y, Gally D, Forsman-Semb K & Uhlin BE (2000a) Regulatory cross-talk between adhesin operons in *Escherichia coli*: inhibition of type 1 fimbriae expression by the PapB protein. *EMBO J* 19(7):1450-1457.

Yoon S-i, Kurnasov O, Natarajan V, Hong M, Gudkov AV, Osterman AL & Wilson IA (2012) Structural basis of TLR5-flagellin recognition and signaling. *Science* 335(6070):859-864.

Zhang G, Meredith TC & Kahne D (2013) On the essentiality of lipopolysaccharide to Gram-negative bacteria. *Current Opinion in Microbiology* 16(6):779-785.

Zhao K, Liu M & Burgess RR (2005) The global transcriptional response of *Escherichia coli* to induced σ32 protein involves σ32 regulon activation followed by inactivation and degradation of σ32 in vivo. *Journal of Biological Chemistry* 280(18):17758-17768.

Zhou G, Mo W-J, Sebbel P, Min G, Neubert TA, Glockshuber R, Wu X-R, Sun T-T & Kong X-P (2001a) Uroplakin Ia is the urothelial receptor for uropathogenic *Escherichia coli*: evidence from in vitro FimH binding. *Journal of Cell Science* 114(22):4095-4103.

Zhou Z, Li X, Liu B, Beutin L, Xu J, Ren Y, Feng L, Lan R, Reeves PR & Wang L (2010) Derivation of *Escherichia coli* O157:H7 from its O55:H7 precursor. *PLoS One* 5(1):e8700.

Zuker M (2003) Mfold web server for nucleic acid folding and hybridization prediction. *Nucleic Acids Research* 31(13):3406-3415.

12   ANNEXE I Combined role of SPATES during infection

Pour cet article, j'ai participé dans les infections d'animaux et le criblage par PCR pour la présence des SPATES chez les souches UPEC et APEC. J'ai également contribué à l'analyse des données, la rédaction et la critique du manuscrit.

Three new serine-protease autotransporters of *Enterobacteriaceae* (SPATEs) from extra-intestinal pathogenic *Escherichia coli* and combined role of SPATEs for cytotoxicity and colonization of the mouse kidney

Hajer Habouria, Pravil Pokharel, Segolène Maris, Amélie Garénaux, Hicham Bessaiah, Sébastien Houle, Frédéric J. Veyrier, Stéphanie Guyomard-Rabenirina, Antoine Talarmin & Charles M. Dozois

Three new serine-protease autotransporters of *Enterobacteriaceae* (SPATEs) from extra-intestinal pathogenic *Escherichia coli* and combined role of SPATEs for cytotoxicity and colonization of the mouse kidney

Hajer Habouria, Pravil Pokharel, Segolène Maris, Amélie Garénaux, Hicham Bessaiah, Sébastien Houle, Frédéric J. Veyrier, Stéphanie Guyomard-Rabenirina, Antoine Talarmin & Charles M. Dozois

Taylor & Francis
Taylor & Francis Group

Three new serine-protease autotransporters of *Enterobacteriaceae* (SPATEs) from extra-intestinal pathogenic *Escherichia coli* and combined role of SPATEs for cytotoxicity and colonization of the mouse kidney

Hajer Habouria[*a,b], Pravil Pokharel[*a,b], Segolène Maris[a,b], Amélie Garénaux[a,b], Hicham Bessaiah[a,b], Sébastien Houle[a,b], Frédéric J. Veyrier[a,c], Stéphanie Guyomard-Rabenirina[c,d], Antoine Talarmin[c,d], and Charles M. Dozois[a,b,c]

[a]Institut national de recherche scientifique (INRS)-Institut Armand Frappier, Laval, Quebec, Canada; [b]Centre de recherche en infectiologie porcine et avicole (CRIPA); [c]Institut Pasteur International Network; [d]Unité Environnement Santé, Institut Pasteur de Guadeloupe, Les Abymes, Guadeloupe, France

ABSTRACT

Serine protease autotransporters of *Enterobacteriaceae* (SPATEs) are secreted proteins that contribute to virulence and function as proteases, toxins, adhesins, and/or immunomodulators. An extra-intestinal pathogenic *E. coli* (ExPEC) O1:K1 strain, QT598, isolated from a turkey, was shown to contain *vat, tsh*, and three uncharacterized SPATE-encoding genes. Uncharacterized SPATEs: Sha (Serine-protease hemagglutinin autotransporter), TagB and TagC (tandem autotransporter genes B and C) were tested for activities including hemagglutination, autoaggregation, and cytotoxicity when expressed in *E. coli* K-12. Sha and TagB conferred autoaggregation and hemagglutination activities. TagB, TagC, and Sha all exhibited cytopathic effects on a bladder epithelial cell line. In QT598, *tagB* and *tagC* are tandemly encoded on a genomic island, and were present in 10% of UTI isolates and 4.7% of avian *E. coli*. Sha is encoded on a virulence plasmid and was present in 1% of UTI isolates and 20% of avian *E. coli*. To specifically examine the role of SPATEs for infection, the 5 SPATE genes were deleted from strain QT598 and tested for cytotoxicity. Loss of all five SPATEs abrogated the cytopathic effect on bladder epithelial cells, although derivatives producing any of the 5 SPATEs retained cytopathic activity. In mouse infections, *sha* gene-expression was up-regulated a mean of sixfold in the bladder compared to growth *in vitro*. Loss of either *tagBC* or *sha* did not reduce urinary tract colonization. Deletion of all 5 SPATEs, however, significantly reduced competitive colonization of the kidney supporting a cumulative role of SPATEs for QT598 in the mouse UTI model.

Introduction

Escherichia coli is a common commensal of the gastrointestinal tract of mammals and birds, and is also a versatile pathogen associated with a variety of intestinal and extra-intestinal infections. Pathogenic *E. coli* belong to two main groups: intestinal pathogenic *E. coli*, and extra-intestinal pathogenic *E. coli* (ExPEC) [1,2]. Among ExPEC, the strains have been classified into pathotypes based on the sites of infection or the animal species they have infected, although these different ExPEC subgroups often share certain traits [3–8]. Such pathotypes include neonatal meningitis *E. coli* (NMEC), uropathogenic *E. coli* (UPEC), and avian pathogenic *E. coli* (APEC) [2,9,10]. Avian pathogenic *E. coli* (APEC) are a subset of ExPEC that cause respiratory infections and septicemia in poultry [4,10–12]. The genomes of a number of APEC strains and their virulence plasmids have been sequenced and share

similarities to some human ExPEC isolates and their plasmids [13–18]. The plasticity of the *E. coli* genome has led to the emergence of numerous combinations of genes that can be encoded on genomic islands or harbored on plasmids that can contribute to fitness, adaptability, and virulence of a variety of ExPEC strains [19–21].

APEC and human ExPEC strains share multiple virulence factors that promote survival and colonization of the host during extraintestinal infections. These include fimbriae, iron acquisition systems, autotransporter (AT) proteins, capsular polysaccharides, O-antigens, toxins and secretion systems [1,2,9,11,12]. Most APEC strains also contain conjugative colicin V (ColV) or similar plasmids that encode multiple virulence genes that have been shown to contribute to virulence in poultry [11,22,23], and also to urinary tract infection or systemic infection in rodent models [6,24,25]. The shared battery of virulence genes and the close phylogenetic relatedness of some

APEC and human ExPEC strains suggest that some APEC may be potential zoonotic pathogens for humans [6,7,25–28].

Among pathogenic *E. coli* virulence factors, AT proteins comprise a large family that falls into three main categories: SPATEs (Serine Protease Autotransporters of *Enterobacteriaceae*), trimeric AT proteins, and the self-associating autotransporters (SAATs), such as AIDA-1 and Antigen43 (Ag43) [29–31]. AT proteins are exported by the type V secretion system, which can be classified into 5 subgroups: Va for the monomeric autotransporters which includes SPATEs, Vb for the two-partner secretion system, Vc for the trimeric AT, Ve for the ATs that are homologous to both type Va and type Vb, and Vd for the intimins and invasins which have a reverse order of domains [32]. The export process of the AT may also require additional proteins such as the BAM and TAM assembly systems [33,34]. SPATEs consist of three specific domains: (i) a signal peptide which translocates the protein from cytoplasm to periplasm by the Sec-dependant pathway (ii) a functional passenger domain which contains a conserved serine protease motif (GDSGS), and (iii) a β-barrel domain which is localized in the outer membrane acting as a pore-forming domain that translocates the passenger domain [35]. SPATEs have been grouped into two main classes; class 1 SPATEs consist of cytotoxic proteins, whereas class 2 SPATEs represent immunomodulator proteins [32]. Certain SPATEs including the secreted autotransporter toxin (Sat), vacuolating autotransporter protein (Vat), temperature-sensitive hemagglutinin (Tsh), which has also been called hemoglobin protease (Hbp) [36], and protein involved in colonization (Pic) [37] have been previously reported in APEC and human ExPEC.

The SPATEs comprise a diverse group of autotransporter proteins that contribute to the virulence of pathogenic *E. coli* and *Shigella* spp., and other Enterobacteria [2,22,32,37–43]. Some SPATEs were shown to be important virulence factors in disseminated infection of ExPEC due to their proteolytic activity, which can promote the degradation of host cell substrates and elicit an inflammatory response [32,44]. In ExPEC, SPATE proteins have previously been characterized and have been shown to be associated with infections of both humans and other animals including poultry. SPATEs identified in uropathogenic *E. coli* include Sat [44], Vat [45,46] and PicU [41]. The *sat* gene encodes a vacuolating toxin and *sat* sequences were present in 55% of UPEC strains [40] but were not identified in a collection of APEC isolates [47]. PicU is homologous to the Pic protein identified in *Shigella* and enteroaggregative *E. coli* (EAEC) [37]. *PicU* was found in 22% of UPEC isolates [41] and 9% of APEC strains [47]. The Vat autotransporter was first discovered in APEC [45], was present in 60–70% of ExPEC from human infections

[46,48] and 33% of APEC strains [47]. The Vat toxin was shown to contribute to virulence, respiratory infection, and cellulitis in broiler chickens [45]. Both *pic* and *vat* were shown to contribute to the fitness of UPEC in a mouse model of systemic infection [43]. Tsh was the first SPATE identified in *E. coli* [49] and was shown to contribute to the development of respiratory lesions in the air sacs of chickens [22]. The *tsh* gene is located on ColV-type plasmids, was present in 50% of APEC strains [47], is less commonly associated with human ExPEC, but can be associated with certain human ExPEC strains [18,50–52].

In this report, analysis of the genome sequence of an APEC O1 strain, QT598, revealed that it contained 5 distinct SPATEs. Three of these, two chromosomally encoded SPATE genes (we name *tagB* and *tagC*) and a novel plasmid-encoded SPATE gene *(sha)* have not been previously characterized. The remaining two SPATEs were the previously characterized Vat and Tsh proteins. Herein, we have characterized the three novel SPATEs, determined their prevalence among avian and human urinary tract isolates, and investigated the role of these SPATEs for cytotoxicity and in the colonization of the murine urinary tract.

Results

Genomic analysis identifies five predicted SPATEs encoded by *E. coli* strain QT598

Strain QT598 was initially isolated from an infected turkey poult in France as MT156 [53]. It is a phylogenetic group B2 strain belonging to serogroup O1, a common serogroup among ExPEC strains causing infections in both poultry and humans. This APEC strain was sequenced initially because it contains most of the known APEC-associated virulence genes and was previously found to be virulent in one-day-old chicks [54]. QT598 belongs to sequence type (ST) 1385. Other strains belonging to ST1385 include other APEC O1 isolates, a canine urinary isolate, and environmental isolates (http://enterobase.warwick.ac.uk/). Interestingly, ST1385 strains are related to other STs including ST91, which contains some strains from human extra-intestinal infections and *E. coli* F54, an O18:K1 human fecal isolate sharing many virulence genes found in ExPEC from neonatal meningitis [55].

The genome of QT598 contains five SPATE-encoding sequences (Figure 1). Two of the SPATE genes, *tsh* and a novel SPATE which we have called *sha* (for **s**erine-protease **h**emaglutinin **a**utotransporter), are located on a ColV-type plasmid (pEC598). The *vat* gene was also identified on a genomic island. Finally, a genomic region was identified containing two distinct SPATE-encoding sequences in close proximity to each other, which we have
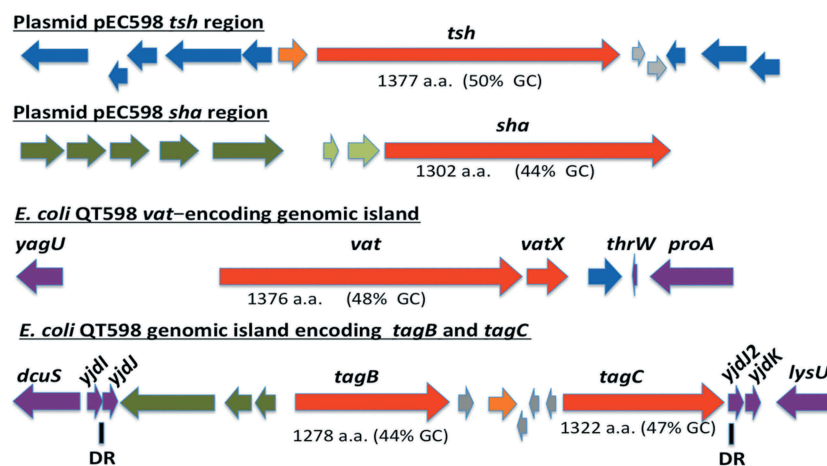
Figure 1. Regions containing the five SPATE-encoding genes in *E. coli* QT598.

The *tsh* and *sha* genes are located on a ColV-type plasmid (pEC598). The *vat*, *tagB*, and *tagC* genes are located on genomic islands. Arrows indicate open reading frames (ORFs). SPATE encoding ORFs and regulatory gene *vatX* are in red. Predicted full amino acid lengths and GC content of the SPATE ORFs are indicated below arrows. Blue ORFs are related to insertion elements, integrases, or mobile elements. Dark green ORFs are predicted fimbrial proteins. Light green ORFS are predicted EAL-domain proteins. Grey ORFS are hypothetical uncharacterized ORFs. Orange ORFs are hypothetical regulatory proteins. Purple ORFs are genes conserved in *E. coli* K-12 that border the SPATE-encoding genomic regions. Direct repeats (DR) are indicated for the region containing the *tag* AT genes.

named *tagB* and *tagC* (for **t**andem **a**utotransporter **g**enes B and C).

The *tsh* open reading frame on plasmid pEC598 shares highest identity to *tsh* from plasmid pACN001-B (accession number KC853435.1) [56] and similar sequences in the NCBI database, differing in only 1 nucleotide, a Gly_{1177}-Ser_{1177} substitution. Compared to the characterized Tsh (Hbp) proteins, Tsh from APEC strain χ7122 [22] and hemoglobin protease (Hbp) from ExPEC strain EB1 [36], Tsh_{QT598} contains 4 and 2 amino acid differences, respectively. In QT598, *tsh* is also flanked by sequences related to transposases and insertional sequences (Figure 1) that also flank *tsh* on other IncFII plasmids [22,36]. The *sha* gene is also located on pEC598 and has a 44% GC content. Sequence analysis of the *sha* gene revealed an open reading frame (ORF) of 3909 bp encoding a predicted precursor protein of 1302 amino acids with an N-terminal domain signal peptide (residues 1–51), a passenger domain (residues 52–1026) (predicted molecular mass of 105.7 kDa) containing a consensus serine protease motif ^{256}GDSGS, and β-barrel domain (residues 1027–1302). Interestingly, the highly conserved SPATE cleavage site of two consecutive asparagines "EV**NN**LNK", found between the passenger domain and the β-barrel of most SPATEs [57], is absent in Sha. Sha is more closely related to Tsh and Vat proteins than to other SPATEs (Figure 2). The global alignment of Sha with Tsh_{QT598} has 43% identity/56% similarity with 237 gaps, whereas the global alignment of Sha with Vat_{QT598} is 38% identity/52% similarity with 252 gaps.

The *vat* gene from QT598 is present on a genomic island that includes the *vatX* regulatory gene, and is located between the *E. coli* conserved genes *yagU* and *proA* adjacent to the *thrW*-tRNA gene (Figure 1). This is a conserved insertion site for *vat*-encoding genomic islands [58]. Vat_{QT598} is a predicted 1376 aa precursor with a single substitution (His_{534}-Arg_{534}) compared to Vat from UPEC strain CFT073 (accession number AAN78874.1). At least 41 predicted Vat protein sequences from different *E. coli* strains share an identical predicted Vat_{QT598} sequence, indicating it is a common allelic variant of Vat (Supplemental Table 2). These entries include sequences from strains isolated from fecal samples and infections of poultry and two human UTIs that are labeled as "Hbp" or "SepA" proteins in the databank.

The two new chromosomal-encoded SPATE genes were named *tagB* and *tagC*, **T**andem **a**utotransporter **g**enes (Tag) because of their tandem co-localization in the genome of QT598 as well as in various other *E. coli* strains such as: multidrug-resistant CTX-M-15-producing ST131 isolate *E. coli* JJ1886 (Accession number CP006784), porcine *E. coli* PCN033 (Accession number CP006632), and *E. coli* CI5 (Accession number CP011018). The *tagB* and *tagC* SPATE-encoding genes from QT598 are located on a genomic island between the *E. coli* conserved genes *yjdI* and *yjdK* (Figure 1). This genomic island has a mean GC content of 41%, which is considerably lower than the 50% GC of *E. coli*, suggesting horizontal gene transfer. This genomic region is also bordered by direct repeat (DR) sequences that correspond to duplication of *yjdJ* sequences bordering each side of the genomic island (Figure 1).
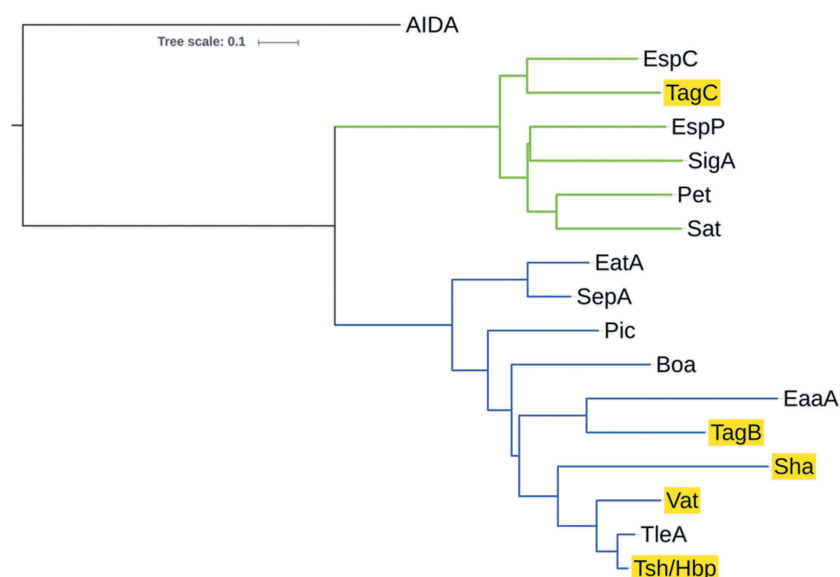
Figure 2. Phylogenetic analysis of new SPATEs identified in the QT598 genome.

The evolutionary history of passenger domains of QT598 SPATEs (highlighted in yellow) as well as other characterized SPATEs was inferred using the Neighbor-Joining method [98]. The optimal tree with the sum of branch length = 8.78918031 is shown. The tree is drawn to scale, with branch lengths in the same units as those of the evolutionary distances used to infer the phylogenetic tree. The evolutionary distances were computed using the JTT matrix-based method [99] and are in the units of the number of amino acid substitutions per site. The analysis involved 17 amino acid sequences. All positions containing gaps and missing data were eliminated. There were a total of 723 positions in the final dataset. Evolutionary analyses were conducted in MEGA6 [85]. Multiple sequence alignment was performed by Clustal W, and the tree was constructed using the Mega6 software with PhyML/bootstrapping. A cluster of cytotoxic SPATEs (class 1) comprise the green branches, while immunomodulator SPATEs (class 2) are in blue branches. DNA regions encoding SPATE protein sequences are available in NCBI database as follows: EspC, GenBank Accession No. AAC44731, TagB and TagC, MH899681; EspP, NP_052685; SigA, AF200692; Pet, SJK83553; Sat, AAG30168; EatA, CAI79539, SepA, Z48219; Pic, ALT57188; Boa, AAW66606; EaaA, AAF63237; Sha, MH899684; Vat, MH899682; TleA, KF494347; Tsh/Hbp, MH899683.

Related genomic islands containing similar SPATE encoding genes at this insertion site are present in other *E. coli* genome sequences including antibiotic-resistant strains isolated from the urinary tract and other infections in humans (Supplemental Table 3). The predicted TagB and TagC proteins share the closest identity to the EaaA [59] and EspC [60], respectively (Figure 2). TagB shares 46% identity/63% similarity to EaaA with 84 gaps over its full length. TagC shares 60% identity/74% similarity to EspC with 22 gaps. TagB comprises a predicted signal peptide (residues 1–58), a passenger domain from residues 59–1006 (predicted molecular mass of 101 kDa) containing a consensus serine protease motif ^{253}GDSGS, and a β-barrel domain from residues 1007–1283. TagC comprises a predicted signal peptide (residue 1–53), a passenger domain from residues 55–1032 (predicted molecular mass of 105.14 kDa) with a consensus serine protease motif ^{250}GDSGS, and β-barrel domain ranging between 1033 and 1309 residues. Both TagB and TagC contain the conserved twin asparagine (N-N) residues in the linker domain connecting passenger and β-barrel domains, EIN^{1006}NLNDRM and EVN^{1032}NLNKRM, respectively.

Prevalence of new SPATE genes in human uropathogenic and avian pathogenic *E. coli*

To determine the distribution of the SPATE sequences among *E. coli* clinical isolates, the presence of these three new SPATE sequences as well as *vat, sat,* and *tsh* were detected by PCR in a collection of UPEC isolates from Guadeloupe (697 isolates) [61] and from avian pathogenic *E. coli* (299 isolates) [22]. For the UPEC isolates, *tagB* sequences were present in 70 isolates (10%), whereas *tagC* sequences were present in 80 isolates (11.5%). Interestingly, 96.8% (69/70) of the *tagB*-positive isolates were also *tagC*-positive. Furthermore, 68 of the *tagB* isolates belonged to phylogenetic group B2, with one isolate from group B1 and one untypable isolate. The 11 isolates that contained *tagC* but not *tagB* sequences belonged to groups other than B2: B1 (3 isolates), D (3 isolates), F (4 isolates), or A (1 isolate). *Sha* was the least common sequence, and was present in only 6 UTI isolates (0.9%), all of which belonged to group B2 and were also *vat*-positive. Five of the *sha*-positive strains also contained *tagB* and *tagC*, whereas *vat* and *sat* sequences were more common and found in 333 isolates (47.8%) and 217 isolates (31.1%), respectively. The *tsh* gene was present in 41 UPEC isolates (5.9%). In summary, in

UPEC, *tagB* and *tagC* were found together in a subset of strains belonging to phylogenetic group B2, although some strains belonging to other phylogenetic groups were only *tagC* positive.

With regards to the APEC strains, *tagB* sequences were present in 14 isolates (4.7%) and *tagC* sequences were present in 21 isolates (7%). All 14 *tagB*-positive APEC were also *tagC*-positive, and 13/14 of these belonged to phylogenetic group B2. Among these, 10 strains belonged to serogroup O1, 1 was serogroup O78, and 3 were of undetermined serogroup. Interestingly, among the 299 APEC strains that were screened, comprised of 109 from chickens, 175 from turkeys, and 15 from ducks, all of the *tagB* or *tagC*-positive isolates were exclusively from infections in turkeys. Overall, similar to UPEC, *tagB*, and *tagC* were specifically present in a subset of APEC strains, mainly belonging to group B2, although some strains belonging to other phylogenetic groups only contained *tagC* sequences.

The *sha* sequences were present in 61 APEC strains (20%). The majority, 42 strains, belonged to phylogenetic group A, 11 strains belonged to group B1, 5 strains belonged to group B2, and 3 strains belonged to group D. Among these *sha*-containing strains, 35 belonged to serogroup O78, 3 were from serogroup O1, 2 strains each belonged to serogroups O11, O54, O21, and O8, and one belonged to serogroup O55. The remaining 12 strains were from undetermined serogroups. The *sha* gene is, therefore, clearly more prevalent among APEC than UPEC in the subset of strains we analyzed.

Cloning and production of SPATEs in culture supernatants

All five of the predicted SPATE-encoding genes and promoter regions were cloned to determine their expression and for use in a variety of phenotypic tests. Each of the five SPATE genes, when cloned into *E. coli* BL21, produced a high-molecular-weight protein (>100 kDa) in culture supernatants that corresponded to the expected product (Figure 3). In addition, derivatives of strain QT598 wherein these SPATE-encoding genes were inactivated were generated. Analysis of supernatant fractions of QT598, by SDS-PAGE, revealed the presence of SPATE proteins expressed under laboratory conditions, as demonstrated by visualization of bands with a high molecular mass (>100 kDa) secreted in the external milieu. By contrast, no such bands were observed in the supernatant extracts of the SPATE-free, Δ5ATs, derivative of QT598 (Figure 3). The purity of concentrated supernatant filtrate was also evaluated by silver staining (Supplemental Fig. S1). Protein bands of the newly identified SPATEs were extracted from gels and sampled by mass spectrometry for peptide analysis following trypsin digestion

(Supplemental Fig. S2). For Sha, peptides corresponding to the mature secreted protein spanned from amino acids 52 to 1009. Despite not containing the twin asparagine (N-N) cleavage site present in most SPATEs, peptide profiles suggest the cleavage site from the β-barrel domain likely resides within the 1010–1020 region. This region contains two adjacent polar amino acids, Ser1015 and Asp1016, that may serve as the cleavage site. For TagB, peptide scans suggest that the mature secreted protein spans from amino acids 54 to 1006 based on the twin Asp1006-Asp1007 location. For TagC, peptide scans suggest that the mature secreted protein spans from at least amino acid 60 to 1026 with a predicted twin Asp1032-Asp 1033 cleavage site. As expected, peptides corresponding to the predicted amino-terminal signal peptides and the carboxy-terminal predicted β-barrel domains of the Sha, TagB, and TagC SPATEs were not identified from peptide analysis of the secreted proteins (Supplemental Fig. S2).

## Cleavage of oligopeptides by SPATE proteins

To determine the protease substrate cleavage specificity of the new SPATEs, we used synthetic polypeptides conjugated with *p*NA at the C-terminus. Purified proteins from supernatants of each SPATE were incubated with N-Succinyl-Ala-Ala-Ala-p-nitroanilide (elastase substrate), N-Benzoyl-L-arginine 4-nitroanilide (trypsin substrate) and N-succinyl-ala-ala-pro-phe-p-nitroanilide (chymotrypsin substrate) (Sigma-Aldrich, St. Louis, MO, USA). TagB and TagC demonstrated trypsin-like activity and efficiently cleaved N-Benzoyl-L-arginine 4-nitroanilide, similarly to the EspC protein (Figure 4(a)). By contrast, Sha demonstrated significant elastase-like activity toward N-Succinyl-Ala-Ala-Ala-p-nitroanilide, as did the Vat and Tsh proteins (Figure 4(a)). The cleavage activity of high-molecular-weight supernatant fractions from WT strain QT598 and SPATE mutant derivatives was also determined (Figure 4(b)). QT598 demonstrated both trypsin-like and elastase-like activity, whereas the Δ5ATs mutant had lost these activities. By contrast, a strain which had lost only *tagBC* demonstrated only elastase-like activity conferred by *vat, tsh*, and *sha* (Figure 4(b)). In addition, pre-incubation of these supernatants with PMSF eliminated or sharply inhibited oligo-peptide cleavage indicating the activity demonstrated was due to the SPATE proteins produced by the strains (Supplemental Fig. S3)

Multiple alignment of the new autotransporters with other SPATEs places TagC within the class 1, cytotoxic and enterotoxic SPATEs, along with the EspC SPATE from Enteropathogenic *E. coli* (EPEC) (Figure 2). EspC was previously shown to cleave spectrin, Factor V, pepsin and hemoglobin [42,62] and as with TagC and TagB, similarly demonstrated trypsin-like protease activity (Figure 4(a)). The SPATE sharing closest identity to TagB
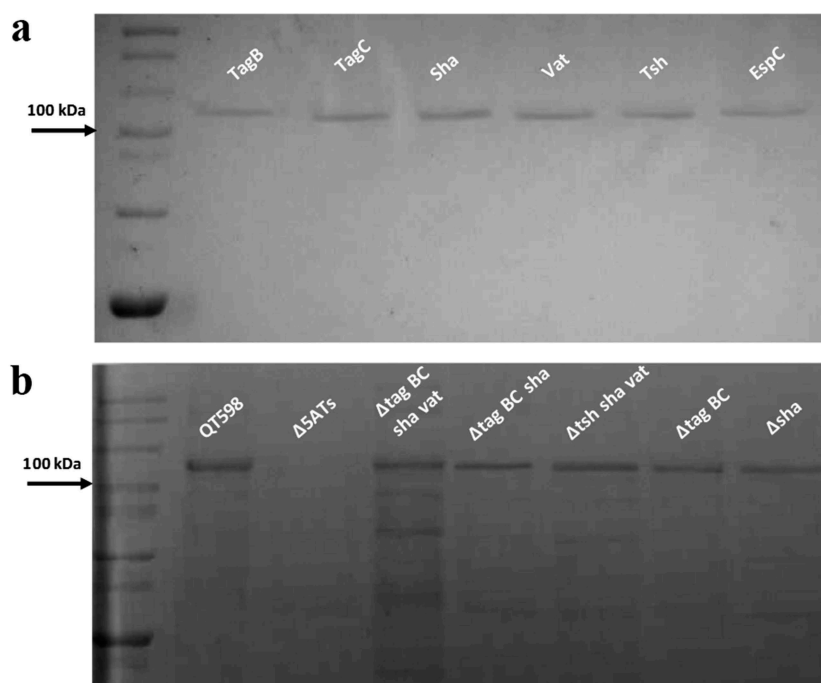
Figure 3. Detection of SPATE proteins by SDS-PAGE A. SDS-PAGE analysis of cloned SPATE genes.

a. Clones expressing SPATE proteins were produced in the BL21 background with high-copy plasmid pBCsk+. Supernatants were filtered then concentrated through Amicon filters with 50 kDa cutoff. Samples containing 5 μg protein were migrated with protein marker (10–200 kDa) and stained with Coomassie blue (arrow represents 100 kDa size marker). b. Detection of SPATEs from supernatants of strain QT598 and various SPATE gene mutant derivatives. Supernatants from an overnight culture of the respective mutants were filtered, concentrated and run on SDS-polyacrylamide gels and stained with Coomassie blue to visualize proteins.
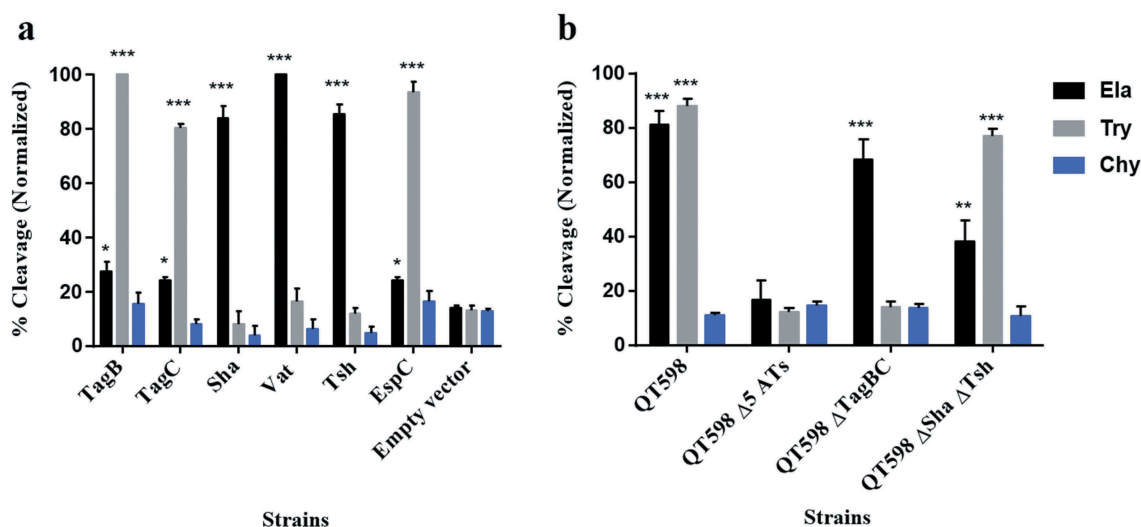
Figure 4. Oligopeptide cleavage profiles of SPATEs.

a. Enzymatic activity of cloned SPATEs. Five μg of each SPATE-containing supernatant was incubated at 37°C for 3 h with 1mM of synthetic oligopeptide specifically recognized by the following enzymatic activities: Elastase (Ela)-(N-Suc-Ala-Ala-Ala-pNA); Trypsin (Try)-(N-Ben-L-arginine-pNA); or Chymotrypsin (Chy)-(N-Suc-Ala-Ala-Pro-Phe-pNA). Absorbance at 410nm was normalized to the maximum absorbance value. b. Enzymatic activity of supernatants from strain QT598 and SPATE gene mutant derivatives. Samples were tested as described above. Data are the means of three independent experiments, and error bars represent the standard errors of the means (* $p < 0.05$, **$p < 0.01$, ***$p < 0.001$ one-way ANOVA with multiple comparisons vs pBCsk+ (A) or QT598Δ5ATs (B)).

is the class 2 SPATE EaaA, identified from commensal *E. coli* ECOR-9 [59] (Figure 2). Sha shares more identity to class 2 SPATEs Tsh/Hbp (66% identity) [36,63], TleA (60% identity) [64] and Vat (56% identity) [45]. As such, Sha is likely to share other properties more similar to Tsh (adhesin, hemagglutinin) and Vat (cytotoxin), and the elastase-like substrate specificity of Sha, also shown for Tsh and Vat, is in line with this.

To predict the 3D structure of the passenger domain of new SPATEs, we used the I-Tasser program to generate a 3D structure model and UCSF chimera to compare structures [65,66]. We found that the Sha protein is also predicted to contain the small domain 2 that was identified in Tsh/Hbp and was considered to be characteristic of class 2 SPATEs [32] (Figure 5). This domain was however absent in predicted models of TagB and TagC (Fig. S4).
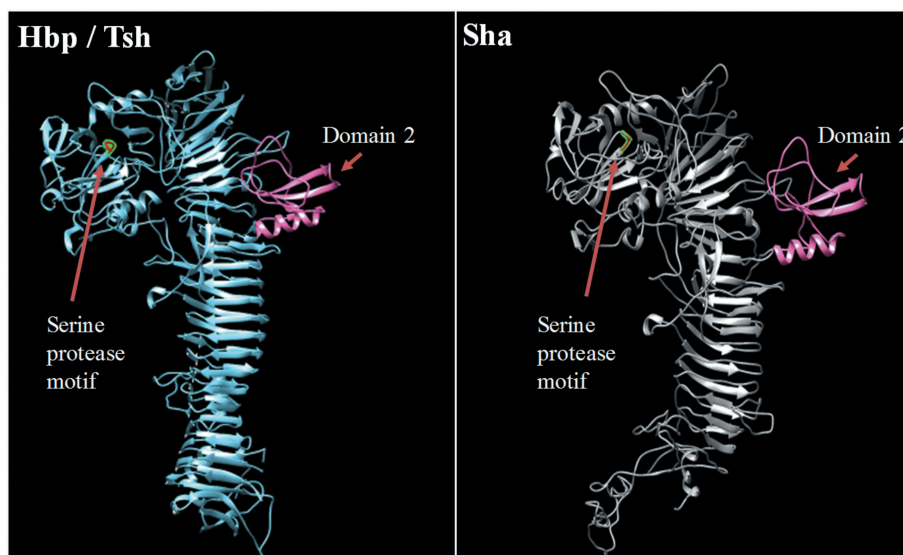
Figure 5. Stereo ribbon diagram showing the predicted three-dimensional structure of the Sha SPATE passenger domain derived from the Hbp/Tsh crystal structure.

Crystal structure of the Heme-binding protein (Hbp) (PDB 1WXR), which is near identical to Tsh, was used to model a homologous structure based on alignment with the Sha protein sequence. The model was generated using the I-TASSER server with 100.0% confidence by the single highest scoring template. Sha is shown to harbor a conserved domain, domain 2 (shown in pink), which is characteristic of class 2 SPATEs.
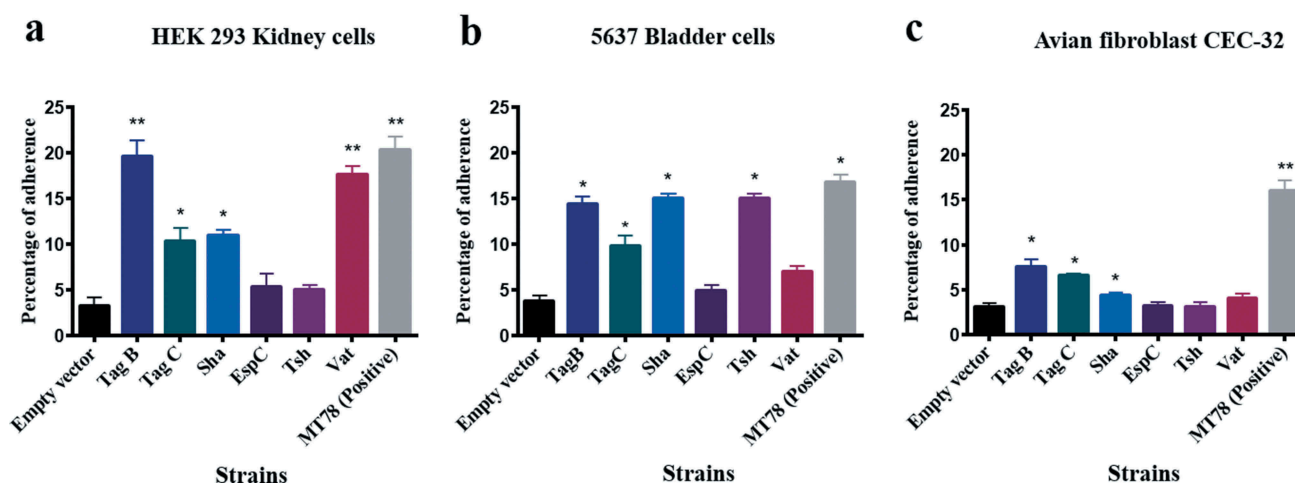
Figure 6. TagB, TagC, and Sha SPATEs promote adherence to the human kidney (HEK-293) and bladder (5637) epithelial, and avian fibroblast (CEC-32) cell lines.

Cell monolayers were infected with *E. coli* fim-negative ORN172 expressing SPATE proteins at a multiplicity of infection (MOI) of 10 and incubated at 37°C at 5% CO_2 for 2 h. Adherent bacteria were enumerated by plating on LB agar. Empty vector (pBCsk+) was used as a negative-control and APEC MT78 [80] as a positive control for adherence to cell lines. Data are the averages of three independent experiments. Error bars represent standard errors of the means. (*$p < 0.05$, **$p < 0.01$, ***$p < 0.001$ vs empty vector by one-way ANOVA).

Increased adherence to epithelial cells is mediated by SPATEs

Some AT proteins can promote adherence to host cells [31,67]. To investigate this with TagB, TagC, and Sha, the different SPATE encoding genes were cloned in the *fim*-negative *E. coli* K-12 strain ORN172 and tested for increased adherence to avian fibroblasts (CEC-32), human kidney (HEK-293) and bladder (5637) epithelial cells (Figure 6). Clones expressing either TagB, TagC, Sha, or Vat adhered significantly to kidney cells, whereas Tsh and EspC did not significantly increase adherence (Figure 6(a)). For the bladder cells, all SPATEs tested except for Vat and EspC significantly increased adherence (Figure 6(b)). By contrast, for avian fibroblasts, only TagB and TagC increased adherence (Figure 6(c)). These cell culture-based results suggest that TagB, TagC, and Sha, as well as Vat and Tsh, may contribute to host cell interactions in the urinary tract, and that TagBC may also contribute to adherence to tissues in poultry. Although some individual SPATEs were shown to increase adherence to host cells, loss of all 5 SPATEs did not reduce adherence of strain QT598 (Fig. S5).

Sha, TagB, Vat, and Tsh are hemagglutinins

Tsh has been previously shown to hemagglutinate chicken and sheep erythrocytes [22,49,68]. To assess whether other SPATEs also show hemagglutinin activity, we verified hemagglutination by the different SPATEs with erythrocytes from a variety of species. Interestingly, Sha, Tsh, and Vat all demonstrated hemagglutinin activities against sheep, bovine, pig, dog, chicken, turkey, rabbit, horse, and human blood (type O and A groups). In addition, TagB and TagC hemagglutinated sheep, bovine and pig erythrocytes, but not human, turkey, rabbit, dog, chicken, or horse erythrocytes (Table 1). However, the titer for TagC was very low for any erythrocytes tested and EspC demonstrated no hemagglutination.

TagB, TagC, and Sha mediate autoaggregation, but only Sha increases biofilm formation

Some AT proteins such as AIDA-1 and Ag43 mediate cell–cell interactions and autoaggregation, which can contribute to virulence and facilitate host cell adherence [69–71]. We observed that the absorbance of clones expressing Sha, TagB, and TagC dropped rapidly similar to the positive control AIDA-1(Figure 7(a)). An aggregative adherence pattern was also observed on interaction with bladder epithelial cell culture (Figure 7(b)). As these SPATEs demonstrated autoaggregation, we were interested to know if these plasmids could also confer autoaggregation to ExPEC QT598. However, the introduction of these plasmids did not lead to an autoaggregation phenotype in QT598 (Figure 7(a)).

Proteins involved in autoaggregation can also increase biofilm formation [69]. We, therefore, checked biofilm forming capacity of these new SPATE clones at different temperatures (25°C, 30°C, 37°C, and 42°C). TagB and TagC did not increase biofilm formation. However, Sha, Vat, and Tsh significantly increased biofilm production at lower temperatures (25°C and 30°C), but no significant differences in biofilm production were observed at higher temperatures of 37°C and 42°C (Figure 8).

### Assessment of the cytopathic effect of 5 different SPATEs on bladder cells

Since some SPATEs produce cytopathic activity on host cells, we assessed the cytopathic effect of extracts of supernatants of the different SPATEs as well as the supernatant of wild-type strain QT598 and SPATE-free Δ5ATs mutant, on the human bladder 5637 cell line. Incubation of SPATEs from concentrated filtered supernatant (Figure 3(b)) of strain QT598 with bladder cells triggered a cytopathic effect, characterized by the dissolution of cytoplasm and enlargement of the nucleus (Figure 9(a)), after 5 h of incubation. After 12 h, the majority of the cells were affected and showed similar morphological changes. These phenotypes were absent upon the treatment with the supernatant of the Δ5AT SPATE-free mutant or with culture media alone.

Further, we assessed the cytopathic effect of individual SPATEs that were from recombinant clones. Following 12 h of interaction, cells incubated with TagB or TagC proteins elicited distinct cytopathic changes including

Table 1. Hemagglutination activities of different SPATEs.

	Erythrocytes – Species (titer dilution)[a]								
SPATEs	Sheep	Bovine	Pig	Chicken	Turkey	Rabbit	Horse	Dog	Human
Vat	6	5	4	3	3	7	4	7	7
Tsh	8	7	6	7	4	7	7	7	7
Sha	6	3	5	6	4	3	3	5	5
TagB	6	3	3	-	-	-	-	-	-
TagC	0–1	1	0–1	-	0–1	-	-	-	-
EspC	-	-	-	-	-	-	-	-	-
pBCsk+ vector	-	-	-	-	-	-	-	-	-

a- Clones expressing SPATEs in *E. coli* ORN172 were adjusted to an O.D.$_{600nm}$ of 0.6 and then concentrated 100-fold. Samples were then diluted twofold in microwell plates containing final suspensions of 3% erythrocytes from different species. Titers are the average maximal dilution showing agglutination. Both human A and O blood gave similar titers. 0–1: little or no detectable agglutination. See Methods section for details.
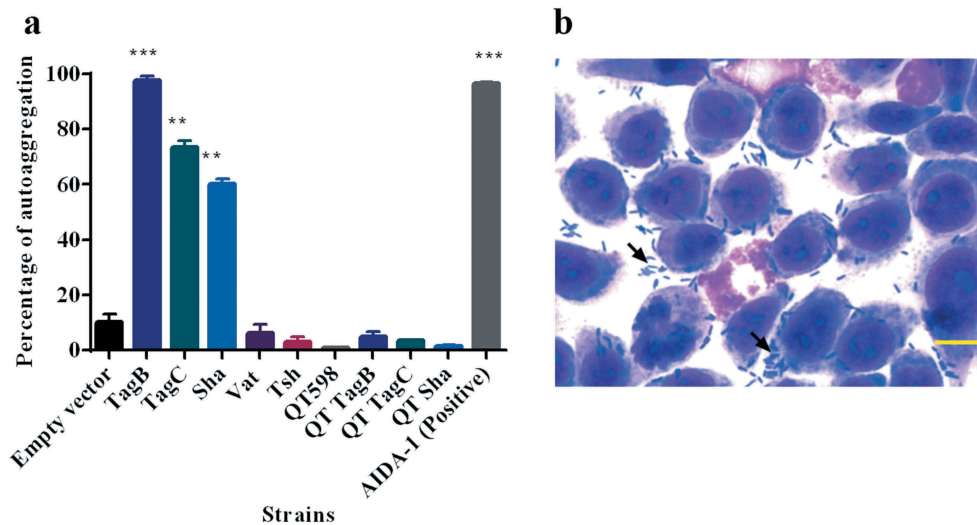
Figure 7. TagB, TagC, and Sha are autoaggregating proteins.

a. Clones of *E. coli fim*-negative strain ORN172 expressing SPATE proteins were grown 18 h and adjusted to OD_{600} of 1.5 and left to rest at 4° C. Samples were taken at 1 cm from the top surface of the cultures after 3 h to determine the change in OD_{600}. Assays were performed in triplicate, and the rate of autoaggregation was determined by the mean decrease in OD after 3 h. The autoaggregation phenotype was absent when plasmids expressing *tagB, tagC*, or *sha* were introduced into APEC strain QT598 (QT TagB, QT TagC, QT Sha respectively). Empty vector (pBCsk+) was used as a negative control and the AIDA-1 AT as a positive control for autoaggregation. Error bars represent standard errors of the means (* $p < 0.05$, **$p < 0.01$, ***$p < 0.001$ compared to empty vector using one-way ANOVA). b. Giemsa stain of the 5637 bladder cell line infected with a *tagB* expressing clone after 2 h demonstrates an aggregative adherence pattern to bladder cells (arrow head). A similar pattern was found for *tagC* and *sha* expressing clones (not shown here). Bar represents 50 μm.

dissolution of cytoplasm, nuclear enlargement and vacuolation in the nucleus, cells treated with Sha were rounded, and Vat-treated cells showed numerous vacuoles within the cytoplasm (Figure 9(b)). By contrast, cells exposed to Tsh did not show distinct morphological changes. These results suggest that TagB, TagC, Sha and Vat proteases demonstrate cytopathic effects that alter bladder cell morphology, whereas Tsh was less cytopathic to this cell line. We further investigated the cytopathic effect of these SPATEs by measuring the release of lactate dehydrogenase (LDH) after 5 h and 12 h following exposure to supernatant extracts. The release of LDH after 5 h was demonstrated only following exposure to either TagB or TagC (Figure 9(c)). Interestingly, although LDH was not
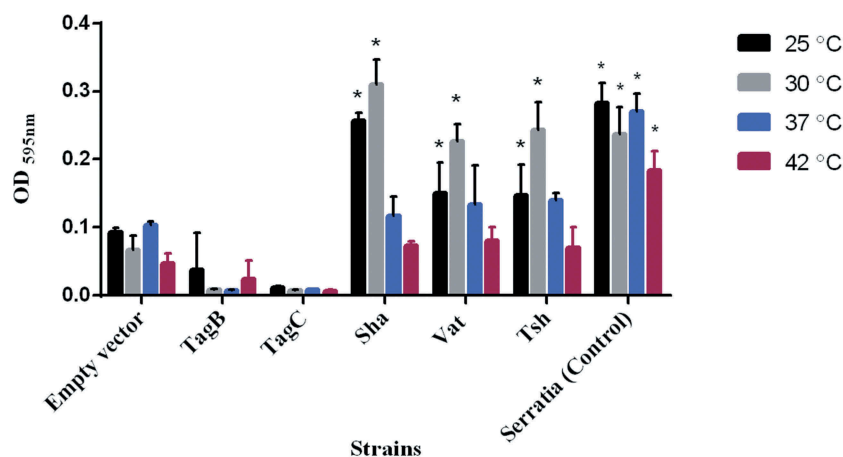
Figure 8. Sha, Vat, and Tsh promote biofilm formation.

Clones of *E. coli fim*-negative strain ORN172 expressing SPATE proteins were grown at different temperatures (25°C, 30°C, 37°C, and 42°C) in polystyrene plate wells for 48 h and then stained with crystal violet. Remaining crystal violet after washing with acetone was measured as absorbance at 595 nm. Data are the means of three independent experiments, and error bars represent standard errors of the means. Empty vector (pBCsk+) was used as a negative control, and a string biofilm producing *Serratia* strain [100] served as a positive control for biofilm formation (* $p < 0.05$, **$p < 0.01$, ***$p < 0.001$ compared to empty vector using one-way ANOVA).
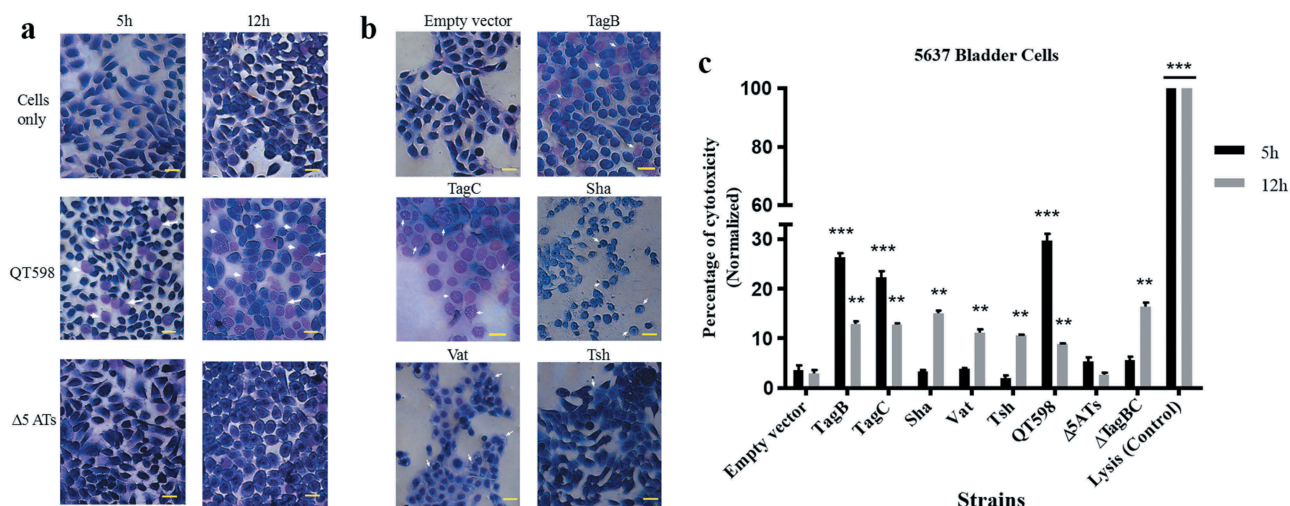
Figure 9. All five different SPATEs from strain QT598 induce cytopathic effects.

a. Concentrated supernatants (30 μg of protein per well) from wild type QT598 as well SPATE free Δ5ATs were incubated with human bladder cell line 5637 for 5 h and 12 h. Cytopathic cells (arrowheads) were found in the cells treated with QT598 supernatant while there were no morphological changes in the cells treated with supernatant of Δ5ATs. b. Concentrated supernatants of *E. coli* BL21 pBCsk+ (30 μg of protein per well) clones overexpressing different SPATEs were incubated with monolayers of 5637 bladder cell lines for 12 h at 37℃. TagB, TagC, Sha, and Vat showed more cytopathic effect (arrowheads) compared to Tsh and empty vector. c. LDH release by 5637 cells after incubation with culture filtrates of different clones (30 μg of protein per well) expressing SPATEs or from supernatants from wild-type *E. coli* strain QT598 and Δ5ATs mutant derivatives with 5637 human bladder cells at 37℃ for 5 h and 12 h. Empty vector (pBCsk+) was used as a negative control. Lysis solution was added as a positive control for maximum LDH release. Data are the means of three independent experiments, and error bars represent the standard errors of the means (* $p < 0.05$, **$p < 0.01$, ***$p < 0.001$ vs empty vector using one-way ANOVA). Bar represents 50 μm.

detected from samples exposed to Vat, Tsh and Sha after 5 h (Figure 9(c)), some LDH release was observed after 12 h of exposure, suggesting these SPATEs may demonstrate a delayed cytotoxic effect. Hence, all 5 SPATEs elicited some cytotoxicity that corresponded with cytotoxic effects that were observed in cells following Giemsa staining. Of further interest, the concentrated supernatant filtrates from ExPEC strain QT598 showed early toxicity comparable to the concentrated supernatant filtrates from *tagB* or *tagC* expressing clones. However, loss of *tagB* and *tagC* resulted in only a late onset cytotoxic effect at 12 h, and loss of all 5 SPATEs abrogated LDH release at either early or late time points (Figure 9(c)). Taken together, these results indicate TagB and TagC can mediate an early (5 h) cytotoxicity, whereas Vat, Tsh, and Sha mediate late onset (12 h) cytotoxicity, and that these 5 SPATES collectively mediate the overall cytotoxic effects of ExPEC QT598 on bladder epithelial cells.

Cumulative role of SPATEs for colonization during urinary infection in mice

In order to determine the potential role of SPATEs during UTI, we tested isogenic mutants with deletions of the *tagB, tagC,* and *sha* genes in a murine transurethral infection model. We observed no significant differences in colonization of the wild-type compared to *tagB, tagC* or *sha*

knockout mutants (Figure 10). To determine the collective role of the SPATEs in UTI for QT598, we deleted all five SPATE encoding genes and did transurethral infections. We again observed no significant difference in the colonization of kidneys or bladder following single-strain infections. By contrast, when a co-infection model was used (1 mouse died after 24 h), the Δ5ATs mutant was significantly outcompeted by the wild-type by more than 10-fold in kidneys ($p = 0.0037$) (Figure 10)

Sha gene expression is upregulated during infection in the mouse bladder

The level of expression of SPATE encoding genes from samples grown in different culture conditions as well as from infected mouse bladders was determined. All 5 SPATE genes were expressed in LB medium as well as in minimal M63-glycerol medium. Interestingly, the *vat* gene was upregulated by 10-fold in the minimal medium compared to LB. In bladder samples from infected mice, all the SPATE genes were detected and expressed during infection. Interestingly, the *sha* gene was upregulated 6-fold in the bladder (Figure 11). However, expression levels of the four other SPATE genes were not significantly different in bladders when compared to expression during culture in LB.
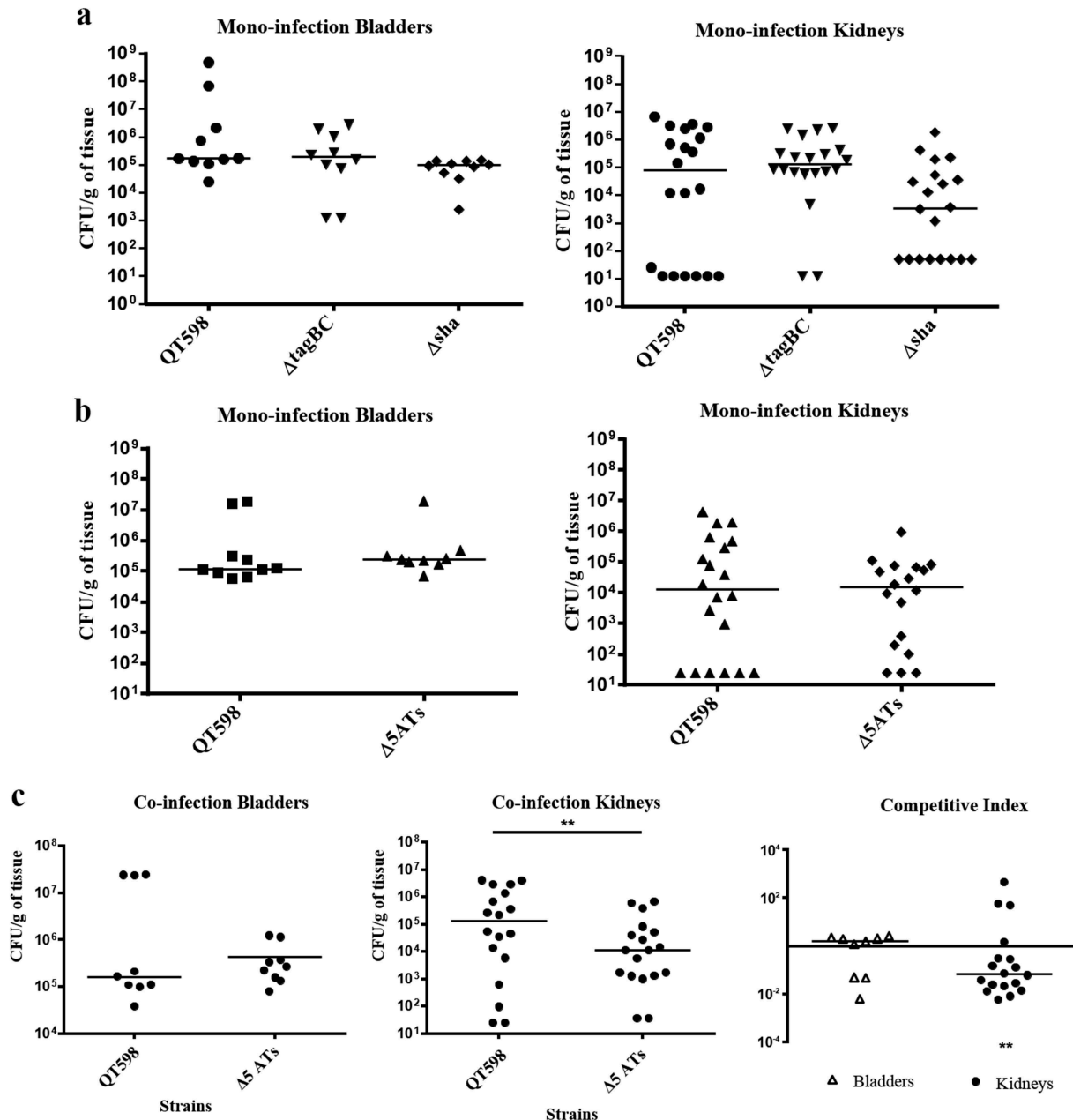
Figure 10. Role of SPATEs for *E. coli* QT598 in the murine model of ascending UTI.

CBA/J mice were challenged transurethrally with QT598 and isogenic strains ΔtagBC, Δsha, or Δ5ATs (wherein all 5 SPATE genes are inactivated). Mice were euthanized after 48 h, and bladder and kidneys were harvested for colony counts. a. Single-strain infections to compare wild-type strain QT598 to ΔtagBC, Δsha mutants. There were no significant differences in bacterial numbers in either the bladders or kidneys. b. Single-strain infections to compare wild-type strain QT598 to the Δ5ATs mutant. Similarly, there were no significant differences in colonization observed. c. Co-infection experiments between the QT598Δlac and the Δ5ATs mutant. The Δ5ATs mutant colonized the bladder at similar levels to the wild-type (Δlac) strain; however, the Δ5ATs strain was outcompeted in the kidneys by over 10-fold (Data are means ± standard errors of the means of 10 mice (* p < 0.05, ** p < 0.01, Mann–Whitney Test).

Discussion

Some pathogenic *E. coli* produce multiple SPATEs, and this may provide a greater capacity to infect different host species or tissues. Having a combination of SPATEs may also allow a reserve of functions that may include both specific and redundant functions which may importantly be differentially regulated during infection or colonization. UPEC strain CFT073 has 10 autotransporter proteins including 3 SPATEs: Sat, Vat and PicU [41]. *Shigella flexneri* also contains 3 SPATEs: SepA, Pic and SigA [37,72,73]. Similarly, *Citrobacter rodentium*, a model for A/E lesions of EPEC and Enterohemorrhagic *E. coli* (EHEC) also produces 3 SPATEs [74]. The ExPEC strain QT598 we investigated in this report produces a total of 5
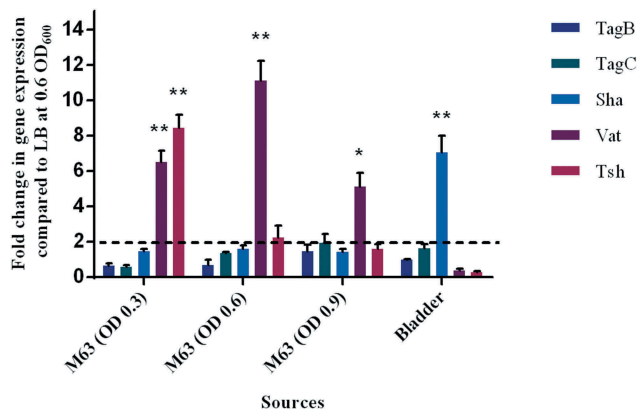
Figure 11. Differential expression of some SPATE genes occurs *in vitro* and in mouse bladder.

qRT-PCR analysis of SPATE gene transcription from QT598 strain grown in different conditions. Growth in rich medium (LB) to OD_{600} of 0.6 was used as a standard and compared to growth in M63 minimal medium (with glycerol as carbon) at different growth phases (OD_{600} of 0.3, 0.6. and 0.9). RNAs were also extracted from infected mouse bladder. Transcription of *tsh* and *vat* genes were significantly increased in minimal medium. Further, the *sha* gene was shown to be significantly upregulated in the mouse bladder. (* $p < 0.05$, ** $p < 0.01$, error bars indicate standard deviations, Student *t*-test). Expression of other SPATE genes was tested under similar conditions. See methods section for details concerning the calculation of gene expression levels. Expressions of other SPATE genes were similar under all conditions tested. The dashed line corresponds to the cutoff for a significant difference in expression.

SPATEs including three previously uncharacterized members: Sha, TagB, and TagC. Each of the 5 SPATEs demonstrated individual as well as shared properties or functions. Sha, located on a ColV-type plasmid (pEC598), is a class 2 SPATE, and it is closely related to Tsh and Vat proteins. We found this new AT has a modified cleavage site lacking twin asparagine (NN) sites between the passenger domain and the β-barrel. This absence of a typical cleavage site was also seen in *rpeA* (Rabbit-specific enteropathogenic *Escherichia coli* (REPEC) plasmid-encoded autotransporter) [75], indicating that the passenger domain is not cleaved from the outer membrane. However, in the case of Sha when cloned in BL21, a band was detected in polyacrylamide gel indicating that the modified cleavage site contributes to the separation of the passenger domain from the β-barrel.

TagB and TagC were found on a genomic island between the conserved *E. coli* genes *yjdI* and *yjdK*. Prevalence of the SPATE sequences among UPEC and APEC demonstrated that *tagB* and *tagC* sequences were present in at least 10% of the UPEC strains and that these genes were largely associated with strains belonging to phylogenetic group B2. Interestingly, genomic islands harboring *tagB* and *tagC* are also present in the genomes of

Table 2. Strains and plasmids used in this study.

Strains	Characteristic(s)	References
ORN172	thr-1 leuB thi-1Δ(argF-lac)U169 xyl-7 ara-13 mtl-2 gal-6 rpsL tonA2 supE44Δ(fimBEACDFGH)::Km pilG1	[101]
BL21	fhuA2 [lon] ompT gal [dcm] ΔhsdS	New England Biolabs
QT1603	HB101 with AIDA-1 operon	[92]
QT598	APEC O1:K, serum resistant	[53]
MT78	APEC O2:K1	[80]
QT2799	*Serratia liquefaciens*	ATCC27592
QT4567	QT598 ΔlacZYA	This study
QT4726	QT598 ΔtagBC::kan, Km^R	This study
QT5187	QT598ΔtagBC::FRT	This study
QT5188	QT598ΔtagBCΔvat::cat, Cm^R	This study
QT5189	QT598ΔtagBCΔvat::cat Δsha::kan, Cm^R Km^R	This study
QT5182	Δ5ATs or QT598ΔtagBCΔvat:: cat Δsha:: kan Δtsh::tetAR(B) Cm^R Km^R Tc^R	This study
QT5190	QT598Δsha:: kan Δtsh:: tetAR(B) Km^R Tc^R	This study
QT5191	QT598ΔtagBC Δvat:: cat Δtsh:: tetAR(B) Cm^R Km^R Tc^R	This study
QT5192	QT598Δsha:: kan Km^R	This study
QT5193	QT598Δtsh:: tetAR(B) Tc^R	This study
QT12	ORN172/pBCsk+	This study
QT4750	ORN172/pIJ551, (Expressing vat)	This study
QT4751	ORN172/pIJ552 (Expressing tsh)	This study
QT4767	ORN172/pIJ553 (Expressing sha)	This study
QT5194	BL21/pIJ548 (Expressing tagB)	This study
QT5195	BL21/pIJ549 (Expressing tagC)	This study
QT5197	BL21/pIJ550 (Expressing espC)	This study
QT5198	ORN172/pIJ548 (Expressing tagB)	This study
QT5199	ORN172/pIJ549 (Expressing tagC)	This study
QT5201	ORN172/pIJ550 (Expressing espC)	This study
QT5431	BL21/pIJ551 (Expressing vat)	This study
QT5432	BL21/pIJ552 (Expressing tsh)	This study
QT5433	BL21/pIJ553 (Expressing sha)	This study
Plasmids		
pKD3	Plasmid used for amplification of *cat* cassette	[89]
pKD4	Plasmid used for amplification of *kan* cassette	[89]
pKD13	Plasmid used for amplification of *kan* cassette	[89]
pKD46	λ Red plasmid; Amp^r	[89]
pCP20	FLP recombinase, Amp^r	[89]
pBCsk+	Cloning vector; Cm^r	Stratagene, La Jolla, CA
pIJ548	pBCsk+::tagB	This study
pIJ549	pBCsk+::tagC	This study
pIJ550	pBCsk+::espC	This study
pIJ551	pBCsk+::vat	This study
pIJ552	pBCsk+::tsh	This study
pIJ553	pBCsk+::sha	This study

numerous multi-resistant clinical isolates including members of the *E. coli* ST131 pandemic clone such as *E. coli* JJ1877 [76] and many other CTX-producing clinical isolates from urinary tract infections or sepsis (Supplemental Table 2). Further investigation into the potential role of these newly identified SPATE toxins for the virulence of such human ExPEC is therefore warranted.

Although *tagB* and *tagC* were less prevalent in APEC, the strains carrying those genes were mostly O1 strains belonging to phylogenetic group B2 and were all isolated from diseased turkeys. Although *sha* was only present in 1% of UPEC, it was present in 20% of APEC strains. As with Tsh, Sha is plasmid-encoded and these ColV-type plasmids are present in nearly all APEC but are less common in UPEC [77]. Similar phenotypes were observed for

the Tsh, Vat, and Sha autotransporters, including hemagglutination, adherence, protease activity, biofilm formation, and cytopathic effects. As such, the role of these three SPATEs may also be cumulative for some APEC strains.

We assessed the cumulative role of SPATEs in APEC strain QT598 with cell cytotoxicity assays and infection experiments in the murine UTI model. It has been shown that certain APEC strains are highly similar to human ExPEC and can belong to the same clonal groups and contain similar virulence gene profiles [2,6,9,11,12,14,24,25]. Previous reports have also tested APEC strains in the mouse UTI model [78–81]. QT598 is a serogroup O1 strain, which is a common serogroup of both APEC and human ExPEC strains, and is clonally related to some human ExPEC, further supporting verification of the role of SPATEs for this strain in a UTI model. QT598 was initially isolated from a young turkey poult and was virulent by subcutaneous infection of 1-day-old chicks. We initially tested QT598 strain in a 3-week-old chicken air sac inoculation model. However, the strain only caused very limited disease and was rapidly cleared in this model. It is possible that the strain is only able to infect very young chicks or it may be more specific for infection of turkeys than chickens. It will be of interest to investigate this in the future.

By cloning each of the SPATE encoding genes in E. coli K-12, specific activities of individual SPATEs could be determined. Protease cleavage using oligopeptides demonstrated that Sha, as well as Tsh and Vat, demonstrated elastase-like activity, whereas TagB and TagC demonstrated trypsin-like activity, similar to the EspC autotransporter (Figure 4). Oligopeptide degradation was also observed in strain QT598 with TagB and TagC being required for trypsin-like activity, whereas the Class 2 SPATEs contributed to Elastase-like activity. As such, the combination of these SPATEs provides an expanded spectrum of protease activity. However, adding a serine protease inhibitor (PMSF) to the supernatant of the SPATEs neutralized their effect on the cleavage of these oligopeptides. Further, when the catalytic site of the ATs was mutated (serine was replaced by alanine) proteolytic activity was absent, indicating that the serine protease motif is important for the activity of these SPATEs (Supplemental Fig. S3). Previously, Tsh was shown to be proteolytic to substrates including mucin and factor V, whereas EspC could cleave other proteins such as pepsin and spectrin [62]. This suggests that the combination of SPATEs produced by QT598 can target multiple substrates. It will be of interest to more specifically investigate cleavage of different host substrates by the newly characterized SPATEs Sha, TagB, and TagC to try to identify their mechanisms of

interaction with host cells. Adherence to host cell lines was also increased by the production of SPATEs. In particular, TagB, TagC, and Sha increased adherence to both human and avian epithelial cells, whereas Tsh only increased adherence to bladder cells, and Vat only increased adherence to kidney cells (Figure 6). Interestingly, in addition to promoting general adherence to host cells, TagB, TagC, and Sha also mediated bacterial aggregation, suggesting a self-associating phenotype similar to the AIDA-1 autotransporter (Figure 7). Although Tsh and Vat were less effective at general adherence to different epithelial cells, these SPATEs as well as Sha were effective hemagglutinins for erythrocytes of a variety of animal species and also demonstrated increased biofilm formation, whereas production of TagB and TagC only conferred limited hemagglutination activity (Table 2) and no increase in biofilm formation (Figure 8). It is interesting to note that some class 2 SPATEs have been shown to recognize a variety of glycans on leukocyte surfaces [82]. As similar carbohydrates may be present on erythrocyte surfaces, it is not surprising that Sha as well as Tsh and Vat autotransporters demonstrated extensive hemagglutination activity for a variety of erythrocytes. It will be of interest to further determine if these SPATEs can also recognize glycosylated surface receptors on either human or avian leukocytes that may alter host immune function.

Notably, some phenotypes such as autoaggregation, hemagglutination, and biofilm formation were only present when the genes were expressed in high-copy vectors but were absent in the clinical strain. Cloning in a higher copy vector provides a means to constitutively express proteins in vitro, whereas these proteins or systems may not always be expressed when in a single copy or on a native plasmid in the clinical strain under in vitro growth conditions. Also, in the wild-type clinical strain, there can be a great deal of redundancy of function with multiple proteins (both the autotransporters and other outer membrane proteins and fimbrial adhesins that may similarly mediate hemagglutination to different erythrocytes or adherence to host cells).

Interestingly all of the SPATEs demonstrated cytopathic effects on epithelial cells. However, the class 2 SPATEs, Vat, Tsh, and Sha, only caused delayed cell death after 12 h exposure, compared to the TagB and TagC SPATEs that demonstrated cytotoxicity within 5 h of interaction (Figure 9). Importantly, loss of all 5 of the SPATE encoding genes from QT598 was required to abrogate the cytopathic effect (Figure 9). However, the "slow acting" cytopathic effect may be due to a less directed or non-specific internalization such as pinocytosis for some of the SPATEs and since this effect only occurs after long-term 12-h exposure it may indicate that the cytotoxic capacity of these SPATEs may be limited and that the

roles of such SPATEs may be more specifically linked to other protease functions such as mucinase activity or immunomodulatory roles as has been proposed as the main function of some of the Class-2 SPATEs. Similarly, a slow effect was seen in the case of EspC, when it was internalized slowly into the cells by pinocytosis, and no receptor was required for this process [83]. Further experiments are in progress to elucidate the cytopathic effects of Sha, TagB, and TagC.

Of further note, loss of all 5 SPATEs resulted in decreased fitness in the kidneys of infected mice (Figure 10), whereas loss of individual SPATEs did not have any reduction in virulence or fitness. This suggests that collectively these SPATEs can provide a selective advantage during kidney infection for QT598 in the murine UTI model. The levels of expression of the 5 SPATEs were different depending on the growth conditions – all 5 SPATEs were expressed in LB broth, mass spectrometry results have confirmed that Tsh (48% of coverage) and Vat (22% of coverage) proteins were highly expressed compared to the other SPATE proteins. In minimal M63-glycerol medium, the *vat* gene was upregulated by 10-fold compared to LB, and the *sha* gene was upregulated six-fold in infected bladder compared to culture in LB. These results indicate that SPATE-encoding genes can be subjected to environmental changes that influence their regulation. However, other than the *vat* gene [58], there is very limited information concerning identification of factors that regulate the expression of different SPATEs.

In conclusion, we investigated the role of three new SPATEs in an APEC strain, TagB, TagC, and Sha, which were present in some APEC and UPEC strains. These SPATEs may confer fitness and capabilities to infect multiple hosts. Our findings highlight the potential role of these proteins in virulence and show they significantly contribute to autoaggregation, hemagglutination, adherence to epithelial cell lines and also exhibit cytopathic effects. Furthermore, we have shown, in combination, all five ATs contribute to fitness and colonization of QT598 during urinary tract infection in the mouse model. In future studies, it will be of interest to determine mechanisms of action of the TagB, TagC, and Sha autotransporters, identify specific targets, and determine the effects of these SPATEs on host immune responses.

Materials and methods

Strains, media, and PCR screening

Strains and plasmids are listed in Table 2. The 697 *E. coli* strains isolated from urinary tract infections were clinical isolates from Guadeloupe. Strains were collected by laboratories or hospitals over a period of 17 months and included

community or nosocomial urinary tract infection isolates [61]. The 299 APEC strains were previously described elsewhere [22]. MT156 (QT598) is an APEC serogroup O1 strain that was isolated from the liver of a young turkey poult [53]. *E. coli* DH5α, ORN172, and BL21 were used for gene cloning and phenotypic tests. Bacteria were grown at 37°C on solid or liquid Luria-Bertani medium (Alpha Bioscience, Baltimore, MD, USA) supplemented with the appropriate antibiotics when required at concentrations of 100μg/ml ampicillin, 30 μg/ml chloramphenicol, or 50 μg/ml of kanamycin. For mice infection studies, QT598 and mutant derivatives were grown in brain heart infusion broth (Alpha Bioscience). M63-glycerol minimal medium contained the following per liter: 5.3 g KH_2PO_4, 13.9 g $K_2HPO_4 \cdot 3H_2O$, and 2.0 g $(NH_4)_2SO_4$. The pH was adjusted to 7.5 with KOH, and the medium was supplemented with 1 mM $MgSO_4$, 1 mM $CaCl_2$, 1 mM thiamine, and 0.6% (wt/vol) glycerol.

Multiplex PCR was performed to determine the prevalence of different ATs within clinical isolates using primers listed in Supplemental Table 1. PCR amplification was done in a 25 μl reaction mixture containing 10 mM of primers, 1X of Taq FroggaMix (FroggaBio, Toronto, ON, Canada), DNA templates and deionized water when necessary. To detect *sat, tsh, tagB* and *tagC* genes, the reaction mixture was placed in a thermocycler (Eppendorf, Mississauga, ON, Canada) and set for initial denaturation at 95°C for 2 min followed by 30 cycle of denaturation at 95°C for 30 sec, annealing at 58°C for 40 sec and extension at 72°C for 30 sec. A final extension step was added at 72°C for 5 min. In order to detect *sha* gene, PCR was set for initial denaturation at 95°C for 2 min, 35 cycle of denaturation (95°C, 30 sec), annealing (56°C, 40 sec) and extension (72°C, 1 min), and a final extension step at 72°C for 5 min. To detect *vat* gene, PCR was set for initial denaturation at 95°C for 2 min, 30 cycle of denaturation (95°C, 30 sec), annealing (60°C, 40 sec) and extension (72°C, 30 sec), and a final extension step at 72°C for 5 min. The phylogenetic group of strains was determined by multiplexed PCR as described [84]. Amplified samples were separated by electrophoresis on 0.8% agarose gel stained with gel stain (Civic Bioscience, Beloeil, QC, Canada) and DNA was visualized using Gel Doc (Syngene Chemi Genius, Frederick, MD, USA) at 400 nm.

DNA and genetic manipulations

Plasmid DNA was extracted using the EZ DNA Miniprep kit (Bio Basic, Markham, ON, Canada). PCR products and DNA were purified using the EZ-10 Spin Column PCR Product Purification Kit (Bio Basic). DNA for SPATE-encoding genes was amplified using Q5 High Fidelity-

DNA polymerase (New England Biolabs, Whitby, ON, Canada).

Bioinformatic analysis

Presence of AT sequences *in silico* was determined in *E. coli* genomes available from the NCBI database by Blast analyses using the *tagB, tagC* and *sha* sequences from the QT598 genome. Phylogenetic analyses of the predicted full-length passenger domain sequence of each SPATE were performed by Clustal W, and the phylogenetic tree was constructed using PhyML/bootstrapping in MEGA6 [85]. The Conserved Domain Database (CDD) and SignalP were used to predict the three domains of the AT proteins [86,87]. The I-TASSER server and chimera were used for three-dimensional (3D) structure [65,66] visualization of the predicted Sha AT protein, and the Protein Data Bank (PDB) server was used to obtain the predicted 3-D structure of the Sha protein for comparison to Hbp [88]. Amino acid sequence comparisons were performed using Clone Manager Suite 7 (SciED, Denver, CO, USA) and online BLAST programs available from the National Center for Biotechnology Information (NCBI).

Construction of plasmids

AT-encoding genes were amplified by PCR using specific primers (listed in Supplemental Table 2). The *tagB, tagC, sha, vat,* and *tsh* genes were amplified from QT598. The *espC* gene was amplified from EPEC strain E2348/69 (Accession number AF297061) [60]. To clone *tagB, tagC, espC, sha, tsh,* and *vat,* PCR products contained 15 bp extensions homologous to the pBCsk+ multi-cloning site. Linearized pBCsk+ digested with *Xho*I and *Bam*HI was used to clone inserts by fusion reaction with the Quick-fusion cloning kit (Biotool, Houston, TX, USA). All the recombinant plasmids (pIJ548, pIJ549, pIJ550, pIJ551, pIJ552, pIJ553) were first transformed into *E. coli* DH5α then the plasmids were extracted using a Miniprep kit according to the manufacturer's recommendations (Bio Basic) and transformed into *E. coli* BL21 for protein expression into culture supernatants and into the *fim*-negative *E. coli* strain ORN172 for other phenotypic assays.

Mutagenesis of SPATE-encoding genes

Mutants were generated using the lambda red recombinase method [89]. The *tagBC* genes were first replaced with a kanamycin resistance cassette, from plasmid pKD13 with knock out primers: 2094 and 2095 (Supplemental Table 1). PCR products were electroporated into QT598 containing the lambda red recombinase-expressing plasmid pKD46. Deletion of the *tagB* and *tagC* was confirmed by PCR with screening primers (Supplemental Table 1). The kanamycin resistance cassette, flanked by FLP recombination target (FRT) sequences, was removed by the introduction of plasmid pCP20 expressing the FLP recombinase [90]. Then, the *vat* gene was replaced by a chloramphenicol resistance cassette amplified from pKD4 in the background QT598Δ*tagBC*::FRT (QT5187) using the same approach. Similarly, kanamycin resistance cassette amplified from plasmid pKD3 was used to replace the *sha* gene in QT598 Δ*tagBC* Δ*vat::cat* (QT5188). Finally, the *tsh* gene was replaced with a tetracycline-resistance cassette by allelic exchange as detailed in [22] in QT598 Δ*tagBC* Δ*vat::cat* Δ*sha::kan* (QT5189) generating the five SPATE genes, Δ5*ATs* mutant (QT598 Δ*tagBC* Δ*vat::cat* Δ*sha::kan* Δ*tsh::tetAR*(B)) (QT5182).

Protein preparation and analysis

Culture supernatants, from LB broth cultures of *E. coli* BL21 expressing AT proteins were centrifuged at 7500 × g for 15 min at 4°C. Supernatants were filtered through 0.22 μm filters and concentrated through 50 kDa Amicon filters (Millipore Sigma, St. Louis, MO, USA). Protein concentrations were determined using the Pierce Coomassie Plus Assay Reagent kit (Thermo Fisher Scientific, St. Laurent, QC, Canada) and proteins were visualized on SDS-PAGE by Coomassie blue as well as silver staining and identified based on the protein markers (10–200 kDa) (Bio Basic). To identify the proteins, bands were excised from denatured gels. Protein digestion by the trypsin, peptide labeling, and mass spectrometry analyses was performed by the proteomics platform of the Institut de Recherche en Immunologie et en Cancérologie (IRIC) of the Université de Montréal (Montréal, QC, Canada). The data were visualized and analyzed using Scaffold 4 Proteomics software.

Oligopeptide cleavage assays

Synthetic peptide cleavage was performed as previously described in [91] with slight modifications. Briefly, 5 μg/ml of each SPATES was added to 200 μl of three different pNA-conjugated oligopeptides: N-Succinyl-Ala-Ala-Ala-p-nitroanilide, N-Benzoyl-L-arginine 4-nitroanilide and N-succinyl-ala-ala-pro-phe-p-nitroanilide (Millipore Sigma) at 1 mM concentration in a buffer containing 0.2 M NaCl, 0.01 mM$ZnSO_4$, 0.1 M MOPS (3-(N-morpholino) propanesulfonic acid), pH 7.3 were incubated at 37°C for 3 h and absorbance readings were determined at 410 nm. Readings were normalized to the maximum absorbance of positive control. All reactions were performed in triplicate.

Autoaggregation

The autoaggregation test was carried out as described before [92]. Briefly, overnight cultures were adjusted to an OD_{600} of 1.5. A volume of 10 ml of each culture was placed in sterile 20 ml glass tubes. Tubes were then vortexed for 5 s then left at 4°C for 3 h. Samples 1 cm from the top were taken, and the percentage of change in OD_{600} was used as the value for autoaggregation.

Hemagglutination tests

Hemagglutination in microtiter plates was performed as described by [93] with some modifications. Human, chicken, turkey, pig, bovine, canine, rabbit, horse and sheep red blood cells (RBCs) were washed and resuspended in PBS at a final concentration of 3%. The E. coli fim-negative K-12 strain ORN172 expressing different SPATEs was grown overnight at 37°C in LB medium, harvested and adjusted to an optical density (O.D.$_{600}$) of 60. Suspensions were serially diluted in 96-well round bottom plates containing 20 μl of PBS mixed with 20 μl of 3% red blood cells and incubated for 30 min at 4°C.

Biofilm assay

Biofilm formation on polystyrene surfaces was assessed in 96-well plates as previously described [67]. Strains were grown at various temperatures (25°C, 30°C, 37°C, and 42°C) for 48 h under static conditions in LB medium. Wells were washed and stained with 0.1% crystal violet (Millipore Sigma) for 15 min, then 200 μl of ethanol-acetone (80:20) solution was added, followed by measuring at an optical density at OD_{595}.

Adherence assays

The 5637 human bladder cells (ATCC HTB-9), human embryonic kidney cells HEK-293 (ATCC® CRL-1573™), and the avian fibroblast cell line (CEC-32) were used to determine adherence of E. coli ORN172 expressing different SPATEs as described before [94]. The 5637 cells were maintained in RPMI 1640 (Thermo Fisher Scientific) supplemented with 10% heat-inactivated fetal bovine serum (FBS) at 37°C in 5% CO_2, and 2×10^5 cells/well were seeded into 24-well cell culture plates. Cell lines were washed twice with phosphate-buffered saline (pH 7.2) and then incubated at a multiplicity of infection (MOI) of 10 at 37°C for 2 h in RPMI 1640 medium with 10% FBS. Non-adherent bacteria were removed by washing with PBS three times. Cells were then exposed to 1% Triton X-100 for 5 min, and serial dilutions were plated on LB agar plus an antibiotic. For HEK-293 cells, Eagle's Minimum Essential Medium supplemented with 10% of FBS was used. For CEC-32 cells Dulbecco's Modified Eagle's medium supplemented with 10% of FBS was used. The adherence assays were done in triplicate for each sample.

Determination of cytopathic effects

The 5637 cells were maintained in RPMI 1640 medium (Thermo Fisher Scientific) supplemented with 10% heat-inactivated FBS at 37°C in 5% CO_2, and 2×10^5 cells/well were seeded into eight-well chamber slides (Thermo Fisher Scientific) and allowed to grow to 75% confluence. Thirty μg/ml of each SPATE (final concentration) was added directly to monolayers and incubated for 5 h or 12 h at 37°C with 5% CO_2. Cells were then washed twice with PBS (phosphate-buffered saline), fixed with 70% methanol, and stained with Giemsa stain.

Lactate dehydrogenase (LDH) release assay

Culture supernatants were incubated with monolayers of 5637 cells in RPMI 1640 supplemented with 10% heat-inactivated FBS at 37°C in 5% CO_2 for up to 12 h. Release of LDH was quantified by CytoTox 96® Non-Radioactive Cytotoxicity Assay kit (Promega, Madison, WI, USA) at 5 h and 12 h. A lysis solution (provided in the kit) was added to the non-infected cells to generate the maximum LDH release control from lysed cells.

Ascending urinary tract infection in mice

For single strain infections with the wild-type parent QT598 and isogenic SPATE mutants QT598ΔtagBC and QT598Δsha, 25 μl (10^9 CFU) were tested in an ascending UTI model adapted from [95] with 10 mice in each group. Similarly, a murine ascending UTI model with 10 mice in each group was used for co-infection, in which a virulent ΔlacZYA derivative of QT598 was co-infected with the Δ5ATs strain, a QT598-derivative lacking all 5 SPATE-encoding genes. Twenty-five μl (10^9 CFU) of a mixed culture containing equal amounts of each strain were inoculated through a catheter in six-week-old CBA/J female mice. Mice were euthanized after 48 h, and bladders and kidneys were harvested aseptically, homogenized, diluted and plated on MacConkey agar plates. Bladder samples were frozen at −80°C in TRIzol® reagent (Thermo Fisher Scientific) for RNA extraction.

qRT-PCR analysis of SPATE gene expression in vivo and in vitro

Expression of the 5 SPATE-encoding genes was determined after growth in LB medium, minimal M63

medium, and from infected mouse bladders. Total RNAs from bacterial samples were extracted in the EZ-10 Spin Column Total RNA Miniprep Kit (Bio Basic) as described elsewhere [96]. Briefly, to extract RNA from infected bladder, samples were homogenized with TRIzol® reagent (Thermo Fisher Scientific), centrifuged for 30 sec at $12,000 \times g$, the supernatant was incubated with ethanol (95–100%) and transferred into Zymo-Spin™ IICR Column to extract RNA using Direct-zol RNA Miniprep kit (Zymo Research, Irvine, CA, USA) according to the manufacturer's recommendations. All RNA samples were treated with TURBO DNase (Thermo Fisher Scientific). PCR (35 cycles) was used to verify DNA contamination. cDNAs were synthesized by using the Iscript™ Reverse transcription supermix according to the manufacturer's protocol (Bio-Rad Life Science, Mississauga, ON, Canada). The RNA polymerase sigma factor *rpoD* gene was used as a housekeeping control. Primers designed to amplify *rpoD, tagB, tagC, vat, tsh,* and *sha* (Supplemental Table 1) were used. For each sample, 50 ng of cDNA and 100 nM concentrations of each primer set were mixed with 10 µl of SsoFast Evagreen supermix (Bio-Rad Life Science) per well. Assays were performed in triplicate on a Corbett Rotorgene (Thermo Fisher Scientific) instrument. All data were normalized to *rpoD* expression levels. Melting-curve analysis was verified to differentiate accumulation of Evagreen-bound DNA and determine that signal was gene-amplification specific and not due to the primer-dimer formation. The data were analyzed by the $2^{-\Delta\Delta CT}$ method [97].

Statistical analyses

Experimental data were expressed as a mean ± standard error of the mean (SEM) in each group. The means of groups were combined and analyzed by a two-tailed Student *t*-test for pairwise comparisons and analysis of variance (ANOVA) to compare means of more than two populations. For mouse infection experiments, the Mann–Whitney test was used to compare the samples by pairs, and the Kruskal–Wallis test was used to compare groups. A *P* value of <0.05 was considered statistically significant. All data were analyzed with the Graph Pad Prism 7 software (GraphPad Software, San Diego, CA, USA).

Ethics statement

The protocol for mice urinary tract infection was approved by the animal ethics evaluation committee – *Comité Institutionel de Protection des Animaux* (CIPA No 1608–02) of the INRS-Institut Armand-Frappier.

Nucleotide accession numbers

Sections of the genome of *E. coli* strain QT598 containing the five different SPATE-encoding genes were submitted to NCBI Genbank from the analysis of whole-genome survey sequence. The corresponding accession numbers are *tsh* (MH899683), *sha* (MH899684), *vat* (MH899682), and *tagB* and *tagC* (MH899681) genetic regions.

Disclosure statement

No potential conflict of interest was reported by the authors.

References

[1] Croxen MA, Finlay BB. Molecular mechanisms of *Escherichia coli* pathogenicity. Nat Rev Microbiol. 2010;8(1):26–38.
[2] Kaper JB, Nataro JP, Mobley HL. Pathogenic *Escherichia coli*. Nature Rev Microbiol. 2004;2(2):123.
[3] Bauchart P, Germon P, Bree A, et al. Pathogenomic comparison of human extraintestinal and avian pathogenic *Escherichia coli*–search for factors involved in host specificity or zoonotic potential. Microb Pathog. 2010;49(3):105–115.
[4] Bélanger L, Garenaux A, Harel J, et al. *Escherichia coli* from animal reservoirs as a potential source of human extraintestinal pathogenic *E. coli*. FEMS Immunol Med Microbiol. 2011;62(1):1–10.
[5] Clermont O, Olier M, Hoede C, et al. Animal and human pathogenic *Escherichia coli* strains share common genetic backgrounds. Infect Genet Evol. 2011;11 (3):654–662.
[6] Ewers C, Li G, Wilking H, et al. Avian pathogenic, uropathogenic, and newborn meningitis-causing *Escherichia coli*: how closely related are they?. Int J Med Microbiol. 2007;297(3):163–176.
[7] Moulin-Schouleur M, Schouler C, Tailliez P, et al. Common virulence factors and genetic relationships between O18: K1:H7 *Escherichia coli* isolates of human and avian origin. J Clin Microbiol. 2006;44(10):3484–3492.

[8] Nandanwar N, Janssen T, Kuhl M, et al. Extraintestinal pathogenic *Escherichia coli* (ExPEC) of human and avian origin belonging to sequence type complex 95 (STC95) portray indistinguishable virulence features. Int J Med Microbiol. 2014;304(7):835–842.

[9] Johnson JR, Russo TA. Extraintestinal pathogenic *Escherichia coli*:"the other bad *E.coli*". J Lab Clin Med. 2002;139(3):155–162.

[10] Guabiraba R, Schouler C. Avian colibacillosis: still many black holes. FEMS Microbiol Lett. 2015;362(15): fnv118.

[11] Dho-Moulin M, Fairbrother JM. Avian pathogenic *Escherichia coli* (APEC). Vet Res. 1999;30 (2–3):299–316.

[12] Dziva F, Stevens MP. Colibacillosis in poultry: unravelling the molecular basis of virulence of avian pathogenic *Escherichia coli* in their natural hosts. Avian Pathol. 2008;37(4):355–366.

[13] Dziva F, Hauser H, Connor TR, et al. Sequencing and functional annotation of avian pathogenic *Escherichia coli* serogroup O78 strains reveal the evolution of *E.coli* lineages pathogenic for poultry via distinct mechanisms. Infect Immun. 2013;81(3):838–849.

[14] Johnson TJ, Kariyawasam S, Wannemuehler Y, et al. The genome sequence of avian pathogenic *Escherichia coli* strain O1: K1: H7 shares strong similarities with human extraintestinal pathogenic *E.coli* genomes. J Bacteriol. 2007;189(8):3228–3236.

[15] Johnson TJ, Nolan LK. Pathogenomics of the virulence plasmids of *Escherichia coli*. Microbiol Mol Biol Rev. 2009;73(4):750–774.

[16] Johnson TJ, Wannemuehler YM, Johnson SJ, et al. Plasmid replicon typing of commensal and pathogenic *Escherichia coli* isolates. Appl Environ Microbiol. 2007;73(6):1976–1983.

[17] Mellata M, Touchman JW, Curtiss R. Full sequence and comparative analysis of the plasmid pAPEC-1 of avian pathogenic *E.coli* chi7122 (O78: K80:H9). PLoS One. 2009;4(1):e4232.

[18] Peigne C, Bidet P, Mahjoub-Messai F, et al. The plasmid of *Escherichia coli* strain S88 (O45: K1:H7) that causes neonatal meningitis is closely related to avian pathogenic *E.coli* plasmids and is associated with high-level bacteremia in a neonatal rat meningitis model. Infect Immun. 2009;77(6):2272–2284.

[19] Cordoni G, Woodward MJ, Wu H, et al. Comparative genomics of European avian pathogenic *E.coli* (APEC). BMC Genomics. 2016;17(1):960.

[20] Leimbach A, Hacker J, Dobrindt U. *E.coli* as an all-rounder: the thin line between commensalism and pathogenicity. Curr Top Microbiol Immunol. 2013;358:3–32.

[21] Mokady D, Gophna U, Ron EZ. Extensive gene diversity in septicemic *Escherichia coli*strains. J Clin Microbiol. 2005;43(1):66–73.

[22] Dozois CM, Dho-Moulin M, Bree A, et al. Relationship between the Tsh autotransporter and pathogenicity of avian *Escherichia coli* and localization and analysis of the Tsh genetic region. Infect Immun. 2000;68 (7):4145–4154.

[23] Dozois CM, Daigle F, Curtiss R 3rd. Identification of pathogen-specific and conserved genes expressed in vivo by an avian pathogenic *Escherichia coli* strain. Proc Natl Acad Sci U S A. 2003;100(1):247–252.

[24] Johnson TJ, Johnson SJ, Nolan LK. Complete DNA sequence of a ColBM plasmid from avian pathogenic *Escherichia coli* suggests that it evolved from closely related ColV virulence plasmids. J Bacteriol. 2006;188 (16):5975–5983.

[25] Krishnan S, Chang AC, Hodges J, et al. Serotype O18 avian pathogenic and neonatal meningitis *Escherichia coli* strains employ similar pathogenic strategies for the onset of meningitis. Virulence. 2015;6(8):777–786.

[26] Johnson TJ, Wannemuehler Y, Johnson SJ, et al. Comparison of extraintestinal pathogenic *Escherichia coli* strains from human and avian sources reveals a mixed subset representing potential zoonotic pathogens. Appl Environ Microbiol. 2008;74(22):7043–7050.

[27] Mellata M. Human and avian extraintestinal pathogenic *Escherichia coli*: infections, zoonotic risks, and antibiotic resistance trends. Foodborne Pathog Dis. 2013;10 (11):916–932.

[28] Rodriguez-Siek KE, Giddings CW, Doetkott C, et al. Comparison of *Escherichia coli* isolates implicated in human urinary tract infection and avian colibacillosis. Microbiology. 2005;151(Pt 6):2097–2110.

[29] Henderson IR, Navarro-Garcia F, Nataro JP. The great escape: structure and function of the autotransporter proteins. Trends Microbiol. 1998;6(9):370–378.

[30] Klemm P, Vejborg RM, Sherlock O. Self-associating autotransporters, SAATs: functional and structural similarities. Int J Med Microbiol. 2006;296(4–5):187–195.

[31] Wells TJ, Totsika M, Schembri MA. Autotransporters of *Escherichia coli*: a sequence-based characterization. Microbiology. 2010;156(8):2459–2469.

[32] Ruiz-Perez F, Nataro JP. Bacterial serine proteases secreted by the autotransporter pathway: classification, specificity, and role in virulence. Cell Mol Life Sci. 2014;71(5):745–770.

[33] Albenne C, Ieva R. Job contenders: roles of the beta-barrel assembly machinery and the translocation and assembly module in autotransporter secretion. Mol Microbiol. 2017;106(4):505–517.

[34] Bernstein HD. Looks can be deceiving: recent insights into the mechanism of protein secretion by the autotransporter pathway. Mol Microbiol. 2015;97(2):205–215.

[35] Henderson IR, Navarro-Garcia F, Desvaux M, et al. Type V protein secretion pathway: the autotransporter story. Microbiol Mol Biol Rev. 2004;68(4):692–744.

[36] Otto BR, Van Dooren SJ, Nuijens JH, et al. Characterization of a hemoglobin protease secreted by the pathogenic *Escherichia coli* strain EB1. J Exp Med. 1998;188(6):1091–1103.

[37] Henderson IR, Czeczulin J, Eslava C, et al. Characterization of Pic, a Secreted Protease of *Shigella flexneri* and Enteroaggregative *Escherichia coli*. Infect Immun. 1999;67(11):5587–5596.

[38] Brunder W, Schmidt H, Karch H. EspP, a novel extracellular serine protease of enterohaemorrhagic *Escherichia coli* O157: H7 cleaves human coagulation factor V. Mol Microbiol. 1997;24(4):767–778.

[39] Eslava C, Navarro-García F, Czeczulin JR, et al. Pet, an autotransporter enterotoxin from enteroaggregative *Escherichia coli*. Infect Immun. 1998;66(7):3155–3163.

[40] Guyer DM, Henderson IR, Nataro JP, et al. Identification of sat, an autotransporter toxin produced by uropathogenic *Escherichia coli*. Mol Microbiol. 2000;38(1):53–66.

[41] Parham NJ, Srinivasan U, Desvaux M, et al. PicU, a second serine protease autotransporter of uropathogenic *Escherichia coli*. FEMS Microbiol Lett. 2004;230(1):73–83.

[42] Stein M, Kenny B, Stein MA, et al. Characterization of EspC, a 110-kilodalton protein secreted by enteropathogenic *Escherichia coli* which is homologous to members of the immunoglobulin A protease-like family of secreted proteins. J Bacteriol. 1996;178(22):6546–6554.

[43] Subashchandrabose S, Smith SN, Spurbeck RR, et al. Genome-wide detection of fitness genes in uropathogenic *Escherichia coli* during systemic infection. PLoS Pathog. 2013;9(12):e1003788.

[44] Guyer DM, Radulovic S, Jones F-E, et al. Sat, the secreted autotransporter toxin of uropathogenic *Escherichia coli*, is a vacuolating cytotoxin for bladder and kidney epithelial cells. Infect Immun. 2002;70(8):4539–4546.

[45] Parreira VR, Gyles CL. A novel pathogenicity island integrated adjacent to the *thrW* tRNA gene of avian pathogenic *Escherichia coli* encodes a vacuolating autotransporter toxin. Infect Immun. 2003;71(9):5087–5096.

[46] Parham NJ, Pollard SJ, Desvaux M, et al. Distribution of the serine protease autotransporters of the Enterobacteriaceae among extraintestinal clinical isolates of *Escherichia coli*. J Clin Microbiol. 2005;43(8):4076–4082.

[47] Restieri C, Garriss G, Locas MC, et al. Autotransporter-encoding sequences are phylogenetically distributed among *Escherichia coli* clinical isolates and reference strains. Appl Environ Microbiol. 2007;73(5):1553–1562.

[48] Spurbeck RR, Dinh PC Jr., Walk ST, et al. *Escherichia coli* isolates that carry *vat*, *fyuA*, *chuA*, and *yfcV* efficiently colonize the urinary tract. Infect Immun. 2012;80(12):4115–4122.

[49] Provence DL, Curtiss R. Isolation and characterization of a gene involved in hemagglutination by an avian pathogenic *Escherichia coli* strain. Infect Immun. 1994;62(4):1369–1380.

[50] Cyoia PS, Rodrigues GR, Nishio EK, et al. Presence of virulence genes and pathogenicity islands in extraintestinal pathogenic *Escherichia coli* isolates from Brazil. J Infect Dev Ctries. 2015;9(10):1068–1075.

[51] Maluta RP, Logue CM, Casas MR, et al. Overlapped sequence types (STs) and serogroups of avian pathogenic (APEC) and human extra-intestinal pathogenic (ExPEC) *Escherichia coli* isolated in Brazil. PLoS One. 2014;9(8):e105016.

[52] Otto BR, van Dooren SJ, Dozois CM, et al. *Escherichia coli* hemoglobin protease autotransporter contributes to synergistic abscess formation and heme-dependent growth of *Bacteroides fragilis*. Infect Immun. 2002;70(1):5–10.

[53] Marc D, Dho-Moulin M. Analysis of the *fim* cluster of an avian O2 strain of *Escherichia coli*: serogroup-specific sites within *fimA* and nucleotide sequence of *fimI*. J Med Microbiol. 1996;44(6):444–452.

[54] Dozois CM, Fairbrother JM, Harel J, et al. *pap*-and *pil*-related DNA sequences and other virulence determinants associated with *Escherichia coli* isolated from septicemic chickens and turkeys. Infect Immun. 1992;60(7):2648–2656.

[55] Dobrindt U, Agerer F, Michaelis K, et al. Analysis of genome plasticity in pathogenic and commensal *Escherichia coli* isolates by use of DNA arrays. J Bacteriol. 2003;185(6):1831–1840.

[56] Wang X, Wei L, Wang B, et al. Complete genome sequence and characterization of avian pathogenic *Escherichia coli* field isolate ACN001. Stand Genomic Sci. 2016;11:13.

[57] Kostakioti M, Stathopoulos C. Role of the alpha-helical linker of the C-terminal translocator in the biogenesis of the serine protease subfamily of autotransporters. Infect Immun. 2006;74(9):4961–4969.

[58] Nichols KB, Totsika M, Moriel DG, et al. Molecular characterization of the vacuolating autotransporter Toxin in Uropathogenic *Escherichia coli*. J Bacteriol. 2016;198(10):1487–1498.

[59] Sandt CH, Hill CW. Four Different Genes Responsible for Nonimmune Immunoglobulin-Binding Activities within a Single Strain of *Escherichia coli*. Infect Immun. 2000;68(4):2205–2214.

[60] Mellies JL, Navarro-Garcia F, Okeke I, et al. espC pathogenicity island of enteropathogenic *Escherichia coli* encodes an enterotoxin. Infect Immun. 2001;69(1):315–324.

[61] Guyomard-Rabenirina S, Malespine J, Ducat C, et al. Temporal trends and risks factors for antimicrobial resistant Enterobacteriaceae urinary isolates from outpatients in Guadeloupe. BMC Microbiol. 2016;16(1):121.

[62] Dutta PR, Cappello R, Navarro-García F, et al. Functional comparison of serine protease autotransporters of Enterobacteriaceae. Infect Immun. 2002;70(12):7105–7113.

[63] Stathopoulos C, Provence DL, Curtiss R. Characterization of the Avian Pathogenic *Escherichia coli* Hemagglutinin Tsh, a Member of the Immunoglobulin A Protease-Type Family of Autotransporters. Infect Immun. 1999;67(2):772–781.

[64] Gutierrez D, Pardo M, Montero D, et al. TleA, a Tsh-like autotransporter identified in a human enterotoxigenic *Escherichia coli* strain. Infect Immun. 2015;83(5):1893–1903.

[65] Yang J, Yan R, Roy A, et al. The I-TASSER Suite: protein structure and function prediction. Nat Methods. 2015;12(1):7.

[66] Pettersen EF, Goddard TD, Huang CC, et al. UCSF Chimera—a visualization system for exploratory research and analysis. J Comput Chem. 2004;25(13):1605–1612.

[67] Genevaux P, Muller S, Bauda P. A rapid screening procedure to identify mini-Tn10 insertion mutants of *Escherichia coli* K-12 with altered adhesion properties. FEMS Microbiol Lett. 1996;142(1):27–30.

[68] Kostakioti M, Stathopoulos C. Functional analysis of the Tsh autotransporter from an avian pathogenic *Escherichia coli* strain. Infect Immun. 2004;72(10):5548–5554.

[69] Sherlock O, Vejborg RM, Klemm P. The TibA adhesin/invasin from enterotoxigenic *Escherichia coli* is self recognizing and induces bacterial aggregation and biofilm formation. Infect Immun. 2005;73(4):1954–1963.

[70] Hasman H, Chakraborty T, Klemm P. Antigen-43-mediated autoaggregation of *Escherichia coli* is blocked by fimbriation. J Bacteriol. 1999;181(16):4834–4841.

[71] Benz I, Schmidt MA. Cloning and expression of an adhesin (AIDA-I) involved in diffuse adherence of enteropathogenic *Escherichia coli*. Infect Immun. 1989;57 (5):1506–1511.

[72] Al-Hasani K, Henderson IR, Sakellaris H, et al. The *sigA* gene which is borne on the *she* pathogenicity island of *Shigella flexneri* 2a encodes an exported cytopathic protease involved in intestinal fluid accumulation. Infect Immun. 2000;68(5):2457–2463.

[73] Benjelloun-Touimi Z, Sansonetti PJ, Parsot C. SepA, the major extracellular protein of *Shigella flexneri*: autonomous secretion and involvement in tissue invasion. Mol Microbiol. 1995;17(1):123–135.

[74] Vijayakumar V, Santiago A, Smith R, et al. Role of class 1 serine protease autotransporter in the pathogenesis of *Citrobacter rodentium* colitis. Infect Immun. 2014;82 (6):2626–2636.

[75] Leyton DL, Adams LM, Kelly M, et al. Contribution of a novel gene, *rpeA*, encoding a putative autotransporter adhesin to intestinal colonization by rabbit-specific enteropathogenic *Escherichia coli*. Infect Immun. 2007;75 (9):4664–4669.

[76] Johnson TJ, Aziz M, Liu CM, et al. Complete genome sequence of a CTX-M-15-producing *Escherichia coli* strain from the H30Rx subclone of sequence type 131 from a patient with recurrent urinary tract infections, closely related to a lethal urosepsis isolate from the patient's sister. Genome Announc. 2016;4(3):e00334–16.

[77] Johnson TJ, Siek KE, Johnson SJ, et al. DNA sequence of a ColV plasmid and prevalence of selected plasmid-encoded virulence genes among avian *Escherichia coli* strains. J Bacteriol. 2006;188(2):745–758.

[78] Jakobsen L, Hammerum AM, Frimodt-Møller N. Virulence of *Escherichia coli* B2 isolates from meat and animals in a murine model of ascending urinary tract infection (UTI): evidence that UTI is a zoonosis. J Clin Microbiol. 2010;48(8):2978–2980.

[79] Mellata M, Johnson J, Curtiss III R. *Escherichia coli* isolates from commercial chicken meat and eggs cause sepsis, meningitis and urinary tract infection in rodent models of human infections. Zoonoses Public Health. 2018;65(1):103–113.

[80] Pavanelo DB, Houle S, Matter LB, et al. The periplasmic trehalase affects type 1 fimbriae production and virulence of the extraintestinal pathogenic *E.coli* strain MT78. Infect Immun. 2018;IAI:00241.

[81] Skyberg JA, Johnson TJ, Johnson JR, et al. Acquisition of avian pathogenic *Escherichia coli* plasmids by a commensal *E.coli* isolate enhances its abilities to kill chicken embryos, grow in human urine, and colonize the murine kidney. Infect Immun. 2006;74(11):6287–6292.

[82] Ruiz-Perez F, Wahid R, Faherty CS, et al. Serine protease autotransporters from *Shigella flexneri* and pathogenic *Escherichia coli* target a broad range of leukocyte glycoproteins. Proc Nat Acad Sci. 2011;108 (31):12881–12886.

[83] Vidal JE, Navarro-García F. Efficient translocation of EspC into epithelial cells depends on enteropathogenic *Escherichia coli* and host cell contact. Infect Immun. 2006;74(4):2293–2303.

[84] Clermont O, Christenson JK, Denamur E, et al. The Clermont *Escherichia coli* phylo-typing method revisited: improvement of specificity and detection of new phylogroups. Environ Microbiol Rep. 2013;5(1):58–65.

[85] Tamura K, Stecher G, Peterson D, et al. MEGA6: molecular evolutionary genetics analysis version 6.0. Mol Biol Evol. 2013;30(12):2725–2729.

[86] Bendtsen JD, Nielsen H, von Heijne G, et al. Improved prediction of signal peptides: signalP 3.0. J Mol Biol. 2004;340(4):783–795.

[87] Marchler-Bauer A, Lu S, Anderson JB, et al. CDD: a Conserved Domain Database for the functional annotation of proteins. Nucleic Acids Res. 2010;39(suppl_1): D225–D9.

[88] Kouranov A, Xie L, de la Cruz J, et al. The RCSB PDB information portal for structural genomics. Nucleic Acids Res. 2006;34(suppl_1):D302–D5.

[89] Datsenko KA, Wanner BL. One-step inactivation of chromosomal genes in *Escherichia coli* K-12 using PCR products. Proc Nat Acad Sci. 2000;97(12):6640–6645.

[90] Cherepanov PP, Wackernagel W. Gene disruption in *Escherichia coli*: Tc R and Km R cassettes with the option of Flp-catalyzed excision of the antibiotic-resistance determinant. Gene. 1995;158(1):9–14.

[91] Benjelloun-Touimi Z, Tahar MS, Montecucco C, et al. SepA, the 110 kDa protein secreted by *Shigella flexneri*: two-domain structure and proteolytic activity. Microbiology. 1998;144(7):1815–1822.

[92] Charbonneau M-È, Berthiaume F, Mourez M. Proteolytic processing is not essential for multiple functions of the *Escherichia coli* autotransporter adhesin involved in diffuse adherence (AIDA-I). J Bacteriol. 2006;188 (24):8504–8512.

[93] Provence D, Curtiss R. Role of *crl* in avian pathogenic *Escherichia coli*: a knockout mutation of *crl* does not affect hemagglutination activity, fibronectin binding, or curli production. Infect Immun. 1992;60(11):4460–4467.

[94] Matter LB, Barbieri NL, Nordhoff M, et al. Avian pathogenic *Escherichia coli* MT78 invades chicken fibroblasts. Vet Microbiol. 2011;148(1):51–59.

[95] Hagberg L, Engberg I, Freter R, et al. Ascending, unobstructed urinary tract infection in mice caused by pyelonephritogenic *Escherichia coli* of human origin. Infect Immun. 1983;40(1):273–283.

[96] Porcheron G, Habib R, Houle S, et al. The small RNA RyhB contributes to siderophore production and virulence of uropathogenic *Escherichia coli*. Infect Immun. 2014;82(12):5056–5068.

[97] Livak KJ, Schmittgen TD. Analysis of relative gene expression data using real-time quantitative PCR and the 2−ΔΔCT method. Methods. 2001;25(4):402–408.

[98] Saitou N, Nei M. The neighbor-joining method: a new method for reconstructing phylogenetic trees. Mol Biol Evol. 1987;4(4):406–425.

[99] Jones DT, Taylor WR, Thornton JM. The rapid generation of mutation data matrices from protein sequences. Bioinformatics. 1992;8(3):275–282.

[100] Labbate M, Queck SY, Koh KS, et al. Quorum sensing-controlled biofilm development in *Serratia liquefaciens* MG1. J Bacteriol. 2004;186(3):692–698.

[101] Woodall LD, Russell PW, Harris SL, et al. Rapid, synchronous, and stable induction of type 1 piliation in *Escherichia coli* by using a chromosomal *lacUV5* promoter. J Bacteriol. 1993;175(9):2770–2778.

13 ANNEXE II SPATES internalization in epithelial cells

En tant que troisième auteur de cet article, j'ai contribué à l'analyses des données, la rédaction et la révision de l'article.

Article

The Serine Protease Autotransporters TagB, TagC, and Sha from Extraintestinal Pathogenic *Escherichia coli* Are Internalized by Human Bladder Epithelial Cells and Cause Actin Cytoskeletal Disruption

Pravil Pokharel [1,2], Juan Manuel Díaz [2,3], Hicham Bessaiah [1,2], Sébastien Houle [1,2], Alma Lilián Guerrero-Barrera [3] and Charles M. Dozois [1,2,4,*]

[1] Institut national de recherche scientifique (INRS)-Centre Armand-Frappier Santé Biotechnologie, Laval, QC H7V 1B7, Canada; Pravil.Pokharel@iaf.inrs.ca (P.P.); Hicham.Bessaiah@iaf.inrs.ca (H.B.); Sebastien.Houle@iaf.inrs.ca (S.H.)

[2] Department of Veterinary Medicine, Centre de recherche en infectiologie porcine et avicole (CRIPA), Faculty of Veterinary Medicine, Saint-Hyacinthe, QC J2S 2M2, Canada; jmdv93@hotmail.com

[3] Laboratorio de Biología Celular y Tisular, Departamento de Morfología, Universidad Autónoma de Aguascalientes (UAA), Aguascalientes 20131, Mexico; alguerre@correo.uaa.mx

[4] Department of Biology, Institut Pasteur International Network, Laval, QC H7V 1B7, Canada

* Correspondence: charles.dozois@iaf.inrs.ca

check for updates

Abstract: TagB, TagC (*t*andem *a*utotransporter *genes B* and *C*), and Sha (*S*erine-protease *h*emagglutinin *a*utotransporter) are recently described members of the SPATE (serine protease autotransporters of *Enterobacteriaceae*) family. These SPATEs can cause cytopathic effects on bladder cells and contribute to urinary tract infection in a mouse model. Bladder epithelial cells form an important barrier in the urinary tract. Some SPATEs produced by pathogenic *E. coli* are known to breach the bladder epithelium. The capacity of these newly described SPATEs to alter bladder epithelial cells and the role of the serine protease active site were investigated. All three SPATE proteins were internalized by bladder epithelial cells and altered the distribution of actin cytoskeleton. Sha and TagC were also shown to degrade mucin and gelatin respectively. Inactivation of the serine catalytic site in each of these SPATEs did not affect secretion of the SPATEs from bacterial cells, but abrogated entry into epithelial cells, cytotoxicity, and proteolytic activity. Thus, our results show that the serine catalytic triad of these proteins is required for internalization in host cells, actin disruption, and degradation of host substrates such as mucin and gelatin.

Keywords: SPATEs; UTIs; cytotoxicity; serine proteases; 5637 bladder cells; mucin; gelatin; actin

1. Introduction

Urinary tract infections (UTIs) present a broad range of symptoms and include urosepsis, pyelonephritis (or upper UTI, with infection in the kidney), and cystitis (or lower UTI, with bacteria infecting the bladder) [1,2]. Uropathogenic *Escherichia coli* (UPEC) is the main cause of community-acquired UTIs (about 80–90%) [3], and the ability of UPEC to establish a UTI is due to the expression of a variety of virulence factors. These factors include type 1 and P fimbriae (pili), flagella, capsular polysaccharides, iron acquisition systems, and toxins including hemolysin, cytotoxic necrotizing factor (CNF), and serine protease autotransporters of *Enterobacteriaceae* (SPATEs) [4].

The bladder urothelium constitutes a physical barrier to ascending urinary tract infections [5]. UPEC can produce toxins that damage bladder tissue and can lead to release of host nutrients and

Article

The Serine Protease Autotransporters TagB, TagC, and Sha from Extraintestinal Pathogenic *Escherichia coli* Are Internalized by Human Bladder Epithelial Cells and Cause Actin Cytoskeletal Disruption

Pravil Pokharel [1,2], **Juan Manuel Díaz** [2,3], **Hicham Bessaiah** [1,2], **Sébastien Houle** [1,2], **Alma Lilián Guerrero-Barrera** [3] **and Charles M. Dozois** [1,2,4,*]

1   Institut national de recherche scientifique (INRS)-Centre Armand-Frappier Santé Biotechnologie, Laval, QC H7V 1B7, Canada; Pravil.Pokharel@iaf.inrs.ca (P.P.); Hicham.Bessaiah@iaf.inrs.ca (H.B.); Sebastien.Houle@iaf.inrs.ca (S.H.)
2   Department of Veterinary Medicine, Centre de recherche en infectiologie porcine et avicole (CRIPA), Faculty of Veterinary Medicine, Saint-Hyacinthe, QC J2S 2M2, Canada; jmdv93@hotmail.com
3   Laboratorio de Biología Celular y Tisular, Departamento de Morfología, Universidad Autónoma de Aguascalientes (UAA), Aguascalientes 20131, Mexico; alguerre@correo.uaa.mx
4   Department of Biology, Institut Pasteur International Network, Laval, QC H7V 1B7, Canada
*   Correspondence: charles.dozois@iaf.inrs.ca

check for updates

Abstract: TagB, TagC (*t*andem *a*utotransporter *g*enes *B* and *C*), and Sha (*S*erine-protease *h*emagglutinin *a*utotransporter) are recently described members of the SPATE (serine protease autotransporters of *Enterobacteriaceae*) family. These SPATEs can cause cytopathic effects on bladder cells and contribute to urinary tract infection in a mouse model. Bladder epithelial cells form an important barrier in the urinary tract. Some SPATEs produced by pathogenic *E. coli* are known to breach the bladder epithelium. The capacity of these newly described SPATEs to alter bladder epithelial cells and the role of the serine protease active site were investigated. All three SPATE proteins were internalized by bladder epithelial cells and altered the distribution of actin cytoskeleton. Sha and TagC were also shown to degrade mucin and gelatin respectively. Inactivation of the serine catalytic site in each of these SPATEs did not affect secretion of the SPATEs from bacterial cells, but abrogated entry into epithelial cells, cytotoxicity, and proteolytic activity. Thus, our results show that the serine catalytic triad of these proteins is required for internalization in host cells, actin disruption, and degradation of host substrates such as mucin and gelatin.

Keywords: SPATEs; UTIs; cytotoxicity; serine proteases; 5637 bladder cells; mucin; gelatin; actin

1. Introduction

Urinary tract infections (UTIs) present a broad range of symptoms and include urosepsis, pyelonephritis (or upper UTI, with infection in the kidney), and cystitis (or lower UTI, with bacteria infecting the bladder) [1,2]. Uropathogenic *Escherichia coli* (UPEC) is the main cause of community-acquired UTIs (about 80–90%) [3], and the ability of UPEC to establish a UTI is due to the expression of a variety of virulence factors. These factors include type 1 and P fimbriae (pili), flagella, capsular polysaccharides, iron acquisition systems, and toxins including hemolysin, cytotoxic necrotizing factor (CNF), and serine protease autotransporters of *Enterobacteriaceae* (SPATEs) [4].

The bladder urothelium constitutes a physical barrier to ascending urinary tract infections [5]. UPEC can produce toxins that damage bladder tissue and can lead to release of host nutrients and

counter host defenses and innate immunity. A pore-forming toxin HlyA, can lyse erythrocytes and nucleated host cells [6], induce apoptosis [7], promote exfoliation of bladder epithelial cells and cause extensive uroepithelial damage [8–11]. Another UPEC toxin, cytotoxic necrotizing factor 1 (CNF1), has been reported to mediate bacterial entry into host epithelial cells [12], induce apoptotic death of bladder epithelial cells [13], and potentially promote bladder cell exfoliation [13]. SPATEs such as Sat, Pic, and Vat were also shown to affect bladder or kidney epithelial cells [14–16].

An important step to understand the role of SPATEs in UPEC pathogenesis is to elucidate molecular mechanisms underlying their effect on the bladder epithelium and during urinary tract colonization. The proteolytic activity of SPATEs is mediated by a serine protease catalytic triad of aspartic acid (D), serine (S), and histidine (H), wherein serine is the nucleophile, and aspartic acid interacts with histidine [17]. Mutations within the catalytic triad have been shown to abolish proteolytic activity in a number of SPATEs [15,17–19].

Recently, members of our group identified three new SPATEs: TagB, TagC (*t*andem *a*utotransporter *g*enes *B* and *C*), and Sha (*S*erine-protease *h*emagglutinin *a*utotransporter) in some strains of extra-intestinal pathogenic *E. coli* (ExPEC). In ExPEC strain QT598, *tagB* and *tagC* are tandemly encoded on a genomic island, and were present in 10% of UTI isolates and 4.7% of avian pathogenic *E. coli* (APEC) that we screened [20]. Further, Sha, which is encoded on a virulence plasmid in strain QT598 was present in 1% of UTI isolates and 20% of avian pathogenic *E. coli* [20]. The *tagBC* genes are also present in the genomes of sequenced UPEC strains such as multidrug-resistant CTX-M-15-producing ST131 isolate *E. coli* JJ1886 (Accession number CP006784), *E. coli* CI5 (Accession number CP011018), and multidrug-resistant uropathogenic *E. coli* strain NA114 (Accession number CP002797.2). When cloned into *E. coli* K-12, TagB, TagC, and Sha mediated autoaggregation, hemagglutination, and adherence to human HEK 293 renal and 5637 bladder cell lines, but did not contribute significantly to biofilm production [20]. Further, TagB and TagC exhibited cytopathic effects on the bladder epithelial cell line [20]. Following transurethral infection of CBA/J mice with a *tagBC* mutant or *sha* mutant, no significant difference in colonization was observed. However, the competitive fitness of a mutant derivative lacking all of the SPATEs present in QT598 was significantly lower in the kidney [20].

The purpose of this report was to more fully investigate the effects of the TagB, TagC, and Sha SPATEs on the 5637 bladder epithelial cell line focusing on the actin cytoskeleton. We also investigated potential entry of SPATE proteins within these bladder epithelial cells and whether they demonstrate mucinase or gelatinase activity.

2. Results

2.1. Processing and Secretion of TagB, TagC, and Sha Is Independent of the Serine Protease Motif

To evaluate the importance of the serine protease motif for processing and secretion of three novel SPATEs, we generated variant proteins of TagB, TagC, and Sha lacking the serine catalytic site. Plasmids expressing TagB, TagC, or Sha [20] were used as the templates for construction of site-directed mutant clones where the serine site was substituted for an alanine at residue S255, S252, and S258 respectively (Figures S1 and S2). Each of these three plasmids expressing mutant SPATEs, produced a high-molecular-weight protein (>100 kDa) in culture supernatants that corresponded to the expected size of the native protein, and also lacked breakdown products that are present in samples containing native SPATEs that exhibit some autoproteolytic activity (Figure 1A, asterisks). This demonstrated that the serine protease motif is not necessary for SPATE secretion and release from bacterial cells.

To further localize each of the SPATEs expressed from plasmids in *E. coli* BL21 on the bacterial cell surface, we used immunogold labeling and transmission electron microscopy. Polyclonal antibodies against the entire secreted Vat SPATE [20] were used as they were shown to strongly cross-react and recognize conserved epitopes of the other SPATEs. Thus, we used these polyclonal "SPATE antibodies" for the detection of other SPATEs in our experiments.

E. coli BL21 pBCsk+ expressing TagB, TagC, and Sha were immunogold-labeled (Figure 1B–D); demonstrating localization of these SPATEs on the bacterial surface, as well as release into culture

supernatant. The inset depicts the heavily concentrated proteins on the bacterial surface that appears to cluster around each other and produce fiber-like aggregates on the cell surface (white chevron, Figure 1B–D). *E. coli* BL21 bacteria containing only the empty plasmid vector were not labeled after immunogold labeling with anti-SPATE antibodies and secondary anti-rabbit immunoglobulin conjugated to 10-nm gold particles (Figure 1E).
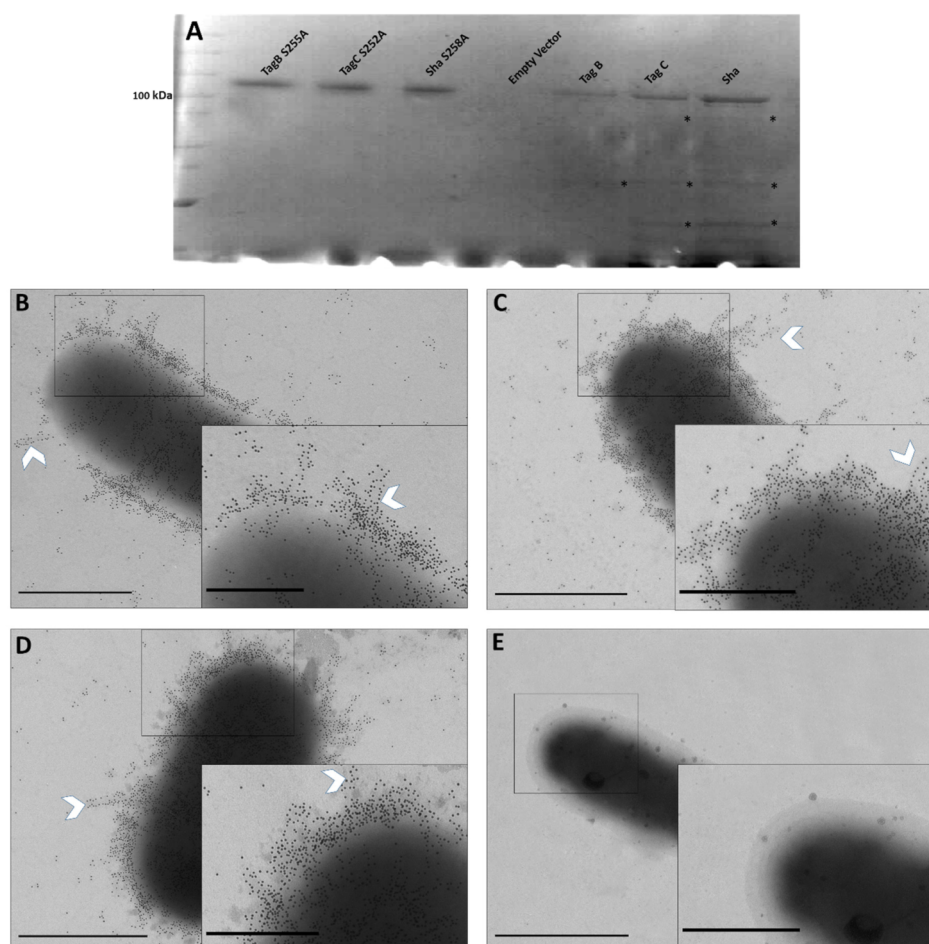

Figure 1. (**A**) Silver stained SDS-PAGE analysis of concentrated supernatants of *E. coli* BL21 expressing SPATE proteins. Filtered supernatants from clones expressing TagB, TagC, and Sha or the variant TagB S255A, TagC S252A, and Sha S258A proteins were concentrated through Amicon filters with a 50 kDa cutoff. Samples containing 5 μg of protein were migrated and stained with silver stain. (**B–E**) Immunogold Electron Microscopy (EM) of SPATEs (Serine protease autotransporters of *Enterobacteriaceae*) localized to the outer membrane and extracellular medium. Immunogold-TEM micrographs of SPATEs using SPATE-specific antiserum. Bacteria were cultured to 0.6 OD$_{600nm}$ in Luria-Bertani medium. *E. coli* BL21 pBCsk+ expressing TagB (**B**), TagC (**C**), and Sha (**D**) labelled with immunogold particles. (**E**) *E. coli* BL21 pBcsk+ (vector only control) shows no immunogold staining. Insets represents boxed areas of higher magnification showing clustering of SPATE proteins. All images were acquired at ×17,000 magnification; scale bars represent 1 μm, and 0.5 μm (Insets).

2.2. The Serine Catalytic Motif of SPATEs Is Not Required for Autoaggregation or Hemagglutination Activity

To determine if the serine catalytic site of each of the three SPATEs is involved in autoaggregation or hemagglutination activity, we tested these phenotypes with our mutant SPATEs as described in [20]. Macroscopic analysis of autoaggregation of *E. coli* BL21 expressing TagB S255A, TagC S252A, or Sha S258A showed that bacterial cells settled at the bottom of the tube under static incubation similar to their respective native protein-expressing clones. The percentage of reduction in turbidity is given as

a percentage of the initial OD_{600} value and was similar for both mutant and native proteins (Figure 2). The reduction in turbidity of the negative control *E. coli* BL21 pBCsk+ was significantly lower compared to clones expressing TagB, TagC, Sha, or AIDA-1 (positive control) (Figure 2). AIDA-1 (Adhesin Involved in Diffuse Adherence) of *E. coli* is a characterized self-associating autotransporter protein which mediates bacterial cell–cell interactions and autoaggregation [21].

These results show that inactivation of the serine catalytic site in each SPATE does not affect autoaggregation. It is therefore likely that other motifs or residues present in these proteins contribute to autoaggregation of bacterial cells.
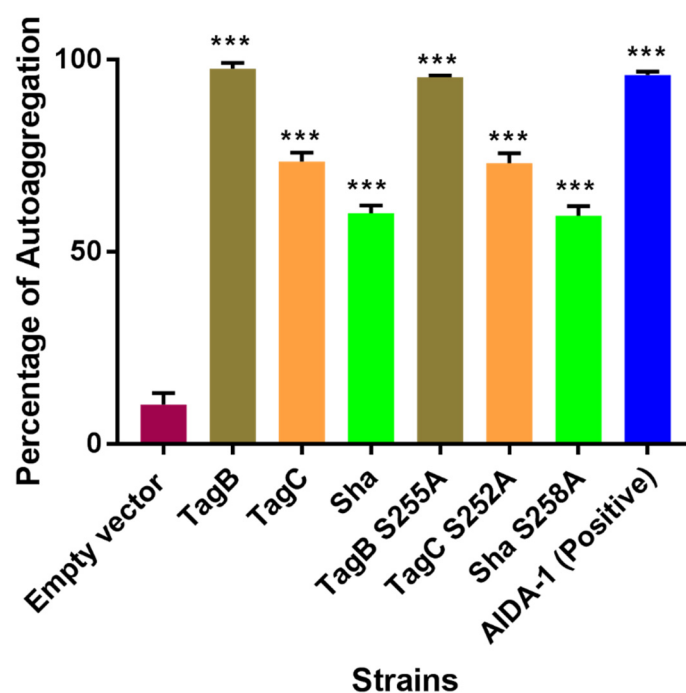

Figure 2. The autoaggregation phenotype is independent of the serine protease motif. Clones of *E. coli* BL21 expressing TagB, TagC, Sha, or their respective serine-site mutants were grown 18 h and adjusted to an OD_{600} of 1.5 and left to rest at 4 °C. Samples were taken at 1 cm from the top surface of the cultures after 3 h to determine the change in OD_{600}. Assays were performed in triplicate, and the rate of autoaggregation was determined by the mean decrease in OD_{600nm} after 3 h. *E. coli* BL21 pBCsk+ vector without insert (empty vector) was used as a negative control and the AIDA-1 autotransporter was the positive control for autoaggregation. Error bars represent standard errors of the means (*** $p < 0.001$ compared to empty vector using one-way ANOVA).

Likewise, Sha S258A showed similar hemagglutination of human blood as reported previously for the Sha native protein [20]. When cloned in the hemagglutination negative *E. coli* strain ORN172, there was no hemagglutination activity for either the native or mutant TagB or TagC proteins. In addition to autoaggregation and hemagglutination activity, the adherence capability of the serine catalytic site mutants of the SPATEs to 5637 human bladder epithelial cells was not affected (Figure S3). Hence, loss of the serine catalytic site did not affect autoaggregation, adherence, or hemagglutination phenotypes associated with each of the SPATEs compared to the native proteins.

2.3. Cytopathic Effect of TagB and TagC Requires the Serine Protease Motif

To assess the role of the serine protease motif for the cytopathic effect of SPATEs, extracts of supernatants of the different SPATEs (30 µg of protein per well) were incubated with human bladder epithelial cell line 5637 for 5h. Then the cells were fixed, stained with Giemsa stain, and observed by light microscopy. Cytopathic changes (dissolution in cytoplasm, enlargement of the nucleus

with vacuoles) observed under the microscope for TagB and TagC (Figure 3A) were absent from cells treated with either TagB or TagC proteins lacking the serine protease active site. In addition, no significant morphological changes were observed with cells treated with either Sha or the mutant, Sha S258A, protein. No cytopathic effect was observed after treatment of cells with concentrated filtered supernatant from *E. coli* BL21 pBCsk+ (empty vector) or media alone (Figure 3A). To examine this cytopathic effect quantitatively, we measured lactate dehydrogenase (LDH) release from epithelial cells incubated with each of SPATEs or their respective catalytic site mutant proteins. There was release of LDH after 5 h upon exposure of cells to TagB or TagC. However, the catalytic site mutant proteins did not release LDH from cells (Figure 3B). Further, no LDH release was detected from cells treated with either Sha or its catalytic site mutant variant (Figure 3B), indicating that cytotoxicity to human bladder epithelial cells by TagB and TagC was dependent on the serine protease catalytic site.
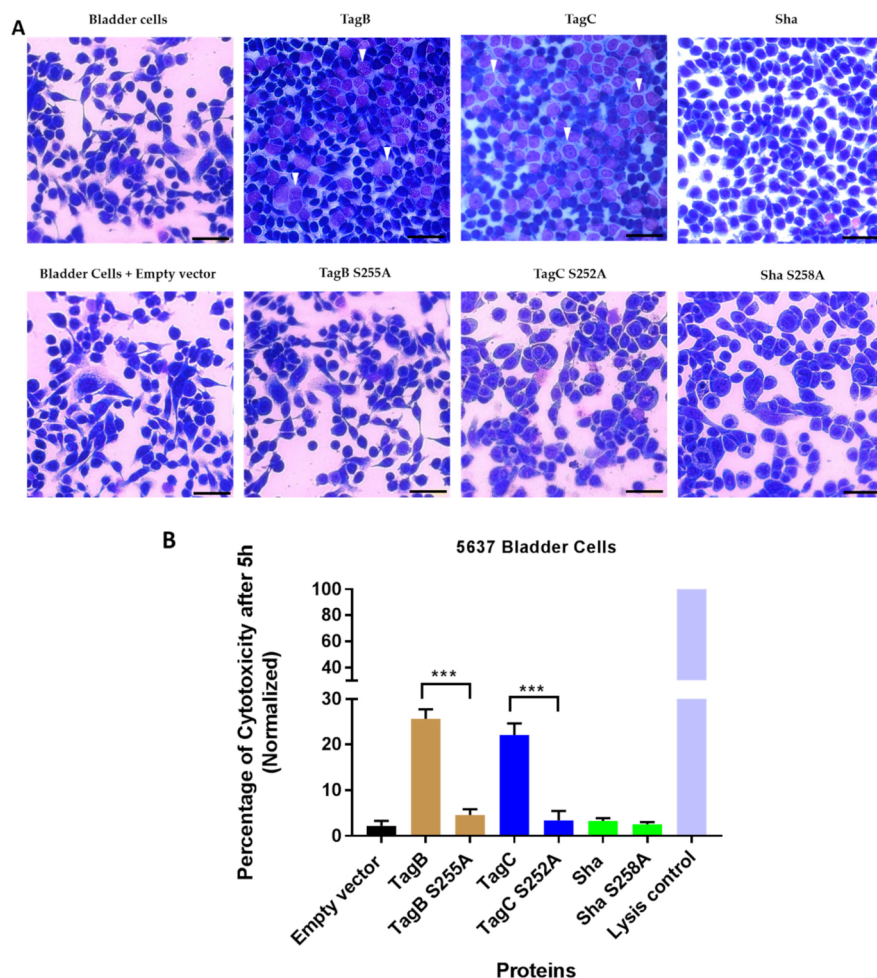
Figure 3. The serine catalytic site is necessary for the cytopathic effect of TagB and TagC. (**A**) Concentrated supernatants containing 30 μg of protein per well derived from *E. coli* BL21 clones expressing TagB, TagC, Sha, or their respective serine mutant variant proteins were incubated with monolayers of the 5637 human bladder epithelial cell line for 5 h at 37 °C. Cytopathic effects (white triangle) were absent in cells treated with the serine catalytic site mutant variants of TagB or TagC. The empty vector (pBCsk+) without insert was used as a negative control. The scale bar represents 20 μm. (**B**) Cytotoxicity measured by LDH release from 5637 human bladder cells after incubation with supernatant filtrates of different clones (30 μg of protein per well) at 37 °C for 5 h. Empty vector (pBCsk+) was used as a negative control and maximum LDH release (positive control) was determined by treatment with lysis solution. Data are the means of three independent experiments, and error bars represent the standard errors of the means. Significant differences between lysis caused by native and mutant SPATEs were determined using Student's *t*-test with *** $p < 0.001$.

2.4. Exposure to TagB, TagC, or Sha Alters Actin Distribution in Bladder Epithelial Cells

Based on the cellular changes seen with bladder epithelial cells after exposure to TagB and TagC, we hypothesized that TagB and TagC could alter the distribution of cytoskeletal components such as actin, with actin being one of the most abundant intracellular proteins in the eukaryotic cell. So, to examine the effect on F-actin cytoskeleton organization, 5637 bladder cells were incubated with native and mutant TagB, TagC, or Sha (30 μg of protein per well) for 5 h at 37 °C, stained with fluorescently labeled phalloidin, and then observed under confocal microscopy. Cells treated with the supernatant extract from the empty vector containing clone were uniform, smooth-edged, and contained clearly visible actin stress fibers (yellow triangle) and strong actin staining around the cell (Figure 4A). By contrast, bladder cells treated with TagB showed reduced actin stress fibers and less actin staining (Figure 4A). Bladder cells treated with TagC, also had a pronounced effect on the cytoskeleton as demonstrated by the absence of actin stress fibers and reduced levels of actin staining. Sha treated cells showed a loss of actin stress fibers and the presence of punctate patterns of actin within the cytoplasm of the cells (yellow arrowheads, Figure 4A). By contrast, the TagB, TagC, and Sha mutants lacking the serine protease catalytic sites demonstrated no changes in the actin cytoskeleton and had actin stress fibers similar to negative control cells, indicating that the serine protease activity of these SPATEs mediates the changes in actin distribution within bladder cells. To quantify the level of phalloidin binding, we measured the staining intensity and distribution of fluorescence of phalloidin around each cell using ImageJ software [22]. Fluorescence intensity for cells was calculated using the channel for actin staining. In comparison with the negative control (empty vector), the density of F-actin staining was significantly lower in cells treated with TagB, TagC, or Sha. Cells treated with the serine catalytic site mutant proteins, demonstrated F-actin staining that was greater when compared to cells treated with the native SPATE proteins (Figure 4B). Overall, these results demonstrate that these SPATEs alter the cytoskeleton and reduce the distribution of actin in bladder epithelial cells.
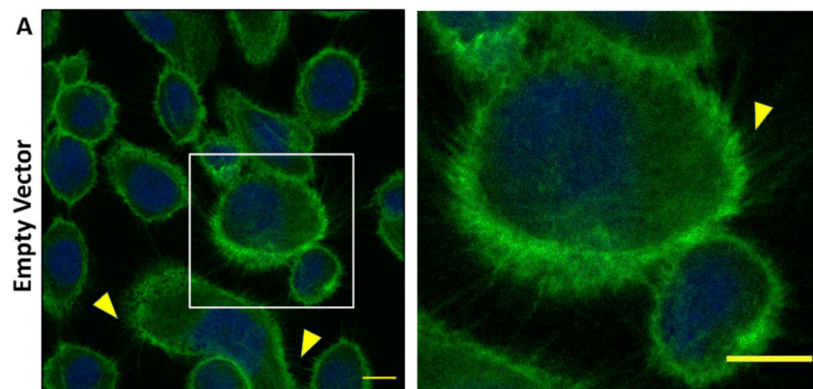

Figure 4. *Cont.*
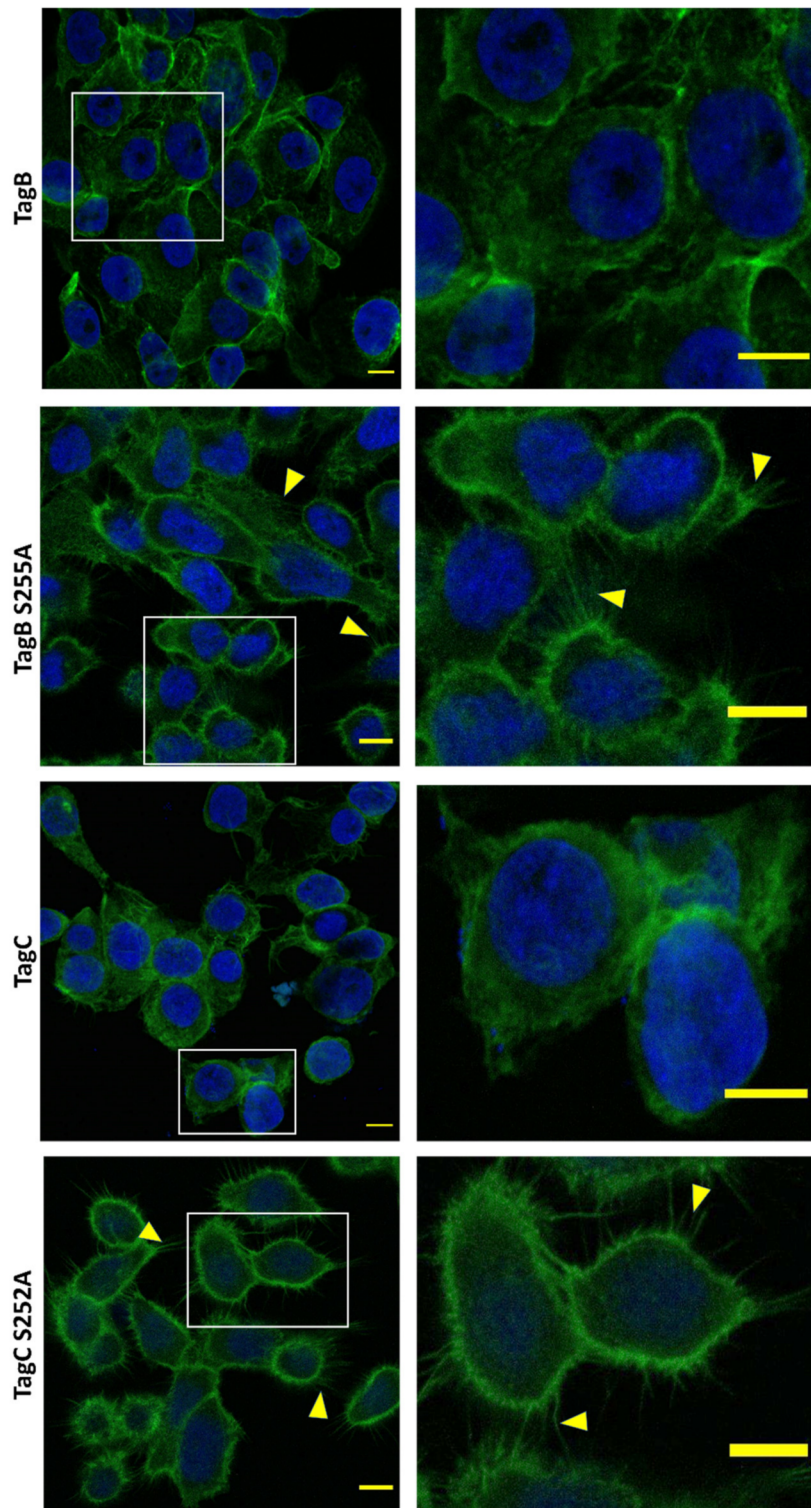
Figure 4. *Cont.*
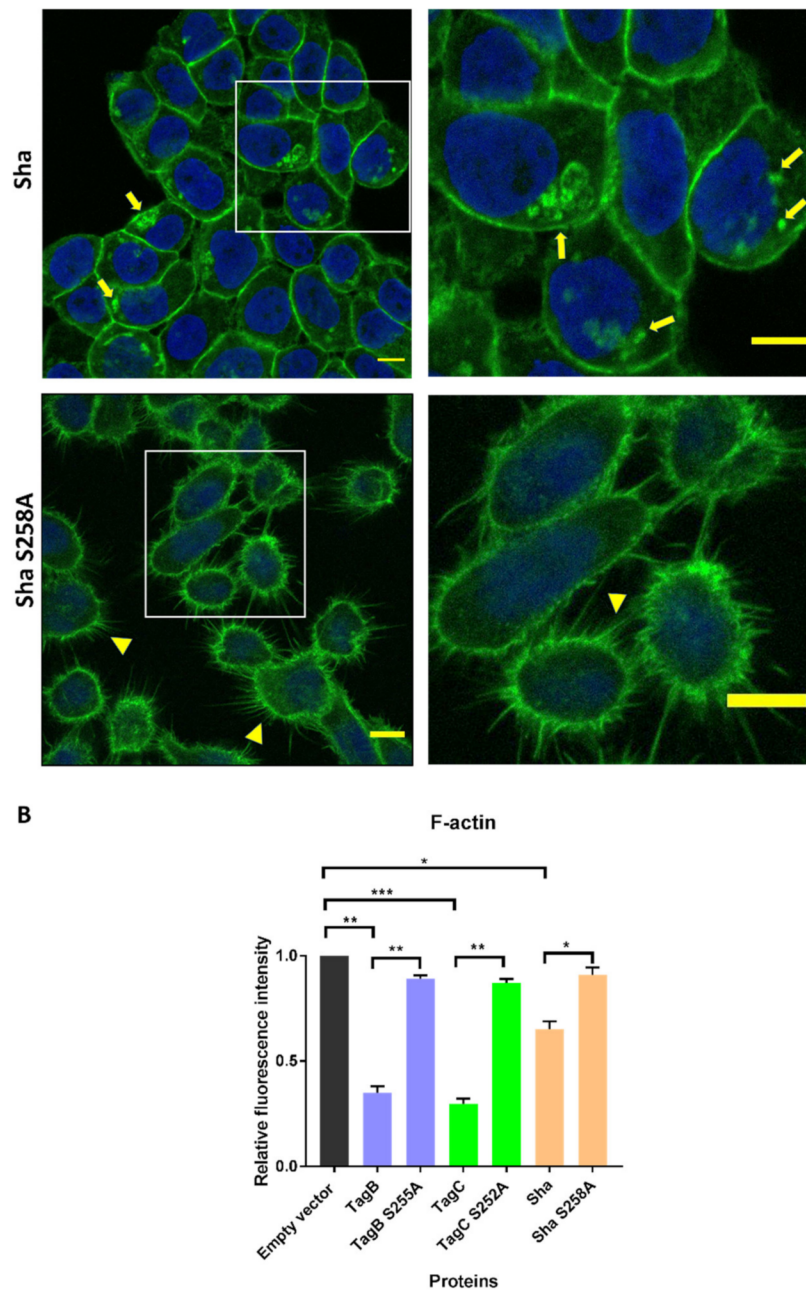
Figure 4. Effects of TagB, TagC, and Sha on the actin cytoskeleton of bladder epithelial cells is serine-protease-motif dependent. (**A**) Concentrated supernatant extracts (30 μg of protein per well) from *E. coli* BL21 clones expressing TagB, TagC, or Sha and their respective serine catalytic site mutants were incubated with monolayers of human bladder (5637) epithelial cells for 5 h at 37 °C. After incubation, cells were fixed and permeabilized. Actin was stained with fluorescently labeled phalloidin (green) and the nucleus was stained by DAPI (blue). Cells treated with the filtered supernatant of *E. coli* BL21 pBCsk+ without insert (empty vector) were used as a negative control. Slides were observed by confocal microscopy. Inset images from the left panels are magnified in the panels to the right. Bars represent 10 μm. (**B**) Quantitative analysis of fluorescence intensity of F-actin. Analysis of fluorescent intensity was done at the original magnification by measuring the mean gray value with ImageJ software [22] with an *n* value of at least 10 cells. Data values represent the mean ± SEM of at least three independent experiments. (* $p < 0.05$, ** $p < 0.01$, *** $p < 0.001$ one-way ANOVA with multiple comparisons).

2.5. SPATE Entry into Bladder Epithelial Cells Is Dependent on the Serine Protease Active Site

We previously showed that TagB and TagC demonstrated cytotoxicity as measured by lactate dehydrogenase (LDH) release from epithelial cells within 5 h [20]. This toxicity could be due to the interaction of the SPATEs with targets inside host cells. So, to gain insight into the potential internalization of these SPATEs, we employed immunofluorescence labeling of proteins followed by visualization using confocal or immunogold electron microscopy. Firstly, confocal Z-sections (optical slices) of 5637 bladder cells treated with SPATEs were examined to determine if SPATEs were translocated within cells. After 5 h of incubation, TagB, TagC, and Sha (red color) were found within cells as evidenced by cell sectioning analysis (Figure 5A). By contrast, the serine active-site mutant variants were unable to enter epithelial cells and were not detected (absence of red staining) (Figure 5A), suggesting that serine protease activity is needed for the entry of SPATEs within cells. Interestingly, TagB within cells also co-localized with actin (green color) in the outer border of the cell (Figure 5A). Further, cells incubated with serine mutant variants of SPATEs did not enter cells, and these cells also produced actin stress fibers (Figure 5).
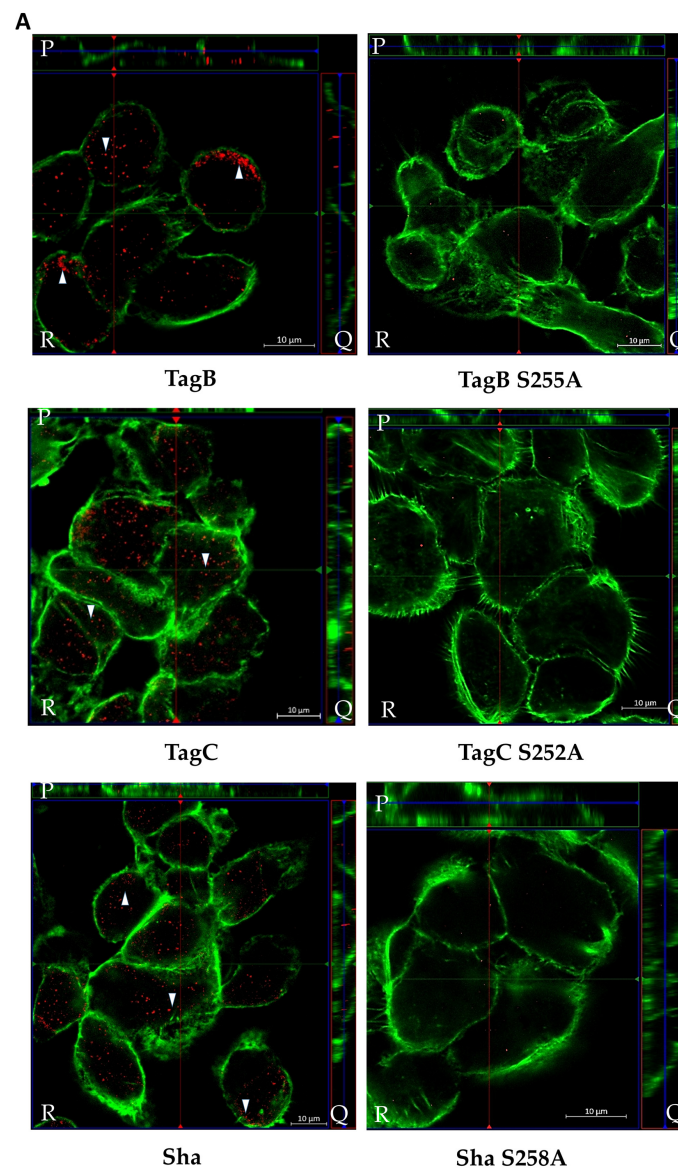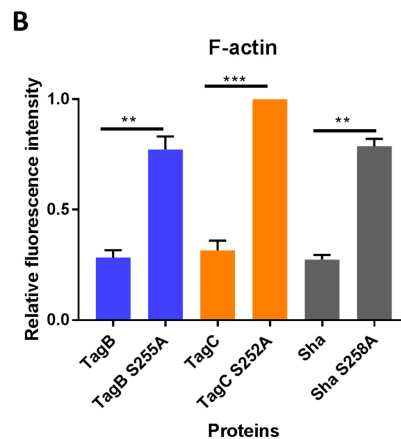

A

TagB   TagB S255A

TagC   TagC S252A

Sha   Sha S258A

Figure 5. *Cont.*

Figure 5. Intracellular localization of TagB, TagC, and Sha determined by confocal microscopy. (**A**) Z-stack imaging showing the localization of TagB, TagC, and Sha and their respective serine active site mutant variants during interaction with 5637 bladder epithelial cells after 5 h of incubation. SPATEs were detected by Alexa Fluor 594 (white arrowheads, red fluorescence) using anti-mouse secondary antibody and actin was stained by Alexa Fluor 488- phalloidin (green fluorescence). Images are displayed in a 3D section view with large Z-sections in the X-Y direction (R), Z-projection in the X–Z direction (P), and Z-projection in the Y–Z direction (Q). The green and red lines in R indicate the orthogonal planes of the X–Z and Y–Z projection. For each selected section, the signal was gathered from a span of 5 μm. Scale bar: 10 μm (**B**) Quantitative analysis of fluorescence intensity of F-actin in the cells treated with native or mutant SPATEs. Analysis of fluorescence intensity was done in green channel by measuring the mean gray value on ImageJ. Data represent the mean ± SEM of at least three independent experiments. Significant differences between fluorescence intensity of each native and mutant SPATE treated cell was determined using Student's t-test with ** $p < 0.01$, *** $p < 0.001$.

Analysis of thin-sections of SPATE-treated cells using immunogold staining and transmission electron microscopy (TEM) also confirmed the intracellular localization of all three SPATEs within cells. TagB and Sha were found in the cytoplasm, whereas TagC was present in the nucleus (Figure 6). However, in multiple independent experiments, we failed to detect the presence of serine mutant variants of TagB, TagC, or Sha within cells. The serine catalytic-site mutant proteins when visualized were almost exclusively observed on the extracellular surface of cells as seen in cells treated with TagB S255A (Figure 6D).
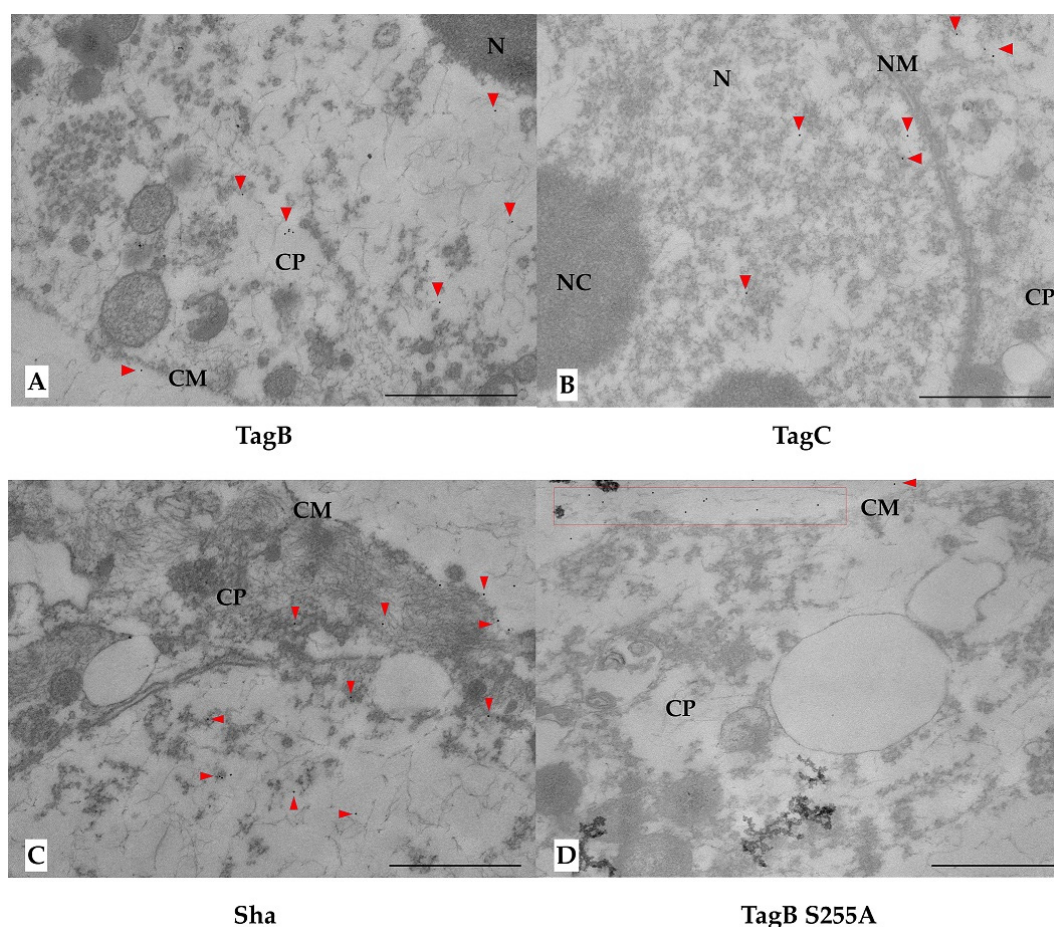
Figure 6. Transmission electron micrographs of 5637 bladder cells showing internalized SPATEs, immunolabelled with 10-nm-diameter gold particles after 5 h of incubation. Gold particles are highlighted with red triangles. (**A**) TagB is principally located in the cytoplasm (CP). (**B**) For Tag C, gold particles were associated with the nucleus (N) and cytoplasm (CP). (**C**) Sha was located mainly in the cytoplasm (CP). (**D**) For the serine mutant variants of TagB, TagC, and Sha, gold particles were only localized on the extracellular surface of cells (red box). Only the TagB S255A mutant protein localization is shown. Cell membrane (CM), Cytoplasm (CP), Nuclear Membrane (NM), Nucleus (N), Nucleolus (NC) Bars, 1 μm.

2.6. Sha Exhibits Serine Protease-Dependent Mucinase Activity

Epithelial cell damage caused by SPATEs was shown to require protease activity, and some other SPATEs were previously shown to demonstrate activity against host proteins such as mucin or gelatin [18,23]. Further, we also tested for mucinase activity, since two of the novel SPATEs identified in APEC QT598, Sha and TagB [20], belong to the class 2 SPATE family whose members have been shown to demonstrate mucinolytic activity. Clones of *E. coli* BL21 expressing each of the SPATEs were grown on agar plates containing 0.5% porcine gastric mucin for 24 h at 37 °C, followed by amido black-staining. Plates containing clones growing on discs expressing Sha revealed clear zones of mucin lysis (Figure 7A) and the lysis zone produced by Sha was intermediate when compared to clones expressing either Tsh (positive control) or Vat. Mucin containing plates had a clearing zone with a diameter of 3.9 ± 0.1 cm after exposure to Sha expressing bacteria, which was less than following exposure to Tsh expressing cells (4.2 ± 0.1 cm), but more than following exposure to Vat expressing cells (3.7 ± 0.2 cm). By contrast, TagB and TagC were mucinase-negative as evidenced by the absence of any clearing zones (Figure 7B). Further, the critical role of the serine catalytic site of Sha for mucinase activity was demonstrated with the clone expressing Sha S258A, which did not produce a zone of

mucin lysis (Figure 7B). The clone containing only the empty vector (negative control) did not grow well in the presence of mucin and also demonstrated no clearing zone. When mucin was treated with culture filtrates of SPATE proteins (Figure 7C), it was not degraded by either TagB, TagC, or in the negative control (empty vector). Sha as well as Tsh and Vat degraded mucin, whereas the serine protease mutant of Sha, Sha S258A, did not. Hence, the serine catalytic site of Sha is required for mucinase activity.
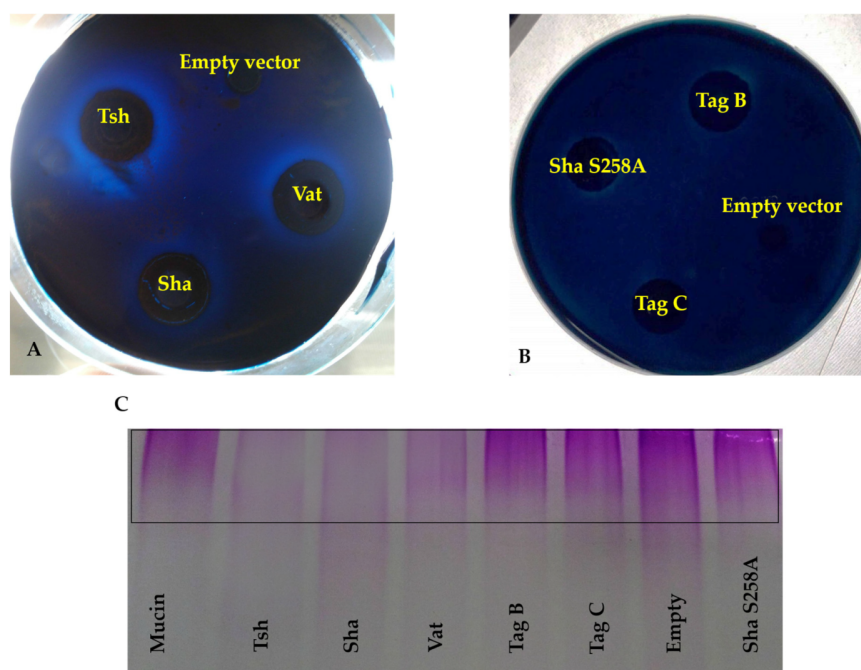
Figure 7. Sha demonstrates serine-protease dependent mucinase activity, but not TagB nor TagC. Mucinase activity was tested in a medium containing 1.5% agarose and 0.5% porcine gastric mucin. Filter discs inoculated with clones containing the empty vector, expressing Sha, Vat, Tsh, (**A**) TagB, TagC, or Sha S258A (**B**) were placed on the agar surface and incubated overnight at 37 °C. Mucin lysis zones were visualized by staining with 0.1% amido-black in 3.5 M acetic acid for 15 min, followed by destaining with 5% acetic acid and 0.5% glycerol for 6 h to overnight. (**C**) Zones of 0.5% porcine gastric mucin hydrolysis are visible in the stacking region of the SDS-PAGE gel (boxed area), concentrated supernatant extracts of SPATEs (5 µg of protein per well) were incubated at 37 °C for 48 h with mucin prior to migration. The gel was stained with a PAS glycoprotein staining kit.

2.7. TagC Exhibits Serine Protease-Dependent Gelatinase Activity

Some SPATEs were previously reported to degrade extracellular matrix proteins such as collagen and gelatin [23]. We previously demonstrated that TagB, TagC, and Sha could mediate increased adherence to chicken fibroblasts [20], which are cells that are associated with connective tissues and produce extracellular matrix proteins such as collagen. The hydrolyzed form of collagen—gelatin was used as a substrate to test for potential gelatinase activity from supernatant extracts containing SPATEs. Culture supernatant filtrate from *Pseudomonas aeruginosa* was used as a positive control, since it is known to demonstrate gelatinase activity [24]. Samples were incubated with 1% bovine gelatin for 48 h at 37 °C. Culture filtrates containing TagC as well as other SPATEs EspC, Tsh, and Vat demonstrated gelatinase activity (Figure 8A). By contrast, neither TagB nor Sha demonstrated gelatinase activity, since high-molecular-weight bands, indicating intact gelatin, remained after exposure to these SPATEs. Further, gelatinase activity from TagC was shown to be dependent on the serine protease motif, since the *E. coli* clone expressing a serine active site mutant protein, TagC S252A, did not generate a hydrolysis zone on medium containing 1% gelatin, whereas the TagC expressing clone did exhibit a hydrolysis zone (Figure 8B).
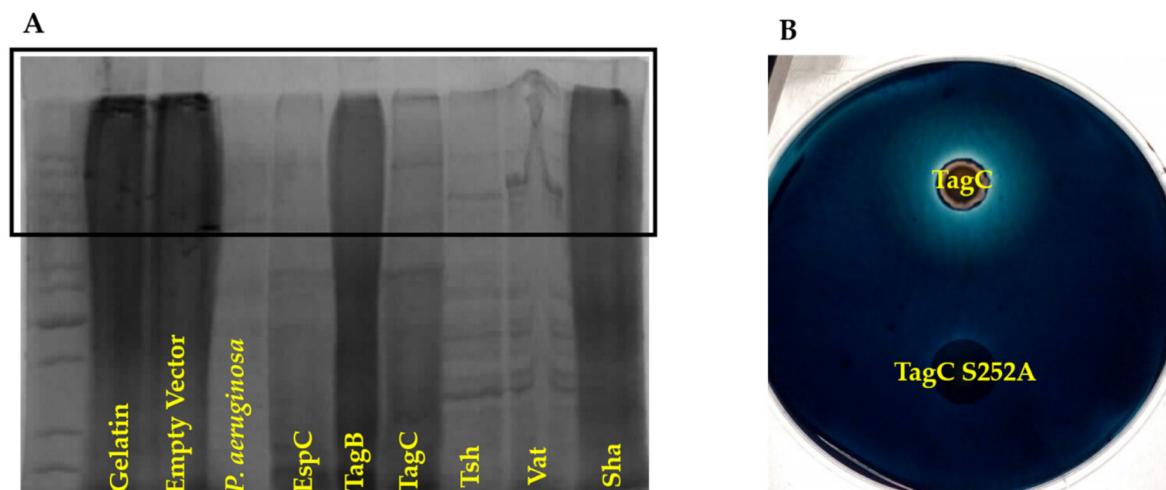
Figure 8. TagC demonstrates serine-protease dependent gelatinase activity, but not TagB nor Sha. (**A**) Zones of 1% bovine skin gelatin hydrolysis are visible in the stacking region of the SDS-PAGE gel (boxed area), concentrated supernatant extracts of SPATEs (5 μg of protein per well) were incubated at 37 °C for 48 h prior to migration. (**B**) Gelatinase activity of TagC was tested in a medium containing 1.5% agarose and 1% bovine skin gelatin. The disc inoculated with a clone expressing TagC or its serine catalytic site mutant variant, TagC S252A, were inoculated on the agar surface and were incubated for 48 h at 37 °C. Zones of gelatin lysis were visualized by staining with 0.1% amido-black in 3.5 M acetic acid for 15 min, followed by destaining with 5% acetic acid and 0.5% glycerol for 6 h.

3. Discussion

Colonization of the bladder is vital for UTI pathogenesis and UPEC deploys an array of virulence factors to infect and colonize the bladder, including secreted toxins [25]. Hemolysin A [8,9], UpxA (TosA) [26], cytotoxic necrotizing factor-1 (CNF-1) [27,28], and a variety of SPATEs (serine-protease autotransporters of *Enterobacteriaceae*) [29] are known toxins of host cells that are produced by some UPEC strains. The recent identification of new members of the SPATEs family present in some pathogenic *E. coli* and their cytotoxic activity on bladder cell lines [20], led us to further investigate mechanisms underlying the cytotoxic and proteolytic activity of the TagB, TagC, and Sha SPATEs on an established human urinary bladder cell line [30,31] and other properties of these virulence-associated proteins.

TagB, TagC, and Sha proteins demonstrated autoaggregating activity, and also promoted adherence of *E. coli* strain BL21 to the human HEK 293 renal and 5637 bladder human cell lines. Further, Sha also contributed to increased biofilm production [20]. SPATEs present on the bacterial surface are likely to contribute to the autoaggregation phenomenon. (Figure 1A). TagB and TagC also exhibited cytopathic effects on the bladder epithelial cell line. Further, we also previously determined that proteolytic activity of these SPATEs was strongly inhibited upon addition of serine protease inhibitor (PMSF), providing evidence for the importance of the serine protease motif in the activity of these SPATEs [20]. To further investigate the role of the serine protease activity, we generated catalytic site mutants of these three SPATEs. It is of note that the serine protease consensus motif (GDSGS) is conserved among different members of SPATEs [20,32–35]. Importantly, loss of the serine active site did not affect the processing or secretion of the SPATE proteins into the extracellular milieu (Figure 1A). Further, loss of the serine active site also eliminated any autoproteolytic activity (Figure 1A). Similarly, autoproteolytic activity has also been reported for other SPATEs including EspP, Sat, Pic [36], and for AspA autotransporter from *Neisseria meningitidis* [37]. Thus, from our results, it is clear that the processing of the passenger domain across the bacterial surface and autocatalytic activities of the TagB, TagC, and Sha is independent of the proteolytic serine site.

We investigated the role of the serine catalytic site of TagB, TagC, and Sha in autoaggregation or hemagglutination, as either SPATE protease activity on the bacterial or host cell surfaces could have possibly mediated these phenotypes. For instance, cleavage could have led to certain domains within the protein, leading to exposure of hydrophobic sites which could promote aggregation [38]. However, the serine protease site was not required for TagB, TagC, or Sha-mediated aggregation (Figure 2). These results indicate that other specific SPATE structural domains are likely to be responsible for aggregation. However, importantly, the autoaggregation phenotype is not a generalized phenotype of SPATEs, since in previous experiments, both the Tsh and Vat SPATEs did not demonstrate any autoaggregation phenotype [20]. Currently, the molecular mechanism of autoaggregation of TagB, TagC, and Sha is unknown. Unlike the three SPATEs described herein, loss of the active site serine of the Hap adhesin, a *Haemophilus influenzae* serine protease autotransporter, abrogated autoproteolytic processing leading to retention of this AT protein on the bacterial cell surface [39]. In fact, the increase in Hap present on the bacterial surface also increased aggregation, formation of microcolonies, and adherence of *H. influenzae* to host cells [40]. With regards to hemagglutination activity of the Sha protein, the serine active site was also dispensable. We found that Sha S258A hemagglutinated human blood with a similar titer to the native Sha protein. Similarly, a Tsh S259A variant protein was also able to bind to avian erythrocytes, turkey hemoglobin, collagen IV, fibronectin, and laminin [41]. Considering that the TagB S255A, TagC S252A, and Sha S258A variant SPATEs all retained the respective phenotypes present in the native SPATE proteins, this suggests that, despite lacking catalytic activity, that these variants are likely to have maintained a properly folded conformation.

In contrast to adherence or aggregation phenotypes, the presence of a serine protease motif was clearly required for cytotoxicity and entry of the SPATE proteins into bladder epithelial cells. In this study, the TagB S255A and TagC S252A mutant proteins were no longer cytopathic. Our results are similar to those described for other SPATEs [15,41,42] which have demonstrated a key role for the serine active site with regards to any native proteolytic or cytopathic activity of SPATEs on protein substrates or host cells.

Since TagC shares 60% identity/74% similarity with another SPATE, EspC, a non-LEE-encoded enterotoxin of enteropathogenic *E. coli* (EPEC) which causes cytotoxic effects and cleavage of cytoskeletal actin-associated protein [43]; we explored potential cellular targets in relation to the cytopathic effect observed in bladder epithelial cells. Following treatment with either TagB, TagC, or Sha, reorganization of the cytoskeleton and loss of actin stress fibers were seen in bladder epithelial cells (Figure 4). The effect of TagC was severe with faint staining remaining for actin compared to TagB interaction with cells. Exposure to Sha caused punctate localization of actin within the cytoplasm. Diminished actin staining and the formation of punctate actin accumulation suggests that each of these SPATEs are targeting the actin cytoskeleton or other cellular targets that lead to modifications in actin fiber formation or distribution within bladder cells. As expected, alterations in actin distribution were absent from bladder cells exposed to the serine catalytic site mutant variant proteins TagB S255A, TagC S252A, or Sha S258A, confirming the critical cytopathic role of serine protease activity.

Many pathogens exploit host actin for various stages of infection, including cellular invasion, intracellular replication, and dissemination by different mechanisms [44,45]. Specifically, during UTIs, UPEC utilizes the Rho family GTPase member Rac1 to mediate actin polymerization for *E. coli* bladder epithelial cell invasion [46]. It has been well documented that there is a relation between intracellular growth of UPEC in the bladder epithelium and the host F-actin cytoskeleton [47]. Based on the observation of actin rearrangement observed in bladder cells, it is also possible that the TagB, TagC, and Sha SPATEs might also contribute to UPEC invasion of the bladder epithelium, as these proteases may promote adhesion and loss of integrity of the protective epithelial barrier which could increase bacterial entry into epithelial cells as well as increase entry and systemic spread of the bacteria to other tissue sites during infection.

Before reaching the epithelial cell surface in the urinary tract, bacteria must cross the protective mucus layer that is coated with mucin [48]. Mucin serves as a primary antibacterial defense in the

bladder and contributes to host innate defense by providing a barrier and by trapping bacteria [49]. Many pathogens can invade or reduce the viscosity of mucin by cleaving it [50–52]. Certain SPATEs, belonging to the Class 2 family, including Pic [18,53], PicC of *Citrobacter rodentium* [53], and Tsh, demonstrate mucinase activity [54]. We, therefore, tested whether any of the three novel SPATEs were mucinolytic, and only Sha was identified as a mucinase (Figure 7). The zone of mucinolytic activity of Sha was intermediate when compared to Vat and Tsh and, as has been shown for Pic [18], the serine catalytic site of Sha was required for mucinase activity. From this standpoint, it is interesting to note that in strain QT598, 3 of the 5 SPATEs (Tsh, Vat, and Sha) demonstrate mucinase activity [20] which might facilitate bacterial colonization by degrading mucus to overcome the mucous barrier at the interface of epithelial surfaces. TagC was also shown to degrade gelatin, which is the hydrolyzed form of collagen, although this activity was absent from Sha and TagB. Collagen is an abundant and ubiquitous extracellular matrix protein that forms an essential component of connective tissues [55]. From this standpoint, the TagC protease may contribute to tissue invasion and systemic spread of ExPEC by degradation of extracellular matrix proteins. As expected, the activity of TagC on gelatin was also dependent on the active serine catalytic site. Similarly, Pic [23] also demonstrated gelatinase activity that required an active serine catalytic site.

Previous reports have described different mechanisms of internalization of SPATEs and types of cytoskeletal damage in various epithelial cells in vitro. The Pet SPATE from enteroaggregative *E. coli* (EAEC) is internalized by a retrograde trafficking pathway [56] through the Pet host cell receptor, cytokeratin 8 [57]. Once internalized, Pet causes loss of actin stress fibers due to the breakdown of spectrin [58,59]. Internalization of EspC by EPEC requires the type 3 secretion system [60] and leads to cleavage of cytoskeletal proteins [43]. Sat is secreted by UPEC, enters the cell by an unknown mechanism, and localizes to the cytoskeletal fraction of fodrin/spectrin and integrin present within bladder and kidney epithelial cells [15]. In the present report, we have demonstrated that TagB, TagC, and Sha are also internalized in bladder epithelial cells by a mechanism that requires an active serine catalytic domain. We used confocal Z-sections to verify the intracellular localization of the SPATEs within human bladder epithelial cells. Of note, we observed the internalization of TagB, TagC, and Sha within bladder cells after 5 h and this was concomitant with diminished fluorescence staining of actin in the vicinity of the localized SPATEs. This observation was pronounced following exposure to TagB, and TagB was shown to be closely associated with actin. Furthermore, to confirm the internalization of SPATEs within bladder epithelial cells, we carried out immunogold TEM of cross-sections of cells to demonstrate SPATE proteins within epithelial cells. TEM demonstrated localization of TagB and Sha in the cytoplasm, whereas TagC targeted the nucleus. We speculate that, since TagC has previously been shown to promote nuclear enlargement [20], TagC may alter nuclear targets and elicit a significant increase in nuclear size. The entry of these SPATEs into host bladder cells does not require a type 3 secretion mechanism since it is absent from *E. coli* QT598 and *E. coli* BL21, and SPATE proteins from bacterial supernatants entered bladder epithelial cells directly. Future studies will elucidate the cytoplasmic or nucleo-cytoplasmic shuttling pathways that mediate the entry and trafficking of these three SPATEs. Importantly, the serine catalytic site was required for cell entry and cytotoxicity of all three SPATEs, since serine protease active site mutants were unable to enter cells or cause any cytopathic effects, further demonstrating a critical role for the serine catalytic site of these SPATEs.

Taken together, the TagB, TagC, and Sha SPATE proteins mediate multiple activities. These include adhesion, aggregation, cytopathic effects, mucinase and gelatinase activities that may collectively contribute to different stages of bacterial infection including initial colonization, invasion of host epithelia, and an increased potential for systemic infection.

4. Materials and Methods

4.1. Ethics Statement

This study was performed in accordance with the ethical standards of the University of Quebec, INRS. A protocol for obtaining biological samples from human blood donors was reviewed and approved by the ethics committee—*Comité d'éthique en recherche* (CER 19-507, approved November 19, 2019) of INRS.

4.2. Bacterial Strains, Plasmids, and Growth Conditions

E. coli clones expressing TagB, TagC, or Sha were described previously [20]. All DNA constructs were transformed into *E. coli* strain BL21 or the type 1 fimbriae *fim*-negative *E. coli* strain ORN172. Strains were grown at 37 °C on solid or liquid Luria-Bertani medium (Alpha Bioscience, Baltimore, MD, USA) supplemented with the appropriate antibiotics when required at concentrations of 100 μg/mL ampicillin, 30 μg/mL chloramphenicol, or 50 μg/mL of kanamycin. Strains, plasmids, and primers are listed in Table 1.

Table 1. Strains and plasmids used in this study.

Strains	Characteristic(s)	Reference
QT598	APEC O1: K1, serum resistant	[61]
ORN172	*thr-1 leuB thi-1Δ (argF-lac)U169 xyl-7 ara-13 mtl-2 gal-6 rpsL tonA2 supE44Δ (fimBEACDFGH)::Km pilG1*	[62]
BL21	*fhuA2 [lon] ompT gal [dcm] ΔhsdS*	New England Biolabs
QT1603	HB101 with AIDA-1 operon	[63]
QT4767	ORN172/pIJ553 (Expressing *sha*)	
QT5194	BL21/pIJ548 (Expressing *tagB*)	
QT5195	BL21/pIJ549 (Expressing *tagC*)	
QT5197	BL21/pIJ550 (Expressing *espC*)	
QT5198	ORN172/pIJ548 (Expressing *tagB*)	[20]
QT5199	ORN172/pIJ549 (Expressing *tagC*)	
QT5431	BL21/pIJ551 (Expressing *vat*)	
QT5432	BL21/pIJ552 (Expressing *tsh*)	
QT5433	BL21/pIJ553 (Expressing *sha*)	
QT5437	BL21 + pIJ554 (Expressing *tagB S255A*)	This study
QT5438	BL21 + pIJ555 (Expressing *tagC S252A*)	This study
QT5439	BL21 + pIJ556 (Expressing *sha S258A*)	This study
QT5598	ORN172 + pIJ554 (Expressing *tagB S255A*)	This study
QT5599	ORN172 + pIJ555 (Expressing *tagC S252A*)	This study
QT5600	ORN172 + pIJ556 (Expressing *sha S258A*)	This study
QT3046	*Pseudomonas aeruginosa* PA14	Eric Déziel, INRS
Plasmids		

Table 1. *Cont.*

pBCsk+	Cloning vector; Cm^r	Stratagene, La Jolla, CA
pIJ548	pBCsk+::*tagB*	[20]
pIJ549	pBCsk+::*tagC*	
pIJ551	pBCsk+::*vat*	
pIJ552	pBCsk+::*tsh*	
pIJ553	pBCsk+::*sha*	
pIJ554	pBCsk+::*tagB S255A*	This study
pIJ555	pBCsk+::*tagC S252A*	This study
pIJ556	pBCsk+::*sha S258A*	This study

4.3. Site-Directed Mutagenesis

Site-directed mutagenesis was performed using the Q5® Site-Directed Mutagenesis kit as specified by the manufacturer. pIJ548, pIJ544, and pIJ553 were used as a template for the construction of the serine catalytic site mutants TagB S255A (pIJ554), TagC S252A (pIJ555), and Sha S258A (pIJ556) at 25 to 50 ng per reaction with 10 pmol of each of the complementary primers. Primers used to generate the single point mutation substituting alanine for serine for TagB were 5′-TCCCGGTGACGCCGGCTCTCCT-3′ and 5′-GTACCGTAGGTTGAGAGTG-3′; TagC were 5′-AGGAGGAGACGCCGGTTCCGGA-3′ and 5′-GTCACTTCATTATAAAATCCACC-3′; and Sha were 5′-GGCTGGTGATGCCGGTTCTCCGC-3′ and 5′-TCACCATAGATCGGTAATAC-3′. Following mutagenesis, all constructs were verified by sequencing at the proteomics platform of the Institut de Recherche en Immunologie et en Cancérologie (IRIC) of the Université de Montréal (Montréal, QC, Canada).

4.4. Recombinant Protein and Antibody Preparation

Expression and purification of SPATE proteins from concentrated filtered culture supernatant fractions were obtained as described previously [20] and the extract was checked by silver staining before each assay. Antibodies against ~ 112 kDa Vat protein were used to generate a Vat-specific rabbit polyclonal antibody, according to a standard protocol [64] (Laboratorio de Biología Celular y Tisular, Departamento de Morfología, Universidad Autónoma de Aguascalientes (UAA), Aguascalientes, Mexico). Since SPATE proteins contain some highly conserved epitopes, anti-Vat antibodies were used to detect and label each of the SPATE proteins. The alignment of the passenger domain of Vat with TagB, TagC, and Sha share identities of 39%, 30%, 56%, respectively. Specific epitopes are not established but Vat-antibodies demonstrate multiple conserved residues (Figure S4) and strong immune cross-reactivity. Cross-reactivity of antibodies raised against other SPATEs have also been reported. Antibodies raised against Pet protein (45% identity with EspC and 60 gaps) cross-reacted with EspC [65]. Likewise in the supernatant of CFT073, anti-Pic (44% identity with Vat and 76 gaps) antibodies were used to detect Vat and PicU SPATEs [66]. Polyclonal antisera adsorption was done by incubating the filtered supernatant of *E. coli* BL21 pBCsk+ without insert with a 1:50 dilution of the Vat polyclonal antiserum for 1 h at room temperature under mild agitation followed by centrifugation at 2000× *g* for 5 min at 4 °C.

4.5. Autoaggregation and Hemagglutination Tests

Autoaggregation of bacterial cells was measured by a settling assay as performed previously [20]. The sedimentation of 10 mL of each culture of *E. coli* BL21 cells expressing native or serine active site mutant SPATEs were adjusted to an OD$_{600nm}$ 1.5 from an overnight culture grown at 37 °C in liquid Luria-Bertani medium. Then, they were monitored for a reduction in turbidity from the top of the tube which was left at 4 °C for 3 h. The reduction of turbidity was plotted as a ratio against the initial turbidity.

For hemagglutination assays, human blood cells (RBCs) were washed and resuspended in PBS at a final concentration of 3% using a protocol adapted from [67]. The *E. coli fim*-negative K-12 strain ORN172 expressing either native or serine active site mutant SPATEs was grown overnight at 37 °C in Luria-Bertani medium, harvested and adjusted to an optical density (O.D.$_{600nm}$) of 60. Suspensions were serially diluted in 96-well round-bottom plates containing 20 μL of PBS mixed with 20 μL of 3% red blood cells and incubated for 30 min at 4 °C.

4.6. Epithelial Cell Culture

The 5637 bladder epithelial cell line was routinely cultured in RPMI 1640 medium (Thermo Fisher Scientific) supplemented with 10% heat-inactivated FBS at 37 °C in humidified 5% CO_2, and 2×10^5 cells/well were seeded into eight-well chamber slides (Thermo Fisher Scientific, Waltham, MA, USA) and allowed to grow to 75% confluence.

To determine cytopathic effects on bladder cells, a final concentration of 30 μg/mL of native SPATEs or the serine catalytic site mutants were added directly to monolayers and incubated for 5 h in RPMI 1640 medium at 37 °C with 5% CO_2. Cells were then washed twice with PBS (phosphate-buffered saline), fixed with 70% methanol, and stained with Giemsa stain. Cell morphology was analyzed at a magnification of ×20 with standard bright-field light microscopy. For the lactate dehydrogenase assay, supernatant from cells treated with native or mutant SPATEs were collected and the release of LDH in cell culture supernatants were quantified by using the CytoTox 96® Non-Radioactive Cytotoxicity Assay kit (Promega, Madison, WI, USA). Maximum LDH release (positive control) was determined by adding lysis solution (provided in the kit) to the non-infected cells.

For fluorescence actin-staining and immunostaining assays, cells were fixed with 3.0%–4.0% formaldehyde in PBS, washed, permeabilized by addition of 0.1% Triton X-100-PBS, stained with 0.05 μg of Alexa Fluor 488-phalloidin/mL (AAT Bioquest, Sunnyvale, CA, USA) at 37 °C for 1 h and counterstained with ProLong Gold/DAPI antifade reagent (Invitrogen, Carlsbad, CA, USA). After image acquisition using confocal microscope, the actin staining intensity was quantified by measuring mean gray value (mean pixel intensity) in ImageJ (https://imagej.nih.gov/ij/) [22]. The cells of interest as well as background with no fluorescence were selected manually to analyze the areas integrated intensities and mean gray value. The value was then corrected and total fluorescence (CTF) was calculated as CTF = Integrated Density – (Area of selected cell X Mean fluorescence of background readings). The averaged corrected mean gray value was used to generate relative quantitative comparison of fluorescence intensity.

SPATE protein localization in bladder cells was detected by immunofluorescence. Treated cells were fixed, permeabilized, and incubated with blocking solution (PBS with 5% BSA) for 1 h at 37 °C. Samples were then incubated with rabbit anti-SPATE polyclonal antibodies (UAA, Mexico) for 2 h at 37 °C. This was followed by incubation with secondary antibody Alexa Fluor 594-labeled goat anti-rabbit IgG antibody (Thermo Fisher Scientific, Waltham, MA, USA). Samples were mounted and imaged with the 60X objective of an LSM780 confocal microscope (Carl Zeiss microscopy Gmbh, Jena, Germany). Images were processed with ZEN 2012 software (Carl Zeiss microscopy Gmbh, Jena, Germany).

4.7. Electron Microscopy

Immunogold labeling of bacteria was carried out by culturing *E. coli* BL21 expressing different SPATEs in Luria-Bertani medium supplemented with 30 μg/mL chloramphenicol for 5 h. Bacterial suspensions (50 μL) were spotted on nickel-coated TEM grids. After 15 min, liquid was wicked away with bibulous paper and blocked with drops of PBS containing 1% ovalbumin for 15 min. A blocking solution was exchanged with a drop of SPATE antiserum diluted 1:100 in PBS. After 15 min, excess fluid was wicked away with bibulous paper and exchanged for PBS containing 1% ovalbumin drops for 5 min. The wash was repeated and then incubated in suitable goat anti-rabbit IgG (H+L), Alexa Fluor 488–10 nm colloidal gold secondary antibodies (Thermo Fisher Scientific, Waltham, MA, USA) diluted 1:250 in incubation solution. After 15 min, grids were washed twice with PBS drops and rinsed

twice with distilled water. Grids were dried with bibulous paper and imaged on a Philips CM-100 transmission electron microscope.

For immunogold labeling of epithelial cell thin sections, cells were fixed in 0.1% glutaraldehyde + 4% paraformaldehyde in cocodylate buffer at pH 7.2, and post-fixed in 1.3% osmium tetroxide in collidine buffer. After dehydration by successive passages through 25, 50, 75, and 95% solutions of acetone in water (for 15–30 min each) samples were immersed for 16–18 h in SPURR: acetone (1:1). Samples were then embedded in BEEM capsules using SPURR resin with the ELR-4221 kit (Polysciences Inc, Warrington, PA, USA) followed by placing the capsules at 60–65 °C for 20–30 h to polymerize the resin. After resin polymerization, samples were cut using an ultramicrotome (Ultratome) and were put onto Formvar and carbon covered-copper 200-mesh grids treated with sodium metaperiodate and were blocked with 1% BSA in PBS. Grids were then incubated with primary antibodies, washed, and incubated with goat anti-rabbit IgG (H+L), Alexa Fluor 488–10 nm colloidal gold secondary antibodies (Thermo Fisher Scientific, Waltham, MA, USA). After washing, samples were contrasted with uranyl acetate and lead citrate and subsequently visualized using a Philips EM 300 transmission electron microscope.

4.8. Cleavage of Protein Substrates

For mucinase activity, cultures of *E. coli* BL21 expressing SPATEs were incubated for 24 h at 37 °C on a medium containing 1.5% agarose and 0.5% porcine gastric mucin (Sigma-Aldrich, St. Louis, MI, USA). Plates were subsequently stained with 0.1% amido-black in 3.5 M acetic acid for 15 min, followed by destaining with 5% acetic acid and 0.5% glycerol for 6 h to overnight. Zones of mucin lysis were visualized as discolored halos around colonies. For the Periodic Acid Schiff (PAS) assay to detect mucin degradation [53], 5 μg of each SPATE protein were incubated with 5 μg of 0.5% porcine gastric mucin (Sigma-Aldrich) in 30 μL of MOPS buffer and incubated for 48 h at 37 °C. Treated samples were electrophoresed on an 8% SDS-PAGE gel and the gel staining was developed using a colorimetric Pierce™ Glycoprotein Staining kit (ThermoFisher Scientific, Waltham, MA, USA).

For gelatinase activity, 5 μg of each SPATE protein were incubated with 5 μg of bovine skin gelatin (Sigma-Aldrich, St. Louis, MI, USA) in 30 μL of MOPS buffer and incubated for 48 h at 37 °C. Samples were then boiled with Laemmli sample buffer, were electrophoresed on an 8% SDS-PAGE gel and then resolved by Coomassie blue staining. In addition, gelatinase activity was also tested by growing the clones on agar plates containing 1.5% agarose and 1% bovine skin gelatin for 48 h at 37 °C. Plates were subsequently stained with 0.1% amido-black in 3.5 M acetic acid for 15 min, followed by destaining with 5% acetic acid and 0.5% glycerol for 6 h to overnight. Zones of gelatin lysis consist of discolored halos around colonies.

4.9. Statistical Analysis

Experimental data were expressed as a mean ± standard error of the mean (SEM) in each group. The means of groups were combined and analyzed by a two-tailed Student *t*-test for pairwise comparisons and analysis of variance (ANOVA) to compare means of more than two populations. A *p* value of <0.05 was considered statistically significant. All data were analyzed with the Graph Pad Prism 7 software (GraphPad Software, San Diego, CA, USA).

5. Conclusions

In conclusion, TagB, TagC, and Sha are novel SPATEs that demonstrate different proteolytic activities on different substrates as well as distinct cytopathic effects on bladder epithelial cells. Additional molecular *in vitro* and *in vivo* studies are in progress in an effort to understand the link between protease activity of the TagB, TagC, and Sha SPATEs and how these proteases disrupt or alter the actin cytoskeleton during ExPEC infections. It will be of further interest to also investigate their potential interactions with other host cells or extracellular matrix proteins, and determine how these relatively large proteins (generally greater than 100 kDa) manage to enter host cells through

serine protease activity and what specific trafficking pathways may be involved in their localization or association with specific cellular compartments.

Abbreviations

AIDA-I	Adhesin involved in diffuse adherence
ANOVA	Analysis of variance
APEC	Avian pathogenic *E. coli*
CNF1	Cytotoxic necrotizing factor 1
DAPI	4′,6-Diamidino-2-phenylindole
EAEC	Enteroaggregative *E. coli*
EPEC	Enteropathogenic *E. coli*
ExPEC	Extra-intestinal pathogenic *E. coli*
LDH	Lactate dehydrogenase
LEE	Locus of enterocyte effacement
LPS	Lipopolysaccharides
OD	Optical density
PAS	Periodic acid–Schiff
PMSF	Phenylmethylsulfonyl fluoride
SDS-PAGE	Sodium dodecyl sulfate-polyacrylamide gel electrophoresis
SPATEs	Serine protease autotransporters of *Enterobacteriaceae*
TEM	Transmission electron microscopy
UPEC	Uropathogenic Escherichia coli
UTIs	Urinary tract infections

References

1. Foxman, B.; Brown, P. Epidemiology of Urinary Tract Infections: Transmission and Risk Factors, Incidence, and Costs. *Infect. Dis. Clin. North Am.* **2003**, *17*, 227–241. [CrossRef]

2. Foxman, B. Urinary Tract Infection Syndromes: Occurrence, Recurrence, Bacteriology, Risk Factors, and Disease Burden. *Infect. Dis. Clin. North Am.* **2014**, *28*, 1–13. [CrossRef] [PubMed]

3. Flores-Mireles, A.L.; Walker, J.N.; Caparon, M.; Hultgren, S.J. Urinary Tract Infections: Epidemiology, Mechanisms of Infection and Treatment Options. *Nature Rev. Microbiol.* **2015**, *13*, 269–284. [CrossRef] [PubMed]

4. O'Brien, V.P.; Hannan, T.J.; Nielsen, H.V.; Hultgren, S.J. Drug and Vaccine Development for the Treatment and Prevention of Urinary Tract Infections. *Microbiol. Spectr.* **2016**, *4*. [CrossRef]

5. Lewis, S.A. Everything You Wanted to Know About the Bladder Epithelium but Were Afraid to Ask. *Am. J. Physiol. Ren. Physiol.* **2000**, *278*, F867–F874. [CrossRef]

6. Keane, W.F.; Welch, R.; Gekker, G.; Peterson, P.K. Mechanism of *Escherichia coli* Alpha-Hemolysin-Induced Injury to Isolated Renal Tubular Cells. *Am. J. Pathol.* **1987**, *126*, 350.

7. Russo, T.A.; Davidson, B.A.; Genagon, S.A.; Warholic, N.M.; MacDonald, U.; Pawlicki, P.D.; Beanan, J.; Olson, M.R.; Holm, B.A.; Knight, P.R., 3rd. *E. coli* Virulence Factor Hemolysin Induces Neutrophil Apoptosis and Necrosis/Lysis in Vitro and Necrosis/Lysis and Lung Injury in a Rat Pneumonia Model. *Am. J. Physiol. Lung Cell. Mol. Physiol.* **2005**, *289*, L207–L216. [CrossRef]

8.   Smith, Y.C.; Rasmussen, S.B.; Grande, K.K.; Conran, R.M.; O'Brien, A.D. Hemolysin of Uropathogenic *Escherichia coli* Evokes Extensive Shedding of the Uroepithelium and Hemorrhage in Bladder Tissue within the First 24 Hours after Intraurethral Inoculation of Mice. *Infect. Immun.* **2008**, *76*, 2978–2990. [CrossRef]

9.   Dhakal, B.K.; Mulvey, M.A. The Upec Pore-Forming Toxin A-Hemolysin Triggers Proteolysis of Host Proteins to Disrupt Cell Adhesion, Inflammatory, and Survival Pathways. *Cell Host Microbe* **2012**, *11*, 58–69. [CrossRef] [PubMed]

10.   Wiles, T.J.; Mulvey, M.A. The Rtx Pore-Forming Toxin A-Hemolysin of Uropathogenic *Escherichia coli*: Progress and Perspectives. *Future Microbiol.* **2013**, *8*, 73–84. [CrossRef]

11.   Ristow, L.C.; Welch, R.A. Hemolysin of Uropathogenic *Escherichia coli*: A Cloak or a Dagger? *Biochim. Biophys. Acta Biomembr.* **2016**, *1858*, 538–545. [CrossRef] [PubMed]

12.   Visvikis, O.; Boyer, L.; Torrino, S.; Doye, A.; Lemonnier, M.; Lorès, P.; Rolando, M.; Flatau, G.; Mettouchi, A.; Bouvard, D. Escherichia coli Producing Cnf1 Toxin Hijacks Tollip to Trigger Rac1-Dependent Cell Invasion. *Traffic* **2011**, *12*, 579–590. [CrossRef] [PubMed]

13.   Mills, M.; Meysick, K.C.; O'Brien, A.D. Cytotoxic Necrotizing Factor Type 1 of Uropathogenic *Escherichia coli* Kills Cultured Human Uroepithelial 5637 Cells by an Apoptotic Mechanism. *Infect. Immun.* **2000**, *68*, 5869–5880. [CrossRef] [PubMed]

14.   Guyer, D.M.; Radulovic, S.; Jones, F.-E.; Mobley, H.L.T. Sat, the Secreted Autotransporter Toxin of Uropathogenic *Escherichia coli*, Is a Vacuolating Cytotoxin for Bladder and Kidney Epithelial Cells. *Infect. Immun.* **2002**, *70*, 4539–4546. [CrossRef]

15.   Maroncle, N.M.; Sivick, K.E.; Brady, R.; Stokes, F.-E.; Mobley, H.L.T. Protease Activity, Secretion, Cell Entry, Cytotoxicity, and Cellular Targets of Secreted Autotransporter Toxin of Uropathogenic *Escherichia coli*. *Infect. Immun.* **2006**, *74*, 6124–6134. [CrossRef]

16.   Heimer, S.R.; Rasko, D.A.; Lockatell, C.V.; Johnson, D.E.; Mobley, H.L.T. Autotransporter Genes Pic and Tsh Are Associated with *Escherichia coli* Strains That Cause Acute Pyelonephritis and Are Expressed During Urinary Tract Infection. *Infect. Immun.* **2004**, *72*, 593–597. [CrossRef]

17.   Carter, P.; Wells, J.A. Dissecting the Catalytic Triad of a Serine Protease. *Nature* **1988**, *332*, 564. [CrossRef]

18.   Gutierrez-Jimenez, J.; Arciniega, I.; Navarro-García, F. The Serine Protease Motif of Pic Mediates a Dose-Dependent Mucolytic Activity after Binding to Sugar Constituents of the Mucin Substrate. *Microb. Pathog.* **2008**, *45*, 115–123. [CrossRef]

19.   Navarro-Garcia, F.; Gutierrez-Jimenez, J.; Garcia-Tovar, C.; Castro, L.A.; Salazar-Gonzalez, H.; Cordova, V. Pic, an Autotransporter Protein Secreted by Different Pathogens in the *Enterobacteriaceae* Family, Is a Potent Mucus Secretagogue. *Infect. Immun.* **2010**, *78*, 4101–4109. [CrossRef]

20.   Habouria, H.; Pokharel, P.; Maris, S.; Garénaux, A.; Bessaiah, H.; Houle, S.; Veyrier, F.J.; Guyomard-Rabenirina, S.; Talarmin, A.; Dozois, C.M. Three New Serine-Protease Autotransporters of *Enterobacteriaceae* (SPATEs) from Extra-Intestinal Pathogenic *Escherichia coli* and Combined Role of Spates for Cytotoxicity and Colonization of the Mouse Kidney. *Virulence* **2019**, *10*, 568–587. [CrossRef]

21.   Benz, I.; Alexander Schmidt, M. Aida-I, the Adhesin Involved in Diffuse Adherence of the Diarrhoeagenic *Escherichia coli* Strain 2787 (O126: H27), Is Synthesized Via a Precursor Molecule. *Mol. Microbiol.* **1992**, *6*, 1539–1546. [CrossRef] [PubMed]

22.   Abràmoff, M.D.; Magalhães, P.J.; Ram, S.J. Image Processing with Imagej. *Biophotonics Int.* **2004**, *11*, 36–42.

23.   Henderson, I.R.; Czeczulin, J.; Eslava, C.; Noriega, F.; Nataro, J.P. Characterization of Pic, a Secreted Protease Ofshigella Flexneri and Enteroaggregative *Escherichia coli*. *Infect. Immun.* **1999**, *67*, 5587–5596. [CrossRef] [PubMed]

24.   Pickett, M.J.; Greenwood, J.R.; Harvey, S.M. Tests for Detecting Degradation of Gelatin: Comparison of Five Methods. *J. Clin. Microbiol.* **1991**, *29*, 2322–2325. [CrossRef] [PubMed]

25.   Xicohtencatl-Cortes, J.; Saldaña, Z.; Deng, W.; Castañeda, E.; Freer, E.; Tarr, P.I.; Finlay, B.B.; Puente, J.L.; Girón, J.A. Bacterial Macroscopic Rope-Like Fibers with Cytopathic and Adhesive Properties. *J. Biol. Chem.* **2010**, *285*, 32336–32342. [CrossRef]

26.   Vigil, P.D.; Wiles, T.J.; Engstrom, M.D.; Prasov, L.; Mulvey, M.A.; Mobley, H.L.T. The Repeat-in-Toxin Family Member Tosa Mediates Adherence of Uropathogenic *Escherichia coli* and Survival During Bacteremia. *Infect. Immun.* **2012**, *80*, 493–505. [CrossRef]

27. Rippere-Lampe, K.E.; O'Brien, A.D.; Conran, R.; Lockman, H.A. Mutation of the Gene Encoding Cytotoxic Necrotizing Factor Type 1 (Cnf 1) Attenuates the Virulence of Uropathogenic Escherichia coli. *Infect. Immun.* **2001**, *69*, 3954–3964. [CrossRef]

28. Davis, J.M.; Rasmussen, S.B.; O'Brien, A.D. Cytotoxic Necrotizing Factor Type 1 Production by Uropathogenic *Escherichia coli* Modulates Polymorphonuclear Leukocyte Function. *Infect. Immun.* **2005**, *73*, 5301–5310. [CrossRef]

29. Pokharel, P.; Habouria, H.; Bessaiah, H.; Dozois, C.M. Serine Protease Autotransporters of the Enterobacteriaceae (SPATEs): Out and About and Chopping It Up. *Microorganisms* **2019**, *7*, 594. [CrossRef]

30. Martinez, J.J.; Mulvey, M.A.; Schilling, J.D.; Pinkner, J.S.; Hultgren, S.J. Type 1 Pilus-Mediated Bacterial Invasion of Bladder Epithelial Cells. *EMBO J.* **2000**, *19*, 2803–2812. [CrossRef]

31. Mulvey, M.A.; Schilling, J.D.; Hultgren, S.J. Establishment of a Persistent *Escherichia coli* Reservoir During the Acute Phase of a Bladder Infection. *Infect. Immun.* **2001**, *69*, 4572–4579. [CrossRef] [PubMed]

32. Eslava, C.; Navarro-García, F.; Czeczulin, J.R.; Henderson, I.R.; Cravioto, A.; Nataro, J.P. Pet, an Autotransporter Enterotoxin from Enteroaggregative *Escherichia coli*. *Infect. Immune.* **1998**, *66*, 3155–3163. [CrossRef]

33. Brunder, W.; Schmidt, H.; Karch, H. Espp, a Novel Extracellular Serine Protease of Enterohaemorrhagic *Escherichia coli* O157: H7 Cleaves Human Coagulation Factor, V. *Mol. Microbiol.* **1997**, *24*, 767–778. [CrossRef]

34. Dozois, C.M.; Dho-Moulin, M.; Brée, A.; Fairbrother, J.M.; Desautels, C.; Curtiss, R. Relationship between the Tsh Autotransporter and Pathogenicity of Avian *Escherichia coli* and Localization and Analysis of the Tsh Genetic Region. *Infect. Immun.* **2000**, *68*, 4145–4154. [CrossRef] [PubMed]

35. Stein, M.; Kenny, B.; Stein, M.A.; Finlay, B.B. Characterization of Espc, a 110-Kilodalton Protein Secreted by Enteropathogenic *Escherichia coli* Which Is Homologous to Members of the Immunoglobulin a Protease-Like Family of Secreted Proteins. *J. Bacteriol.* **1996**, *178*, 6546–6554. [CrossRef]

36. Dutta, P.R.; Cappello, R.; Navarro-García, F.; Nataro, J.P. Functional Comparison of Serine Protease Autotransporters of Enterobacteriaceae. *Infect. Immun.* **2002**, *70*, 7105–7113. [CrossRef] [PubMed]

37. Turner, D.P.J.; Wooldridge, K.G.; Ala'Aldeen, D.A.A. Autotransported Serine Protease a of Neisseria Meningitidis: An Immunogenic, Surface-Exposed Outer Membrane, and Secreted Protein. *Infect. Immun.* **2002**, *70*, 4447–4461. [CrossRef]

38. Jonsson, P.; Wadström, T. Cell Surface Hydrophobicity Ofstaphylococcus Aureus Measured by the Salt Aggregation Test (Sat). *Curr. Microbiol.* **1984**, *10*, 203–209. [CrossRef]

39. Hendrixson, D.R.; De La Morena, M.L.; Stathopoulos, C.; St Geme, J.W., 3rd. Structural Determinants of Processing and Secretion of the Haemophilus Influenzae Hap Protein. *Mol. Microbiol.* **1997**, *26*, 505–518. [CrossRef]

40. Hendrixson, D.R.; St Geme, J.W., 3rd. The Haemophilus Influenzae Hap Serine Protease Promotes Adherence and Microcolony Formation, Potentiated by a Soluble Host Protein. *Mol. Cell* **1998**, *2*, 841–850. [CrossRef]

41. Kostakioti, M.; Stathopoulos, C. Functional Analysis of the Tsh Autotransporter from an Avian Pathogenic *Escherichia coli* Strain. *Infect. Immun.* **2004**, *72*, 5548–5554. [CrossRef]

42. Brockmeyer, J.; Spelten, S.; Kuczius, T.; Bielaszewska, M.; Karch, H. Structure and Function Relationship of the Autotransport and Proteolytic Activity of Espp from Shiga Toxin-Producing *Escherichia coli*. *PLoS ONE* **2009**, *4*, e6100. [CrossRef] [PubMed]

43. Navarro-Garcia, F.; Serapio-Palacios, A.; Vidal, J.E.; Salazar, M.I.; Tapia-Pastrana, G. Espc Promotes Epithelial Cell Detachment by Enteropathogenic *Escherichia coli* Via Sequential Cleavages of a Cytoskeletal Protein and Then Focal Adhesion Proteins. *Infect. Immun.* **2014**, *82*, 2255–2265. [CrossRef] [PubMed]

44. Gruenheid, S.; Finlay, B.B. Microbial Pathogenesis and Cytoskeletal Function. *Nature* **2003**, *422*, 775. [CrossRef]

45. Rottner, K.; Stradal, T.E.B.; Wehland, J. Bacteria-Host-Cell Interactions at the Plasma Membrane: Stories on Actin Cytoskeleton Subversion. *Dev. Cell* **2005**, *9*, 3–17. [CrossRef] [PubMed]

46. Martinez, J.J.; Hultgren, S.J. Requirement of Rho-Family Gtpases in the Invasion of Type 1-Piliated Uropathogenic *Escherichia coli*. *Cell. Microbiol.* **2002**, *4*, 19–28. [CrossRef] [PubMed]

47. Eto, D.S.; Sundsbak, J.L.; Mulvey, M.A. Actin-Gated Intracellular Growth and Resurgence of Uropathogenic *Escherichia coli*. *Cell. Microbiol.* **2006**, *8*, 704–717. [CrossRef]

48. Balish, M.J.; Jensen, J.; Uehling, D.T. Bladder Mucin: A Scanning Electron Microscopy Study in Experimental Cystitis. *J. Urol.* **1982**, *128*, 1060–1063. [CrossRef]

49. Parsons, C.L.; Greenspan, C.; Moore, S.W.; Grant, S. Mulholland. Role of Surface Mucin in Primary Antibacterial Defense of Bladder. *Urology* **1977**, *9*, 48–52. [CrossRef]

50. Lehker, M.W.; Sweeney, D. Trichomonad Invasion of the Mucous Layer Requires Adhesins, Mucinases, and Motility. *Sex. Transm. Infect.* **1999**, *75*, 231–238. [CrossRef]

51. Mantle, M.; Husar, S.D. Binding of Yersinia Enterocolitica to Purified, Native Small Intestinal Mucins from Rabbits and Humans Involves Interactions with the Mucin Carbohydrate Moiety. *Infect. Immun.* **1994**, *62*, 1219–1227. [CrossRef]

52. Finkelstein, R.A.; Boesman-Finkelstein, M.; Holt, P. Vibrio Cholerae Hemagglutinin/Lectin/Protease Hydrolyzes Fibronectin and Ovomucin: Fm Burnet Revisited. *Proc. Natl. Acad. Sci. USA* **1983**, *80*, 1092–1095. [CrossRef] [PubMed]

53. Bhullar, K.; Zarepour, M.; Yu, H.; Yang, H.; Croxen, M.; Stahl, M.; Finlay, B.B.; Turvey, S.E.; Vallance, B.A. The Serine Protease Autotransporter Pic Modulates Citrobacter Rodentium Pathogenesis and Its Innate Recognition by the Host. *Infect. Immun.* **2015**, *83*, 2636–2650. [CrossRef] [PubMed]

54. Kobayashi, R.K.T.; Gaziri, L.C.J.; Vidotto, M.C. Functional Activities of the Tsh Protein from Avian Pathogenic *Escherichia coli* (APEC) Strains. *J. Vet. Sci.* **2010**, *11*, 315–319. [CrossRef] [PubMed]

55. Ricard-Blum, S. The Collagen Family. *Cold Spring Harbor Perspect. Biol.* **2011**, *3*, a004978. [CrossRef]

56. Navarro-García, F.; Canizalez-Roman, A.; Burlingame, K.E.; Teter, K.; Vidal, J.E. Pet, a Non-Ab Toxin, Is Transported and Translocated into Epithelial Cells by a Retrograde Trafficking Pathway. *Infect. Immun.* **2007**, *75*, 2101–2109.

57. Nava-Acosta, R.; Navarro-Garcia, F. Cytokeratin 8 Is an Epithelial Cell Receptor for Pet, a Cytotoxic Serine Protease Autotransporter of Enterobacteriaceae. *MBio* **2013**, *4*, e00838-13. [CrossRef]

58. Navarro-García, F.; Sears, C.; Eslava, C.; Cravioto, A.; Nataro, J.P. Cytoskeletal Effects Induced by Pet, the Serine Protease Enterotoxin of Enteroaggregative *Escherichia coli*. *Infect. Immun.* **1999**, *67*, 2184–2192.

59. Dutta, P.R.; Sui, B.Q.; Nataro, J.P. Structure-Function Analysis of the Enteroaggregative *Escherichia coli* Plasmid-Encoded Toxin Autotransporter Using Scanning Linker Mutagenesis. *J. Biol. Chem.* **2003**, *278*, 39912–39920. [CrossRef]

60. Vidal, J.E.; Navarro-García, F. Espc Translocation into Epithelial Cells by Enteropathogenic *Escherichia coli* Requires a Concerted Participation of Type V and Iii Secretion Systems. *Cell. Microbiol.* **2008**, *10*, 1975–1986. [CrossRef]

61. Marc, D.; Dho-Moulin, M. Analysis of the Fim Cluster of an Avian O2 Strain of *Escherichia coli*: Serogroup-Specific Sites within Fima and Nucleotide Sequence of Fimi. *J. Med Microbiol.* **1996**, *44*, 444–452. [CrossRef]

62. Woodall, L.D.; Russell, P.W.; Harris, S.L.; Orndorff, P.E. Rapid, Synchronous, and Stable Induction of Type 1 Piliation in *Escherichia coli* by Using a Chromosomal Lacuv5 Promoter. *J. Bacteriol.* **1993**, *175*, 2770–2778. [CrossRef] [PubMed]

63. Charbonneau, M.-È.; Berthiaume, F.; Mourez, M. Proteolytic Processing Is Not Essential for Multiple Functions of the *Escherichia coli* Autotransporter Adhesin Involved in Diffuse Adherence (Aida-I). *J. Bacteriol.* **2006**, *188*, 8504–8512. [CrossRef] [PubMed]

64. Nakazawa, M.; Mukumoto, M.; Miyatake, K. Production and Purification of Polyclonal Antibodies. *Methods Mol. Biol. (Clifton, N.J.)*. **2016**. [CrossRef]

65. Mellies, J.L.; Navarro-Garcia, F.; Okeke, I.; Frederickson, J.; Nataro, J.P.; Kaper, J.B. Espc Pathogenicity Island of Enteropathogenic *Escherichia coli* Encodes an Enterotoxin. *Infect. Immun.* **2001**, *69*, 315–324. [CrossRef] [PubMed]

66. Parham, N.J.; Srinivasan, U.; Desvaux, M.; Foxman, B.; Marrs, C.F.; Henderson, I.R. Picu, a Second Serine Protease Autotransporter of Uropathogenic Escherichia coli. *FEMS Microbiol. Lett.* **2004**, *230*, 73–83. [CrossRef]

67. Provence, D.L.; Curtiss, R., 3rd. Role of Crl in Avian Pathogenic *Escherichia coli*: A Knockout Mutation of Crl Does Not Affect Hemagglutination Activity, Fibronectin Binding, or Curli Production. *Infect. Immun.* **1992**, *60*, 4460–4467. [CrossRef]

14 ANNEXE III Review article on SPATES

En tant que troisième auteur de cet article de revue, j'ai participé dans la rédaction et j'ai apporté mes commentaires sur l'ensemble de la revue avant soumission.

microorganisms

MDPI

Review

Serine Protease Autotransporters of the *Enterobacteriaceae* (SPATEs): Out and About and Chopping It Up

Pravil Pokharel [1,2,†], Hajer Habouria [1,2,†], Hicham Bessaiah [1,2] and Charles M. Dozois [1,2,3,*]

1   Institut National de Recherche Scientifique (INRS)-Centre Armand-Frappier Santé Biotechnologie, Laval, QC H7V 1B7, Canada; micropravil@gmail.com (P.P.); hajer.hbr2@gmail.com (H.H.); hicham.bessaiah@iaf.inrs.ca (H.B.)
2   Centre de Recherche en Infectiologie Porcine et Avicole (CRIPA), Saint-Hyacinthe, QC J2S 2M2, Canada
3   Institut Pasteur International Network, Laval, QC H7V 1B7, Canada
*   Correspondence: charles.dozois@iaf.inrs.ca
†   These authors contributed equally to this work.

check for updates

Abstract: Autotransporters are secreted proteins with multiple functions produced by a variety of Gram-negative bacteria. In *Enterobacteriaceae*, a subgroup of these autotransporters are the SPATEs (serine protease autotransporters of *Enterobacteriaceae*). SPATEs play a crucial role in survival and virulence of pathogens such as *Escherichia coli* and *Shigella* spp. and contribute to intestinal and extra-intestinal infections. These high molecular weight proteases are transported to the external milieu by the type Va secretion system and function as proteases with diverse substrate specificities and biological functions including adherence and cytotoxicity. Herein, we provide an overview of SPATEs and discuss recent findings on the biological roles of these secreted proteins, including proteolysis of substrates, adherence to cells, modulation of the immune response, and virulence in host models. In closing, we highlight recent insights into the regulation of expression of SPATEs that could be exploited to understand fundamental SPATE biology.

Keywords: serine protease autotransporters of *Enterobacteriaceae* (SPATE); autotransporters; cytotoxins; adhesins; *E. coli*; gene regulation

1. Introduction

Bacteria have acquired a capacity to export and secrete proteins and other molecules to the cell surface in order to interact with the extracellular environment. The transport of proteins to the cell surface is achieved through a number of highly specialized protein secretion systems that release them into the extracellular milieu. In Gram-negative bacteria, which have an inner and outer membrane that contains a periplasmic space, secretion can be a two-step process involving export to the periplasmic space, and in some cases, subsequent secretion through the outer membrane. Autotransporter (AT) proteins comprise a large family with more than 1000 members that have been characterized [1]. AT proteins represent the largest family of secreted polypeptides in Gram-negative bacteria and serine protease autotransporters of *Enterobacteriaceae* (SPATEs) are a subclass of AT proteins that contain a protease domain belonging to the trypsin-like family, which typically contains a serine in the catalytic motif [1]. In recent years, considerable information has been obtained about how these proteins are assembled and secreted. Here, we review the latest findings on the AT secretion system with a recent model for transporting SPATE cargo out of the bacterial cell and in-depth updates of members of SPATEs including studies on genomic distribution, gene regulation, classification, and fate of the protein during in vitro or in vivo host interaction.

Review

Serine Protease Autotransporters of the *Enterobacteriaceae* (SPATEs): Out and About and Chopping It Up

Pravil Pokharel [1,2,†], **Hajer Habouria** [1,2,†], **Hicham Bessaiah** [1,2] and **Charles M. Dozois** [1,2,3,*]

1   Institut National de Recherche Scientifique (INRS)-Centre Armand-Frappier Santé Biotechnologie, Laval, QC H7V 1B7, Canada; micropravil@gmail.com (P.P.); hajer.hbr2@gmail.com (H.H.); hicham.bessaiah@iaf.inrs.ca (H.B.)
2   Centre de Recherche en Infectiologie Porcine et Avicole (CRIPA), Saint-Hyacinthe, QC J2S 2M2, Canada
3   Institut Pasteur International Network, Laval, QC H7V 1B7, Canada
*   Correspondence: charles.dozois@iaf.inrs.ca
†   These authors contributed equally to this work.

check for updates

Abstract: Autotransporters are secreted proteins with multiple functions produced by a variety of Gram-negative bacteria. In *Enterobacteriaceae*, a subgroup of these autotransporters are the SPATEs (serine protease autotransporters of *Enterobacteriaceae*). SPATEs play a crucial role in survival and virulence of pathogens such as *Escherichia coli* and *Shigella* spp. and contribute to intestinal and extra-intestinal infections. These high molecular weight proteases are transported to the external milieu by the type Va secretion system and function as proteases with diverse substrate specificities and biological functions including adherence and cytotoxicity. Herein, we provide an overview of SPATEs and discuss recent findings on the biological roles of these secreted proteins, including proteolysis of substrates, adherence to cells, modulation of the immune response, and virulence in host models. In closing, we highlight recent insights into the regulation of expression of SPATEs that could be exploited to understand fundamental SPATE biology.

Keywords: serine protease autotransporters of *Enterobacteriaceae* (SPATE); autotransporters; cytotoxins; adhesins; *E. coli*; gene regulation

1. Introduction

Bacteria have acquired a capacity to export and secrete proteins and other molecules to the cell surface in order to interact with the extracellular environment. The transport of proteins to the cell surface is achieved through a number of highly specialized protein secretion systems that release them into the extracellular milieu. In Gram-negative bacteria, which have an inner and outer membrane that contains a periplasmic space, secretion can be a two-step process involving export to the periplasmic space, and in some cases, subsequent secretion through the outer membrane. Autotransporter (AT) proteins comprise a large family with more than 1000 members that have been characterized [1]. AT proteins represent the largest family of secreted polypeptides in Gram-negative bacteria and serine protease autotransporters of *Enterobacteriaceae* (SPATEs) are a subclass of AT proteins that contain a protease domain belonging to the trypsin-like family, which typically contains a serine in the catalytic motif [1]. In recent years, considerable information has been obtained about how these proteins are assembled and secreted. Here, we review the latest findings on the AT secretion system with a recent model for transporting SPATE cargo out of the bacterial cell and in-depth updates of members of SPATEs including studies on genomic distribution, gene regulation, classification, and fate of the protein during in vitro or in vivo host interaction.

2. The Autotransporter Secretion Pathway

AT secretion through the outer membrane is mediated by the type V secretion system (T5SS) or AT secretion pathway. The T5SS pathway has been subdivided into five subtypes: (i) T5SS of monomeric ATs is classed as type Va secretion; (ii) two-partner secretion is classed as type Vb secretion; (iii) trimeric AT secretion is classed as type Vc secretion [2]; (iv) secretion of ATs homologous to both type Va and type Vb is described as type Vd [3]; and (v) secretion of intimins and invasins is classed as subtype Ve [4]. SPATEs are monomeric ATs that are secreted by the type Va secretion pathway.

The figure below depicts the major differences between these subtypes, which includes the variations in alignments of different domains (Figure 1). In type Va ATs, release of the N-terminal passenger domain is assisted by a C-terminal translocation domain or autoprocessed and liberated into the external milieu (explained in detail below) [1]. Type Vb is a split variant of the type Va system as the passenger domain and translocation domain are located in different polypeptide chains, and the translocated domain contains periplasmic polypeptide transport-associated (POTRA) motifs. As such, the type Vb class has also been described as a two-partner secretion system [5]. The type Vc class comprises ATs that form trimers and are also called trimeric autotransporter adhesins [2]. Type Vd ATs differ from type Va due to the presence of additional periplasmic domains between the passenger domain and the translocation domain, which is homologous to the periplasmic domains present in type Vb proteins [3]. Likewise, in type Ve ATs, the domains have a reverse order, wherein the passenger domain is at the C-terminal and translocation domain is N-terminal [4].
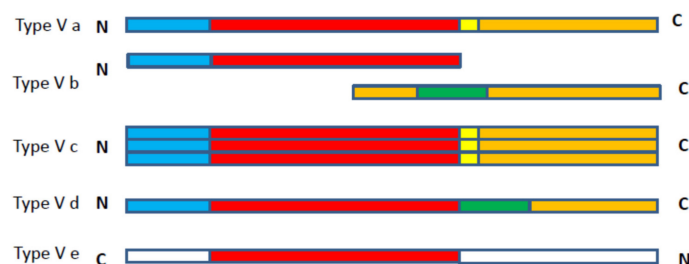

Figure 1. Scheme presenting domain organization among the subclasses of type-V bacterial autotransporter proteins. The labeling includes the conserved domains, colored blocks correspond to: Signal peptide (blue), passenger domain (red), polypeptide transport associated (POTRA) domain (green), linker domain (yellow) and translocation domain (orange). Adapted from [1,4].

Understanding the biogenesis of the SPATEs is of great interest for the isolation, purification, and characterization of these proteins. Over the last two decades, a diversity of predicted AT proteins, including SPATES, have been identified through the sequencing of many bacterial genomes and through bioinformatics analysis. However, only a few SPATEs have been more extensively studied with regards to their biological functions and structural characterization. The crystal structure of the passenger domain of three SPATEs has been determined: EspP from an *Escherichia coli* O157:H7 strain [6], Hbp (also called Tsh) from an extra-intestinal pathogenic *E. coli* (ExPEC) strain [7] and Pet from enteroaggregative *E. coli* (EAEC) strains [8]. Based upon these crystal structures, general models of structure and translocation have been proposed, although, whether such models derived from only a few SPATE structures collectively represent all other SPATEs remains to be determined.

The general structure of AT proteins, including SPATES, comprises three functional domains: The signal peptide, which mediates the Sec-dependent transport of the protein into the periplasm; the N-terminal passenger domain (also called the α-domain), which is the mature protein that is exposed at the surface of the outer membrane and/or released extracellularly; and the pore forming carboxyl-terminal translocator domain (also called as β-barrel), which provides the channel through which the passenger domain is translocated to the surface of the outer membrane [9]. Initial proposals of ATs as autonomously secreted proteins have been rejected due to recent findings, indicating a role for accessory proteins located in the inner membrane [10], the periplasm [11] and the outer membrane [10] which facilitate or mediate translocation of AT proteins to the cell surface.

ATs are exported into the periplasmic space through the Sec-dependent pathway [1], and export can occur co-translationally or follow autotransporter synthesis into the cytoplasm [12]. Immediate export following translation could improve export by preventing premature folding and degradation in the cytoplasm. Upon reaching the periplasm via the Sec-translocon and cleavage of the signal sequence, AT proteins are then protected by conserved periplasmic chaperones such as Skp, SurA, and DegP and directed toward the β-barrel assembly machinery (Bam) complex, which catalyzes the insertion and assembly of the outer membrane protein (Figure 2) [13,14]. A "Hybrid barrel-model" (Figure 2) has been proposed to explain the translocation of the passenger domain through the outer membrane. It has been shown that passenger domain secretion does not appear to use ATP, but that vectorial folding of the C-terminal of the passenger domain may contribute the necessary energy required for transmembrane passage and folding [15].
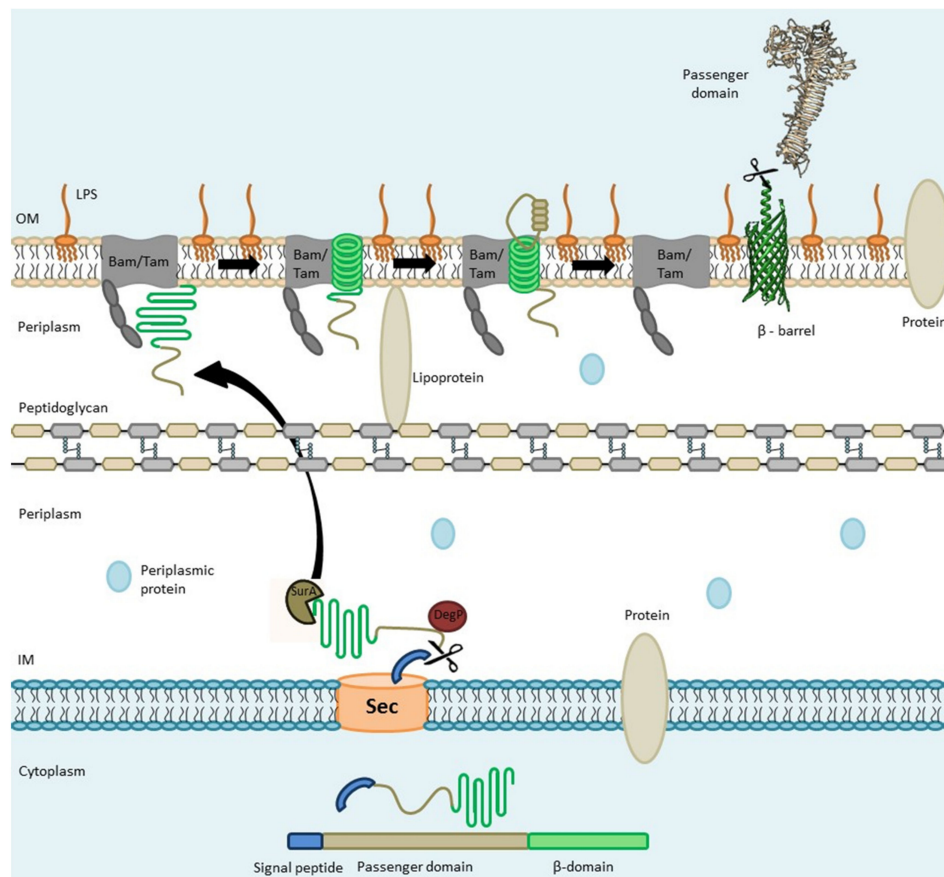
Figure 2. Schematic overview of Autotransporter (AT) processing, export, and secretion: The Signal peptide (SP) mediated by the Sec apparatus, guides translocation of the autotransporter to the periplasmic space. In the periplasm, the AT is kept in a "translocation competent state" by recruiting chaperones such as Skp, SurA, and DegP. Further, the Bam complex assists in the integration of the β-domain into the outer membrane and promotes the translocation of the passenger domain across the outer membrane through a hybrid-barrel mechanism wherein the AT β-barrel and Bam/Tam protein domains interact. Periplasmic chaperones such as SurA and DegP deliver an unfolded autotransporter to BamA/TamA. POTRA domains (gray in beaded structure) are contact sites for the AT protein to be transported. A hybrid-barrel is then formed by insertion of the AT β-strand through the gate region between strands 1 and 16 of the BamA/TamA barrel. Barrel expansion results in pore opening and the passenger domain can then protrude through the hybrid barrel. Subsequently, the passenger domain is released from the hybrid structure and may remain on the bacterial cell surface or can be cleaved for release from the bacterial cell. Adapted from [13,14].

2.1. Sec-Dependent Export of AT Proteins through the Inner Membrane

The N-terminal signal peptide of all autotransporters mediates insertion through the inner membrane through a Sec-dependent mechanism that is common to many other exported or secreted proteins. Generally, the N-terminal signal sequences in proteins show a tripartite organization of n, h, and c regions which corresponds to N-terminal, hydrophobic, and cleavage sites [16,17]. Analysis of signal sequence mutants revealed that a hydrophobic, H region is an essential part for targeting and membrane insertion [16].

The signal peptide sequence has the function of targeting or protein translocation to the inner membrane. In *E. coli*, protein export through the Sec pathway can involve two distinct pathways: (i) The SecB/SecA pathway wherein the chaperone SecB, prevents premature aggregation or folding, keeping the protein in a "translocation—competent state" and leads to transfer to Sec A [18], (ii) the SRP (Signal Recognition Particle) pathway in which the SRP nucleoprotein complex mediates co-translational targeting by interacting with a highly hydrophobic signal sequence following translation from ribosome towards the translocon [19].

2.2. AT Protein Transit through the Periplasm

The mechanism of secretion from the periplasm and the transitional state of ATs while localized in the periplasm is still debated. In fact, in the periplasmic space, these proteins are prone to immature folding or aggregation and degradation by periplasmic proteases. Misfolding or degradation of ATs can be prevented apparently either by prolonged interaction with the Sec-translocon or by interaction with periplasmic chaperones [11], or both. The periplasmic localization of ATs is likely to be very transient, and translocation to the outer membrane may occur rapidly following export and processing of the signal peptide through the cytoplasmic membrane.

2.3. Transport of ATs through the Outer Membrane (The Hybrid-Barrel Model)

Proteins of the Omp85 superfamily such as BamA promote the insertion and folding of β-barrel outer-membrane proteins (OMPs) including AT proteins across the bacterial outer membrane [14,20]. BamA possesses five periplasmic POTRA domains which are believed to recognize substrates mediated by β-strand augmentation [21,22]. In addition to BamA, TamA has been implicated in the translocation of autotransporters [10]. TamA has structural similarities to BamA and also contains domains associated with catalytic functions like insertase and chaperone foldase activity [23]. Thus, a similar model of AT translocation has been proposed for both the BamA and TamA translocation systems.

Despite the lack of a satisfactory model for autotransporter delivery at the outer membrane, the hybrid barrel model (Figure 2) provides a plausible mechanistic model which is based on interactions with the open 16-stranded BamA and TamA barrels. The unzipped strands of these proteins can incorporate β-strands of autotransporter by β-augmentation, creating a hybrid-barrel of the AT protein with BamA/TamA. The resulting hybrid-barrel would form a pore through which the AT passenger domain would be translocated. Subsequent to passenger domain translocation through the outer membrane, a final unzipping of the hybrid complex would separate the two barrels, releasing the assembled autotransporter laterally into the outer membrane and returning BamA/ TamA to its free, uncoupled state [23,24].

2.4. Passenger Domain Cleavage

At the bacterial surface, the fate of AT proteins can be dependent on the specific proteins themselves as well as the physiological conditions or the environmental niche. Some ATs remain associated with the outer membrane surface whereas others, such as the Pet and EspP SPATEs, show autocatalytic activity within the β-barrel leading to cleavage of the linker and release of the passenger domain from the bacterial cell surface [25,26]. Cleavage of the passenger domain from the β-domain can take place by various mechanisms. In the case of the SPATES, the cleavage site is generally conserved.

2.5. A Cleavage Site is Located in the "Linker Domain" of SPATE Proteins

The linker domain encompasses an invariant 14-residue segment that spans the passenger domain and translocation domain junction in the SPATEs, and studies have shown that the cleavage site is conserved in this domain. Analysis of the (^{1021}EVNNLNKRMGDL^{1032}) sequence motif of EspP showed that the passenger domain is cleaved after the first asparagine residue [27,28]. The mutation in the linker peptide resulted in impaired passenger domain cleavage of EspP [28]. Similar mutations impaired passenger domain cleavage and passenger domain translocation of another SPATE, Tsh [29]. These findings suggest that the linker domain and sequence plays an important role in processing of the passenger domain. However, some SPATEs lack a twin asparagine sequence. For instance, RpeA, from a rabbit enteropathogenic *E. coli* (EPEC) strain lacks the twin asparagine residues within its linker domain and it was reported that this protein was not released into the supernatant [30]. By contrast, a recently identified SPATE called Sha (Serine protease hemagglutinin autotransporter) lacks the twin asparagine residues, but was released into the culture supernatant [31], suggesting motifs other than the twin asparagine site may be recognized for cleavage of certain SPATEs.

3. SPATEs

Members of the SPATE family are autotransporter proteins from a variety of enterobacterial species that all contain a consensus serine protease motif, and they have most notably been described from pathogenic *Escherichia coli* and *Shigella* spp. Although some other SPATEs have also been described in other enterobacteria including *Serratia marcescens* [32], *Salmonella bongori* [33], *Citrobacter rodentium* [34], and *Edwardsiella tarda* [35].

Other conserved architecture in SPATEs include: (1) A highly conserved secretion domain/translocation domain called a β-domain. Overall, protein homology ranges from 25% to 55% but in the case of the β-domain, homology ranges from 60% to 90% identity [36]; (2) A conserved serine protease motif (consensus GDSGSP where S is the catalytic serine) at similar positions in their N-terminal passenger domain between residues 250–270 [25,26,37,38]; (3) The serine protease motif of SPATEs does not have a role in the cleavage of the passenger domain from the β-domain [33]; (4) The passenger domain of the SPATEs are cleaved from the β-domain from a conserved cleavage site between the two asparagines [25,39]; (5) All SPATEs have unusually long signal sequences (>50 amino acids) that have been shown to facilitate post-translational targeting [40]; (6) In contrast to the classical autotransporter IgA1protease, none of the SPATEs can cleave IgA1; (7) SPATEs are highly immunogenic proteins having specific phenotypes [41].

3.1. Classification of SPATES

SPATEs are subdivided into class 1 and class 2 on the basis of structural and functional properties. The class 1 SPATEs are cytopathic/cytotoxic toxins (eliciting cellular changes such as cytoplasmic shrinkage, loss of membrane integrity and activation of apoptosis), likely caused by cleavage of cytoskeletal proteins such as spectrin/fodrin [41]. Further, class 1 SPATEs are believed to show cytotoxic activity primarily through targeting of intracellular substrates. On the other hand, class 2 SPATEs, the larger phylogenetic cluster, comprise O-glycoproteases that cleave mucin and other O-glycoproteins present not only on epithelial cells but also on the surface of hematopoietic cells [42]. Thus, due to mucinolytic activity, class 2 SPATEs can impart a subtle competitive advantage in mucosal colonization [41]. Sat, Pet, EspP, EspC, and SigA SPATEs belong to class 1 whereas Pic, PicU, Tsh/Hbp, Vat, EatA, and SepA belong to class 2 SPATEs.

3.2. Distribution of SPATEs among Intestinal and Extra-Intestinal Pathogenic E. coli

Some SPATEs are present in one or more pathotypes of *E coli* (Figure 3). Generally, the following SPATES are found in various groups: EspP (extracellular serine protease plasmid (pO157-encoded) from enterohemorrhagic *E. coli* (EHEC) [26], Pet (plasmid-encoded toxin) from enteroaggregative

E. coli (EAEC) [25], Pic (protein involved in intestinal colonization) from EAEC and uropathogenic
E. coli (UPEC) and *Shigella* [39], EspC (EPEC secreted protein C) from enteropathogenic *E. coli* (EPEC),
EatA (ETEC autotransporter A) from enterotoxinogenic *E. coli* (ETEC) [43], Tsh (temperature-sensitive
hemagglutinin)/ Hbp (hemoglobin protease) mainly in avian pathogenic *E. coli* (APEC) and some ExPEC
(MNEC-UPEC) [37,44], Sat (secreted autotransporter toxin) from UPEC [45], and Vat (vacuolating
autotransporter toxin), TagBC (Tandem autotransporter genes B and C), and Sha (Serine-protease
hemagglutinin autotransporter) from APEC and UPEC strains [31,46].
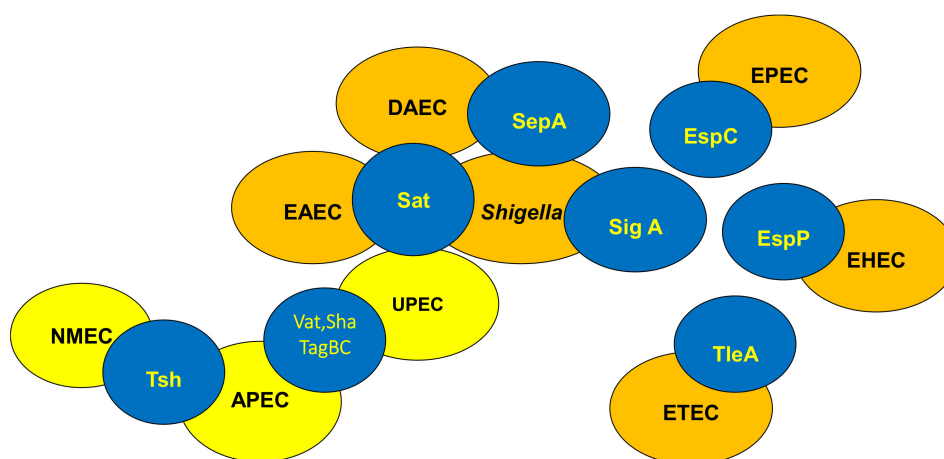
Figure 3. Distribution of SPATEs among intestinal and extra-intestinal pathogenic *E. coli.* SPATEs have
been found not only in all recognized intestinal *E. coli* pathotypes (highlighted in orange) but also
in extra-intestinal *E. coli* pathotypes (highlighted in yellow). The recent availability of many more
bacterial genome sequences, has led to identification of new and previously described SPATE proteins
among both human and animal pathogens, including *Salmonella*, *Citrobacter*, and *Edwarsiella*, as well
as some commensal *E. coli* strains. (APEC, Avian pathogenic *E. coli*; DAEC, Diffuse Adhering *E. coli*;
UPEC, Uropathogenic *E. coli*; NMEC, Neonatal meningitis *E. coli*; EAEC, Enteroaggregative *E. coli*;
EHEC, Enterohemorrhagic *E. coli*; EPEC; Enteropathogenic *E. coli*, ETEC, Enterotoxigenic *E. coli*).

3.3. Allelic Variation

Phylogenetic comparisons of SPATE sequences available in the National Center for Biotechnology
Information (NCBI) databases demonstrate that these proteins share high homology among their fellow
members because of the high degree of amino acid identity in the C-terminal β-domains [47]. If we
consider only the passenger domain, the percentage of homology drops considerably and signifies
that different members contain distinct regions and have differing biological functions (Figure 4).
In addition, some predicted SPATEs are related allelic variants of some of the characterized SPATEs.
Despite demonstrating some closer identity to some of the characterized SPATEs, only functional
testing of these proteins can confirm their specific bioactivities.
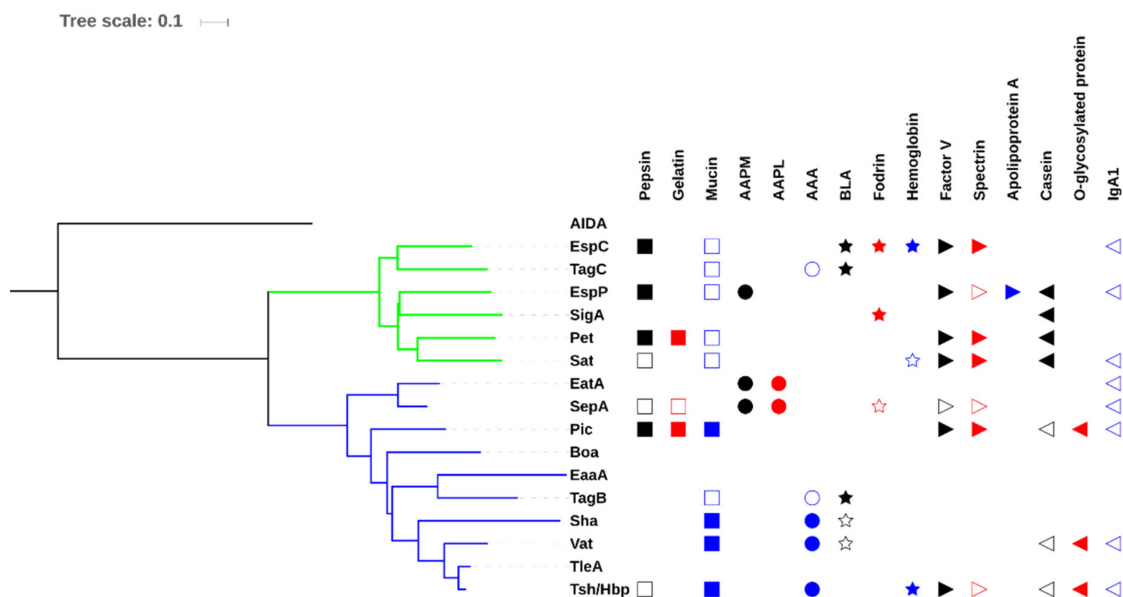
Figure 4. Evolutionary relationships of SPATEs based on passenger domain sequences and presentation of known protease substrates. The evolutionary history of passenger domains of characterized SPATEs was inferred using the neighbor-joining method [48]. The tree is drawn to scale, with branch lengths in the same units as those of the evolutionary distances used to infer the phylogenetic tree. The evolutionary distances were computed using the JTT matrix-based method [49] and are in the units of the number of amino acid substitutions per site. The analysis involved 17 protein sequences. All positions containing gaps and missing data were eliminated. Evolutionary analyses were conducted in MEGA6 [50]. Multiple sequence alignment was performed by Clustal W and the tree was constructed using the Mega6 software with PhyML/bootstrapping and iTOL [51]. Cluster of cytotoxic SPATEs (class 1) are in green branches while immunomodulator SPATEs (class 2) are in blue branches. SPATE protein sequences are available in NCBI database as follows: EspC, GenBank Accession No. AAC44731; EspP, NP_052685; SigA, AF200692; Pet, SJK83553; Sat, AAG30168; EatA, CAI79539, SepA, Z48219; Sha, MH899684; Pic, ALT57188; Boa, AAW66606; TagB and TagC, MH899681; EaaA, AAF63237; Vat, AY151282; TleA, KF494347; Tsh/Hbp, AF218073; AIDA, ABS20376; AAPM: MeOSuc-Ala-Ala-Pro-Met-pNA, AAPL: Suc-Ala-Ala-Pro-Leu-pNA, AAA: N-Succinyl-Ala-Ala-Ala-p-nitroanilide, BLA: N-Benzoyl-L-arginine 4-nitroanilide. The cleaved substrates, substrates that were negative for cleavage, and those untested substrates are represented by filled symbol, unfilled symbol and no symbol respectively. This comparison shows that some of the activities are phylogenetically distributed.

3.4. Confusion Due to Improper Annotation of Uncharacterized SPATE Encoding Proteins

Due to the presence of conserved domains and similarities in protein sequences among SPATEs, there are some cases where SPATE protein sequences were misnamed or given the name of a related, but distinct SPATE. For example, Vat (GenBank Accession No. AAN78874) was annotated as Tsh/Hbp in the UPEC CFT073 genome although this protein shares 78% identity with Tsh/Hbp [33,52,53]. Similarly, in the genome of *E. coli* PCN033, which was isolated from a pig with meningitis, a putative SPATE gene (GenBank Accession No. AKK51062) is named as EspC, despite this protein only having 59% identity with EspC (GenBank Accession No. WP_109867760). So, for annotations in some enterobacterial genomes, it is unfortunate that numerous uncharacterized SPATEs are incorrectly labeled as specific characterized SPATEs, despite sharing a limited degree of identity, particularly in the absence of demonstration of any biological or experimentally confirmed activities.

4. SPATEs Demonstrate a Diversity of Biological Activities Associated with Virulence

Since the discovery of the first SPATE, Tsh, two decades ago, research has focused on characterizing SPATEs by determining their biological activities and substrate specificities and in some cases, structural

properties have been studied through crystallography. Serine protease activity is due to the GDSGS motif and this activity is inhibited by phenylmethane sulfonyl fluoride (PMSF), but not by the metalloprotease inhibitor, Ethylene diamine tetra acetic acid (EDTA) [26]. The virulence properties of SPATEs may in part be attributed to proteolytic activity. However, it is now clear that there is a staggering diversity in biological substrates and modes of action. In the next sections, we focus on specific characteristics and functions of various SPATEs (summarized in Table 1) and their possible roles in enterobacterial pathogenesis.

Table 1. Summary of characteristics of different SPATEs.

SPATEs	Organism [a]	Biological Functions	References
EatA	ETEC	Enterotoxin	[54]
EspC	EPEC	Cytotoxin, Enterotoxin Cleavage of fodrin, hemoglobin, pepsin, coagulation factor V, translocator components (EspA/EspD) of T3SSCell rounding and cell detachment	[41,55–58]
Pet	EAEC	Mucosal cytoxicity, Cleavage of spectrin, pepsin, factor V	[25,41,59–61]
Pic	Shigella, EAEC	Serum resistance Mucinase, Hemagglutination Colonization, Cleavage of gelatin, factor V, O-glycans: PSGL-1, CD44, CD45, CD93 and CX3CL1	[39,41,42,52,62,63]
EspP	EHEC, STEC	Cleaved pepsin, factor V, apolipoprotein, complement factors: C3/C3b and C5	[26,41,64–66]
Tsh/Hbp	APEC	Hemagglutinin, Binding to Caco-2 cells and to EMPs (laminin, fibronectin, and collagen IV) and heme Cleavage of mucin, factor V and O-glycosylated proteins in leukocyte	[37,41,63,67]
Sha	APEC, UPEC	Autoaggregation, hemagglutination, biofilm formation, proteolytic activity on synthetic peptide: N-Succinyl-Ala-Ala-Ala-p-nitroanilide, adherence and cytopathic effects on bladder epithelial cell line	[31]
TleA		Binding to Caco-2 cells Cleavage of bovine submaxillary mucin, leukocyte surface glycoproteins CD45 and P-selectin glycoprotein ligand 1	[68]
Vat	APEC, UPEC	Vacuolating cytotoxin, Agglutinate leukocyte Cleavage of O-glycosylated proteins in leukocyte	[46,63]
Sat	UPEC	Vacuolating cytotoxin on HK-2, HEp-2 and Vero monkey kidney cells Cleavage of casein, factor V and spectrin	[41,45,69]
SepA	*Shigella flexneri*	Intestinal inflammation, proteolytic activity toward synthetic peptides: Suc-Ala-Ala-Pro-Phe-pNA, Suc-Val-Pro-Phe-pNA and Suc-Phe-Leu-Phe-pNA	[70,71]
SigA	*Shigella flexneri*	Cytotoxin, Cleavage of casein, recombinant human α II spectrin Cell rounding and cell detachment	[72,73]
Boa	*Salmonella bongori*	Unknown	[74]
TagBC	UPEC, APEC	Autoaggregation, proteolytic effect on synthetic peptide: N-Benzoyl-L-arginine 4-nitroanilide cytopathic effect on human bladder cell lines	[31]

[a] Bacteria known to produce these SPATEs. APEC, Avian pathogenic *E. coli*; DAEC, Diffuse Adhering *E. coli*; STEC, Shiga toxin-producing *E. coli*; UPEC, Uropathogenic *E. coli*; NMEC, Neonatal meningitis *E. coli*; EAEC, Enteroaggregative *E. coli*; EHEC, Enterohemorrhagic *E. coli*; EPEC, Enteropathogenic *E. coli*; ETEC, Enterotoxigenic *E. coli*.

4.1. EaaA/EaaC

The EaaA and EaaC SPATEs (GenBank Accession No. Protein AAF63237.1, Nucleotide AF151091) were first identified from *Escherichia coli* reference strain ECOR-9, a human commensal intestinal isolate. These two SPATE-encoding genes were found to be associated with genes encoding non-immune immunoglobulin binding proteins that were also associated with prophages [75]. The EaaA and EaaC SPATEs are very similar 1335 aa proteins, sharing 99% identity (only 8 aa substitutions). Other than identification of these genes in ECOR-9, *eaa* gene sequences were also shown to be present in other ECOR strains (ECOR-2, ECOR-5, and ECOR-12) belonging to phylogenetic group A, but these SPATE sequences were not identified in a variety of clinical isolates [76]. However, screening of genomic sequence databases indicates EaaA/EaaC sequences are present in a diversity of *E. coli* strains (at least 50 entries of highly similar proteins identified from uniprot.org). Other than identification of the sequences in different strains, no phenotypic or biochemical properties of Eaa SPATEs have been investigated thus far.

4.2. EatA

EatA for ETEC autotransporter A (GenBank Accession No. CAI79539, Q84GK0; AY163491.2) is secreted by some ETEC strains and has been shown to contribute to virulence in the rabbit ileal loop model of infection, since an *eatA* mutant demonstrated less marked and slowed fluid accumulation [43]. The *eatA* sequence was identified on a plasmid, pCS1, in *E. coli* strain H10407. The EatA protein shares over 80% identity to the SepA SPATE from *Shigella flexneri*. EatA was found to degrade a bacterial adhesin EtpA, which could reduce intestinal colonization, but in parallel increased access of ETEC toxins at the host cell surface [54]. EatA was also shown to be highly immunogenic and could contribute to ETEC virulence by degrading the MUC2 protein at the small intestinal mucous layer, which could further promote access of ETEC toxins to epithelial cell surfaces [77]. The EatA protein was also shown to be present in most ETEC (over 70%) [78] and has been identified less commonly in some EAEC strains (4.1% of isolates) [79]. EatA has vaccine potential for prevention of ETEC, as it generated a high antibody response and protection against ETEC intestinal infection [77].

4.3. EspC

The EspC (EPEC secreted protein C) passenger domain is a 110 kDa protein (GenBank Accession No. AAC44731, U69128.1), and one of the first proteins reported to be secreted by EPEC [38]. As with other SPATEs, although EspC shares some sequence homology to IgA proteases, it cannot cleave IgA nor is the catalytic serine GDSDG motif required for release of the passenger domain from the β-domain into the external milieu [38]. It was also shown that EspC is not involved in EPEC generation of attaching and effacing (A/E) lesions, nor is it required for adherence or invasion of tissue culture cells. EspC demonstrated enterotoxic activity and increased tissue PD (potential difference) and Isc (short circuit current) of rat jejunum mounted in Ussing chambers [80]. EspC enterotoxic activity was nullified by pre-incubation with an antiserum against another SPATE, Pet [80]. Similar to Pet, EspC produced cytotoxic effects on cultured epithelial cells but with three times higher dose (120 μg/mL) than Pet. The actin cytoskeleton was disrupted, resulting in cell contraction and cell detachment. This overall effect was caused by the serine protease motif of EspC [55]. Also, similar to Pet, EspC cleaved an intracellular target, α-fodrin but the cleavage sites were different. Pet cleaves fodrin within the calmodulin binding domain between M^{1198} and V^{1199} [61]. EspC cleavage of fodrin occurred outside of the calmodulin binding domain [55]. Once inside the cells, kinetics of protein degradation indicate that purified EspC cleaves fodrin at two sites (within the 11th repetitive unit between Q^{1219} and $L1^{220}$ and within the 9th repetitive unit between D^{938} and L^{939}) which then results in disruption of focal adhesion including dephosphorylation and degradation of paxillin and FAK; leading to cell rounding and detachment [58]. However, entry to a target cell (cytosol) is critical for EspC cytotoxicity. Though internalization of purified EspC by pinocytosis was shown by [81], it cannot be considered as

a natural physiological phenomenon for infection, as it took 8 h of incubation for insertion while EPEC infection delivers EspC into the cells after 30 min. Interestingly, EspC is secreted into the milieu by the T5SS and then incorporated into the T3SS translocon for entry into host cells [82]. Further, EspC has a relevant role in cell death induced by EPEC. EspC is able to induce apoptosis and necrosis in epithelial cells [56] and apoptosis could be the first event which can manifest to increased necrosis. Also, EspC was shown to interfere with the caspase cascade required for induction of apoptosis which was partially dependent on serine protease activity.

A number of biological targets recognized by EspC which are relevant to its diarrheagenic activity have been identified. Purified EspC cleaved human hemoglobin at an optimum pH between 5 and 6 [57]; although correlation of this biological property for EPEC virulence is yet to be established. EspC has also been shown to cleave other substrates like pepsin, glycoprotein coagulation factor V, and spectrin [41]. Apart from cleaving different biological substrates, EspC also cleaves bacterial components of the secretion system. EspC was found to target EspA/EspD which are translocator components of the Type III secretion system (T3SS) and control of pore formation and cytotoxicity by T3SS for the host cell [83]. The T3SS acts as a molecular syringe, comprised of pore-forming translocator proteins EspB and EspD which insert into the host cell plasma membrane and EspA which forms a hollow structure connecting the T3SS needle into the cell [84]. This result indicates that control of pore formation by EspC can support bacterial colonization, by mediating a controlled release of effector proteins from the T3SS to limit host cell death, since this could increase the immune response and potential clearance of EPEC at an early stage of infection.

4.4. Pet

Pet (Plasmid encoded toxin) is a 104 kDa enterotoxin produced by EAEC (GenBank Accession No. SJK83553), which has been found to increase jejunal potential difference (PD) and Isc (short circuit currents) accompanied by mucosal damage, exfoliation of cells and development of crypt abscesses [25]. Pet is encoded on the pAA plasmid and comprises a 52 aa N-terminal signal peptide and the secreted passenger domain (amino acids 53–1018), which cleaves from the β-domain between N^{1018} and N^{1019} [25].

A host-specific factor is required for proper folding of the Pet autotransporter. Interestingly, clones of *E. coli* HB101 produced both folded and misfolded variants of Pet but the wild-type EAEC only produced the properly folded active Pet, suggesting that the accessory protein from EAEC may be absent or non-functional in strain HB101 [85]. This observation shows that correct protein folding is not required for AT secretion but that accessory proteins are necessary for folding ATs in the right conformation [11,13,86]. X–ray structure of the Pet passenger domain was resolved and when compared with the most similar SPATE, EspP (50% sequence identity); Pet harbors a β-pleated sheet from residues 181–1900 whereas EspP has a coiled loop. Further, the Pet passenger domain showed more β-sheets between residues 135–143 compared to EspP [8]. These β-helices are presumed to confer functionality to the protein.

Pet produced changes in host cytoskeletal architecture in both HEp-2 and HT29 epithelial cells characterized by time and dose dependent cell elongation followed by cell rounding and detachment from the substrate, which was dependent on serine protease activity [60]. Cellular morphological changes were visible after 2 h of incubation with Pet (25 μg/mL). Pet also contributes to pathology at the mucosa which is characterized by dilation of crypt opening, extrusion of colonic enterocytes, development of intercrypt crevices and loss of apical mucus from goblet cells as a result of contraction of interlinking cytoskeleton integrity and loss of actin stress fibers and focal contacts [59]. These cytopathic effects may be due to internalization in host cells by the vesicular system as Pet activity completely vanished following incubation with brefeldin A [87]. Pet interaction with host cells requires a two-hour time lag leading to cell damage and requires a sequence of events: (1) Binding to the cell. (2) Entry into the cell by clathrin-dependent receptor-mediated endocytosis. (3) Entry into early endosomes. (4) Passage to the Golgi apparatus from endosomes. (5) Retrograde vesicular transport from the

Golgi complex to the ER. (6) Delivery to the cytosol through the ER-associated degradation (ERAD) pathway [61,88]. Once internalized, loss of actin microfilaments takes place due to breakdown of cellular spectrin [60,89]. Similar to Pet, EspC also produces cytotoxic activities on epithelial cells, although the dose of EspC was three times higher and a longer incubation time was required to produce a similar result [55]. Subsequently, it was shown that the d2 subdomain of the passenger domain is required for Pet internalization by recognizing the Pet host cell receptor, cytokeratin 8 [90]; the d1 subdomain is the largest domain having a serine protease motif and was incapable of binding the cell surface without the aid of d2 subdomain [90,91]. Pet preferentially cleaves α-fodrin between M^{1198} and V^{1199} residues within the calmodulin-binding domain of fodrin's 11th repetitive unit [61,92]. Pet-mediated cleavage of α-fodrin (spectrin) has been suggested to induce enterocyte death via apoptosis [93,94]. Together, this phenotype of Pet could explain the cellular alteration during EAEC pathogenesis [92]. Recent studies have shown that the spice, curcumin, can also affect the secretion of Pet on the bacterial surface and subsequent internalization into the epithelial cells [95].

4.5. Pic

Protein involved in colonization (Pic) is a 109.8 kDa extracellular protein secreted by both EAEC (GenBank Accession No. ALT57188, AF097644.1), and *Shigella flexneri* 2a [39] and also atypical EPEC [96]. Pic catalyzed mucin degradation and has also been shown to confer serum resistance and hemagglutination [39]. Further, Pic also cleaved gelatin, but did not demonstrate any activity against human immunoglobulins. In addition to Pic identified in diarrheagenic *E. coli*, another highly similar SPATE named PicU (96% amino acid identity to Pic) has been identified in some uropathogenic isolates. PicU was functionally similar to Pic from EAEC, degraded mucin and contributed to colonization during urinary tract infection (UTI) [52,62]. Interestingly, mucinase activity was not only important as a virulence factor but also may contribute to nutrient availability, since the *pic* mutant was less able to grow when compared to the wild-type strain [97]. The Pic mucinase (from all groups EAEC, UPEC, and *Shigella flexneri*) is responsible for increased secretion of mucus in the intestinal lumina of rat ileal loops by increasing mucus production in goblet cells even though this activity was independent of the serine protease motif [98]. This secretory activity of Pic favors the formation of biofilm by EAEC, a hallmark of EAEC infection. The mucolytic activity of Pic not only contributed to damage of the intestinal mucosal layer, but also cleaved mucin-type O-glycans of the immune system, including PSGL-1, CD44, CD45, CD93, and CX3CL1 [42,63]. Further, Pic significantly reduced complement activation by cleaving complement cascade factors- C3, C4 and C2 [99]. Downregulation of complement activation by Pic may contribute to EAEC, *Shigella* and UPEC infections. To add to its virulence potential, Pic was also shown to induce polymorphonuclear leucocytes/neutrophil (PMN) activation and programmed T-cell death [42].

PicU was identified in a UPEC strain and also demonstrates mucinase activity that may contribute to UTI pathogenesis [62]. To support this observation, a *picU* mutant of *E. coli* CFT073 was less able to colonize compared to wild-type parent although differences were not statistically significant. In addition, pepsin and coagulation factor V are other cleavage substrates for PicU [62]

Interestingly, a SPATE in *Citrobacter rodentium* similar to Pic and PicU, named PicC (79% identity at amino acid level), was shown to demonstrate mucinolytic activity [100]. The *picC* mutant actually outcompeted the wild-type and elicited more colitis. The PicC protease may therefore be an important immune regulator that could function to decrease stimulation of the host immune system during infection [100].

4.6. EspP

The extracellular serine protease plasmid (pO157-encoded) (EspP) was isolated from the culture supernatant of EHEC O157: H7 EDL933 associated with hemolytic uremic syndrome (HUS) (GenBank Accession No. NP_052685; CAA66144, X97542.1) [26] and Shiga toxin-producing *Escherichia coli* (STEC) [64,101]. PssA (protease secreted by STEC) is the homologue of EspP which differs by a single

amino acid change and was found to be cytotoxic for Vero cells [102]. EspP is generally associated with STEC, EHEC and atypical EPEC [103]. In silico analysis suggests that the signal sequence of EspP is cleaved between residues A^{55} and A^{56} [26] and the 104 kDa passenger domain contains a chaperone motif and a 30 AA linker domain that connects the β-domain and the passenger domain [104]. It was later shown that biogenesis and export of EspP was not self-mediated but also required additional periplasmic chaperones SurA and DegP, which aided in the proper folding of the AT passenger domain during translocation through the Bam complex [105].

EspP proteins have been classified as four distinct alleles, namely EspPα, EspPβ, EspPγ, and EspPδ, where EspPα is associated with highly virulent EHEC O157: H7 and major non-O157 EHEC and can contribute to biofilm formation by forming macroscopic rope-like polymers which were refractory to antibiotics and showed adhesive and cytopathic effects [106]; EspPγ cleaved pepsin and human coagulation factor V, although EspPβ and EspPδ were either not secreted or proteolytically inactive [64]. Interestingly, EspPα was more prevalent in human isolates (84%) than in environmental isolates (47%) but EspPγ was more prevalent in the environment (40%) than from human sources (11%) [64,107]. The diversity of EspP alleles with different proteolytic activities necessitates specific subtyping for the screening of *espP* genes. The crystal structure of the EspP passenger domain was solved at 2.5 Å, and revealed a large β-helical stalk and a globular subdomain with the catalytic triad [6] and shared overall structure to the previously crystallized Hbp protein [7]. However, in contrast to Hbp, the active site of EspPα is slightly wider, deeper and more exposed, suggesting that it likely interacts with larger substrates [6].

Esp was shown to cleave substrates such as coagulation factor V [26], porcine pepsin A [26], apolipoprotein [65], major complement factor proteins C3/C3b but not factors H and I [66]. A valid argument for prolonged hemorrhage due to EspPα is strengthened by the ability of EspPα to cleave various serpins (serine protease inhibitors) from human plasma which are involved in blood coagulation [108]. Cleavage was specific, targeting only procoagulatory serpins such as α2-AP and α1-PI [108]. Like EspPα, EspI, another SPATE from STEC also cleaved α2-AP and α1-PI [65], but unlike EspPα, EspI mediated cleavage was not complete due to the formation of an inhibitory serpin-enzyme-complex [108]. Further, EspP was found to stimulate electrogenic ion transport in human colonoid monolayers, although this activity was Ca^{2+} dependent but independent of serine protease activity [109]. Taken together, the role of EspP in blood coagulation, pathophysiology and immunomodulation can contribute to pathogenesis of EHEC.

4.7. Tsh/Hbp

The first characterized SPATE, temperature-sensitive hemagglutinin (Tsh) was identified on a ColV-type plasmid in APEC strain χ7122 [37,110]. The *tsh* gene (GenBank Accession No. AF218073) encodes a protein of 1377 amino acids with a molecular weight of approximately 148-kDa. It is composed of a leader sequence that is cleaved between residues A^{52} and A^{53}, a 106-kDa passenger domain that encompasses the serine protease motif (S_{259}) extending from residues 53 to 1100, and a β-barrel domain of 33-kDa that extends from residues 1101 to 1377 [37]. Based on the sequence homology, Tsh was also reported in some UPEC strains [52]. However, Heimer et al. were actually screening for *vat* not *tsh*, and they erroneously named the *vat* gene in CFT073 and other UPEC as *tsh*. However, it has been reported in one study that some human ExPEC strains from newborn meningitis (11 to 50 percent) also contain *tsh* located on large plasmids similar to ColV plasmids [111]. A Tsh-like protein sharing 60% aa identity with *E. coli* Tsh was also reported in *Edwardsiella tarda*, a fish pathogen [35]. Despite the 60% identity of this SPATE from *Edwardsiella tarda* to Tsh, the bioactivity of this protein and its role in virulence fish may be quite distinct.

The production of Tsh in *E. coli* K-12 was found to be higher at low temperature (26 °C) and it conferred the capacity to agglutinate chicken erythrocytes in a mannose resistant manner. However, at higher temperatures, Tsh was released into the supernatant medium and this agglutination activity was lost leading the name, temperature-sensitive hemagglutinin [37]. Interestingly,

the hemagglutination phenotype was also observed for Tsh with sheep [112], bovine, pig, turkey, rabbit, horse, and dog [31] and human erythrocytes [63]. Furthermore, Tsh promoted adherence to Caco-2 cells and to extracellular matrix proteins such as laminin, fibronectin, and collagen IV [112]. Sequence analyses indicated that Tsh is a homologue to IgA proteases (56% of similarity) of *Hemophilus influenzae* and *Neisseria gonorrhoea* [113], but was unable to cleave IgA. Tsh was shown to cleave mucin, factor V [41] and O-glycosylated proteins such as CD43, CD44, CD45, CD93, CD162, and CX3CL1 in vitro [42,63], suggesting diverse roles in cellular and immune functions. Tsh seems to also contribute directly to APEC infection, as its presence accelerates the progression of the infection and could lead to the development of lesions and deposition of fibrin in avian air sacs [37,112]. In addition to these functions, Tsh was shown to have potential enterotoxin function to induce fluid accumulation in a rabbit ligated illeal loop assay [114], although the significance of this role for Tsh in mammalian enteric disease is unknown.

Hbp (hemoglobin protease) is a near-identical variant of Tsh that was isolated from a patient with an intra-abdominal wound infection, and only differs by two amino acids (Q209K and A842T) (GenBank Accession No. AJ223631) [44]. Like *tsh*, the *hbp* gene is located on a virulence plasmid, pColV-K30. Hbp was shown to cleave hemoglobin and acquire heme in an iron depleted host niche [44]. Heme captured by Hbp could also promote growth of *Bacteroides fragilis*. *B. fragilis* was shown to contain a specific receptor that recognizes the heme-Hbp complex and it is capable of exploiting heme liberated from host complexes and cause intra-abdominal abscesses in patients [67].

4.8. TleA

Tsh-like ETEC autotransporter or TleA (GenBank Accession No. KF494347) is an AT that was identified in an ETEC strain [68]. It is a 4110-bp gene that encodes a 1369-amino-acid precursor. Sequence analyses have shown that TleA contains a signal peptide from residues 1 to 52, a passenger domain from residues 53 to 1092 with a serine protease motif GDSGS from residues 257 to 261 and a β-barrel domain from residues 1093 to 1369. The alignment of the passenger domain sequences of the other members of SPATEs indicated that TleA is a class 2 SPATE and shares 97% identity with the Tsh autotransporter [68]. TleA may have a role in intestinal colonization and immunomodulation as it was shown to degrade bovine submaxillary mucin and leukocyte surface glycoproteins CD45 and P-selectin glycoprotein ligand 1. Further, nonadherent *E. coli* HB101 expressing TleA conferred the capacity to adhere to Caco-2 cells, while such adherence was not observed in the wild-type ETEC strain 1766a [68].

4.9. Vat

Vacuolating autotransporter toxin (Vat) is a 140 kDa class II SPATE that was found to be encoded on a pathogenicity island from APEC *E. coli* Ec222, and was shown to contribute to respiratory tract infection, cellulitis and septicemia in poultry [46]. The *vat* gene is located on a pathogenicity island (VAT-PAI) between the *proA* and *yagU* genes (GenBank Accession No. AY151282). The *vat* pathogenicity island in Ec222 contains 33 ORFs wherein *vat* is ORF27. Interestingly, ORF26 share 44% aa identity with the PapX regulator from UPEC strains [46]. The *vat* predicted gene product also shares 97% identity with an AT present in UPEC strain CFT073, which was annotated mistakenly as Tsh/Hbp. However, the new annotation has been corrected as Vat-ExPEC [33,52,53]. Vat shares 77.5% identity to Tsh/Hbp of APEC [44,110], which explains why Vat has sometimes been mislabeled as Tsh for certain strains or genome sequences.

Unlike Tsh/Hbp, the secreted 111.8-kDa Vat passenger domain was unable to cleave casein-based substrate [46]. Compared to the *vat* mutant, APEC Ec222 exhibited a robust cytotoxic effect on chicken embryonic fibroblast (CEF) cells. Cytotoxic activity involved vacuole formation in cells that was visualized from 2–24 h after exposure [46]. In a cellulitis infection model, chickens challenged with *E. coli* Ec222 developed cellulitis, whereas none of the chickens developed cellulitis when infected with the *vat* mutant [46]. In UPEC, Vat elicits an antibody response in some urosepsis patients, and

the titer of Vat-specific IgG was higher in the plasma of patients compared to the titer found in controls and patients infected with *vat*-negative UPEC strains [115]. Vat contributed to fitness in UPEC during murine systemic infection [116]. Further, a role for Vat in combination with other SPATEs was demonstrated for fitness in murine kidney colonization and cytotoxicity [31]. Vat has also been shown to mediate agglutination of erythrocytes and cleavage of O-glycoproteins in vitro [63].

Vat (Vat-AIEC) from an adherent invasive *E. coli* (AIEC) associated with Crohn's disease, is 97% similar to Vat from APEC Ec222 and contains a modification in the serine catalytic domain to GDSGSP instead of the conserved ATSGSP motif present in Vat [117]. Vat-AIEC acts as a mucinase and inactivation of *vat* reduced gut colonization by one-log in a mouse model [117].

4.10. Sha

A recently identified SPATE-encoding gene, *sha* (serine-protease hemaglutinin autotransporter), is located on a distinct region of a ColV-type plasmid [31]. The *sha* gene (GenBank Accession No. MH899684) was more common among APEC (present in 20% of 299 APEC strains) than in UPEC (0.9% of 697 strains). Sha is more closely related to Tsh (43% identity) and Vat proteins (38% identity) than to other SPATEs. Similar to Vat and Tsh, Sha showed elastase-like activity by cleaving N-Succinyl-Ala-Ala-Ala-p-nitroanilide. In addition, Sha increased adherence to both human and avian epithelial cells, whereas Tsh only increased adherence to bladder cells, and Vat only increased adherence to kidney cells. Sha also demonstrated hemagglutation for erythrocytes of a variety of animal species (sheep, bovine, pig, dog, chicken, turkey, rabbit, horse, and human), contributed to increased biofilm formation, and delayed cytotoxicity (release of LDH after 12 h from bladder epithelial cells). As similar carbohydrates may be present on erythrocyte surfaces, it is not surprising that Sha as well as Tsh and Vat autotransporters demonstrated extensive hemagglutination activity for a variety of erythrocytes. We believe that the contrasting phenotype when Sha is expressed in high copy vector—agglutination with erythrocytes by the protein present on the bacterial surface as well as the cytopathic effects of released protein in culture supernatant could be explained by the presence of protein both the bacterial surface and released in the supernatant (Figure 5). Although, loss of *sha* didn't affect competitive fitness during colonization of the urinary tract of female mice, *sha* expression was upregulated six-fold in infected bladder compared to culture in lysogeny broth (LB) [31].
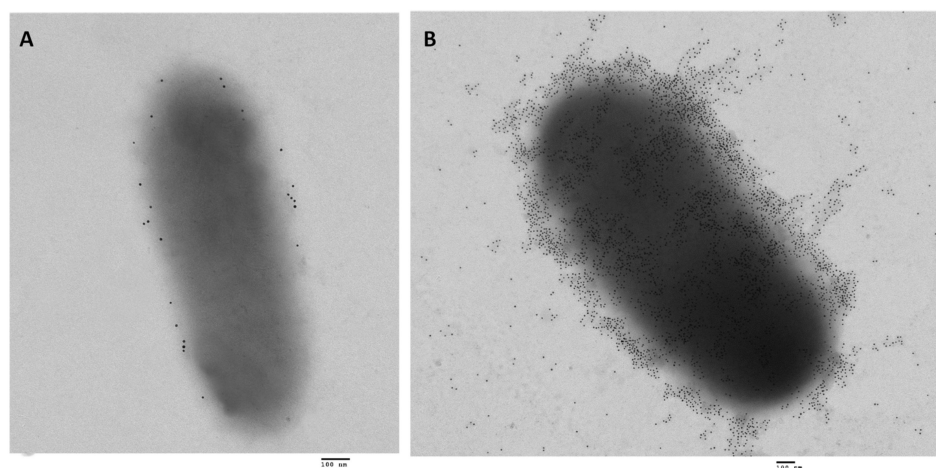
Figure 5. Transmission electron micrographs of *E. coli* BL21 expressing the Sha autotransporter [31] immunolabelled with 10-nm-diameter gold particles (**A**) The negative control, adsorbed serum was used for the primary incubation with *E. coli* BL21 empty vector and shows very low background of gold particles. (**B**) Gold-labelling with AT-specific antibodies shows that when Sha is constitutively expressed, proteins are localized on the surface as well as released in the supernatant. So, the protein released can gain access to host cell targets, whereas the protein associated with bacterial cells can mediate agglutination, autoaggregation, and adherence to host cells. Bar 100 nm.

4.11. Sat

A Secreted autotransporter toxin (Sat) was identified in UPEC strain CFT073 [45] and later also described in *Shigella*, EAEC, DEAC and neonatal septicemia *E. coli* strains [118]. The 3885-bp *sat* gene (GenBank Accession No. AAG30168) is located on a pathogenicity island that also carries a *pap* fimbrial gene cluster. The *sat* gene product is a 1295-amino-acid precursor with a molecular weight of 142 kDa [45]. Sat was unable to agglutinate human erythrocytes and did not cleave glycoproteins CD43 and CD162 from Jurkat cells [63]. Sat was also shown to cleave casein, coagulation factor V and nonerythroid spectrin, but not pepsin or mucin [41,45]. Like Vat, Sat also exhibited cytotoxicity on epithelial cells, including HK-2, HEp-2 and Vero cells, characterized by vacuole formation, autophagy and cell detachment [45,69,119]. Cytotoxicity included disruption of actin and other cytoskeletal and nuclear proteins and was dependent on the serine protease active site [120]. Sat is internalized by an unknown mechanism, and shown to be localized specifically to the cytoskeletal fraction of bladder and kidney epithelial cells [120].

The autophagy in HeLa epithelial cells triggered by Sat led to disruption of the F-actin cytoskeleton [119]. Sat also modified tight junction-associated proteins ZO-1, ZO-2 and occludins in human polarized epithelial intestinal Caco-2 and TC7 cells, resulting in increased paracellular permeability [121]. In addition, Sat induced a strong immune response in a murine model of ascending urinary tract infection, although a *sat* mutant colonized urine, bladder and kidneys as well as the wild-type strain [45]. However, kidneys of mice infected with the wild-type strain showed dissolution of the glomerular membrane and vacuolation of proximal tubules and these lesions were absent in kidneys infected with the *sat* mutant [69]. In addition, Sat from a Diffusely adhering *E. coli* (DAEC) strain triggered pronounced fluid accumulation and villous necrosis in rabbit ileal tissue [122]. Taken together, Sat plays an important role as a cytotoxin in the pathogenicity of urinary tract infection as well as in intestinal infections. Still, the role of Sat as an enterotoxin is paradoxical, since Sat is also present in the probiotic strain *Escherichia coli* Nissle 1917 even though it was shown to be a functioning protease and was expressed during colonization of the mouse intestine [123].

4.12. SepA

Shigella extracellular protein A (SepA) was identified in *Shigella flexneri*, which causes diarrhea (shigellosis) in humans [70] and also in some enteroaggregative *E. coli* (EAEC) strains [103]. The *sepA* gene (GenBank Accession No. Z48219) is located on the 200 kb virulence plasmid pWR100 and encodes a 1366 a.a. precursor of 146 kDa [70]. SepA exhibited protease activity of some synthetic peptides such as Suc-Val-Pro-Phe-pNA [71], although no protease activity was found on natural substrates such as gelatin, IgA1 [70], angiotensin-I, egg lysozyme [71], fibronectin, mucin, pepsin, factor V, spectrin, or fodrin [41]. Unlike other class-2 SPATEs, SepA did not cleave O-linked glycoproteins from leucocytes such as CD43, CD44, CD45, CD93, CD162, and CX3CL1 [63]. Deletion of *sepA* did not affect entry of *S. flexneri* into epithelial cells or cell-to-cell spread; however, the *sepA* mutant showed a decrease in fluid accumulation and inflammation in the rabbit ileal loop model compared to the wild type [70]. Furthermore, in a human explant model, the *sepA* mutant demonstrated reduced mucosal damage and a significant reduction in desquamation of intestinal epithelial barrier [124]. SepA also induced disruption of the apical pole of a polarized epithelial barrier and facilitated invasion of intestinal cells by *Shigella* [125]. This was associated with a decrease in LIMK1 leading to increased accumulation of colifin, a protein involved in actin dynamics [125,126].

4.13. SigA

Shigella IgA-like protease homologue or SigA is another SPATE identified in *Shigella flexneri* 2a [72] (GenBank Accession No. AF200692). The *sigA* gene is located on the *she* pathogenicity island and encodes a 103 kDa protein [72,74]. SigA imparts cytotoxic and enterotoxic effects and was shown to cleave casein [72] and recombinant human α II spectrin (α-fodrin) [73], indicating that it might

contribute to patho-physiological manifestation of *Shigella*. SigA shares 56% identity to the Pet. A *S. flexneri* 2a *sigA* mutant had 30% reduction in fluid accumulation in a rabbit ileal loop model. It was also shown that immunogenic SigA can bind to HEp-2 cells and induce cell rounding and detachment, phenotypes similar to purified Pet toxin from enteroaggregative *E. coli*, suggesting that SigA could play a key role in the virulence of *S. flexneri* [72,73]. Owing to the immunogenic properties of SigA [127], a computational approach has been used to identify potential epitopes for generation of a peptide vaccine against *Shigella* [128]. Due to their high immunogenicity, the potential of SigA and other SPATEs as vaccine targets is warranted.

4.14. Boa

Although most SPATEs identified to date were characterized from different pathotypes of *E. coli* and *Shigella* spp., Boa represents the only SPATE identified in *Salmonella spp*. Boa is present in *Salmonella bongori*, a Salmonella species associated mainly with reptiles, but which have been reported to infect some animals and humans. Surprisingly, no other SPATEs have been identified in all other *Salmonella enterica* serovars. It has been suggested that Boa may have been acquired by horizontal gene transfer from another Enterobacteria such as *E. coli* [74]. The *boa* gene encodes a 1384 protein (GenBank Accession No. AAW66606, FR877557) predicted to have a long signal peptide of 57 residues, a passenger domain of 1050 residues containing a serine protease GDSGS motif from residues 262 to 266 and a β-barrel domain of 277 residues [74,129]. To date, the biological properties of the Boa protein or its potential role for *Salmonella bongori* pathogenesis have not been determined.

4.15. TagBC

Recently, two new SPATEs referred to as "tandem autotransporter genes, *tagB* and *tagC*, located adjacent to each other on a genomic island between the conserved *E. coli* genes *yjdI* and *yjdK* in an APEC O1:K1 strain were identified [31]. Genome analysis and screening for *tagB* and *tagC* (GenBank Accession No. MH899681) indicate that these SPATE genes are present in APEC as well as UPEC strains [31]. Among 697 UPEC isolates, *tagB* sequences were present in 70 isolates (10%), whereas *tagC* sequences were present in 80 isolates. While amongst 299 APEC strains, *tagB* sequences were present in 14 isolates (4.7%) and *tagC* sequences were present in 21 isolates (7%). Interestingly, all of the *tagB* or *tagC*-positive APEC isolates were exclusively from infections in turkeys. Both proteins showed trypsin-like activity and efficiently cleaved N-Benzoyl-L-arginine 4-nitroanilide, similarly to the activity of EspC protein. Further, TagB and TagC were autoaggregating, hemagglutinating, could promote adherence to the HEK 293 renal and 5637 bladder cell lines as well as cytotoxic to human bladder cell lines when expressed in *E. coli* K-12 (with early release of LDH after 5 h). Neither of them required a functional serine protease motif for secretion [31]. In spite of these in vitro phenotypes, loss of TagBC did not have any appreciable effect on virulence or fitness of the mutant in bladder and kidneys of infected mice.

5. Regulation of Expression of SPATEs

Although numerous SPATEs have been characterized and their roles in infection and cell toxicity have been reported, determination of the mechanisms of regulation of SPATEs has been limited. In general, most SPATEs are thermally regulated and are better expressed under conditions similar to the host infection sites and upon contact with host cells, in tissue culture medium and at neutral to alkaline pH (7 to 9). EspP, EspC, Tsh, Pic, SigA, SepA are thermoregulated, although mechanisms of regulation remain to be elucidated [26,37,39,57,113]. Expression of the *vat-AIEC* gene was upregulated when grown at pH 7.5 with bile salts and mucin, which are similar to conditions in the distal ileal segment of the GI tract [117]. Expression of EspP in culture supernatant was higher in lysogeny broth (LB) than in minimal essential medium (MEM) as well as higher at 37 °C than at 20 °C [26,130]. Further, when EHEC 5236/96 (O26:H11) was grown in contact with human intestinal epithelial HCT-8 cells, *espP* expression was upregulated more than 35-fold [131]. Likewise, transcription of *pet* expression was

increased in tryptone-containing medium, which might be of clinical significance for the milk-drinking pediatric population that can be infected with EAEC. Similarly, *tsh* and *vat* expression was shown to be upregulated in minimal medium when compared to rich LB medium [31]. Despite determining what conditions increase expression of some SPATEs, defining which regulatory mechanisms control SPATE expression has been limited. Specific aspects of regulation of expression of some SPATEs are presented below.

5.1. Regulation by LER

The locus of enterocyte effacement (LEE) encoded regulator (Ler) regulates the LEE pathogenicity island of EPEC and EHEC which produce attaching and effacing lesions on host intestinal epithelial cells. Ler activates the transcription of various LEE operons [132]. Apart from regulating operons associated with the LEE and its Type 3 secretion system, Ler also strongly activates the *espC* promoter (by 31-fold) and hence increases the production of the EspC SPATE in EPEC [133].

5.2. Regulation by H-NS

Histones are small, abundant, highly conserved proteins that have been recognized as DNA binding proteins. They play a role in compacting DNA into the nucleosome, the main structures to form chromosomes, in eukaryotic cell nuclei [134,135]. In bacteria, such as *E. coli*, some proteins have been described as histone-like proteins. They may not share the same functions as compacting prokaryotic DNA but it was shown that they play a role in the regulation of genes by competing for binding to their promoter, and these genes could be associated with virulence, osmoregulation, pH and temperature sensing [136]. Based on sequence homology, four major groups of histone-like proteins were described: histone-like proteins *Escherichia coli* U93 (HU), histone-like nucleoid structuring proteins (H-NS), integration host factors (IHF), and factors for inversion stimulation (FIS). Among these, a role for H-NS has been reported for regulation of different AT encoding genes including regulation of the SPATE Vat.

H-NS has been shown to regulate different trimeric autotransporters [137–139]. Further, H-NS repressed the expression of *vat*; in UPEC strain CFT073, as a Δ*hns* mutant was shown to secrete a significantly higher level of Vat than the wild type strain [115]. Further, sequence analysis of the *vat* promoter region predicted the presence of three potential H-NS binding sites in the *vat* promoter region [115]. It seems H-NS could also potentially directly regulate other SPATE genes, as there are predicted putative H-NS binding sites present in SPATE gene promoter regions (Table 2). However, further experimental evidence will be required to confirm whether or not regulation of expression of SPATEs by H-NS is a common phenomenon.

Table 2. The potential H-NS binding sites on the promoter region of SPATEs as predicted by Virtual Footprint Software [a].

SPATEs	Potential H-NS Binding Sites
boa	$^{-97}$GCAATAAACC^{-88} (−), $^{-96}$GCAATAAAAT^{-87} (−),$^{-80}$GCTATAAAAA^{-71} (−)
sigA	$^{-179}$TGGTTAGATA^{-170} (−),$^{-170}$GTGATTGATT^{-161} (−), $^{-19}$CCGATATTTC^{-10} (−)
pic	$^{-159}$CAGATAAAAC^{-150} (+), $^{-109}$TGCATTAATG^{-100} (−), $^{-35}$GGGATATAAA^{-26} (−)
sepA	$^{-176}$ATGATAAAAA^{-167}(+), $^{-35}$AAGATTAATT^{-26} (−)
tsh/hbp	$^{-164}$CACATAAAGT^{-155} (−), $^{-28}$AAAATAAAAT^{-19} (−), $^{-10}$GTAATTAAAA^{-1} (+)
espC	$^{-300}$ACCATTAAAA^{-291} (+), $^{-299}$CCATTAAAAT^{-290} (+), $^{-111}$GCCACAAACT^{-102} (−)
espP	$^{-280}$TCGATTGTTA^{-271} (−), $^{-96}$CAGATAAATG^{-87} (−), $^{-46}$CTGATACATT^{-37} (+)
pet	$^{-177}$ATGATTAATT^{-168} (+),$^{-42}$AGGATTAAGA^{-33} (−),$^{-24}$TCAATAAATG^{-15} (+)
sat	$^{-177}$ACGATCAATT^{-168} (+),$^{-166}$ACGATCAATT^{-157} (+),$^{-24}$TCAATAAATG^{-15} (+)
eatA	$^{-88}$GCTATCTATT^{-79} (+),$^{-71}$ACAATAAATG^{-62} (+),$^{-40}$TCCACACAAC^{-31} (−)

Table 2. *Cont.*

SPATEs	Potential H-NS Binding Sites
eaaA	$^{-314}$ACCATACAGC^{-305} (−),$^{-124}$GCGGTAAAAA^{-115} (−)
tagB	$^{-304}$ACGAAAAAAA^{-295} (−),$^{-161}$CTGATAAATA^{-152} (−),$^{-128}$TCGATAAATG^{-119} (+)
tagC	$^{-256}$GCAATTAATA^{-247} (+),$^{-62}$TCGCTATATT^{-53} (+),$^{-56}$ACTATAAATA^{-47} (−)
sha	$^{-187}$CCCACAAATC^{-178} (−),$^{-48}$TCCTTATATT^{-39} (+),$^{-32}$TCAATAGATA^{-23} (−)
vat	$^{-296}$TCCATATATC^{-287} (+),$^{-295}$TGGATATATG^{-286} (−),$^{-107}$GCTATATAAT^{-98} (−)

ᵃ Virtual Footprint software [140] was used for in silico analysis of different SPATEs promoter region for putative regulatory H-NS binding sites and additional experimentation is required to confirm a role for H-NS in regulation of SPATE gene regulation. Pattern matching tool Virtual Footprint used specific position weight matrices (PWMs) to generate the top three potential binding sites upstream to the start codon with high scoring matches. (+/− strand).

5.3. Regulation of Vat by the MarR-Related Protein VatX

The multiple antibiotic resistance regulator (MarR) family are proteins that regulate the expression of many genes involved in resistance to multiple antibiotics including tetracycline, chloramphenicol, β-lactams, nalidixic acid, penicillins, fluoroquinolones, toxic substances, organic solvents, oxidative stress agents and pathogenic factors [115,141–145]. In *E. coli*, MarR is located in the chromosome in the *mar* locus and consists of an operator marO and two divergent transcriptional units marC and marRAB [146]. Besides, the possible role of H-NS as a negative regulator of Vat, an open reading frame was located downstream of the *vat* gene designated as ORF26 in the VAT-PAI from Ec222 [46] and c0392 in CFT073 [53]. This ORF shares 44% amino acid identity to the protein PapX (P pilus-associated transcriptional regulatory) from CFT073 [115,147]. PapX has been described as a member of the MarR family, it regulates flagella by binding to the *flhDC* promoter region [115,147]. Considering identity to PapX, the ORF was named VatX. The *vatX* gene is present and adjacent to the *vat* gene in many strains. The VatX protein contains a MarR protein family (PFAM) domain (PF01047) and a helix-turn-helix motif that is characteristic of DNA binding proteins and was classified in a different clade of MarR family regulators, and is more closely related to the PapX, SfaX, and FocX fimbria-associated regulators. In UPEC strain CFT073, overexpression of VatX increased expression of Vat 3-fold compared to wild-type levels. Interestingly, in the absence of H-NS, the *vat* and *vatX* genes were both co-transcribed, suggesting VatX may compete with H-NS to promote expression of *vat* [115].

5.4. Co-Regulation of SPATEs by CRP and FIS Proteins

The cyclic AMP receptor protein (CRP) is a global transcription factor which is required by *E. coli* in carbon metabolism [148,149]. CRP binds as a homodimer to a 16-bp DNA binding site, is allosterically activated by cAMP binding and interacts with RNA polymerase as either an activator or a repressor of transcription initiation [150]. CRP has been identified as a key transcription factor for the *pet* gene in EAEC strain 042 [151]. In addition, transcription from the *pet* promoter was found to be co-dependent on CRP and Fis regulators and the synergy between these regulators was due to the non-optimal position for transcription initiation of CRP and the additional required binding of the Fis regulator [151]. Fis is a versatile transcription factor and is involved in site-specific recombination events, organization of local DNA topology in bacterial chromosomes, and as a global transcription factor [152,153]. It binds DNA as a homodimer that recognizes a degenerate 15-bp binding sequence often found in many promoter regions [154]. Through a co-activation mechanism, Fis was also shown to co-regulate SPATE genes with CRP including the *sat* gene from UPEC and *sigA* from *Shigella sonnei* [155].

Clearly, further investigation of regulation of SPATE expression by either DNA-binding proteins, transcriptional factors and mechanisms controlling expression of different SPATE proteins is needed. Further, potential cross-talk or hierarchical production of different SPATES needs to be considered and to what extent other virulence proteins affect the trafficking and secretion of SPATEs, if they are

using the same secretion machinery such as BAM/TAM systems for their export and biogenesis at the bacterial cell surface.

6. Some SPATEs Can Also Mediate Degradation of Bacterial Protein Targets

The perspective of considering SPATEs uniquely as virulence proteins specifically produced to damage host cells and promote infection has been called into question in recent years. A newly described role for some SPATEs has been identified to be the degradation of bacterial proteins and secretion systems. Protease activity of SPATEs has mainly been determined for host proteins, however, importantly, some SPATEs can play an important role in infection through targeting of other bacterial substrates. The EatA SPATE from ETEC degrades the ETEC EtpA adhesin which can lead to reduced intestinal colonization [54]. Reduced colonization may be an advantage for ETEC to quickly deliver enterotoxin without causing extensive damage and may reduce inflammation and decrease the host immune response – acting as hit and run strategy of the bacteria. Similar activity was shown by EspC, wherein EspC reduced secretion of EspA and EspD, which are effector proteins of the EPEC T3SS [83]. In this case, EspC contributed to reducing pore formation and cytotoxicity by degrading EspA and EspD. A similar interchangeable activity was found for EspP [83]. Therefore, these SPATEs can also contribute to EPEC/EHEC infections by degrading other bacterial secreted proteins secreted by the T3SS before they contact the host cell. Another example of interference with other bacterial virulence factors is EspPα present in EHEC, which has been shown to degrade the pore-forming repeats-in-toxin (RTX)-protein hemolysin Ehx (EHEC- Hly) [156] in its free and vesicle-bound form [131]. EspP mediated cleavage was specific to the Ehx hydrophobic domain, which is crucial for interaction with the host cell membrane and pore formation [157]. Similarly, the reduction in the level of active pore-forming toxin may also alter the host immune response and contribute to intestinal colonization and pathogenesis.

7. Conclusions

Improved technologies and affordability of DNA sequencing and other methods to investigate bacterial/host interactions has greatly advanced our understanding of many aspects of bacterial pathogenesis in recent years. The large amount of data from genome sequences has also resulted in the determination of new putative SPATEs, which may also contribute to host colonization and infection. Two decades after the characterization of the first SPATE, much progress has been made in the study of SPATEs by combining in silico bioinformatics, bacteriology, molecular biology, biochemistry and cellular biology and pathogenesis studies. Within the SPATE family, all members may share a similar global structure, but each SPATE may mediate distinct functional properties and substrate specificities and be associated with certain bacterial pathotypes, the type of the disease they cause, and host animal species they infect. One would expect that the variety of host and tissues niches could result in diversification of SPATE functions. Further, these pathogens can also differ in their interactions with the host, with some SPATE-producing pathogens remaining extracellular during infection, whereas others may invade cells or survive in host phagocytes. Many questions remain to be answered about the molecular basis for substrate recognition and specificity of SPATEs and also fundamentally understanding how these proteins are regulated. It is also unclear to what extent these SPATEs may modulate or alter proteins and the bacterial surface and effect pathogenesis. Moreover, the SPATE proteins are also frequently present in certain enterobacterial pathogens commonly associated with both enteric and systemic diseases in humans and animal hosts. As these proteins are highly immunogenic, it stands to reason that the SPATEs or their conserved epitopes can be targeted for potential approaches to develop vaccines to prevent such diseases.

References

1. Henderson, I.R.; Navarro-Garcia, F.; Desvaux, M.; Fernandez, R.C.; Ala'Aldeen, D. Type V protein secretion pathway: The autotransporter story. *Microbiol. Mol. Biol. Rev.* **2004**, *68*, 692–744. [CrossRef] [PubMed]

2. Linke, D.; Riess, T.; Autenrieth, I.B.; Lupas, A.; Kempf, V.A. Trimeric autotransporter adhesins: Variable structure, common function. *Trends Microbiol.* **2006**, *14*, 264–270. [CrossRef] [PubMed]

3. Salacha, R.; Kovačić, F.; Brochier-Armanet, C.; Wilhelm, S.; Tommassen, J.; Filloux, A.; Voulhoux, R.; Bleves, S. The Pseudomonas aeruginosa patatin-like protein PlpD is the archetype of a novel Type V secretion system. *Environ. Microbiol.* **2010**, *12*, 1498–1512. [PubMed]

4. Leo, J.C.; Grin, I.; Linke, D. Type V secretion: Mechanism (s) of autotransport through the bacterial outer membrane. *Phil. Trans. R. Soc. B* **2012**, *367*, 1088–1101. [CrossRef] [PubMed]

5. Jacob-Dubuisson, F.; Locht, C.; Antoine, R. Two-partner secretion in Gram-negative bacteria: A thrifty, specific pathway for large virulence proteins. *Mol. Microbiol.* **2001**, *40*, 306–313. [CrossRef] [PubMed]

6. Khan, S.; Mian, H.S.; Sandercock, L.E.; Chirgadze, N.Y.; Pai, E.F. Crystal structure of the passenger domain of the *Escherichia coli* autotransporter EspP. *J. Mol. Biol.* **2011**, *413*, 985–1000. [CrossRef]

7. Otto, B.R.; Sijbrandi, R.; Luirink, J.; Oudega, B.; Heddle, J.G.; Mizutani, K.; Park, S.-Y.; Tame, J.R. Crystal structure of hemoglobin protease, a heme binding autotransporter protein from pathogenic *Escherichia coli*. *J. Biol. Chem.* **2005**, *280*, 17339–17345. [CrossRef]

8. Meza-Aguilar, J.D.; Fromme, P.; Torres-Larios, A.; Mendoza-Hernández, G.; Hernandez-Chiñas, U.; Campos, C.A.E.; Fromme, R. X-ray crystal structure of the passenger domain of plasmid encoded toxin (Pet), an autotransporter enterotoxin from enteroaggregative *Escherichia coli* (EAEC). *Biochem. Biophys. Res. Commun.* **2014**, *445*, 439–444. [CrossRef]

9. Veiga, E.; Sugawara, E.; Nikaido, H.; de Lorenzo, V.; Fernández, L.A. Export of autotransported proteins proceeds through an oligomeric ring shaped by C-terminal domains. *EMBO J.* **2002**, *21*, 2122–2131. [CrossRef]

10. Selkrig, J.; Mosbahi, K.; Webb, C.T.; Belousoff, M.J.; Perry, A.J.; Wells, T.J.; Morris, F.; Leyton, D.L.; Totsika, M.; Phan, M.-D. Discovery of an archetypal protein transport system in bacterial outer membranes. *Nat. Struct. Mol. Biol.* **2012**, *19*, 506. [CrossRef]

11. Ruiz-Perez, F.; Henderson, I.R.; Leyton, D.L.; Rossiter, A.E.; Zhang, Y.; Nataro, J.P. Roles of periplasmic chaperone proteins in the biogenesis of serine protease autotransporters of Enterobacteriaceae. *J. Bacteriol.* **2009**, *191*, 6571–6583. [CrossRef]

12. Sijbrandi, R.; Urbanus, M.L.; Corinne, M.; Bernstein, H.D.; Oudega, B.; Otto, B.R.; Luirink, J. Signal recognition particle (SRP)-mediated targeting and Sec-dependent translocation of an extracellular *Escherichia coli* protein. *J. Biol. Chem.* **2003**, *278*, 4654–4659. [CrossRef] [PubMed]

13. Purdy, G.E.; Fisher, C.R.; Payne, S.M. IcsA surface presentation in Shigella flexneri requires the periplasmic chaperones DegP, Skp, and SurA. *J. Bacteriol.* **2007**, *189*, 5566–5573. [CrossRef] [PubMed]

14. Sauri, A.; Soprova, Z.; Wickström, D.; de Gier, J.-W.; Van der Schors, R.C.; Smit, A.B.; Jong, W.S.; Luirink, J. The Bam (Omp85) complex is involved in secretion of the autotransporter haemoglobin protease. *Microbiology* **2009**, *155*, 3982–3991. [CrossRef] [PubMed]

15. Peterson, J.H.; Tian, P.; Ieva, R.; Dautin, N.; Bernstein, H.D. Secretion of a bacterial virulence factor is driven by the folding of a C-terminal segment. *Proc. Natl. Acad. Sci. USA* **2010**, *107*, 17739–17744. [CrossRef]

16. Michaelis, S.; Hunt, J.; Beckwith, J. Effects of signal sequence mutations on the kinetics of alkaline phosphatase export to the periplasm in *Escherichia coli*. *J. Bacteriol.* **1986**, *167*, 160–167. [CrossRef]

17. Martoglio, B.; Dobberstein, B. Signal sequences: More than just greasy peptides. *Trends Cell Biol.* **1998**, *8*, 410–415. [CrossRef]

18. Randall, L.; Hardy, S. SecB, one small chaperone in the complex milieu of the cell. *Cell. Mol. Life Sci. Cmls* **2002**, *59*, 1617–1623. [CrossRef]

19. Valent, Q.A.; Scotti, P.A.; High, S.; de Gier, J.W.L.; von Heijne, G.; Lentzen, G.; Wintermeyer, W.; Oudega, B.; Luirink, J. The *Escherichia coli* SRP and SecB targeting pathways converge at the translocon. *EMBO J.* **1998**, *17*, 2504–2512. [CrossRef]

20. Bredemeier, R.; Schlegel, T.; Ertel, F.; Vojta, A.; Borissenko, L.; Bohnsack, M.T.; Groll, M.; Von Haeseler, A.; Schleiff, E. Functional and phylogenetic properties of the pore-forming β-barrel transporters of the Omp85 family. *J. Biol. Chem.* **2007**, *282*, 1882–1890. [CrossRef]

21. Fleming, P.J.; Patel, D.S.; Wu, E.L.; Qi, Y.; Yeom, M.S.; Sousa, M.C.; Fleming, K.G.; Im, W. BamA POTRA domain interacts with a native lipid membrane surface. *Biophys. J.* **2016**, *110*, 2698–2709. [CrossRef] [PubMed]

22. Albrecht, R.; Schütz, M.; Oberhettinger, P.; Faulstich, M.; Bermejo, I.; Rudel, T.; Diederichs, K.; Zeth, K. Structure of BamA, an essential factor in outer membrane protein biogenesis. *Acta Crystallogr. Sect. D Biol. Crystallogr.* **2014**, *70*, 1779–1789. [CrossRef] [PubMed]

23. Gruss, F.; Zähringer, F.; Jakob, R.P.; Burmann, B.M.; Hiller, S.; Maier, T. The structural basis of autotransporter translocation by TamA. *Nat. Struct. Mol. Biol.* **2013**, *20*, 1318. [CrossRef] [PubMed]

24. Noinaj, N.; Kuszak, A.J.; Balusek, C.; Gumbart, J.C.; Buchanan, S.K. Lateral opening and exit pore formation are required for BamA function. *Structure* **2014**, *22*, 1055–1062. [CrossRef]

25. Eslava, C.; Navarro-García, F.; Czeczulin, J.R.; Henderson, I.R.; Cravioto, A.; Nataro, J.P. Pet, an autotransporter enterotoxin from enteroaggregative *Escherichia coli*. *Infect. Immun.* **1998**, *66*, 3155–3163.

26. Brunder, W.; Schmidt, H.; Karch, H. EspP, a novel extracellular serine protease of enterohaemorrhagic *Escherichia coli* O157: H7 cleaves human coagulation factor V. *Mol. Microbiol.* **1997**, *24*, 767–778. [CrossRef]

27. Dautin, N.; Barnard, T.J.; Anderson, D.E.; Bernstein, H.D. Cleavage of a bacterial autotransporter by an evolutionarily convergent autocatalytic mechanism. *EMBO J.* **2007**, *26*, 1942–1952. [CrossRef]

28. Dautin, N.; Bernstein, H.D. Residues in a conserved α-helical segment are required for cleavage but not secretion of an *Escherichia coli* serine protease autotransporter passenger domain. *J. Bacteriol.* **2011**, *193*, 3748–3756. [CrossRef]

29. Kostakioti, M.; Stathopoulos, C. Role of the α-helical linker of the C-terminal translocator in the biogenesis of the serine protease subfamily of autotransporters. *Infect. Immun.* **2006**, *74*, 4961–4969. [CrossRef]

30. Leyton, D.L.; Adams, L.M.; Kelly, M.; Sloan, J.; Tauschek, M.; Robins-Browne, R.M.; Hartland, E.L. Contribution of a novel gene, rpeA, encoding a putative autotransporter adhesin to intestinal colonization by rabbit-specific enteropathogenic *Escherichia coli*. *Infect. Immun.* **2007**, *75*, 4664–4669. [CrossRef]

31. Habouria, H.; Pokharel, P.; Maris, S.; Garénaux, A.; Bessaiah, H.; Houle, S.; Veyrier, F.J.; Guyomard-Rabenirira, S.; Talarmin, A.; Dozois, C.M. Three new serine-protease autotransporters of Enterobacteriaceae (SPATEs) from extra-intestinal pathogenic *Escherichia coli* and combined role of SPATEs for cytotoxicity and colonization of the mouse kidney. *Virulence* **2019**, *10*, 568–587. [CrossRef] [PubMed]

32. Ohnishi, Y.; Beppu, T.; Horinouchi, S. Two genes encoding serine protease homologues in Serratia marcescens and characterization of their products in *Escherichia coli*. *J. Biochem.* **1997**, *121*, 902–913. [CrossRef] [PubMed]

33. Parham, N.J.; Pollard, S.J.; Desvaux, M.; Scott-Tucker, A.; Liu, C.; Fivian, A.; Henderson, I.R. Distribution of the serine protease autotransporters of the Enterobacteriaceae among extraintestinal clinical isolates of *Escherichia coli*. *J. Clin. Microbiol.* **2005**, *43*, 4076–4082. [CrossRef] [PubMed]

34. Vijayakumar, V.; Santiago, A.; Smith, R.; Smith, M.; Robins-Browne, R.M.; Nataro, J.P.; Ruiz-Perez, F. Role of class 1 serine protease autotransporter in the pathogenesis of Citrobacter rodentium colitis. *Infect. Immun.* **2014**, *82*, 2626–2636. [CrossRef]

35. Hu, Y.-H.; Zhou, H.-Z.; Jin, Q.-W.; Zhang, J. The serine protease autotransporter Tsh contributes to the virulence of Edwardsiella tarda. *Vet. Microbiol.* **2016**, *189*, 68–74. [CrossRef]

36. Dautin, N. Serine protease autotransporters of enterobacteriaceae (SPATEs): Biogenesis and function. *Toxins* **2010**, *2*, 1179–1206. [CrossRef]

37. Dozois, C.M.; Dho-Moulin, M.; Brée, A.; Fairbrother, J.M.; Desautels, C.; Curtiss, R. Relationship between the Tsh autotransporter and pathogenicity of avian *Escherichia coli* and localization and analysis of the Tsh genetic region. *Infect. Immun.* **2000**, *68*, 4145–4154. [CrossRef]

38. Stein, M.; Kenny, B.; Stein, M.A.; Finlay, B.B. Characterization of EspC, a 110-kilodalton protein secreted by enteropathogenic *Escherichia coli* which is homologous to members of the immunoglobulin A protease-like family of secreted proteins. *J. Bacteriol.* **1996**, *178*, 6546–6554. [CrossRef]

39. Henderson, I.R.; Czeczulin, J.; Eslava, C.; Noriega, F.; Nataro, J.P. Characterization of Pic, a Secreted Protease ofShigella flexneri and Enteroaggregative *Escherichia coli*. *Infect. Immun.* **1999**, *67*, 5587–5596.

40. Peterson, J.H.; Szabady, R.L.; Bernstein, H.D. An unusual signal peptide extension inhibits the binding of bacterial presecretory proteins to the signal recognition particle, trigger factor, and the SecYEG complex. *J. Biol. Chem.* **2006**, *281*, 9038–9048. [CrossRef]

41. Dutta, P.R.; Cappello, R.; Navarro-García, F.; Nataro, J.P. Functional comparison of serine protease autotransporters of Enterobacteriaceae. *Infect. Immun.* **2002**, *70*, 7105–7113. [CrossRef] [PubMed]

42. Ruiz-Perez, F.; Wahid, R.; Faherty, C.S.; Kolappaswamy, K.; Rodriguez, L.; Santiago, A.; Murphy, E.; Cross, A.; Sztein, M.B.; Nataro, J.P. Serine protease autotransporters from Shigella flexneri and pathogenic *Escherichia coli* target a broad range of leukocyte glycoproteins. *Proc. Natl. Acad. Sci. USA* **2011**, *108*, 12881–12886. [CrossRef] [PubMed]

43. Patel, S.K.; Dotson, J.; Allen, K.P.; Fleckenstein, J.M. Identification and molecular characterization of EatA, an autotransporter protein of enterotoxigenic *Escherichia coli*. *Infect. Immun.* **2004**, *72*, 1786–1794. [CrossRef]

44. Otto, B.R.; Van Dooren, S.J.; Nuijens, J.H.; Luirink, J.; Oudega, B. Characterization of a hemoglobin protease secreted by the pathogenic *Escherichia coli* strain EB1. *J. Exp. Med.* **1998**, *188*, 1091–1103. [CrossRef] [PubMed]

45. Guyer, D.M.; Henderson, I.R.; Nataro, J.P.; Mobley, H.L. Identification of sat, an autotransporter toxin produced by uropathogenic *Escherichia coli*. *Mol. Microbiol.* **2000**, *38*, 53–66. [CrossRef] [PubMed]

46. Parreira, V.; Gyles, C. A novel pathogenicity island integrated adjacent to the thrW tRNA gene of avian pathogenic *Escherichia coli* encodes a vacuolating autotransporter toxin. *Infect. Immun.* **2003**, *71*, 5087–5096. [CrossRef] [PubMed]

47. Ruiz-Perez, F.; Nataro, J.P. Bacterial serine proteases secreted by the autotransporter pathway: Classification, specificity, and role in virulence. *Cell. Mol. Life Sci.* **2014**, *71*, 745–770. [CrossRef]

48. Saitou, N.; Nei, M. The neighbor-joining method: A new method for reconstructing phylogenetic trees. *Mol. Biol. Evol.* **1987**, *4*, 406–425.

49. Jones, D.T.; Taylor, W.R.; Thornton, J.M. The rapid generation of mutation data matrices from protein sequences. *Bioinformatics* **1992**, *8*, 275–282. [CrossRef]

50. Tamura, K.; Stecher, G.; Peterson, D.; Filipski, A.; Kumar, S. MEGA6: Molecular evolutionary genetics analysis version 6.0. *Mol. Biol. Evol.* **2013**, *30*, 2725–2729. [CrossRef]

51. Ciccarelli, F.D.; Doerks, T.; Von Mering, C.; Creevey, C.J.; Snel, B.; Bork, P. Toward automatic reconstruction of a highly resolved tree of life. *Science* **2006**, *311*, 1283–1287. [CrossRef] [PubMed]

52. Heimer, S.R.; Rasko, D.A.; Lockatell, C.V.; Johnson, D.E.; Mobley, H.L. Autotransporter genes pic and tsh are associated with *Escherichia coli* strains that cause acute pyelonephritis and are expressed during urinary tract infection. *Infect. Immun.* **2004**, *72*, 593–597. [CrossRef] [PubMed]

53. Welch, R.A.; Burland, V.; Plunkett, G.; Redford, P.; Roesch, P.; Rasko, D.; Buckles, E.; Liou, S.-R.; Boutin, A.; Hackett, J. Extensive mosaic structure revealed by the complete genome sequence of uropathogenic *Escherichia coli*. *Proc. Natl. Acad. Sci. USA* **2002**, *99*, 17020–17024. [CrossRef] [PubMed]

54. Roy, K.; Kansal, R.; Bartels, S.R.; Hamilton, D.J.; Shaaban, S.; Fleckenstein, J.M. Adhesin degradation accelerates delivery of heat-labile toxin by enterotoxigenic E. coli. *J. Biol. Chem.* **2011**, *286*, 29771–29779. [CrossRef]

55. Navarro-García, F.; Canizalez-Roman, A.; Sui, B.Q.; Nataro, J.P.; Azamar, Y. The serine protease motif of EspC from enteropathogenic *Escherichia coli* produces epithelial damage by a mechanism different from that of Pet toxin from enteroaggregative E. coli. *Infect. Immun.* **2004**, *72*, 3609–3621. [CrossRef]

56. Serapio-Palacios, A.; Navarro-Garcia, F. EspC, an autotransporter protein secreted by enteropathogenic *Escherichia coli*, causes apoptosis and necrosis through caspase and calpain activation, including direct procaspase-3 cleavage. *MBio* **2016**, *7*, e00479-16. [CrossRef]

57. Elisa Drago-Serrano, M.; Gavilanes Parra, S.; Angel Manjarrez-Hernández, H. EspC, an autotransporter protein secreted by enteropathogenic *Escherichia coli* (EPEC), displays protease activity on human hemoglobin. *FEMS Microbiol. Lett.* **2006**, *265*, 35–40. [CrossRef]

58. Navarro-Garcia, F.; Serapio-Palacios, A.; Vidal, J.E.; Salazar, M.I.; Tapia-Pastrana, G. EspC promotes epithelial cell detachment by enteropathogenic *Escherichia coli* via sequential cleavages of a cytoskeletal protein and then focal adhesion proteins. *Infect. Immun.* **2014**, *82*, 2255–2265. [CrossRef]

59. Henderson, I.R.; Hicks, S.; Navarro-Garcia, F.; Elias, W.P.; Philips, A.D.; Nataro, J.P. Involvement of the Enteroaggregative *Escherichia coli* Plasmid-Encoded Toxin in Causing Human Intestinal Damage. *Infect. Immun.* **1999**, *67*, 5338–5344.

60. Navarro-García, F.; Sears, C.; Eslava, C.; Cravioto, A.; Nataro, J.P. Cytoskeletal effects induced by pet, the serine protease enterotoxin of enteroaggregative *Escherichia coli*. *Infect. Immun.* **1999**, *67*, 2184–2192.

61. Canizalez-Roman, A.; Navarro-García, F. Fodrin CaM-binding domain cleavage by Pet from enteroaggregative *Escherichia coli* leads to actin cytoskeletal disruption. *Mol. Microbiol.* **2003**, *48*, 947–958. [CrossRef] [PubMed]

62. Parham, N.J.; Srinivasan, U.; Desvaux, M.; Foxman, B.; Marrs, C.F.; Henderson, I.R. PicU, a second serine protease autotransporter of uropathogenic *Escherichia coli*. *FEMS Microbiol. Lett.* **2004**, *230*, 73–83. [CrossRef]

63. Ayala-Lujan, J.L.; Vijayakumar, V.; Gong, M.; Smith, R.; Santiago, A.E.; Ruiz-Perez, F. Broad spectrum activity of a lectin-like bacterial serine protease family on human leukocytes. *PLoS ONE* **2014**, *9*, e107920. [CrossRef] [PubMed]

64. Brockmeyer, J.; Bielaszewska, M.; Fruth, A.; Bonn, M.L.; Mellmann, A.; Humpf, H.-U.; Karch, H. Subtypes of the plasmid-encoded serine protease EspP in Shiga toxin-producing *Escherichia coli*: Distribution, secretion, and proteolytic activity. *Appl. Environ. Microbiol.* **2007**, *73*, 6351–6359. [CrossRef] [PubMed]

65. Schmidt, H.; Zhang, W.-L.; Hemmrich, U.; Jelacic, S.; Brunder, W.; Tarr, P.; Dobrindt, U.; Hacker, J.; Karch, H. Identification and characterization of a novel genomic island integrated at selC in locus of enterocyte effacement-negative, Shiga toxin-producing *Escherichia coli*. *Infect. Immun.* **2001**, *69*, 6863–6873. [CrossRef] [PubMed]

66. Orth, D.; Ehrlenbach, S.; Brockmeyer, J.; Khan, A.B.; Huber, G.; Karch, H.; Sarg, B.; Lindner, H.; Würzner, R. EspP, a serine protease of enterohemorrhagic *Escherichia coli*, impairs complement activation by cleaving complement factors C3/C3b and C5. *Infect. Immun.* **2010**, *78*, 4294–4301. [CrossRef]

67. Otto, B.R.; Van Dooren, S.J.; Dozois, C.M.; Luirink, J.; Oudega, B. *Escherichia coli* hemoglobin protease autotransporter contributes to synergistic abscess formation and heme-dependent growth of Bacteroides fragilis. *Infect. Immun.* **2002**, *70*, 5–10. [CrossRef]

68. Gutiérrez, D.; Pardo, M.; Montero, D.; Oñate, A.; Farfán, M.J.; Ruiz-Pérez, F.; Del Canto, F.; Vidal, R. TleA, a Tsh-like autotransporter identified in a human enterotoxigenic *Escherichia coli* strain. *Infect. Immun.* **2015**, *83*, 1893–1903. [CrossRef]

69. Guyer, D.M.; Radulovic, S.; Jones, F.-E.; Mobley, H.L. Sat, the secreted autotransporter toxin of uropathogenic *Escherichia coli*, is a vacuolating cytotoxin for bladder and kidney epithelial cells. *Infect. Immun.* **2002**, *70*, 4539–4546. [CrossRef]

70. Benjelloun-Touimi, Z.; Sansonetti, P.J.; Parsot, C. SepA, the major extracellular protein of Shigella flexneri: Autonomous secretion and involvement in tissue invasion. *Mol. Microbiol.* **1995**, *17*, 123–135. [CrossRef]

71. Benjelloun-Touimi, Z.; Tahar, M.S.; Montecucco, C.; Sansonetti, P.J.; Parsot, C. SepA, the 110 kDa protein secreted by Shigella flexneri: Two-domain structure and proteolytic activity. *Microbiology* **1998**, *144*, 1815–1822. [CrossRef] [PubMed]

72. Al-Hasani, K.; Henderson, I.R.; Sakellaris, H.; Rajakumar, K.; Grant, T.; Nataro, J.P.; Robins-Browne, R.; Adler, B. The sigA gene which is borne on the shepathogenicity island of Shigella flexneri 2a encodes an exported cytopathic protease involved in intestinal fluid accumulation. *Infect. Immun.* **2000**, *68*, 2457–2463. [CrossRef] [PubMed]

73. Al-Hasani, K.; Navarro-Garcia, F.; Huerta, J.; Sakellaris, H.; Adler, B. The immunogenic SigA enterotoxin of Shigella flexneri 2a binds to HEp-2 cells and induces fodrin redistribution in intoxicated epithelial cells. *PLoS ONE* **2009**, *4*, e8223. [CrossRef] [PubMed]

74. Yen, Y.T.; Kostakioti, M.; Henderson, I.R.; Stathopoulos, C. Common themes and variations in serine protease autotransporters. *Trends Microbiol.* **2008**, *16*, 370–379. [CrossRef]

75. Sandt, C.H.; Hill, C.W. Four Different Genes Responsible for Nonimmune Immunoglobulin-Binding Activities within a Single Strain of *Escherichia coli*. *Infect. Immun.* **2000**, *68*, 2205–2214. [CrossRef]

76. Restieri, C.; Garriss, G.; Locas, M.-C.; Dozois, C.M. Autotransporter-encoding sequences are phylogenetically distributed among *Escherichia coli* clinical isolates and reference strains. *Appl. Environ. Microbiol.* **2007**, *73*, 1553–1562. [CrossRef]

77. Kumar, P.; Luo, Q.; Vickers, T.J.; Sheikh, A.; Lewis, W.G.; Fleckenstein, J.M. EatA, an immunogenic protective antigen of enterotoxigenic *Escherichia coli*, degrades intestinal mucin. *Infect. Immun.* **2014**, *82*, 500–508. [CrossRef]

78. Del Canto, F.; Valenzuela, P.; Cantero, L.; Bronstein, J.; Blanco, J.E.; Blanco, J.; Prado, V.; Levine, M.; Nataro, J.; Sommerfelt, H. Distribution of classical and nonclassical virulence genes in enterotoxigenic *Escherichia coli* isolates from Chilean children and tRNA gene screening for putative insertion sites for genomic islands. *J. Clin. Microbiol.* **2011**, *49*, 3198–3203. [CrossRef]

79. Andrade, F.B.; Abreu, A.G.; Nunes, K.O.; Gomes, T.A.; Piazza, R.M.; Elias, W.P. Distribution of serine protease autotransporters of Enterobacteriaceae in typical and atypical enteroaggregative *Escherichia coli*. *Infect. Genet. Evol.* **2017**, *50*, 83–86. [CrossRef]

80. Mellies, J.L.; Navarro-Garcia, F.; Okeke, I.; Frederickson, J.; Nataro, J.P.; Kaper, J.B. espC pathogenicity island of enteropathogenic *Escherichia coli* encodes an enterotoxin. *Infect. Immun.* **2001**, *69*, 315–324. [CrossRef]

81. Vidal, J.E.; Navarro-García, F. Efficient translocation of EspC into epithelial cells depends on enteropathogenic *Escherichia coli* and host cell contact. *Infect. Immun.* **2006**, *74*, 2293–2303. [CrossRef] [PubMed]

82. Vidal, J.E.; Navarro-García, F. EspC translocation into epithelial cells by enteropathogenic *Escherichia coli* requires a concerted participation of type V and III secretion systems. *Cell. Microbiol.* **2008**, *10*, 1975–1986. [CrossRef] [PubMed]

83. Guignot, J.; Segura, A.; Van Nhieu, G.T. The serine protease EspC from enteropathogenic *Escherichia coli* regulates pore formation and cytotoxicity mediated by the type III secretion system. *PLoS Pathog.* **2015**, *11*, e1005013. [CrossRef] [PubMed]

84. Garmendia, J.; Frankel, G.; Crepin, V.F. Enteropathogenic and enterohemorrhagic *Escherichia coli* infections: Translocation, translocation, translocation. *Infect. Immun.* **2005**, *73*, 2573–2585. [CrossRef]

85. Nemec, K.N.; Scaglione, P.; Navarro-García, F.; Huerta, J.; Tatulian, S.A.; Teter, K. A host-specific factor is necessary for efficient folding of the autotransporter plasmid-encoded toxin. *Biochimie* **2010**, *92*, 171–177. [CrossRef]

86. Wagner, J.K.; Heindl, J.E.; Gray, A.N.; Jain, S.; Goldberg, M.B. Contribution of the periplasmic chaperone Skp to efficient presentation of the autotransporter IcsA on the surface of Shigella flexneri. *J. Bacteriol.* **2009**, *191*, 815–821. [CrossRef]

87. Navarro-García, F.; Canizalez-Roman, A.; Luna, J.; Sears, C.; Nataro, J.P. Plasmid-Encoded Toxin of Enteroaggregative *Escherichia coli* is Internalized by Epithelial Cells. *Infect. Immun.* **2001**, *69*, 1053–1060. [CrossRef]

88. Navarro-García, F.; Canizalez-Roman, A.; Burlingame, K.E.; Teter, K.; Vidal, J.E. Pet, a non-AB toxin, is transported and translocated into epithelial cells by a retrograde trafficking pathway. *Infect. Immun.* **2007**, *75*, 2101–2109. [CrossRef]

89. Dutta, P.R.; Sui, B.Q.; Nataro, J.P. Structure-function analysis of the enteroaggregative *Escherichia coli* plasmid-encoded toxin autotransporter using scanning linker mutagenesis. *J. Biol. Chem.* **2003**, *278*, 39912–39920. [CrossRef]

90. Nava-Acosta, R.; Navarro-Garcia, F. Cytokeratin 8 is an epithelial cell receptor for Pet, a cytotoxic serine protease autotransporter of Enterobacteriaceae. *MBio* **2013**, *4*, e00838-13. [CrossRef]

91. Chavez-Dueñas, L.; Serapio-Palacios, A.; Nava-Acosta, R.; Navarro-Garcia, F. The subdomain 2 of the autotransporter Pet is the ligand site for recognizing Pet receptor on the epithelial cell surface. *Infect. Immun.* **2016**, *84*, 2012–2021. [CrossRef] [PubMed]

92. Villaseca, J.M.; Navarro-García, F.; Mendoza-Hernández, G.; Nataro, J.P.; Cravioto, A.; Eslava, C. Pet toxin from enteroaggregative *Escherichia coli* produces cellular damage associated with fodrin disruption. *Infect. Immun.* **2000**, *68*, 5920–5927. [CrossRef] [PubMed]

93. Martin, S.J.; O'Brien, G.A.; Nishioka, W.K.; McGahon, A.J.; Mahboubi, A.; Saido, T.C.; Green, D.R. Proteolysis of fodrin (non-erythroid spectrin) during apoptosis. *J. Biol. Chem.* **1995**, *270*, 6425–6428. [CrossRef] [PubMed]

94. Wang, K.K.; Posmantur, R.; Nath, R.; McGinnis, K.; Whitton, M.; Talanian, R.V.; Glantz, S.B.; Morrow, J.S. Simultaneous degradation of αII-and βII-spectrin by caspase 3 (CPP32) in apoptotic cells. *J. Biol. Chem.* **1998**, *273*, 22490–22497. [CrossRef]

95. Sanchez-Villamil, J.I.; Navarro-Garcia, F.; Castillo-Romero, A.; Gutierrez-Gutierrez, F.; Tapia-Pastrana, G. Curcumin blocks cytotoxicity of enteroaggregative and enteropathogenic *Escherichia coli* by blocking Pet and EspC proteolytic release from bacterial outer membrane. *Front. Cell. Infect. Microbiol.* **2019**, *9*, 334. [CrossRef]

96. Abreu, A.G.; Abe, C.M.; Nunes, K.O.; Moraes, C.T.; Chavez-Dueñas, L.; Navarro-Garcia, F.; Barbosa, A.S.; Piazza, R.M.; Elias, W.P. The serine protease Pic as a virulence factor of atypical enteropathogenic *Escherichia coli*. *Gut Microbes* **2016**, *7*, 115–125. [CrossRef]

97. Harrington, S.M.; Sheikh, J.; Henderson, I.R.; Ruiz-Perez, F.; Cohen, P.S.; Nataro, J.P. The Pic protease of enteroaggregative *Escherichia coli* promotes intestinal colonization and growth in the presence of mucin. *Infect. Immun.* **2009**, *77*, 2465–2473. [CrossRef]

98. Navarro-Garcia, F.; Gutierrez-Jimenez, J.; Garcia-Tovar, C.; Castro, L.A.; Salazar-Gonzalez, H.; Cordova, V. Pic, an autotransporter protein secreted by different pathogens in the Enterobacteriaceae family, is a potent mucus secretagogue. *Infect. Immun.* **2010**, *78*, 4101–4109. [CrossRef]

99. Abreu, A.G.; Fraga, T.R.; Granados Martínez, A.P.; Kondo, M.Y.; Juliano, M.A.; Juliano, L.; Navarro-Garcia, F.; Isaac, L.; Barbosa, A.S.; Elias, W.P. The serine protease Pic from enteroaggregative *Escherichia coli* mediates immune evasion by the direct cleavage of complement proteins. *J. Infect. Dis.* **2015**, *212*, 106–115. [CrossRef]

100. Bhullar, K.; Zarepour, M.; Yu, H.; Yang, H.; Croxen, M.; Stahl, M.; Finlay, B.B.; Turvey, S.E.; Vallance, B.A. The serine protease autotransporter pic modulates citrobacter rodentium pathogenesis and its innate recognition by the host. *Infect. Immun.* **2015**, *83*, 2636–2650. [CrossRef]

101. Brockmeyer, J.; Spelten, S.; Kuczius, T.; Bielaszewska, M.; Karch, H. Structure and function relationship of the autotransport and proteolytic activity of EspP from Shiga toxin-producing *Escherichia coli*. *PLoS ONE* **2009**, *4*, e6100. [CrossRef] [PubMed]

102. Djafari, S.; Ebel, F.; Deibel, C.; Krämer, S.; Hudel, M.; Chakraborty, T. Characterization of an exported protease from Shiga toxin-producing *Escherichia coli*. *Mol. Microbiol.* **1997**, *25*, 771–784. [CrossRef] [PubMed]

103. Boisen, N.; Ruiz-Perez, F.; Scheutz, F.; Krogfelt, K.A.; Nataro, J.P. High prevalence of serine protease autotransporter cytotoxins among strains of enteroaggregative *Escherichia coli*. *Am. J. Trop. Med. Hyg.* **2009**, *80*, 294–301. [CrossRef] [PubMed]

104. Velarde, J.J.; Nataro, J.P. Hydrophobic residues of the autotransporter EspP linker domain are important for outer membrane translocation of its passenger. *J. Biol. Chem.* **2004**, *279*, 31495–31504. [CrossRef]

105. Ruiz-Perez, F.; Henderson, I.R.; Nataro, J.P. Interaction of FkpA, a peptidyl-prolyl cis/trans isomerase with EspP autotransporter protein. *Gut Microbes* **2010**, *1*, 339–344. [CrossRef]

106. Xicohtencatl-Cortes, J.; Saldaña, Z.; Deng, W.; Castañeda, E.; Freer, E.; Tarr, P.I.; Finlay, B.B.; Puente, J.L.; Girón, J.A. Bacterial macroscopic rope-like fibers with cytopathic and adhesive properties. *J. Biol. Chem.* **2010**, *285*, 32336–32342. [CrossRef]

107. Khan, A.B.; Naim, A.; Orth, D.; Grif, K.; Mohsin, M.; Prager, R.; Dierich, M.P.; Würzner, R. Serine protease espP subtype α, but not β or γ, of Shiga toxin-producing *Escherichia coli* is associated with highly pathogenic serogroups. *Int. J. Med Microbiol.* **2009**, *299*, 247–254. [CrossRef]

108. Weiss, A.; Joerss, H.; Brockmeyer, J. Structural and functional characterization of cleavage and inactivation of human serine protease inhibitors by the bacterial SPATE protease EspPα from enterohemorrhagic E. coli. *PLoS ONE* **2014**, *9*, e111363. [CrossRef]

109. Tse, C.; In, J.; Yin, J.; Donowitz, M.; Doucet, M.; Foulke-Abel, J.; Ruiz-Perez, F.; Nataro, J.; Zachos, N.; Kaper, J. Enterohemorrhagic E. coli (EHEC)—Secreted Serine Protease EspP Stimulates Electrogenic Ion Transport in Human Colonoid Monolayers. *Toxins* **2018**, *10*, 351. [CrossRef]

110. Provence, D.L.; Curtiss, R. Isolation and characterization of a gene involved in hemagglutination by an avian pathogenic *Escherichia coli* strain. *Infect. Immun.* **1994**, *62*, 1369–1380.

111. Nicholson, B.A.; West, A.C.; Mangiamele, P.; Barbieri, N.; Wannemuehler, Y.; Nolan, L.K.; Logue, C.M.; Li, G. Genetic characterization of ExPEC-like virulence plasmids among a subset of NMEC. *PLoS ONE* **2016**, *11*, e0147757. [CrossRef] [PubMed]

112. Kostakioti, M.; Stathopoulos, C. Functional analysis of the Tsh autotransporter from an avian pathogenic *Escherichia coli* strain. *Infect. Immun.* **2004**, *72*, 5548–5554. [CrossRef] [PubMed]

113. Stathopoulos, C.; Provence, D.L.; Curtiss, R. Characterization of the Avian Pathogenic *Escherichia coli* Hemagglutinin Tsh, a Member of the Immunoglobulin A Protease-Type Family of Autotransporters. *Infect. Immun.* **1999**, *67*, 772–781. [PubMed]

114. Maluta, R.P.; Gatti, M.S.V.; Joazeiro, P.P.; De Paiva, J.B.; Rojas, T.C.G.; Silveira, F.; Houle, S.; Kobayashi, R.K.T.; Dozois, C.M.; Dias da Silveira, W. Avian extraintestinal *Escherichia coli* exhibits enterotoxigenic-like activity in the in vivo rabbit ligated ileal loop assay. *Foodborne Pathog. Dis.* **2014**, *11*, 484–489. [CrossRef]

115. Nichols, K.B.; Totsika, M.; Moriel, D.G.; Lo, A.W.; Yang, J.; Wurpel, D.J.; Rossiter, A.E.; Strugnell, R.A.; Henderson, I.R.; Ulett, G.C. Molecular characterization of the vacuolating autotransporter toxin in uropathogenic *Escherichia coli*. *J. Bacteriol.* **2016**, *198*, 1487–1498. [CrossRef]

116. Subashchandrabose, S.; Smith, S.N.; Spurbeck, R.R.; Kole, M.M.; Mobley, H.L. Genome-wide detection of fitness genes in uropathogenic *Escherichia coli* during systemic infection. *PLoS Pathog.* **2013**, *9*, e1003788. [CrossRef]

117. Gibold, L.; Garenaux, E.; Dalmasso, G.; Gallucci, C.; Cia, D.; Mottet-Auselo, B.; Faïs, T.; Darfeuille-Michaud, A.; Nguyen, H.T.T.; Barnich, N. The Vat-AIEC protease promotes crossing of the intestinal mucus layer by Crohn's disease-associated *Escherichia coli*. *Cell. Microbiol.* **2016**, *18*, 617–631. [CrossRef]

118. Tapader, R.; Chatterjee, S.; Singh, A.; Dayma, P.; Haldar, S.; Pal, A.; Basu, S. The high prevalence of serine protease autotransporters of Enterobacteriaceae (SPATEs) in *Escherichia coli* causing neonatal septicemia. *Eur. J. Clin. Microbiol. Infect. Dis.* **2014**, *33*, 2015–2024. [CrossRef]

119. Liévin-Le Moal, V.; Comenge, Y.; Ruby, V.; Amsellem, R.; Nicolas, V.; Servin, A.L. Secreted autotransporter toxin (Sat) triggers autophagy in epithelial cells that relies on cell detachment. *Cell. Microbiol.* **2011**, *13*, 992–1013. [CrossRef]

120. Maroncle, N.M.; Sivick, K.E.; Brady, R.; Stokes, F.-E.; Mobley, H.L. Protease activity, secretion, cell entry, cytotoxicity, and cellular targets of secreted autotransporter toxin of uropathogenic *Escherichia coli*. *Infect. Immun.* **2006**, *74*, 6124–6134. [CrossRef]

121. Guignot, J.; Chaplais, C.; Coconnier-Polter, M.H.; Servin, A.L. The secreted autotransporter toxin, Sat, functions as a virulence factor in Afa/Dr diffusely adhering *Escherichia coli* by promoting lesions in tight junction of polarized epithelial cells. *Cell. Microbiol.* **2007**, *9*, 204–221. [CrossRef] [PubMed]

122. Taddei, C.R.; Fasano, A.; Ferreira, A.J.; Trabulsi, L.R.; Martinez, M.B. Secreted autotransporter toxin produced by a diffusely adhering *Escherichia coli* strain causes intestinal damage in animal model assays. *FEMS Microbiol. Lett.* **2005**, *250*, 263–269. [CrossRef] [PubMed]

123. Toloza, L.; Giménez, R.; Fábrega, M.J.; Alvarez, C.S.; Aguilera, L.; Cañas, M.A.; Martín-Venegas, R.; Badia, J.; Baldomà, L. The secreted autotransporter toxin (Sat) does not act as a virulence factor in the probiotic *Escherichia coli* strain Nissle 1917. *BMC Microbiol.* **2015**, *15*, 250. [CrossRef] [PubMed]

124. Coron, E.; Flamant, M.; Aubert, P.; Wedel, T.; Pedron, T.; Letessier, E.; Galmiche, J.P.; Sansonetti, P.J.; Neunlist, M. Characterisation of early mucosal and neuronal lesions following Shigella flexneri infection in human colon. *PLoS ONE* **2009**, *4*, e4713. [CrossRef] [PubMed]

125. Maldonado-Contreras, A.; Birtley, J.R.; Boll, E.; Zhao, Y.; Mumy, K.L.; Toscano, J.; Ayehunie, S.; Reinecker, H.-C.; Stern, L.J.; McCormick, B.A. Shigella depends on SepA to destabilize the intestinal epithelial integrity via cofilin activation. *Gut Microbes* **2017**, *8*, 544–560. [CrossRef]

126. Huang, T.Y.; DerMardirossian, C.; Bokoch, G.M. Cofilin phosphatases and regulation of actin dynamics. *Curr. Opin. Cell Biol.* **2006**, *18*, 26–31. [CrossRef]

127. Scorza, F.B.; Colucci, A.M.; Maggiore, L.; Sanzone, S.; Rossi, O.; Ferlenghi, I.; Pesce, I.; Caboni, M.; Norais, N.; Di Cioccio, V. High yield production process for Shigella outer membrane particles. *PLoS ONE* **2012**, *7*, e35616.

128. Oany, A.R.; Pervin, T.; Mia, M.; Hossain, M.; Shahnaij, M.; Mahmud, S.; Kibria, K. Vaccinomics approach for designing potential peptide vaccine by targeting Shigella spp. serine protease autotransporter subfamily protein SigA. *J. Immunol. Res.* **2017**, *2017*, 6412353. [CrossRef]

129. Fookes, M.; Schroeder, G.N.; Langridge, G.C.; Blondel, C.J.; Mammina, C.; Connor, T.R.; Seth-Smith, H.; Vernikos, G.S.; Robinson, K.S.; Sanders, M. Salmonella bongori provides insights into the evolution of the Salmonellae. *PLoS Pathog.* **2011**, *7*, e1002191. [CrossRef]

130. Ebel, F.; Deibel, C.; Kresse, A.U.; Guzman, C.A.; Chakraborty, T. Temperature-and medium-dependent secretion of proteins by Shiga toxin-producing *Escherichia coli*. *Infect. Immun.* **1996**, *64*, 4472–4479.

131. Brockmeyer, J.; Aldick, T.; Soltwisch, J.; Zhang, W.; Tarr, P.I.; Weiss, A.; Dreisewerd, K.; Müthing, J.; Bielaszewska, M.; Karch, H. Enterohaemorrhagic *Escherichia coli* haemolysin is cleaved and inactivated by serine protease EspPα. *Environ. Microbiol.* **2011**, *13*, 1327–1341. [CrossRef] [PubMed]

132. Friedberg, D.; Umanski, T.; Fang, Y.; Rosenshine, I. Hierarchy in the expression of the locus of enterocyte effacement genes of enteropathogenic *Escherichia coli*. *Mol. Microbiol.* **1999**, *34*, 941–952. [CrossRef] [PubMed]

133. Elliott, S.J.; Sperandio, V.; Girón, J.A.; Shin, S.; Mellies, J.L.; Wainwright, L.; Hutcheson, S.W.; McDaniel, T.K.; Kaper, J.B. The Locus of enterocyte effacement (LEE)-encoded regulator controls expression of both LEE-and non-LEE-encoded virulence factors in enteropathogenic and enterohemorrhagic *Escherichia coli*. *Infect. Immun.* **2000**, *68*, 6115–6126. [CrossRef] [PubMed]

134. Drlica, K.; Rouviere-Yaniv, J. Histonelike proteins of bacteria. *Microbiol. Rev.* **1987**, *51*, 301.

135. Workman, J.; Kingston, R. Alteration of nucleosome structure as a mechanism of transcriptional regulation. *Annu. Rev. Biochem.* **1998**, *67*, 545–579. [CrossRef]

136. Anuchin, A.; Goncharenko, A.; Demidenok, O.; Kaprelyants, A. Histone-like proteins of bacteria (review). *Appl. Biochem. Microbiol.* **2011**, *47*, 580–585. [CrossRef]

137. Allsopp, L.P.; Beloin, C.; Ulett, G.C.; Valle, J.; Totsika, M.; Sherlock, O.; Ghigo, J.-M.; Schembri, M.A. Molecular characterization of UpaB and UpaC, two new autotransporter proteins of uropathogenic *Escherichia coli* CFT073. *Infect. Immun.* **2012**, *80*, 321–332. [CrossRef]

138. Allsopp, L.P.; Beloin, C.; Moriel, D.G.; Totsika, M.; Ghigo, J.-M.; Schembri, M.A. Functional heterogeneity of the UpaH autotransporter protein from uropathogenic *Escherichia coli*. *J. Bacteriol.* **2012**, *194*, 5769–5782. [CrossRef]

139. Totsika, M.; Wells, T.J.; Beloin, C.; Valle, J.; Allsopp, L.P.; King, N.P.; Ghigo, J.-M.; Schembri, M.A. Molecular characterization of the EhaG and UpaG trimeric autotransporter proteins from pathogenic *Escherichia coli*. *Appl. Environ. Microbiol.* **2012**, *78*, 2179–2189. [CrossRef]

140. Münch, R.; Hiller, K.; Grote, A.; Scheer, M.; Klein, J.; Schobert, M.; Jahn, D. Virtual Footprint and PRODORIC: An integrative framework for regulon prediction in prokaryotes. *Bioinformatics* **2005**, *21*, 4187–4189. [CrossRef]

141. George, A.; Levy, S. Gene in the major cotransduction gap of the *Escherichia coli* K-12 linkage map required for the expression of chromosomal resistance to tetracycline and other antibiotics. *J. Bacteriol.* **1983**, *155*, 541–548. [PubMed]

142. Cohen, S.P.; McMurry, L.; Hooper, D.; Wolfson, J.; Levy, S. Cross-resistance to fluoroquinolones in multiple-antibiotic-resistant (Mar) *Escherichia coli* selected by tetracycline or chloramphenicol: Decreased drug accumulation associated with membrane changes in addition to OmpF reduction. *Antimicrob. Agents Chemother.* **1989**, *33*, 1318–1325. [CrossRef] [PubMed]

143. George, A.M.; Levy, S.B. Amplifiable resistance to tetracycline, chloramphenicol, and other antibiotics in *Escherichia coli*: Involvement of a non-plasmid-determined efflux of tetracycline. *J. Bacteriol.* **1983**, *155*, 531–540. [PubMed]

144. Asako, H.; Nakajima, H.; Kobayashi, K.; Kobayashi, M.; Aono, R. Organic solvent tolerance and antibiotic resistance increased by overexpression of marA in *Escherichia coli*. *Appl. Environ. Microbiol.* **1997**, *63*, 1428–1433. [PubMed]

145. Ariza, R.; Cohen, S.; Bachhawat, N.; Levy, S.; Demple, B. Repressor mutations in the marRAB operon that activate oxidative stress genes and multiple antibiotic resistance in *Escherichia coli*. *J. Bacteriol.* **1994**, *176*, 143–148. [CrossRef]

146. Cohen, S.P.; Hächler, H.; Levy, S. Genetic and functional analysis of the multiple antibiotic resistance (mar) locus in *Escherichia coli*. *J. Bacteriol.* **1993**, *175*, 1484–1492. [CrossRef]

147. Simms, A.N.; Mobley, H.L. PapX, a P fimbrial operon-encoded inhibitor of motility in uropathogenic *Escherichia coli*. *Infect. Immun.* **2008**, *76*, 4833–4841. [CrossRef]

148. Gosset, G.; Zhang, Z.; Nayyar, S.; Cuevas, W.A.; Saier, M.H. Transcriptome analysis of Crp-dependent catabolite control of gene expression in *Escherichia coli*. *J. Bacteriol.* **2004**, *186*, 3516–3524. [CrossRef]

149. Green, J.; Stapleton, M.R.; Smith, L.J.; Artymiuk, P.J.; Kahramanoglou, C.; Hunt, D.M.; Buxton, R.S. Cyclic-AMP and bacterial cyclic-AMP receptor proteins revisited: Adaptation for different ecological niches. *Curr. Opin. Microbiol.* **2014**, *18*, 1–7. [CrossRef]

150. Won, H.-S.; Lee, Y.-S.; Lee, S.-H.; Lee, B.-J. Structural overview on the allosteric activation of cyclic AMP receptor protein. *Biochim. Biophys. Acta (BBA) Proteins Proteom.* **2009**, *1794*, 1299–1308. [CrossRef]

151. Rossiter, A.E.; Browning, D.F.; Leyton, D.L.; Johnson, M.D.; Godfrey, R.E.; Wardius, C.A.; Desvaux, M.; Cunningham, A.F.; Ruiz-Perez, F.; Nataro, J.P. Transcription of the plasmid-encoded toxin gene from Enteroaggregative *Escherichia coli* is regulated by a novel co-activation mechanism involving CRP and Fis. *Mol. Microbiol.* **2011**, *81*, 179–191. [CrossRef] [PubMed]

152. Koch, C.; Kahmann, R. Purification and properties of the *Escherichia coli* host factor required for inversion of the G segment in bacteriophage Mu. *J. Biol. Chem.* **1986**, *261*, 15673–15678. [PubMed]

153. Travers, A.; Schneider, R.; Muskhelishvili, G. DNA supercoiling and transcription in *Escherichia coli*: The FIS connection. *Biochimie* **2001**, *83*, 213–217. [CrossRef]

154. Kahramanoglou, C.; Seshasayee, A.S.; Prieto, A.I.; Ibberson, D.; Schmidt, S.; Zimmermann, J.; Benes, V.; Fraser, G.M.; Luscombe, N.M. Direct and indirect effects of H-NS and Fis on global gene expression control in *Escherichia coli*. *Nucleic Acids Res.* **2010**, *39*, 2073–2091. [CrossRef] [PubMed]

155. Rossiter, A.E.; Godfrey, R.E.; Connolly, J.A.; Busby, S.J.; Henderson, I.R.; Browning, D.F. Expression of different bacterial cytotoxins is controlled by two global transcription factors, CRP and Fis, that co-operate in a shared-recruitment mechanism. *Biochem. J.* **2015**, *466*, 323–335. [CrossRef] [PubMed]

156. Schmidt, H.; Beutin, L.; Karch, H. Molecular analysis of the plasmid-encoded hemolysin of *Escherichia coli* O157: H7 strain EDL 933. *Infect. Immun.* **1995**, *63*, 1055–1061. [PubMed]

157. Welch, R. RTX toxin structure and function: A story of numerous anomalies and few analogies in toxin biology. In *Pore-Forming Toxins*; Springer: Berlin/Heidelberg, Germany, 2001.